Oxazaborolidines in Organocatalysis

The Importance of Noncovalent Interactions in the Corey-Bakshi-Shibata Reduction

Dissertation zur Erlangung des Doktorgrades der
Naturwissenschaftlichen Fachbereiche

(Fachbereich 08 – Biologie und Chemie)

der Justus-Liebig-Universität Gießen

vorgelegt von

Christian Eschmann

aus Gießen

Gießen 2022

Die vorliegende Arbeit wurde in der Zeit von April 2016 bis Januar 2022 am Institut für Organische Chemie der Justus-Liebig-Universität Gießen unter Anleitung von Herrn Prof. Dr. Peter R. Schreiner, Ph.D. angefertigt.

Eidesstattlich Erklärung nach §17 der Promotionsordnung

„Ich erkläre: Ich habe die vorgelegte Dissertation selbständig und ohne unerlaubte fremde Hilfe und nur mit den Hilfen angefertigt, die ich in der Dissertation angegeben habe. Alle Textstellen, die wörtlich oder sinngemäß aus veröffentlichten Schriften entnommen sind, und alle Angaben, die auf mündlichen Auskünften beruhen, sind als solche kenntlich gemacht. Bei den von mir durchgeführten und in der Dissertation erwähnten Untersuchungen habe ich die Grundsätze guter wissenschaftlicher Praxis, wie sie in der „Satzung der Justus-Liebig-Universität Giessen zur Sicherung guter wissenschaftlicher Praxis“ niedergelegt sind, eingehalten.“

Ort, Datum Unterschrift

Table of Contents

Summary 1

Zusammenfassung 3

Introduction

1. Organocatalysis – Catalysis with Amino Acids and Peptides 5

1.1. Oxazaborolidines in Organocatalysis 10

1.1.1. The Corey-Bakshi-Shibata (CBS) Reduction 10

1.1.2. Oxazaborolidines in C-C Bond Formations 16

2. Noncovalent Interactions 21

2.1.1. Hydrogen Bonding 22

2.1.2. London Dispersion 25

3. References 29

Chapter 1 Adamantane-Based Oxazaborolidines

1. Motivation 34

2. Results 35

3. Summary & Outlook 51

4. Experimental Section 54

5. Computational Data 71

6. Spectra 73

7. References 86

Chapter 2 Peptide-Based Oxazaborolidines

1. Motivation 90

2. Results 91

3. Summary and Outlook 109

4. Experimental Section 113

5. Spectra 130

6. References 146

Chapter 3 London Dispersion Interactions Rather than Steric Hindrance Determine the Enantioselectivity of the Corey-Bakshi-Shibata Reduction

1. Introduction 150

2. Results and Discussion 152

3. Conclusion 166

4. Computational Methods 167

5. Acknowledgements 167

6. References 168

7. Supporting Information 170

Part 2 Lewis Acid Enhancement in the House-Meinwald Rearrangement of Epoxides

1. Introduction 234

2. Motivation 239

3. Results 240

4. Summary & Outlook 263

5. Experimental Section 266

6. Spectra 288

7. References 316

Abbreviations and Acronyms 318

Acknowledgements 321

Summary

Part 1: Oxazaborolidines in Organocatalysis

The major part of this thesis deals with oxazaborolidines (OXB) as chiral organocatalysts for asymmetric Diels-Alder reactions and Corey-Bakshi-Shibata reductions. In order to expand the library of catalytically active OXB, the first two chapters describe the synthesis of new types of chiral OXB, which were then tested in catalysis. In the third chapter we investigated the noncovalent interactions (NCIs) in the CBS reduction and provide a novel explanation for the high selectivity of proline-based CBS catalysts.

Chapter 1 Adamantane-Based Oxazaborolidines

In the first chapter we envisaged establishing adamantane-based OXB as catalysts in order to combine the catalytic activity of OXB with the physicochemical properties of adamantane (lipophilicity, dispersion energy donor). For this purpose, we present synthetic routes to various enantiomerically enriched, vicinal adamantane amino alcohols. The amino alcohols were then used as precursors for the conversion to catalytically active OXB. Therefore, we investigated *in situ* protocols with different boronic acids and borane. The OXB obtained were finally employed in catalytic CBS reductions, but only provide poor enantioselectivities.

Chapter 2 Peptide-Based Oxazaborolidines

Based on the natural amino acid L-serine, we developed new precursors for OXB that can be attached to peptides. The peptide-bound precursors were converted to catalytically active OXB in an *in situ* synthesis with phenylboron dichloride and tested in asymmetric Diels-Alder reactions of α,β-unsaturated dienophiles and cyclopentadiene. The catalysis results show a strong influence of the peptide structure on activity and selectivity, respectively. The best selectivity is achieved by the OXB based on Ts-L-Ser-L-Phe-OMe with up to 58% *ee*.

In the second part of this chapter we investigated *trans*-4-hydroxy-L-proline as an OXB precursor, attachable to peptides *via* a Steglich esterification. The resulting peptide-bound OXB catalyze CBS reductions in high enantioselectivities with up to 88% *ee*. Thereby, the chiral peptide backbone hardly influences the enantioselectivity, which could enable the development of site-selective reductions or a multicatalysis approach.

Chapter 3 London Dispersion Interactions Rather than Steric Hindrance Determine the Enantioselectivity of the Corey-Bakshi-Shibata Reduction

Published as: C. Eschmann, L. Song, P. R. Schreiner, *Angew. Chem. Int. Ed.* **2021**, *60*, 4823–4832.

We investigated the origin of the outstanding enantioselectivity of established proline-based OXBs in CBS reduction. Therefore, we question Corey's often cited mechanistic hypothesis, which assumes steric repulsion as the main reason that determines selectivity. Utilizing detailed computational and experimental studies, we show that attractive London Dispersion (LD) interactions between catalyst and substrate are the main reason for the high selectivity. By functionalizing the CBS catalysts with dispersion energy donors (DED) in the *meta*-positions of the aryl groups, we can increase the selectivity of the CBS reduction for various substrates.

Part 2: Lewis Acid Enhancement in the House-Meinwald Rearrangement of Epoxides

The second part of this thesis deals with titanium Lewis acids, the catalytic activity of which can be enhanced by coordination to thioureas or BINOL ligands. We developed a protocol for the *in situ* formation of the complexes and verified their structure *via* NMR spectroscopy. The complexes were employed in the catalytic House-Meinwald rearrangement of epoxides. For complexes consisting of ureas or thioureas, we observed a dependency of the catalytic activity on the pK_A value. Therefore, the best results are obtained with Schreiner's thiourea. Squaramides and thiosquaramides generally deliver lower conversion. The use of chiral BINOL ligands leads to a kinetic resolution of the epoxides. Substitution in the 3,3‘-position of the BINOL ligands determines the quantitative enantioselectivity of the rearrangement, as well as the absolute configuration of the rearrangement products.

Zusammenfassung

Teil 1: Oxazaborolidine in der Organokatalyse

Der Hauptteil dieser Arbeit beschäftigt sich mit Oxazaborolidinen (OXB) als chirale Organokatalysatoren für asymmetrische Diels-Alder Reaktionen und Corey-Bakshi-Shibata-Reduktionen. Um die Bibliothek von katalytisch wirksamen OXB zu erweitern, beschreiben die ersten beiden Kapitel Synthesen zu neuartigen chiralen OXB, die dann in der Katalyse getestet wurden. Im dritten Kapitel untersuchen wir die nichtkovalenten Wechselwirkungen in der CBS-Reduktion und liefern eine neue Erklärung für die hohe Selektivität prolinbasierter CBS-Katalysatoren.

Kapitel 1 Adamantan-basierte Oxazaborolidine

Im ersten Kapitel beabsichtigten wir Adamantan-basierte OXB als neue Katalysatoren zu etablieren, um die katalytische Aktivität der OXB mit den physikochemischen Eigenschaften von Adamantan (Lipophilie, Dispersions-Energie-Donor) zu kombinieren. Dazu stellen wir Syntheserouten zu verschiedenen enantiomerenangereicherten, vicinalen Adamantan-Aminoalkoholen vor. Die Aminoalkohole wurden anschließend als Vorläufer für die Umsetzung zu katalytisch aktiven OXB verwendet. Dabei testeten wir *in situ* Synthesen mit verschiedenen Boronsäuren, sowie auch Boran. Die erhaltenen OXB wurden schließlich in katalytischen CBS-Reduktionen eingesetzt, liefern allerdings nur niedrige Enantioselektivitäten.

Kapitel 2 Peptidbasierte Oxazaborolidine

Ausgehend von der natürlichen Aminosäure L-Serin entwickelten wir neue Vorläufer für OXB, die sich an Peptide binden lassen. Die peptidgebundenen Vorläufer wurden in einer *in situ* Synthese mit Dichlorphenylboran zu katalytisch aktiven OXB umgesetzt und in asymmetrischen Diels-Alder Reaktionen von α,β-ungesättigten Dienophilen und Cyclopentadien getestet. Die Katalyse-Ergebnisse zeigen einen starken Einfluss der Peptidstruktur sowohl auf Aktivität und Selektivität. Die beste Selektivität erzielt das OXB basierend auf Ts-L-Ser-L-Phe-OMe mit bis zu 58% *ee*.

Im zweiten Teil dieses Kapitels untersuchten wir *trans*-4-Hydroxy-L-Prolin als OXB-Vorläufer, welcher über eine Steglich-Veresterung an Peptide gebunden werden kann. Die resultierenden peptidgebundenen OXB katalysieren CBS-Reduktionen in hohen Enantioselektivitäten mit bis zu 88% *ee*. Das chirale Peptidrückgrat nimmt dabei kaum Einfluss auf die Enantioselektivität, was die Entwicklung von Ort-selektiven Reduktionen oder einem Multikatalyse-Ansatz ermöglichen könnte.

Kapitel 3 London Dispersionswechselwirkungen anstatt sterischer Abstoßung bestimmen die Enantioselektivität der Corey-Bakshi-Shibata Reduktion

Publiziert als: C. Eschmann, L. Song, P. R. Schreiner, *Angew. Chem. Int. Ed.* **2021**, *60*, 4823–4832.

Wir untersuchten den Grund der herausragenden Enantioselektivität von bereits etablierten prolin-basierten OXBs in der CBS-Reduktion. Dazu hinterfragen wir Coreys oft zitierte mechanistische Hypothese, welche von sterischer Abstoßung als selektivitätsbestimmenden Hauptgrund ausgeht. Mit Hilfe von detaillierten computergestützten Berechnungen und experimentellen Studien zeigen wir, dass attraktive LD Wechselwirkungen zwischen Katalysator und Substrat den Hauptgrund für die hohe Selektivität bilden. Durch Funktionalisieren der CBS-Katalysatoren mit Dispersions-Energie-Donoren (DED) in den *meta*-Positionen der Arylgruppen können wir die Selektivität der CBS-Reduktion für verschiedene Substrate steigern.

Teil 2: Lewis-Säure Verstärkung in der House-Meinwald Umlagerung von Epoxiden

Der zweite Teil dieser Thesis beschäftigt sich mit Titan-Lewis-Säuren, deren katalytische Aktivität durch Koordination an Thioharnstoffe oder BINOL-Liganden verstärkt werden kann. Wir entwickelten ein Protokoll zur *in situ* Herstellung der Komplexe und verifizierten deren Struktur per NMR-Spektroskopie. Die Komplexe wurden in der katalytischen House-Meinwald Umlagerung von Epoxiden eingesetzt. Für Komplexe bestehend aus Harnstoffen oder Thioharnstoffen stellten wir eine Abhängigkeit der katalytischen Aktivität vom pK_S-Wert fest. Daher erhalten wir die besten Umsätze mit Schreiners Thioharnstoff. Quadratsäureamide und Thioquadratsäureamide liefern generell niedrigere Umsätze. Die Verwendung chiraler BINOL-Liganden führt zu einer kinetischen Racematspaltung der Epoxide. Substitution in 3,3‘-Position der BINOL-Liganden bestimmt die quantitative Enantioselektivität der Umlagerung sowie auch die absolute Konfiguration der Umlagerungsprodukte.

Introduction

In times of climate change, scarcity of resources, and *Fridays for future* demonstrations, the desire for sustainability and efficiency is a central aspect of various areas of our current society. Chemistry, in particular, has a responsibility to contribute to innovative, economical, and resource efficient methods in organic synthesis. To meet this obligation, huge advancements in the synthesis of chiral compounds have been made. Whether on millimolar laboratory or large industrial scale, asymmetric catalysis has extensively replaced the stoichiometric use of reagents and auxiliaries for the generation of chiral compounds.[1–3] Utilization of transition metals has led to numerous cross coupling reactions and asymmetric hydrogenations, whereas biocatalysts such as enzymes offer economic and environmental benefits for asymmetric synthesis of pharmaceutical compounds.[4] In addition to metal catalysis and biocatalysis, organocatalysis represents the third important pillar of asymmetric catalysis, making use of readily available small organic molecules like alkaloids, phosphoric acids, ureas, amino acids, and peptides.[2,3,5–8]

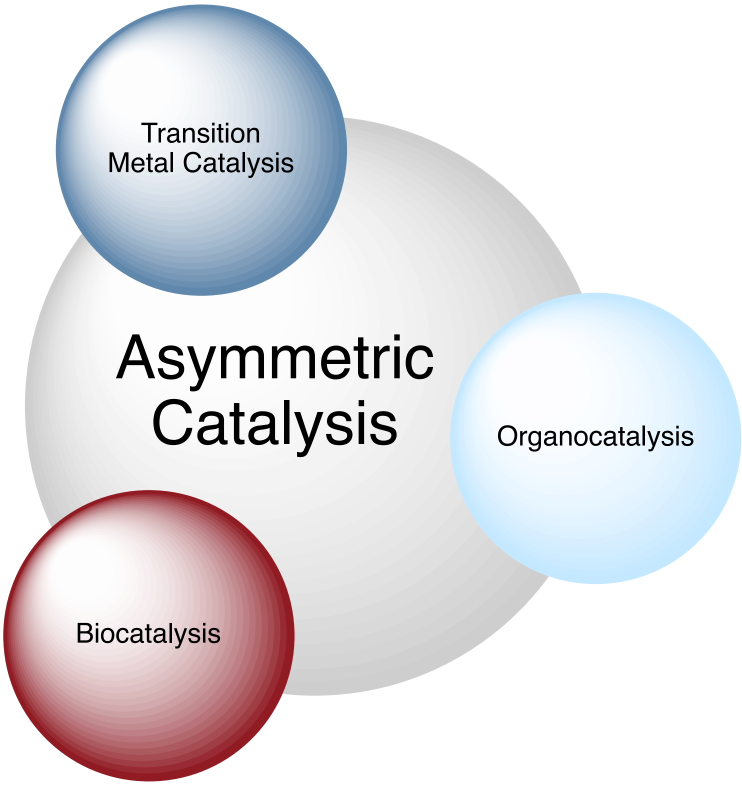

1. Organocatalysis – Catalysis with Amino Acids and Peptides

Asymmetric organocatalysis describes the use of small organic molecules (e.g., alkaloids, ureas, amino acids, peptides, or phosphoric acids) to catalyze organic transformations in enantioselective synthesis.[9] In general, chiral organocatalysts are non-toxic compounds, which are naturally available or cheap and easily to prepare in both enantiomeric forms.

Organocatalyzed reactions can be performed under mild reaction conditions without the need for transition metals. For this reason, organocatalysis has become attractive especially for pharmaceutical and medicinal chemistry, as no complex purification steps are necessary to remove toxic metals.

Publications on organocatalytic reactions have been known sporadically since the beginning of the 19th century. Classic examples include Wöhler's and Liebig's cyanide catalyzed formation of benzoin in 1832[10] or the proline catalyzed Hajos-Parrish-Eder-Sauer-Wiechert reaction for the synthesis of steroid precursors.[11] The term "*Organische Katalyse*" was first coined by Wolfang Langenbeck in 1927, who reported on isatin derivatives as catalysts for the dehydrogenation of amino acids.[12,13] However, the step towards a separate research topic started with the renaissance of organocatalysis in 2000 by the respective publications of MacMillan[14] and List, Lerner, and Barbas.[15] These seminal contributions initiated growing interest and further developments in this field, eventually culminating in the bestowal of the Nobel Prize in chemistry to List and MacMillan in 2021.

MacMillan reported the Diels-Alder reaction of α,β-unsaturated aldehyde **1** with cyclopentadiene (**2**) catalyzed by (*S*)-phenylalanine derived imidazolidinone **3** (Scheme 1a). LUMO lowering activation of **1** *via* formation of an iminium ion facilitated the [4+2] cycloaddition in excellent yield and enantioselectivity with up to 93% *ee*. Barbas and List developed the first proline (**7**) catalyzed direct intermolecular asymmetric aldol reaction between acetone (**5**) and *p*-nitrobenzaldehyde (**6**) *via* an enamine mechanism (Scheme 1b).

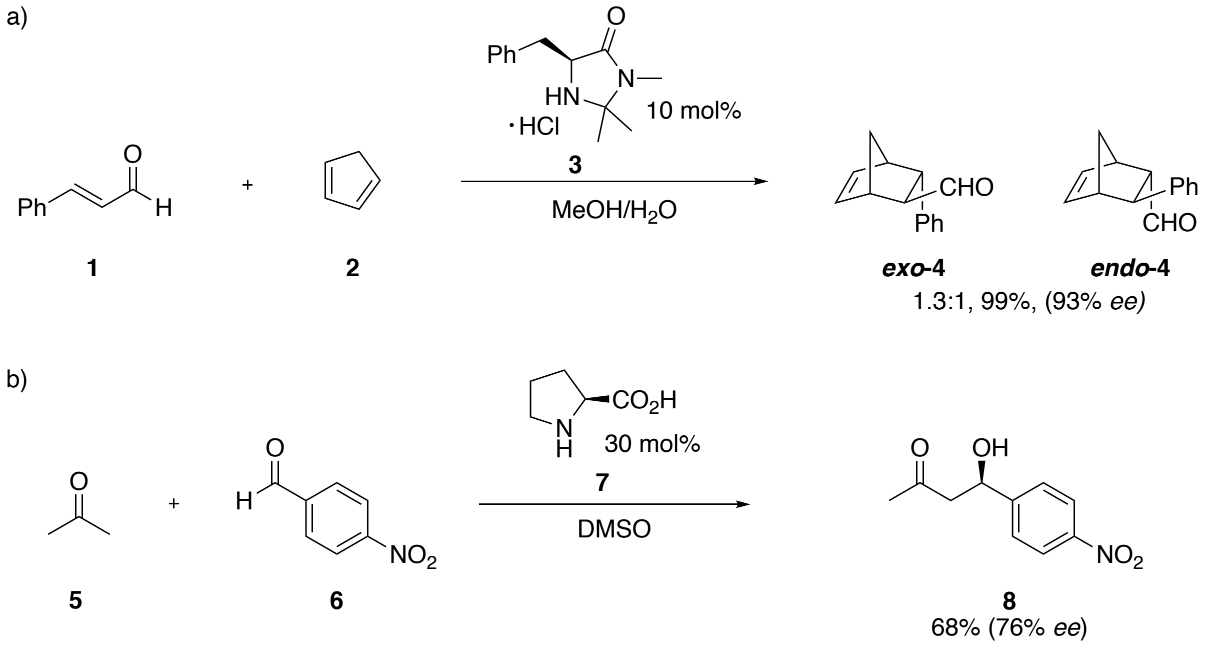

Scheme 1 a) MacMillan's organocatalyzed Diels-Alder reaction[14] and b) the asymmetric aldol reaction by Barbas and List.[15]

Organocatalytic modes are typically classified in covalent and noncovalent activation.[3] Catalysts such as amines and *N*-heterocyclic carbenes[16,17] (NHCs) form new covalent bonds with the substrates, whereby activated intermediates (enamines, iminium ions, acylium ions, enolates) are generated. On the other hand, common noncovalent organocatalysts include phase transfer catalysts[18–20] (PTC), hydrogen bond donors such as Brønsted acids[21,22], thioureas[23–26] or squaramides,[27] and chiral Lewis acids like oxazaborolidines (OXB).[28–31] Both covalent and noncovalent organocatalysts are often based on simple amino acids. Proline, in particular, forms the basis for many well-known organocatalysts. In addition to the already mentioned enamine catalysis by Barbas and List, it forms the basic structure of many established diarylprolinol derivatives, such as, for example, the Jørgensen-Hayashi catalysts.[32,33] These catalysts were independently developed by Jørgensen and Hayashi for iminium ion catalysis. Hayashi and coworkers employed diphenylprolinol silyl ether **9a** as organocatalyst for the asymmetric Michael reaction of aldehyde **10** with nitroalkene **11** (Scheme 2a). They observed that silylation of the prolinol dramatically improved the catalytic activity.[33] At the same time, Jørgensen and colleagues used trifluoromethyl substituted diphenylprolinol silyl ether **9b** as efficient organocatalyst for the direct enantioselective sulfenylation of aldehydes **13** (Scheme 2b).[32]

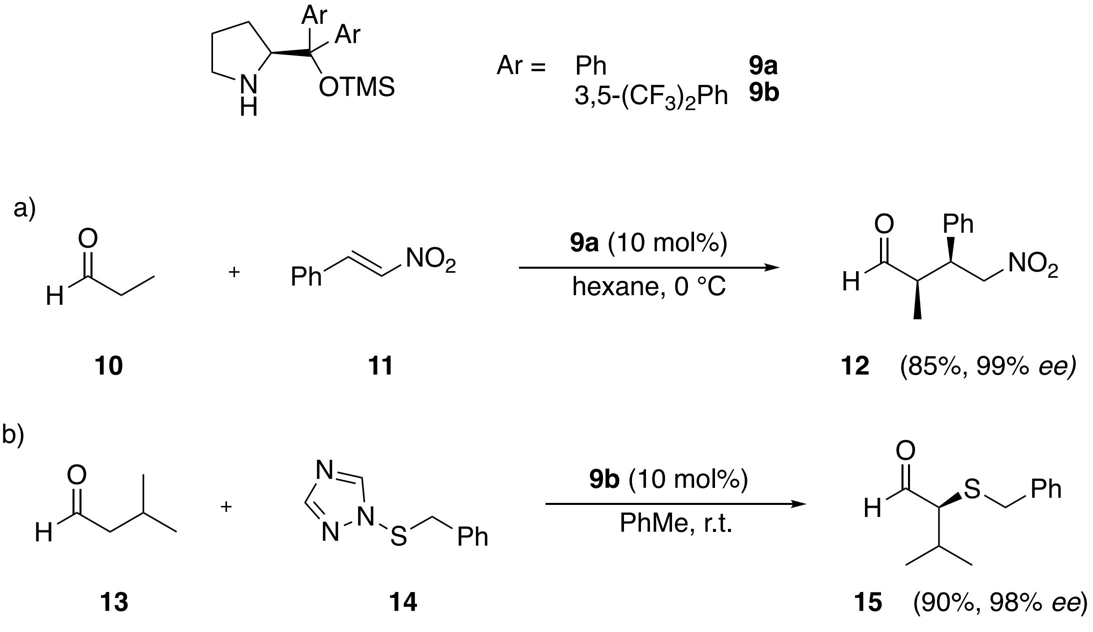

Scheme 2 a) **9a** catalyzed asymmetric Michael reaction by Hayashi[33] and b) **9b** catalyzed enantioselective sulfenylation by Jørgensen.[32]

Amino acids also form the basis for some noncovalent organocatalysts. Especially OXBs like the Corey-Bakshi-Shibata (CBS) catalysts operate as chiral Lewis acids in various reductions and cycloadditions and are mostly based on valine, proline, tryptophan, or threonine derivatives.[29,34]

While, on the one hand, with small organic molecules such as the mentioned diarylprolinol derivatives emphasis is placed on rigid, bulky structures in order to achieve high selectivities, larger catalysts rather provide structural flexibility as design element. Catalysts that adapt to substrates to maximize attractive noncovalent interactions for the stabilization of transition structures were reserved to enzyme catalysis for a long time.[35] Inspired by nature's enzyme and biocatalysis, chemists have successfully utilized synthetic oligopeptides as asymmetric catalysts for many chemical transformations including epoxidations, acylations, and C-C bond formations. Peptide catalysts consisting of chiral amino acids are able to perform highly stereoselective reactions. Moreover, chirality can be transferred by adopting secondary and tertiary structures in solution. In connection with their simple synthesis by solution-phase or solid phase peptide synthesis (SPPS) with readily available amino acids as building blocks, peptide catalysts can easily be tailored to specific substrates.[36,37]

In pioneering studies, Inoue and Oku already reported in 1979 the peptide catalyzed stereoselective hydrocyanation of aldehydes.[38] Since then, countless other reactions catalyzed by peptides have been reported, for example, the Morita-Baylis-Hillman reaction,[39] Friedel-Crafts alkylations,[40] or acyl transfer reactions.[41,42] During the last two decades, the development of efficient peptide catalysts was mainly driven by the groups of Miller, Wennemers, and Schreiner. Miller *et al.* established chiral oligopeptides bearing *π*-methyl-L-histidine (Pmh), a modified synthetic amino acid, as catalytic moiety for several group transfer reactions (e.g., acylation, phosphorylation, and sulfinylation).[42] The group of Wennemers employed peptides containing a Pro-Pro sequence as highly selective catalysts in enamine catalysis.[43] Schreiner developed a range of lipophilic peptide catalysts, which were able to perform the kinetic resolution of diols[41,44] and the first enantioselective Dakin-West reaction.[45] These catalysts, containing the nonproteinogenic amino acid γ-adamantyl glycine, provide a dynamic binding pocket for substrates. Moreover, he could show that attractive noncovalent interactions (NCIs) namely hydrogen bonding and London dispersion (LD) between the peptide catalyst and substrate facilitate the kinetic resolution of *trans*-diols, leading to high selectivity factors > 50.[46] In a recent publication, these peptides were also used to functionalize more complex carbohydrates in a site-selective manner. In the acylation of 4,6-*O*-benzylidene-α-D-glucopyranoside (**19**), chiral peptide catalyst **17** overwrites the intrinsic reactivity of *N*-methylimidazole (NMI) **16**, so that a selective acylation of the 2-position leading to **20** is possible (Scheme 3).[47] By incorporating an azo moiety into the peptide catalyst, it was also possible to show that the selectivity in the acylation of glucopyranosides can be controlled and changed by light.[48]

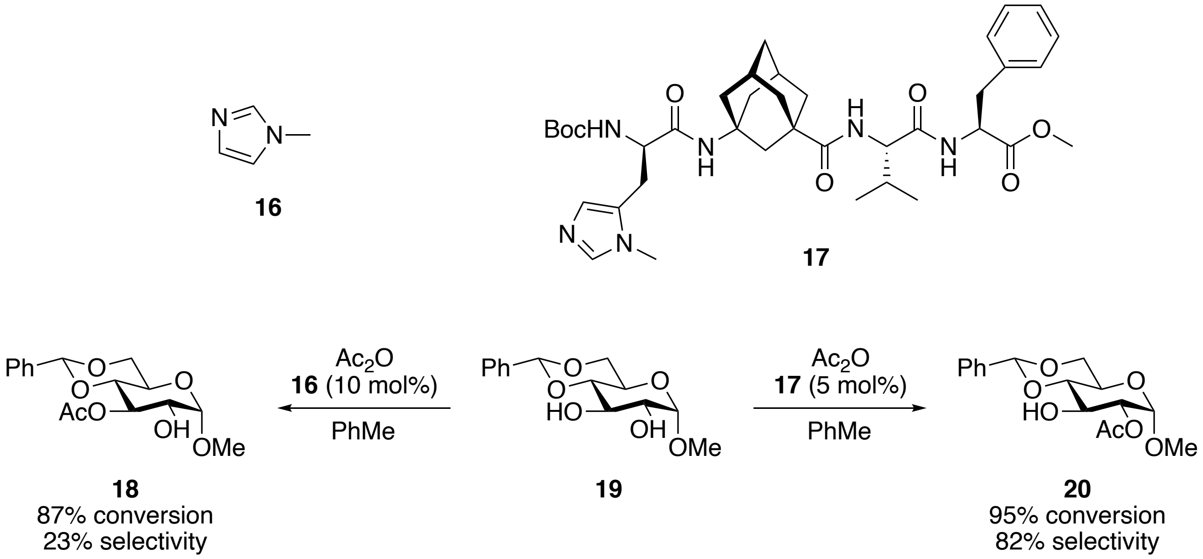

Scheme 3 Site-selective acylation of pyranosides **19** with oligopeptide catalyst **17**.[47]

Due to the modular structure of peptide catalysts and their chiral backbone, they offer the basis for multicatalysts. For this concept, several independently reactive catalytic moieties are attached to a single catalyst backbone, to promote complex multistep reactions in one pot. It is important here that an orthogonal reactivity of the catalytic motifs is ensured. This avoids time-consuming intermittent work-up steps and can lead to better atom- and redox economy by reducing waste.[49] The group of Schreiner refined their peptide catalysts to develop multicatalysts for the synthesis of enantiomerically enriched *trans*-diols and the enantioselective oxidative esterification of aldehydes.[50–52] In a proof of principle, aldehyde **22** is first oxidized by the TEMPO moiety to provide mixed anhydride **23**, which is then enantioselectively transferred onto *trans*-cycloalkane-1,2-diol by the Pmh moiety of the same catalyst **21** (Scheme 4). Importantly, the multicatalyst sequence provided similar yield and just slightly reduced enantioselectivities compared to the reaction sequence with individual catalysts, demonstrating the potential of multicatalysts to convert reactive intermediates that arise after the first catalytic step.

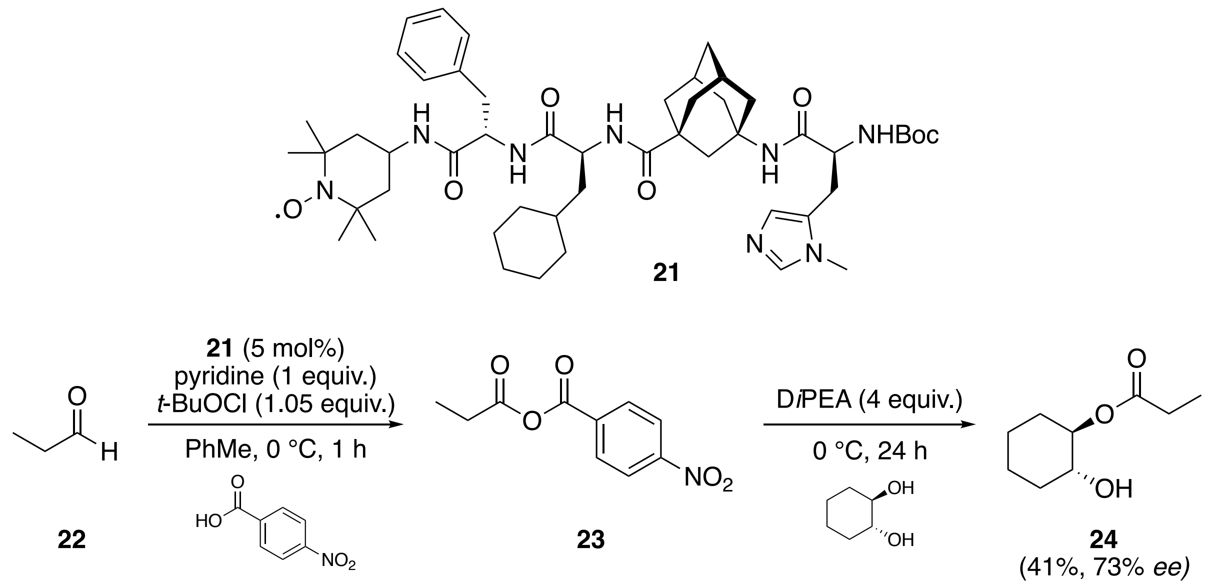

Scheme 4 Schreiner's peptide-based multicatalyst for oxidation and selective esterification.

These selected examples show the great advantages of amino acids and peptide-based catalysts in organocatalysis. They represent a green and sustainable approach and offer a variety of modes of activation for numerous reaction types. Moreover, the possibility of making chiral peptide catalysts tailored to specific substrate types holds great potential for addressing substrates that have previously reacted with only low selectivities.

1.1. Oxazaborolidines in Organocatalysis

Even though the term organocatalysis is naturally not directly associated with oxazaborolidines (OXB), they precisely fit into the concept of organocatalysis. OXBs are heterocyclic five-membered rings bearing oxygen, nitrogen and boron. They are often derived from natural amino acids and can act as chiral organocatalytic Lewis acids in various types of reactions.

1.1.1. The Corey-Bakshi-Shibata (CBS) Reduction

In 1981 Itsuno *et al.* first reported the asymmetric reduction of prochiral ketones by the stoichiometric use of amino alcohols such as (*S*)-prolinol, (*S*)-valinol, (*S*)-leucinol, and (*S*)-phenylalaninol, and two equivalents of $BH_3 \cdot THF$.[53–55] In a study to optimize the selectivity, they introduced two phenyl groups *via* a Grignard reaction to (*S*)-valine methyl ester and established (*S*)-diarylvalinol as ligand, which in cooperation with $BH_3 \cdot THF$ enabled reductions of aromatic ketones **25** with up to 94% *ee* (Scheme 5a).[56] They proposed formation of complex **28a** upon addition of $BH_3 \cdot THF$ to the corresponding amino alcohol **27** (Scheme 5b), which then can act as chiral reducing agent. The formation of the five-membered OXB ring occurs with release of H_2, which in addition to the formation of the thermodynamically stable B-O bond (192 kcal·mol^{-1}) represents the entropic driving force of the reaction.[57] Despite the excellent yield and high selectivity of the reduction, no mechanistic clarification or general application in asymmetric synthesis were reported.

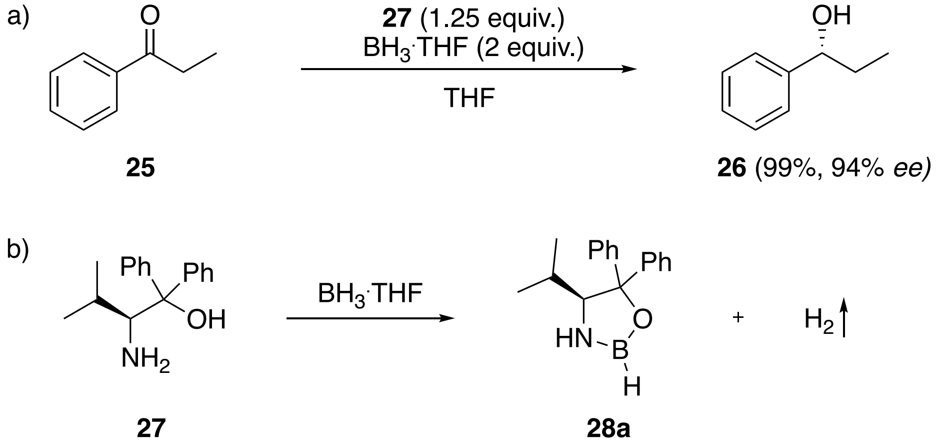

Scheme 5 a) Asymmetric reduction of aromatic ketones with stoichiometric amounts of (*S*)-diarylvalinol **27** and 2 equivalents of BH_3. b) Proposed complexation of borane by hydrogen extrusion leads to the chiral reducing agent **28a**.

A few years later, Itsuno's initial work was further investigated by Corey and coworkers. *Via* ^1H an ^{11}B NMR spectroscopy, they identified and thus proved OXB **28a**. However, by just using a stoichiometric amount of **28a**, they were not able to reduce any of the ketones in satisfying yield, even after several hours at 23 °C. It was only when they used a mixture of BH_3·THF and OXB **28a** that they were able to reproduce Itsuno's results. From these results they concluded that an additional complexation of the electrophilic borane with the OXB takes place, thus creating activated species **28a·BH₃** (Scheme 6). Considering this, they developed a protocol that allowed using catalytic amounts of the amino alcohol **27** and stoichiometric amounts of BH_3 as reducing agent, which ultimately became known as the Corey-Bakshi-Shibata (CBS) reduction.[28]

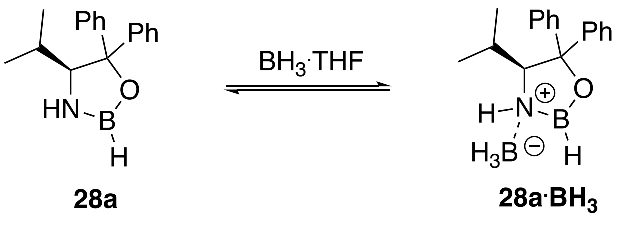

Scheme 6 Complexation of an additional equivalent of BH_3 generates the activated catalytic species **28a·BH₃**.

They further established a new catalyst based on (*S*)-diphenylprolinol. With this catalyst and optimized reaction conditions, they achieved outstanding enantioselectivities in the reduction of aromatic ketones, while only 10 mol% of the amino alcohol were necessary (Scheme 7).[28]

In the original protocol, OXB **31a** was synthesized by addition of BH_3 to (*S*)-diphenylprolinol *via* hydrogen extrusion. However, the resultant OXB **31a** is extremely sensitive to moisture and therefore has to be synthesized *in situ* prior to catalysis. As a result, Corey established OXBs **31b** and **31c** derived from boronic acids with Me or *n*-Bu substituents, which are stable under ambient conditions and therefore can be isolated and stored, while providing similar selectivity as **31a**.[58,59]

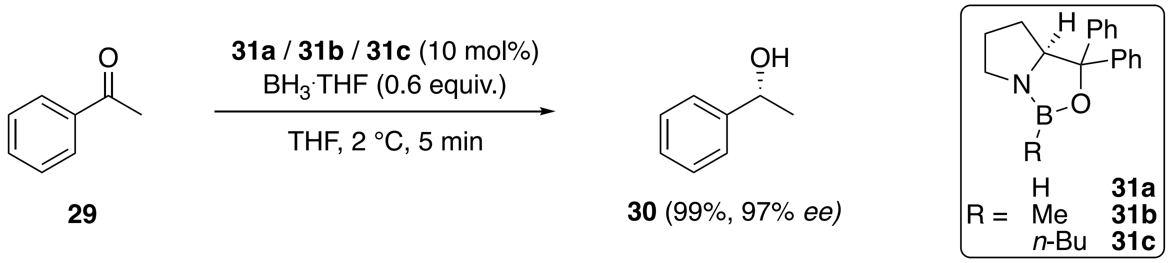

Scheme 7 Corey's CBS catalysts **31a**-**c** for the reduction of acetophenone.

Based on ^{11}B NMR, single-crystal X-ray diffraction analysis and the stereochemical results, Corey eventually proposed a mechanistic model, which explains the high rate and enantioselectivity of the reaction (Fig. 2).[60,61] While OXB **31b** is catalytically too unreactive, coordination of a further electrophilic BH_3 to the Lewis basic nitrogen forms complex **31b·BH3**, which acts as the activated catalyst species, whose Lewis acidity is strongly enhanced. Complex **31b·BH3** then coordinates acetophenone **29** in a six-membered boat-like transition structure **TSR**. The following hydride transfer from the coordinated BH_3 to the carbonyl carbon is the selectivity-determining step, which leads to intermediate **32**. Finally, product release can occur *via* two different pathways: either by dissociation to regenerate OXB **31b** or by the addition of a further equivalent of BH_3 to species **33**, which decomposes to the complex **31b·BH3** by releasing product **34**. Acidic workup of **34** then provides enantiomerically enriched alcohol **30**.

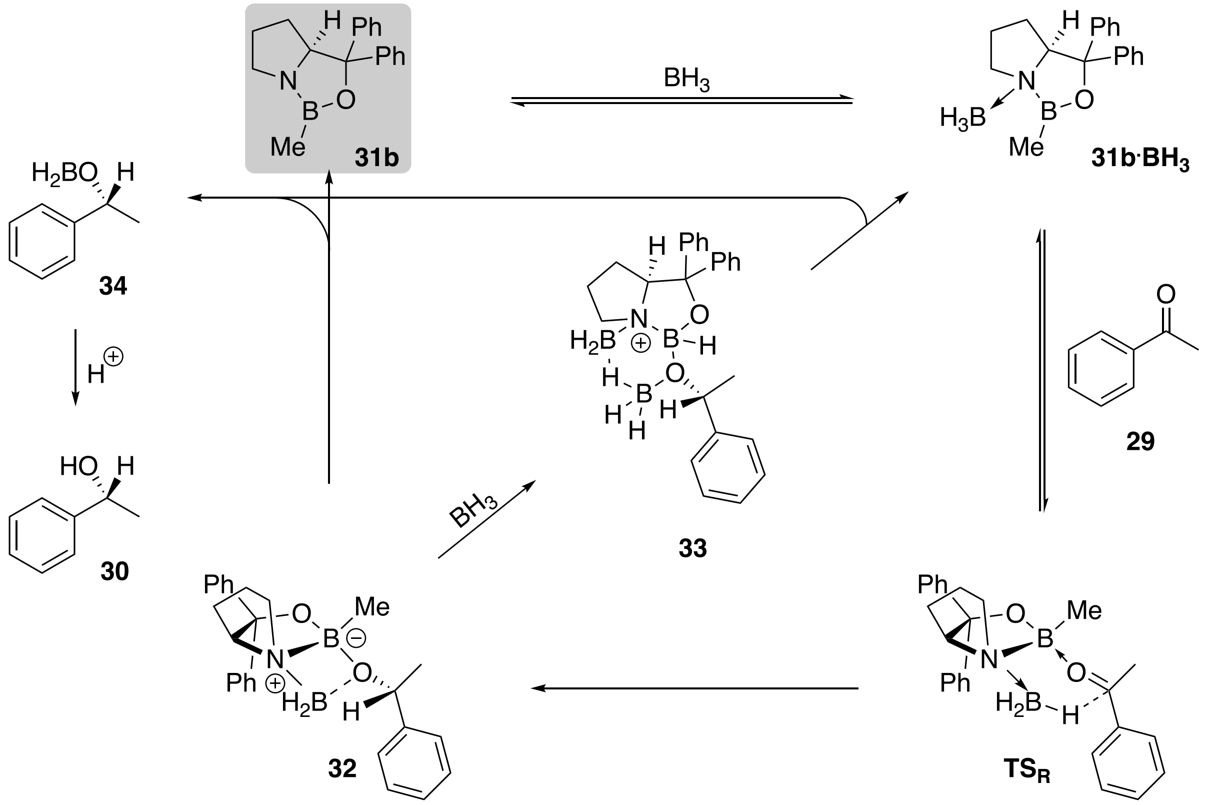

Figure 2 Corey’s proposed mechanism for the CBS reduction.

According to Corey’s model, the coordination of the ketone occurs in a six-membered boat-like transition structure **TS$_\text{R}$** at the s*terically more accessible lone pair* to minimize steric repulsion between the ketone substituents (**R$_\text{S}$, R$_\text{L}$**) and the boron substituent (**R**) of the catalyst (Fig. 3).[62,63] This model allows the prediction of the absolute stereochemistry and offers an explanation for the high enantioselectivity for a large number of substrates, which eventually made the CBS reduction extremely popular and led to its application in several total syntheses.[34,64]

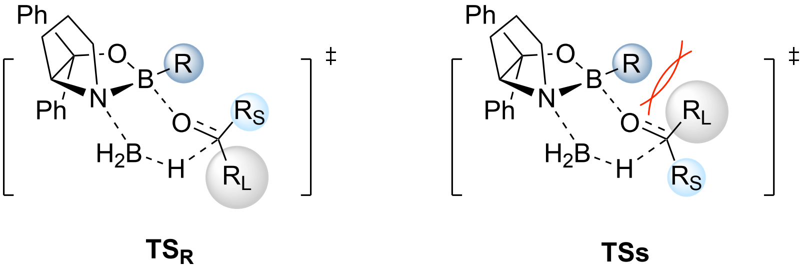

Figure 3 Corey’s proposed transition structures (**TS**) for the hydride transfer.

However, there are also ketones for which Corey's model does not provide a sufficient explanation for the high enantioselectivity. Despite bearing substituents similar in size, the reduction of cyclopropyl isopropyl ketone and *p*-methoxy-*p*’-nitro-3-benzophenone delivers the respective (*R*)-enantiomers **35** and **36** in high selectivities (Fig. 4).[63] This indicates that the enantioselectivity is not solely based on steric repulsion. An additional indication for further interactions is provided by the reduction of trichloroacetophenone, which also provides the (*R*)-enantiomer **37** in high selectivity.[62] Accordingly, the phenyl ring as $\mathbf{R_S}$ faces the *n*-Bu substituent of **31c** and the trichloromethyl acts as the $\mathbf{R_L}$ pointing away from the boron substituent in the transition state. This contradicts Corey's original model and rather suggests noncovalent interactions based on electronic effects. Further supporting this hypothesis, it was observed that electron deficient ketones are reduced with lower selectivity despite being more activated towards reduction. Moreover, tuning the electronic properties of the catalyst also improved the selectivity for other challenging substrates.[65]

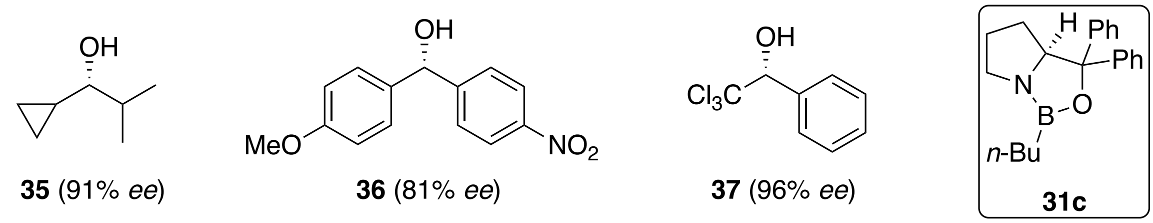

35 (91% *ee*) **36** (81% *ee*) **37** (96% *ee*) **31c**

Figure 4 CBS Reduction of substrates that contradict Corey's traditional model for enantioselectivity.

As a result, many other groups started to elucidate the key factors responsible for the high enantioselectivity in the CBS reduction, including experimental studies of the influence of reaction temperature[66] or borane source.[67] For example, reductions with catecholborane as the reducing agent must be carried out at low temperatures (–78 °C) in order to achieve high selectivities. In contrast, reductions with BH_3 perform best at slightly elevated temperatures (up to 50 °C), which is justified by a faster product release rate.[66] In some cases, the rate of ketone addition has also affected selectivity.[68] Ideally, the substrates should be added slowly over time (for example with a syringe pump), to prevent an uncatalyzed nonselective background reaction with BH_3.

Kinetic isotope effects (KIE) were investigated proposing that Corey's steric model may be too simplistic.[69,70] A few groups also conducted quantum mechanical computations to study the "origin of enantioselectivity" in oxazaborolidine catalyzed reductions. In a theoretical study, Liotta *et al.* reported in 1993, that the prolinol substituents (phenyl in the CBS catalysts) are highly important for the transition state arrangement and therefore for selectivity.[71] They suggested chair-like transition structures with the phenyl group of the substrate lying parallel to the prolinol phenyl group in the favored transition structure $\mathbf{TS_R}$ (Fig. 5).

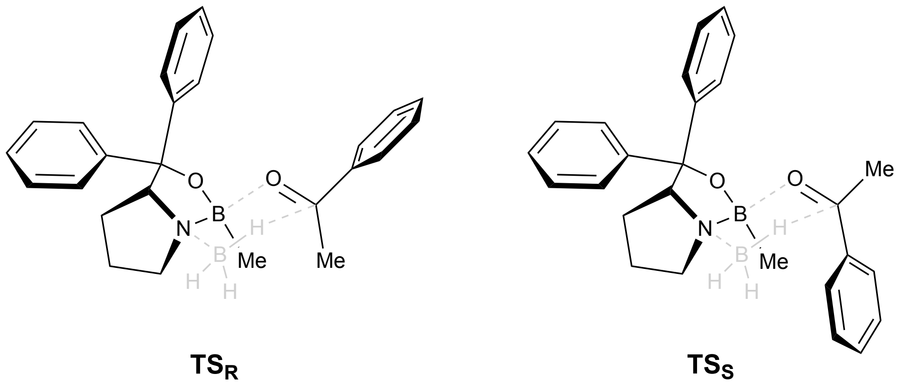

Figure 5 Liotta's suggested transition structures for the CBS reduction.[71]

Lachtar *et al.* performed density functional theory (DFT) calculations to show that stabilizing NCIs lead to the favored transition structure.[72] However, they used just a simplified catalyst structure, so that a precise examination of the NCIs in the CBS reduction is still missing. Obviously the high enantioselectivity stems from a complex interplay of many different parameters.

In addition to the mechanistic studies on enantioselectivity, considerable effort was also made to extend the catalyst scope by using new amino alcohol precursors. Further OXB based on chiral amino acids like L-threonine[73] and other natural substances such as pinene[74], fenchone,[74] or indane[75] have been developed (Fig. 6a). Instead of looking for completely new catalyst structures, many groups also modified the original CBS catalyst. However, changing the prolinol substituents from phenyl to alkyl, *ortho*-substituted aryl, or fluorinated groups generally decreased the enantioselectivity of the catalyst.[34] Only β-naphthyl or *all-meta* phenyl substitution provided similarly good results to phenyl (Fig. 6b).[34,59,76] Taking Corey's model of the transition state into account, the boron substituent was also modified with the intention to maximize steric repulsion and thereby the enantioselectivity. Therefore, Me, *n*-Bu,[58,59,64] methoxy and phenol,[76] and trialkylsilyl[77] substituents have been investigated (Fig. 6b). However, no general significant effect of the more sterically demanding substituents could be observed, so that H, Me, and *n*-Bu substituents still give the best selectivities for most substrates. Further reports also covered the optimization of the *in situ* catalyst formation protocol[78] and different sources of reductants. The use of catecholborane allowed the reduction at low temperatures and thus allowed the use of more reactive substrates like α,β-ynones.[77] Other borane sources such as $BH_3 \cdot SMe_2$ or BH_3·diethylaniline, with lower sensitivity to moisture, led to easier handling and better reproducibility of the CBS reduction.[79–81] Recent investigations include the immobilization of CBS catalysts to C_3-symmetric dendrimers,[82] ionic liquids **38**,[83] or acrylic polymer beads **39**[84,85] to enhance catalyst recycling (Fig. 6c).

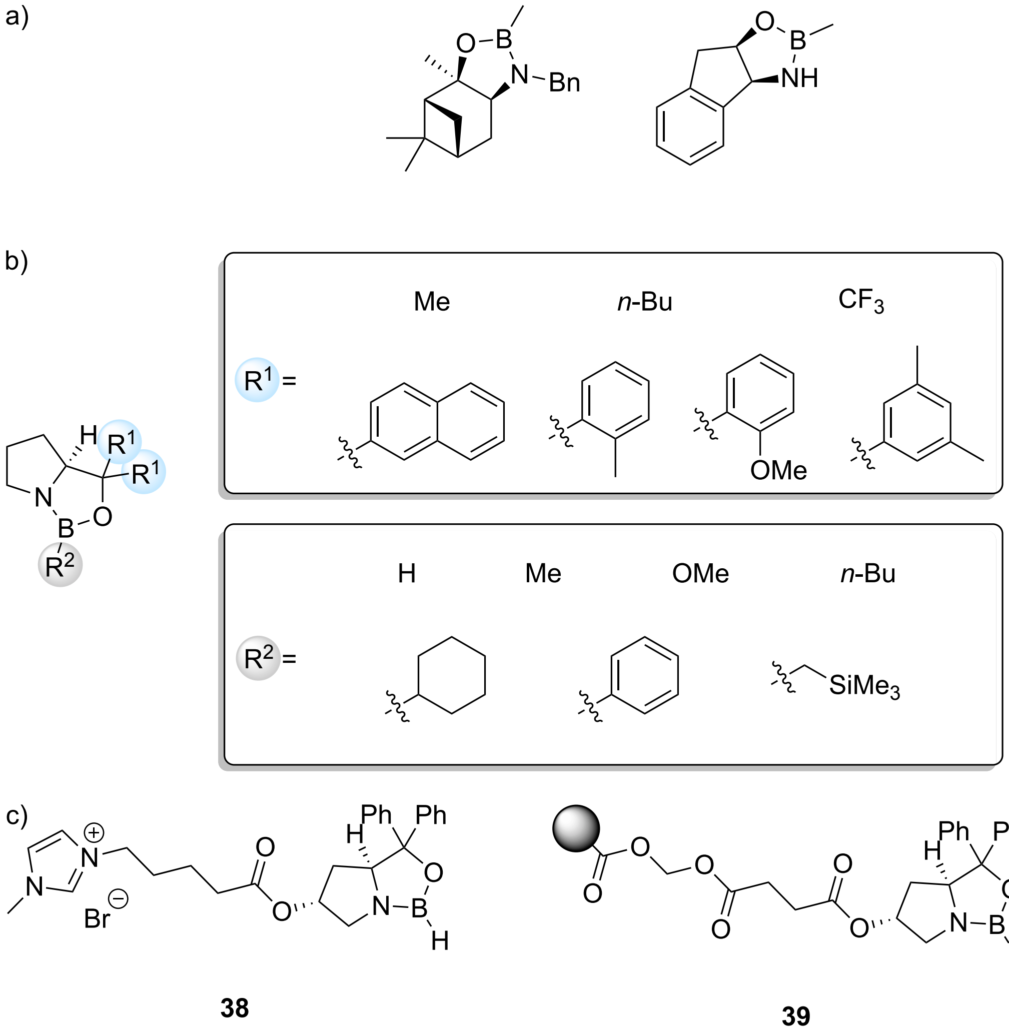

Figure 6 Further catalyst structures / precursors.

However, in the majority of these publications only the same common substrates such as acetophenone derivatives, 3,3-dimethylbutan-2-one or α-tetralone were reduced, which generally provide high selectivities, though the simplest but most challenging ketones are *n*-aliphatic ketones (e.g., 2-butanone, 2-pentanone, etc.). For a catalyst it is hard to differentiate between two small *n*-aliphatic substituents. These ketones are usually reduced with low selectivities and often require derivatization or alternative routes to provide high enantioselectivities.[86] In order to selectively reduce such ketones a comprehensive understanding of the selectivity determining factors, like noncovalent interactions, is necessary.

1.1.2. Oxazaborolidines in C-C Bond Formations

Corey's discovery of the catalytic CBS reduction demonstrated that OXBs react like chiral borenium Lewis acids by complexation and thus activation of carbonyl compounds. With this in mind, Corey reported the first OXB catalyzed Diels-Alder reaction in 1990.[87] In contrast to the previous CBS reduction, in which vicinal amino alcohols were used as catalyst precursors, Corey and coworkers employed the amino acid L-tryptophan, to create OXB **42**. By adding an electron deficient tosyl group to the heterocyclic nitrogen, they were able to enhance the Lewis acidity of the boron center and therefore the catalytic activity of the OXB. With only 5 mol% of this powerful catalyst they achieved excellent yields, diastereo- and enantioselectivities in the cycloaddition of α,β-unsaturated 2-bromoacrolein (**40**) and cyclopentadiene (**41**) (Scheme 8). They suggested a combination of attractive as well as repulsive interactions to be responsible for the high enantioselectivity. In his proposed transition structure **TS**, the indole ring of tryptophane is in parallel orientation to the dienophile resulting in an attractive π-π interaction (Scheme 8).

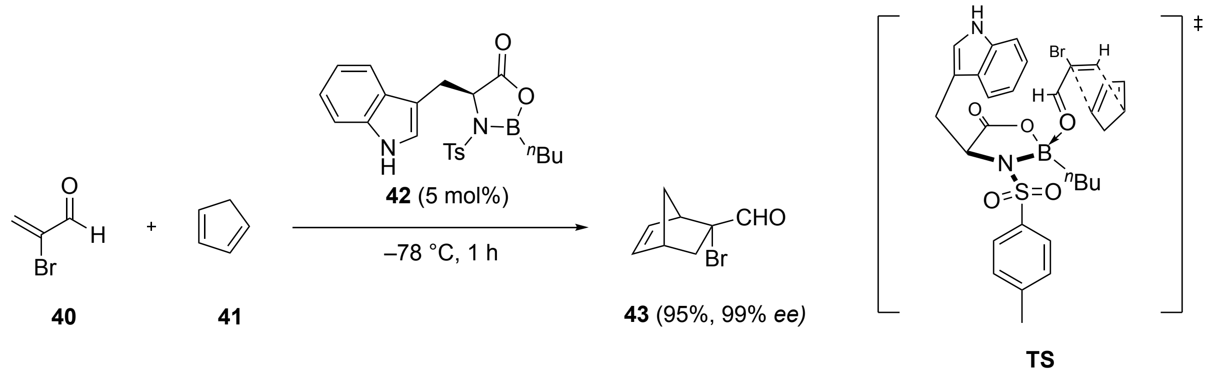

Scheme 8 Oxazaborolidinone catalyzed Diels-Alder reaction with a proposed transition structure.

In addition to Diels-Alder reactions, this tryptophane derived OXB **42** was also applied to the Mukaiyama aldol reaction of benzaldehyde (**44**) with 1-trimethylsilyloxycyclopentene (**45**) affording the product in good yield and with excellent selectivity (Scheme 9). Corey assumed that the aldol reaction proceeds *via* a similar arrangement like in the Diels-Alder **TS** shown in Scheme 8. The high selectivity of the reaction with several aldehydes and various trimethylsilyl enol ethers proved the broad applicability of this OXB catalyst.[87–89]

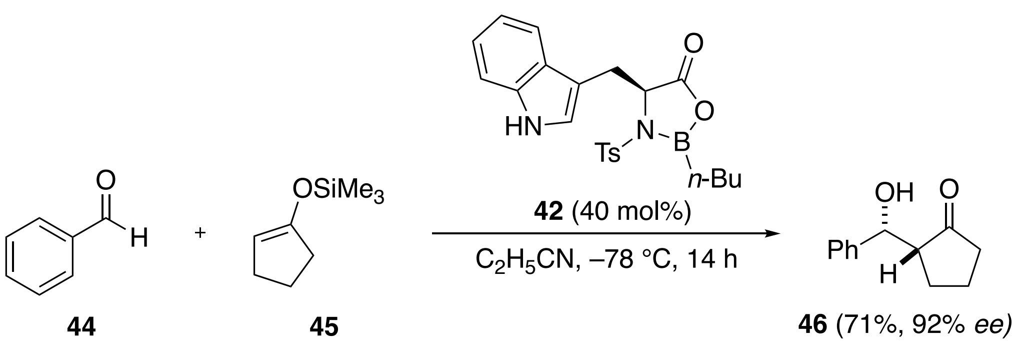

Scheme 9 Mukaiyama aldol reaction catalyzed by tryptophane derived OXB **42**.

Inspired by this new type of catalyst, further research has been devoted to enhance the scope, activity, and applicability of OXBs. The group of Toshiro Harada focused on the development of *O*-acyl-*allo*-threonine derived OXB **50**. They reported an easy synthesis of the precursors starting from commercially available L-*allo*-threonine methyl ester hydrochloride and simple catalyst modification in the acylation step. Like Corey, they used *N*-tosylation for electronic activation of the catalyst, but employed dibromophenylborane for clean and quantitative OXB formation.[90] These catalysts provided good yields and high enantioselectivities in the enantioselective Mukaiyama-Michael reaction of various acyclic enones **47** with trimethylsilyl ketene *S*,*O*-acetal **48** (Scheme 10).[91] Moreover, these OXBs proved to be valuable catalysts for asymmetric Diels-Alder reactions.[92] As the source of enantioselectivity, Harada proposed a **TS** similar to Corey's tryptophane based OXB. However, in accordance with his experimental observations he suggested that attractive π-π interactions do not play a major role for enantioselectivity, but rather steric shielding of the *si* face by the *O*-aroyl moiety is responsible for selective nucleophile attack at the *re* face (Scheme 10).[91,92]

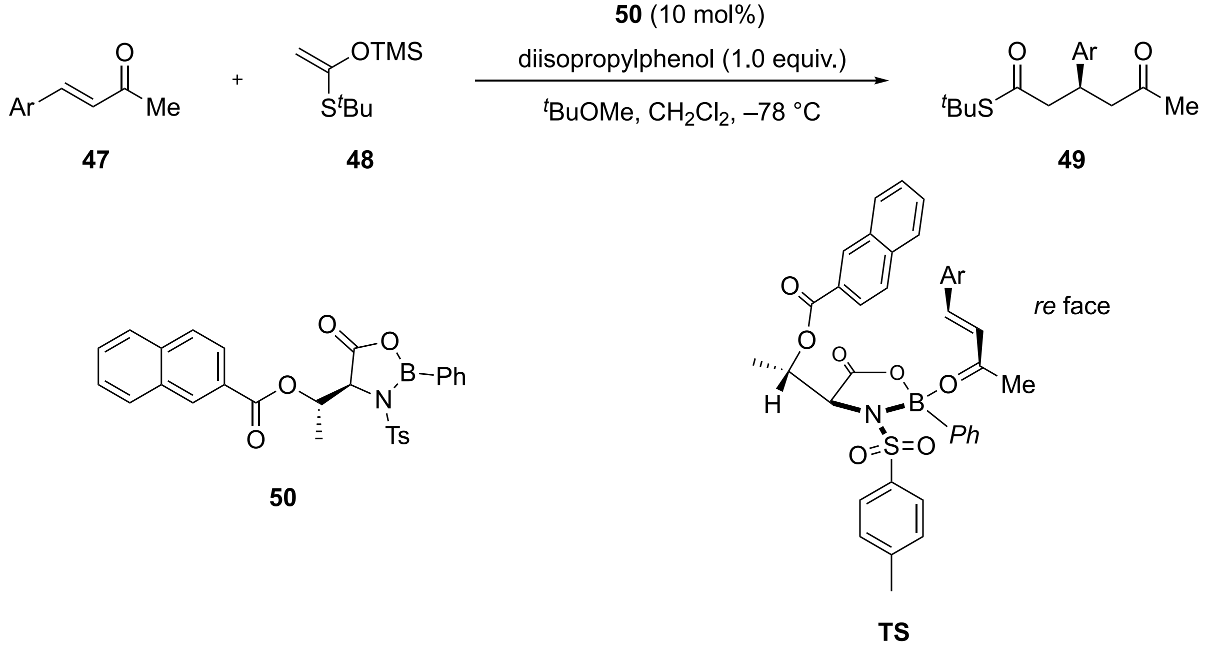

Scheme 10 Harada's *allo*-threonine derived OXB **50** in the Mukaiyama Michael reaction of enones.[91]

Corey further refined his diphenylprolinol based CBS catalysts to also use them in C-C bond formations. Therefore he used strong Brønsted acids like triflic acid or triflimide as activators to form protonated species **53a**, acting as a potent chiral "Lewis superacid" because of its cationic character. With this Brønsted acid assisted Lewis acid catalyst **53a** (BLA), Corey achieved nearly quantitative yield and excellent selectivities in the Diels-Alder reaction of various dienes and α,β-unsaturated ketones. Even the cycloaddition with less reactive dienes such as cyclohexadiene (**51**) with trifluoroethyl acrylate (**52**) were catalyzed in high yields and excellent stereoselectivity (Scheme 11a). Again, Corey proposed a mechanistic transition structure model to predict the absolute configuration of the Diels-Alder products.[93–95]

Around the same time, Hisashi Yamamoto published an analogous Lewis acid assisted Lewis acid catalyst **56a** (LLA). He used various Lewis acids such as $AlCl_3$, Et_2AlCl, $FeCl_3$, $Sc(OTf)_3$, $SnCl_4$, $[CpTiCl_3]$, or $TiCl_4$ as activator to promote Diels-Alder reactions of simple α,β-unsaturated ketones **55** and cyclopentadiene (**41**), but with extremely low catalyst loadings of only 1 mol% (Scheme 11b).[30]

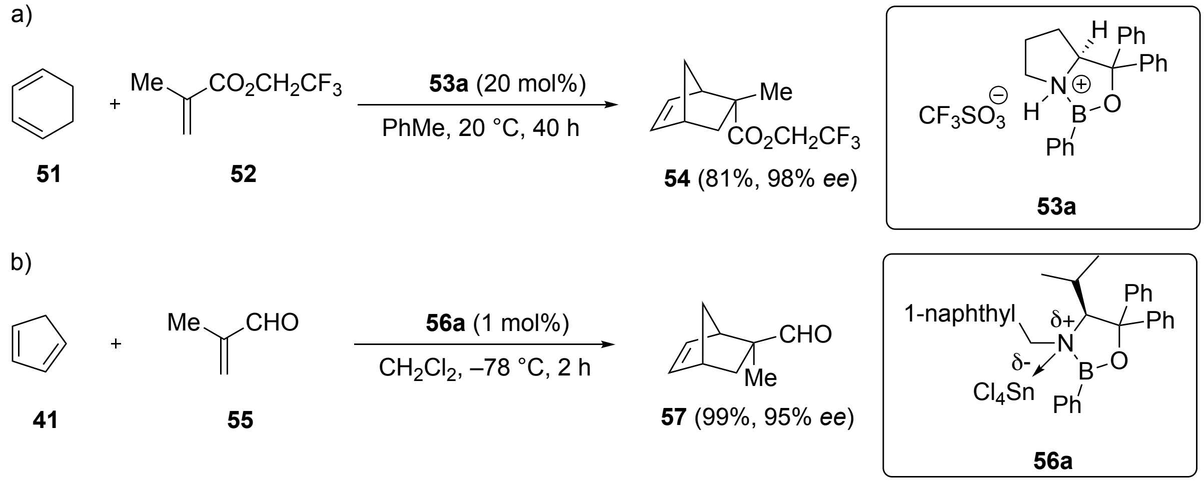

Scheme 11 a) Corey's BLA OXB **53a** and b) Yamamoto's LLA OXB **56a**.

The easy access and general utility of these effective OXB catalysts along with the predictable absolute configuration of the reaction products has led to the application in [4+2] cycloadditions of a wide range of substrates, such as α,β-unsaturated aldehydes, ketones, esters, lactones, and quinones with various dienes. Additionally, the OXBs have also shown to catalyze [3+2] cycloadditions of 2,3-dihydrofurans with benzoquinones and [2+2] cycloadditions of 2,3-dihydofurans with acrylates in high selectivity.[96,97] As a result, Corey's BLA catalysts have been employed in several natural product syntheses.[98] The total synthesis of Oseltamivir, an anti-influenza neuramidase inhibitor, could be greatly improved by utilization of an OXB catalyzed chiral cycloaddition in the first step, so that inexpensive and readily available 1,3-butadiene and acrylic acid can be used as starting materials. The authors showed that the cycloaddition can be carried out on a multigram scale in excellent yield and enantioselectivity. Furthermore, the use of dangerous azide reagents could be avoided by this new synthesis route.[99] The contraceptive desogestrel is produced industrially by total synthesis. Therefore, an intermolecular OXB catalyzed Diels-Alder reaction as enantioselective key step helped to create a shorter and more effective synthetic route.[100] Also in the total synthesis of (+)-estrone and the odorants georgyone and arborone OXB catalyzed cycloaddition is employed as key step (Fig. 5).[100,101] The synthesis of dolabellane is accomplished by an intramolecular Diels-Alder reaction creating an 11-membered ring. The reaction proceeds with Corey's BLA catalyst in high yield and excellent enantioselectivity of 90% *ee*, whereas strong Lewis acids like $EtAlCl_2$, Me_2AlCl, and $BF_3·Et_2O$ do not catalyze the reaction at all.[102]

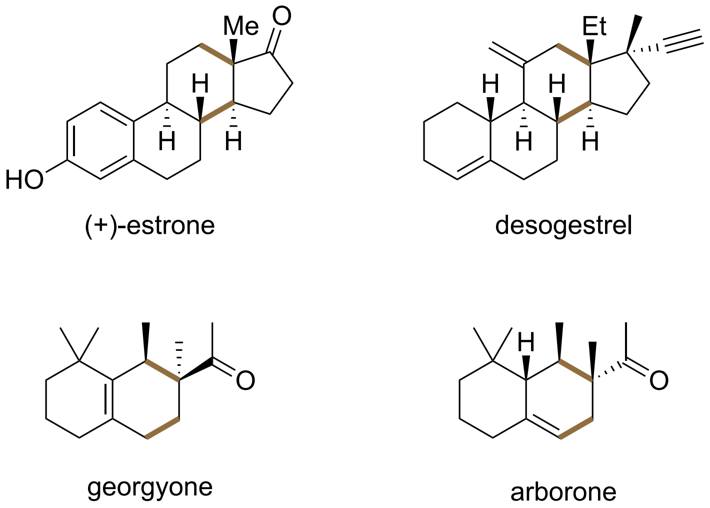
(+)-estrone desogestrel
georgyone arborone

Figure 5 Natural products which are synthesized *via* an OXB catalyzed asymmetric cycloaddition as key step. The bonds formed by the OXB catalyzed cycloaddition are colored.

Several groups also performed theoretical investigations to shed light on the activity and enantioselectivity of the OXB catalyzed Diels-Alder reactions. Based on X-ray crystallographic studies of a tryptophan-based OXB-BF_3 complex with benzaldehyde, Corey suggested that a formyl C-H···O hydrogen bond determines the transition state assembly **TS 42** (Fig. 6a).[103] This finding was confirmed by *ab initio* and DFT computations by Wong. In addition to the formyl C-H···O hydrogen bond they observed stabilizing π-stacking of the α,β-unsaturated aldehyde to the tryptophane's indole ring in the transition state **TS 42** (Fig. 6a).[104] Sherburn as well as Houk extended the quantum mechanical studies to Corey's prolinol based BLA OXB **53a** and observed similar results (Fig. 5). They identified these two interactions, together with the boron-ketone complexation, as key features for the high enantioselectivity of the Diels-Alder reaction.[105,106]

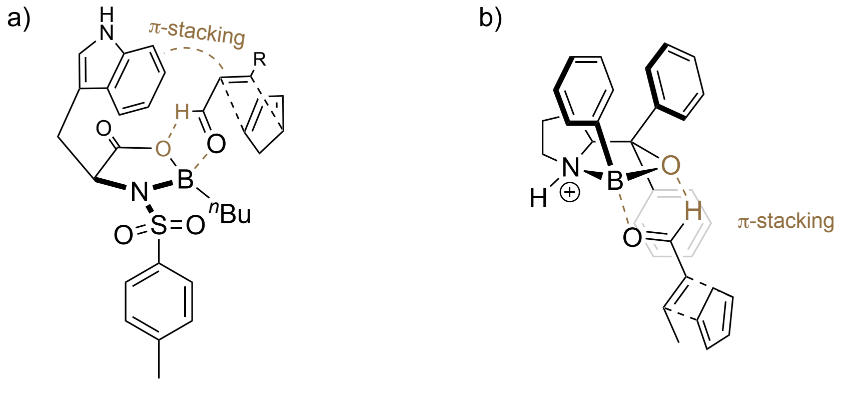
TS 42 **TS 53a**

Figure 6 a) Transition structure of the tryptophane based OXB **42** based on X-ray crystallography.[103] b) Computed transition structure of the prolinol based OXB **53a**.[105,106]

Recent trends and advancements in this field include second generation OXB catalysts as well as further core structures (Fig. 7). The second generation analogues **58** and **59** possess a greatly enhanced Lewis acidity resulting from fluorination of the OXB at either the proline core, the prolinol substituents, or the boron substituent.[107] However, the fluorination reduces the basicity of the OXB and thus makes protonation to the activated catalytic species more difficult. To ensure complete protonation to the activated catalytic species, an equimolar combination of triflimide and $TiCl_4$ has shown to be superior. This allows highly selective reactions with just low catalyst loadings of 1-2 mol%.[108] In 2017, a novel sulfur containing borenium Lewis acid was established. Kumar *et al.* used (thiolan-2-yl)diphenylmethanol and phenylboron dichloride with $AlCl_3$ as halophil to form oxathiaborolium **60** in one step (Fig. 7). Since sulfur is a weaker π-electron donor as nitrogen, they suggested an increased Lewis acidity of the catalyst. Indeed, catalyst **60** showed high activity and selectivity in a range of [4+2] cycloadditions, but was stable only at low temperature.[109] In a further study, Yamamoto published novel OXB catalysts based on 1,1'-bi-2-naphthol (BINOL). In contrast to other borenium Lewis acids, these rely on a chiral boronic acid and achiral amino alcohols. They showed that despite the chiral BINOL backbone, modification of the amino alcohol substituents could improve the enantioselectivity in Diels-Alder reactions. Furthermore they created catalyst **61** with two OXB moieties for dual activation (Fig. 7).[110]

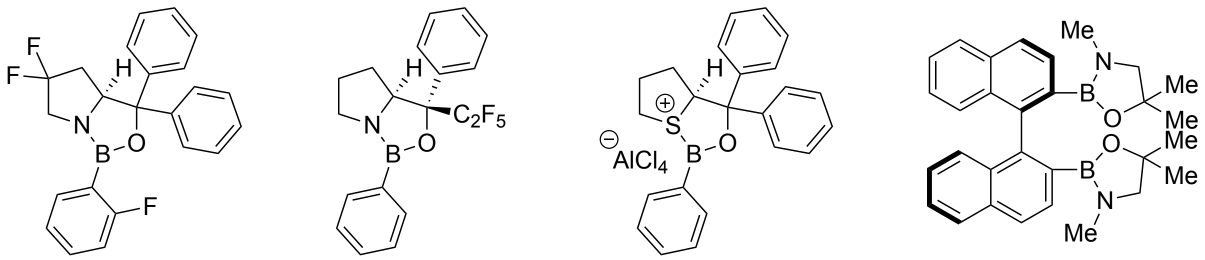

58 **59** **60** **61**

Figure 7 Second generation OXBs **58** and **59**, oxathiaborolium **60**, and BINOL-based dual OXB **61**.

These examples clearly testify that, in addition to CBS reductions, OXBs are exceptional and versatile borenium Lewis acid catalysts for C-C bond forming reactions. They are cheap and easily accessible and possess high catalytic activity. Especially in Diels-Alder reactions these types of catalysts provide excellent yields and high selectivities for α,β-unsaturated dienophiles. However, most of the published OXBs are based on a common core structure and therefore are only effective for similar substrates.

2. Noncovalent Interactions

Noncovalent interactions (NCIs) are mainly divided into hydrogen bonding, electrostatics and van der Waals (vdW) interactions, which in turn can be subdivided into a repulsive part (steric repulsion, Pauli exchange) and in an attractive part (London dispersion). NCIs are omnipresent in biological and chemical systems. They affect the chemical stability and reactivity of organic molecules and often dictate the mechanism and thus the outcome of chemical reactions. The control of selectivities in asymmetric catalysis, be it site selectivity, diastereoselectivity, or enantioselectivity, is also governed by NCIs. They may determine the geometry and stability of the transition structure and thus of the selectivity-determining steps.[35]

Historically, NCIs in catalysis were mostly reduced to steric repulsion, which was considered as the main factor influencing selectivity. As a result, catalyst design mostly consisted of maximizing steric repulsion by adding rigid, bulky elements. However, it is well-known that attractive NCIs are omnipresent and are utilized, for example, by enzymes in their substrate recognition.[111] An multitude of functionalities at the enzyme's active site enable NCIs such as hydrogen bonding, hydrophobic interactions, and vdW interactions to selectively control highly complex transformations. For a few years now, an understanding of attractive NCIs in asymmetric catalysis has been developed. It was found that a precise balance between attractive and repulsive interactions is ultimately responsible for the experimental selectivities in many reactions. The utilization of attractive NCIs eventually led to the design of some new and efficient catalysts.

The following chapter mainly focus on the two attractive interactions, namely hydrogen bonding and London dispersion, that play a pivotal role for the studies described in the present thesis.

2.1.1. Hydrogen Bonding

Hydrogen bonding is based on an electrostatic dipole-dipole interaction between a hydrogen (donor) to a hydrogen acceptor – an electronegative atom with a lone pair.[112] This ubiquitous interaction determines structures and properties of a variety of compounds in chemistry, but also in biology. The properties of water and the crystal structure of ice are the result of a network of hydrogen bonds.[113] Cellulose consists of long chains of glucose units, which are arranged in fibers due to hydrogen bonds, which is responsible for its mechanical strength.[114] Intramolecular hydrogen bonds between individual amino acids in peptides ensure protein folding into defined tertiary structures, which eventually determine the specific function of the protein.[115] Kevlar® is an extremely strong synthetic fiber based on poly(*p*-phenylene terephthalamide) chains which are linked into a lattice by strong hydrogen-bonding. The highly ordered structure leads to a high thermal and mechanical stability.[116]

In addition to its structure determining and stabilizing essentiality, hydrogen bonding plays an important role in catalysis. Similar to Lewis acids, small molecule hydrogen bond donors are used for the acceleration of chemical transformations. Typically by decreasing the electron density *via* hydrogen bonding, electrophiles are activated towards nucleophilic attack.[117] Thiourea derivatives are one class of popular hydrogen bond donor organocatalysts. The catalytic activity of thioureas results from the high acidity of the N-H protons, leading to strong catalyst-substrate interactions.[118] The 3,5-bis-(trifluoromethyl)phenyl motif has a strong electron withdrawing effect. It increases the polarity of the catalyst and stabilizes the hydrogen bond interactions in the transition state and has therefore proven to be a privileged motif for a large number of hydrogen bond donor catalysts.[25,119,120] Based on these properties, Schreiner successfully employed thiourea catalyst **62** in the diastereoselective cycloaddition of dienophile **63** with cyclopentadiene (**41**) (Scheme 12).[121]

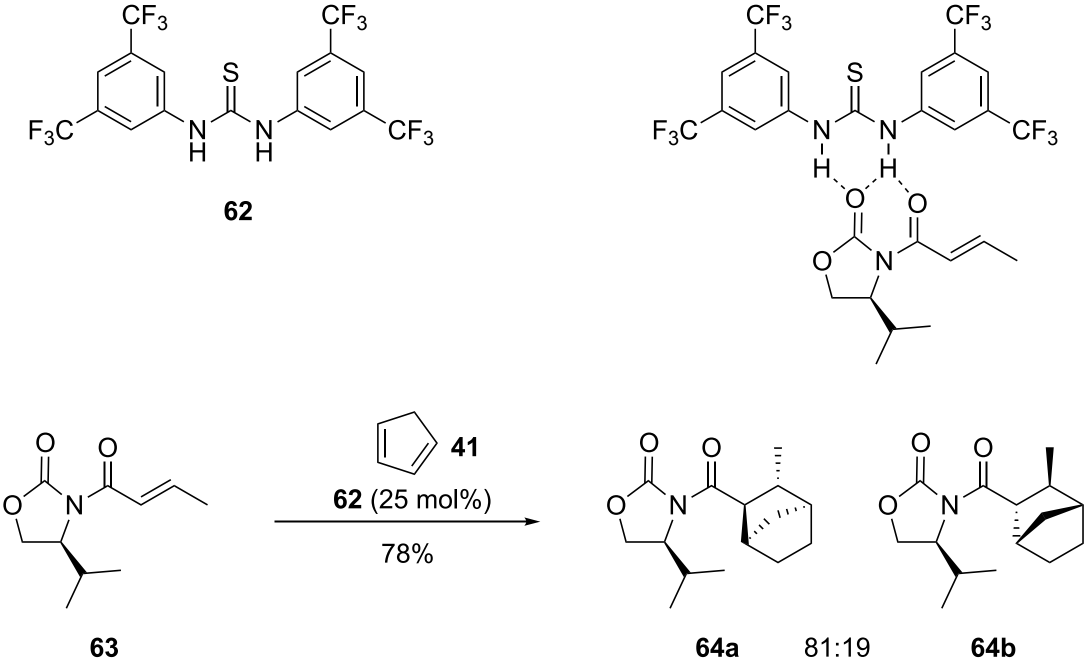

Scheme 12 Diastereoselective cycloaddition catalyzed by thiourea **62**.

After the establishment of **62** in organocatalysis, many other thiourea catalysts have been developed and mainly used in addition reactions.[117,122] Takemoto developed chiral thiourea **65**, which was first employed in the asymmetric Michael addition of malonic acid esters to nitroolefins. By incorporating the tertiary amine function as a hydrogen bond acceptor, a bifunctional thiourea was obtained (Fig. 8).[123] Other popular chiral hydrogen bond donor organocatalysts include diols and biphenols, which are often derived from BINOL **66**. In 2003, McDougal and Schaus were the first who reported on (*R*)-BINOL as hydrogen bond donor catalyst in the asymmetric Morita-Baylis-Hillman reaction of cyclohexanone with aldehydes.[124] Since then, optimization studies of several groups have revealed further 3,3-substituted derivatives for various stereoselective transformations.[117] Furthermore, the BINOL backbone initiated the establishment of chiral phosphoric acids **67** (CPA) as highly reactive and selective Brønsted acid catalysts, whose reactivity can be correlated to their acidity. The remarkable versatility originates from their simple modifiability at the BINOL backbone or by replacing the phosphoric acid with more acidic moieties such as phosphoramides.[6]

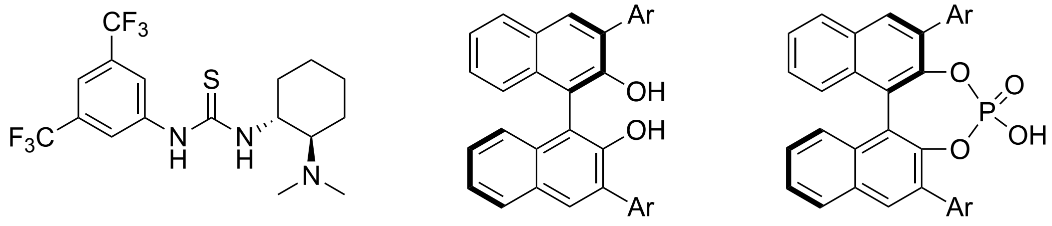

65 **66** **67**

Ar = 3,5-$(CF_3)_2$Ph
3,5-$(CH_3)_2$Ph,
4-(2-Np)Ph

Figure 8 Takemoto's chiral bifunctional thiourea **65**, BINOL **66**, and CPA **67** catalysts.

In addition to the bare catalytic activation by hydrogen bond donors, catalysts also determine the stereoselectivity of reactions *via* specific hydrogen bonding. Substrate-catalyst hydrogen bonds often adjust the transition structure geometry in proline and peptide catalyzed transformations.[42,125,126] Moreover, oligopeptides may adopt secondary and tertiary structures through intramolecular hydrogen bonds that are key for stereoselectivity. Miller established a range of oligopeptide catalysts **68**-**70** for the kinetic resolution of amino alcohols,[127] the addition of allenoates to *N*-acyl imines,[128] and the methanolysis of oxazol-5(4*H*)-ones (Fig. 9).[129] All peptide catalysts adopt a β-turn secondary structure, which is stabilized by intramolecular hydrogen bonds.

Akin to enzymes, oligopeptide catalysts may utilize hydrogen bonds also for site-selective transformations. In Schreiner's recent publication on the site-selective acylation of pyranosides with oligopeptide catalysts (Scheme 3), hydrogen bonding interactions are expected to be a major factor contributing to the observed selectivity.[47] Also in the design of site-selective metal complexes, hydrogen bond donors are used as a design element to target specific functionalities. For example in a recent publication an urea moiety incorporated into a novel rhodium(II) complex enables the site-selective aziridination of farnesol carbamate.[130]

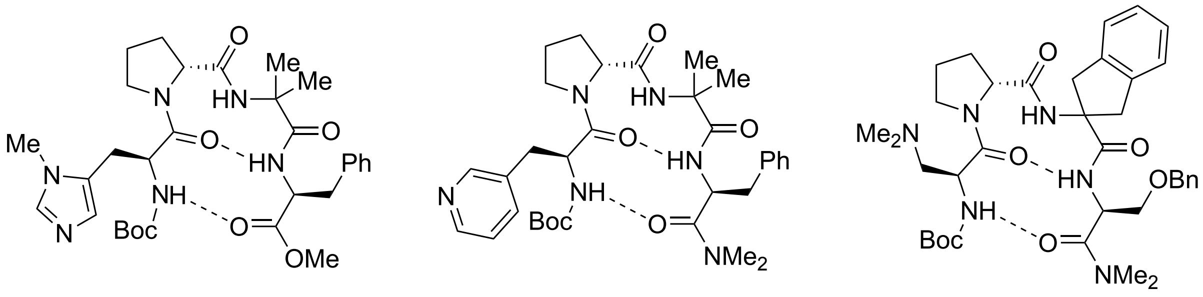

68 **69** **70**

Figure 9 Miller's peptides are stabilized in a β-turn conformation by intramolecular hydrogen bonds.

2.1.2. London Dispersion

The attractive part of the vdW potential can be mainly attributed to three NCI. It is the result of the interactions between

- permanent dipoles (Keesom interaction),
- a permanent dipole and a polarizable atom (Debye interaction),
- two polarizable atoms (London dispersion).

London dispersion (LD) was first introduced by Fritz London in 1930.[131] It is an electron correlation effect based on induced-dipole-induced-dipole attraction and therefore not restricted to specific functional groups.[132] Moreover, LD is ubiquitously present in molecules and does not cancel even in solution.[133–135] In contrast to steric repulsion and electrostatic interactions, dispersion is often considered to be small and therefore insignificant. However, the strength of LD grows rapidly with increasing molecule size, so that LD becomes meaningful especially for larger fragments.

Much research has been carried out on dispersion interactions over the past few years and with the help of modern spectroscopic and computational methods it was demonstrated that LD is not negligible, but rather a balance between repulsion and attraction is important for the reactivity and stability of molecules. For example in nature, LD interactions ensure a stabilized spatial alignment of ladderanes in cell the walls of anammox bacteria, an important participant in the nitrogen cycle.[136] Moreover, LD describes the attractive properties of π-π stacking or σ-π interactions, determines the stability and reactivity of various molecules and compounds, and may even influence the selectivity of reactions.[137]

Extensive research has established so-called dispersion energy donors (DED), bulky and polarizable substituents, which can thermodynamically stabilize compounds by their pairwise attractive LD interactions.[137–139] This can lead to the stabilization of otherwise labile molecules and bonding situations, such as extremely long carbon-carbon bonds in alkanes[140,141] or short intermolecular H···H contacts.[142] Hexaphenylethane **71a** (Scheme 13, R = H), a molecule with a quite long history in chemistry, could never be isolated despite simple theoretical synthesis routes.[143] It was only through modification of the phenyl rings to sterically more crowded all-*meta*-^{t}Bu substituted derivatives that the synthesis, isolation, and characterization of hexaphenylethane **71d** (Scheme 13, R = *tert*-butyl) by means of X-ray was made possible.[144] Spectroscopic and computational investigations revealed strong stabilization by LD interactions of many CH···CH contacts of bulky and highly polarizable *tert*-butyl **71d**, cyclohexyl **71e**, and adamantyl groups **71f**, preventing the dissociation into the corresponding trityl radicals **72** (Scheme 13).[145,146]

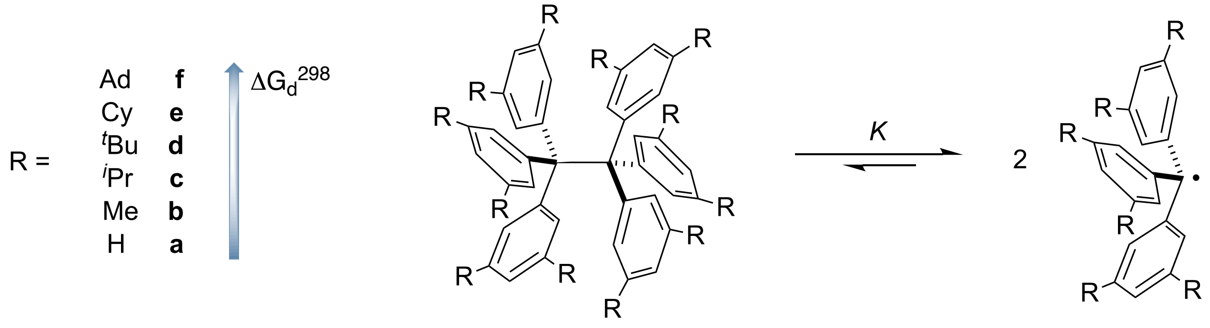

71 **72**

Scheme 13 The computed free dissociation energies ΔG_d^{298} of all-*meta*-substituted hexaphenylethane derivatives **71a**-**f** increases with bulky, polarizable substituents.[145]

In a recent report, the group of Wennemers presented the synthesis of a novel peptide-metal framework. Usually, the conformational flexibility prevents the use of peptides as ligands or integral part of metal-organic frameworks (MOFs). In their publication, the authors showed that intermolecular LD interactions between helical proline ligands ensure defined secondary structures, which are aligned into a crystalline network by metal ion complexation.[147]

In connection with the stabilizing abilities, LD interactions also make an impact on isomerization processes. Wegner *et al.* reported about the impact of LD on the *Z*↔*E* isomerization of azobenzene switches. Therefore, various azobenzene switches equipped with DED were synthesized and after photoirradiation to the *Z* isomer, the thermal *Z*↔*E* isomerization rate was investigated in various solvents. The authors observed that the isomerization rate became slower with increasing DED capability and thus a higher stabilization of the *Z* isomer.[148] Additionally, they showed that linear alkyl chains also provide sufficient stabilization up to a threshold, where the entropic penalty of the conformational flexibility overcompensates the dispersion part.[149]

As LD interactions may be attenuated, but do not cancel in solution, a crucial role of LD interactions in asymmetric catalysis seems obvious. Indeed, in recent years there has been an increasing recognition of LD in catalysis. Schreiners oligopeptide **73** catalyzes the kinetic resolution of *trans*-cycloalkane-1,2-diols **74** with high stereoselectivity (Fig. 10). To investigate the origins of the selectivity of peptide **73**, detailed spectroscopic studies have been carried out by the group of Thiele.[46] Therefore, a combination of NMR methods, such as nuclear Overhauser effect (NOE), residual dipolar coupling (RDC), and diffusion-ordered spectroscopy (DOSY), as well as specially designed pure shift EASY ROESY (efficient adiabatic symmetrized rotating frame Overhauser effect spectroscopy)[150] experiments were employed to elucidate the key NCIs, which are responsible for the selectivity. The γ-adamantyl glycine of **73** induces a dynamic binding pocket for the diol. In addition to hydrogen bonds, the intermolecular contacts between the cyclohexyl moiety of **73** and the *trans*-cycloalkane-1,2-diol **74** could be attributed to stabilizing LD interactions (Fig. 10). These results are in accordance with the experimental observation that hydrophobic groups (like cyclohexyl) lead to higher enantioselectivity. Eventually, these spectroscopic studies confirmed the preliminary assumptions and computations by the Schreiner group that attractive LD is a decisive factor for the high selectivity of the reaction.[44]

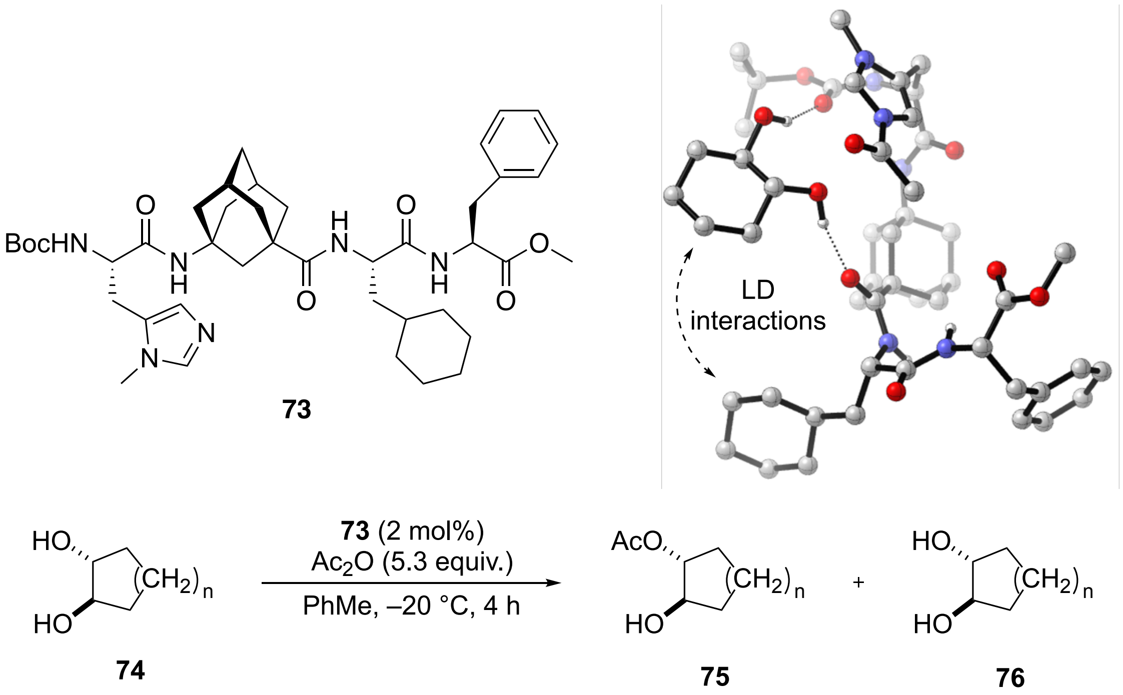

Figure 10 Kinetic resolution of *trans*-cycloalkane-1,2-diols **74** catalyzed by oligopeptide **73**. Hydrogen bonding and LD interactions in the transition structure facilitate the high stereoselectivity.

In a few recent publications, the key NCIs being responsible for the selectivity of some already known asymmetric catalyzed reactions have been investigated. The group of Gschwind performed a thorough study of BINOL derived CPAs catalysis by detailed NMR spectroscopy and quantum mechanical calculations. They found that an ensemble of steric repulsion and stabilizing dispersion interactions by the 3,3'-substituents on the BINOL backbone determine the geometry of the CPA/imine complexes, which are responsible for the selectivity in the transfer hydrogenation of ketimines.[151] In 2013, Buchwald reported an asymmetric hydroamination of a variety of olefins catalyzed by copper(I) hydride (CuH) with bidentate phosphine ligands.[152] The transformation features low catalyst loadings, a broad substrate scope, and excellent enantioselectivities. However, the authors noticed that employing inactivated aliphatic or internal olefins **77**, the hydroamination to **78** worked only well with extremely bulky phosphine ligands such as DTBM-SEGPHOS. To understand the observed ligand effects, a detailed computational investigation was performed.[153] DFT calculations showed that bulky 3,5-di-*tert*-butyl substituents on the ligand reduced the activation barrier of the hydrocupration because of stabilizing *intermolecular* ligand substrate interactions, while the *intramolecular* interactions remained constant (Fig. 11). A subsequent energy decomposition analysis revealed that these through-space interactions are dominated by Pauli- and electrostatic repulsion as well as attractive LD. The use of bulky and polarizable ligand substituents such as 3,5-di-*tert*-butyl phenyl, leads to an amplification of attractive dispersion, which overcompensates the repulsion. This ultimately results in a reduction of the energy barrier and enables efficient hydroamination.

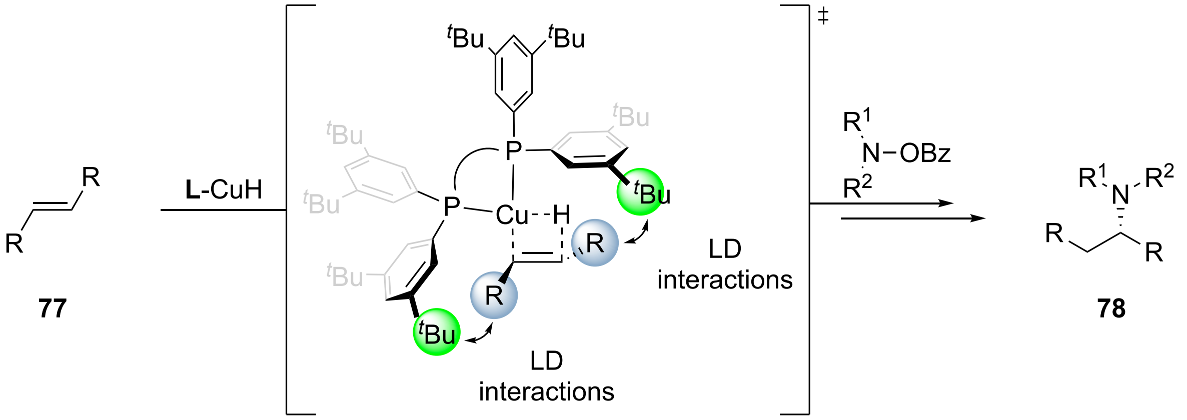

Figure 11 Bulky and polarizable ligands enable the copper catalyzed hydroamination of olefins through LD interactions.

A further comprehensive quantum mechanical investigation by Bistoni *et al.* dealt with the identification of the key NCIs of the enantioselective DA reaction of cinnamate esters catalyzed by either binaphthyl-allyl-tetrasulfone (BALT) or imidodiphosphorimidate (IDPi) organocatalysts.[154] In a self-compiled computational protocol they first identified the conformers and transition state geometries using molecular meta-dynamics simulations *via* xTB. Subsequent free energy calculations with DFT and coupled-cluster methods for the conformers provided theoretical selectivities of the transformation that were in accordance with the experimental results. For the analysis of the key interactions, they finally performed a local energy decomposition (LED) analysis. For both, the rigid BALT as well as the more flexible IDPi, they found that attractive LD interactions have a large influence on the selectivity of the cycloaddition by stabilization of the transition structures. They finally stated that with the new understanding of attractive NCIs, LD by highly polarizable substituents represents a new design element for catalyst development.

The increasing number of publications emphasizing the use of hydrogen bond donors/acceptors or DED as design elements shows the enormous potential of NCIs in controlling reactivity and selectivity in organocatalysis. The goal of this thesis was to combine the concepts of NCIs with the development of new chiral OXBs as versatile Lewis acid organocatalysts. On the one hand, we wanted to establish a new OXB moiety attached to a chiral peptide backbone. On the other hand, we investigated if we can utilize DED as a design element for oxazaborolidines to develop innovative and efficient catalysts for cycloaddition reactions and the reduction of ketones, which are still hard to reduce selectively.

3. References

[1] B. M. Trost, *Proc. Natl. Acad. Sci. U.S.A.* **2004**, *101*, 5348–5355.
[2] D. L. Hughes, *Org. Process Res. Dev.* **2018**, *22*, 574–584.
[3] B. Han, X. H. He, Y. Q. Liu, G. He, C. Peng, J. L. Li, *Chem. Soc. Rev.* **2021**, *50*, 1522–1586.
[4] R. A. Sheldon, J. M. Woodley, *Chem. Rev.* **2018**, *118*, 801–838.
[5] F. Giacalone, M. Gruttadauria, P. Agrigento, R. Noto, *Chem. Soc. Rev.* **2012**, *41*, 2406–2447.
[6] D. Parmar, E. Sugiono, S. Raja, M. Rueping, *Chem. Rev.* **2014**, *114*, 9047–9153.
[7] B. F. Sun, *Tetrahedron Lett.* **2015**, *56*, 2133–2140.
[8] J. Alemán, S. Cabrera, *Chem. Soc. Rev.* **2013**, *42*, 774–793.
[9] P. I. Dalko, L. Moisan, *Angew. Chem. Int. Ed.* **2001**, *40*, 3726–3748.
[10] Wöhler, Liebig, *Ann. der Pharm.* **1832**, *3*, 249–282.
[11] U. Eder, G. Sauer, R. Wiechert, *Angew. Chem. Int. Ed.* **1971**, *10*, 496–497.
[12] W. Langenbeck, *Ber. Dtsch. Chem. Ges.* **1927**, *60*, 930–934.
[13] W. Langenbeck, *Die Organischen Katalysatoren Und Ihre Beziehungen Zu Den Fermenten*, Springer, Berlin, Heidelberg, **1935**.
[14] K. A. Ahrendt, C. J. Borths, D. W. C. MacMillan, *J. Am. Chem. Soc.* **2000**, *122*, 4243–4244.
[15] B. List, R. A. Lerner, C. F. Barbas, *J. Am. Chem. Soc.* **2000**, *122*, 2395–2396.
[16] X. Y. Chen, Q. Liu, P. Chauhan, D. Enders, *Angew. Chem. Int. Ed.* **2018**, *57*, 3862–3873.
[17] Q. Z. Li, R. Zeng, B. Han, J. L. Li, *Chem.Eur. J.* **2021**, *27*, 3238–3250.
[18] C. M. Starks, *J. Am. Chem. Soc.* **1971**, *93*, 195–199.
[19] E. V. Dehmlow, *Angew. Chem. Int. Ed.* **1974**, *13*, 170–179.
[20] C. M. Starks, C. L. Liotta, M. E. Halpern, *Phase-Transfer Catalysis*, Springer, Dordrecht, **1994**.
[21] M. Rueping, A. Kuenkel, I. Atodiresei, *Chem. Soc. Rev.* **2011**, *40*, 4539–4549.
[22] R. Maji, S. C. Mallojjala, S. E. Wheeler, *Chem. Soc. Rev.* **2018**, *47*, 1142–1158.
[23] P. R. Schreiner, *Chem. Soc. Rev.* **2003**, *32*, 289–296.
[24] Z. G. Zhang, P. R. Schreiner, *Chem. Soc. Rev.* **2009**, *38*, 1187–1198.
[25] Z. Zhang, Z. Bao, H. Xing, *Org. Biomol. Chem.* **2014**, *12*, 3151–3162.
[26] A. Shakeel, *J. Drug Des. Med. Chem.* **2016**, *2*, 10–20.
[27] J. P. Malerich, K. Hagihara, V. H. Rawal, *J. Am. Chem. Soc.* **2008**, *130*, 14416–14417.
[28] E. J. Corey, R. K. Bakshi, S. Shibata, *J. Am. Chem. Soc.* **1987**, *109*, 5551–5553.
[29] E. J. Corey, *Angew. Chem. Int. Ed.* **2009**, *48*, 2100–2117.
[30] K. Futatsugi, H. Yamamoto, *Angew. Chem. Int. Ed.* **2005**, *44*, 1484–1487.
[31] T. S. De Vries, A. Prokofjevs, E. Vedejs, *Chem. Rev.* **2012**, *112*, 4246–4282.
[32] M. Marigo, T. C. Wabnitz, D. Fielenbach, K. A. Jørgensen, *Angew. Chem. Int. Ed.* **2005**, *44*, 794–797.
[33] Y. Hayashi, H. Gotoh, T. Hayashi, M. Shoji, *Angew. Chem. Int. Ed.* **2005**, *44*, 4212–4215.
[34] E. J. Corey, C. J. Helal, *Angew. Chem. Int. Ed.* **1998**, *37*, 1986–2012.
[35] J. M. Crawford, M. S. Sigman, *Synthesis* **2019**, *51*, 1021–1036.
[36] E. A. C. Davie, S. M. Mennen, Y. Xu, S. J. Miller, *Chem. Rev.* **2007**, *107*, 5759–5812.
[37] A. J. Metrano, A. J. Chinn, C. R. Shugrue, E. A. Stone, B. Kim, S. J. Miller, *Chem. Rev.* **2020**, *120*, 11479–11615.
[38] J. Oku, N. Ito, S. Inoue, *Macromol. Chem. Phys.* **1979**, *180*, 1089–1091.
[39] M. M. Vasbinder, J. E. Imbriglio, S. J. Miller, *Tetrahedron* **2006**, *62*, 11450–11459.
[40] K. Akagawa, R. Suzuki, K. Kudo, *Adv. Synth. Catal.* **2012**, *354*, 1280–1286.
[41] C. E. Müller, L. Wanka, K. Jewell, P. R. Schreiner, *Angew. Chem. Int. Ed.* **2008**, *47*, 6180–6183.
[42] E. A. C. Davie, S. M. Mennen, Y. Xu, S. J. Miller, *Chem. Rev.* **2007**, *107*, 5759–5812.
[43] H. Wennemers, *Chem. Commun.* **2011**, *47*, 12036–12041.
[44] C. E. Müller, D. Zell, R. Hrdina, R. C. Wende, L. Wanka, S. M. M. Schuler, P. R. Schreiner, *J. Org. Chem.* **2013**, *78*, 8465–8484.
[45] R. C. Wende, A. Seitz, D. Niedek, S. M. M. Schuler, C. Hofmann, J. Becker, P. R. Schreiner, *Angew. Chem. Int. Ed.* **2016**, *55*, 2719–2723.
[46] E. Procházková, A. Kolmer, J. Ilgen, M. Schwab, L. Kaltschnee, M. Fredersdorf, V. Schmidts, R. C. Wende, P. R. Schreiner, C. M. Thiele, *Angew. Chem. Int. Ed.* **2016**, *55*, 15754–15759.
[47] A. Seitz, R. C. Wende, E. Roesner, D. Niedek, C. Topp, A. C. Colgan, E. M. McGarrigle, P. R. Schreiner, *J. Org. Chem.* **2021**, *86*, 3907–3922.
[48] D. Niedek, F. R. Erb, C. Topp, A. Seitz, R. C. Wende, A. K. Eckhardt, J. Kind, D. Herold, C. M. Thiele, P. R. Schreiner, *J. Org. Chem.* **2020**, *85*, 1835–1846.
[49] R. C. Wende, P. R. Schreiner, *Green Chem.* **2012**, *14*, 1821–1849.
[50] C. Hofmann, S. M. M. Schuler, R. C. Wende, P. R. Schreiner, *Chem. Commun.* **2014**, *50*, 1221–1223.
[51] C. Hofmann, J. M. Schümann, P. R. Schreiner, *J. Org. Chem.* **2015**, *80*, 1972–1978.

[52] R. Hrdina, C. E. Müller, R. C. Wende, L. Wanka, P. R. Schreiner, *Chem. Commun.* **2012**, *48*, 2498–2500.

[53] A. Hirao, S. Itsuno, S. Nakahama, N. Yamazaki, *J. Chem. Soc. Chem. Commun.* **1981**, 315–317.

[54] S. Itsuno, A. Hirao, S. Nakahama, N. Yamazaki, *J. Chem. Soc. Perkin Trans. 1* **1983**, 1673–1676.

[55] S. Itsuno, M. Nakano, K. Miyazaki, H. Masuda, K. Ito, A. Hirao, S. Nakahama, *J. Chem. Soc. Perkin Trans. 1* **1985**, 2039–2044.

[56] S. Itsuno, K. Ito, A. Hirao, S. Nakahama, *J. Chem. Soc., Chem. Commun.* **1983**, 469–470.

[57] L. Brewer, G. M. Rosenblatt, *Advances in High Temperature Chemistry*, **1969**, pp. 1–83.

[58] E. J. Corey, R. K. Bakshi, S. Shibata, C. P. Chen, V. K. Singh, *J. Am. Chem. Soc.* **1987**, *109*, 7925–7926.

[59] E. J. Corey, J. O. Link, *Tetrahedron Lett.* **1989**, *30*, 6275–6278.

[60] E. J. Corey, M. Azimioara, S. Sarshar, *Tetrahedron Lett.* **1992**, *33*, 3429–3430.

[61] E. J. Corey, J. O. Link, R. K. Bakshi, *Tetrahedron Lett.* **1992**, *33*, 7107–7110.

[62] E. J. Corey, J. O. Link, R. K. Bakshi, *Tetrahedron Lett.* **1992**, *33*, 7107–7110.

[63] E. J. J. E. J. E. J. Corey, C. J. Helal, *Tetrahedron Lett.* **1995**, *36*, 9153–9156.

[64] E. . Corey, J. O. Link, *Tetrahedron Lett.* **1990**, *31*, 601–604.

[65] Xu, Wei, Zhang, *J. Org. Chem.* **2004**, *69*, 6860–6866.

[66] J. Zhao, X. Bao, X. Liu, B. Wan, X. Han, C. Yang, J. Hang, Y. Feng, B. Jiang, *Tetrahedron Asymmetry* **2000**, *11*, 3351–3359.

[67] X. Wang, J. Du, H. Liu, D.-M. Du, J. Xu, *Heteroat. Chem.* **2007**, *18*, 740–746.

[68] Xu, Wei, Zhang, *J. Org. Chem.* **2003**, *68*, 10146–10151.

[69] M. P. Meyer, *Org. Lett.* **2009**, *11*, 4338–4341.

[70] T. Giagou, M. P. Meyer, *Chem.Eur. J.* **2010**, *16*, 10616–10628.

[71] D. K. Jones, D. C. Liotta, I. Shinkai, D. J. Mathre, *J. Org. Chem.* **1993**, *58*, 799–801.

[72] Z. Lachtar, A. Khorief Nacereddine, A. Djerourou, *Struct. Chem.* **2020**, *31*, 253–261.

[73] M. Shimizu, Y. Ikari, A. Wakabayashi, *J. Chem. Soc. Perkin 1* **2001**, *1*, 2519–2520.

[74] D. Hobuß, A. Baro, S. Laschat, W. Frey, *Tetrahedron* **2008**, *64*, 1635–1640.

[75] N. J. Gilmore, S. Jones, M. P. Muldowney, *Org. Lett.* **2004**, *6*, 2805–2808.

[76] Y. Kawanami, Y. Mikami, K. Kiguchi, Y. Harauchi, R. C. Yanagita, *Tetrahedron Asymmetry* **2011**, *22*, 1891–1894.

[77] C. J. Helal, P. A. Magriotis, E. J. Corey, *J. Am. Chem. Soc.* **1996**, *118*, 10938–10939.

[78] Y. Kawanami, S. Murao, T. Ohga, N. Kobayashi, *Tetrahedron* **2003**, *59*, 8411–8414.

[79] D. J. Mathre, T. K. Jones, L. C. Xavier, T. J. Blacklock, R. A. Reamer, J. J. Mohan, E. T. T. Jones, K. Hoogsteen, M. W. Baum, E. J. J. Grabowski, *J. Org. Chem.* **1991**, *56*, 751–762.

[80] A. M. Salunkhe, E. R. Burkhardt, *Tetrahedron Lett.* **1997**, *38*, 1523–1526.

[81] X. Wang, J. Du, H. Liu, D.-M. Du, J. Xu, *Heteroat. Chem.* **2007**, *18*, 740–746.

[82] Y. N. Niu, Z. Y. Yan, G. Q. Li, H. L. Wei, G. L. Gao, L. Y. Wu, Y. M. Liang, *Tetrahedron Asymmetry* **2008**, *19*, 912–920.

[83] M. S. Chauhan, S. Singh, *J. Mol. Catal. A Chem.* **2015**, *398*, 184–189.

[84] R. J. Kell, P. Hodge, P. Snedden, D. Watson, *Org. Biomol. Chem.* **2003**, *1*, 3238–3243.

[85] S. Degni, C. E. Wilén, A. Rosling, *Tetrahedron Asymmetry* **2004**, *15*, 1495–1499.

[86] B. T. Cho, D.-J. Kim, *Bull. Korean Chem. Soc.* **2004**, *25*, 1385–1391.

[87] E. J. Corey, T. P. Loh, *J. Am. Chem. Soc.* **1991**, *113*, 8966–8967.

[88] E. J. Corey, C. L. Cywin, T. D. Roper, *Tetrahedron Lett.* **1992**, *33*, 6907–6910.

[89] E. J. Corey, T. P. Loh, *Tetrahedron Lett.* **1993**, *34*, 3979–3982.

[90] T. Harada, C. Inui, *J. Org. Chem.* **2006**, *71*, 1277–1279.

[91] X. Wang, S. Adachi, H. Iwai, H. Takatsuki, K. Fujita, M. Kubo, A. Oku, T. Harada, *J. Org. Chem.* **2003**, *68*, 10046–10057.

[92] R. S. Singh, S. Adachi, F. Tanaka, T. Yamauchi, C. Inui, T. Harada, *J. Org. Chem.* **2008**, *73*, 212–218.

[93] E. J. Corey, T. Shibata, T. W. Lee, *J. Am. Chem. Soc.* **2002**, *124*, 3808–3809.

[94] D. H. Ryu, T. W. Lee, E. J. Corey, *J. Am. Chem. Soc.* **2002**, *124*, 9992–9993.

[95] D. H. Ryu, E. J. Corey, *J. Am. Chem. Soc.* **2003**, *125*, 6388–6390.

[96] G. Zhou, E. J. Corey, *J. Am. Chem. Soc.* **2005**, *127*, 11958–11959.

[97] E. Canales, E. J. Corey, *J. Am. Chem. Soc.* **2007**, *129*, 12686–12687.

[98] E. J. Corey, *Angew. Chem. Int. Ed.* **2009**, *48*, 2100–2117.

[99] Yeung, S. Hong, E. J. Corey, *J. Am. Chem. Soc.* **2006**, *128*, 6310–6311.

[100] Q. Y. Hu, P. D. Rege, E. J. Corey, *J. Am. Chem. Soc.* **2004**, *126*, 5984–5986.

[101] S. Hong, E. J. Corey, *J. Am. Chem. Soc.* **2006**, *128*, 1346–1352.

[102] S. A. Snyder, E. J. Corey, *J. Am. Chem. Soc.* **2006**, *128*, 740–742.

[103] E. J. Corey, T. W. Lee, *Chem. Commun.* **2001**, 1321–1329.

[104] M. W. Wong, *J. Org. Chem.* **2005**, *70*, 5487–5493.
[105] M. N. Paddon-Row, L. C. H. Kwan, A. C. Willis, M. S. Sherburn, *Angew. Chem. Int. Ed.* **2008**, *47*, 7013–7017.
[106] M. N. Paddon-Row, C. D. Anderson, K. N. Houk, *J. Org. Chem.* **2009**, *74*, 861–868.
[107] K. Mahender Reddy, E. Bhimireddy, B. Thirupathi, S. Breitler, S. Yu, E. J. Corey, *J. Am. Chem. Soc.* **2016**, *138*, 2443–2453.
[108] B. Thirupathi, S. Breitler, K. Mahender Reddy, E. J. Corey, *J. Am. Chem. Soc.* **2016**, *138*, 10842–10845.
[109] S. N. Kumar, I. F. Yu, R.-J. Chein, *Org. Lett.* **2017**, *19*, 22–25.
[110] Y. Shimoda, H. Yamamoto, *Synthesis* **2016**, *49*, 175–180.
[111] A. Kohen, J. P. Klinman, *Acc. Chem. Res.* **1998**, *31*, 397–404.
[112] E. Arunan, G. R. Desiraju, R. A. Klein, J. Sadlej, S. Scheiner, I. Alkorta, D. C. Clary, R. H. Crabtree, J. J. Dannenberg, P. Hobza, *Pure Appl. Chem.* **2011**, *83*, 1637–1641.
[113] S. Thomas, *Angew. Chem. Int. Ed.* **2002**, *41*, 48–76.
[114] K. H. Gardner, J. Blackwell, *Biochim. Biophys. Acta - Gen. Subj.* **1974**, *343*, 232–237.
[115] R. E. Hubbard, M. Kamran Haider, *Encyclopedia of Life Sciences*, Wiley, Chichester, **2010**.
[116] S. Rebouillat, J. C. . Peng, J.-B. Donnet, *Polymer.* **1999**, *40*, 7341–7350.
[117] M. S. Taylor, E. N. Jacobsen, *Angew. Chem. Int. Ed.* **2006**, *45*, 1520–1543.
[118] G. Jakab, C. Tancon, Z. Zhang, K. M. Lippert, P. R. Schreiner, *Org. Lett.* **2012**, *14*, 1724–1727.
[119] A. Wittkopp, P. R. Schreiner, *Chem.Eur. J.* **2003**, *9*, 407–414.
[120] K. M. Lippert, K. Hof, D. Gerbig, D. Ley, H. Hausmann, S. Guenther, P. R. Schreiner, *Eur. J. Org. Chem.* **2012**, 5919–5927.
[121] P. R. Schreiner, A. Wittkopp, *Org. Lett.* **2002**, *4*, 217–220.
[122] C. Uyeda, E. N. Jacobsen, *J. Am. Chem. Soc.* **2008**, *130*, 9228–9229.
[123] T. Okino, Y. Hoashi, Y. Takemoto, *J. Am. Chem. Soc.* **2003**, *125*, 12672–12673.
[124] N. T. McDougal, S. E. Schaus, *J. Am. Chem. Soc.* **2003**, *125*, 12094–12095.
[125] L. Albrecht, H. Jiang, K. A. Jorgensen, *Chem.Eur. J.* **2014**, *20*, 358–368.
[126] C. E. Jakobsche, G. Peris, S. J. Miller, *Angew. Chem. Int. Ed.* **2008**, *120*, 6809–6813.
[127] G. T. Copeland, E. R. Jarvo, S. J. Miller, *J. Org. Chem.* **1998**, *63*, 6784–6785.
[128] B. J. Cowen, L. B. Saunders, S. J. Miller, *J. Am. Chem. Soc.* **2009**, *131*, 6105–6107.
[129] A. J. Metrano, S. J. Miller, *J. Org. Chem.* **2014**, *79*, 1542–1554.
[130] J.-P. Berndt, Y. Radchenko, J. Becker, C. Logemann, D. R. Bhandari, R. Hrdina, P. R. Schreiner, *Chem. Sci.* **2019**, *10*, 3324–3329.
[131] F. London, *Z. Phys.* **1930**, *63*, 245–279.
[132] J. N. Israelachvili, *Intermolecular and Surface Forces*, Academic Press, London ; San Diego, **1991**.
[133] L. Yang, C. Adam, G. S. Nichol, S. L. Cockroft, *Nat. Chem.* **2013**, *5*, 1006.
[134] J. M. Schümann, J. P. Wagner, A. K. Eckhardt, H. Quanz, P. R. Schreiner, *J. Am. Chem. Soc.* **2021**, *143*, 41–45.
[135] R. Pollice, M. Bot, I. J. Kobylianskii, I. Shenderovich, P. Chen, *J. Am. Chem. Soc.* **2017**, *139*, 13126–13140.
[136] J. P. Wagner, P. R. Schreiner, *J. Chem. Theory Comput.* **2014**, *10*, 1353–1358.
[137] J. P. Wagner, P. R. Schreiner, *Angew. Chem. Int. Ed.* **2015**, *54*, 12274–12296.
[138] S. Grimme, R. Huenerbein, S. Ehrlich, *ChemPhysChem* **2011**, *12*, 1258–1261.
[139] S. Grimme, P. R. Schreiner, *Angew. Chem. Int. Ed.* **2011**, *50*, 12639–12642.
[140] P. R. Schreiner, L. V. Chernish, P. A. Gunchenko, E. Y. Tikhonchuk, H. Hausmann, M. Serafin, S. Schlecht, J. E. P. Dahl, R. M. K. Carlson, A. A. Fokin, *Nature* **2011**, *477*, 308–311.
[141] A. A. Fokin, L. V. Chernish, P. A. Gunchenko, E. Y. Tikhonchuk, H. Hausmann, M. Serafin, J. E. P. Dahl, R. M. K. Carlson, P. R. Schreiner, *J. Am. Chem. Soc.* **2012**, *134*, 13641–13650.
[142] S. Rösel, H. Quanz, C. Logemann, J. Becker, E. Mossou, L. Cañadillas-Delgado, E. Caldeweyher, S. Grimme, P. R. Schreiner, *J. Am. Chem. Soc.* **2017**, *139*, 7428–7431.
[143] M. Gomberg, *Ber. Dtsch. Chem. Ges.* **1900**, *33*, 3150–3163.
[144] B. Kahr, D. Van Engen, K. Mislow, *J. Am. Chem. Soc.* **1986**, *108*, 8305–8307.
[145] S. Rösel, C. Balestrieri, P. R. Schreiner, *Chem. Sci.* **2017**, *8*, 405–410.
[146] S. Rösel, J. Becker, W. D. Allen, P. R. Schreiner, *J. Am. Chem. Soc.* **2018**, *140*, 14421–14432.
[147] T. Schnitzer, E. Paenurk, N. Trapp, R. Gershoni-Poranne, H. Wennemers, *J. Am. Chem. Soc.* **2021**, *143*, 644–648.
[148] L. Schweighauser, M. A. Strauss, S. Bellotto, H. A. Wegner, *Angew. Chem. Int. Ed.* **2015**, *54*, 13436–13439.
[149] M. A. Strauss, H. A. Wegner, *Angew. Chem. Int. Ed.* **2019**, *58*, 18552–18556.
[150] C. M. Thiele, K. Petzold, J. Schleucher, *Chem.Eur. J.* **2009**, *15*, 585–588.
[151] M. Melikian, J. Gramüller, J. Hioe, J. Greindl, R. M. Gschwind, *Chem. Sci.* **2019**, *10*, 5226–5234.

[152] S. Zhu, N. Niljianskul, S. L. Buchwald, *J. Am. Chem. Soc.* **2013**, *135*, 15746–15749.
[153] G. Lu, R. Y. Liu, Y. Yang, C. Fang, D. S. Lambrecht, S. L. Buchwald, P. Liu, *J. Am. Chem. Soc.* **2017**, *139*, 16548–16555.
[154] D. Yepes, F. Neese, B. List, G. Bistoni, *J. Am. Chem. Soc.* **2020**, *142*, 3613–3625.

Chapter 1

Adamantane-Based Oxazaborolidines

1. Motivation

The adamantane scaffold has received tremendous attention as building block for the synthesis of bioactive compounds.[1] Because of its high lipophilicity, adamantane helps to improve the pharmacological activity, while at the same time provides chemical stability.[2] Moreover, the inexpensive, symmetrical shape, and electron-rich nature of adamantane makes it an attractive candidate for catalyst design. Several applications for ligand design in transition metal catalysis or as building block for organocatalysts have been reported.[3–8] Due to new insights in the field of noncovalent interactions (NCIs), adamantane is now not only used because of its sterical demand, but also because of its excellent properties as an dispersion energy donor (DED).[9–11]

Common OXBs are without exception based on simple amino acids like proline, valine, or tryptophan, which usually possess a certain conformational flexibility. While conformationally dynamic peptide catalysts might be well suited for imparting selectivity, a high degree of conformational flexibility in small molecules can also inhibit the selectivity of a catalyst.[12–14] In this work, we envisaged to establish an unprecedented adamantane based oxazaborolidine catalyst, to make use of adamantanes rigidity, therefore preventing conformational flexibility and at the same time exploiting the DED capacities of the purely aliphatic and polarizable framework. However, the formation of an OXB requires either an accessible vicinal amino alcohol or amino acid moiety. While monosubstitution or disubstitution at the tertiary adamantane carbon atoms can be easily achieved by oxidation with subsequent substitution or by Ritter-type reaction a selective 1,2-disubstitution is a formidable challenge.[2]

In 2007, the group of Rohde reported the synthesis of an adamantane based vicinal amino alcohol as building block for various adamantane 11β-hydroxysteroid dehydrogenase type 1 inhibitors.[15] The key step in the synthesis is a rhodium catalyzed nitrenoid insertion previously established by Espino and Du Bois.[16] Inspired by this C-H functionalization of the adamantane cage, Hrdina *et al.* developed a synthetic strategy to access various 1,2-disubstituted adamantane derivatives.[17–19] This work accompanied with the progress of OXB chemistry set the starting point for our project.

2. Results

2.1. Preliminary Considerations

The preparation of OXBs for catalysis can be achieved in many different ways.[20–22] While few derivatives are stable at ambient conditions and can be isolated, most derivatives are sensitive towards hydrolysis and must be handled under exclusion of moisture, which makes purification steps difficult.[20,23,24] To avoid hydrolysis a lot of research has been done to establish effective procedures for the generation and usage of OXBs without the need for a purification step. Thus, a quantitative and clean formation of the OXB is essential to obtain reproducible results in the subsequent catalysis.

A common strategy is the *in situ* formation of the active catalyst directly prior to catalysis. Thereby, stoichiometric amounts of a catalyst precursor (*e.g.*, a stable and weighable vicinal amino alcohol) and borane are allowed to react by hydrogen extrusion or boronic acids by condensation to yield the OXB (Fig. 1).[23–27] First, we investigated if an adamantane based amino alcohol is an appropriate precursor. In this regard, we tested whether a vicinal adamantane amino alcohol can be transformed into an OXB in a clean and quantitative fashion with sufficient purity for catalysis.

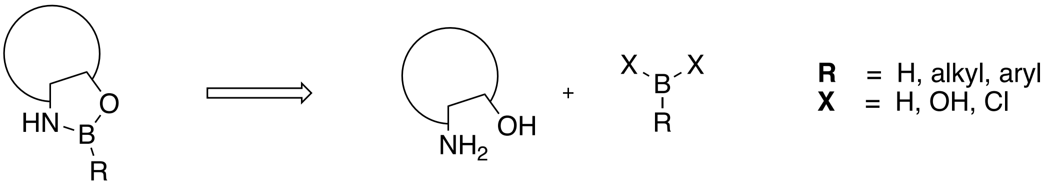

Figure 1 Retrosynthesis of OXBs by reaction of vicinal amino alcohols with boronic acid derivatives.

2.2. Synthesis of Racemic Catalyst Precursors

We started with the synthesis of racemic adamantane amino alcohols which should then act as catalyst precursors. Using the literature known protocol by Rhode *et al.*, adamantane-1-ol (**1**) was converted with trichloroacetyl isocyanate in a nucleophilic substitution to adamantane-1-carbisocyanate, which was then hydrolyzed to carbamate **2**. The following rhodium catalyzed nitrenoid insertion provided racemic adamantane oxazolidinone ***rac*-3** in high yield (Scheme 1).[15]

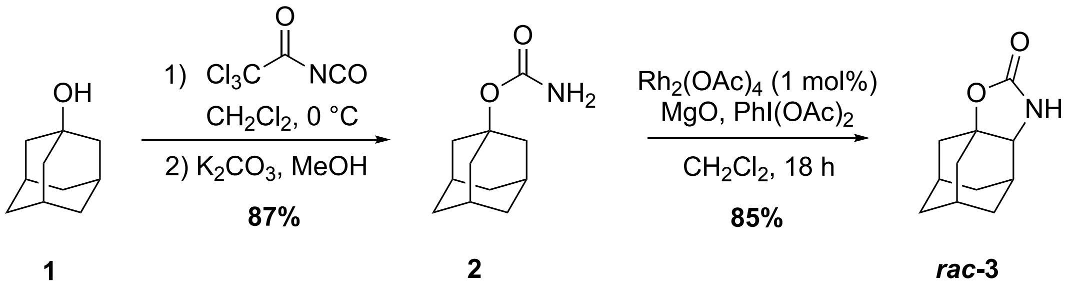

Scheme 1 Synthesis of adamantane carbamate **2** with subsequent rhodium catalyzed C-H insertion to adamantane oxazolidinone ***rac*-3**.

After hydrolysis of oxazolidinone ***rac*-3** under basic conditions amino alcohol ***rac*-4** was isolated in 95% yield. Additionally, we synthesized a mono-*N*-benzylated amino alcohol. We chose *N*-benzyl substitution at the target catalyst precursor since electron donating groups at the amine have shown to enhance the following OXB formation with boronic acids, because of the increased nucleophilicity of the nitrogen atom. Furthermore, nitrogen substitution of OXBs may also effect enantioselectivity.[28,29] Reductive amination with benzaldehyde and $NaBH_4$ provided racemic secondary amino alcohol ***rac*-4a** in moderate yield (Scheme 2).

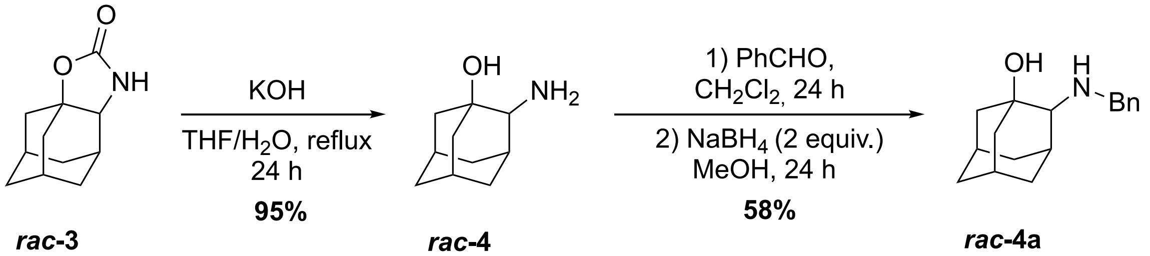

Scheme 2 Hydrolysis of adamantane oxazolidinone ***rac*-3** to amino alcohol ***rac*-4** followed by reductive amination with benzaldehyde to ***rac*-4a**.

2.3. NMR Investigation of Catalyst Formation

With the racemic catalyst precursors in hand, we envisioned to verify the presence of a catalytically active OXB *via* NMR spectroscopy. For that purpose, we refluxed amino alcohol ***rac*-4** with a stoichiometric amount of phenylboronic acid in toluene using a micro Soxhlet extractor filled with CaH_2 to remove H_2O (Fig. 2). This is a common protocol for condensation reactions, which has proven useful for the generation of OXBs.[30] Afterwards the solvent was distilled off and an NMR sample was prepared under Ar. For preparation of the NMR samples, we employed quartz glass NMR tubes, as normal NMR tubes consist of borosilicate glass and therefore are not appropriate for ^{11}B-NMR investigation. A range of ^{1}H, ^{13}C, and ^{11}B NMR spectra were measured and selected spectra are discussed below.

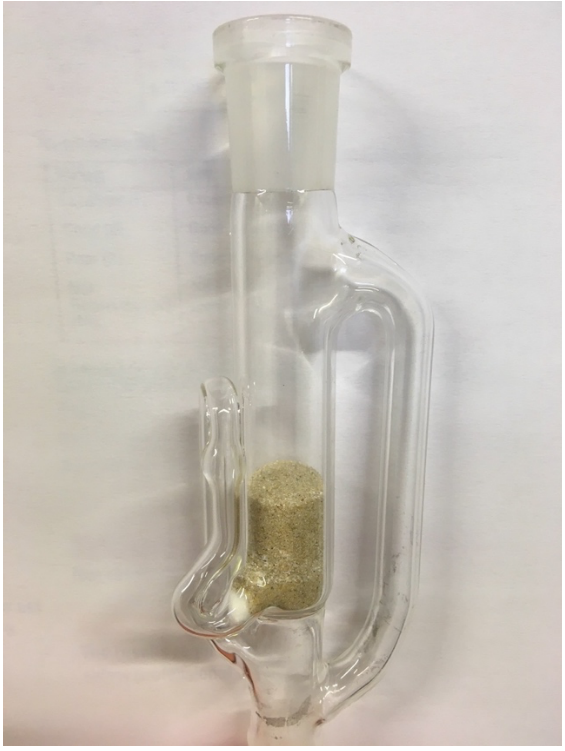

Figure 2 *In situ* formation of the OXB catalyst *via* condensation through a micro Soxhlet filled with CaH_2 and sand.

By comparison of the ^{13}C NMR spectra of amino alcohol ***rac*-4** and OXB ***rac*-5** we assumed deshielding and thereby a downfield shift of the tertiary and quaternary adamantyl carbons due to the Lewis acidic character of boron. Indeed, two new downfield shifted signals at 76.2 ppm and 61.5 ppm appeared, which could be assigned to the desired OXB (Fig. 3). However, even after several hours of azeotropic distillation, we did not achieve full conversion to the OXB, but rather obtained a mixture with starting material.

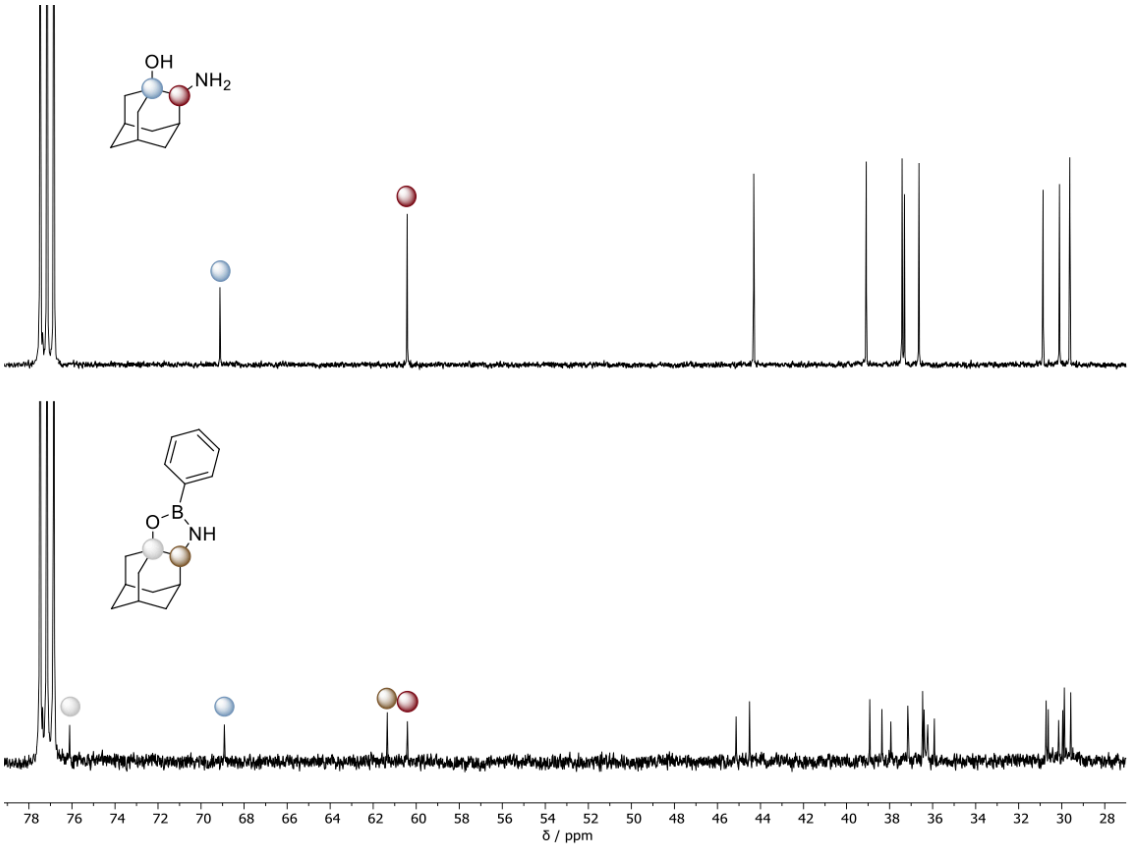

Figure 3 ^{13}C NMR spectra of the amino alcohol precursor (top) and the reaction mixture (bottom).

Next, we employed phenylboron dichloride, the more reactive analogue of the boronic acid, as chlorines are better leaving groups and therefore should facilitate the substitution towards the OXB. To trap HCl and prevent formation of the hydrochloride we used two equivalents of D*i*PEA as a mild base. Initial addition of D*i*PEA to amino alcohol ***rac*-4** did not provide a change in the NMR spectrum. Consecutive addition of phenylboron dichloride did not lead to any noticeable change of the amino alcohol ***rac*-4** chemical shifts in the ^{1}H and ^{13}C NMR spectra, but we observed a change of multiplicity of the D*i*PEA signals. The heptet at 3.00 ppm and the quartet at 2.45 ppm appeared as broad singlets. The aromatic signals of phenylboron dichloride shifted upfield, observable in both ^{1}H and ^{13}C NMR spectra (Fig. 4). Unfortunately, the signals of the amino alcohol ***rac*-4** remained completely unchanged. It can be concluded, that we only observed the formation of the Lewis acid-base adduct of phenylboron dichloride and D*i*PEA, while the amino alcohol remained unchanged.

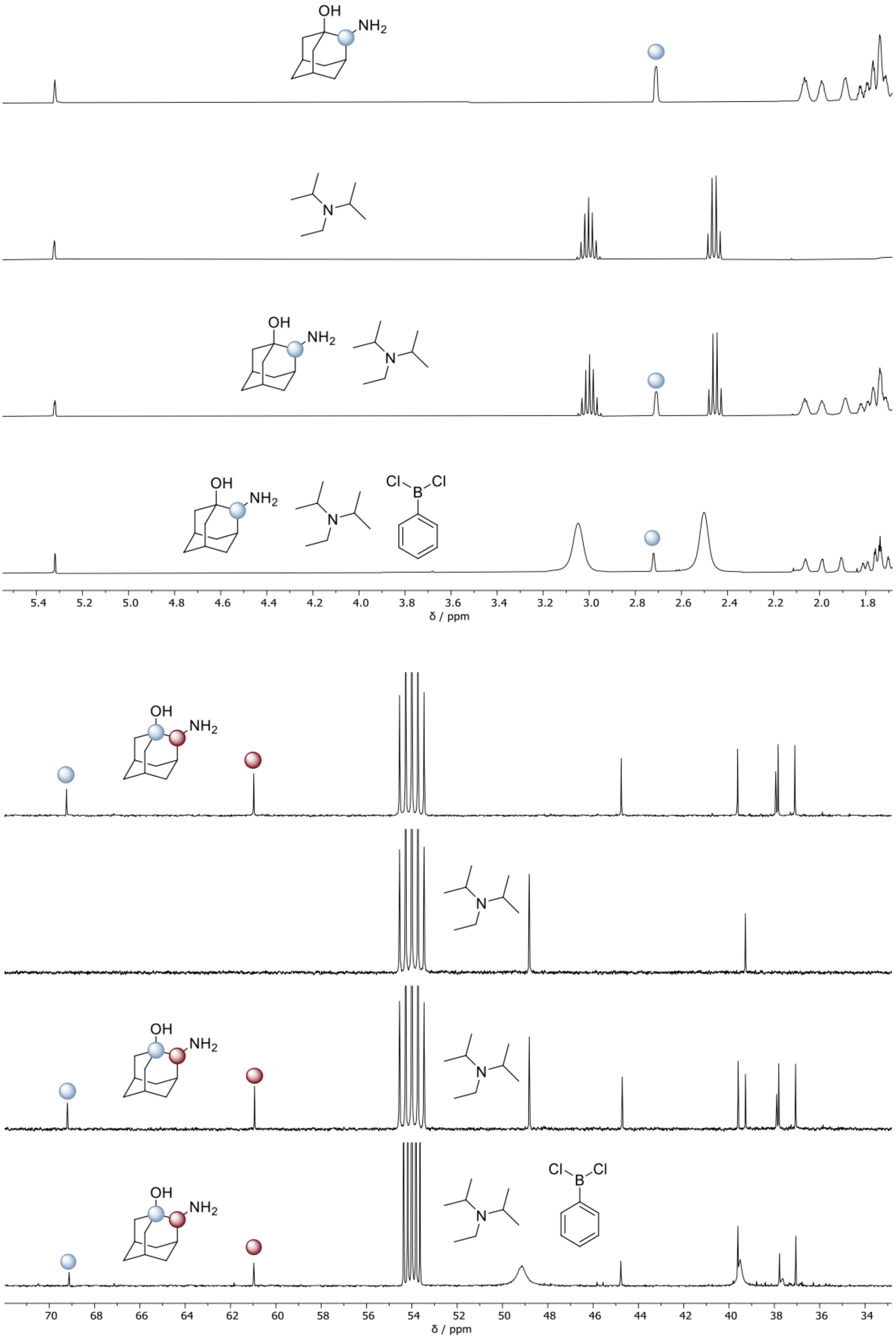

Figure 4 Comparison of ^{1}H and ^{13}C NMR spectra of the OXB formation.

In a last NMR experiment, we examined the catalyst formation with $BH_3{\cdot}SMe_2$, which is usually employed for the *in-situ* formation of OXBs in the CBS reduction. Hydrogen extrusion as driving force ensures clean and quantitative formation of a wide range of OXBs.[25] To this end, a quartz glass NMR tube was loaded with a sample of the amino alcohol and $BH_3 \cdot SMe_2$ under Ar. The ^{11}B NMR spectra were calibrated using $BF_3 \cdot Et_2O$ (0.0 ppm) as external reference. BH_3 became visible as a quartet around –20.5 ppm. First, we performed a test experiment with $BH_3 \cdot SMe_2$ and adamantan-1-ol as reference (Fig. 5). As expected, after adding adamantan-1-ol to $BH_3 \cdot SMe_2$, a sharp signal became visible at around 25.2 ppm, indicating oxygen substitution at the boron center.[31] The broadened area between 30 ppm and –10 ppm arises from the boron-containing probe head of the NMR spectrometer.

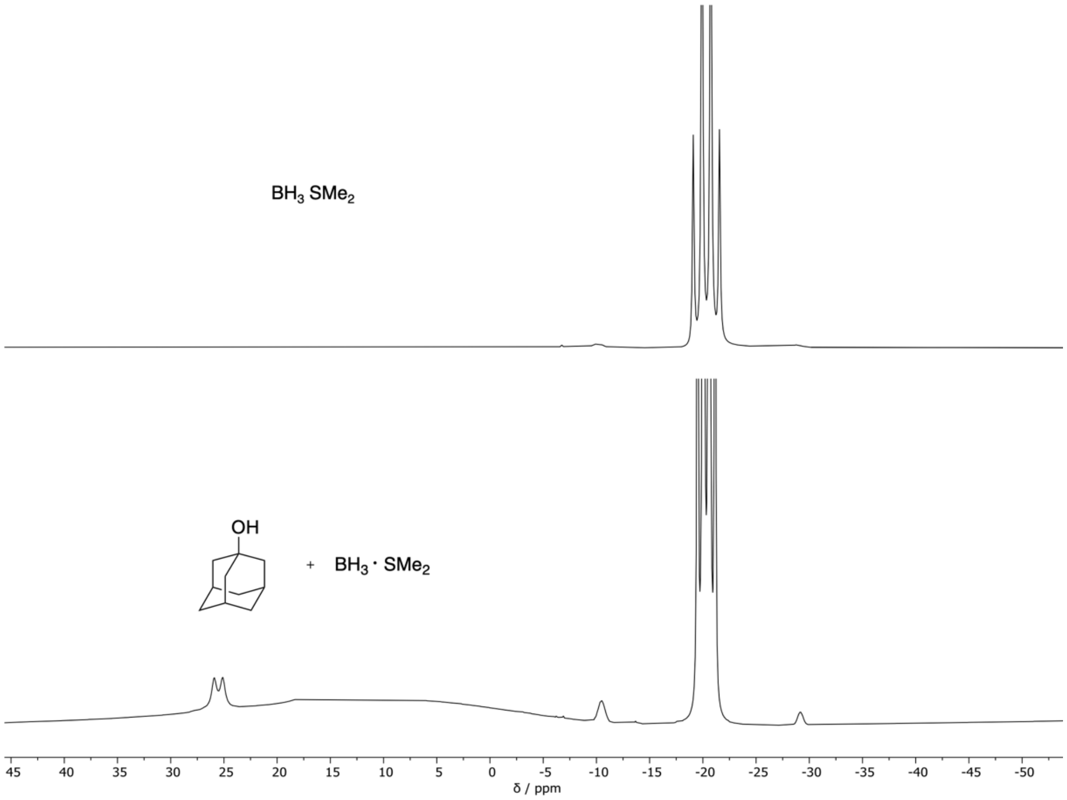

Figure 5 ^{11}B NMR spectra of $BH_3 \cdot SMe_2$ and a mixture of adamantan-1-ol and $BH_3 \cdot SMe_2$.

Next, we performed the experiment with amino alcohol ***rac*-4** and $BH_3 \cdot SMe_2$ (Fig. 6). As observed in the case of adamantan-1-ol, a broadened area between 30 ppm and –10 ppm is visible, arising from the boron-containing probe head of the NMR spectrometer. Certainly, we did not observe a sharp signal for a substituted boron, which indicates, that no reaction or coordination took place. This is extremely exceptional, because the high oxophilicity of boron should at least enforce the coordination to oxygen.

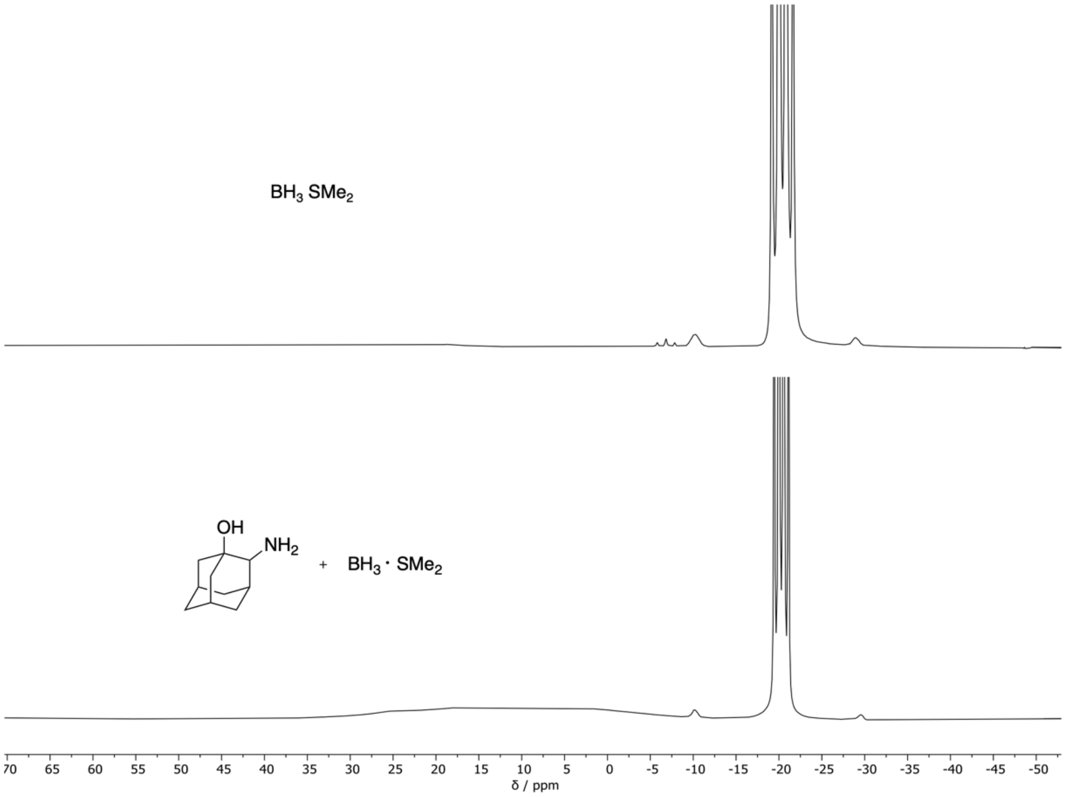

Figure 6 ^{11}B NMR spectra of $BH_3\cdot SMe_2$ and a mixture of amino alcohol ***rac*-4** and $BH_3\cdot SMe_2$.

2.4. Diels-Alder Reaction as Benchmark for Catalyst Formation

A further common strategy to proof the OXB formation is to perform catalyzed benchmark reactions and check for conversion or selectivity as an indicator for catalytic activity and thereby catalyst formation.[22,25,28,32] For this purpose, we chose a simple DA reaction with croton aldehyde as unreactive dienophile as a benchmark. The OXB formation was performed *in situ* directly before catalysis to circumvent catalyst hydrolysis during work up. Therefore, amino alcohol ***rac*-4** was refluxed again with a stochiometric amount of boronic acid in toluene through a micro Soxhlet extractor filled with CaH_2 for 24 h (Fig. 2). Alternatively, we employed phenylboron dichloride in a substitution reaction at room temperature. Afterwards, the solvent was removed and the product redissolved in anhydrous toluene to afford a stock solution, which was employed in the DA reactions.

In previous publications, the boron substituent proved to be important for catalyst formation, stability as well as reactivity and enantioselectivity in cycloaddition reactions. Especially phenyl substituents delivered better results compared to Me or ^{n}Bu.[33] To benchmark the catalyst formation, we investigated the conversion of DA reactions following literature established LLA and BLA protocols, employing 20 mol% of the *in situ* formed catalyst mixture and additionally 20 mol% of co-catalyst at –78 °C in toluene (Table 1).[27,34] We chose cyclopentadiene (**6**) and croton aldehyde (**7**) as substrates, as these do not undergo an uncatalyzed background reaction to **8** (entry 1). Using only OXB ***rac*-4** or ***rac*-4a** without an additional co-catalyst (entries 2 and 9), we did not observe any conversion. In contrast, the co-catalyst alone (entries 3, 5 and 7) promoted the DA reaction to the cycloaddition product **8** albeit with low conversion. Unexpectedly, the combination of OXB ***rac*-5** or ***rac*-5a** and co-catalyst led to even lower or no conversion at all.

Although the combination of an OXB with a co-catalyst should result in an active catalytic species for DA reactions, the OXB did not catalyze the desired transformation but additionally inhibited the co-catalyst in our test reactions. Because it was also not possible to identify ***rac*-5** in NMR experiments, we conclude that we did not form the desired OXB during the *in situ* protocol and the free amine of the starting materials then poisoned the co-catalyst.

Table 1 Benchmark cycloaddition reactions to test the OXB formation.

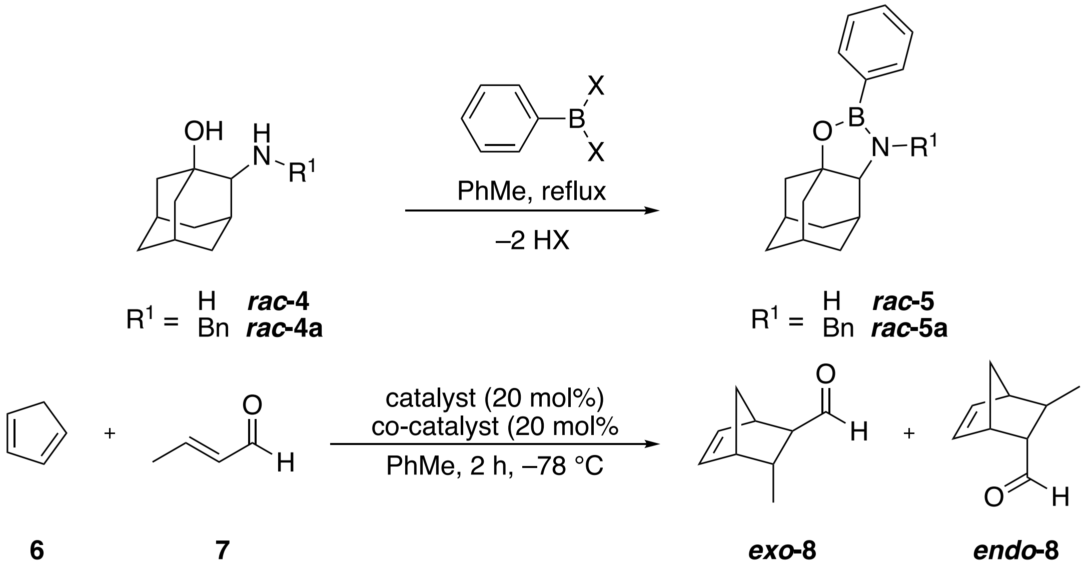
OH
H
N
R1
X
B
X
PhMe, reflux
–2 HX
O
B
N–R1
R1 = H rac-4
Bn rac-4a
R1 = H rac-5
Bn rac-5a
+
O
H
catalyst (20 mol%)
co-catalyst (20 mol%
PhMe, 2 h, –78 °C
O
H
+
O
H
6
7
exo-8
endo-8

Entry	R^1	X	Co-catalyst	Conversion[a] [%]	*endo*:*exo*[a]
1	-	-	-	0	nd
2	H	OH	-	0	nd
3	-	-	$AlCl_3$	12	7:1
4	H	OH	$AlCl_3$	traces	nd
5	-	-	CF_3SO_3H	14	2:1
6	H	OH	CF_3SO_3H	24	5:1
7	-	-	$SnCl_4$	33	9:1
8	H	OH	$SnCl_4$	27	2:1
9	Bn	OH	-	0	nd
10	Bn	OH	CF_3SO_3H	9	4:1
11	Bn	OH[b]	CF_3SO_3H	6	5:1
12	Bn	OH[b]	$AlCl_3$	0	nd
13	Bn	Cl	$AlCl_3$	0	nd
14	Bn	Cl	CF_3SO_3H	20	3:1
15	Bn	Cl[c]	$AlCl_3$	0	nd
16	Bn	Cl[c]	CF_3SO_3H	1	nd

[a] Conversion and diastereoselectivity were determined *via* ^{1}H NMR with *p*-nitro benzaldehyde as internal standard; [b] Triphenyl boroxine (anhydride of the acid) was used as borane source; [c] 0.4 equiv. Et_3N were added to trap HCl.

2.5. CBS Reduction as Chiral Benchmark Reaction for Catalyst Formation

As it was not possible to prove the OXB formation with boronic acids neither in NMR experiment nor in catalyzed Diels-Alder reactions, we envisaged an OXB formation with BH_3 and a chiral precursor for the asymmetric borane reduction of ketones. The formation of OXBs with BH_3 usually proceed efficiently due to extrusion of H_2 as driving force. Observing of enantiomeric excess (*ee*) in the following reduction would be a proof for the formation of a chiral catalyst.

To access the chiral catalyst precursor, a resolution of the racemic oxazolidinone ***rac*-3** was necessary. Therefore, we started with the esterification of the racemic starting material with (*R*)-O-Me-mandelic acid as chiral auxiliary. The use of (*R*)-O-Me-mandelic acid active ester **9** provided clean and quantitative transformation to **3a**. The obtained diastereoisomers **3a** were separated by column chromatography. Afterwards, the single diastereomer **(*S*,*R*)-3a** was hydrolyzed under basic conditions to yield the enantioenriched oxazolidinone **(*S*)-3** (Scheme 3), which was directly employed in the reduction to the vicinal amino alcohol. The absolute stereochemistry of the products was assigned by comparison with literature data.[18]

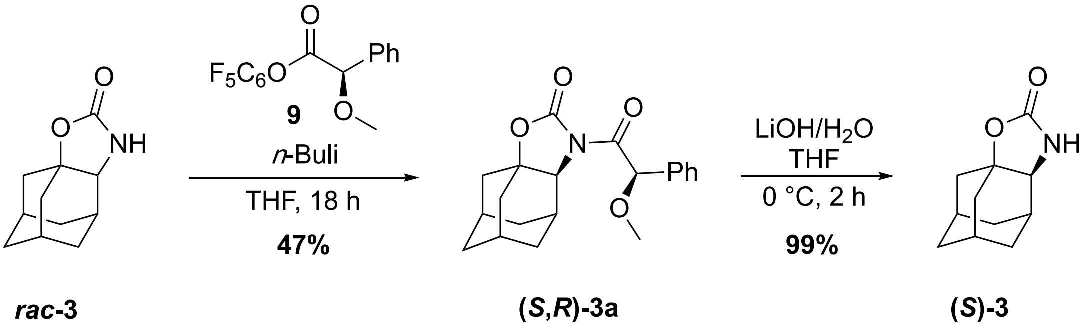

Scheme 3 Chiral resolution of oxazolidinone ***rac*-3** to yield **(*S*)-3**.

Oxazolidinone **(*S*)-3** was further reduced with $LiAlH_4$ to afford the vicinal *N*-methyl amino alcohol **(*S*)-4b** in good yield.[35] However, chiral analysis *via* HPLC revealed only 74% *ee* for **(*S*)-4b** (Scheme 4). This indicates racemization during either the basic cleavage of the auxiliary or the subsequent reduction step. We assume that racemization occurs probably by deprotonation of the amine with a subsequent rearrangement through a noradamantane derivative, but a mechanistic evidence is missing.

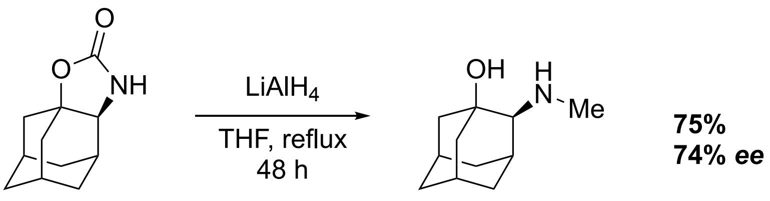

(S)-3 **(S)-4b**

Scheme 4 $LiAlH_4$ reduction of oxazolidinone **(*S*)-3** to enantioenriched vicinal amino alcohol **(*S*)-4b**.

Despite partial racemization, we employed the enantioenriched amino alcohol **(*S*)-4b** in the CBS reduction of acetophenone and 2-butanone (Table 2). We performed the reductions under conditions based on the original protocol by Corey, using 10 mol% of catalyst and 1.1 equivalents of reducing agent in THF.[20,25] Additionally, we chose slightly elevated temperatures, as borane reductions often perform more selectively and at higher rate at elevated temperatures.[36,37] Unfortunately, the reduction of both substrates provided no enantioselectivity. The high conversion can be attributed to background reaction with BH_3. Due to these unpromising results, an additional synthesis and usage of **(*R*)-4b** was not further pursued.

Table 2. CBS reduction of acetophenone and 2-butanone employing catalyst precursor **(*S*)-4b**.

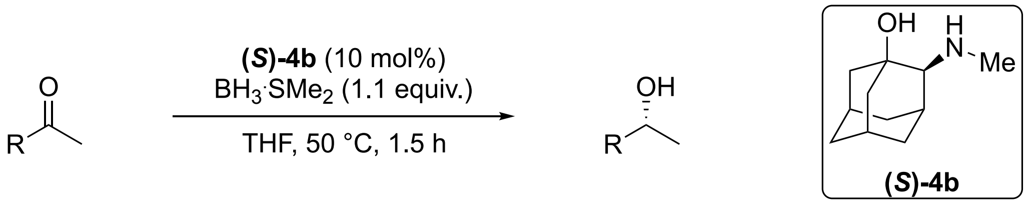

Entry	R	Conversion[a] [%]	*ee*[a] [%]
1	Ph	> 90	0
2	Et	> 90	0

[a] conversion and enantioselectivity were determined *via* chiral stationary phase GC.

Neither in NMR studies, nor in our benchmark reactions, we got any proof for the formation of a catalytically active OXB based on the vicinal adamantane amino alcohols ***rac*-4**, ***rac*-4a** and **(*S*)-4b**. We thus conclude that 1,2-adamantane amino alcohols **4** are not appropriate precursors to form OXBs, probably because of geometric reasons. The dihedral angle between the nitrogen and the oxygen in amino alcohol **(*R*)-4** amounts to 54.1°, while the computed OXB **(*R*)-6** has a dihedral angle of only 35.7° (Fig. 7). We therefore assume that, due to the rigidity of the adamantane framework, the distance is too large to bond boron with nitrogen and oxygen at the same time.

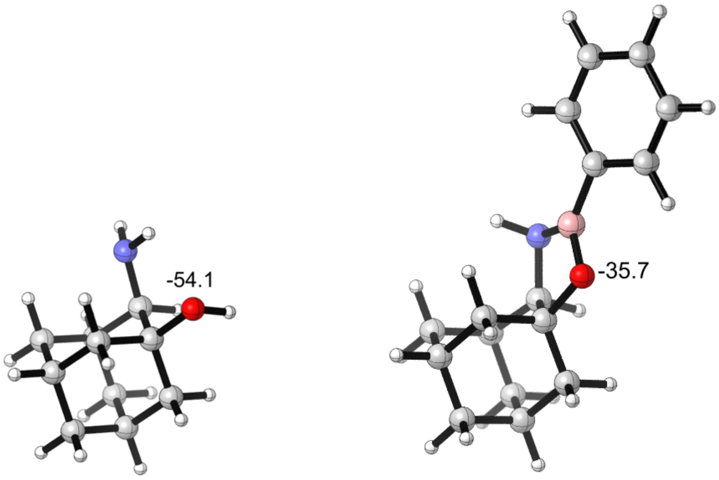

Figure 7 Optimized geometries of amino alcohol **(*R*)-4** (left) and OXB **(*R*)-6** at the B3LYP-D3(BJ)/6-31+G(d,p) level of theory.

2.6. Synthesis and Chiral Resolution of a more Flexible Adamantane Amino Alcohol

In order to establish an adamantane based OXB, we had to overcome the wide dihedral angle of the amino alcohol, combined with the rigidity of the adamantane core. Therefore, we used an adamantane amino alcohol with more flexibility as precursor. Furthermore, we envisaged to create the OXB not directly at the adamantane core, but slightly displaced. Starting from commercially available 2-adamantanone (**10**), we performed a Grignard reaction with benzyl bromide to obtain alcohol **11**, which was transformed to carbamate **12** by substitution with trichloroacetyl isocyanate. In the subsequent rhodium catalyzed C-H amination different C-H insertion products are generally possible. However, the nitrenoid as electron deficient species preferentially inserted into the more electron rich benzylic C-H bond to yield the heterospirocyclic oxazolidinone ***rac*-13** in 65% yield. Resolution of ***rac*-13** was again performed by esterification with the pentafluorophenyl ester of (*R*)-O-Me-mandelic (**9**) as chiral auxiliary, followed by separation of diastereomers *via* column chromatography to yield the pure diastereoisomers **(*R*,*R*)-13a** and **(*S*,*R*)-13a** (Scheme 5). The determination of the absolute configuration was performed at a later stage and is discussed in chapter 2.7.

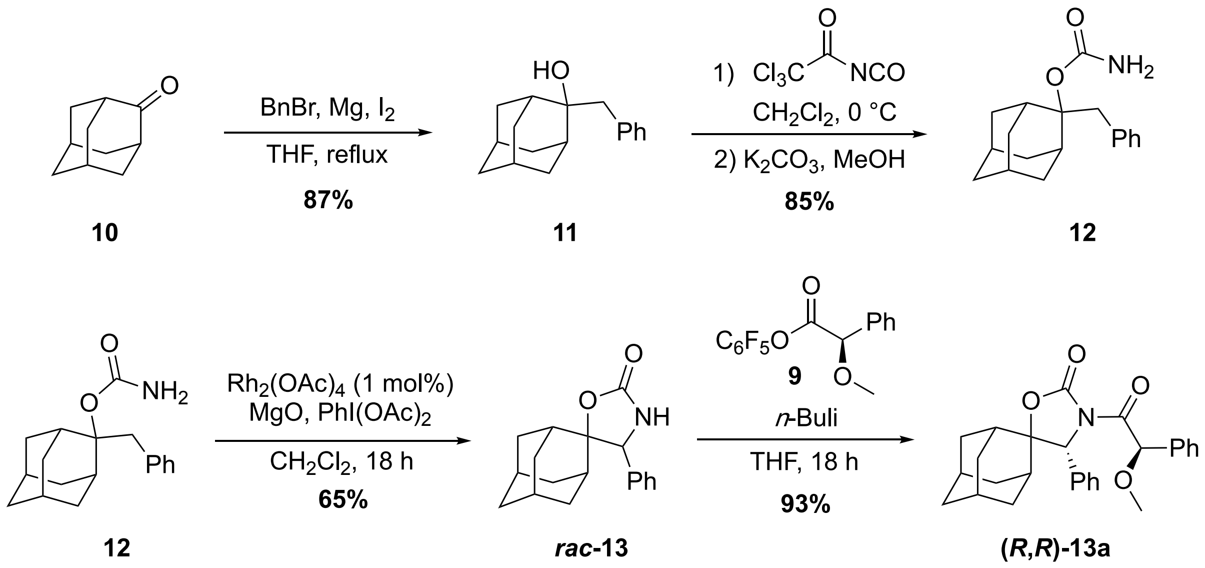
BnBr, Mg, I_2
THF, reflux
87%
1) Cl_3C, NCO
CH_2Cl_2, 0 °C
2) K_2CO_3, MeOH
85%
$Rh_2(OAc)_4$ (1 mol%)
MgO, $PhI(OAc)_2$
CH_2Cl_2, 18 h
65%
C_6F_5O
9
n-Buli
THF, 18 h
93%
10
11
12
12
rac-13
(*R*,*R*)-13a

Scheme 5 Synthesis and chiral resolution of the pure oxazolidinone diastereoisomers **(*R*,*R*)-13a** and **(*S*,*R*)-13a**.

Afterwards, both diastereoisomers **13a** were hydrolyzed separately under basic conditions to yield the enantioenriched oxazolidinones **13** (Table 3). In the synthesis of the previous amino alcohol **(*S*)-4b**, we experienced racemization in either the auxiliary cleavage or reduction step (Scheme 4). As a result, this time we carefully checked every synthetic step for erosion of enantiomeric excess. Indeed, HPLC analysis of the hydrolyzed oxazolidinones **13** revealed racemization of the enantiomers (Table 3). Remarkably, racemization was observed more for **(*S*)-13** (60% *ee*), while **(*R*)-13** was received with over 91% *ee*. Even under the literature optimized protocol for the cleavage of Evan's auxiliaries employing hydrogen peroxide as nucleophile under basic conditions, lower *ee* was always observed for **(*S*)-13** compared to **(*R*)-13** (Tab. 3 entry 4).[38,39] Thus racemization must occur at the diastereomeric state before cleavage of the auxiliary, as enantiomers have same chemical properties and therefore racemize equally fast.

Table 3 Hydroxide (LiOH) and peroxide (LiOH/H_2O_2) mediated hydrolysis of **13a** according to the protocol of Evans.[38,39]

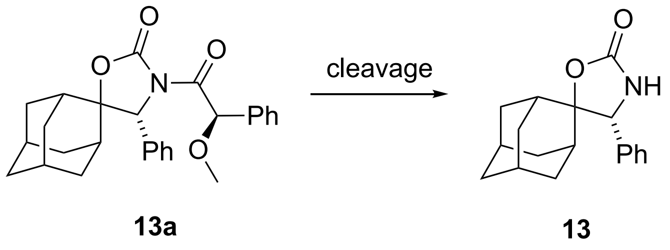
cleavage
13a
13

Entry	Diastereomer	Base	Yield [%]	Enantiomer	*ee*[a] [%]
1	**(*R*,*R*)-13a**	LiOH	70	**(*R*)-13**	90
2	**(*R*,*R*)-13a**	LiOH/H_2O_2	86	**(*R*)-13**	91

3	**(*S*,*R*)-13a**	LiOH	65	**(*S*)-13**	59
4	**(*S*,*R*)-13a**	LiOH/H_2O_2	84	**(*S*)-13**	60

[a] *ee* was determined by chiral stationary phase HPLC

The enantioenriched oxazolidinones **13** were then reduced using $LiAlH_4$ affording the vicinal amino alcohols **14a** in good yield and without further racemization (Table 4).[35] These results suggest that also in case of the previous amino alcohol **(*S*)-4b**, racemization probably occurred in the preceding auxiliary cleavage step (Scheme 3).

Table 4 Reduction of enantioenriched oxazolidinones **13** to amino alcohols **14a.**

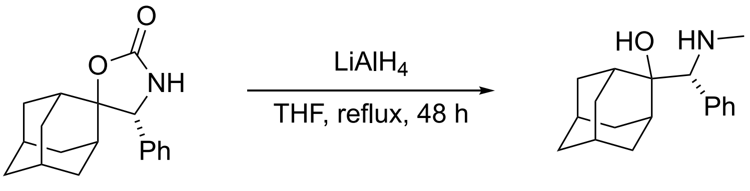

13 **14a**

Entry	Oxazolidinone	*ee* oxazolidinone[a] [%]	Amino alcohol	Yield [%]	*ee*[a] [%]
1	**(*R*)-13**	91	**(*R*)-14a**	78	91
2	**(*S*)-13**	60	**(*S*)-14a**	80	60

[a] *ee* was determined *via* chiral stationary phase HPLC

2.7. Determination of the Absolute Configuration

For asymmetric catalysis, the knowledge of the absolute configuration (AC) of the employed catalyst is of indispensable importance. While numerous analytical techniques exist to determine ACs of chiral molecules, crystal X-ray diffraction (XRD) analysis is one of the most widely used methods. Therefore, the chiral molecule is crystallized with a chiral resolving agent with known configuration. The resulting ionic single crystal can then be examined by XRD analysis and the AC is derived from the known configuration of the chiral resolving agent.[40,41]

We made several attempts to co-crystallize amino alcohol **(*S*)-14a** either with (*S*)- or (*R*)-mandelic acid in various solvents including acetone, dichloromethane, toluene, and *n*-hexane (Scheme 6).[17,42] However, all attempts failed to produce suitable crystals for XRD.

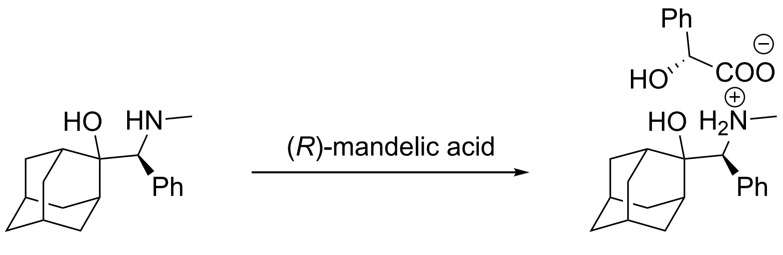

(*S*)-14a **15**

Scheme 6 Attempted co-crystallization of amino alcohol **(*S*)-14a** with (*R*)-mandelic acid.

Another common method for determining ACs of chiral amines or alcohols is the derivatization with an enantiomeric form of α-methoxy-α-trifluoromethylphenylacetic acid (MTPA), also known as Mosher's acid.[43] The resultant pair of diastereomers can then be analyzed by NMR spectroscopy. By precisely assigning and comparing the chemical shifts and coupling constants of the diastereomeric compounds, the respective AC can finally be deduced.[44,45] Certainly, as we utilized an amino alcohol substituted with adamantane and phenyl, the accurate assignment of protons was challenging, because many chemical shifts overlap in the corresponding frequency regions.

Due to these difficulties, we finally decided to make use of vibrational circular dichroism spectroscopy (VCD), which has recently been applied for AC determination of chiral molecules in the Schreiner group.[46–48] VCD spectroscopy detects differences in the absorption of left and right circularly polarized light, passing through a solution of the chiral compound.[49] Because VCD spectra can be simply computed and matched with the experimentally determined spectra, this represents a powerful method with increasing popularity for AC determination. For stereochemical assignment, we employed our amino alcohol **(*R*)-14a** as well as the precursor oxazolidinone **(*R*)-13** to the protocol of the recently published work by Schreiner.[46–48] In order to calculate a VCD spectrum, all conformers of a molecule have to be taken into account. Therefore, all conformers have to be calculated and subjected to a Boltzmann distribution. Due to its rigidity, oxazolidinone **(*R*)-13** is only present in one conformer. The VCD spectrum was computed at the B3LYP/6-311++G(d,p) level of theory. Conformational analysis of amino alcohol **(*R*)-14a** revealed four conformers within 3.0 kcal mol^{-1} using GFN2-xTB methods. For these conformers, VCD spectra were also computed at B3LYP/6-311++G(d,p) and used to simulate the Boltzmann-weighted VCD spectrum. The experimental VCD spectra were measured as solution in CD_2Cl_2 and provided excellent agreement with the computed spectra for both compounds and a consistent stereochemistry, allowing the unequivocal determination of the AC (Fig. 8).

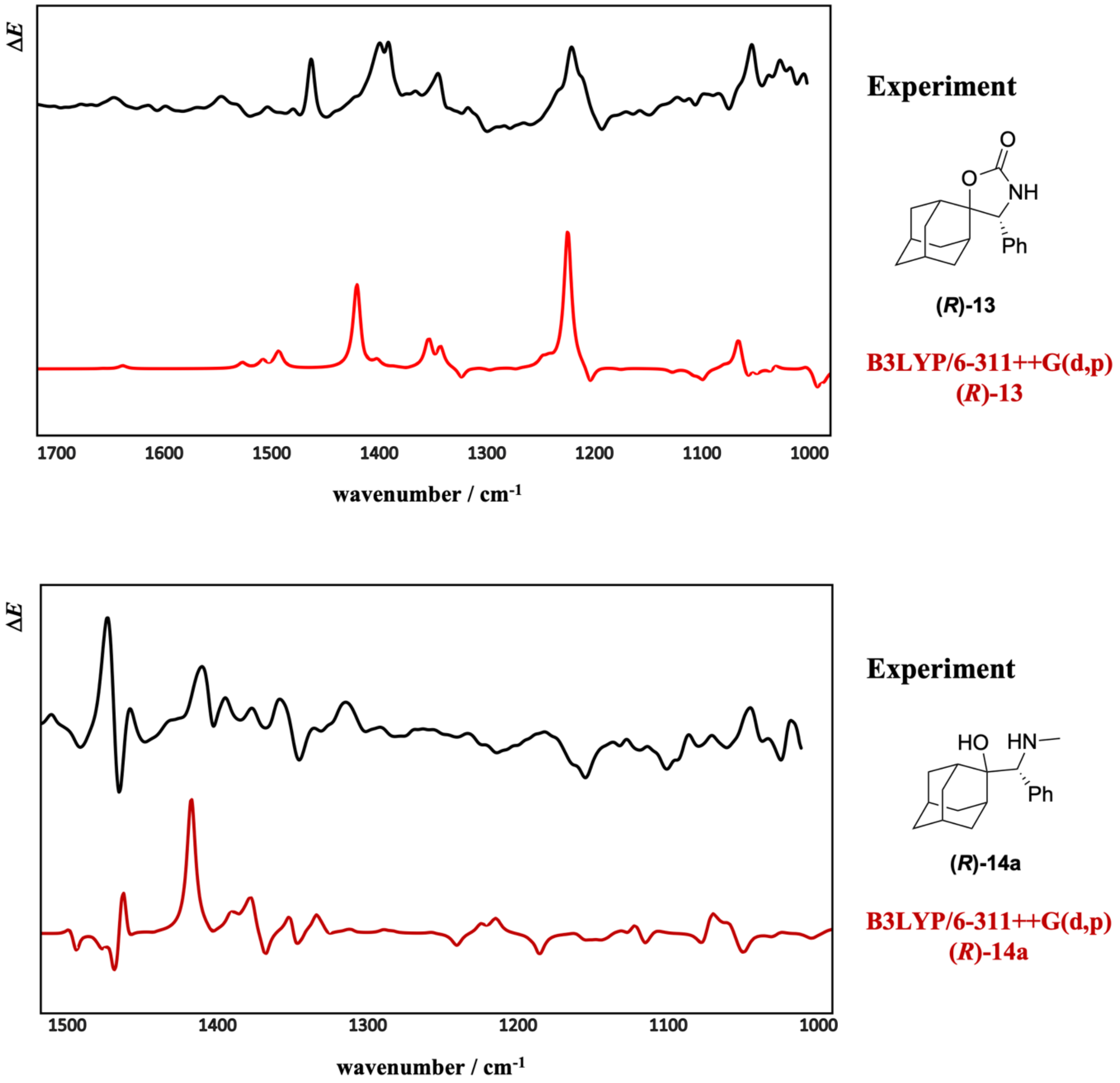

Figure 8 Comparison of the computed (red) and experimental (black) VCD spectra of adamantane oxazolidinone **(*R*)-13** (top) and amino alcohol **(*R*)-14a** (bottom).

2.8. Application in the CBS-Reduction

After having determined the absolute stereochemistry, we employed amino alcohols **(*R*)-14a** and **(*S*)-14a** as catalyst precursors in the CBS reduction of ketones. The results obtained for the reduction of three different ketones with $BH_3 \cdot SMe_2$ as reducing agent in THF at slightly elevated temperatures are summarized in Table 5. The reductions provided the alcohols in high yield (> 90%) but with only poor *ee*. While the reduction of 2-butanone was completely unselective, acetophenone and cyclohexyl ketone were reduced with up to 6% *ee*. In conjunction with the varying AC of the product alcohol by changing the catalyst enantiomer we are quite confident to claim that the adamantane based OXB as catalytically active species is formed. Nevertheless, the selectivities are only marginal, and regarding the effort for synthesis and chiral resolution of the catalyst, the project did not seem worth to continue.

Furthermore, the reaction conditions of the CBS reduction have already been optimized over years and leave little room for further refinement.

Table 5 CBS Reduction employing catalyst precursors **(*R*)-14a** and **(*S*)-14a.**

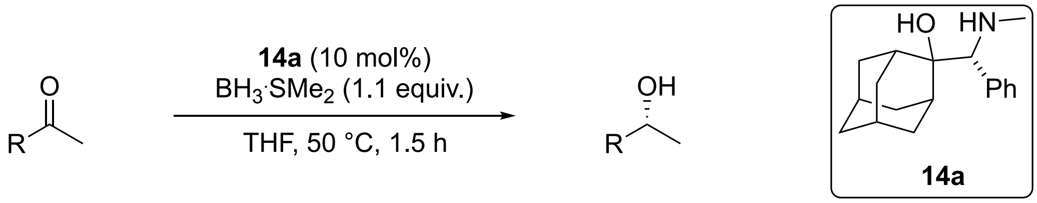

Entry	Amino alcohol	R	*ee*[a] [%]
1	**(*R*)-14a**	Ph	6 (*S*)
2	**(*S*)-14a**	Ph	3 (*R*)
3	**(*R*)-14a**	Cy	6 (*S*)
4	**(*S*)-14a**	Cy	4 (*R*)
5	**(*R*)-14a**	Et	0

conversion was in all cases over 90%

[a] *ee* was determined by chiral stationary phase GC

3. Summary & Outlook

While carrying out this work, we synthesized different adamantane based vicinal amino alcohols (Fig. 9). During the hydrolysis of the enantioenriched oxazolidinones we faced difficulties of racemization even under common reaction conditions, which have been published for many other derivatives.

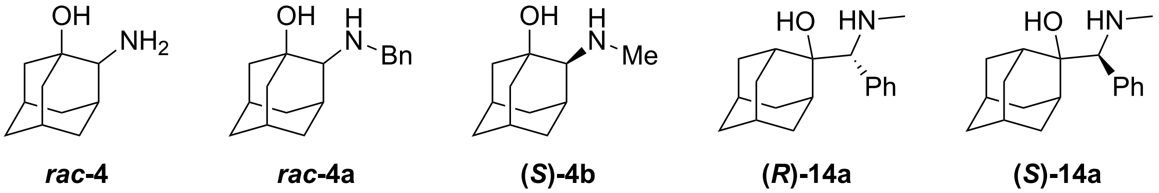

Figure 9 Synthesized adamantane based vicinal amino alcohols.

The vicinal amino alcohols were tested in the formation of OXBs. Therefore, we performed several NMR experiments and employed the amino alcohols as catalyst precursors in DA reactions and CBS reductions. Unfortunately, for amino alcohols **4** neither NMR spectroscopy experiments nor the benchmark reactions pointed to the formation of an OXB as catalytically active species. Wide dihedral angle and the rigidity of the adamantane core prevent the formation of an OXB. Therefore a less rigid and more flexible precursor is necessary.

Indeed, we could show that more flexible vicinal amino alcohols **14** are able to form catalytically active OXBs with BH_3 and can be utilized in CBS reductions (Scheme 7). We conclude, that vicinal amino alcohols based on adamantane are not appropriate precursors for the formation of OXBs in catalysis. On the one hand, amino alcohols **4** do not form the desired OXB, due to geometric restrictions. On the other hand, OXBs derived from amino alcohols **14** only provide poor selectivities in the CBS reduction.

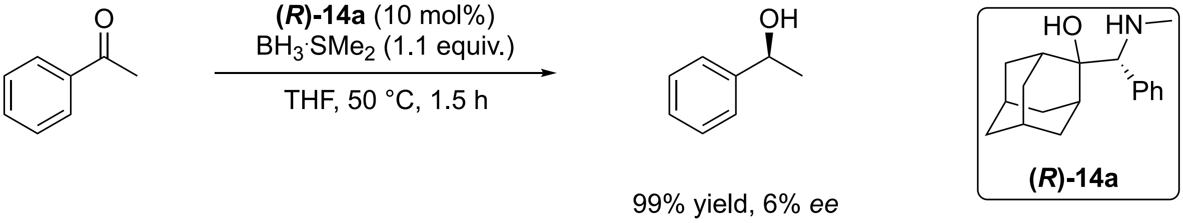

Scheme 7 (*R*)-14a catalyzed CBS reduction of acetophenone.

In 2015 Hrdina *et al.* published an easy route to access the chiral adamantane based amino alcohol **16**, starting from commercially available adamantane carbonic acid **18** (Fig. 11).[17] On the one hand, amino alcohol **16** should also be flexible enough for the formation of an OXB. On the other hand, **16** is not a vicinal amino alcohol and therefore could only provide six-membered OXBs that seemingly possess just inferior catalytic activity compared to their five-membered counterparts.[50] For this reason, we dispensed with synthesizing and testing amino alcohol **16** for OXB formation.

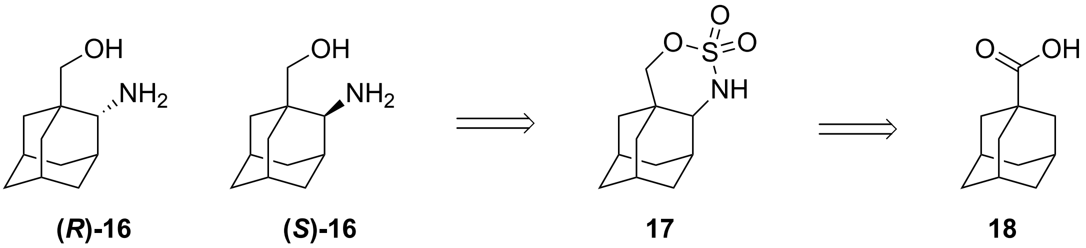

Figure 11 Access to chiral amino alcohol **16** published by Hrdina *et al.*[17]

Instead of striving for an OXB mounted directly on to the adamantane backbone, adamantyl-alanine could be a valuable OXB precursor for catalysis. While proteinogenic L-tryptophane is a common precursor for **19,** which was successfully used in asymmetric Diels-Alder[30] and Mukaiyama-Aldol reactions,[51] non-proteinogenic adamantyl-alanine has not got much attention in catalysis, yet (Fig. 12). Especially in regard of attractive LD interactions, the adamantylalanine derived catalyst **20** may effectively address aliphatic substrates by pure dispersion interactions[11,52,53] analogous to the tryptophan derived catalyst **19**, which facilitates $\sigma - \pi$ interactions for enantiodiscrimination (Fig. 12).[30,54]

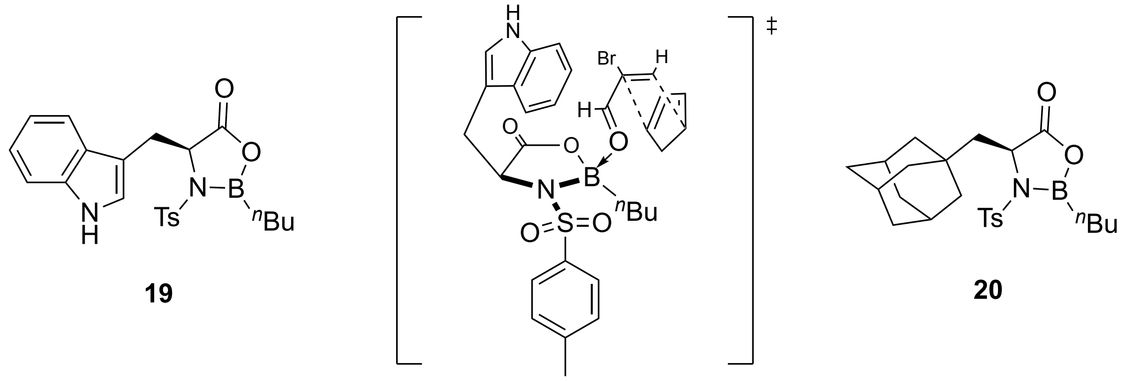

19

20

Figure 12 Tryptophan derived OXB **19** (left) and proposed transition structure in a Diels-Alder reaction[30,54] (middle). Adamantylalanine derived OXB **20** (right).

The synthesis of L-adamantyl alanine (**22**) can be facilitated *via* a modified Strecker synthesis and has been published by the group of Schwyzer in 1979.[55] The synthetic route starting from commercially available L-adamantyl acetaldehyde (**21**) is provided in Scheme 8.

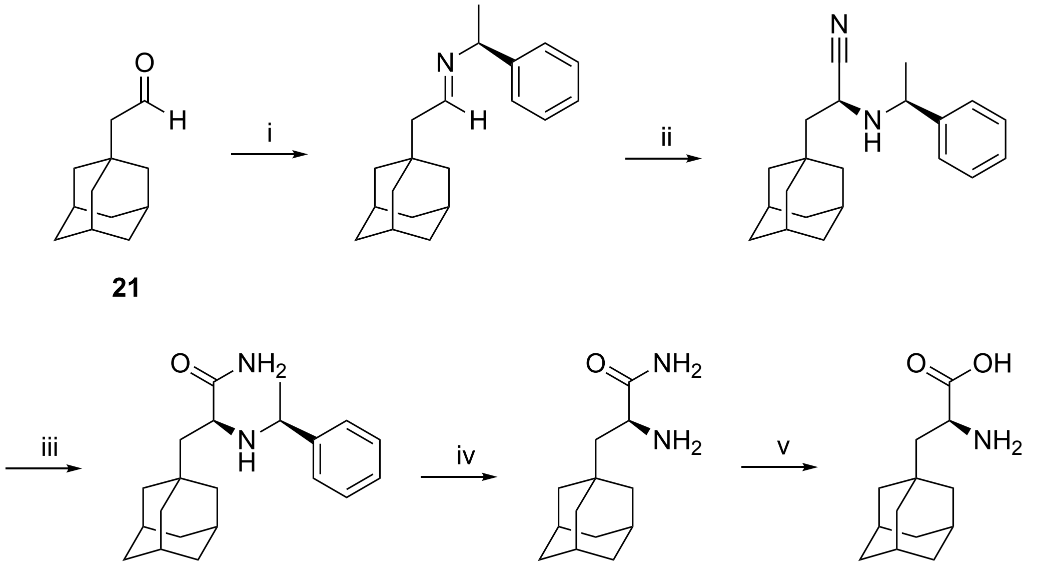

21

22

Scheme 8 Synthetic route to L-adamantyl alanine **22**. i; (*S*)-Methylbenzylamine, Et_2O, r.t., 24 h; ii: HCN, EtOH, r.t., 50 h; iii: HCl (37%), EtOH, r.t. 20 h; iv: H_2, Pd/C, EtOH, r.t. 15 h; v: HCl (37%), 90 °C, 4 h.[55]

4. Experimental Section

4.1. General Information

Unless otherwise noted, chemicals were purchased from Acros Organics, TCI, Alfa Aesar, Lancaster, Merck, or Fluka at the highest purity grade available and were used without further purification. All solvents were distilled prior to use. Toluene, THF, and CH_2Cl_2, were distilled from appropriate drying agents prior to use and stored under argon atmosphere. All catalytic reactions were carried out under an argon atmosphere employing oven- and flame-dried glassware. Column chromatography was conducted using Merck silica gel 60 (0.040 – 0.063 mm).

4.2. Analytical Methods

Thin Layer Chromatography (TLC) was performed on silica coated plates (*Merck*, silica 60 F254) with detection by UV-light (λ = 254 nm) and/or by staining with a cerium ammonium molybdate solution [CAM] and developed by heating.

CAM-staining solution: cerium sulfate tetrahydrate (1.00 g), ammonium molybdate (25.0 g), and concentrated sulfuric acid (25.0 mL) in water (250 mL).

Nuclear Magnetic Resonance (NMR) spectra were recorded at room temperature either on a *Bruker* AV-400 or a *Bruker* AV-400HD. ^1H NMR spectra were referenced to the residual proton signal of $CDCl_3$ (δ = 7.26 ppm). ^{13}C NMR spectra were referenced to the ^{13}C-D triplet of $CDCl_3$ (δ = 77.2 ppm). The following abbreviations for single multiplicities were used: *br* = broad, s = singlet, d = doublet, t = triplet, q = quartet, quint = quintet, sept = septet.

High resolution mass spectrometry (HRMS) was performed employing either a Bruker MicrOToF or a Bruker Impact II using methanol solutions of the respective compounds.

Chiral Gas Chromatography (GC): Enantioselectivities were determined by chiral stationary phase GC analyses on Hewlett Packard 5890 or 6890 gas chromatographs, respectively.

4.3. Standards for Catalysis

4.3.1. Cycloaddition Standards

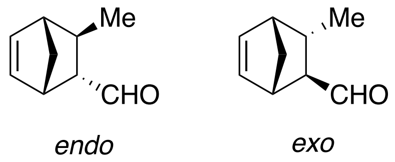

The standards for the Diels-Alder reaction were synthesized according to a published protocol by MacMillan *et al.* employing a chiral amine catalyst.[56] Yield and diastereoselectivity of the catalyzed reactions were determined by ^{1}H NMR studies employing *p*-nitrobenzaldehyde as internal standard.

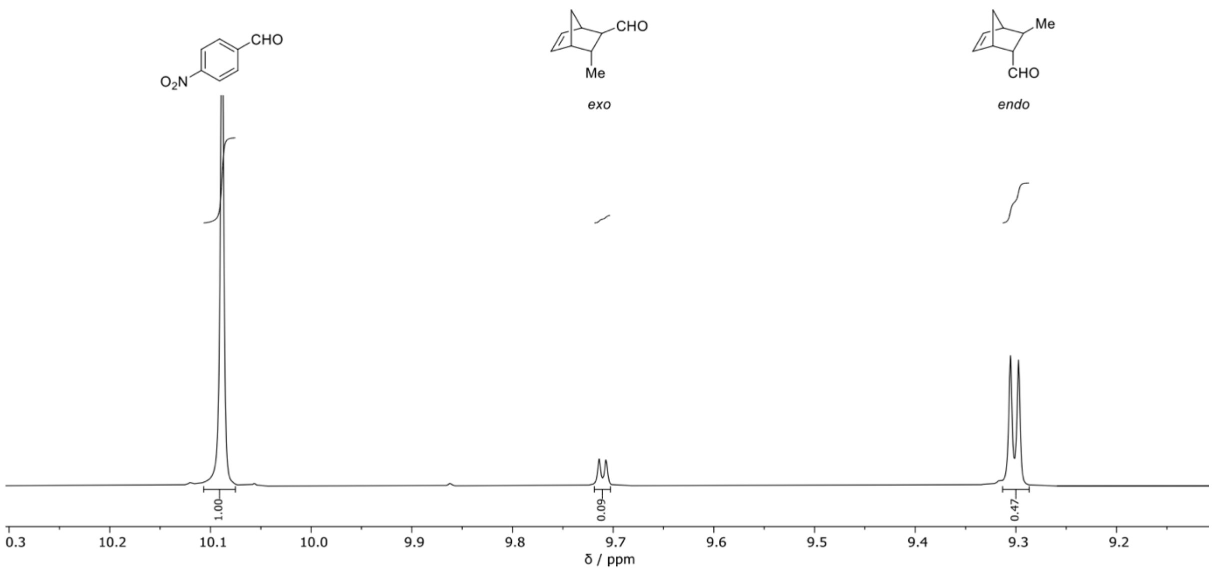

Figure 13 ^{1}H NMR spectrum of the aldehyde shifts of *p*-nitrobenzaldehyde and the *exo* and *endo* cycloaddition products.

4.3.2. Racemic Alcohols for the CBS Reduction

The racemic alcohols were either purchased or synthesized by reduction of the appropriate ketones with $NaBH_4$ in MeOH.

Phenylethanol

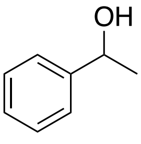

Enantioselectivity was determined *via* chiral stationary phase GC employing a 30 m FS-Hydrodex β-6TBDM column (Macherey Nagel).

T (Injector + Detector) = 250 °C

Splitflow = 80 mL min^{-1}

Precolumn pressure = 0.8 bar

Conditions: 100 °C isothermal, 20 min

Retention Times: (*R*) = 10.8 min; (*S*) = 11.2 min

2-Butanol

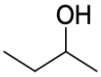

Enantioselectivity was determined by investigation of the benzoylated alcohol *via* chiral stationary phase GC employing a 30 m FS-Hydrodex β-6TBDM column (Macherey Nagel).

T (Injector + Detector) = 250 °C

Splitflow = 80 mL min^{-1}

Precolumn pressure = 0.8 bar

Conditions: 100 °C – 140 °C, 2 °C min^{-1}

Retention Times: (*R*) = 14.3 min; (*S*) = 14.5 min

1-Cyclohexylethanol

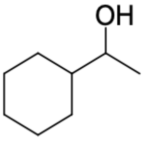

Enantioselectivity was determined *via* chiral stationary phase GC employing a 30 m FS-Hydrodex β-TBDAc column (Macherey Nagel).

T (Injector + Detector) = 250 °C

Splitflow = 80 mL min^{-1}

Precolumn pressure = 0.8 bar

Conditions: 80 °C isothermal, 20 min; 80 – 120 °C, 2 °C min^{-1}

Retention Times: (*R*) = 26.9 min; (*S*) = 27.4 min

4.4. General Procedures

GP1: Formation of carbamates

To a cooled suspension of starting material (1.00 equiv.) in CH_2Cl_2 was added trichloroacetylisocyanate (1.20 equiv.) and the reaction mixture was stirred at r.t. for 24 h. The solvent was evaporated and the colorless solid was diluted with MeOH and sat. aq. K_2CO_3 solution. The reaction mixture was further stirred at 55 °C for 24 h. MeOH was evaporated under reduced pressure and the aqueous phase was extracted with CH_2Cl_2 (3×). The combined organic layers were extracted with sat. aq. NH_4Cl solution and brine, dried over $MgSO_4$, filtered, and the solvent was removed under reduced pressure to provide the product as a crystalline solid.

GP2: Rh catalyzed nitrenoid insertion

An oven dried Schlenk tube was charged with carbamate (1.00 equiv.), $PhI(OAc)_2$ (1.20 equiv.), MgO (2.50 equiv.), and $Rh_2(OAc)_4$ (0.05 equiv.) in 20 mL of dry CH_2Cl_2 under Ar. The suspension was stirred under reflux for 24 h. The suspension was filtered over a plug of silica and the solvent was removed under reduced pressure. The crude product was purified by column chromatography.

GP3: Separation of diastereoisomers

Synthesis of the active ester

A solution of (*R*)-O-Me-mandelic acid (1.00 equiv.), pentafluorophenol (1.00 equiv.), and EDC•HCl (2.00 equiv.) in CH_2Cl_2 was stirred at r.t. for 24 h. The reaction mixture was diluted with EtOAc and extracted with 0.5 M citric acid (3×) solution, sat. aq. $NaHCO_3$ solution (3×), and brine. The organic phase was dried over $MgSO_4$, filtered, and the solvent was removed under reduced pressure to provide the active ester as a colorless liquid.

Esterification of the oxazolidinone

To a cooled solution of starting material (1.00 equiv.) in dry THF under Ar at 0 °C was added *n*-BuLi (1.00 equiv.) and the reaction mixture was stirred at 0 °C for 1 h. Then the pentafluorophenyl ester of (*R*)-O-Me-mandelic acid (1.50 equiv.) dissolved in dry THF was added and the reaction mixture was stirred at r.t. for 18 h. The reaction was quenched by addition of brine and the aqueous phase was extracted with EtOAc (4×). The combined organic phases were dried over $MgSO_4$, filtered, and the solvent was removed under reduced pressure. The crude product was purified by column chromatography to provide separated diastereoisomers.

GP4: Cleavage of the auxiliary

Cleavage with LiOH

To a solution of starting material (1.00 equiv.) in THF were added 4 mL of water and LiOH (16.0 equiv.) and the reaction mixture was stirred at 0 °C for 2 h. The reaction mixture was extracted with EtOAc (4×). The combined organic phases were dried over $MgSO_4$, filtered, and the solvent was removed under reduced pressure to provide the product.

Cleavage with H_2O_2 / LiOH

A solution of starting material (1.00 equiv.) in THF/H_2O (3:1) [0.05 M] was cooled to 0 °C and treated with 30% H_2O_2 (4.60 equiv.) and LiOH (2.00 equiv.) The reaction mixture was stirred at r.t. for 2 h and the excess of peroxide was quenched with a 1.5 M Na_2SO_3 solution (5.00 equiv.) The pH was adjusted to 9-10 by addition of a sat. aq. $NaHCO_3$ solution and THF was evaporated under reduced pressure. The aqueous phase was extracted with CH_2Cl_2 (4×) and the combined organic phases were washed with brine, dried over Na_2SO_4, filtered, and the solvent was removed under reduced pressure to provide the oxazolidinone as a colorless solid.

GP5: Reduction of the oxazolidinone

To a suspension of $LiAlH_4$ (3.00 equiv.) in THF [1 M] was added a solution of the cyclic carbamate (1.00 equiv.) in THF at 0 °C. The reaction mixture was stirred at 70 °C for 48 h. Then the reaction was quenched at 0 °C by addition of EtOAc, 10% NaOH, and H_2O and the mixture was stirred at r.t. for further 5 h. After filtration over a plug of Celite, the solvent was removed under reduced pressure to provide the pure product.

GP6: *In situ* OXB formation with boronic acids

An oven dried Schlenk tube was charged with the corresponding amino alcohol (1.00 equiv.) and the boronic acid (1.00 equiv.) in anhydrous toluene. A micro Soxhlet filled with sand and CaH_2 was placed on top of the flask and the reaction mixture was refluxed for 24 h under Ar. Afterwards, toluene was removed by distillation and the OXB was dried for 1 h under reduced pressure. A stock solution of the OXB was prepared and directly employed in catalysis.

GP7: *In situ* OXB formation with $BH_3{\bullet}SMe_2$ for subsequent CBS reduction

An oven dried Schlenk tube was charged with the corresponding amino alcohol (1.00 equiv.) and $BH_3{\bullet}SMe_2$ (0.60 equiv.) in anhydrous THF under Ar. The reaction mixture was stirred at 50 °C for 1 h. Then a solution of the ketone was slowly added *via* syringe pump over a period of 1.5 h. The reaction was quenched by addition of 0.5 M citric acid solution. The aqueous phase was extracted with CH_2Cl_2 (3×), the combined organic phases were dried over $MgSO_4$, filtered, and solvent was removed under reduced pressure.

4.5. Synthesis of Alcohols

2-Benzyl-2-adamantanol (11)

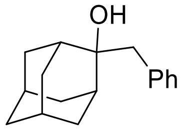

To a suspension of magnesium (0.359 g, 15.0 mmol, 1.50 equiv.) in 10 mL anhydrous Et_2O under Ar was added a crystal of iodine and the mixture was stirred at room temperature for 30 min. Then 5% of a solution of benzyl bromide (1.78 mL, 15.0 mmol, 1.50 equiv.) in 20 mL Et_2O was added and the reaction mixture was stirred under reflux. As soon as the color changed from brown to pale yellow, the remaining solution of benzyl bromide was added dropwise *via* an addition funnel (~ 0.1 mL min^{-1}). The reaction mixture was refluxed for 1 h and then cooled to 0 °C.

To the benzylmagnesium bromide suspension, a solution of 2-adamantanon (1.50 g, 10.0 mmol, 1.00 equiv.) in 20 mL Et_2O was added dropwise (~ 0.1 mL min^{-1}). The reaction mixture was stirred under reflux for 2 h, cooled to 0 °C, and 20 mL sat. aq. NH_4Cl solution was added to quench the reaction. The mixture was then extracted with EtOAc (3×). The combined organic layers were washed with brine, dried over Na_2SO_4, filtered, and the solvent was removed under reduced pressure. The crude product was purified by column chromatography.

***R*f** = 0.32 (Hex:EtOAc /20:1)

^{1}H NMR (400 MHz, $CDCl_3$): δ/ppm = 7.28 – 7.13 (m, 5H), 2.92 (s, 2H), 2.48 (s, 1H), 2.10 (dd, J = 12.5, 3.1 Hz, 2H), 2.04 – 1.98 (m, 2H), 1.86 (s, 1H), 1.75 – 1.69 (m, 3H), 1.66 – 1.59 (m, 3H), 1.50 – 1.40 (m, 2H), 1.35 (s, 1H).

^{13}C NMR (101 MHz, $CDCl_3$): δ/ppm = 137.5, 130.8, 128.4, 126.6, 77.5, 77.2, 76.8, 74.8, 47.1, 44.0, 39.4, 38.6, 37.0, 34.8, 33.1, 27.7, 27.6, 27.5.

HRMS (ESI): calcd for $C_{17}H_{23}O$ $[M+H]^+$: 243.1743; found: 243.1741

4.6. Synthesis of Carbamates

1-Adamantyl carbamate (2)

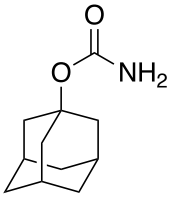

Using GP1, 1-adamantanol (3.04 g, 20.0 mmol, 1.00 equiv.) was reacted with trichloroacetylisocyanate (2.86 mL, 24.0 mmol, 1.20 equiv.) to afford 1-adamantyl carbamate (3.64 g, 18.6 mmol, 93%) as a crystalline, colorless solid.

***R*$_f$** = 0.36 (Hex:EtOAc /2:1)

^{1}H NMR (400 MHz, CDCl$_3$): δ/ppm = 4.44 (brs, 2H); 2.16 (s, 3H); 2.12-2.06 (m, 6H); 1.71-1.60 (m, 6H).

^{13}C NMR (101 MHz, CDCl$_3$): δ/ppm = 156.1 (Cq), 79.7 (Cq), 41.6 (CH$_2$), 36.3 (CH$_2$), 31.0 (CH).

HRMS (ESI): calcd for $C_{11}H_{17}NNaO_2$ [M+Na]$^+$: 218.1158; found: 218.1152

The NMR spectra are in accordance with those reported in the literature.[15]

2-Benzyl-2-adamantyl carbamate (12)

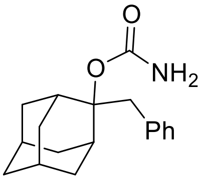

Using GP1, 2-benzyl-2-adamantanol (**11**) (1.84 g, 7.60 mmol, 1.00 equiv.) was reacted with trichloroacetylisocyanate (1.72 mL, 9.12 mmol, 1.20 equiv.) to afford the 2-benzyl-2-adamantyl carbamate **12** (1.85 g, 6.52 mmol, 87%) as a crystalline, colorless solid.

***R*$_f$** = 0.40 (Hex:EtOAc /20:1)

^{1}H NMR (400 MHz, CDCl$_3$): δ/ppm = 7.24 – 7.12 (m, 5H), 4.47 (s, 2H), 3.42 (s, 2H), 2.30 (s, 2H), 2.03 – 1.99 (m, 2H), 1.98 – 1.89 (m, 4H), 1.77 – 1.73 (m, 2H), 1.70 – 1.64 (m, 2H), 1.53 – 1.47 (m, 2H).

^{13}C NMR (101 MHz, CDCl$_3$): δ/ppm = 156.1, 137.6, 130.5, 128.1, 126.3, 87.3, 77.5, 77.2, 76.8, 47.1, 39.4, 38.4, 38.0, 36.4, 34.6, 34.1, 33.3, 27.6, 27.5, 27.0.

HRMS (ESI): calcd for $C_{18}H_{24}NO_2$ [M+H]$^+$: 286.1802; found: 286.1800

4.7. Synthesis of Oxazolidinones

Adamantyl oxazolidin-2-one (*rac*-3)

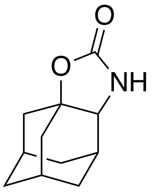

Using GP2, adamantyl-1-carbamat (**2**) (1.00 g, 5.20 mmol, 1.00 equiv.) was treated with PhI(OAc)2 (2.20 g, 6.76 mmol, 1.20 equiv.), MgO (0.524 g, 13.0 mmol, 2.50 equiv.), and $Rh_2(OAc)_4$ (0.114 g 0.260 mmol, 0.05 equiv.) in 20 mL dry CH_2Cl_2. The obtained oil was purified by column chromatography (silica, Hex/EtOAc = 2/1) to afford the product (0.569 g, 2.94 mmol, 57%) as a colorless solid.

***R*f** = 0.15 (Hex:EtOAc / 2:1)

^{1}H NMR (400 MHz, $CDCl_3$): δ/ppm = 5.37 (s, 1H), 3.66 (s, 1H), 2.33 – 2.23 (m, 2H), 2.19 – 1.98 (m, 4H), 1.90 – 1.56 (m, 8H).

^{13}C NMR (101 MHz, $CDCl_3$): δ/ppm = 161.1 (Cq), 80.6 (Cq), 64.2 (CH), 40.2 (CH), 37.3 (CH), 36.4 (CH_2), 36.3 (CH_2), 31.3 (CH_2), 31.1 (CH), 29.2 (CH).

HRMS (ESI): calcd for $C_{11}H_{15}NNaO_2$ $[M+Na]^+$: 216.0996; found: 216.1001

The NMR spectra are in accordance with those reported in the literature.[15]

2-Benzyl-2-adamantyl oxazolidinone (*rac*-13)

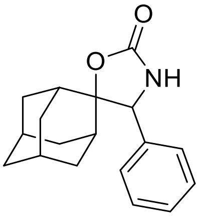

Using GP2, 2-benzyl-2-adamantyl carbamate (**12**) (1.00 g, 3.50 mmol, 1.00 equiv.) was treated with $PhI(OAc)_2$ (1.47 g, 4.55 mmol, 1.30 equiv.), MgO (0.353 g, 8.75 mmol, 2.50 equiv.), and $Rh_2(OAc)_4$ (0.077 g 0.175 mmol, 0.05 equiv.) in 20 mL dry CH_2Cl_2. The obtained oil was purified by column chromatography (silica, Hex/EtOAc = 2/1) to afford the product (0.569 g, 2.94 mmol, 57%) as a colorless solid.

***R*f** = 0.10 (Hex:EtOAc / 2:1)

^{1}H NMR (400 MHz, $CDCl_3$): δ/ppm = 7.41 – 7.28 (m, 5H), 5.37 (s, 1H), 4.64 (s, 1H), 2.32 (dp, J = 12.7, 2.7 Hz, 1H), 2.25 – 2.15 (m, 2H), 2.05 – 1.89 (m, 2H), 1.80 (dq, J = 18.6, 3.2 Hz, 2H), 1.75 – 1.57 (m, 2H), 1.49 (dq, J = 12.7, 2.7 Hz, 1H), 1.34 – 1.23 (m, 2H).

^{13}**C NMR** (101 MHz, $CDCl_3$): δ/ppm = 158.7, 137.8, 128.9, 128.6, 128.5, 90.1, 63.5, 37.3, 36.5, 34.9, 33.8, 33.3, 33.1, 32.7, 26.6, 26.4.

HRMS (ESI): calcd for $C_{18}H_{21}NNaO$ $[M+Na]^+$: 306.1464; found: 306.1464

4.8. Separation of Diastereomers

(*S*,*R*)-3a

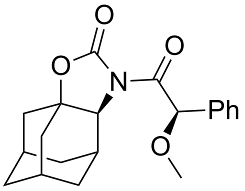

Using GP3, adamantyl oxazolidin-2-one (***rac*-3**) (0.290 g, 1.50 mmol) was esterified and the crude product was purified *via* column chromatography to provide separated diastereomers.

^{1}**H NMR** (400 MHz, $CDCl_3$): δ/ppm = 7.52 – 7.47 (m, 2H), 7.38 – 7.29 (m, 3H), 6.06 (s, 1H), 3.87 (d, *J* = 2.6 Hz, 1H), 3.42 (s, 3H), 3.05 – 2.98 (m, 1H), 2.27 – 2.19 (m, 1H), 2.06 – 1.92 (m, 2H), 1.83 – 1.77 (m, 1H), 1.76 – 1.72 (m, 2H), 1.64 – 1.54 (m, 3H), 1.54 – 1.46 (m, 1H), 1.45 – 1.37 (m, 1H), 1.10 (dq, *J* = 12.2, 2.7 Hz, 1H), 0.97 – 0.88 (m, 1H).

^{13}**C NMR** (101 MHz, $CDCl_3$): δ/ppm = 173.1, 154.6, 137.0, 129.1, 128.8, 128.1, 81.9, 80.0, 66.4, 57.5, 39.5, 38.2, 36.2, 35.6, 30.6, 30.0, 29.3, 28.9.

The NMR spectra are in accordance with those reported in the literature.[18]

(*R*,*R*)-3a

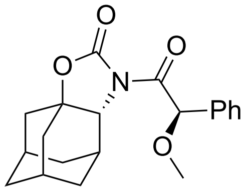

^{1}**H NMR** (400 MHz, $CDCl_3$): δ/ppm = 7.58 – 7.49 (m, 2H), 7.43 – 7.30 (m, 3H), 5.81 (s, 1H), 3.84 (s, 1H), 3.37 (s, 3H), 3.25 (s, 1H), 2.29 (s, 1H), 2.19 (s, 1H), 2.11 (s, 1H), 2.08 – 1.95 (m, 2H), 1.96 – 1.87 (m, 1H), 1.87 – 1.79 (m, 1H), 1.79 – 1.61 (m, 5H).

^{13}**C NMR** (101 MHz, $CDCl_3$): δ/ppm = 172.4, 154.3, 135.5, 129.0, 128.9, 128.5, 81.5, 79.9, 67.4, 57.5, 39.6, 38.5, 36.3, 35.7, 31.0, 30.5, 29.8, 29.1.

The NMR spectra are in accordance with those reported in the literature.[18]

(*S*,*R*)-13a

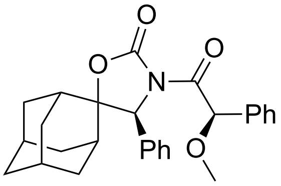

Using GP3, 2-benzyl-2-adamantyl oxazolidinone (0.290 g, 1.50 mmol) was esterified and the crude product was purified *via* column chromatography to provide separated diastereomers.

R

R_f = 0.33 (Hex:EtOAc / 5:1)

^{1}H NMR (400 MHz, $CDCl_3$): δ/ppm = 7.53 – 7.44 (m, 2H), 7.40 – 7.28 (m, 8H), 6.06 (s, 1H), 5.17 (s, 1H), 3.22 (s, 3H), 2.15 – 2.02 (m, 2H), 1.92 – 1.83 (m, 1H), 1.83 – 1.74 (m, 3H), 1.72 – 1.57 (m, 3H), 1.55 – 1.42 (m, 3H), 1.39 – 1.29 (m, 2H).

^{13}C NMR (101 MHz, $CDCl_3$): δ/ppm = 170.9, 152.8, 136.0, 135.3, 129.1, 128.8, 128.7, 128.6, 128.4, 128.4, 89.2, 80.8, 65.2, 57.2, 37.0, 36.2, 35.0, 33.4, 33.1, 32.5, 31.8, 26.4, 26.1.

HRMS (ESI): calcd for $C_{27}H_{29}NNaO_4$ $[M+Na]^+$: 454.1989; found: 454.1991

(*R*,*R*)-13a

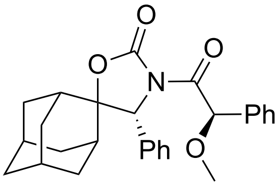

R_f = 0.25 (Hex:EtOAc / 5:1)

^{1}H NMR (400 MHz, $CDCl_3$): δ/ppm = 7.29 – 7.07 (m, 8H), 6.93 (s, 1H), 6.00 (s, 1H), 5.38 (s, 1H), 3.34 (s, 3H), 2.28 (dt, *J* = 13.4, 2.9 Hz, 1H), 2.14 – 2.00 (m, 3H), 2.00 – 1.90 (m, 1H), 1.88 – 1.77 (m, 2H), 1.76 – 1.66 (m, 2H), 1.66 – 1.58 (m, 2H), 1.47 (dq, *J* = 12.9, 2.7 Hz, 1H), 1.35 – 1.23 (m, 3H).

^{13}C NMR (101 MHz, $CDCl_3$): δ/ppm = 170.0, 152.3, 134.6, 134.1, 129.0, 128.8, 128.5, 128.4, 128.1, 88.6, 81.5, 64.6, 57.3, 37.1, 36.8, 34.9, 33.4, 33.1, 32.7, 32.1, 31.7, 26.5, 26.2, 22.8, 14.2.

HRMS (ESI): calcd for $C_{27}H_{29}NNaO_4$ $[M+Na]^+$: 454.1989; found: 454.1991

4.9. Cleavage of the Auxiliary

(*S*)-Adamantyl oxazolidinone ((*S*)-3)

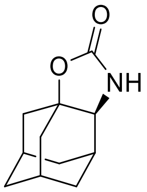

Using GP4, **(*S*,*R*)-3a** (0.117 g 0.343 mmol) was cleaved with LiOH to provide (*S*)-adamantyl oxazolidinone (**(*S*)-3**) (0.066 g, 0.342 mmol, 99%) as a colorless solid. The product was directly used in the next step without further purification.

(*R*)-2-Benzyl-2-adamantyl oxazolidinone ((*R*)-13)

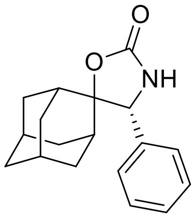

Using GP4, **(*R*,*R*)-13a** (0.127 g, 0.290 mmol) was cleaved with 30% H_2O_2 and LiOH to provide (*R*)-2-benzyl-2-adamantyl oxazolidinone (**(*R*)-13**) (0.071 g, 0.249 mmol, 86%) as a colorless solid with 91% *ee*.

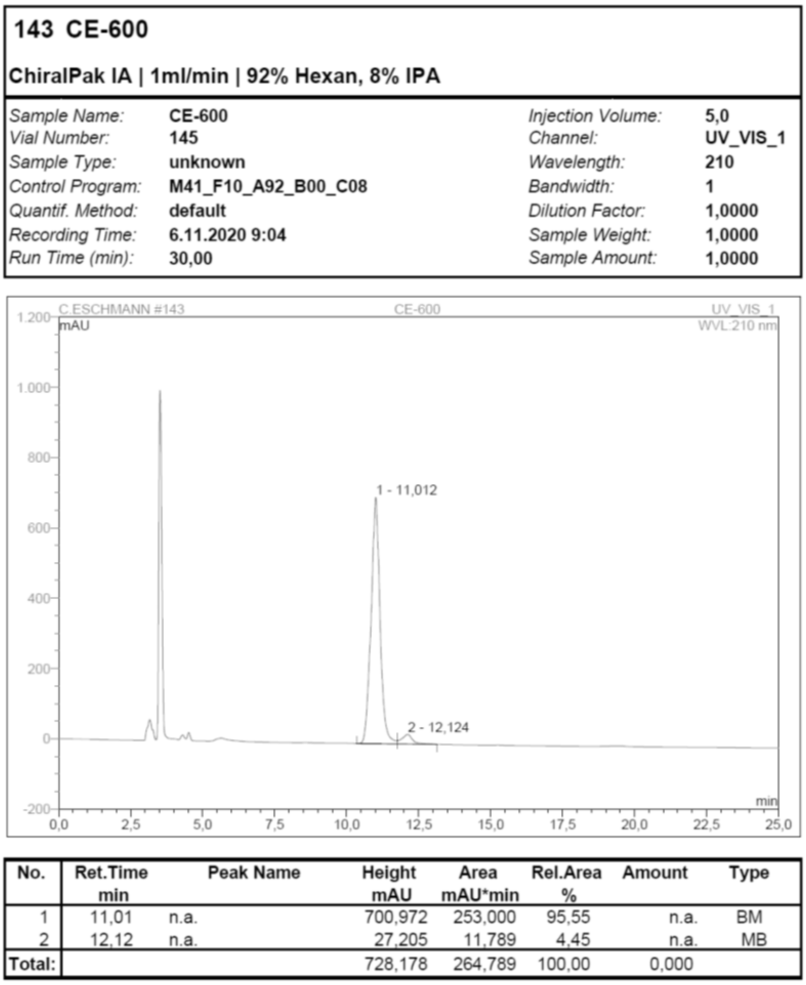

143 CE-600

ChiralPak IA | 1ml/min | 92% Hexan, 8% IPA

Sample Name:	**CE-600**	*Injection Volume:*	**5,0**
Vial Number:	**145**	*Channel:*	**UV_VIS_1**
Sample Type:	**unknown**	*Wavelength:*	**210**
Control Program:	**M41_F10_A92_B00_C08**	*Bandwidth:*	**1**
Quantif. Method:	**default**	*Dilution Factor:*	**1,0000**
Recording Time:	**6.11.2020 9:04**	*Sample Weight:*	**1,0000**
Run Time (min):	**30,00**	*Sample Amount:*	**1,0000**

No.	Ret.Time min	Peak Name	Height mAU	Area mAU*min	Rel.Area %	Amount	Type
1	11,01	n.a.	700,972	253,000	95,55	n.a.	BM
2	12,12	n.a.	27,205	11,789	4,45	n.a.	MB
Total:			728,178	264,789	100,00	0,000	

(*S*)-2-Benzyl-2-adamantyl oxazolidinone ((*S*)-13)

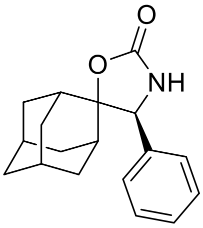

Using GP4, **(*S*,*R*)-13a** (0.067 g, 0.23 mmol) was cleaved with 30% H_2O_2 and LiOH to provide (*S*)-2-benzyl-2-adamantyl oxazolidinone (**(*S*)-13**) (0.037 g, 0.193 mmol, 84%) as a colorless solid with 61% *ee*.

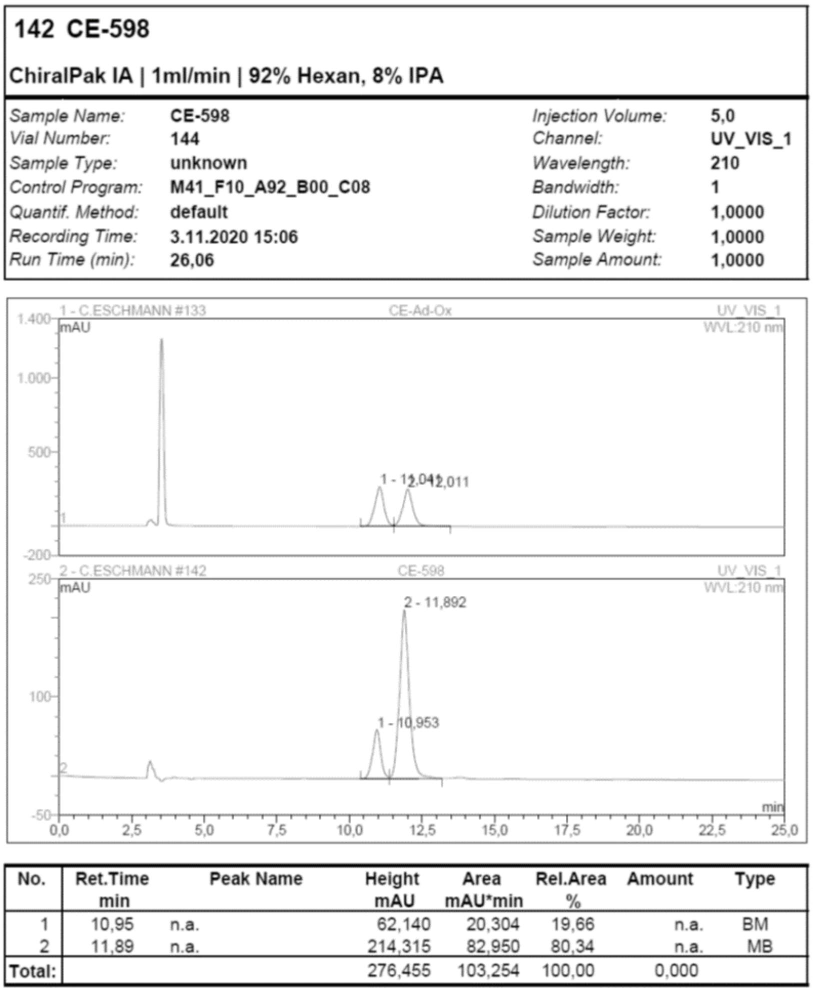

142 CE-598

ChiralPak IA | 1ml/min | 92% Hexan, 8% IPA

Sample Name:	CE-598	*Injection Volume:*	5,0
Vial Number:	144	*Channel:*	UV_VIS_1
Sample Type:	unknown	*Wavelength:*	210
Control Program:	M41_F10_A92_B00_C08	*Bandwidth:*	1
Quantif. Method:	default	*Dilution Factor:*	1,0000
Recording Time:	3.11.2020 15:06	*Sample Weight:*	1,0000
Run Time (min):	26,06	*Sample Amount:*	1,0000

No.	Ret.Time min	Peak Name	Height mAU	Area mAU*min	Rel.Area %	Amount	Type
1	10,95	n.a.	62,140	20,304	19,66	n.a.	BM
2	11,89	n.a.	214,315	82,950	80,34	n.a.	MB
Total:			276,455	103,254	100,00	0,000	

4.10. Synthesis of Aminoalcohols

2-Aminoadamantan-1-ol (*rac*-4)

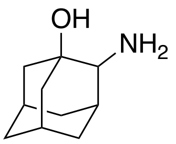

Adamantyl oxazolidine-2-on (***rac*-3**) (0.543 g, 2.81 mmol, 1.00 equiv.) was refluxed in 30 mL 5 M KOH solution for 24 h. The aqueous phase was extracted with 50 mL CH_2Cl_2 (3×). The combined organic layers were dried over Na_2SO_4, filtered, and the solvent was removed under reduced pressure to afford the product (***rac*-4**) (0.446 g, 2.67 mmol, 95%) as a colorless solid.

$\boldsymbol{R_f}$ = 0.05 (Hex/EtOAc 2:1)

^{1}H NMR (400 MHz, $CDCl_3$): δ/ppm = 2.76 (s, 1H), 2.16 – 1.39 (m, 16H).

^{13}C NMR (101 MHz, $CDCl_3$): δ/ppm = 69.1 (Cq), 60.4 (CH), 44.3 (CH_2), 39.1 (CH_2), 37.4 (CH_2), 37.3 (CH_2), 36.6 (CH_2), 30.9 (CH), 30.1 (CH), 29.6 (CH).

HRMS (ESI): calcd for $C_{10}H_{18}NO$ $[M+H]^+$: 168.1383; found: 168.1389

The NMR spectra are in accordance with those reported in the literature.[15]

N-Benzyl-2-aminoadamantan-1-ol (*rac*-4a)

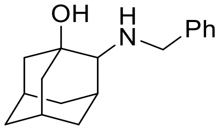

A solution of 2-aminoadamantan-1-ol (***rac*-4a**) (167 mg, 1.00 equiv., 1.00 mmol) and benzaldehyde (0.111 mL, 106 mg, 1.20 equiv., 1.20 mmol) in 10 mL CH_2Cl_2 was stirred at r.t. for 24 h. The solvent was removed under reduced pressure and 10 mL MeOH and $NaBH_4$ (75.6 mg, 2.00 equiv., 2.00 mmol) were added. The solution was stirred at r.t. for further 24 h. The reaction was quenched with 10 mL sat. aq. $NaHCO_3$ solution and MeOH was removed under reduced pressure. The aqueous phase was extracted with 10 mL CH_2Cl_2 (3×) and the combined organic layers were dried over Na_2SO_4, filtered, and the solvent was removed under reduced pressure. After column chromatography (silica, Hex/EtOAc = 2/1) the product (***rac*-4a**) (150 mg, 0.580 mmol, 58%) was obtained as a colorless solid.

^{1}H NMR (400 MHz, $CDCl_3$): δ/ppm = 7.41 – 7.24 (m, 5H), 3.98 (d, 1 H, *J* = 12.8 Hz), 3.74 (d, 1H, *J* = 12.9 Hz), 2.67 (s, 1H), 2.25 – 1.43 (m, 14H).

^{13}C NMR (101 MHz, $CDCl_3$): δ/ppm = 128.7 (CH), 128.5 (CH), 127.4 (CH), 68.5 (Cq), 66.8 (CH), 51.8 (CH_2), 44.3 (CH_2), 40.3 (CH_2), 37.1 (CH_2), 37.3 (CH_2), 36.5 (CH_2), 31.5 (CH), 30.4 (CH), 30.0 (CH_2), 29.7 (CH).

HRMS (ESI): calcd for $C_{17}H_{24}NO$ $[M+H]^+$: 258.1852; found: 258.1853

N-Methyl-2-aminoadamantan-1-ol ((*S*)-4b)

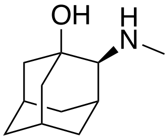

Using GP5, (*S*)-adamantyl oxazolidin-2-on (**(S)-3**) (0.068 g, 0.350 mmol) was reduced to obtain (**(S)-4b**) (0.048g, 0.265 mmol, 76%) as a colorless solid.

^{1}H NMR (400 MHz, $CDCl_3$): δ/ppm = 2.43 (s, 4H), 2.21 – 2.16 (m, 1H), 2.13 – 2.06 (m, 1H), 2.02 – 1.96 (m, 1H), 1.85 – 1.71 (m, 3H), 1.71 – 1.54 (m, 5H), 1.54 – 1.39 (m, 2H).

^{13}C NMR (101 MHz, $CDCl_3$): δ/ppm = 77.4, 69.0, 68.6, 44.4, 40.2, 37.1, 36.6, 34.6, 30.7, 30.5, 29.9, 29.7.

HRMS (ESI): calcd for $C_{11}H_{20}NO$ $[M+H]^+$: 182.1545; found: 182.1551

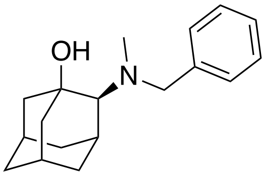

Enantiomeric excess was determined by investigation of the benzylated amino alcohol *via* HPLC employing a ChiralPak IA column.

^{1}H NMR (400 MHz, $CDCl_3$): δ/ppm = 7.36 – 7.29 (m, 4H), 7.28 – 7.21 (m, 1H), 3.83 (s, 2H), 3.52 (brs, 1H), 2.70 (s, 1H), 2.37 (s, 3H), 2.35 – 2.29 (m, 1H), 2.23 – 2.09 (m, 3H), 2.05 – 1.97 (m, 1H), 1.86 – 1.58 (m, 8H), 1.50 (dq, J = 13.2, 2.5 Hz, 1H).

^{13}C NMR (101 MHz, $CDCl_3$): δ/ppm = 140.3, 128.7, 128.5, 127.1, 72.1, 69.6, 62.6, 46.7, 40.9, 40.7, 39.4, 37.1, 32.3, 30.9, 30.8, 30.3.

HRMS (ESI): calcd for $C_{18}H_{26}NO$ $[M+H]^+$: 272.2009; found: 272.2011

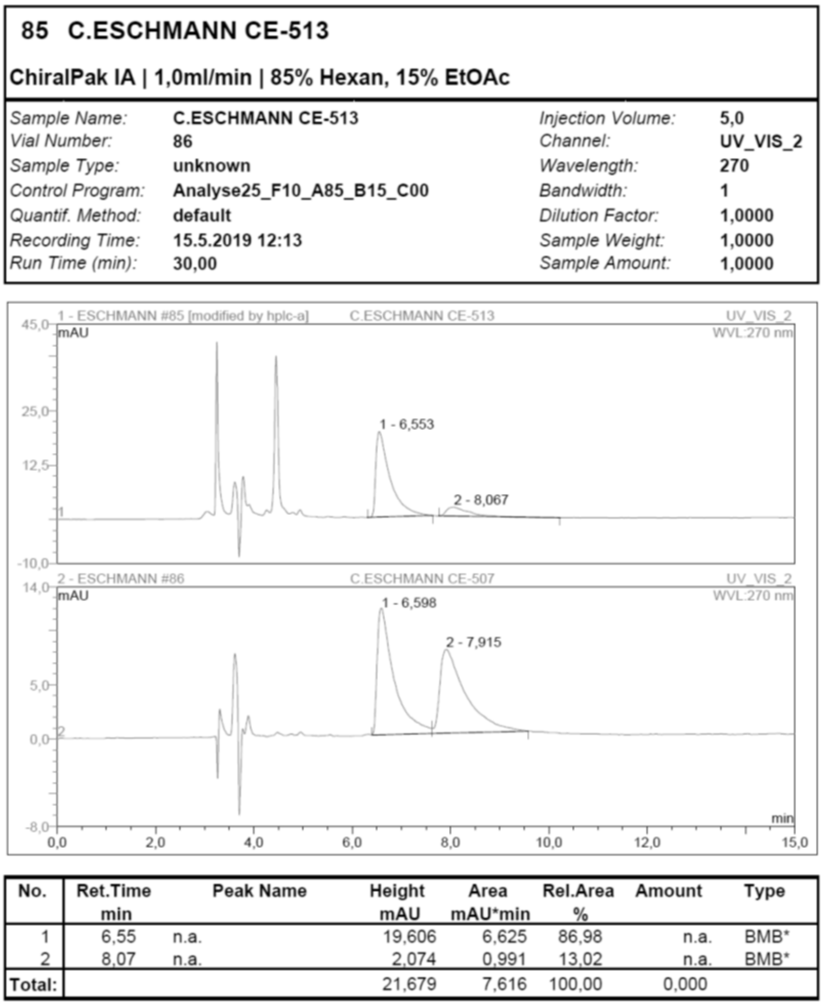

85 C.ESCHMANN CE-513

ChiralPak IA | 1,0ml/min | 85% Hexan, 15% EtOAc

Sample Name:	**C.ESCHMANN CE-513**	*Injection Volume:*	**5,0**
Vial Number:	**86**	*Channel:*	**UV_VIS_2**
Sample Type:	**unknown**	*Wavelength:*	**270**
Control Program:	**Analyse25_F10_A85_B15_C00**	*Bandwidth:*	**1**
Quantif. Method:	**default**	*Dilution Factor:*	**1,0000**
Recording Time:	**15.5.2019 12:13**	*Sample Weight:*	**1,0000**
Run Time (min):	**30,00**	*Sample Amount:*	**1,0000**

No.	Ret.Time min	Peak Name	Height mAU	Area mAU*min	Rel.Area %	Amount	Type
1	6,55	n.a.	19,606	6,625	86,98	n.a.	BMB*
2	8,07	n.a.	2,074	0,991	13,02	n.a.	BMB*
Total:			21,679	7,616	100,00	0,000	

***rac*-14a**

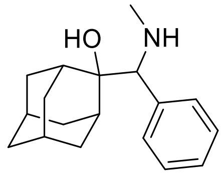

Using GP5, (*S*)-adamantyl oxazolidin-2-on (***rac*-13**) (0.020 g, 0.071 mmol) was reduced to obtain (***rac*-14a**) (0.013g, 0.048 mmol, 67%) as a colorless solid.

^{1}H NMR (400 MHz, MeOH-d$_4$): δ/ppm = 7.52 – 7.39 (m, 2H), 7.38 – 7.22 (m, 3H), 4.20 (s, 1H), 2.33 – 2.23 (m, 3H), 2.17 (s, 3H), 2.15 – 2.03 (m, 3H), 1.93 – 1.81 (m, 2H), 1.80 – 1.68 (m, 3H), 1.67 – 1.46 (m, 1H), 1.40 (s, 2H), 1.17 (s, 1H).

^{13}C NMR (101 MHz, MeOH-d$_4$): δ/ppm = 130.5, 129.1, 128.5, 77.7, 67.6, 39.4, 36.0, 35.3, 35.3, 34.7, 34.2, 34.1, 33.8, 28.6, 28.6.

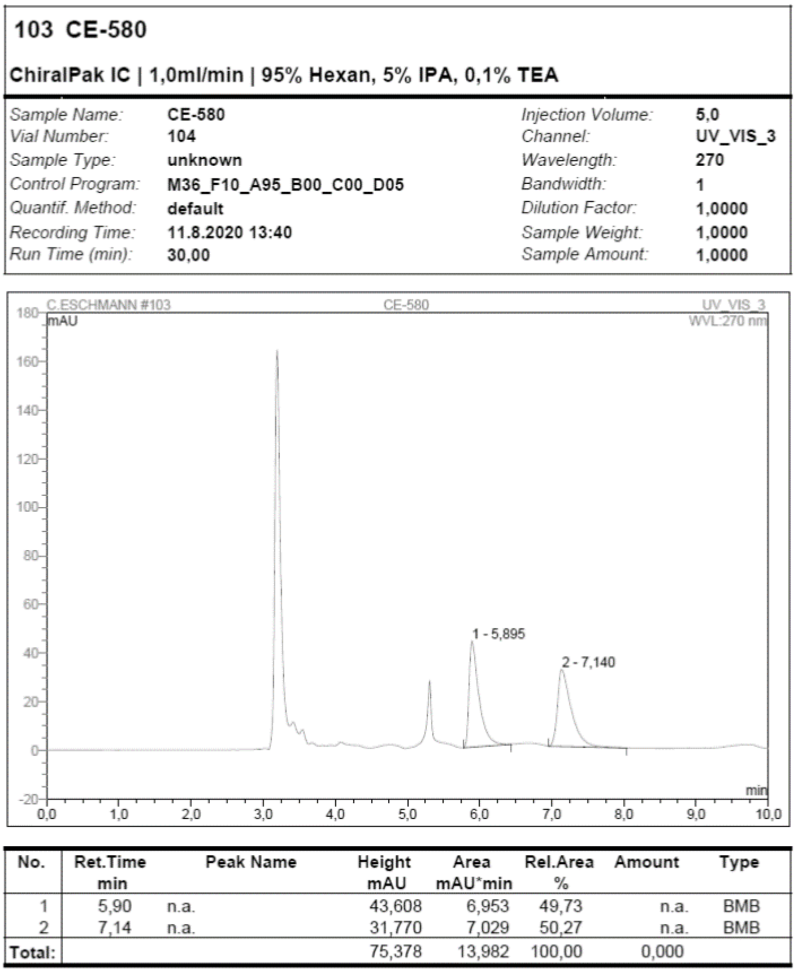

103 CE-580

ChiralPak IC | 1,0ml/min | 95% Hexan, 5% IPA, 0,1% TEA

Sample Name:	**CE-580**	*Injection Volume:*	**5,0**
Vial Number:	**104**	*Channel:*	**UV_VIS_3**
Sample Type:	**unknown**	*Wavelength:*	**270**
Control Program:	**M36_F10_A95_B00_C00_D05**	*Bandwidth:*	**1**
Quantif. Method:	**default**	*Dilution Factor:*	**1,0000**
Recording Time:	**11.8.2020 13:40**	*Sample Weight:*	**1,0000**
Run Time (min):	**30,00**	*Sample Amount:*	**1,0000**

No.	Ret.Time min	Peak Name	Height mAU	Area mAU*min	Rel.Area %	Amount	Type
1	5,90	n.a.	43,608	6,953	49,73	n.a.	BMB
2	7,14	n.a.	31,770	7,029	50,27	n.a.	BMB
Total:			75,378	13,982	100,00	0,000	

5. Computational Data

(*R*)-4

C	2.35163	-0.52214	0.00187
C	2.84734	0.90446	0.27251
C	1.64109	1.86753	0.28282
C	0.87844	1.80634	-1.05826
C	0.38418	0.35479	-1.32087
C	1.66956	-0.47748	-1.37591
C	1.40790	-0.90427	1.15966
C	0.66753	1.44882	1.39925
C	-0.59243	-0.10581	-0.19429
C	0.16478	-0.00618	1.16310
C	-1.42805	-1.41412	-0.47434
N	-2.66845	-1.07638	0.16683
C	-2.83310	0.27014	0.18404
O	-1.66561	0.88904	-0.14317
C	-0.94223	-2.81226	-0.09947
C	-1.50492	-3.60247	0.91353
C	-0.89355	-4.79862	1.32638
C	0.31884	-5.19379	0.77244
C	0.83099	-4.48545	-0.30094
C	0.13848	-3.37781	-0.78896
O	-3.87753	0.85597	0.44010
H	3.19474	-1.22124	-0.02665
H	3.57084	1.19810	-0.49789
H	3.37705	0.93771	1.23239
H	2.00244	2.88664	0.45586
H	1.53459	2.13192	-1.87355
H	0.03514	2.50813	-1.04498
H	-0.13028	0.34293	-2.29046
H	2.36002	-0.02620	-2.10388
H	1.50936	-1.46008	-1.78583
H	1.93805	-0.78679	2.11471
H	1.14079	-1.95641	1.12807
H	-0.17210	2.15263	1.44050
H	1.17415	1.51542	2.36988
H	-0.50084	-0.26613	1.99627
H	-1.68459	-1.44624	-1.54062
H	-3.49828	-1.65148	0.16443
H	-2.43141	-3.31493	1.40803
H	-1.35418	-5.40845	2.09890
H	0.84674	-6.06410	1.15513
H	1.76959	-4.78595	-0.76212
H	0.48912	-2.93931	-1.71087

(*R*)-6

H	-4.40758	-2.16530	-2.16255
C	-4.64585	-1.85947	-1.13664
C	-4.74606	-2.54873	1.26744
C	-4.23250	-0.14264	0.65905
C	-3.95394	-1.28595	1.65312
C	-3.84554	-0.58500	-0.76219
C	-4.32878	-3.00410	-0.14447
H	-5.82314	-2.34119	1.28680
H	-5.29611	0.12487	0.67442
H	-5.71980	-1.64221	-1.10543
H	-4.55490	-3.34705	1.99566
H	-3.66881	0.75008	0.94646
H	-4.22715	-0.96924	2.66643
H	-4.05946	0.21426	-1.48097
H	-4.89720	-3.89636	-0.42998
C	-2.45253	-1.60444	1.60201
H	-2.18859	-2.39562	2.31335
H	-1.87018	-0.71544	1.86362
C	-2.81318	-3.35636	-0.15319
H	-2.60309	-4.14237	0.58122
H	-2.50585	-3.72253	-1.13933
C	-2.37913	-1.02255	-0.87569
H	-2.27349	-1.49014	-1.86992
C	-2.06215	-2.07700	0.18961
O	-0.60713	-2.15830	0.14691
N	-1.24484	-0.09723	-0.72002
B	-0.17303	-0.89394	-0.24327
C	1.34082	-0.51355	-0.12904
C	4.10091	0.08940	0.08717
C	1.78273	0.80687	0.04272
C	2.31141	-1.52853	-0.17675
C	3.67080	-1.22919	-0.07495
C	3.14488	1.10182	0.14997
H	1.06595	1.61732	0.11132
H	1.99539	-2.55975	-0.29087
H	5.15544	0.32034	0.16823
H	3.44624	2.08061	0.27713
H	4.36579	-1.99076	-0.12000
H	-1.47154	0.63559	-0.04773

(*R*)-13

C	2.35163	-0.52214	0.00187
C	2.84734	0.90446	0.27251
C	1.64109	1.86753	0.28282
C	0.87844	1.80634	-1.05826
C	0.38418	0.35479	-1.32087
C	1.66956	-0.47748	-1.37591
C	1.40790	-0.90427	1.15966
C	0.66753	1.44882	1.39925
C	-0.59243	-0.10581	-0.19429
C	0.16478	-0.00618	1.16310
C	-1.42805	-1.41412	-0.47434
N	-2.66845	-1.07638	0.16683
C	-2.83310	0.27014	0.18404
O	-1.66561	0.88904	-0.14317

C	-0.94223	-2.81226	-0.09947
C	-1.50492	-3.60247	0.91353
C	-0.89355	-4.79862	1.32638
C	0.31884	-5.19379	0.77244
C	0.83099	-4.48545	-0.30094
C	0.13848	-3.37781	-0.78896
O	-3.87753	0.85597	0.44010
H	3.19474	-1.22124	-0.02665
H	3.57084	1.19810	-0.49789
H	3.37705	0.93771	1.23239
H	2.00244	2.88664	0.45586
H	1.53459	2.13192	-1.87355
H	0.03514	2.50813	-1.04498
H	-0.13028	0.34293	-2.29046
H	2.36002	-0.02620	-2.10388
H	1.50936	-1.46008	-1.78583
H	1.93805	-0.78679	2.11471
H	1.14079	-1.95641	1.12807
H	-0.17210	2.15263	1.44050
H	1.17415	1.51542	2.36988
H	-0.50084	-0.26613	1.99627
H	-1.68459	-1.44624	-1.54062
H	-3.49828	-1.65148	0.16443
H	-2.43141	-3.31493	1.40803
H	-1.35418	-5.40845	2.09890
H	0.84674	-6.06410	1.15513
H	1.76959	-4.78595	-0.76212
H	0.48912	-2.93931	-1.71087

(*R*)-14a

C	3.56415	-2.41836	-2.67787
C	4.19914	-3.81200	-2.58120
C	3.10770	-4.84551	-2.24219
C	2.05460	-4.84472	-3.36152
C	1.38267	-3.45170	-3.46689
C	2.50620	-2.44672	-3.79927
C	2.42834	-4.46879	-0.90999
C	2.94976	-2.10574	-1.30542
C	0.65549	-3.03464	-2.13729
C	1.77040	-3.05717	-1.01593
C	-0.15459	-1.60591	-2.35674
N	0.42480	-0.53684	-1.50596
O	-0.28864	-4.05556	-1.78186
C	-1.71264	-1.49186	-2.32742
C	-2.61475	-2.55953	-2.25114
C	-4.00764	-2.36252	-2.23093
C	-4.54637	-1.08557	-2.31411
C	-3.69230	-0.00283	-2.43249
C	-2.30689	-0.20841	-2.44921
C	1.00349	0.57869	-2.24165
H	4.33213	-1.67344	-2.91291
H	4.97878	-3.81571	-1.80932
H	4.69009	-4.06618	-3.52828
H	3.56670	-5.83685	-2.16115
H	1.31551	-5.63400	-3.19062
H	2.53643	-5.09198	-4.31697
H	0.65302	-3.49349	-4.28490
H	2.10442	-1.45058	-3.98283
H	2.98666	-2.73892	-4.74198
H	3.17769	-4.46589	-0.10735
H	1.70154	-5.23531	-0.62316
H	2.68519	-1.05725	-1.22991
H	3.71281	-2.23148	-0.52408
H	1.31607	-2.82774	-0.04380
H	0.04185	-1.34264	-3.40509
H	-0.27758	-0.21526	-0.83792
H	0.13606	-4.92524	-1.74442
H	-2.29138	-3.59143	-2.20709
H	-4.66932	-3.22186	-2.15083
H	-5.62215	-0.93848	-2.29700
H	-4.09198	1.00451	-2.51471
H	-1.69527	0.67959	-2.55783
H	1.88073	0.27868	-2.82321
H	1.35516	1.33224	-1.53038
H	0.30680	1.06580	-2.92605

6. Spectra

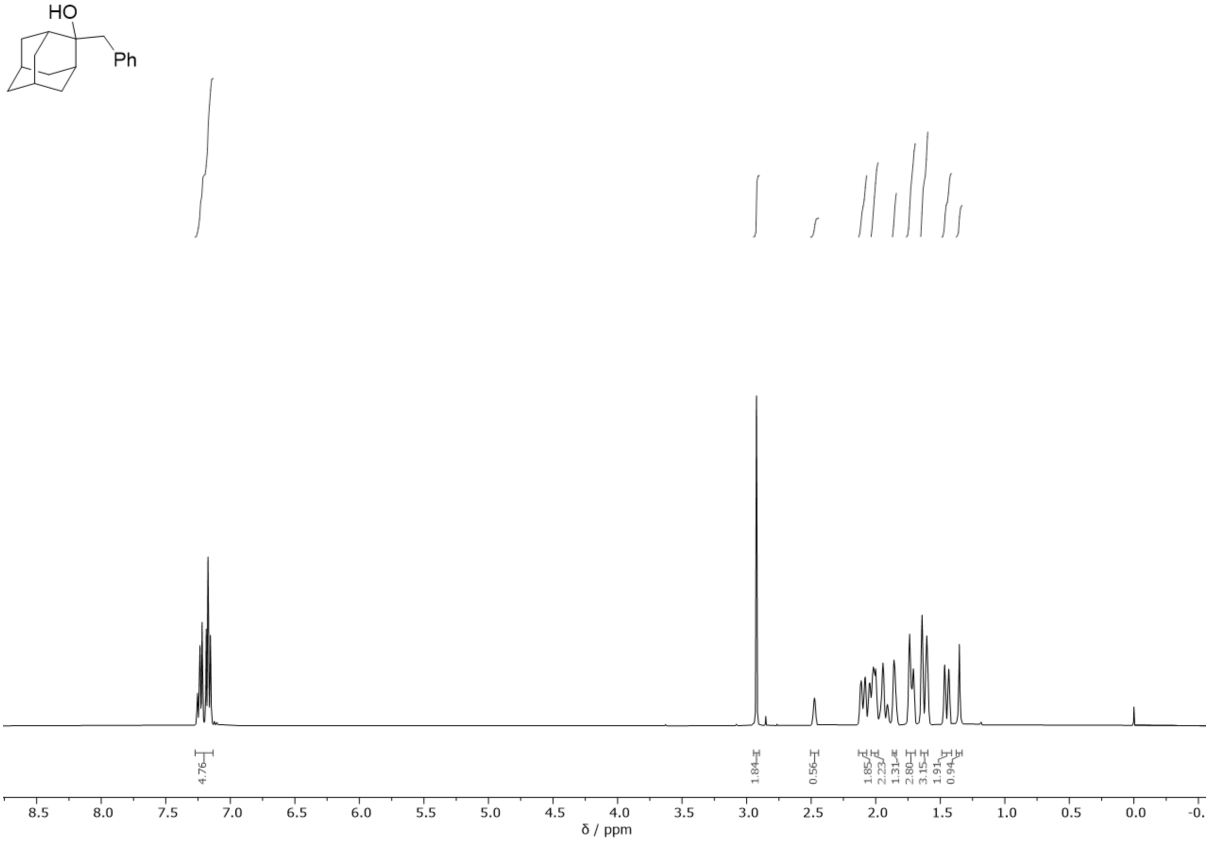
HO
Ph
4.76
1.84
0.56
1.85
2.23
1.31
2.80
3.15
1.91
0.94
8.5 8.0 7.5 7.0 6.5 6.0 5.5 5.0 4.5 4.0 3.5 3.0 2.5 2.0 1.5 1.0 0.5 0.0 -0.
δ / ppm

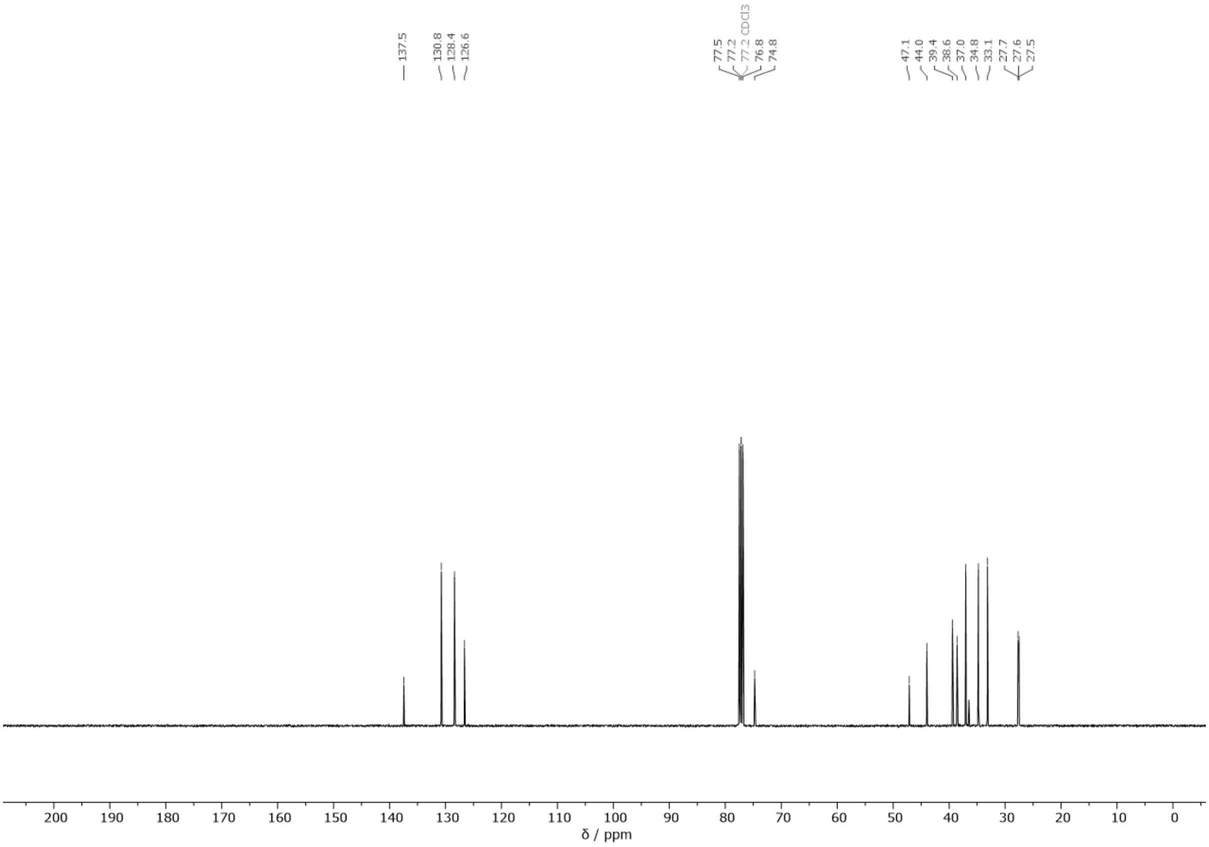
137.5
130.8
128.4
126.6
77.5
77.2
77.2 CDCl3
76.8
74.8
47.1
44.0
39.4
38.6
37.0
34.8
33.1
27.7
27.6
27.5
200 190 180 170 160 150 140 130 120 110 100 90 80 70 60 50 40 30 20 10 0
δ / ppm

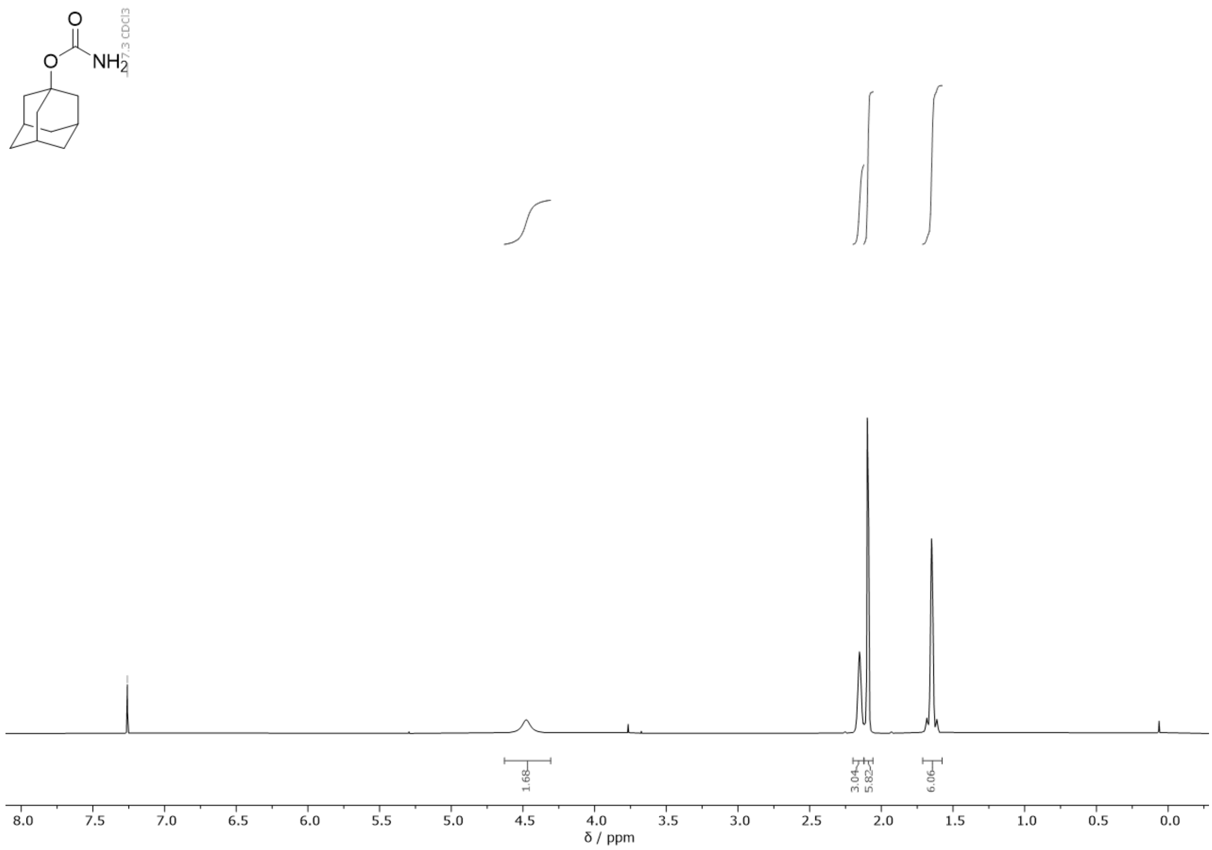
O
O
NH2
7.3 CDCl3
1.68
3.04
5.82
6.06
8.0
7.5
7.0
6.5
6.0
5.5
5.0
4.5
4.0
3.5
3.0
2.5
2.0
1.5
1.0
0.5
0.0
δ / ppm

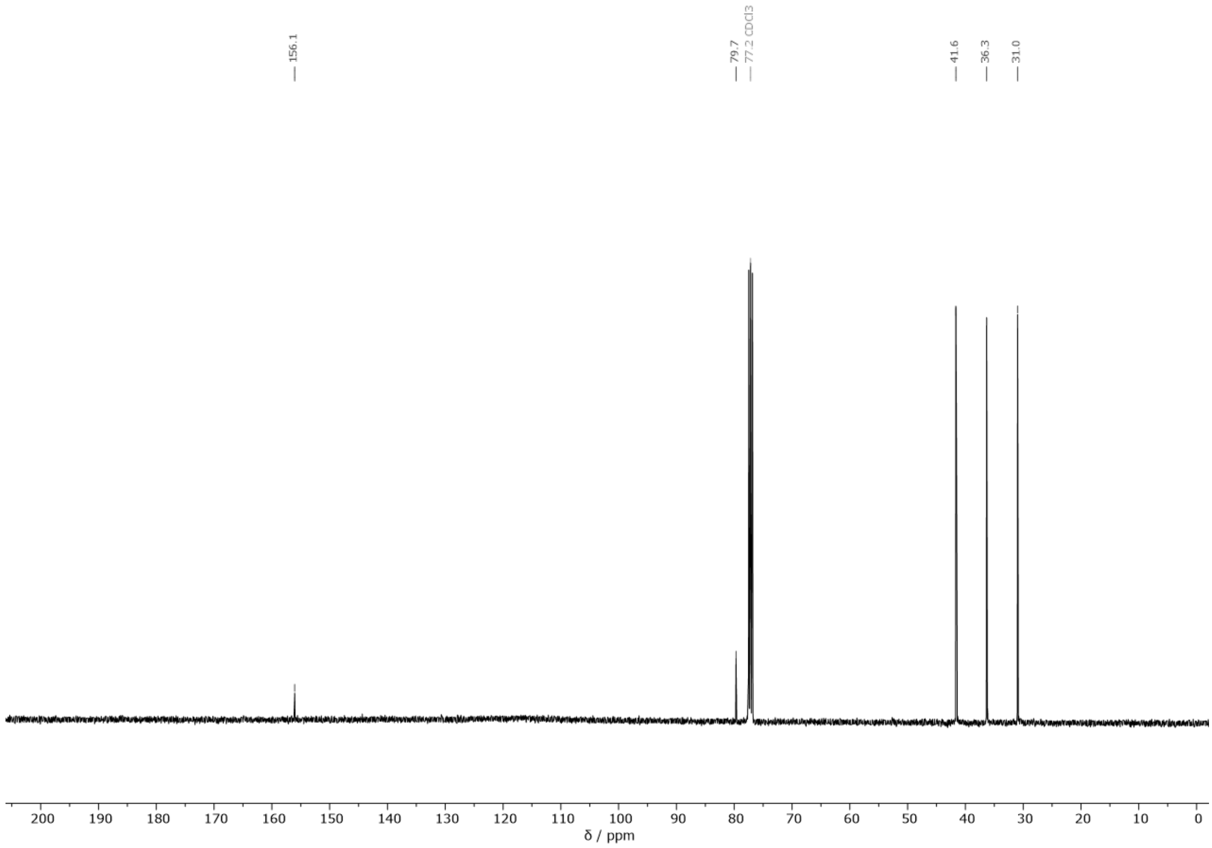
156.1
79.7
77.2 CDCl3
41.6
36.3
31.0
200
190
180
170
160
150
140
130
120
110
100
90
80
70
60
50
40
30
20
10
0
δ / ppm

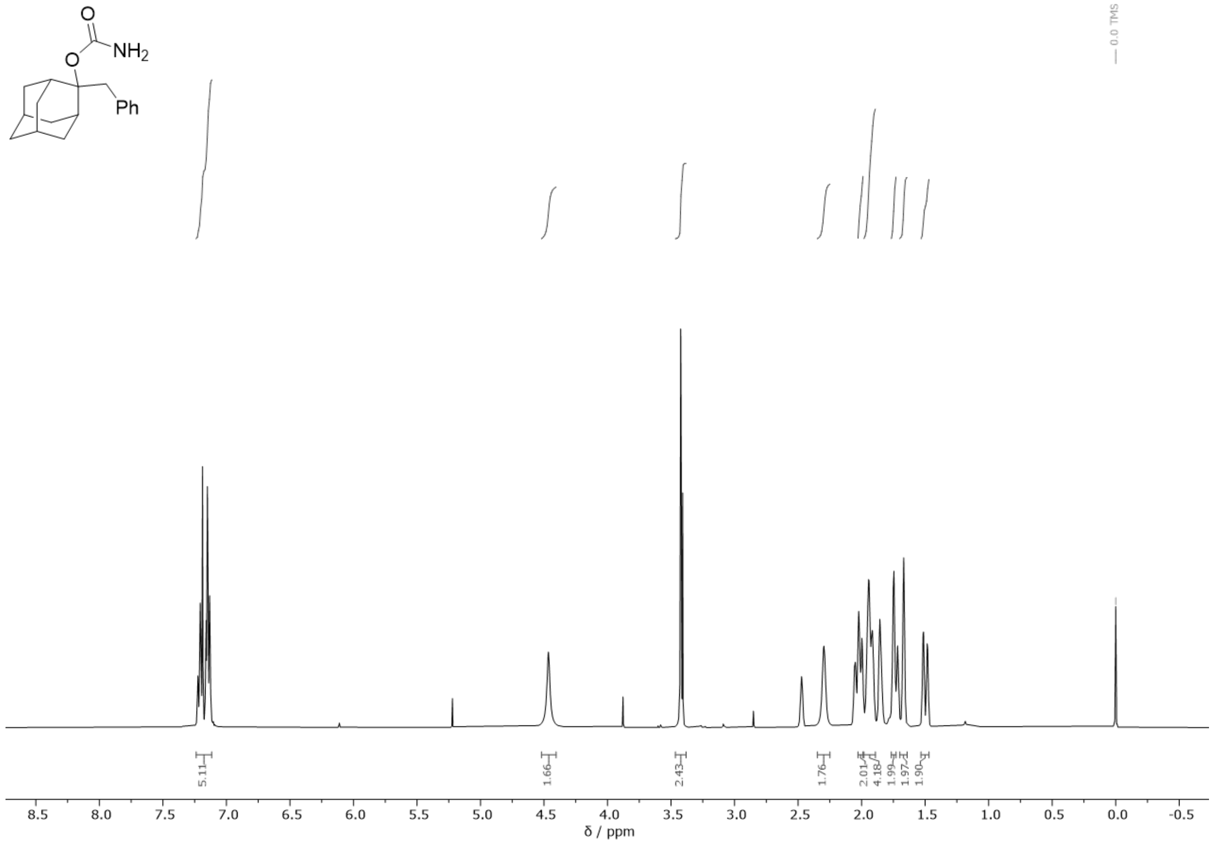
O
O
NH2
Ph
0.0 TMS
5.11
1.66
2.43
1.76
2.01
4.18
1.99
1.97
1.90
8.5
8.0
7.5
7.0
6.5
6.0
5.5
5.0
4.5
4.0
3.5
3.0
2.5
2.0
1.5
1.0
0.5
0.0
-0.5
δ / ppm

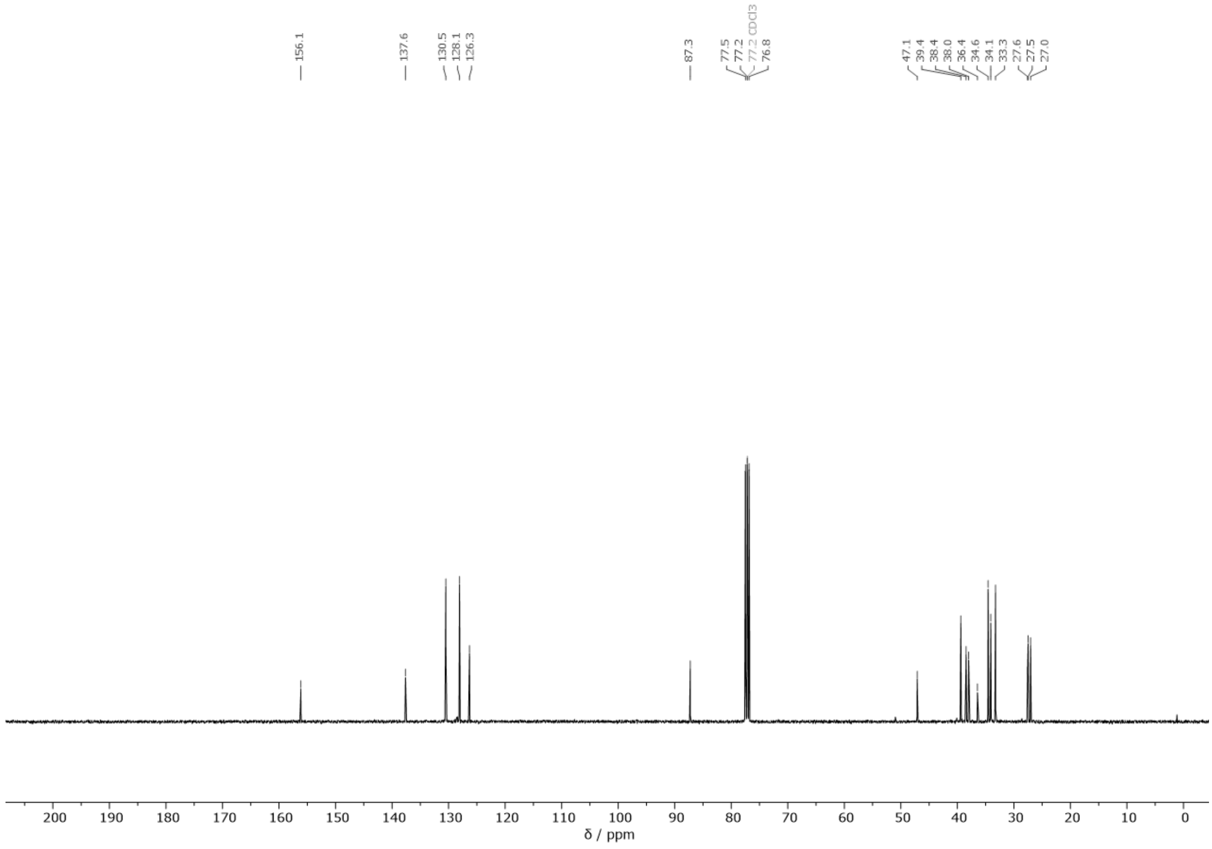
156.1
137.6
130.5
128.1
126.3
87.3
77.5
77.2
77.2 CDCl3
76.8
47.1
39.4
38.4
38.0
36.4
34.6
34.1
33.3
27.6
27.5
27.0
200
190
180
170
160
150
140
130
120
110
100
90
80
70
60
50
40
30
20
10
0
δ / ppm

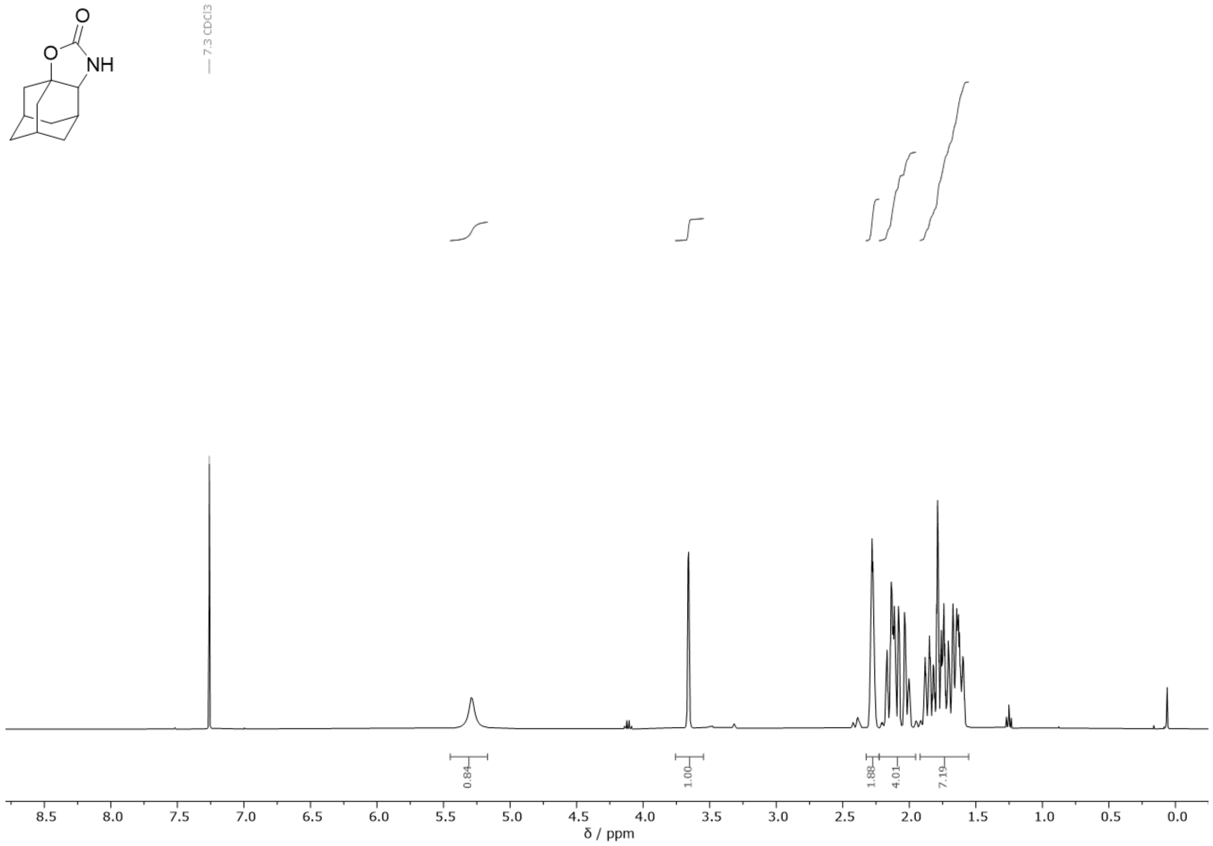
O
O
NH
7.3 CDCl3
0.84
1.00
1.88
4.01
7.19
8.5
8.0
7.5
7.0
6.5
6.0
5.5
5.0
4.5
4.0
3.5
3.0
2.5
2.0
1.5
1.0
0.5
0.0
δ / ppm

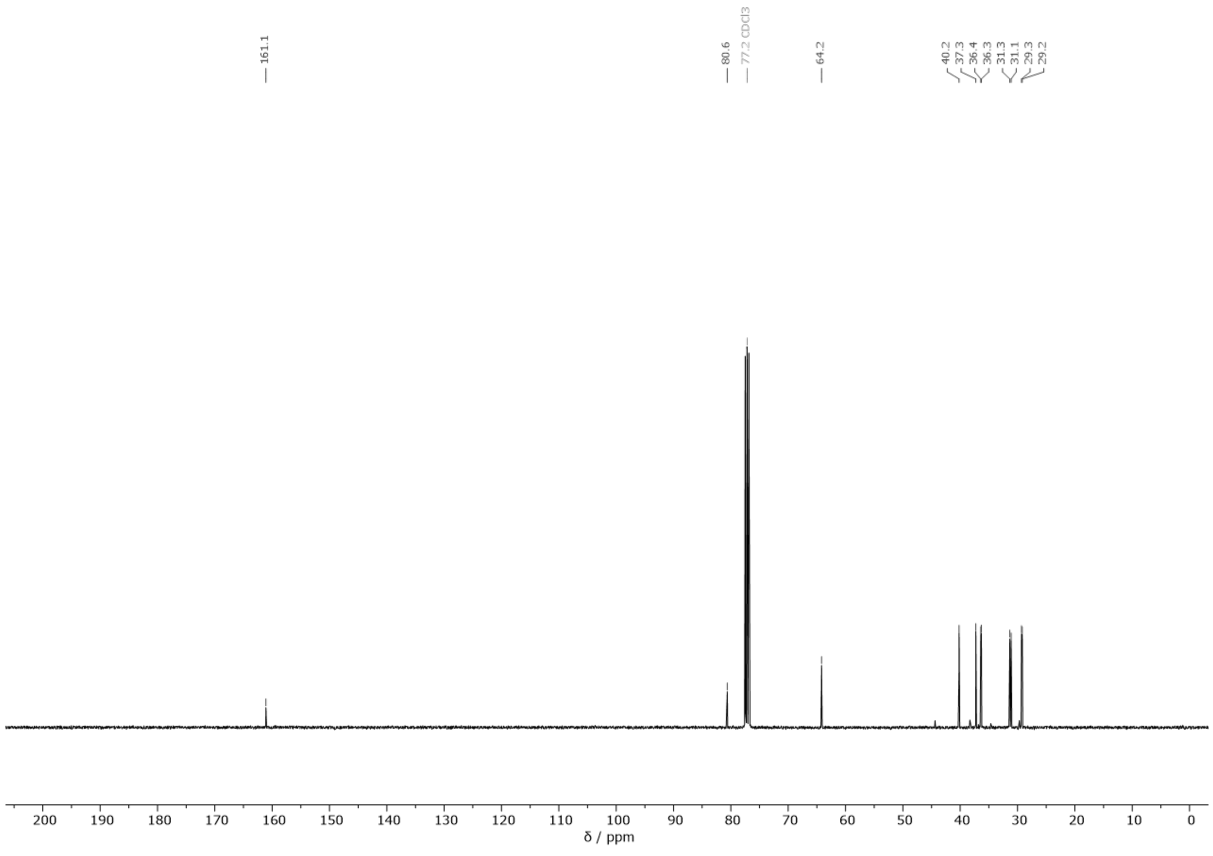
161.1
80.6
77.2 CDCl3
64.2
40.2
37.3
36.4
36.3
31.3
31.1
29.3
29.2
200
190
180
170
160
150
140
130
120
110
100
90
80
70
60
50
40
30
20
10
0
δ / ppm

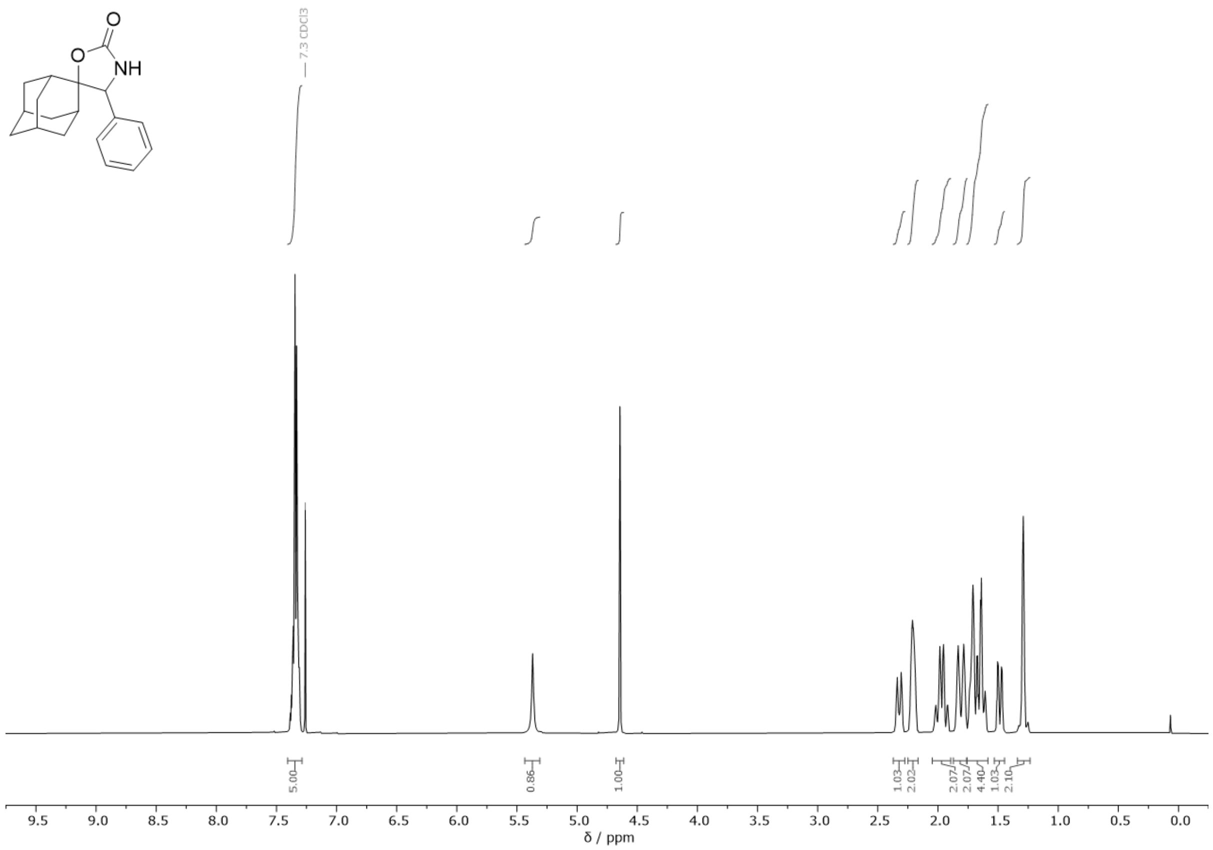
O
O
NH
7.3 CDCl3
5.00
0.86
1.00
1.03
2.02
2.07
2.07
4.40
1.03
2.10
9.5 9.0 8.5 8.0 7.5 7.0 6.5 6.0 5.5 5.0 4.5 4.0 3.5 3.0 2.5 2.0 1.5 1.0 0.5 0.0
δ / ppm

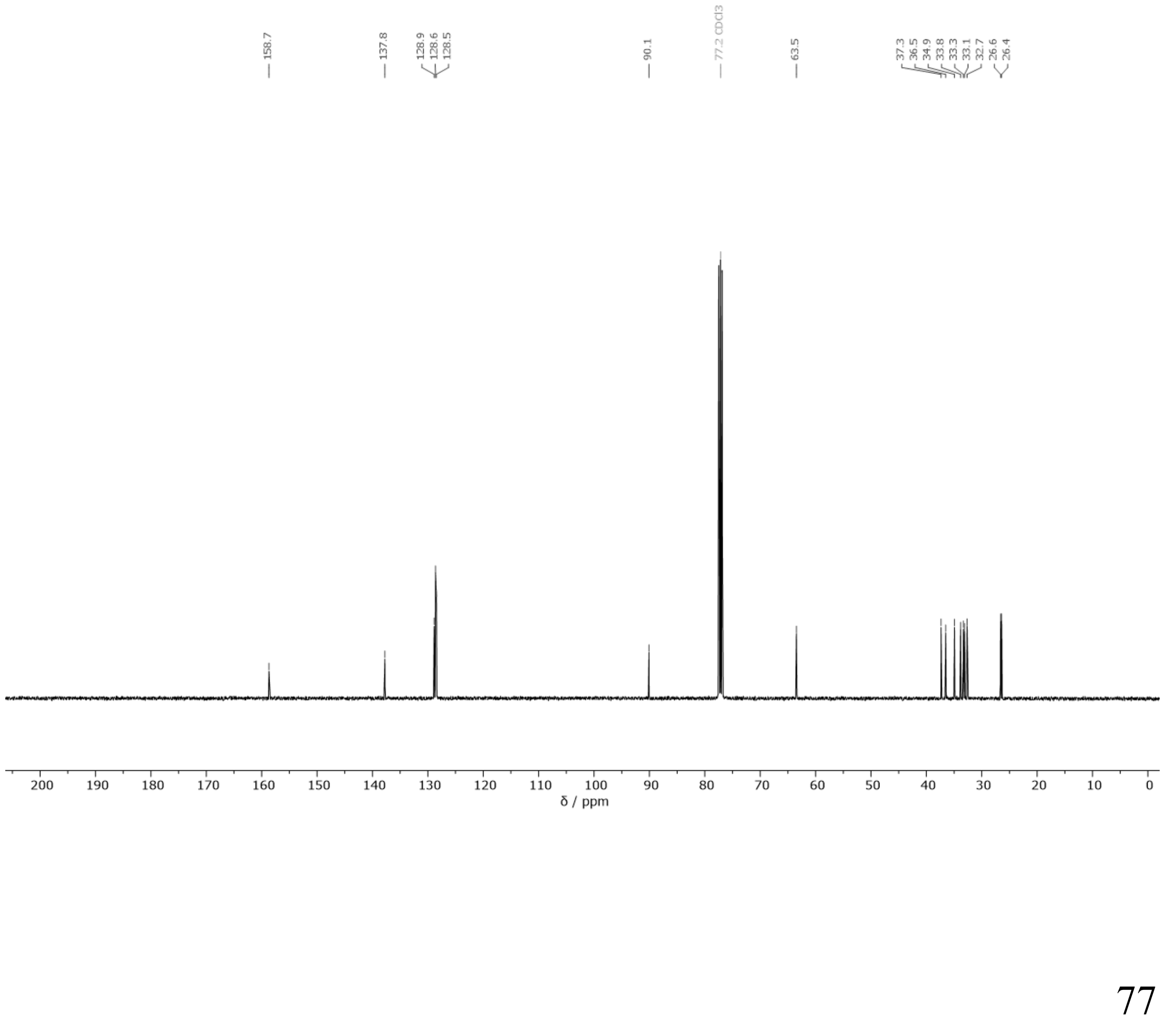
158.7
137.8
128.9
128.6
128.5
90.1
77.2 CDCl3
63.5
37.3
36.5
34.9
33.8
33.3
33.1
32.7
26.6
26.4
200 190 180 170 160 150 140 130 120 110 100 90 80 70 60 50 40 30 20 10 0
δ / ppm

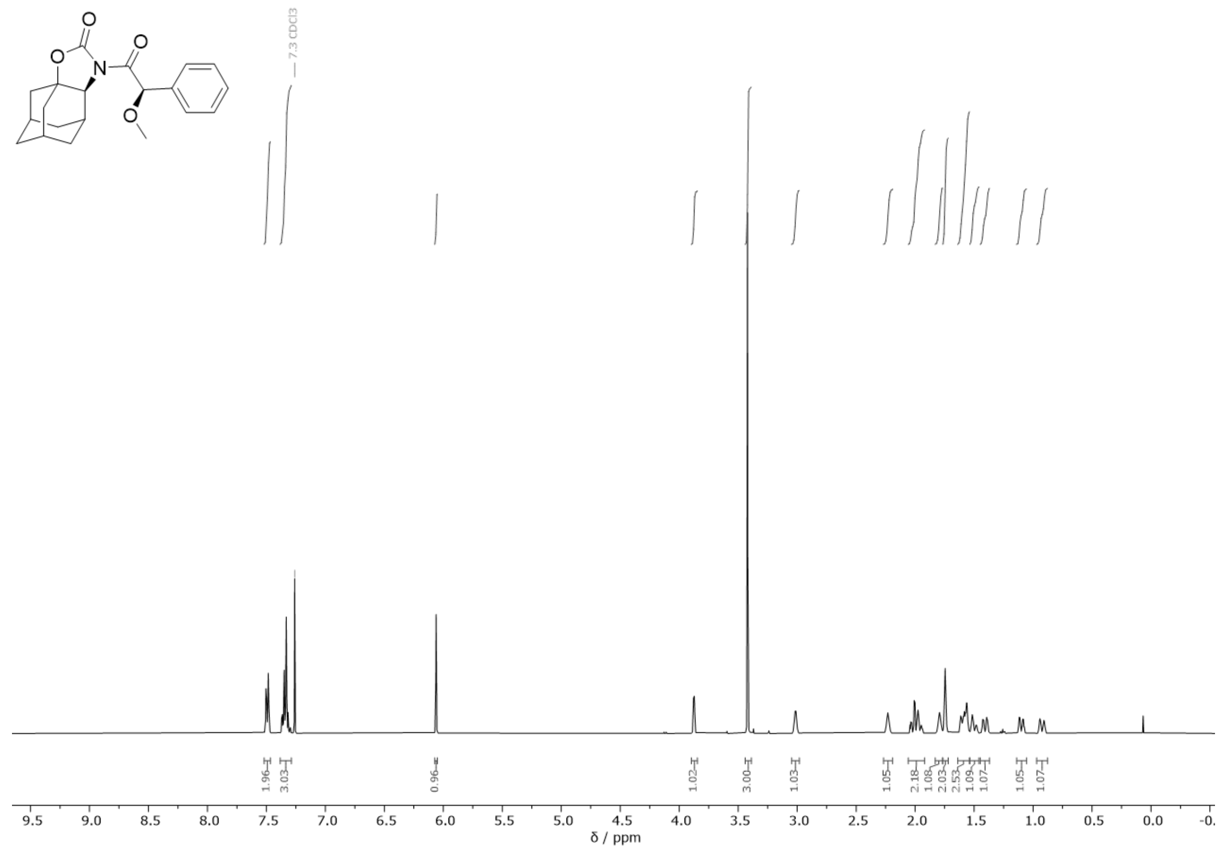
O
O
N
O
O
7.3 CDCl3
1.96
3.03
0.96
1.02
3.00
1.03
1.05
2.18
1.08
2.03
2.53
1.09
1.07
1.05
1.07
9.5
9.0
8.5
8.0
7.5
7.0
6.5
6.0
5.5
5.0
4.5
4.0
3.5
3.0
2.5
2.0
1.5
1.0
0.5
0.0
-0.
δ / ppm

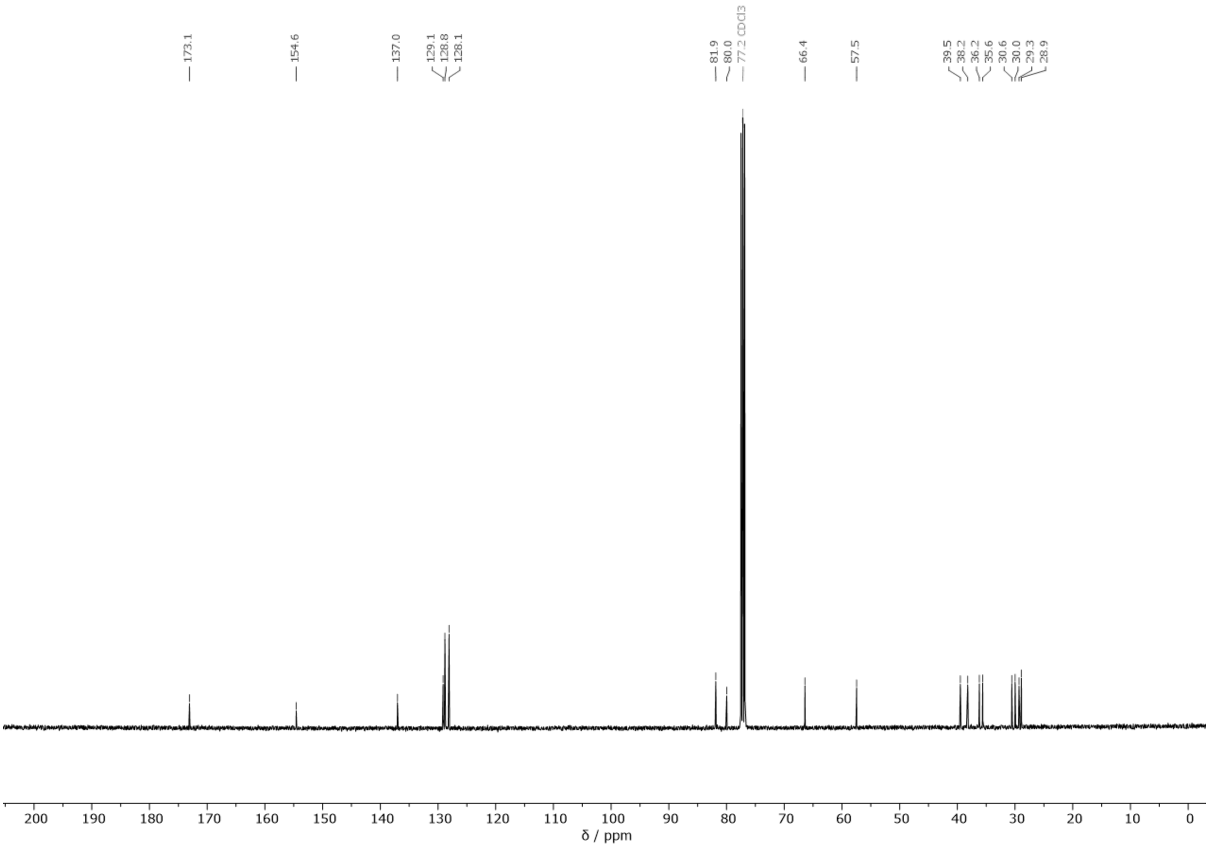
173.1
154.6
137.0
129.1
128.8
128.1
81.9
80.0
77.2 CDCl3
66.4
57.5
39.5
38.2
36.2
35.6
30.6
30.0
29.3
28.9
200
190
180
170
160
150
140
130
120
110
100
90
80
70
60
50
40
30
20
10
0
δ / ppm

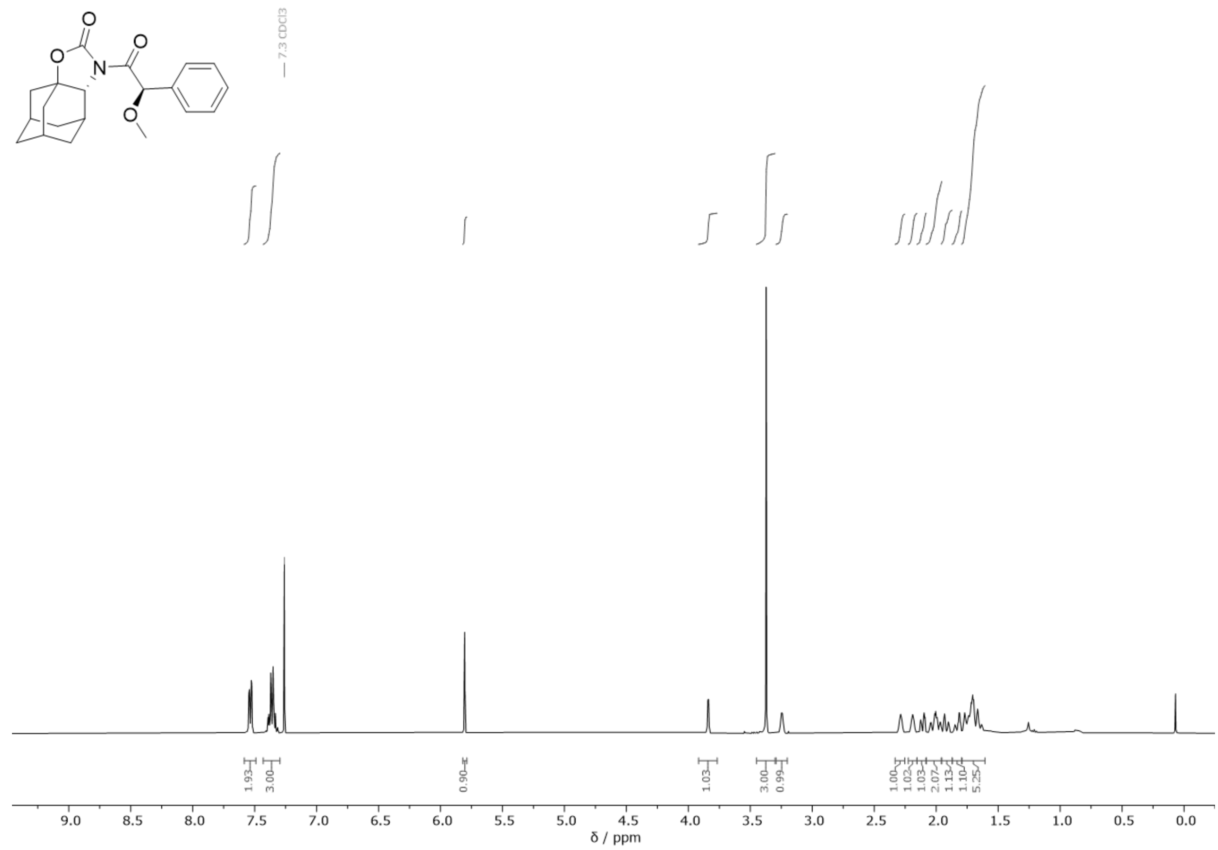
O
O
N
O
O
7.3 CDCl3
1.93
3.00
0.90
1.03
3.00
0.99
1.00
1.02
1.03
2.07
1.13
1.10
5.25
9.0
8.5
8.0
7.5
7.0
6.5
6.0
5.5
5.0
4.5
4.0
3.5
3.0
2.5
2.0
1.5
1.0
0.5
0.0
δ / ppm

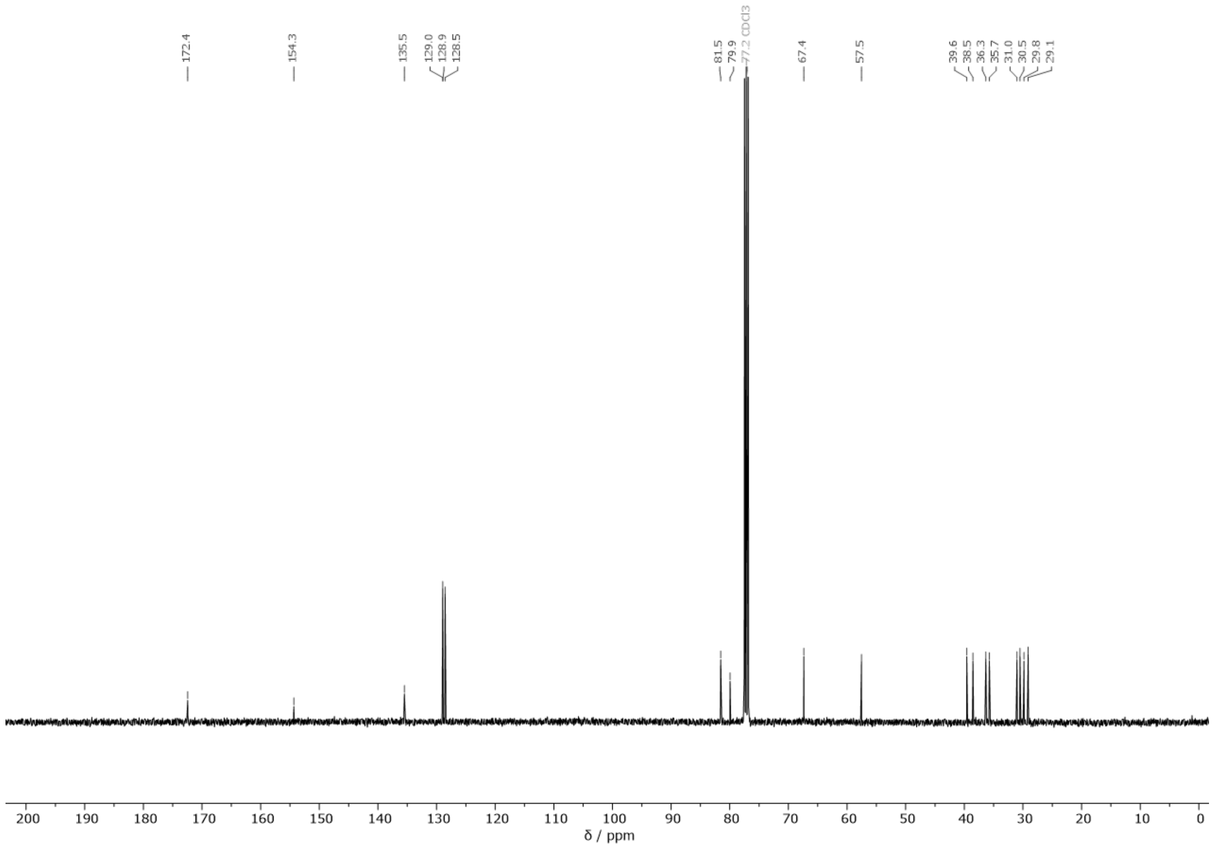
172.4
154.3
135.5
129.0
128.9
128.5
81.5
79.9
77.2 CDCl3
67.4
57.5
39.6
38.5
36.3
35.7
31.0
30.5
29.8
29.1
200
190
180
170
160
150
140
130
120
110
100
90
80
70
60
50
40
30
20
10
0
δ / ppm

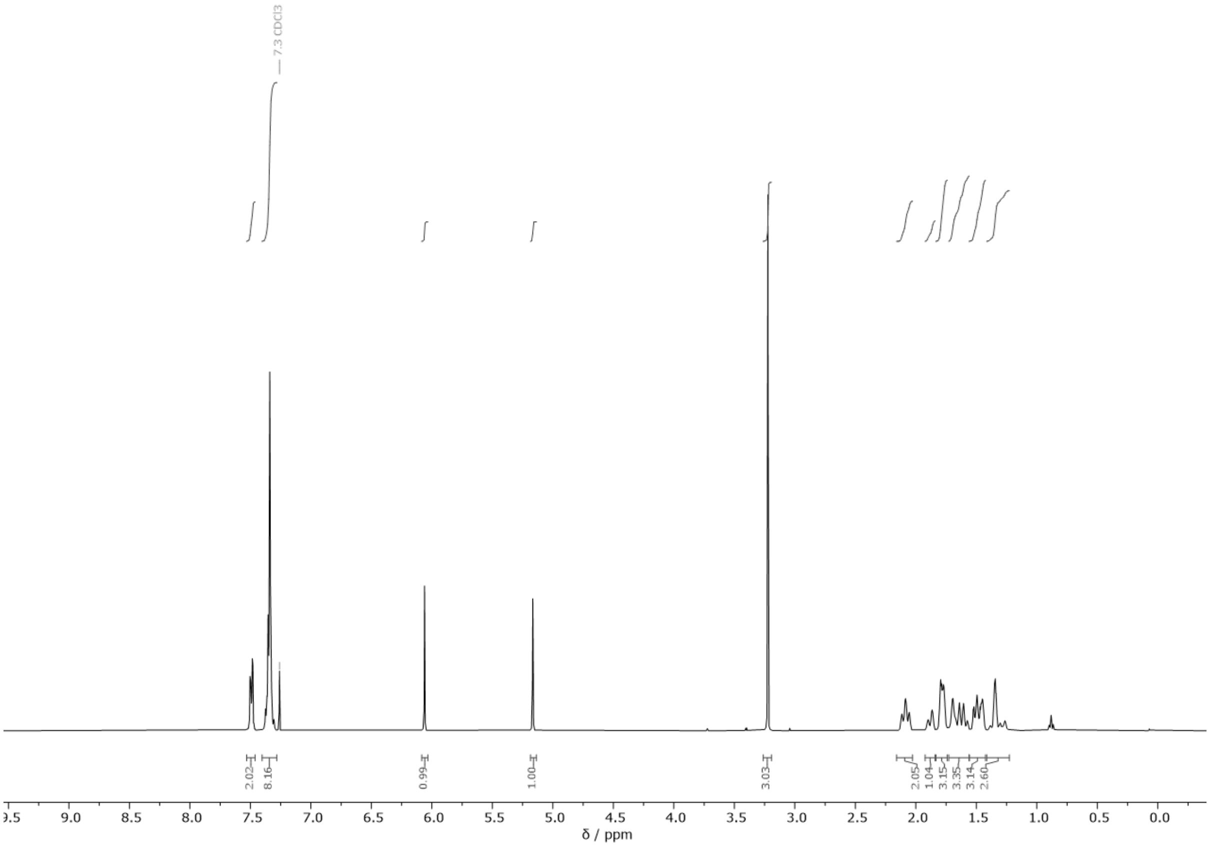
7.3 CDCl3
2.02
8.16
0.99
1.00
3.03
2.05
1.04
3.15
3.35
3.14
2.60
9.5
9.0
8.5
8.0
7.5
7.0
6.5
6.0
5.5
5.0
4.5
4.0
3.5
3.0
2.5
2.0
1.5
1.0
0.5
0.0
δ / ppm

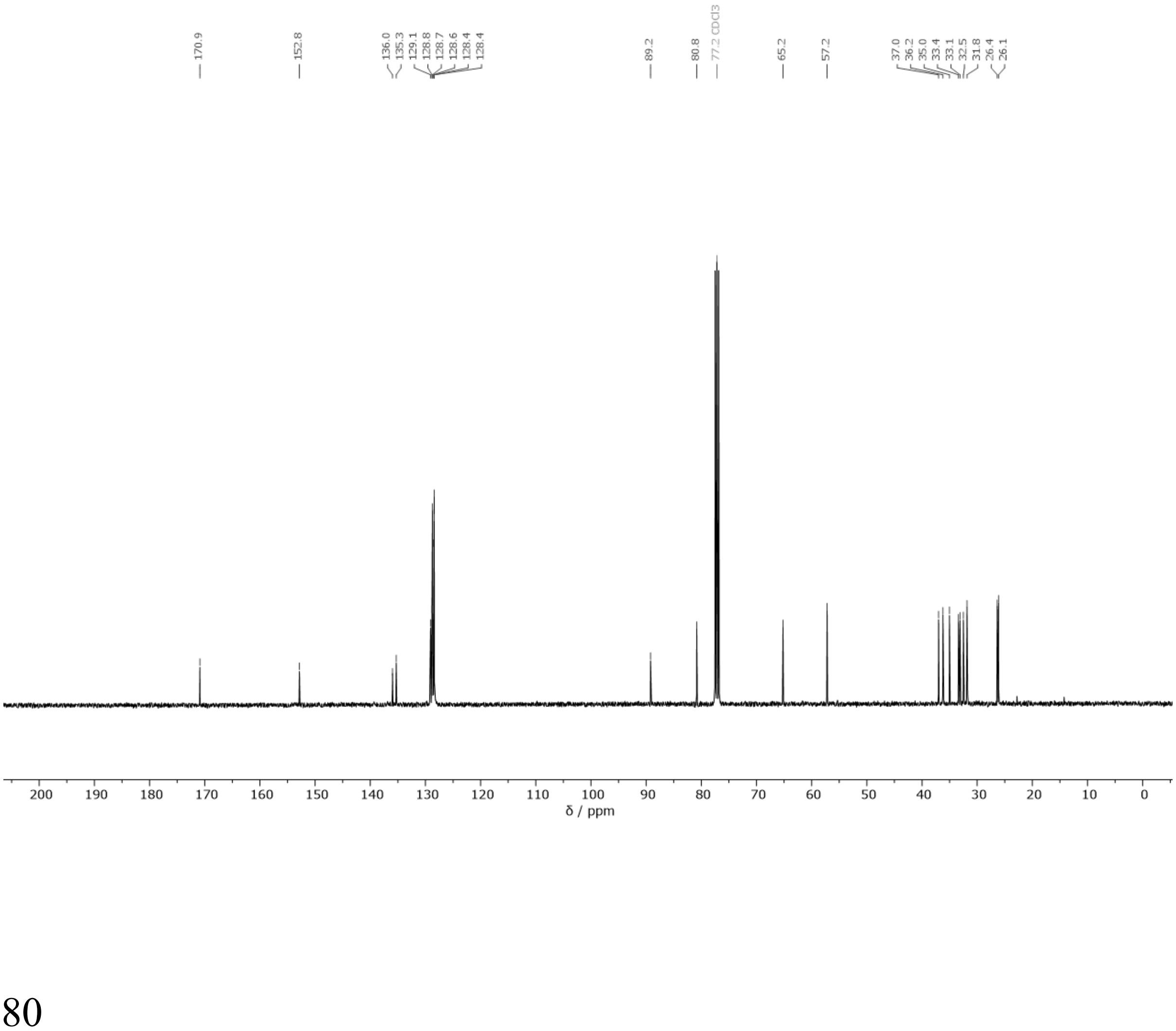
170.9
152.8
136.0
135.3
129.1
128.8
128.7
128.6
128.4
128.4
89.2
80.8
77.2 CDCl3
65.2
57.2
37.0
36.2
35.0
33.4
33.1
32.5
31.8
26.4
26.1
200
190
180
170
160
150
140
130
120
110
100
90
80
70
60
50
40
30
20
10
0
δ / ppm

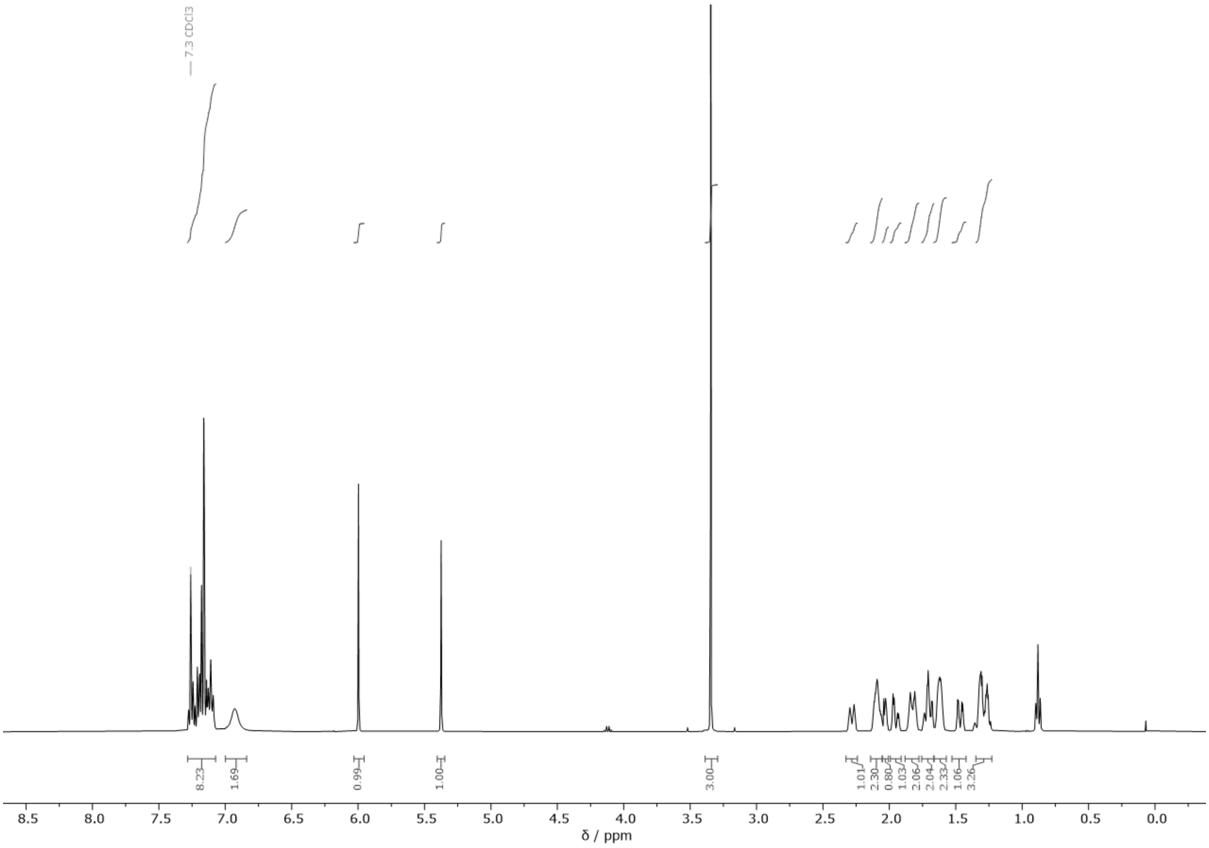
7.3 CDCl3
8.23
1.69
0.99
1.00
3.00
1.01
2.30
0.80
1.03
2.06
2.04
2.33
1.06
3.26
8.5
8.0
7.5
7.0
6.5
6.0
5.5
5.0
4.5
4.0
3.5
3.0
2.5
2.0
1.5
1.0
0.5
0.0
δ / ppm

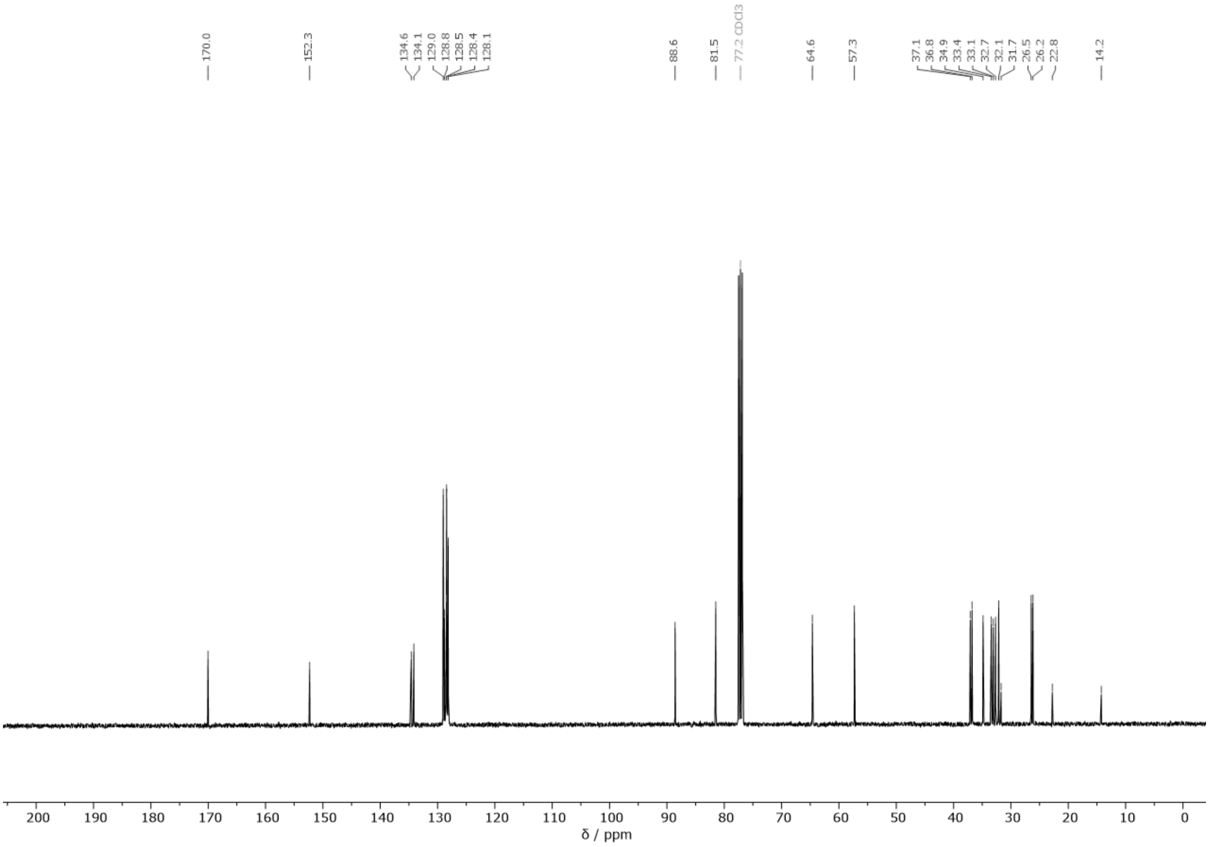
170.0
152.3
134.6
134.1
129.0
128.8
128.5
128.4
128.1
88.6
81.5
77.2 CDCl3
64.6
57.3
37.1
36.8
34.9
33.4
33.1
32.7
32.1
31.7
26.5
26.2
22.8
14.2
200
190
180
170
160
150
140
130
120
110
100
90
80
70
60
50
40
30
20
10
0
δ / ppm

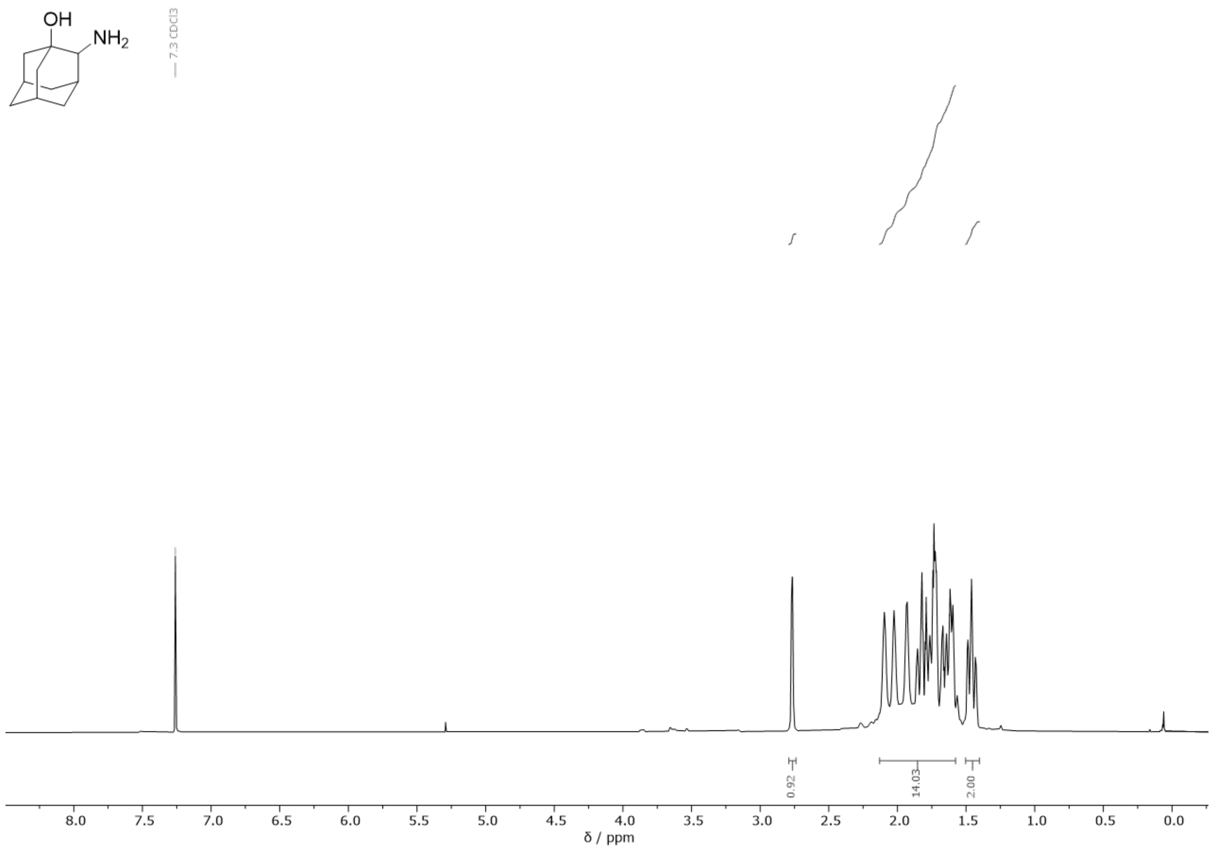
OH
NH2
7.3 CDCl3
0.92
14.03
2.00
8.0
7.5
7.0
6.5
6.0
5.5
5.0
4.5
4.0
3.5
3.0
2.5
2.0
1.5
1.0
0.5
0.0
δ / ppm

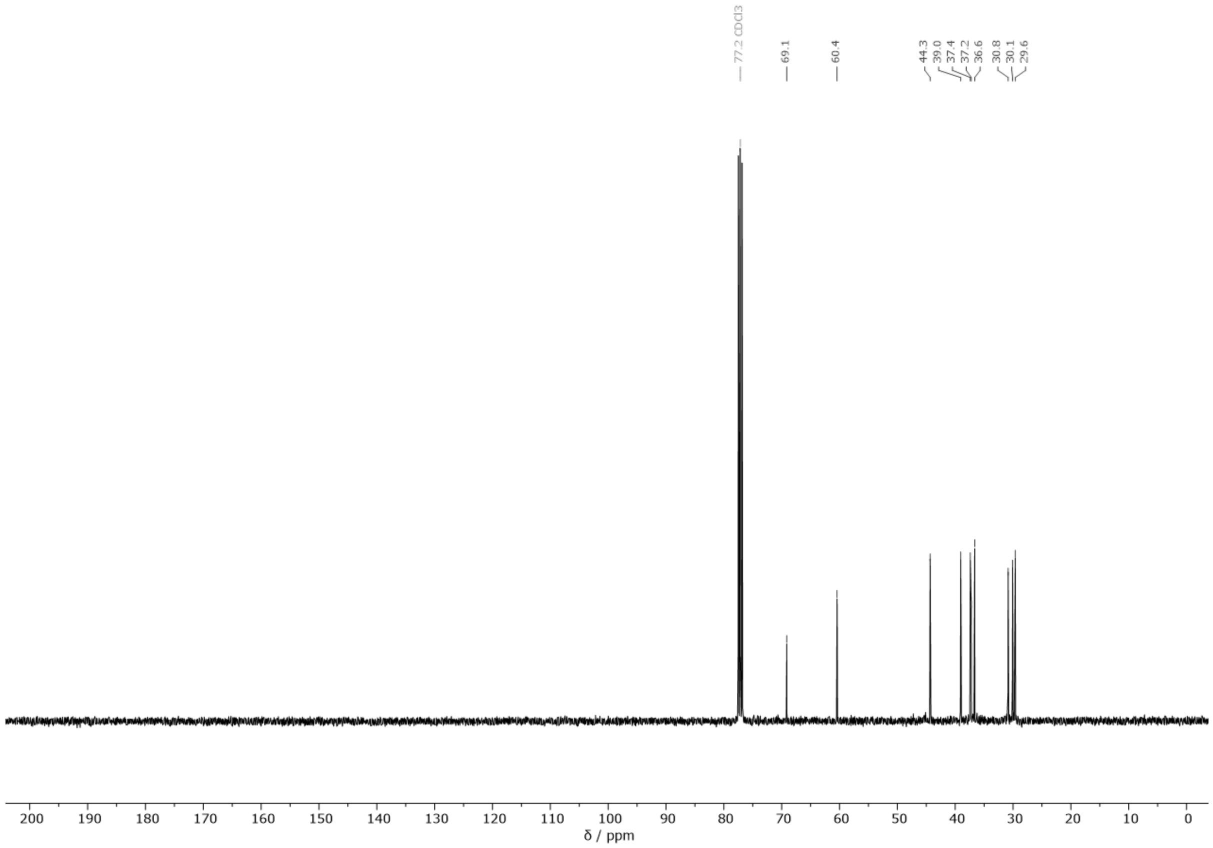
77.2 CDCl3
69.1
60.4
44.3
39.0
37.4
37.2
36.6
30.8
30.1
29.6
200
190
180
170
160
150
140
130
120
110
100
90
80
70
60
50
40
30
20
10
0
δ / ppm

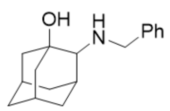
OH
H
N
Ph

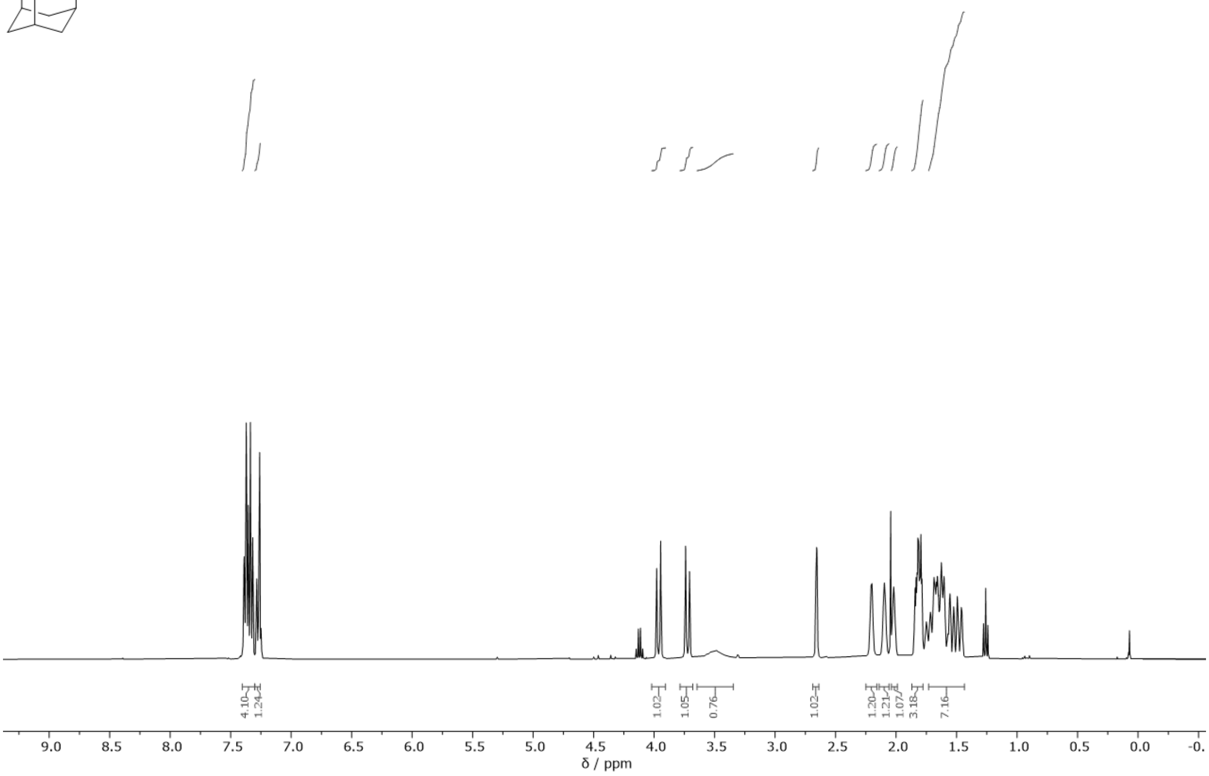
4.10
1.24
1.02
1.05
0.76
1.02
1.20
1.21
1.07
3.18
7.16
9.0
8.5
8.0
7.5
7.0
6.5
6.0
5.5
5.0
4.5
4.0
3.5
3.0
2.5
2.0
1.5
1.0
0.5
0.0
-0.
δ / ppm

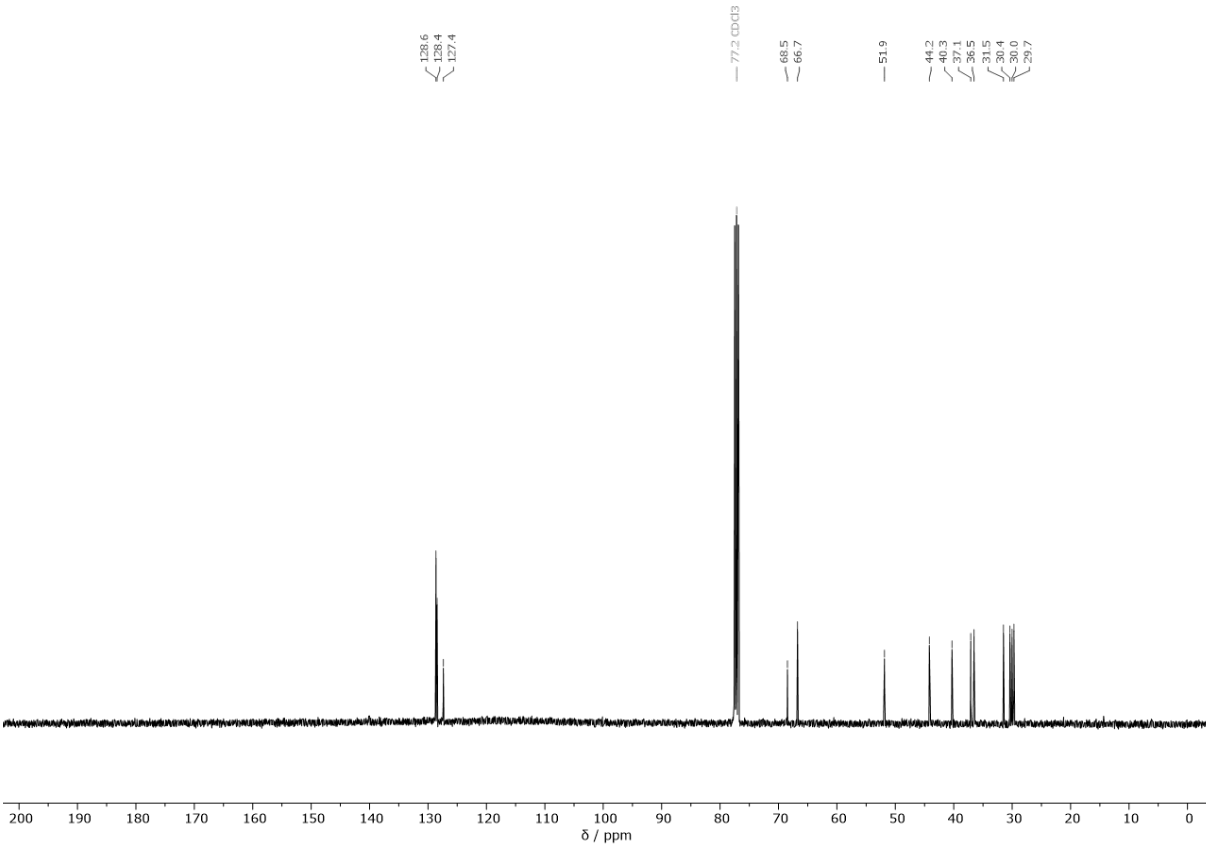
128.6
128.4
127.4
77.2 CDCl3
68.5
66.7
51.9
44.2
40.3
37.1
36.5
31.5
30.4
30.0
29.7
200
190
180
170
160
150
140
130
120
110
100
90
80
70
60
50
40
30
20
10
0
δ / ppm

Spectra

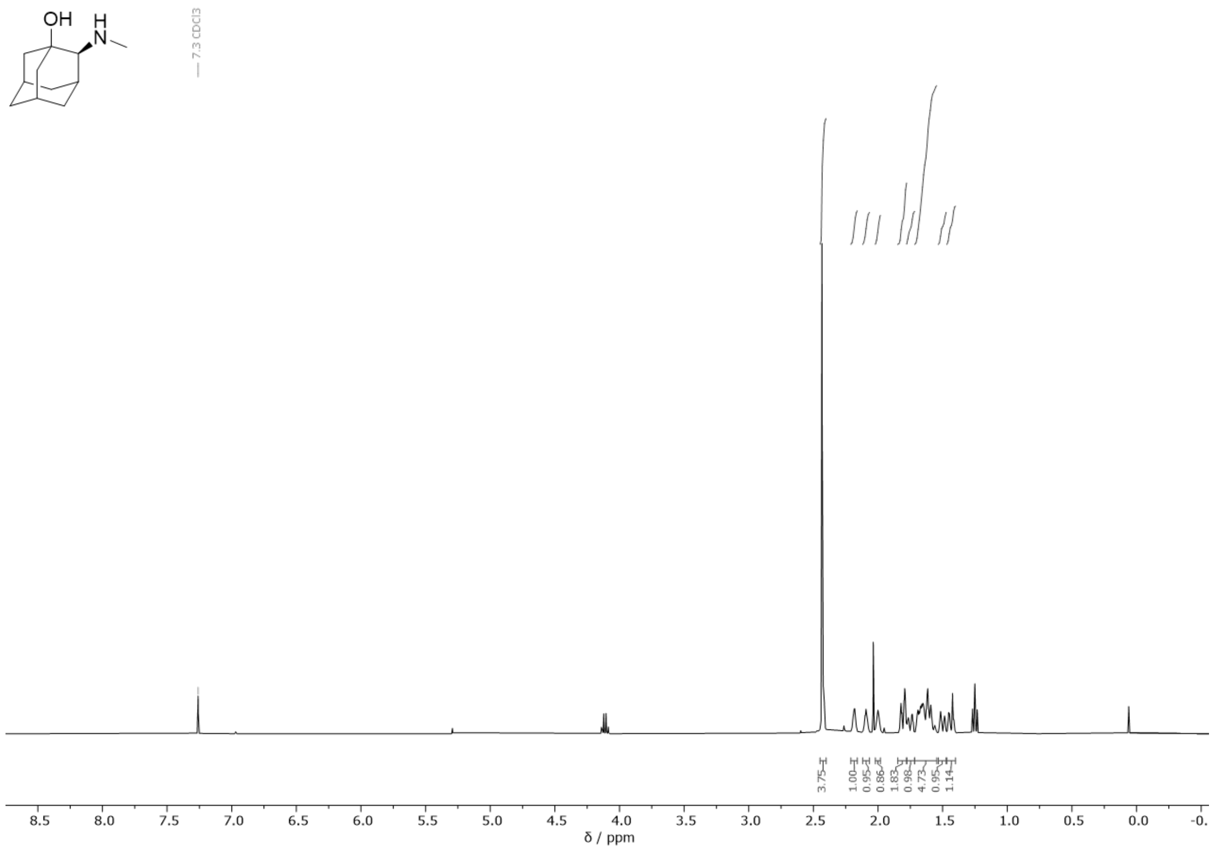
OH
H
N
7.3 CDCl3
3.75
1.00
0.95
0.86
1.83
0.98
4.73
0.95
1.14
8.5
8.0
7.5
7.0
6.5
6.0
5.5
5.0
4.5
4.0
3.5
3.0
2.5
2.0
1.5
1.0
0.5
0.0
-0.
δ / ppm

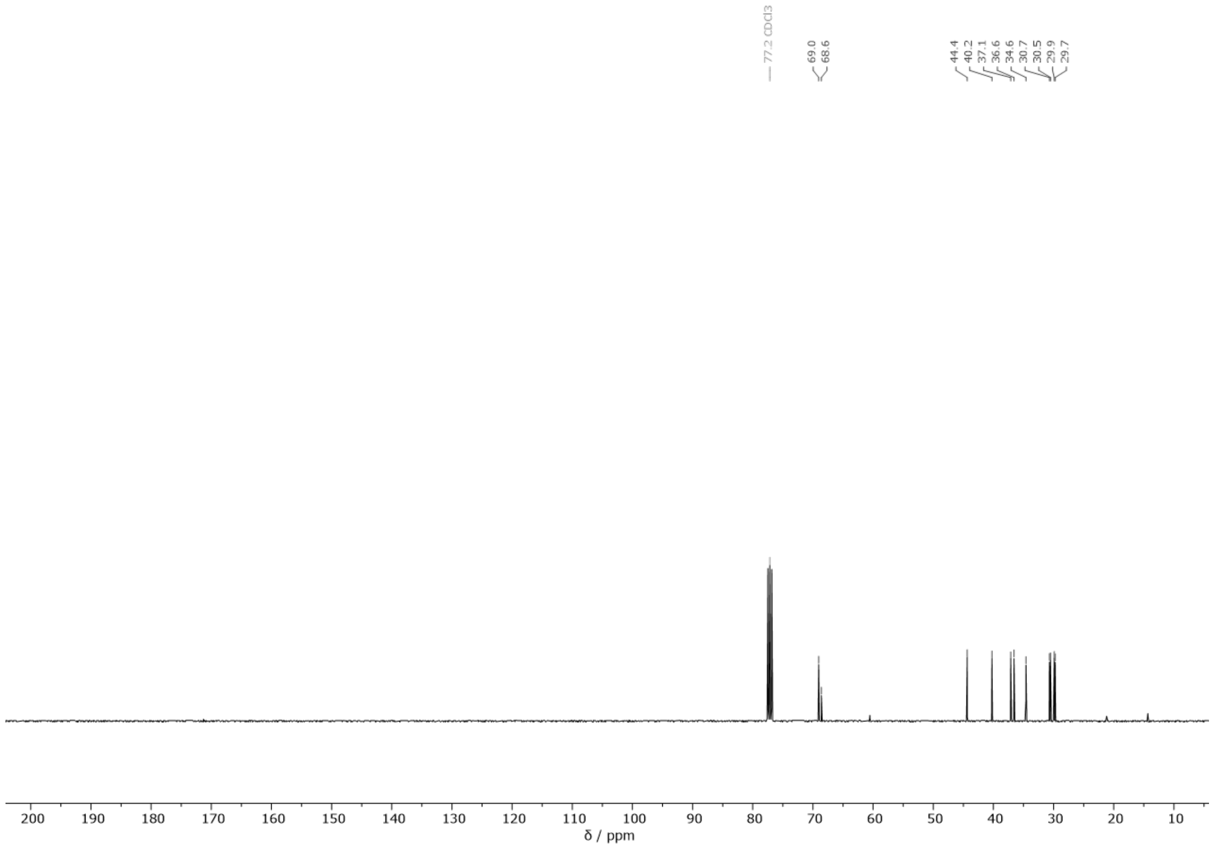
77.2 CDCl3
69.0
68.6
44.4
40.2
37.1
36.6
34.6
30.7
30.5
29.9
29.7
200
190
180
170
160
150
140
130
120
110
100
90
80
70
60
50
40
30
20
10
δ / ppm

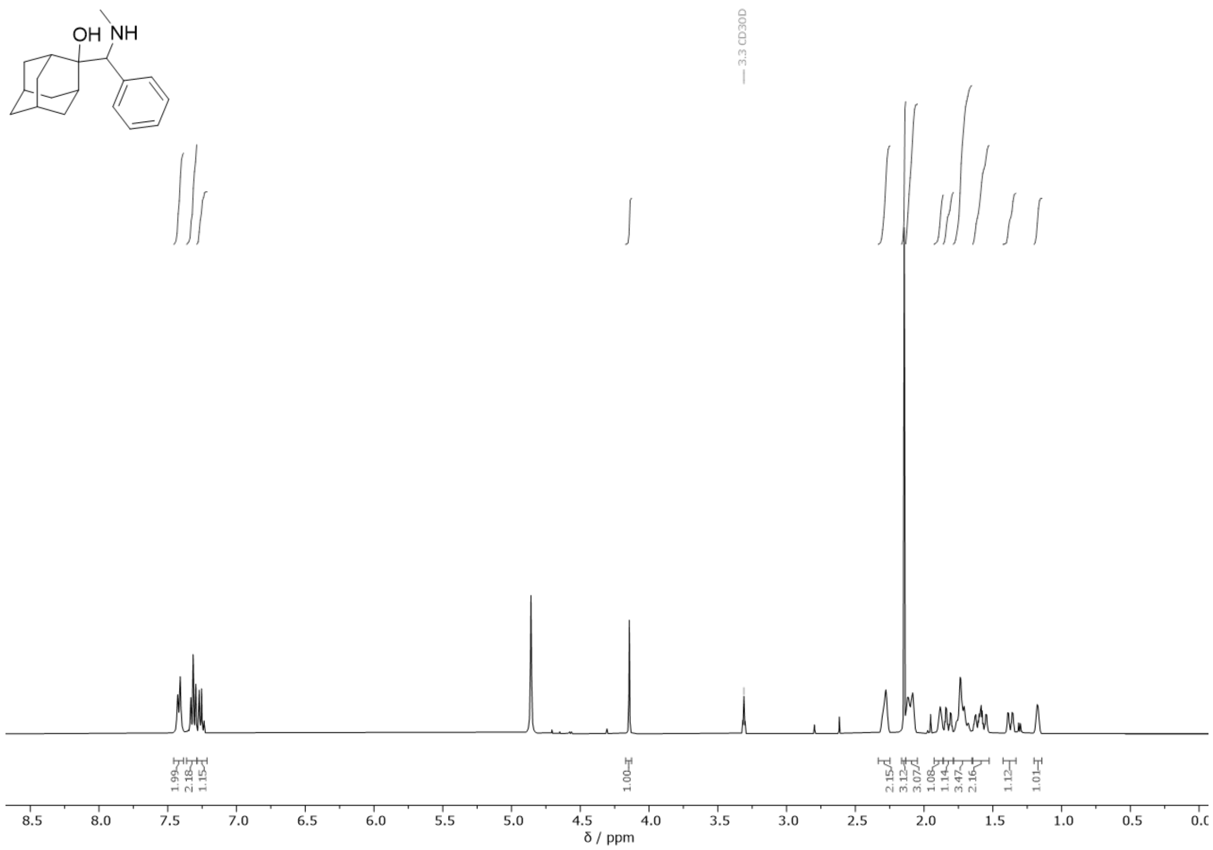
OH
NH
3.3 CD3OD
1.99
2.18
1.15
1.00
2.15
3.12
3.07
1.08
1.14
3.47
2.16
1.12
1.01
8.5
8.0
7.5
7.0
6.5
6.0
5.5
5.0
4.5
4.0
3.5
3.0
2.5
2.0
1.5
1.0
0.5
0.0
δ / ppm

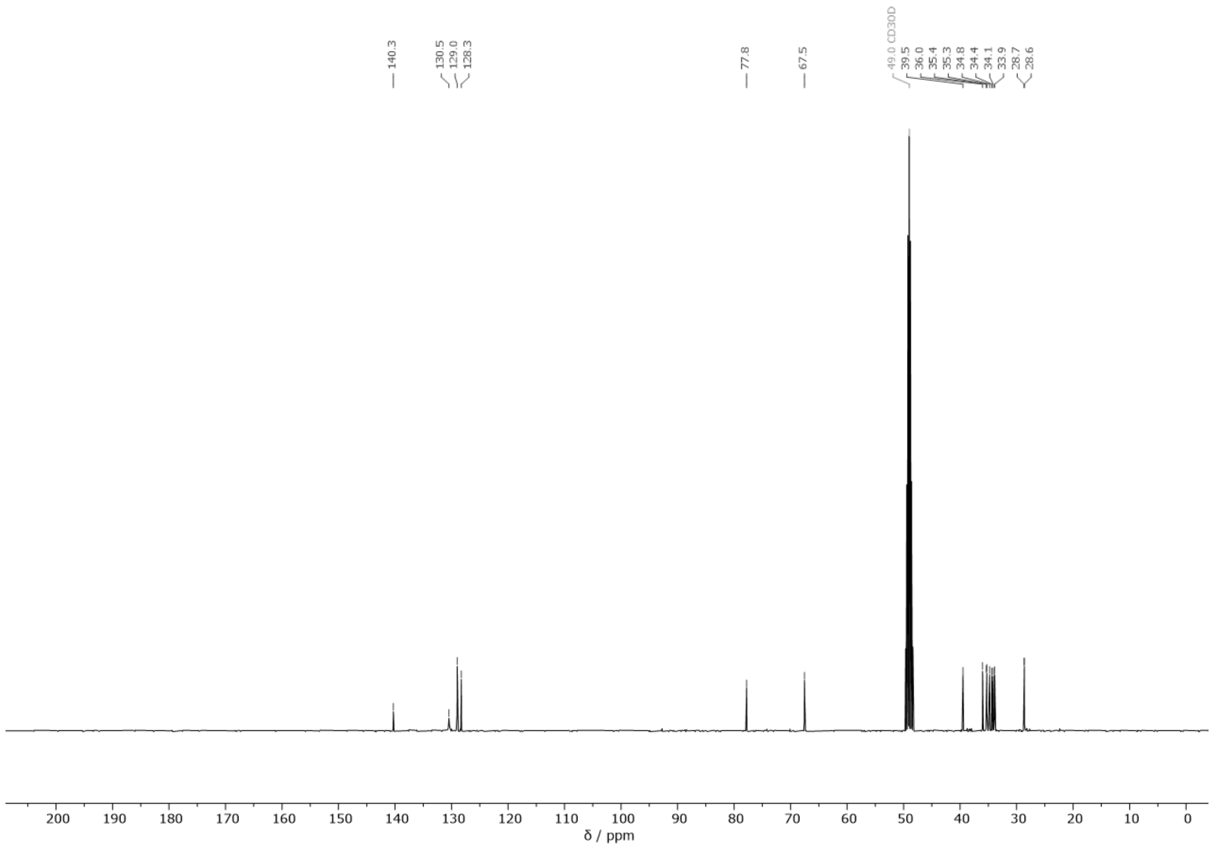
140.3
130.5
129.0
128.3
77.8
67.5
49.0 CD3OD
39.5
36.0
35.4
35.3
34.8
34.4
34.1
33.9
28.7
28.6
200
190
180
170
160
150
140
130
120
110
100
90
80
70
60
50
40
30
20
10
0
δ / ppm

7. References

[1] L. Wanka, K. Iqbal, P. R. Schreiner, *Chem. Rev.* **2013**, *113*, 3516–3604.
[2] H. Schwertfeger, A. A. Fokin, P. R. Schreiner, *Angew. Chem. Int. Ed.* **2008**, *47*, 1022–1036.
[3] K. A. Agnew-Francis, C. M. Williams, *Adv. Synth. Catal.* **2016**, *358*, 675–700.
[4] J.-P. Berndt, Y. Radchenko, J. Becker, C. Logemann, D. R. Bhandari, R. Hrdina, P. R. Schreiner, *Chem. Sci.* **2019**, *10*, 3324–3329.
[5] C. E. Müller, L. Wanka, K. Jewell, P. R. Schreiner, *Angew. Chem. Int. Ed.* **2008**, *47*, 6180–6183.
[6] R. Hrdina, C. E. Müller, R. C. Wende, L. Wanka, P. R. Schreiner, *Chem. Commun.* **2012**, *48*, 2498–2500.
[7] R. C. Wende, A. Seitz, D. Niedek, S. M. M. Schuler, C. Hofmann, J. Becker, P. R. Schreiner, *Angew. Chem. Int. Ed.* **2016**, *55*, 2719–2723.
[8] A. Seitz, R. C. Wende, E. Roesner, D. Niedek, C. Topp, A. C. Colgan, E. M. McGarrigle, P. R. Schreiner, *J. Org. Chem.* **2021**, *86*, 3907–3922.
[9] S. Rösel, C. Balestrieri, P. R. Schreiner, *Chem. Sci.* **2017**, *8*, 405–410.
[10] S. Rösel, J. Becker, W. D. Allen, P. R. Schreiner, *J. Am. Chem. Soc.* **2018**, *140*, 14421–14432.
[11] J. P. Wagner, P. R. Schreiner, *Angew. Chem. Int. Ed.* **2015**, *54*, 12274–12296.
[12] J. M. Crawford, M. S. Sigman, *Synthesis* **2019**, *51*, 1021–1036.
[13] E. R. Jarvo, S. J. Miller, *Tetrahedron* **2002**, *58*, 2481–2495.
[14] E. J. Corey, C. J. Helal, *Angew. Chem. Int. Ed.* **1998**, *37*, 1986–2012.
[15] J. J. Rohde, M. A. Pliushchev, B. K. Sorensen, D. Wodka, Q. Shuai, J. Wang, S. Fung, K. M. Monzon, W. J. Chiou, L. Pan, *J. Med. Chem.* **2007**, *50*, 149–164.
[16] C. G. Espino, J. Du Bois, *Angew. Chem. Int. Ed.* **2001**, *40*, 598–600.
[17] R. Hrdina, F. M. Metz, M. Larrosa, J.-P. Berndt, Y. Y. Zhygadlo, S. Becker, J. Becker, *Eur. J. Org. Chem.* **2015**, 6231–6236.
[18] R. Hrdina, M. Larrosa, C. Logemann, *J. Org. Chem.* **2017**, *82*, 4891–4899.
[19] R. Hrdina, *Synthesis* **2019**, *51*, 629–642.
[20] E. J. Corey, R. K. Bakshi, S. Shibata, C. pin Chen, V. K. Singh, *J. Am. Chem. Soc.* **1987**, *109*, 7925–7926.
[21] Y. Kawanami, R. Yanagita, *Molecules* **2018**, *23*, 2408–2422.
[22] Y. Shimoda, H. Yamamoto, *Synthesis* **2016**, *49*, 175–180.
[23] E. J. Corey, C. J. Helal, *Angew. Chem. Int. Ed.* **1998**, *37*, 1986–2012.
[24] T. Harada, C. Inui, *J. Org. Chem.* **2006**, *71*, 1277–1279.
[25] E. J. Corey, R. K. Bakshi, S. Shibata, *J. Am. Chem. Soc.* **1987**, *109*, 5551–5553.
[26] E. J. Corey, T.-P. Loh, *Tetrahedron Lett.* **1993**, *34*, 3979–3982.
[27] K. Futatsugi, H. Yamamoto, *Angew. Chem. Int. Ed.* **2005**, *44*, 1484–1487.
[28] K. Ishihara, S. Kondo, H. Yamamoto, *Synlett* **1999**, *1999*, 1283–1285.
[29] M. D. Barker, R. A. Dixon, S. Jones, B. J. Marsh, *Tetrahedron* **2006**, *62*, 11663–11669.
[30] E. J. Corey, T. P. Loh, *J. Am. Chem. Soc.* **1991**, *113*, 8966–8967.
[31] G. R. Eaton, *J. Chem. Educ.* **1969**, *46*, 547–556.
[32] M. S. Chauhan, S. Singh, *J. Mol. Catal. A Chem.* **2015**, *398*, 184–189.
[33] E. J. Corey, *Angew. Chem. Int. Ed.* **2002**, *41*, 1650–1667.
[34] E. J. Corey, T. Shibata, T. W. Lee, *J. Am. Chem. Soc.* **2002**, *124*, 3808–3809.
[35] M. Masui, T. Shioiri, *Tetrahedron* **1995**, *51*, 8363–8370.
[36] G. B. Stone, *Tetrahedron Asymmetry* **1994**, *5*, 465–472.
[37] Xu, Wei, Zhang, *J. Org. Chem.* **2003**, *68*, 10146–10151.
[38] D. A. Evans, T. C. Britton, J. A. Ellman, *Tetrahedron Lett.* **1987**, *28*, 6141–6144.
[39] G. L. Beutner, B. M. Cohen, A. J. Delmonte, D. D. Dixon, K. J. Fraunhoffer, A. W. Glace, E. Lo, J. M. Stevens, D. Vanyo, C. Wilbert, *Org. Process Res. Dev.* **2019**, *23*, 1378–1385.
[40] H. D. Flack, G. Bernardinelli, *Chirality* **2008**, *20*, 681–690.
[41] N. Harada, A. Synthesis, *Chirality* **2008**, *20*, 691–723.
[42] L. Pasteur, *Ann. Chim. Phys.* **1848**, *24*, 442–459.
[43] J. A. Dale, H. S. Mosher, *J. Am. Chem. Soc.* **1973**, *95*, 512–519.
[44] I. Ohtani, T. Kusumi, Y. Kashman, H. Kakisawa, *J. Am. Chem. Soc.* **1991**, *113*, 4092–4096.
[45] T. R. Hoye, C. S. Jeffrey, F. Shao, *Nat. Protoc.* **2007**, *2*, 2451–2458.
[46] F. Saito, J. Becker, P. R. Schreiner, *J. Org. Chem.* **2020**, *85*, 4441–4447.
[47] F. Saito, D. Gerbig, J. Becker, P. R. Schreiner, *Org. Lett.* **2020**, *22*, 3895–3899.
[48] F. Saito, D. Gerbig, J. Becker, P. R. Schreiner, *Org. Lett.* **2021**, *23*, 113–117.
[49] P. J. Stephens, F. J. Devlin, J.-J. Pan, *Chirality* **2008**, *20*, 643–663.
[50] D.-S. Lee, *Chirality* **2007**, *19*, 148–151.

[51] E. J. Corey, C. L. Cywin, T. D. Roper, *Tetrahedron Lett.* **1992**, *33*, 6907–6910.
[52] S. Grimme, R. Huenerbein, S. Ehrlich, *ChemPhysChem* **2011**, *12*, 1258–1261.
[53] D. Yepes, F. Neese, B. List, G. Bistoni, *J. Am. Chem. Soc.* **2020**, *142*, 3613–3625.
[54] M. W. Wong, *J. Org. Chem.* **2005**, *70*, 5487–5493.
[55] K. Q. Do, P. Thanei, M. Caviezel, R. Schwyzer, *Helv. Chim. Acta* **1979**, *62*, 956–964.
[56] K. A. Ahrendt, C. J. Borths, D. W. C. MacMillan, *J. Am. Chem. Soc.* **2000**, *122*, 4243–4244.

Chapter 2

Peptide-Based Oxazaborolidines

1. Motivation

During the last two decades, peptides have proven to be a valuable class of organocatalysts in asymmetric synthesis. While the catalytic motif provides the necessary activation of substrates, the chiral peptide backbone induces chirality in chemical transformations and at the same time influences reactivity by additional activation modes like NCIs such as hydrogen bonding or LD. Similar to enzymes, oligopeptide catalysts may adopt secondary or tertiary structures for chirality transfer. Because of the modular nature of peptides, selectivity and reactivity can be modified by replacing or functionalizing single amino acids. Moreover, amino acid sequences can be tailored for specific substrates facilitating highly selective reactions.[1–4]

There are several established catalytic moieties, which are employed in peptide-based transformations. These mainly include various functionalizations *via* enamine catalysis by secondary amines and group transfer reactions, e.g., acylation, phosphorylation, and sulfonylation *via* Lewis base activation by a *N*-π-methylhistidine (Pmh) moiety.[3,5–7] Furthermore, TEMPO mediated oxidations of alcohols as well as Baeyer-Villiger reactions and epoxidations by *in-situ* generated peracids or *via* iminium ion catalysis are well studied.[8–12] Some publications also deal with transition metal catalyzed reactions in which peptides are used as chiral ligands.[13,14] These examples demonstrate, that many catalytic motifs can benefit from incorporation into oligopeptides ultimately enabling selective transformations of molecules, which are hard to address by other small molecule catalysts. Therefore, herein we aimed to incorporate a Lewis acidic OXB moiety into a chiral peptide backbone to create a novel Lewis acidic peptide catalyst for cycloaddition reactions.

2. Results

2.1. Preliminary Considerations

Developing a catalytic moiety for peptide catalysis is a challenging task, because several aspects must be fulfilled. In general, the precursor should either be commercially available or the synthesis should be easily feasible. Furthermore, it must be attachable to the peptide backbone. In the case of OXB formation, the precursor must possess a vicinal amino alcohol, which can condensate with a boronic acid to yield the appropriate catalytic species. Lastly, the catalyst precursor should be functionalizable or derivatizable to tune electronic and steric properties.

In this project, we selected two possible moieties as catalyst precursor, both containing a vicinal amino alcohol and a further functionalizable group for peptide attachment. For both possible moieties, we first investigated their capability for OXB formation, then attached the catalyst precursor to test peptides and finally checked for a possible application in catalysis.

2.2. Serine-Based Catalyst Precursor

For attaching an OXB to a chiral peptide backbone, we chose the proteinogenic amino acid L-serine as catalyst precursor. L-Serine is a naturally occurring amino acid, which is commercially available and cheap. Besides the amino alcohol moiety that is necessary for the OXB formation, it offers a carboxylic acid group by which it is attachable to the peptide.

By functionalization of the nitrogen, the electronic properties of the resultant OXB can be tuned. For a successful application in catalysis, a fine balance of the electronic properties is necessary. While electron withdrawing groups (EWG) at the nitrogen enhance the Lewis acidity of the synthesized OXB, the low nucleophilicity of the amino alcohol precursors make the formation of the OXB difficult. Electron donating groups (EDG) provide opposite reactivity. The formation of the OXB is enhanced, but the resultant catalyst is less Lewis acidic and thereby less active.[15] We started our investigation with the synthesis of four L-serine based amino alcohol precursors. Nucleophilic substitution with trifluoroacetyl chloride and tosyl chloride provided derivatives **1a** and **1b** bearing EWG, whereas reductive amination with benzaldehyde and 1-naphthyl aldehyde provided derivatives **1c** and **1d** equipped with EDG (Fig. 1).

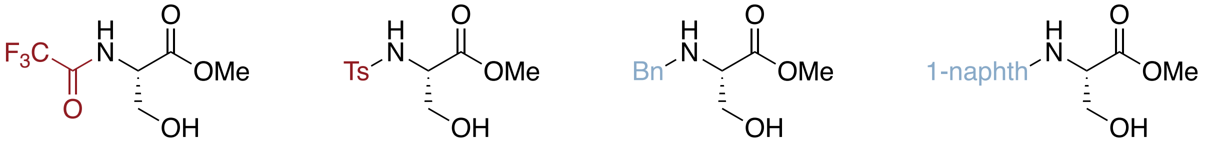

1a **1b** **1c** **1d**

Figure 1 Functionalized derivatives of L-serine used as catalyst precursors.

Subsequently, we tested the precursors in the formation of the corresponding OXBs. Therefore, we performed an azeotropic distillation of amino alcohols **1a-d** with phenyl boronic acid (**2**) in toluene for 24 h (Scheme 1) using a Soxhlet apparatus and CaH for water removal (Chapter 1, Fig. 2).[16] As OXBs are typically very sensitive to moisture, workup or purification steps are hardly possible due to hydrolysis. For this reason, the OXBs are often synthesized *in situ*.[17–19] A clean formation of the desired catalyst is thereby necessary to ensure reproducible results when employed in catalysis.

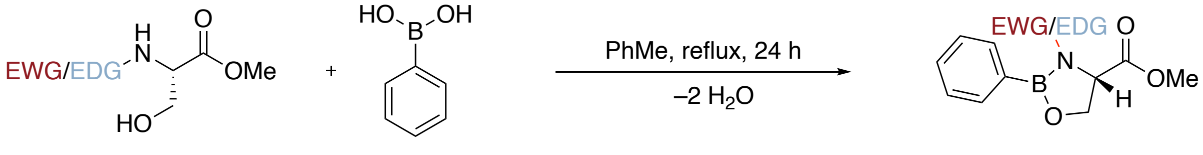

1a-d **2** **3a-d**

Scheme 1 Electron withdrawing groups (EWG) and electron donating groups (EDG) influence OXB formation.

Unfortunately, the azeotropic distillation of the amino alcohols equipped with EWG as substituents (**1a** and **1b**, respectively) did not lead to clean and quantitative formation to the corresponding OXBs **3a** and **3b** as detected by NMR analysis of the crude concentrate. We rather observed complex mixtures of the desired OXB with varying amounts of the partially cyclized analogue and starting material. Only the amino alcohols equipped with EDG as substituents (**1c** and **1d**) led to quantitative conversion to the desired OXBs **3c** and **3d**. After inspection of the NMR spectra, we judged the OXBs to be sufficiently clean for the use in catalysis (Fig. 2 and Fig. 3).

Comparison of the ^{1}H and ^{13}C NMR spectra of amino alcohol **1c** and the crude reaction mixture of OXB **3c** revealed downfield shifting of the vicinal amino alcohol signals, because of increased deshielding by the Lewis acidic boron (Fig. 2 and 3). The signal of the methyl ester remained at around 3.7 ppm, proving that the boron cyclized at the amino alcohol moiety and not *via* the carboxylic ester, which was reported for precursors such as tryptophane or threonine.[20,21]

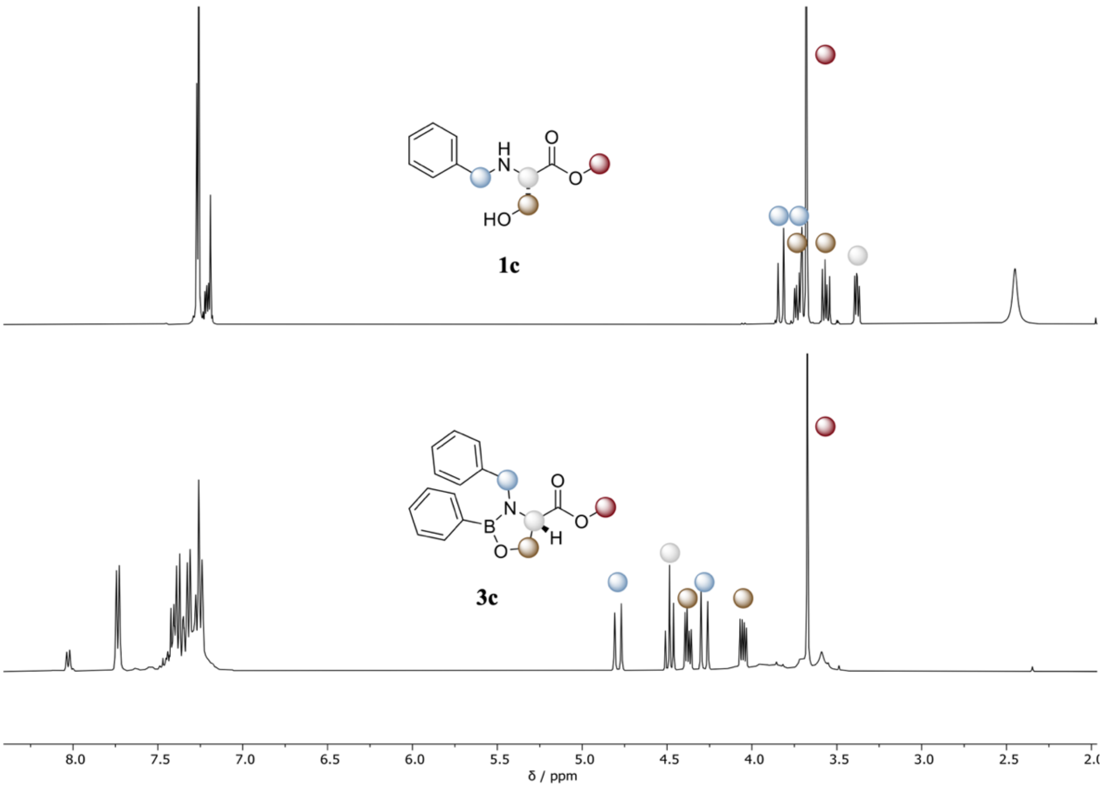

Figure 2 ^{1}H NMR spectra of amino alcohol **1c** and *in situ* generated OXB **3c**.

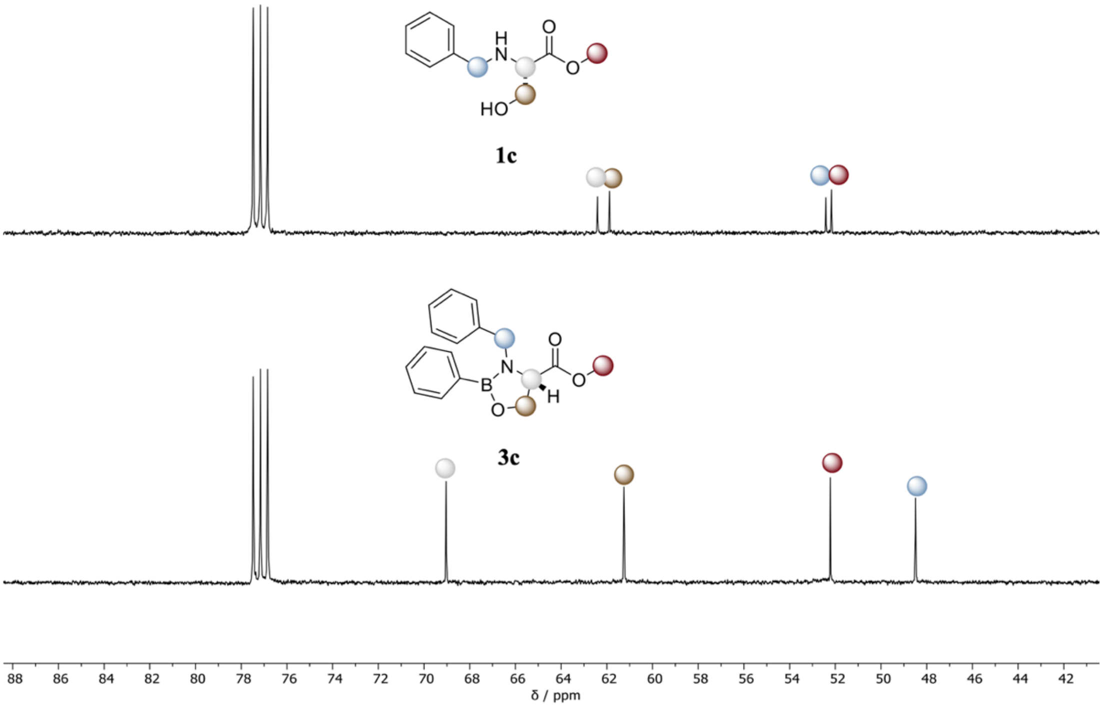

Figure 3 ^{13}C NMR spectra of amino alcohol **1c** and *in situ* generated OXB **3c**.

Encouraged by the simple and reliable OXB generation, we turned our attention towards its catalytic activity. Although the EDG are superior regarding *in situ* formation, they reduce the Lewis acidity and thus the catalytic activity of the cyclic boron.[15] For this reason, further electronic activation of the boron is necessary. Typically, there are two strategies for further activation. One the one hand, the addition of a co-catalyst provides some of the most useful and reactive OXB catalysts up to date. The addition of strong Brønsted acids, e.g., TfOH and HNTf$_2$ leads to a Brønsted acid assisted Lewis acid catalyst (BLA) system **3c•TfOH** (Fig. 4a).[22,23] Equally, the addition of Lewis acids, e.g., SnCl$_4$, AlCl$_3$, Et$_2$AlCl, and TiCl$_4$ provides the corresponding Lewis acid assisted Lewis acid catalyst (LLA) system **3c•AlCl$_3$** (Fig. 4b).[24]

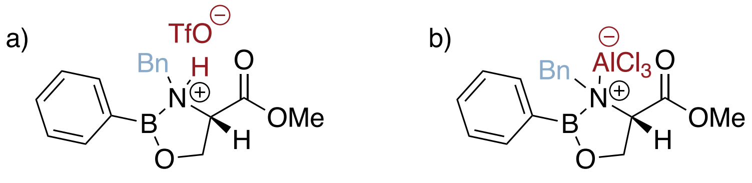

3c·TfOH **3c·AlCl$_3$**

Figure 4 Strategies for increasing the Lewis acidity of the OXB catalyst by Brønsted and Lewis acids. a) Corey's BLA.[22,23] b) Yamamoto's LLA.[24]

On the other hand, activation of OXBs can be achieved directly by using more electron deficient boronic acids like fluorinated analogues such as 3,5-bis(trifluoromethyl)phenylboronic acid or 4-fluorophenylboronic acid (Fig. 5).[19,25,26] Ideally, in addition to catalytic activation, the formation of OXBs **4c** and **5c** should also be affected positively, because of the higher electrophilicity of the fluorinated boronic acid.

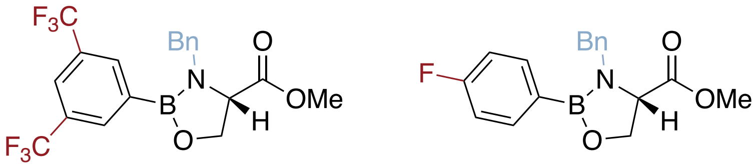

4c **5c**

Figure 5 Further strategies for increasing the Lewis acidity of the OXB catalyst through substitution of boronic acid precursor.[25]

In a first set of experiments, we tested the LLA and BLA systems for our serine derived OXB, regarding catalytic activity. Therefore, we employed 10 mol% of OXB **3c** with different Lewis Acids or Brønsted acids in the Diels-Alder reaction of methacrolein (**6**) and cyclopentadiene (**7**) (Tab. 1). LLA and BLA catalysts were typically synthesized by slowly adding 10 mol% of the co-catalyst to a solution of **3c** with subsequent stirring for 30 min. To exclude an uncatalyzed background reaction of the highly reactive methacrolein, low temperatures were necessary. At –10 °C no background reaction was observed (Table 1, entry 1). Moreover, the pure OXB was not active enough to catalyze the Diels-Alder reaction (entry 2). The pure co-catalysts in turn catalyzed the desired reaction to a small extent (entries 3, 5, and 7). Combining OXB and co-catalysts to LLA systems (entries 4 and 8) and BLA system (entry 6) provided the best conversion to the desired cycloadducts with high *endo* diastereoselectivity. These encouraging results indicate a first proof of principle, that an L-serine derived OXB can easily be synthesized and successfully employed in catalysis.

Table 1 Proof of principle Diels-Alder cycloaddition with catalyst **3c** as LLA or BLA system.

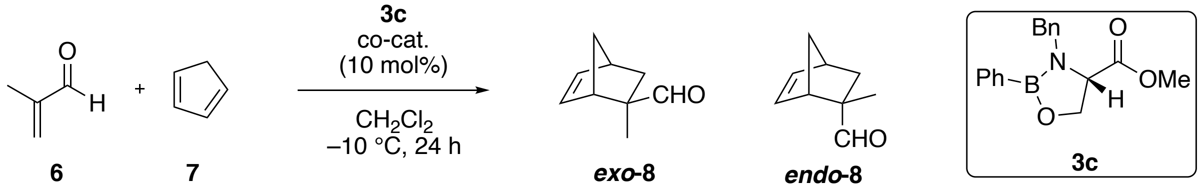

Entry	Cat. loading [mol%]	Co-catalyst	Conversion[a] [%]	*exo*:*endo*[a]
1	-	-	0	-
2	10	-	0	-
3	-	$SnCl_4$	38	1:4
4	10	$SnCl_4$	42	1:6
5	-	TfOH	35	1:34
6	10	TfOH	54	1:53
7	-	$AlCl_3$	15	1:14
8	10	$AlCl_3$	71	1:8

[a] Conversion and diastereoselectivity were determined *via* ^{1}H NMR spectroscopy with *para*-nitrobenzaldehyde as internal standard.

However, the addition of co-catalysts like Lewis acids or strong Brønsted acids to chiral peptides can lead to undesired coordination, racemization, or even decomposition. In addition to that, the utilization of metal based Lewis acids is contradictory to our organocatalytic concept.

Accordingly, we investigated the catalytic activation by more electron deficient boronic acids. The use of 3,5-bis(trifluoromethyl)phenylboronic acid for OXB formation provided catalyst **4c** in quantitative conversion. Purity of the crude reaction mixture was sufficient for use in catalysis. To test catalyst **4c**, we performed Diels-Alder reactions of croton aldehyde (**9**) and cyclopentadiene (**7**) under various reaction conditions (Tab. 2). At 0 °C no uncatalyzed background reaction occurred (entry 1). As expected, concentration and catalyst loading significantly affected the conversion, while the effect of reaction temperature was only marginal. Finally, we were able to achieve up to 96% conversion to the cycloadducts (entry 13). These experiments confirmed the much higher reactivity of OXB **4c** when using an electron deficient system like the 3,5-bis(trifluoromethyl)phenylboronic acid. However it is noteworthy, that in all reactions we achieved ***exo*-10** product as slightly favored diastereomer, which is contrary to the ***endo*-8** diastereoselectivity of the BLA and LLA systems depicted in Table 1.

Table 2 Organocatalytic Diels-Alder cycloaddition of crotonaldehyde **9** and cyclopentadiene **7** employing activated catalyst **4c**.

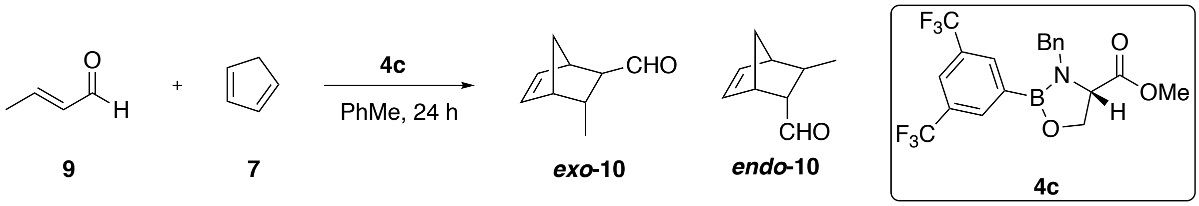

Entry	Conc. [mmol mL^{-1}]	Cat. loading [mol%]	T [°C]	Conversion[a] [%]	*exo*:*endo*[a]
1	1	-	0	0	-
2	3.5	5	−10	23	2.3:1
3	1	30	25	47	1.5:1
4	1	5	25	53	1.4:1
5	2	15	−10	57	2.1:1
6	2	15	0	58	1.8:1
7	3.5	5	25	64	1.4:1
8	2	15	25	83	1.2:1
9	2	30	25	85	1.1:1
10	2	30	−10	88	2.1:1
11	3.5	30	−10	90	2.0:1
12	2	30	0	95	1.5:1
13	2	20	0	96	1.7:1

[a] Conversion and diastereoselectivity were determined *via* ^{1}H NMR spectroscopy with *para*-nitrobenzaldehyde as internal standard.

2.2.1. Incorporation into a Test-Dipeptide

With the optimized procedures for catalyst formation and catalysis in hand, we incorporated the catalytic motif into a chiral peptide. The three-step synthesis for a simple test peptide starting from commercially available Boc-L-Ser-OBzl and L-phenylalanine is illustrated in Scheme 2. We decided to employ *tert*-butyloxycarbonyl (Boc) and benzyl protected L-serine as starting material, due to orthogonal reactivity to the methyl ester protecting group of L-phenylalanine or further amino acids. First, 1-ethyl-3-(3-dimethylaminopropyl)carbodiimide (EDC) promoted peptide coupling afforded dipeptide **13**. After hydrogenation and Boc-deprotection to **14**, we performed a reductive amination with benzaldehyde to yield **15c** as catalyst precursor.

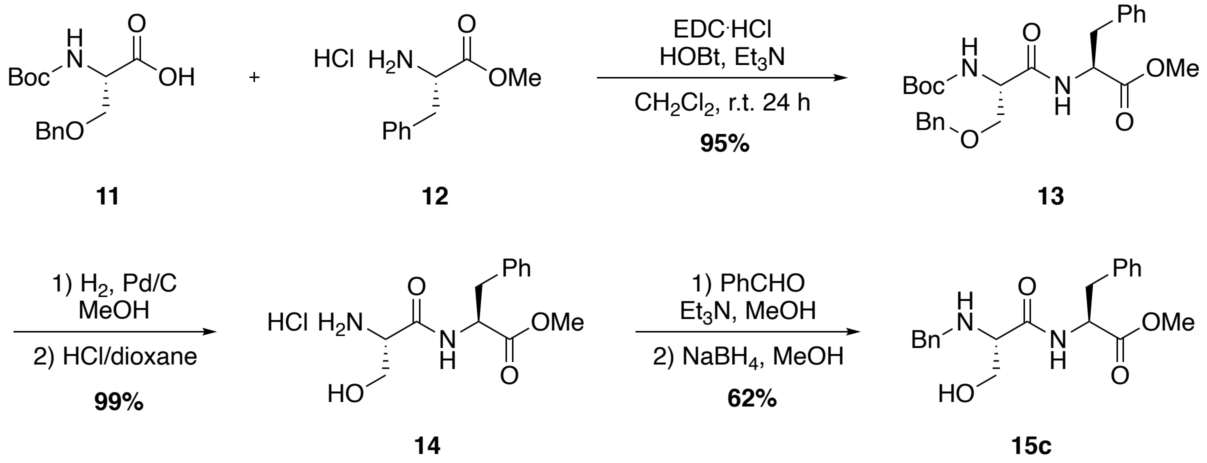

Scheme 2 Synthetic route to test precursor **15c**.

Following the protocol used for OXB formation with L-serine (Scheme 1), we employed dipeptide **15c** and 3,5-bis(trifluoromethyl)phenylboronic acid in an azeotropic condensation in toluene for 24 h (Scheme 3). Whereas the formation with the single amino acid quantitatively provided the desired OXB, the azeotropic distillation with dipeptide **15c** led to complex mixtures of OXB, starting material, and various other coordination adducts. Furthermore, refluxing peptide **15c** for 24 h in toluene led to partial thermal decomposition and racemization, which was monitored by chiral stationary phase HPLC analysis. Further studies at room temperature employing different water trapping agents (e.g., 4 Å molecular sieves, anhydrous $MgSO_4$) did not provide the desired catalyst **16c** in sufficient conversion and purity. Therefore we concluded, that boronic acids are not suitable for the formation of peptide based OXBs, as too harsh reaction conditions are necessary.

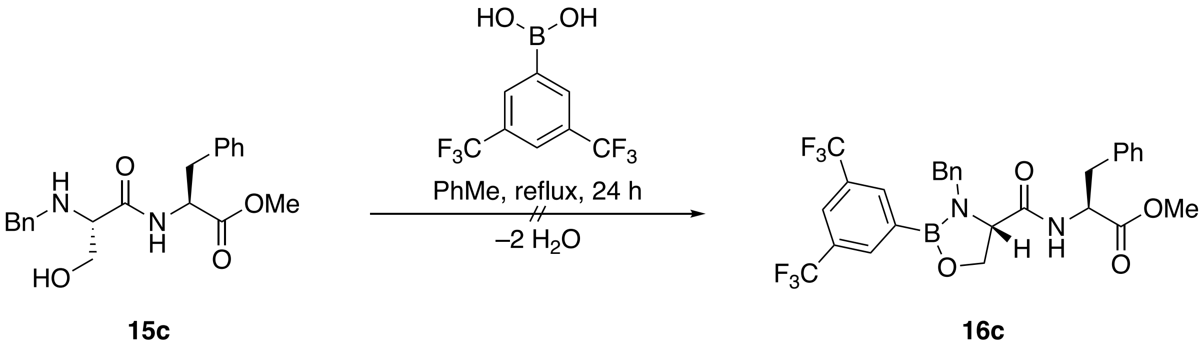

Scheme 3 Azeotropic condensation with peptide **15c** towards catalyst **16c**.

Since boronic acids were too unreactive, we anticipated the use of phenyl boron dichlorides as more reactive analogues. We made several attempts to synthesize electronically activated 3,5-bis(trifluoromethyl)phenyl boron dichloride (**2e**) by treatment of the corresponding boronic acid **2c** with BCl_3 (Scheme 4).[19,26] Unfortunately, **2e** is extremely sensitive towards air and moisture and thus hydrolyzed during the purification step even by distillation under Ar.

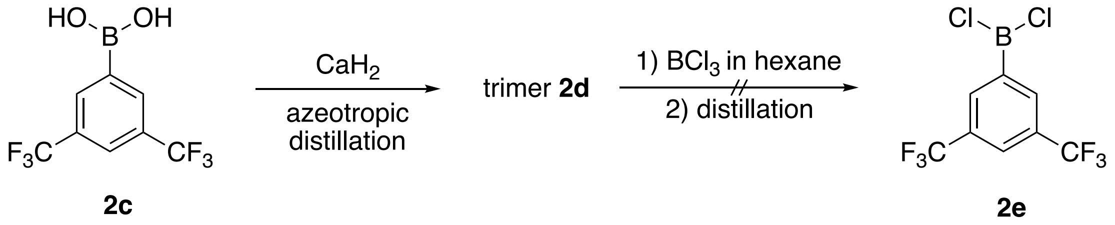

Scheme 4 Synthesis approach of 3,5-bis(trifluoromethyl)phenyl boron dichloride (**2e**).

As final compromise, we went back and chose the strategy of controlling the electronic activation *via* the nitrogen substituent while using commercially available phenyl boron dichloride (**2b**) to ensure OXB formation. Therefore, we functionalized the amine with an electron withdrawing sulfonyl group, instead of the electron donating benzyl group. Nucleophilic substitution of intermediate **14** with tosyl chloride provided precursor **15b** (Scheme 5a), which was then employed in OXB formation with phenyl boron dichloride (Scheme 5b). Therefore, an equimolar amount of the chloride was added to a solution of precursor **15b** at room temperature under Ar. After stirring for two hours, the solvent was removed under reduced pressure and the catalyst was dried. This time, clean and efficient formation of the peptide based OXB **16b** was accomplished.

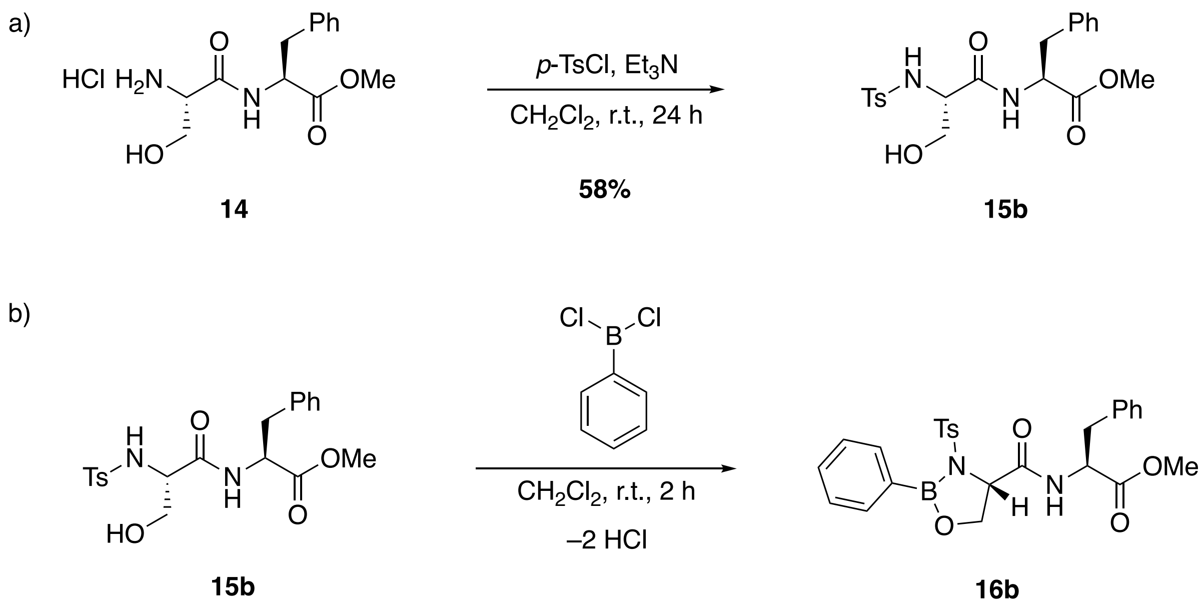

Scheme 5 a) Synthesis of precursor **15b** with tosyl as EWG. b) OXB **16b** formation with phenyl boron dichloride.

For investigation of catalytic efficiency, we employed the *in situ* formed catalyst **16b** in the DA cycloaddition of croton aldehyde (**9**) and cyclopentadiene (**7**) with 10 mol% catalyst loading (Tab. 3). Initially, we chose dichloromethane as solvent, to ensure sufficient solubility for both steps, the *in situ* catalyst formation as well as catalysis. To minimize a possible unselective background reaction, low temperatures were again necessary. At 0 °C, we observed no significant background reaction (Table 3, entry 1). Moreover, an amine catalyzed background reaction with the catalyst precursor could be excluded (entry 2). Phenyl boron dichloride itself provided a moderate background reaction with 47% conversion (entry 3). Therefore it was necessary, to achieve a full consumption of the phenyl boron dichloride in the previous *in situ* catalyst formation. In the presence of catalyst **16b**, the Diels-Alder reaction proceeded with good conversion (75%) but just low selectivity of 15% *ee* (entry 4). To trap remaining traces of HCl from catalyst preparation, we added 2,6-ditertbutylpyridine (D*t*BP) or diisopropylethylamine (D*i*PEA), which slightly decreased conversion but more importantly improved enantioselectivity (entries 5 to 8). Whereas 2.5 mol% of base generally led to good results, higher amounts of base (10 mol% or 20 mol%) greatly reduced the conversion. Utilization of activated 4 Å molecular sieves (MS) did not provide better results, but rather diminished enantioselectivity (entry 9). Best results (55% *ee*) were obtained with 2.5 mol% D*i*PEA at –20 °C (entry 10). Although lower temperatures may lead to higher enantioselectivities, –20 °C represented an acceptable trade-off between results and practicability. These experimental results confirmed, that a chiral peptide can be equipped with an OXB moiety to catalytically promote DA reactions in an enantioselective fashion.

Table 3 Diels-Alder cycloaddition of crotonaldehyde **9** with cyclopentadiene **7** catalyzed by dipeptide catalyst **16b**.

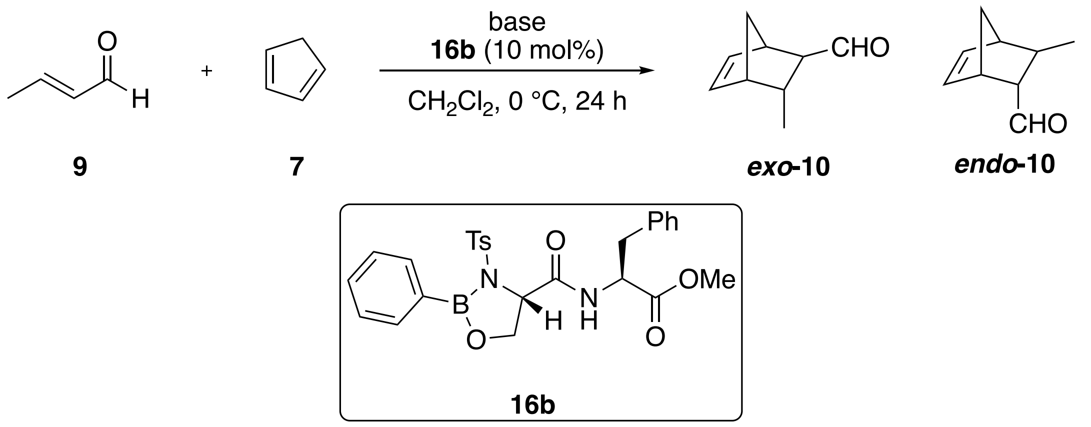

Entry	Base	Conversion[a] [%]	*exo*:*endo*[a]	*ee*[b] [%]
1[c]	-	0	-	-
2[d]	-	0	-	-
3[e]	D*t*BP[e] 10 mol%	48	1:4.0	-
4	-	75	1:3.9	15
5	D*t*BP 2.5 mol%	79	1:2.2	43
6	D*t*BP 10 mol%	56	1:2.2	47
7	D*t*BP 20 mol%	14	1:2.6	35
8	D*i*PEA 2.5 mol%	70	1:2.4	51
9[f]	D*i*PEA 2.5 mol%	55	1:2.9	7
10[g]	DiPEA 2.5 mol%	68	1:2.6	55

[a] Conversion and diastereoselectivity were determined *via* ^{1}H NMR spectroscopy with *para*-nitrobenzaldehyde as internal standard; [b] enantioselectivity was determined *via* chiral stationary phase GC; [c] background reaction; [d] reaction was performed only with the peptide catalyst precursor **15b**; [e] reaction was performed without peptide only with phenyl boron dichloride and base; [f] with 4 Å MS; [g] reaction was performed at –20 °C.

Next, we turned our attention towards the peptide architecture. Further L-serine derived dipeptides were synthesized, all equipped with a tosyl group for electronic activation. Afterwards, we employed the corresponding OXBs **16b**-**16f** in DA cycloadditions under the previously tested conditions (Tab. 4). The L-Serine derived OXB **1b** catalyzed the reaction to 65% yield, but with just 5% enantioselectivity (entry 1). With an attached L-phenylalanine as second amino acid, the selectivity greatly increased to 51-55% *ee* (entries 2-3). Comparing the results of catalyst stereoisomers **16b** and **16c** (entries 3-4), we observed a match/mismatch effect. Since **16c** provided the lower selectivity, D-amino acids should be negligible. Replacement of L-phenylalanine with L-alanine or L-cyclohexylalanine failed to afford catalysts with improved activity or enantioselectivity (entries 5 and 6). In addition to that, when we introduced a bulky achiral adamantyl substituent **16f**, the cycloaddition proceeded nearly racemically (entry 7). When applying our best working catalyst **16b** to methacrolein as substrate, the selectivity decreased to 21% *ee* (entry 8). On the other hand, the reduction of cinnamaldehyde delivered the best selectivity so far with up to 58% *ee* (entry 9).

Table 4 Diels-Alder cycloadditions employing various dipeptide catalysts.

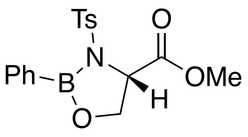

1b

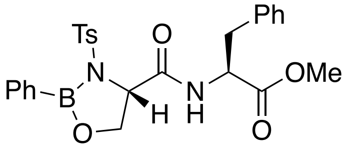

16b

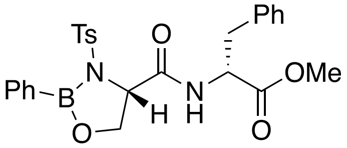

16c

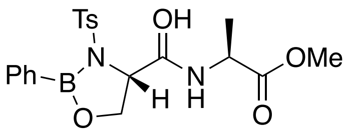

16d

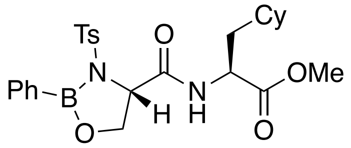

16e

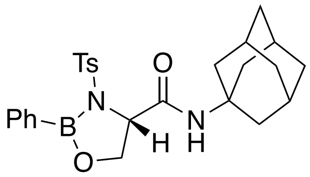

16f

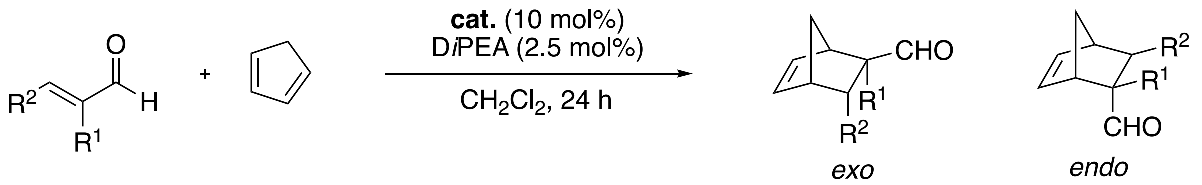

Entry	Catalyst	R^1	R^2	Conversion^a [%]	*exo*:*endo*^{a}	*ee*^{b} [%]
1^c	**1b**	H	CH_3	65	1:2.1	5
2^c	**16b**	H	CH_3	70	1:2.4	51
3	**16b**	H	CH_3	68	1:2.6	55
4	**16c**	H	CH_3	64	1:2.4	34
5	**16d**	H	CH_3	14	1:3.4	12
6	**16e**	H	CH_3	15	1:3.8	21
7	**16f**	H	CH_3	25	1:5.2	1
8	**16b**	CH_3	H	69	1:5.9	21
9	**16b**	H	Ph	60	1:2.1	58

[a] Conversion and diastereoselectivity were determined *via* ^{1}H NMR spectroscopy with *para*-nitrobenzaldehyde as internal standard; [b] enantioselectivity was determined *via* chiral stationary phase GC; [c] reaction was performed at –10 °C.

These results clearly indicate, that the enantioselectivity is determined by a second chiral amino acid or peptide backbone. Moreover, the reaction greatly benefits from L-phenylalanine, as both, conversion and enantioselectivity improve, compared to the L-cyclohexylalanine derivative **16e** or the catalytic moiety **1b** itself. This might be due to stabilizing NCIs in the transition structure of the cycloaddition, which are preferable in the case of L-phenylalanine derivative **16b**, probably because of σ-π interactions. To clarify this issue, conformational analysis using a semiempirical tight binding method (GFN2-xTB) followed by high level density functional theory (DFT) calculations with Grimme's D3-dispersion correction and Becke-Johnson damping function would be necessary.[27–29] These insights could also help to optimize the peptide architecture to maximize enantioselectivity. However, this is highly time consuming and could not be carried out during this project.

2.2.2. Application in Formal Hetero-Diels-Alder reactions

To test the utility of our peptide based OXB approach, we aimed to employ dipeptide **16b** in the synthesis of valuable synthons for natural product synthesis. For this purpose, we selected 1-methoxy-3-trimethylsilyloxy-1,3-butadiene (**17**; Danishefsky diene) as a highly versatile compound in organic synthesis.[30] Its electron-rich nature accounts for the use as reactive reagent, especially in thermally promoted Diels-Alder reactions with α,β-unsaturated aldehydes to chiral cyclohexenones **19a** (Scheme 6a).[31] More importantly, the Lewis acid mediated reaction of **17** with aldehydes enables a Mukaiyama aldol reaction to **20**, which after acidic hydrolysis of the silyl ether cyclizes to 2-substituted 2,3-dihydro-4H-pyran-4-ones **21a** (Scheme 6b).[32] Dihydropyranones are commonly applied synthons in the synthesis of natural products and biologically active compounds.[33–35]

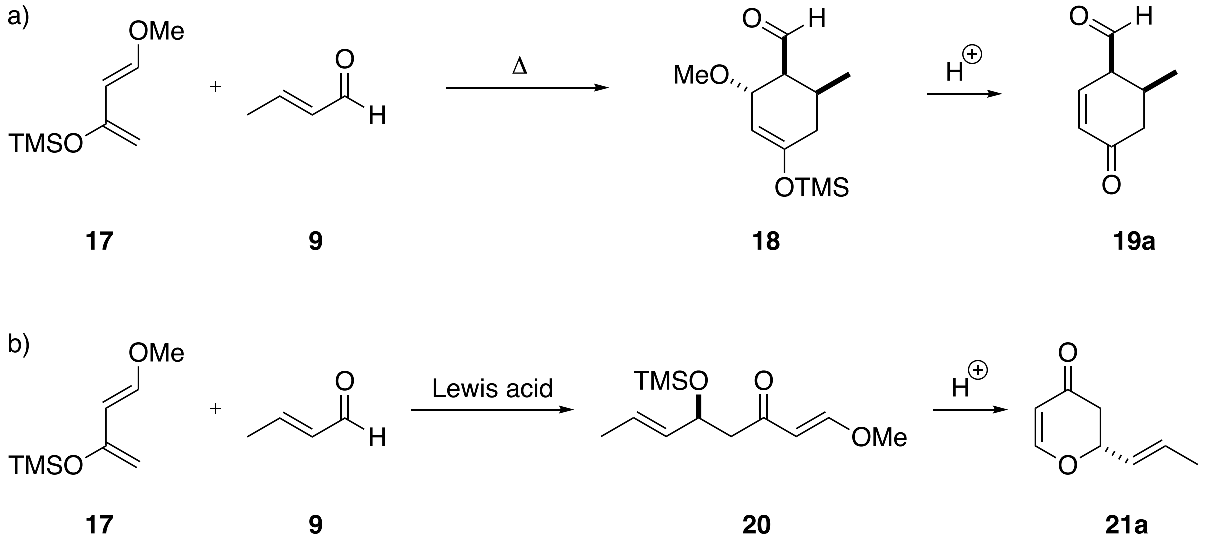

Scheme 6 Differing reactivity of the Danishefsky diene (**17**). a) Thermal treatment provides the [4+2] cycloaddition product **18**, which can be hydrolyzed to cyclohexenone **19a**. b) Lewis acid catalysis enables a two-step Mukaiyama aldol-Michael sequence to dihydropyranone **21a**.

Before testing dipeptide **16b** in the catalytic reactions, we synthesized the corresponding dihydropyranones **21** as racemic mixtures. BF_3 catalyzed aldol reaction at –78 °C, followed by hydrolysis with TFA provided the racemic products **21a-c** in moderate yield (Scheme 7). Afterwards, we separated the enantiomers *via* chiral HPLC.

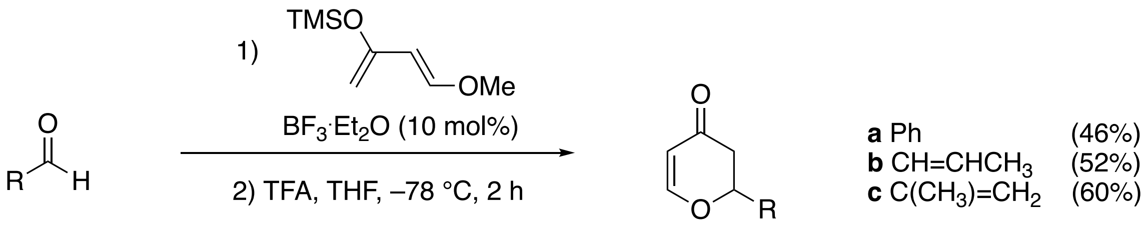
1)
TMSO
OMe
BF3·Et2O (10 mol%)
2) TFA, THF, –78 °C, 2 h
O
R
H
O
O
R
a Ph (46%)
b CH=CHCH3 (52%)
c C(CH3)=CH2 (60%)

21

Scheme 7 Synthesis of racemic dihydropyranone standards **21a**-**c** .

Subsequently, we performed the reactions with chiral dipeptide **16b** in CH_2Cl_2 (Tab. 5). At room temperature low conversion to the thermal mediated cycloaddition products **19** was observed. This background reaction was absent at 0 °C. We employed 10 mol% of catalyst and 2.5 mol% D*i*PEA to trap traces of HCl remaining from the *in situ* catalyst formation. After 24 h, the reactions were quenched and the aldol products were hydrolyzed by addition of TFA. All reactions provided the desired dihydropyranones **21**, but just in low to moderate yield (Tab. 5). Variation of temperature did not play an important role. The aldol reactions with crotonaldehyde and benzaldehyde provided low enantioselectivities (entries 1-4), while the reaction with methacrolein did not deliver any selectivity (entries 5-6).

Table 5 Catalyzed Mukaiyama aldol reaction with subsequent acidic treatment to dihydropyranones **21a**-**c**

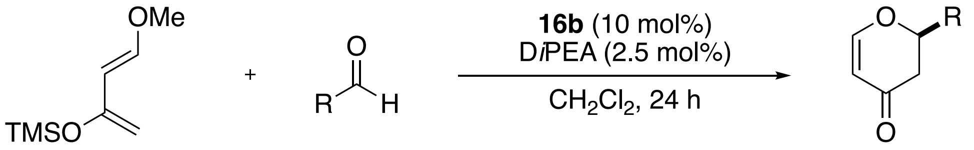
OMe
TMSO
+
O
R
H
16b (10 mol%)
DiPEA (2.5 mol%)
CH2Cl2, 24 h
O
R
O

Entry	T [°C]	Aldehyde	Product	Yield^a [%]	ee^b [%]
1	25	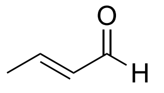	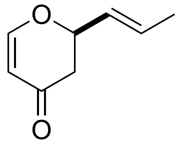	55	4
2	0			48	6
3	25	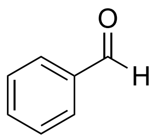	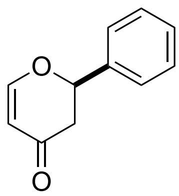	41	8
4	0			40	11
5	25	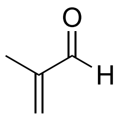	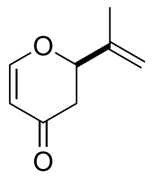	32	0

6	0	30	0

[a] Yield of isolated product; [b] enantioselectivity was determined *via* chiral stationary phase HPLC.

Due to the moderate yields and low selectivities even under the previously optimized reaction conditions, further investigations with Danishefsky diene **17** were not pursued. In addition to that, the high expense for optimization of this new catalytic moiety regarding *in situ* formation and catalysis led us to the conclusion to stop our approach with L-Ser, but rather to rely on a known and more common OXB moiety to a attach at a peptide backbone.

2.3. Prolinol-Based Catalyst Precursor

2.3.1. Synthesis of *trans*-4-Hydroxyproline as Catalyst Precursor

As mentioned before, we had to find a better suitable catalytic moiety without the need for comprehensive optimization of OXB formation and catalytic usage. In comparison to L-serine (Chapter 2.2), diphenylprolinol based OXBs are common catalysts for several catalytic transformations, especially CBS reductions and cycloadditions.[22,24,36] Moreover 4-hydroxy-proline is attachable to peptides *via* the hydroxy group. Therefore, we chose *trans*-4-hydroxyproline as starting material, as there are already a few reports about the successful use as precursor for OXBs.[37,38]

Starting from commercially available *trans*-4-hydroy-L-proline (**22**) we synthesized the methyl ester using thionyl chloride in methanol followed by benzyl protection to yield **23** in almost quantitative yield (Scheme 8). Considering a further functionalization with amino acids and peptides, we selected benzyl as amine protecting group, since reactivity of the benzyl group is orthogonal to fluorenylmethoxycarbonyl (Fmoc) and boc, respectively. Ester **23** was transformed in a double Grignard reaction to diphenylprolinol derivative **24**, which we attached to L-phenylalanine *via* a DMAP mediated Steglich type esterification. Finally, reductive cleavage of the benzyl group provided catalyst precursor **26**. The hydrogenation step required a minimum of 20 mol% of Pd/C and the addition of a small amount of acetic acid was necessary to inhibit catalyst poisoning.[39] With this strategy, the protected catalytic moiety **24** could easily be used as a building block to functionalize amino acids and peptides.

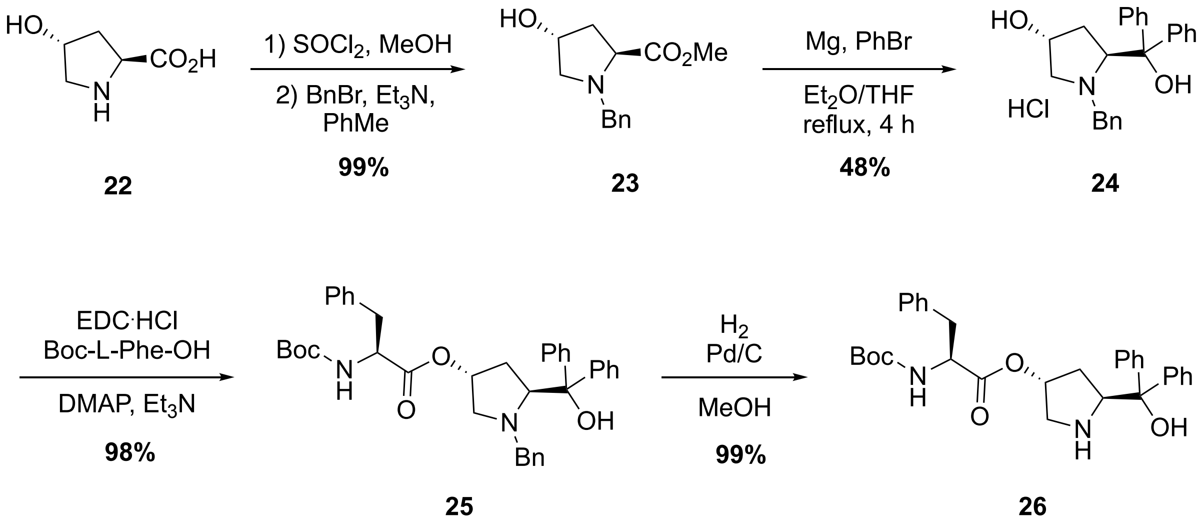
22
1) SOCl2, MeOH
2) BnBr, Et3N, PhMe
99%
23
Mg, PhBr
Et2O/THF reflux, 4 h
48%
24
EDC·HCl
Boc-L-Phe-OH
DMAP, Et3N
98%
25
H2
Pd/C
MeOH
99%
26

Scheme 8 Synthesis of diphenylprolinol-based OXB precursor **26**.

2.3.2. Diels-Alder reaction

With catalyst precursor **26** in hand, we turned our attention to the formation of OXB **27a** (Scheme 9). To circumvent the use of additional co-catalysts (e.g., metal based Lewis acids) in subsequent reactions, we employed 3,5-bis(trifluoromethyl)-phenylboronic acid again to enhance the Lewis acidity of the catalyst's boron center. An azeotropic distillation (cf. Chapter 1, Fig. 2) provided catalyst **27a** with sufficient purity for further catalysis.

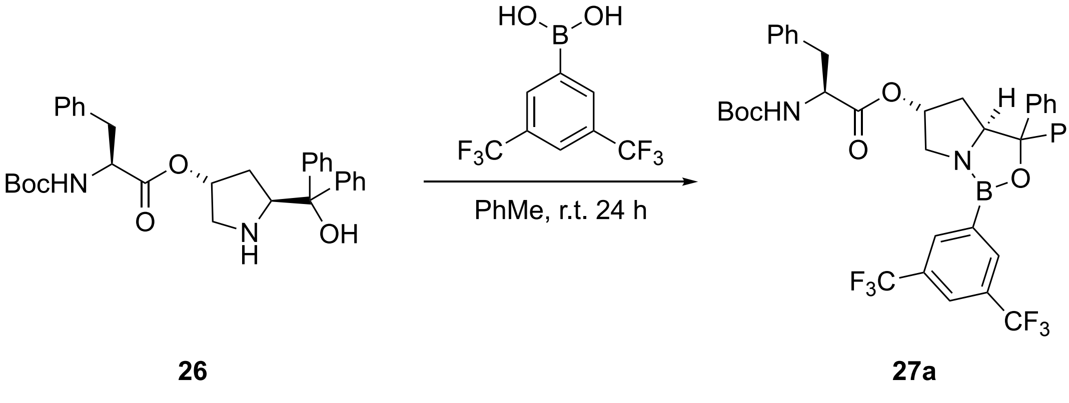
PhMe, r.t. 24 h
26
27a

Scheme 9 Formation of hydroxyproline derived OXB **27a**.

With the working *in situ* formation of **27a**, we performed benchmark cycloadditions of crotonaldehyde (**9**) and cyclopentadiene (**7**) to test for catalytic activity (Tab. 6). To minimize an unselective background reaction, low temperatures were necessary. At 0 °C, no uncatalyzed background reaction occurred (Table 6, entry 1). When employing solely 3,5-bis(trifluoromethyl)phenylboronic acid the cycloaddition proceeded in moderate yield (entry 2).

Unfortunately, the chiral OXB **27a** provided only poor yield and enantioselectivity (entry 3). With a catalyst loading of 20 mol%, we achieved 32% *ee*, but yield remained low (entry 4).

Table 6 Catalyzed Diels-Alder reaction to test the catalytic activity of OXB **27a**.

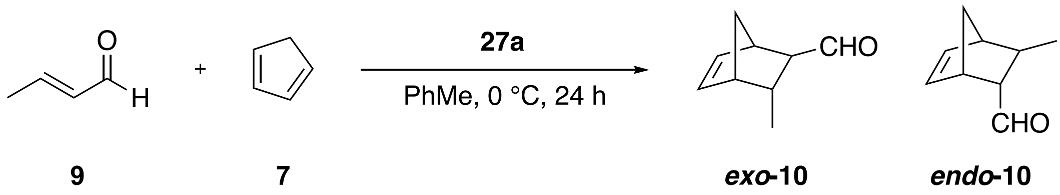

Entry	Cat. loading [mol%]	Conversion[a] [%]	*exo*:*endo*[a]	*ee*[b] [%]
1	-	0	-	-
2	10[c]	40	1:5.6	-
3	10	3	1:2.7	6
4	20	6	1:2.7	32

[a] Conversion and diastereoselectivity were determined *via* ^{1}H NMR spectroscopy with *para*-nitrobenzaldehyde as internal standard; [b] enantioselectivity was determined *via* chiral stationary phase GC; [c] reaction was performed with 10 mol% of bis(trifluoromethyl)boronic acid as catalyst.

This indicates that the catalytic activity of OXB **27a** without a co-catalyst is lower compared to the sole boronic acid and therefore not sufficient for DA cycloadditions with crotonaldehyde (**9**). Even though we could employ more reactive dienophiles (e.g., methacrolein), we would also have to decrease reaction temperature to inhibit background reactions. As the possibilities for further activation of hydroxyproline derived OXBs without the addition of co-catalysts are limited, further optimization of the reaction conditions seemed not promising.

2.3.3. CBS Reduction

Having the *trans*-4-hydroxy-L-proline derived OXB precursor **26** in hand, it was also tested in the CBS reduction of prochiral ketones. The advantage of CBS reductions compared to cycloadditions is that borane can be used as reducing agent as well as reagent for OXB formation. Moreover, the use of borane facilitates the *in situ* catalyst formation by extrusion of hydrogen as driving force. In addition to that, there are no possible impurities from boronic acids and further additives to trap HCl are not necessary.

We compared dipeptide OXB **27b** with the original CBS catalyst **28** in the reduction of several ketones employing $BH_3{\cdot}SMe_2$ as reducing agent. (Tab. 7). We used THF as solvent and performed the reduction at 50 °C, as slightly elevated temperatures have proven to be more beneficial for selectivity in borane reductions (Table 7, entries 1 and 2).[40,41] To minimize the uncatalyzed background reaction with BH_3 itself, we slowly added a solution of the substrate *via* a syringe pump to the catalyst solution. Performing the reductions at 50 °C both catalysts provided quantitative conversion to the corresponding chiral alcohols in all cases. To our delight, the hydroxyproline derived catalyst **27b** facilitated the reductions with selectivities in a comparable range to the original CBS catalyst **28** for all substrates. Ketones bearing rigid cyclic π-electron rich substituents (entries 1, 2, 12, and 13) as well as sterically demanding ketones (entries 3-5 and 8 and 9) were reduced in high selectivities up to 89% *ee*. These ketone substituents account for strong DED, which probably are beneficial to achieve high enantioselectivities. More conformationally flexible ketones bearing aliphatic substituents certainly resulted in lower selectivities in the range of 60-71% *ee* (entries 6, 7 and 10, 11).

Table 7 CBS reduction of several ketones catalyzed by OXBs **27b** and **28**.

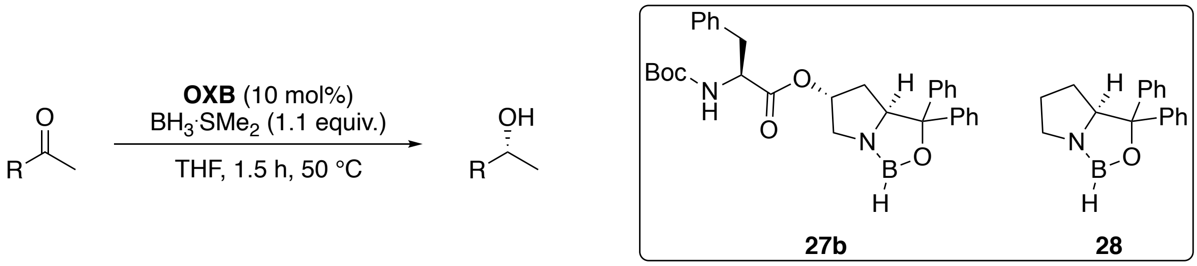

Entry	OXB	R	Conversion[a] [%]	*ee*[a] [%]
1[b]	**27b**	Ph	88	78
2	**27b**	Ph	99	88
3	**28**	Cy	99	86
4	**27b**	Cy	99	85
5[b]	**27b**	Cy	84	68
6	**28**	CH_2CH_2Ph	99	71
7	**27b**	CH_2CH_2Ph	99	65
8	**28**	^{t}Bu	99	98
9	**27b**	^{t}Bu	99	89
10	**28**	*n*-hept	99	60
11	**27b**	*n*-hept	99	62
12	**28**	cyclopropyl	99	91
13	**27b**	cyclopropyl	99	81

[a] Conversion and enantioselectivity were determined *via* chiral stationary phase GC; [b] reaction was performed at 25 °C.

Next we investigated the effect of the attached amino acids. For this purpose, we synthesized additional catalyst precursors *via* the synthesis route discussed in Scheme 8 of Chapter 2.3.1. The corresponding OXBs **27b** and **29b-31b** were employed in the reduction of acetophenone and 2-butanone under the previously used conditions (Tab. 8). In the reduction of acetophenone (entries 1-5), all catalysts achieved high yields, with just minor differences in selectivity. For 2-butanone, the overall selectivity was lower (entries 6-10). This is not surprising, as 2-butanone is just a small molecule with quite similar substituents, hence extremely difficult to differentiate for a catalyst. However, all catalysts performed in a comparable range of selectivity and the peptide-based OXBs **27b** and **29b-31b** catalyzed the reductions with just slightly lower selectivities compared to **28**. Seemingly, it did not play an important role, which amino acids were attached to the catalytic moiety, as even the attached dipeptides **30b** and **31b** hardly influenced the enantioselectivity. This rather demonstrates that just the prolinol core determines the high enantioselectivity of the reduction.

Table 8 CBS reduction of ketones catalyzed by *trans*-4-hydroy-L-proline derived OXBs **27b** and **29b-31b**.

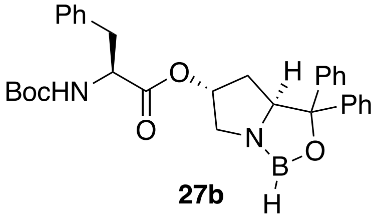
Ph
BocHN
O
O
H Ph
Ph
N
B
O
H

27b

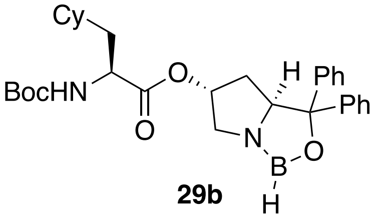
Cy
BocHN
O
O
H Ph
Ph
N
B
O
H

29b

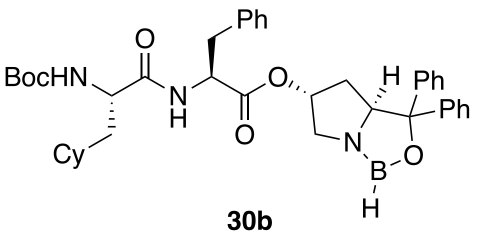
O
Ph
BocHN
N
H
Cy
O
O
H Ph
Ph
N
B
O
H

30b

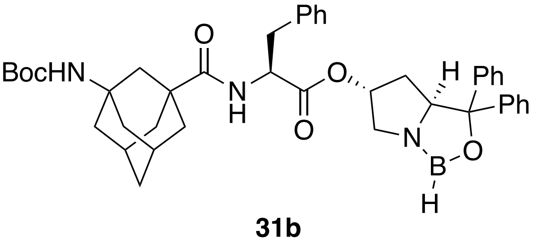
O
Ph
BocHN
N
H
O
O
H Ph
Ph
N
B
O
H

31b

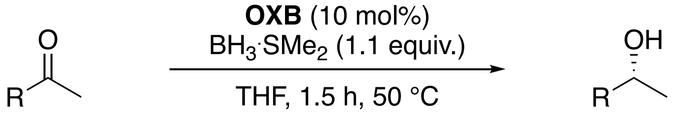
O
R
OXB (10 mol%)
BH3·SMe2 (1.1 equiv.)
THF, 1.5 h, 50 °C
OH
R

Entry	OXB	R	*ee*[c] [%]
1	**28**	Ph	97
2	**27b**	Ph	88
3	**29b**	Ph	84
4	**30b**	Ph	82
5	**31b**	Ph	83
6	**28**	Et	60
7	**27b**	Et	62
8	**29b**	Et	57
9	**30b**	Et	55
10	**31b**	Et	54

[a]: Conversion and enantioselectivity were determined *via* chiral stationary phase GC; unless otherwise noted, conversion was 99%.

3. Summary and Outlook

In this project, a major part of effort focused on the research of an OXB as catalytic moiety, which can be attached to an amino acid or a peptide backbone. As OXBs are highly sensitive towards hydrolysis, it was necessary to investigate an appropriate precursor, which can reliably be transformed into an OXB, even when other functional groups such as amides are present.

In the first part, we developed an *in situ* protocol for the OXB formation based on L-serine as readily available amino acid. L-Serine was easily attachable to other amino acids *via* the carboxylic acid and offered the possibility for OXB formation at the vicinal amino alcohol. Lewis acidity was tuned by EWG/EDG substitution of the amine. It turned out that an EWG such as tosyl is necessary to obtain sufficient catalytic activity. While simple boronic acids were too unreactive, phenyl boron dichloride facilitated the OXB formation in a clean and quantitative fashion. With test peptide **16b** we achieved 68% yield and 55% *ee* in the DA cycloaddition of cyclopentadiene (**7**) and crotonaldehyde (**9**) as benchmark reaction (Scheme 10). In this reaction, the OXB of the single L-serine moiety itself did not provide much selectivity, but rather the attached phenylalanine induced enantioselectivity. This means, that the peptide backbone controlled the selectivity and therefore should be tailored to the needs of specific substrates in the future. However, high optimization effort would be necessary. For future investigations I would recommend to perform quantum mechanical computations of the transition structures employing high level DFT calculations with D3 correction and BJ damping function to determine the present NCIs (e.g., H-bonding, dispersion, sterics), which control the selectivity.[27–29]] Based on these results, a reasonable extension and modification of the peptide, making use of the *chiral pool,* could improve catalytic results. Alternatively, machine learning approaches like conformer dependent quadrant models are a very topical issue, which undisputedly would help to determine most suitable amino acid sequences for peptide catalysts.[42]

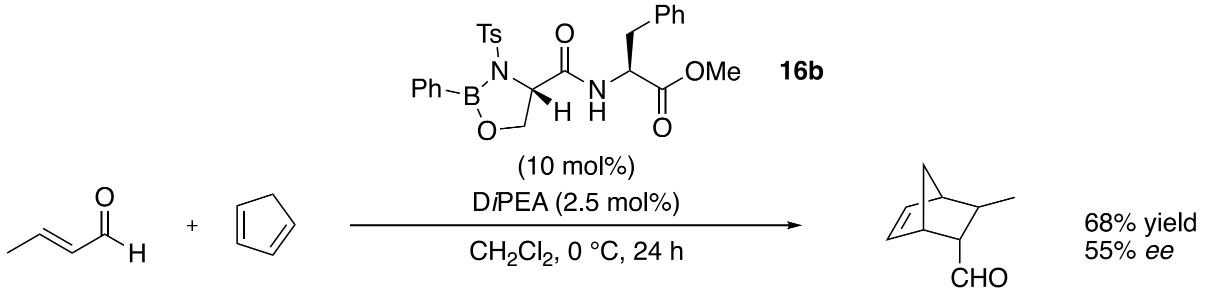

9 **7** ***endo*-10**

Scheme 10 Diels-Alder reaction of cyclopentadiene (**7**) and crotonaldehyde (**9**) catalyzed by the *in situ* formed OXB **16b**.

In the second part of this project, we employed *trans*-4-hydroxy-L-proline as precursor for a peptide based OXB. Analogous to the original proline based CBS catalysts, we transformed *trans*-4-hydroxy-L-proline *via* a double Grignard route to a diphenylprolinol derivative, which worked as an OXB precursor. We attached amino acids and peptides *via* Steglich esterification at the 4-hydroxy function and employed the resulting catalysts in DA reactions of crotonaldehyde (**9**) and cyclopentadiene (**7**) as well as CBS reductions of prochiral ketones. However, the *trans*-4-hydroxy-L-proline derived OXB did not show sufficient catalytic activity to promote DA reactions. On the other hand, CBS reductions were successfully catalyzed with almost quantitative conversion and high enantioselectivity (Scheme 11). In contrast to the L-serine based catalysts in Chapter 2.2, the diphenylprolinol moiety itself determined the enantioselectivity, while the attached amino acids barely influenced the selectivity of the CBS reduction.

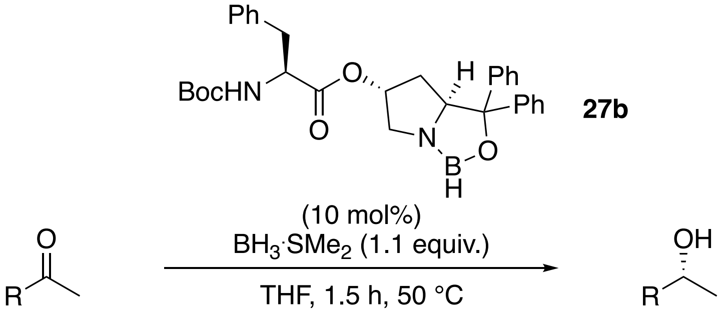

Scheme 11 CBS reduction of prochiral ketones catalyzed by *trans*-4-hydroxy-L-proline derived OXB **27b**.

As additional amino acids did not affect the reactivity or selectivity of the CBS reduction, a multicatalyst approach could be conceivable. However, it must be considered that an orthogonal reactivity of all individual catalytic motifs has to be guaranteed in this case.[43] Since most peptide based organocatalysts commonly bear functional groups such as amines for enamine/iminium activation and acyl transfer, NHCs or thiourea derivatives, orthogonal reactivity with borane cannot be easily realized. Borane is strongly oxophilic and sensitive to nucleophiles, which is why it would react with most catalytic motifs.[44,45] Thus an application for synergistic/dual catalysis and tandem/relay catalysis, in which the reaction conditions are the same in both catalytic steps, should be excluded. The only reasonable application would be sequential multicatalysis in which the asymmetric reduction is the first step. The intermediate, which is an unstable borinate species, could then be further functionalized directly by changing the reaction conditions.

However, the actual advantage of this peptide-based OXB could lie in the area of site-selective and regioselective catalysis. The selective modification of small molecules to deliver complex biomolecules mimics enzymatic catalysis and thus is applicable to peptide catalysis.[46–48] Moreover, site-selective borane reductions are a largely unexplored area. In line with previously published work on the site selective acylation of pyranosides, synthetic organocatalysts that can site-selectively distinguish between different ketones would hence be a logical and valuable extension for peptide- as well as borane chemistry.[48–50] The flexible peptide backbone may control the site selectivity through its secondary structure or binding pocket, while the prolinol motif determines the arrangement of the carbonyl to the reducing agent and thus controls the stereochemistry.

A site- and stereoselective reduction of α-diketones to chiral α-hydroxy ketones could be suitable. Optically active α-hydroxy ketones are useful synthons in organic chemistry, e.g., for natural products synthesis.[51–53] The selective reduction of α-diketones to α-hydroxy ketones can be enzymatically mediated by yeast[54] or by transition metal complexes.[55] Alternatively, access to chiral α-hydroxy ketones is possible *via* an enzyme catalyzed kinetic resolution of their racemic analogues or by kinetic resolution of 1,2-diols with subsequent oxidation.[56,57] However, the substrate scope is rather limited employing these methods. Hence, a direct selective organocatalyzed reduction to α-hydroxy ketones would be an elegant extension. In addition to that, the site-selective reduction of steroidal ketones (e.g., cortisone (**32**)), which are selectively oxidized and reduced by 11β-hydroxysteroid dehydrogenase (11β-HSD) could be possible (Scheme 12).[58]

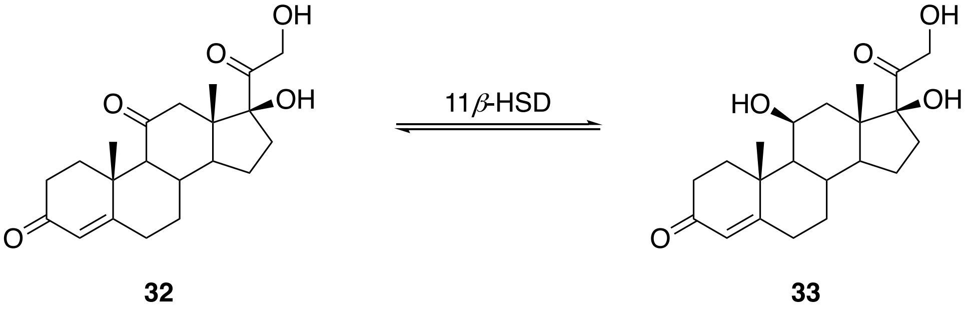

Scheme 12 Site-selective reduction/oxidation of cortisone (**32**) by 11β-hydroxysteroid dehydrogenase (11β-HSD).

As point of entry, the first step is to compare the selectivity of CBS catalyst **28** with peptide-based catalyst **37** in the reduction of α-diketone **35**, decalin **35**, and androstane-3,17-dione (**36**) (Fig. 6) - all ketones are commercially available. The suggested architecture of peptide catalyst **37** bearing an adamantane γ-amino acid in the backbone to provide a dynamic binding pocket is inspired by the work of the Schreiner group.[3] The catalyst can easily be synthesized with building block **24** *via* the synthesis route discussed in Scheme 8 of Chapter 2.3.1.

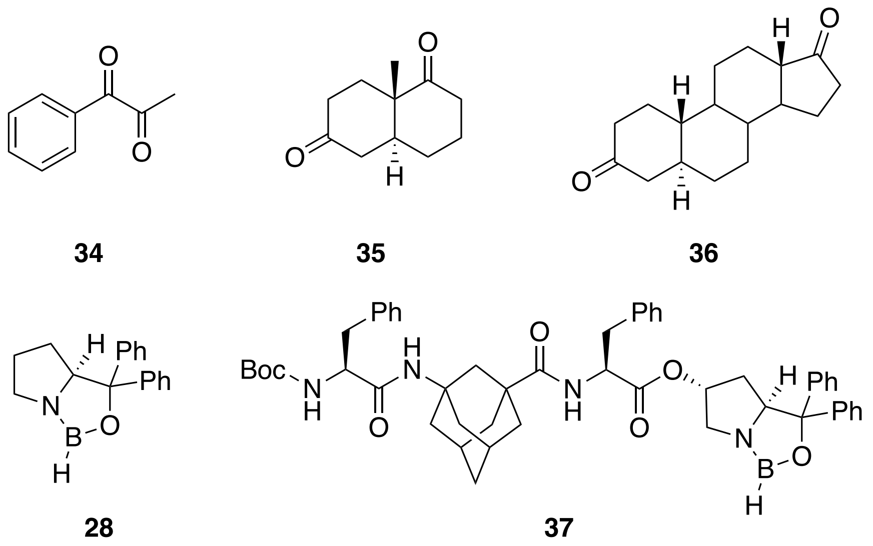

Figure 6 Possible starting point for the investigation of a site-selective CBS reduction.

4. Experimental Section

4.1. General Information

Unless otherwise noted, chemicals were purchased from Acros Organics, TCI, Alfa Aesar, Lancaster, Merck, or Fluka at the highest purity grade available and were used without further purification. All solvents were distilled prior to use. Toluene, THF, and CH_2Cl_2 were distilled from appropriate drying agents prior to use and stored under argon atmosphere. All catalytic reactions were carried out under an argon atmosphere employing oven- and flame-dried glassware. Column chromatography was conducted using Merck silica gel 60 (0.040 – 0.063 mm).

4.2. Analytical Methods

Thin Layer Chromatography (TLC) was performed on silica coated glass plates (*Merck*, silica 60 F254) with detection by UV-light ($\lambda = 254$ nm) and/or by staining with a with a cerium ammonium molybdate solution [CAM] followed by heat treatment.

CAM-staining solution: cerium sulfate tetrahydrate (1.00 g), ammonium molybdate (25.0 g) and concentrated sulfuric acid (25.0 mL) in water (250 mL).

Nuclear Magnetic Resonance-Spectra were recorded at room temperature either on a *Bruker* AV-400, ^{1}H NMR spectra were referenced to the residual proton signal of $CDCl_3$ ($\delta = 7.26$ ppm). ^{13}C NMR spectra were referenced to the ^{13}C-D triplet of $CDCl_3$ ($\delta = 77.16$ ppm). The following abbreviations for single multiplicities were used: *br*-broad, s-singlet, d-doublet, t-triplet, q-quartet, quint-quintet, sept-septet.

High resolution mass spectrometry (HRMS) was performed employing a Bruker MicrOTof using methanol solutions of the respective compounds.

Chiral Gas Chromatography (GC): Enantioselectivities were determined by chiral stationary phase GC analyses on Hewlett Packard 5890 or 6890 gas chromatographs, respective

4.3. Standards for Catalysis

4.3.1. Cycloaddition Standards

The standards for the Diels-Alder reaction were synthesized according to a published protocol by MacMillan *et al*. employing a chiral amine catalyst.[59] Conversion and diastereoselectivity of the catalyzed reactions were determined by ^{1}H NMR spectroscopy employing *p*-nitrobenzaldehyde as internal standard.

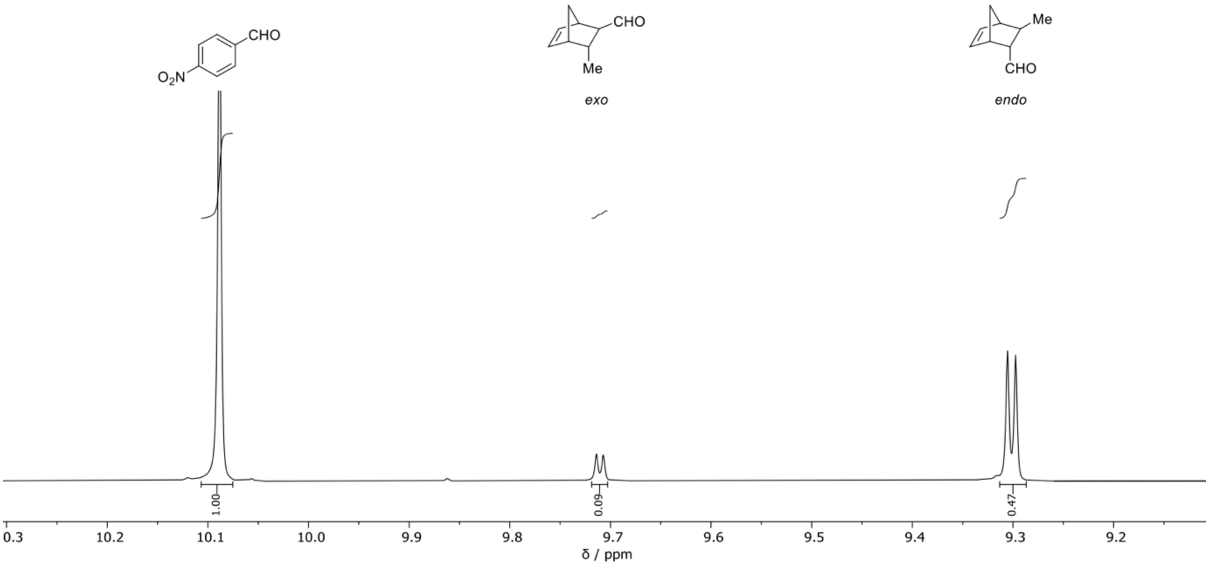

Enantioselectivity was determined *via* chiral stationary phase GC. Retention times were assigned to the absolute stereochemistry by comparison with published results of a known catalyst. [59]

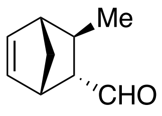

endo

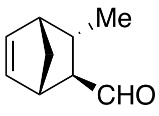

exo

Enantioselectivity was determined *via* chiral stationary phase GC employing a 30 m FS-Hydrodex β-6TBDM column (Macherey Nagel).

T (Injector + Detector) = 250 °C

Splitflow = 80 mL min^{-1}

Precolumn pressure = 0.8 bar

Conditions: 80 – 200 °C, 2 °C min^{-1}

Retention Times: *exo* isomers: 22.4 min; 22.8 min; *endo* isomers: (*R*,*S*) = 23.8 min; (*S*,*R*) = 24.2 min.

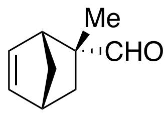

endo

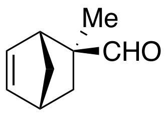

exo

Enantioselectivity was determined *via* chiral stationary phase GC employing a 30 m FS-Hydrodex β-6TBDM column (Macherey Nagel).

T (Injector + Detector) = 250 °C

Splitflow = 80 mL min^{-1}

Precolumn pressure = 0.8 bar

Conditions: 80 – 160 °C, 2 °C min^{-1}

Retention Times: *exo* isomers: 38.1 min; 38.3 min; *endo* isomers: (*R*,*S*) = 40.1 min; (*S*,*R*) = 40.2 min.

4.3.2. Cycloaddition Products of the Danishefsky Diene

A flame dried flask under Ar was charged with the aldehyde (1.00 equiv.) in THF. At –78 °C, Danishefsky's diene (1.00 equiv.) and catalytic amounts of $BF_3{\cdot}Et_2O$ (10 mol%) were added and the reaction mixture was stirred at –78 °C for 2 h. The reaction was quenched by addition of sat. aq. $NaHCO_3$ solution and the aqueous phase was extracted with CH_2Cl_2 (3×). The combined organic layers were treated with trifluoracetic acid (0.037 mL, 0.470 mmol, 1.00 equiv.) and stirred at r.t. for 2 h, and then quenched by the addition of 5 mL sat. aq. $NaHCO_3$ solution. The organic phase was separated, dried over Na_2SO_4, filtered, and the solvent was removed under reduced pressure. After purification by column chromatography the dihydropyrones were obtained as the final product.[32,60]

2,3-Dihydro-2-phenyl-4*H*-pyran-4-one (21a)

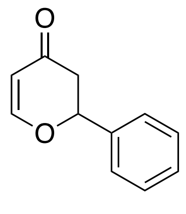

TLC: $R_f = 0.25$ (Hex/EtOAc = 4/1).

HRMS (ESI): calcd for $C_{11}H_{10}NaO_2$ $[M+H]^+$: 197.0573; found: 197.0575

Enantioselectivity was determined *via* chiral stationary phase GC employing a 30 m FS-Hydrodex β-6TBDM column (Macherey Nagel).

T (Injector + Detector) = 250 °C

Splitflow = 80 mL min^{-1}

Precolumn pressure = 0.8 bar

Conditions: 100 – 200 °C, 2

Retention Times: (*S*) = 23.6 min; (*R*) = 24.9 min

2,3-Dihydro-2-(1*E*)-1-propen-1-yl-4*H*-pyran-4-one (21b)

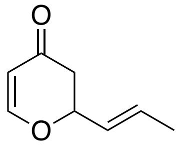

TLC: R_f = 0.61 (Hex/EtOAc = 2/3).

HRMS (ESI): calcd for $C_8H_{10}NaO_2$ [M+Na]$^+$: 161.0573; found: 161.0576

Enantioselectivity was determined *via* chiral stationary phase GC employing a 30 m FS-Hydrodex β-6TBDM column (Macherey Nagel).

T (Injector + Detector) = 250 °C

Splitflow = 80 mL min^{-1}

Precolumn pressure = 0.8 bar

Conditions: 100 – 200 °C, 2 °C min^{-1}

Retention Times: (*S*) = 16.1 min; (*R*) = 17.2 min

2,3-Dihydro-2-(1-methylethenyl)-4*H*-pyran-4-one (21c)

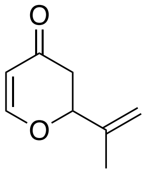

TLC: R_f = 0.61 (Hex/EtOAc = 2/3).

HRMS (ESI): calcd for $C_8H_{10}NaO_2$ [M+Na]$^+$: 161.0573; found: 161.0576

Enantioselectivity was determined *via* chiral stationary phase GC employing a 30 m FS-Hydrodex β-6TBDM column (Macherey Nagel).

T (Injector + Detector) = 250 °C

Splitflow = 80 mL min^{-1}

Precolumn pressure = 0.8 bar

Conditions: 100 – 200 °C, 2 °C min^{-1}

Retention Times: (*S*) = 14.4 min; (*R*) = 14.9 min

4.3.3. Racemic Alcohols for the Catalyzed Borane Reduction

The racemic alcohols were synthesized by reduction of the appropriate commercially available ketones with $NaBH_4$.

Phenylethanol

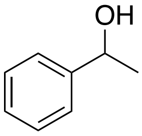

Enantioselectivity was determined *via* chiral stationary phase GC employing a 30 m FS-Hydrodex β-6TBDM column (Macherey Nagel).

T (Injector + Detector) = 250 °C

Splitflow = 80 mL min^{-1}

Precolumn pressure = 0.8 bar

Conditions: 100 °C, 20 min

Retention Times: (*R*) = 10.8 min; (*S*) = 11.2 min

2-Butanol

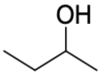

Enantioselectivity was determined by investigation of the benzoylated alcohol *via* chiral stationary phase GC employing a 30 m FS-Hydrodex β-6TBDM column (Macherey Nagel).

T (Injector + Detector) = 250 °C

Splitflow = 80 mL min^{-1}

Precolumn pressure = 0.8 bar

Conditions: 100 °C – 140 °C, 2 °C min^{-1}

Retention Times: (*R*) = 14.3 min; (*S*) = 14.5 min

1-Cyclohexylethanol

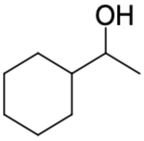

Enantioselectivity was determined *via* chiral stationary phase GC employing a 30 m FS-Hydrodex β-TBDAc column (Macherey Nagel).

T (Injector + Detector) = 250 °C

Splitflow = 80 mL min^{-1}

Precolumn pressure = 0.8 bar

Conditions: 80 °C, 20 min; 80 – 120 °C, 2 °C min^{-1}

Retention Times: (*R*) = 26.9 min; (*S*) = 27.4 min

4.4. General Procedures

GP1: Peptide Coupling

To a solution of 1.0 equiv. of the unprotected acid and 1.0 equiv. of the hydrochloride in CH_2Cl_2 were added 1.1 equiv. HOBt, 1.1 equiv. EDAC·HCl and 1.1 equiv. Et_3N. The reaction mixture was stirred at r.t. for 24 h. The mixture was diluted with EtOAc, washed with 0.5 M citric acid (3×), sat. aq. $NaHCO_3$ solution (3×), and brine. The organic phase was dried with $MgSO_4$, filtered, and the solvent was removed under reduced pressure.

GP2: Boc deprotection

A solution of 1.0 equiv. of the Boc-protected amino acid in 2 mL of hydrogen chloride in 1,4-dioxane (4 M) was stirred at r. t. for 1 h. The reaction flask was closed with a septum and the generated gas was removed occasionally. After 1 h, the solvent was removed under reduced pressure.

GP3: Esterification

To a solution of the alcohol (1.00 equiv.) and the carboxylic acid (1.00 equiv.) at 0 °C was added EDC·HCl (1.10 equiv.) and catalytic amounts of DMAP (0.100 equiv.) First, the reaction mixture was stirred at 0 °C for 1 h and afterwards refluxed for 1 h. The mixture was diluted with EtOAc and the organic layer was extracted with 0.5 M citric acid (3×), sat. aq. $NaHCO_3$ solution (3×), and brine. The organic phase was dried over Na_2SO_4, filtered, and the solvent was removed under reduced pressure.

GP4: Hydrogenation

The benzyl-protected compound was dissolved in methanol and palladium on charcoal (10–20 wt%) was added. The reaction flask was purged with hydrogen gas. After stirring 24 h at room temperature the reaction mixture was filtered through a pad of Celite and washed with small portions of methanol. The solvent was removed under reduced pressure, and the residue was dissolved in EtOAc and extracted with 2 M aqueous sodium hydroxide solution (3 × 50 mL) and with brine, dried over Na_2SO_4, filtered, and the solvent was removed under reduced pressure.

GP5: *N*-Tosyl protection

In a flame dried flask under Ar, starting material (1.00 equiv.) was dissolved in anhydrous CH_2Cl_2. At 0 °C, Et_3N (2.40 equiv.) and *p*-toluenesulfonyl chloride (1.10 equiv.) were added and the reaction mixture was stirred at r.t. over night. The reaction was quenched by addition of 25 mL dest. H_2O and the aqueous phase was extracted with CH_2Cl_2 (3×). The combined organic layers were extracted with 0.5 M citric acid (3×), sat. aq. $NaHCO_3$ solution (3×), and brine. The organic phase was dried over Na_2SO_4, filtered, and the solvent was removed under reduced pressure.

GP6: *In-situ* OXB formation with boronic acids

An oven dried Schlenk tube was charged with the corresponding amino alcohol (1.00 equiv.) and the boronic acid (1.00 equiv.) in anhydrous toluene. A micro Soxhlet filled with sand and CaH_2 was placed on top of the flask and the reaction mixture was refluxed for 24 h under Ar. Afterwards, toluene was removed by distillation and the OXB was dried for 1 h under reduced pressure at the Schlenk line. A stock solution of the OXB was created and directly employed in catalysis.

GP7: *In-situ* OXB formation with phenylboron dichloride

An oven dried Schlenk tube was charged with the corresponding amino alcohol (1.00 equiv.) and phenylboron dichloride (1.00 equiv.) in anhydrous CH_2Cl_2. The reaction mixture was stirred at r.t. for 2 h under Ar. Afterwards, CH_2Cl_2 was removed by distillation and the OXB was dried for 1 h under reduced pressure at the Schlenk line. A stock solution of the OXB was created and directly employed in catalysis.

GP8: *In-situ* OXB formation with $BH_3{\cdot}SMe_2$ for subsequent CBS reduction

An oven dried Schlenk tube was charged with the corresponding amino alcohol (1.00 equiv.) and the $BH_3.SMe_2$ (0.60 equiv.) in anhydrous THF under Ar. The reaction mixture was stirred at 50 °C for 1 h. Then, a solution of the ketone was slowly added *via* syringe pump over a period of 1.5 h. Afterwards, the reaction was quenched by the addition of 0.5 M citric acid. The aqueous phase was extracted with CH_2Cl_2 (3×). The combined organic phases were dried with $MgSO_4$, filtered and solvent was removed under reduced pressure.

4.5. Synthesis of L-Serine derivatives

N-trifluoracetyl serine (1a)

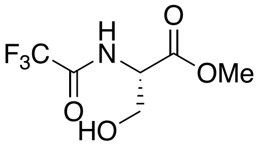

In a flame dried flask under Ar, L-Ser OMe HCl (0.500 g, 3.21 mmol, 1.00 equiv.) was dissolved in 10 mL of anhydrous CH_2Cl_2 and cooled to 0°C. Et_3N (1.34 mL, 9.64 mmol, 3.00 equiv.) and trifluoracetic anhydride (0.893 mL, 6.43 mmol, 2.00 equiv.) were added and the reaction mixture was stirred at r.t. over night. The reaction was quenched with 10 mL of sat. aq. $NaHCO_3$ solution and aqueous phase was extracted with CH_2Cl_2 (3×). The combined organic phases were dried over Na_2SO_4, filtered, and the solvent was removed under reduced pressure to yield an orange oil. After purification by column chromatography (Hex/EtOAc 1:1) the product (0.453 g 2.11 mmol, 66%) was obtained as a colorless oil.

***R*f** = 0.30 (Hex:EtOAc / 1:1).

^{1}H NMR (400 MHz, $CDCl_3$): δ/ppm = 7.53 – 7.31 (m, 1H), 4.67 (dt, J = 7.7, 3.3 Hz, 1H), 4.09 (dd, J = 11.4, 3.3 Hz, 1H), 3.95 (dd, J = 11.4, 3.3 Hz, 1H), 3.82 (s, 3H), 2.55 (s, 1H).

^{13}C NMR (101 MHz, $CDCl_3$): δ/ppm = 169.6, 158.0, 157.6, 157.3, 156.9, 120.0, 117.2, 114.3, 111.5, 62.2, 54.8, 53.3.

N-Tosyl serine (1b)

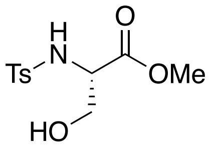

In a flame dried flask under Ar, H-L-Ser-OMe •HCl (0.500 g, 3.21 mmol, 1.00 equiv.) was dissolved in 10 mL of anhydrous CH_2Cl_2 and cooled to 0°C. Et_3N (1.07 mL, 7.71 mmol, 2.40 equiv.) and para-toluene sulfonyl chloride (0.674 g, 3.54 mmol, 1.10 equiv.) were added and the reaction mixture was stirred at r.t. over night. The reaction was quenched with 10 mL of dest. H_2O and the aqueous phase was extracted with CH_2Cl_2 (3×). The combined organic phases were extracted with sat. $NaHCO_3$ solution (3×), 0.5 M citric acid (3×), and brine. The combined organic phases were dried over Na_2SO_4, filtered, and the solvent was removed under reduced pressure to yield an colorless solid. After purification by column chromatography (Hex/EtOAc 1:1) the product (0.769 g 2.81 mmol, 88%) was obtained as a colorless crystalline solid.

***R*f** = 0.25 (Hex:EtOAc / 1:1).

^{1}H NMR (400 MHz, $CDCl_3$): δ/ppm = 7.78 – 7.70 (m, 2H), 7.35 – 7.28 (m, 2H), 5.68 – 5.48 (m, 1H), 3.98 (dt, *J* = 7.4, 3.7 Hz, 1H), 3.89 (d, *J* = 3.8 Hz, 2H), 3.69 – 3.57 (m, 3H), 2.42 (s, 3H).

^{13}C NMR (101 MHz, $CDCl_3$): δ/ppm = 170.3, 144.1, 144.1, 136.6, 130.0, 129.9, 127.4, 63.9, 57.7, 57.7, 53.1, 21.7.

N-Benzyl serine (1c)

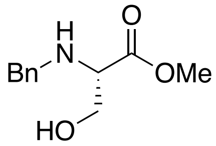

In a flame dried flask under Ar, H-L-Ser-OMe • HCl (1.00 g, 6.43 mmol, 1.00 equiv.) was dissolved in 50 mL of anhydrous CH_2Cl_2. Et_3N (5.65 mL, 38.57 mmol, 6.00 equiv.) and freshly distilled benzaldehyde (0.656 mL, 6.43 mmol, 1.00 equiv.) were added and the reaction mixture was stirred at r.t. over night. The solvent was removed under reduced pressure and the resiue was diluted with 50 mL MeOH. The solution was cooled to 0 °C and $NaBH_4$ (0.243 g, 6.43 mmol, 1.00 equiv.) was added portion wise. After 4 h the reaction was quenched by the addition of 10 mL dest. H_2O. The aqueous phase was extracted with CH_2Cl_2 (3×). The combined organic phases were dried over Na_2SO_4, filtered, and the solvent was removed under reduced pressure. After purification by column chromatography (Hex/EtOAc 1:1) the product (0.709 g 3.39 mmol, 53%) was obtained as a colorless oil.

***R*f** = 0.19 (Hex:EtOAc / 1:1).

^{1}H NMR (400 MHz, $CDCl_3$): δ/ppm = 7.38 – 7.31 (m, 4H), 7.31 – 7.27 (m, 1H), 3.95 – 3.86 (m, 1H), 3.83 – 3.72 (m, 5H), 3.68 – 3.58 (m, 1H), 3.49 – 3.41 (m, 1H), 2.52 (s, 2H).

^{13}C NMR (101 MHz, $CDCl_3$): δ/ppm = 173.2, 138.9, 128.6, 128.4, 127.5, 62.3, 61.8, 52.3, 52.0.

N-1-naphthyl serine (1d)

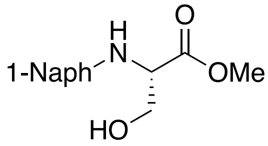

In a flame dried flask under Ar, H-L-Ser-OMe • HCl (0.500 g, 3.21 mmol, 1.00 equiv.) was dissolved in 20 mL of anhydrous CH_2Cl_2 and cooled to 0°C. Et_3N (2.67 mL, 19.28 mmol, 6.00 equiv.) and 1-naphthaldehyde (0.436 mL, 3.21 mmol, 1.00 equiv.) were added and the reaction mixture was stirred at r.t. over night. The solvent was removed under reduced pressure and the residue was diluted with MeOH. The solution was cooled to 0 °C and $NaBH_4$ (0.122 g, 3.21 mmol, 1.00 equiv.) was added portion wise. After 4 h the reaction was quenched by the addition of 10 mL dest. H_2O. The aqueous phase was extracted with CH_2Cl_2 (3×). The combined organic phases were dried over Na_2SO_4, filtered, and the solvent was removed under reduced pressure. After purification by column chromatography (Hex/EtOAc 1:1) the product (0.524 g 2.14 mmol, 63%) was obtained as a colorless oil.

***R*f** = 0.17 (Hex:EtOAc / 1:1).

^{1}H NMR (400 MHz, $CDCl_3$): δ/ppm = 8.21 – 8.13 (m, 1H), 7.90 – 7.84 (m, 1H), 7.83 – 7.76 (m, 1H), 7.58 – 7.38 (m, 4H), 4.36 (d, J = 12.8 Hz, 1H), 4.16 (d, J = 12.8 Hz, 1H), 3.80 (dd, J = 10.5, 4.1 Hz, 1H), 3.76 (s, 3H), 3.65 – 3.52 (m, 2H), 2.61 (s, 2H).

^{13}C NMR (101 MHz, $CDCl_3$): δ/ppm = 173.5, 134.8, 134.0, 131.9, 128.9, 128.4, 126.8, 126.5, 125.9, 125.5, 123.8, 62.7, 62.4, 53.5, 52.3, 50.2.

Ser(OH)-Phe OMe HCl (14)

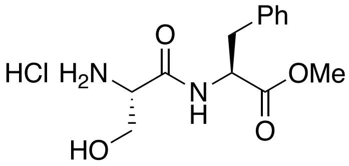

Using GP1, Boc-L-Ser(Bn)-OH (1.00 g, 3.29 mmol, 1.00 equiv.) was coupled with H-L-Phe-OMe • HCl (0.730 g, 3.29 mmol, 1.00 equiv.) to the dipeptide followed by deprotection of the boc and benzyl group using GP2 and GP4 respectively. The obtained product was directly used in the next step without further purification.

Bn-Ser(OH)-Phe OMe (15c)

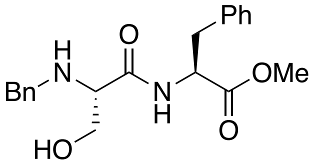

In a flame dried flask under Ar, Ser(OH)-Phe OMe HCl (**14**) (0.500 g, 1.65 mmol, 1.00 equiv.) was dissolved in 10 mL of anhydrous CH_2Cl_2. Et_3N (1.37 mL, 9.91 mmol, 6.00 equiv.) and freshly distilled benzaldehyde (0.169 mL, 1.65 mmol, 1.00 equiv.) were added and the reaction mixture was stirred at r.t. over night. The solvent was removed under reduced pressure and the resiue was diluted with 50 mL MeOH. The solution was cooled to 0 °C and $NaBH_4$ (0.243 g, 6.43 mmol, 1.00 equiv.) was added portion wise. After 4 h the reaction was quenched by the addition of 10 mL dest. H_2O. The aqueous phase was extracted with CH_2Cl_2 (3×). The combined organic phases were dried over Na_2SO_4, filtered, and the solvent was removed under reduced pressure. After purification by column chromatography (Hex/EtOAc 1:2) the product (0.359 g 1.01 mmol, 61%) was obtained as a colorless oil.

***R*f** = 0.21 (Hex:EtOAc / 1:2).

^{1}H NMR (400 MHz, $CDCl_3$): δ/ppm = 7.78 (t, *J* = 7.8 Hz, 1H), 7.30 – 7.12 (m, 9H), 7.11 – 7.03 (m, 2H), 4.87 – 4.71 (m, 1H), 3.72 – 3.58 (m, 6H), 3.28 – 3.08 (m, 2H), 3.08 – 2.93 (m, 1H), 2.67 (s, 2H).

^{13}C NMR (101 MHz, $CDCl_3$): δ/ppm = 172.2, 171.9, 136.1, 129.4, 129.2, 128.9, 128.7, 128.5, 127.8, 127.3, 62.9, 62.7, 62.4, 53.2, 53.0, 52.7, 52.6, 52.1, 52.0, 38.0, 37.6.

HRMS (ESI): calcd for $C_{20}H_{25}N_2O_4$ $[M+H]^+$: 357.1809; found: 357.1811

Ts-Ser(OH)-Phe OMe (15b)

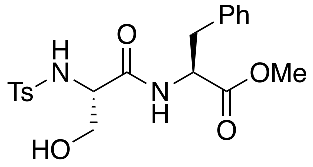

Using GP5, Ser(OH)-Phe OMe HCl (**14**) (1.81 g, 5.98 mmol, 1.00 equiv.) was protected with *p*-toluene sulfonyl chloride (1.25 g, 6.58 mmol, 1.10 equiv.). After purification by column chromatography (Hex/EtOAc 1:1) the product (1.46 g 3.47 mmol, 58%) was obtained as a colorless crystalline solid.

***R*f** = 0.11 (Hex:EtOAc / 1:1).

^{1}H NMR (400 MHz, $CDCl_3$): δ/ppm = 7.65 (d, *J* = 8.3 Hz, 2H), 7.24 – 7.13 (m, 5H), 7.02 – 6.92 (m, 3H), 5.71 (dd, *J* = 7.6, 2.2 Hz, 1H), 4.67 (ddd, *J* = 7.9, 7.0, 5.6 Hz, 1H), 3.77 (dd, *J* =

11.2, 3.9 Hz, 1H), 3.71 – 3.65 (m, 1H), 3.64 (s, 3H), 3.31 (dd, *J* = 11.2, 5.8 Hz, 1H), 3.02 (dd, *J* = 13.9, 5.5 Hz, 1H), 2.92 (dd, *J* = 13.9, 7.0 Hz, 1H), 2.51 (s, 1H), 2.33 (s, 3H).

^{13}C NMR (101 MHz, $CDCl_3$): δ/ppm = ^{13}C NMR (101 MHz, $CDCl_3$) δ 171.7, 169.4, 144.2, 136.4, 135.7, 130.0, 129.3, 128.8, 127.4, 62.9, 57.2, 53.8, 52.7, 37.7, 21.7.

HRMS (ESI): calcd for $C_{20}H_{24}N_2NaO_6S$ $[M+Na]^+$: 443.1247; found: 443.1246

Ts-Ser(OH)-D-Phe OMe (15c)

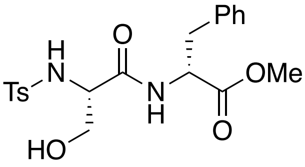

Using GP1, Boc-L-Ser(Bn)-OH (0.886 g, 3.00 mmol, 1.00 equiv.) was coupled with H-D-Phe-OMe • HCl (0.712 g, 3.30 mmol, 1.10 equiv.) to the dipeptide followed by deprotection of the Boc and benzyl group using GP2 and GP4 respectively. The obtained compound was then *N*-tosyl protected using GP5. After column chromatography (Hex/EtOAc 1:1) the product (0.609 g, 1.45 mmol, 45%) was obtained as a colorless solid.

***R*f** = 0.12 (Hex:EtOAc / 1:1).

^{1}H NMR (400 MHz, $CDCl_3$): δ/ppm = 7.75 – 7.69 (m, 2H), 7.34 – 7.26 (m, 5H), 7.16 – 7.11 (m, 2H), 7.09 (d, *J* = 8.3 Hz, 1H), 5.73 (d, *J* = 7.2 Hz, 1H), 4.77 (ddd, *J* = 8.2, 6.5, 5.6 Hz, 1H), 3.90 – 3.83 (m, 1H), 3.72 (s, 3H), 3.71 – 3.69 (m, 1H), 3.28 (dd, *J* = 11.4, 5.1 Hz, 1H), 3.10 (qd, *J* = 13.9, 6.1 Hz, 2H), 2.42 (s, 3H).

^{13}C NMR (101 MHz, $CDCl_3$): δ/ppm = 171.9, 169.6, 144.3, 136.4, 135.5, 130.1, 129.4, 129.0, 127.5, 127.3, 62.8, 57.6, 53.6, 52.7, 37.7, 21.7.

HRMS (ESI): calcd for $C_{20}H_{24}N_2NaO_6S$ $[M+Na]^+$: 443.1247; found: 443.1246

Ts-Ser(OH)-Ala OMe (15d)

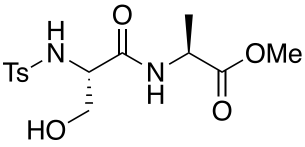

Using GP1, Boc-L-Ser(Bn)-OH (1.67 g, 5.65 mmol, 1.00 equiv.) was coupled with H-L-Phe-OMe • HCl (0.868 g, 6.22 mmol, 1.10 equiv.) to the dipeptide followed by deprotection of the Boc and benzyl group using GP2 and GP4 respectively. The obtained compound was then *N*-tosyl protected using GP5. After column chromatography (Hex/EtOAc 1:1) the product (0.662 g, 1.92 mmol, 34%) was obtained as a colorless solid.

***R*f** = 0.05 (Hex:EtOAc / 1:1).

^{1}H NMR (400 MHz, DMSO): 8.22 (d, *J* = 7.1 Hz, 1H), 7.72 (s, 1H), 7.66 (d, *J* = 8.3 Hz, 2H), 7.37 – 7.28 (m, 2H), 4.81 (t, *J* = 5.6 Hz, 1H), 4.02 (p, *J* = 7.2 Hz, 1H), 3.78 (t, *J* = 6.0 Hz, 1H), 3.58 (s, 3H), 3.46 – 3.34 (m, 2H), 3.32 (s, 2H), 2.36 (s, 3H), 1.12 (d, *J* = 7.3 Hz, 3H).

^{13}C NMR (101 MHz, DMSO): δ/ppm = 172.6, 168.9, 142.4, 138.3, 129.2, 126.7, 62.1, 58.2, 51.8, 47.4, 20.9, 16.9.

HRMS (ESI): calcd for $C_{14}H_{20}N_2NaO_6S$ $[M+Na]^+$: 367.0939; found: 367.0942

Ts-Ser(OH)-CHA OMe (15e)

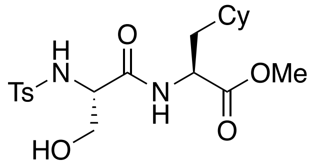

Using GP1, Boc-L-Ser(Bn)-OH (1.42 g, 4.38 mmol, 1.00 equiv.) was coupled with H-L-Cha-OMe •DCHA(2.09 g, 4.82 mmol, 1.10 equiv.) to the dipeptide followed by deprotection of the Boc and benzyl group using GP2 and GP4 respectively. The obtained compound was then *N*-tosyl protected using GP5. After column chromatography (Hex/EtOAc 1:1) the product (0.785 g, 1.84 mmol, 42%) was obtained as a colorless solid.

***R*f** = 0.17 (Hex:EtOAc / 1:1).

^{1}H NMR (400 MHz, DMSO): 8.18 (d, *J* = 7.6 Hz, 1H), 7.71 (d, *J* = 6.6 Hz, 1H), 7.69 – 7.63 (m, 2H), 7.38 – 7.28 (m, 2H), 4.80 (t, *J* = 5.6 Hz, 1H), 4.16 – 4.04 (m, 1H), 3.81 (d, *J* = 6.3 Hz, 1H), 3.57 (s, 3H), 2.36 (s, 3H), 1.59 (t, *J* = 13.0 Hz, 5H), 1.47 – 1.32 (m, 2H), 1.29 – 1.06 (m, 5H), 0.91 – 0.70 (m, 2H).

^{13}C NMR (101 MHz, DMSO): δ/ppm = δ 172.7, 169.2, 142.3, 138.4, 129.2, 126.6, 62.2, 58.2, 51.8, 49.5, 38.4, 33.2, 32.8, 31.7, 30.7, 26.0, 25.6, 25.5, 21.0.

HRMS (ESI): calcd for $C_{20}H_{30}N_2NaO_6S$ $[M+Na]^+$: 449.1717; found: 449.1718

Ts-Ser(OH)-Ad (15f)

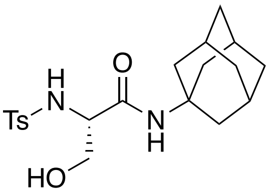

Using GP1, Boc-L-Ser(Bn)-OH (0.781 g, 2.64 mmol, 1.00 equiv.) was coupled with 1-adamantylamine (0.439 g, 2.90 mmol, 1.10 equiv.) to the amide followed by deprotection of the Boc and benzyl group using GP2 and GP4 respectively. The obtained compound was then *N*-tosyl protected using GP5. After column chromatography (Hex/EtOAc 1:1) the product (0.497 g, 1.27 mmol, 48%) was obtained as a colorless solid.

***R*~f~** = 0.21 (Hex:EtOAc / 1:1).

^{1}H NMR (400 MHz, $CDCl_3$): δ/ppm = 7.66 – 7.57 (m, 2H), 7.18 (dd, *J* = 8.4, 3.1 Hz, 2H), 6.55 (d, *J* = 6.7 Hz, 1H), 6.39 (s, 1H), 3.68 – 3.58 (m, 1H), 3.50 – 3.41 (m, 1H), 3.40 – 3.30 (m, 1H), 3.16 (s, 1H), 2.29 (d, *J* = 3.3 Hz, 3H), 1.90 (s, 3H), 1.51 (d, *J* = 3.5 Hz, 6H).

^{13}C NMR (101 MHz, $CDCl_3$): δ/ppm = 168.2, 143.4, 136.5, 129.6, 127.0, 77.5, 77.4, 77.2, 77.1, 76.8, 76.8, 62.6, 58.1, 51.7, 41.0, 36.1, 29.1, 21.3.

HRMS (ESI): calcd for $C_{20}H_{28}N_2NaO_4S$ $[M+Na]^+$: 415.1662; found: 415.1665

4.6. Synthesis of L-Hydroxyproline Derivatives

N-benzyl-*trans*-4-Hydroxy-L-proline methyl ester (23)

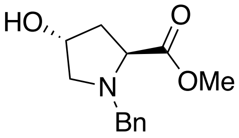

To a solution of *trans*-4-Hydroxy-L-proline (5.00 g, 43.4 mmol, 1.00 equiv.) in methanol (40 mL, 1 M) at 0 °C was added dropwise thionyl chloride (7.87 mL, 109 mmol, 2.50 equiv.) and stirred for 20 h at room temperature. The solvent was removed under reduced pressure and afterwards co-evaporated with toluene (3×). The crude material was diluted with toluene (40 mL, 1 M) and cooled to 0 °C. After DiPEA (14.0 mL, 109 mmol, 2.50 equiv.) and freshly distilled benzyl bromide (5.67 mL, 47.8 mmol, 1.10 equiv.) were added, the reaction mixture was refluxed for 6 h. Sat. $NaHCO_3$ solution was added and the aqueous phase was extracted with CH_2Cl_2 (3×). The combined organic layers were extracted with brine, dried over Na_2SO_4, filtered, and the solvent was removed under reduced pressure to afford the product **23** as brownish oil.

***R*~f~** = 0.15 (Hex:EtOAc / 1:1).

^{1}H NMR (400 MHz, $CDCl_3$): δ/ppm = 7.29 – 7.16 (m, 6H), 4.38 (s, 1H), 3.84 (d, *J* = 12.9 Hz, 1H), 3.60 (s, 3H), 3.58 – 3.53 (m, 1H), 3.26 (dd, *J* = 10.2, 5.6 Hz, 1H), 2.41 (dd, *J* = 10.2, 3.9 Hz, 1H), 2.25 – 2.14 (m, 1H), 2.07 – 1.97 (m, 1H).

^{13}C NMR (101 MHz, $CDCl_3$): δ/ppm = 174.1, 138.1, 129.2, 128.4, 127.3, 70.3, 63.8, 61.2, 58.3, 51.8, 39.7.

HRMS (ESI): calcd for $C_{13}H_{18}NO_3$ $[M+H]^+$: 236.1381; found: 236.1381

(2*S*,4*R*)-4-Hydroxy-α,α-diphenyl-1-(phenylmethyl)-2-pyrrolidinemethanol hydrochloride (24)

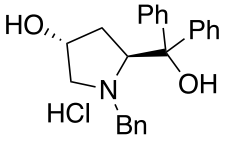

To a suspension of magnesium (0.357 g, 14.9 mmol, 2.50 equiv.) in anhydrous THF under Ar was added a crystal of iodine and stirred at room temperature for 30 min. Then 5% of the solution of bromobenzene (1.56 mL, 14.88 mmol, 2.50 equiv.) in THF was added and the reaction mixture was warmed to 50 °C. As soon as the color changed from brown to pale yellow, the remaining solution of bromobenze was added dropwise *via* an addition funnel (0.1 mL min^{-1}). The reaction mixture was refluxed for 1 h and then cooled to 0 °C.

To the phenylmagnesium bromide suspension, a solution of *N*-benzyl-*trans*-4-Hydroxy-l-proline methyl ester (X) (1.40 g, 5.95 mmol, 1.00 equiv.) in THF was added dropwise (0.1 mL min^{-1}). The reaction mixture was stirred at r.t. for 5h. At 0 °C, sat. NH_4Cl solution was added to quench the reaction and the mixture was then extracted with EtOAc (3×). The combined organic layers were washed with brine, dried over Na_2SO_4, filtered, and the solvent was removed under reduced pressure to afford a light orange solid. The solid was carefully washed with a small amount of cold Et_2O to afford the product **24** (1.28 g, 3.57 mmol, 60%) as colorless solid.

***R*$_f$** = 0.11 (Hex:EtOAc / 4:1).

^{1}H NMR (400 MHz, $CDCl_3$): δ/ppm = 7.72 – 7.66 (m, 2H), 7.54 – 7.49 (m, 2H), 7.24 – 7.00 (m, 9H), 6.97 – 6.92 (m, 2H), 4.87 (s, 1H), 4.32 (t, *J* = 7.8 Hz, 1H), 4.16 (p, *J* = 4.5 Hz, 1H), 3.21 (q, 2H), 3.00 (dd, *J* = 11.2, 4.6 Hz, 1H), 2.44 (dd, *J* = 11.2, 1.3 Hz, 1H), 1.87 – 1.72 (m, 2H), 1.52 (s, 1H).

^{13}C NMR (101 MHz, $CDCl_3$): δ/ppm = 147.8, 146.1, 139.6, 128.9, 128.7, 128.4, 128.4, 128.2, 127.3, 127.1, 126.7, 126.5, 125.7, 125.5, 71.0, 70.6, 66.0, 62.2, 61.4, 38.9, 15.4.

HRMS (ESI): calcd for $C_{24}H_{26}NO_2$ $[M+H]^+$: 360.1958; found: 360.1959

Boc-Phe-HydroxyPro-OH (26)

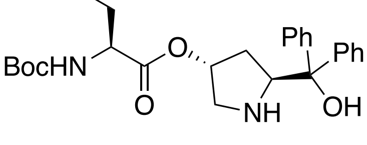

Using GP3, **24** (0.400 g, 1.01 mmol, 1.00 equiv.) was esterified with Boc-Phe-OH (0.268 g, 1.01 mmol, 1.00 equiv.). Afterwards the benzyl group was hydrogenated using GP4. The crude product was purified by column chromatography (Hex/EtOAc 2:1) to afford the final compound **26** (0.339 g, 0.657 mmol, 65%) as colorless solid.

***R*f** = 0.25 (Hex:EtOAc / 2:1).

^{1}H NMR (400 MHz, $CDCl_3$): δ/ppm = 7.58 – 7.53 (m, 2H), 7.43 – 7.38 (m, 2H), 7.36 – 7.27 (m, 4H), 7.25 – 7.18 (m, 5H), 7.18 – 7.12 (m, 2H), 5.14 (d, *J* = 4.9 Hz, 2H), 4.56 (q, *J* = 7.0 Hz, 1H), 4.44 (q, 1H), 3.19 – 2.98 (m, 4H), 1.98 – 1.89 (m, 1H), 1.41 (s, 10H).

^{13}C NMR (101 MHz, $CDCl_3$): δ/ppm = 136.2, 129.4, 128.7, 128.6, 128.3, 127.2, 126.9, 126.2, 125.5, 77.0, 63.7, 52.6, 38.6, 33.1, 28.4.

HRMS (ESI): calcd for $C_{31}H_{36}N_2NaO_5$ $[M+Na]^+$: 539.2516; found: 539.2515

Boc-CHA-HydroxyPro-OH (29)

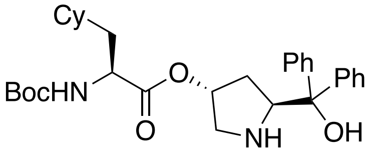

Using GP3, **24** (0.100 g, 0.253 mmol, 1.00 equiv.) was esterified with Boc-Cha-OH •DCHA (0.114 g, 0.253 mmol, 1.00 equiv.). Afterwards the benzyl group was hydrogenated using GP4. The crude product was purified by column chromatography (Hex/EtOAc 2:1) to afford the final compound **29** (0.094 g, 0.179 mmol, 71%) as colorless solid.

***R*f** = 0.28 (Hex:EtOAc / 2:1).

^{1}H NMR (400 MHz, $MeOD_4$): δ/ppm = 7.63 – 7.53 (m, 2H), 7.47 – 7.40 (m, 2H), 7.38 – 7.12 (m, 6H), 5.23 – 5.15 (m, 1H), 4.51 (dd, *J* = 9.7, 6.5 Hz, 1H), 4.11 (q, *J* = 7.2 Hz, 3H), 3.23 (dd, *J* = 12.2, 4.5 Hz, 1H), 3.01 (d, *J* = 12.3 Hz, 1H), 2.02 (s, 3H), 1.78 – 1.72 (m, 3H), 1.58 – 1.52 (m, 2H), 1.45 (s, 8H), 1.25 (t, *J* = 7.1 Hz, 4H), 1.05 – 0.90 (m, 2H).

^{13}C NMR (101 MHz, $MeOD_4$): δ/ppm = 174.8, 173.0, 148.1, 147.1, 129.2, 129.0, 127.8, 127.6, 127.6, 127.1, 126.7, 80.6, 79.2, 77.8, 64.9, 61.5, 53.6, 53.0, 40.1, 35.4, 34.8, 34.6, 33.5, 28.8, 27.5, 27.4, 27.2, 20.9, 14.5.

HRMS (ESI): calcd for $C_{31}H_{42}N_2NaO_5$ $[M+Na]^+$: 545.2986; found: 545.2986

Boc-CHA-Phe-HydroxyPro-OH (30)

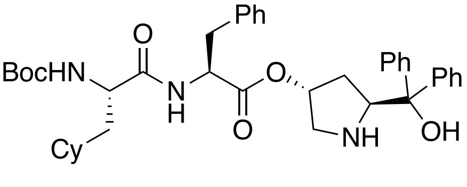

Using GP3, **24** (0.820 g, 2.07 mmol, 1.00 equiv.) was esterified with Boc-Phe-OH (0.549 g, 2.07 mmol, 1.00 equiv.). Afterwards the boc group was removed using GP2. The obtained free amine was esterified with Boc-Cha-OH •DCHA (0.938 g, 2.07 mmol, 1.00 equiv.) using GP3, followed by hydrogenation of the benzyl group using GP4. The crude product was purified by column chromatography (CH_2Cl_2/MeOH 20:1) to afford the final compound **30** (0.339 g, 0.657 mmol, 33%) as colorless foam.

***R*f** = 0.21 (CH_2Cl_2:MeOH / 20:1).

^{1}H NMR (400 MHz, $CDCl_3$): δ/ppm = 7.59 – 7.51 (m, 2H), 7.46 – 7.38 (m, 2H), 7.34 – 7.27 (m, 4H), 7.25 – 7.16 (m, 5H), 7.14 – 7.07 (m, 2H), 6.53 (d, *J* = 7.8 Hz, 1H), 5.12 (s, 1H), 4.85 – 4.69 (m, 2H), 4.38 (dd, *J* = 10.1, 6.3 Hz, 1H), 4.12 (s, 1H), 3.20 (dd, *J* = 12.3, 4.4 Hz, 1H), 3.14 – 3.02 (m, 2H), 3.02 – 2.94 (m, 1H), 1.91 – 1.82 (m, 1H), 1.76 – 1.65 (m, 6H), 1.43 (s, 9H), 1.41 – 1.35 (m, 2H), 1.19 – 1.12 (m, 2H), 1.02 – 0.83 (m, 3H).

^{13}C NMR (101 MHz, $CDCl_3$): 172.5, 144.7, 129.4, 128.7, 128.5, 128.2, 127.3, 126.9, 126.7, 126.2, 125.6, 63.5, 53.3, 52.8, 38.3, 33.8, 33.2, 28.4, 26.5, 26.3, 26.2.

HRMS (ESI): calcd for $C_{40}H_{52}N_3O_6$ $[M+H]^+$: 670.3851; found: 670.3854

Boc-AdGly-Phe-HydroxyPro-OH (31)

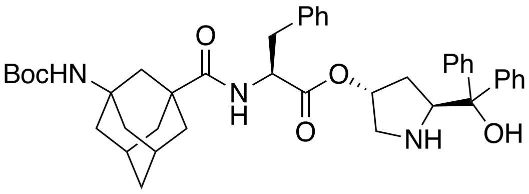

Using GP3, **24** (0.650 g, 1.64 mmol, 1.00 equiv.) was esterified with Boc-Phe-OH (0.436 g, 1.64 mmol, 1.00 equiv.). Afterwards the boc group was removed using GP2. The obtained free amine was esterified with Boc-^{A}Gly-OH (0.485 g, 1.64 mmol, 1.00 equiv.) using GP3, followed by hydrogenation of the benzyl group using GP4. The crude product was purified by column chromatography (CH_2Cl_2/MeOH 20:1) to afford the final compound **31** (0.638 g, 0.919 mmol, 56%) as colorless foam.

***R*f** = 0.25 (CH_2Cl_2:MeOH / 20:1).

^{1}H NMR (400 MHz, CD_2Cl_2): δ/ppm = 7.58 – 7.52 (m, 2H), 7.47 – 7.42 (m, 2H), 7.34 – 7.19 (m, 9H), 7.13 – 7.09 (m, 2H), 6.00 (d, J = 7.5 Hz, 1H), 5.16 – 5.09 (m, 1H), 4.77 – 4.71 (m, 1H), 4.49 – 4.42 (m, 2H), 4.27 (s, 1H), 3.71 (s, 1H), 3.09 (d, J = 6.2 Hz, 2H), 2.19 – 2.16 (m, 2H), 1.98 – 1.87 (m, 5H), 1.84 – 1.77 (m, 3H), 1.73 – 1.68 (m, 4H), 1.64 – 1.57 (m, 4H), 1.40 (s, 9H).

^{13}C NMR (101 MHz, CD_2Cl_2): δ/ppm = 176.40, 171.84, 154.52, 148.33, 145.48, 136.86, 129.93, 129.89, 129.05, 129.02, 128.86, 128.62, 127.59, 127.26, 127.08, 126.51, 125.90, 77.53, 77.21, 63.85, 53.14, 51.20, 43.11, 41.48, 38.74, 38.69, 38.42, 35.87, 33.61, 29.92, 29.90, 28.72.

HRMS (ESI): calcd for $C_{42}H_{51}N_3NaO_6$ $[M+Na]^+$: 716.3670; found: 716.3671

5. Spectra

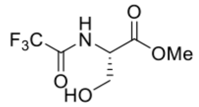
F3C
H
N
O
OMe
O
HO

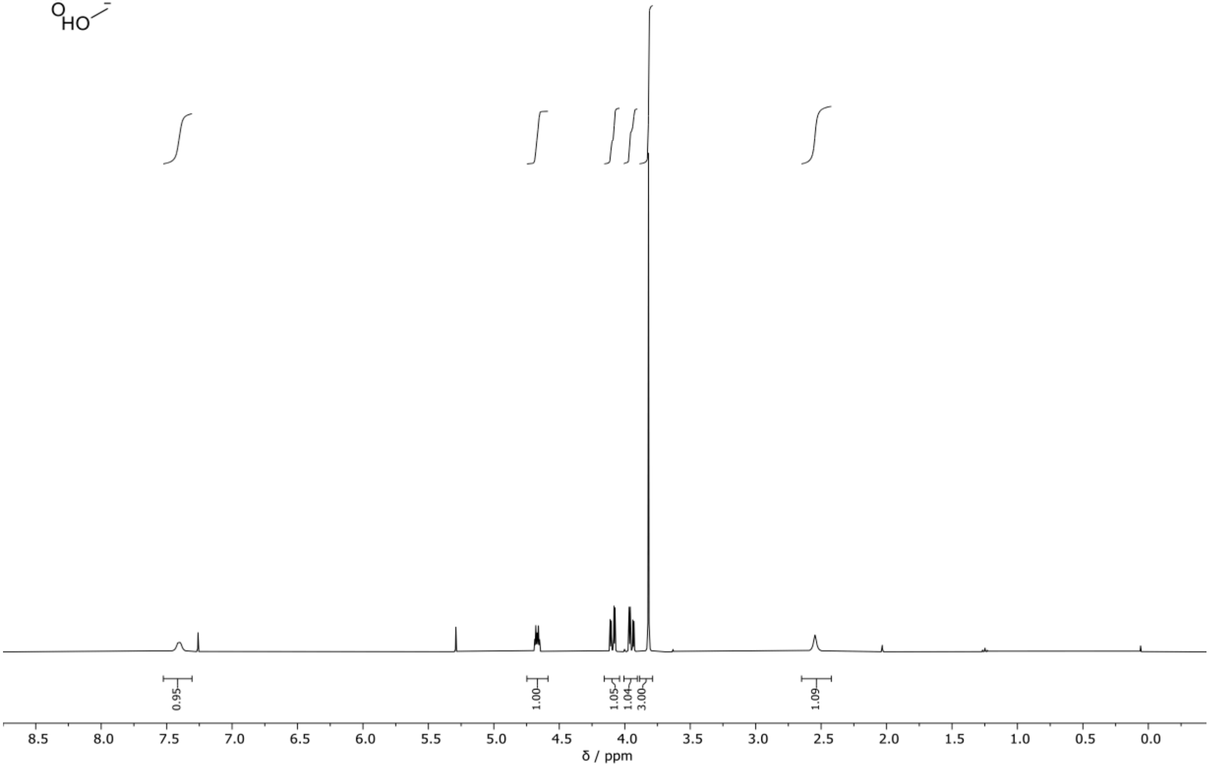
0.95
1.00
1.05
1.04
3.00
1.09
8.5
8.0
7.5
7.0
6.5
6.0
5.5
5.0
4.5
4.0
3.5
3.0
2.5
2.0
1.5
1.0
0.5
0.0
δ / ppm

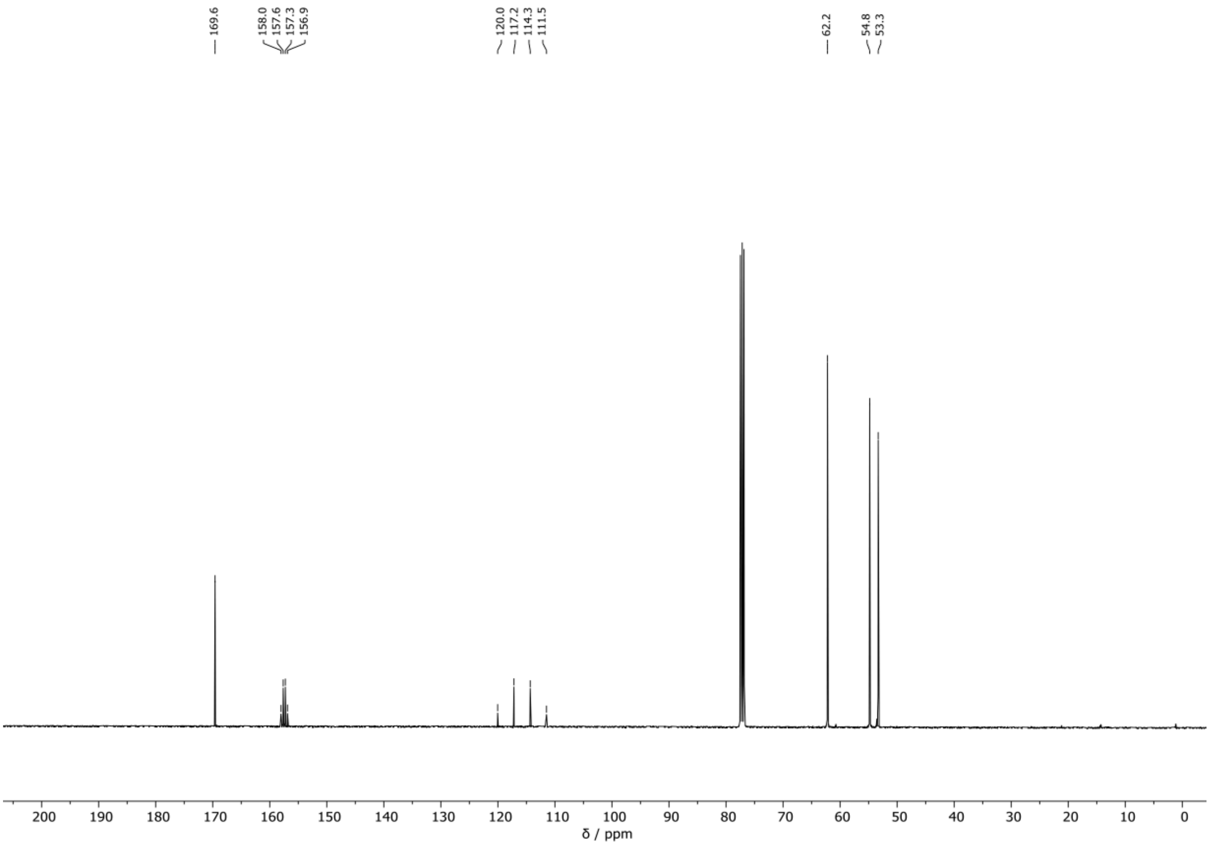
169.6
158.0
157.6
157.3
156.9
120.0
117.2
114.3
111.5
62.2
54.8
53.3
200
190
180
170
160
150
140
130
120
110
100
90
80
70
60
50
40
30
20
10
0
δ / ppm

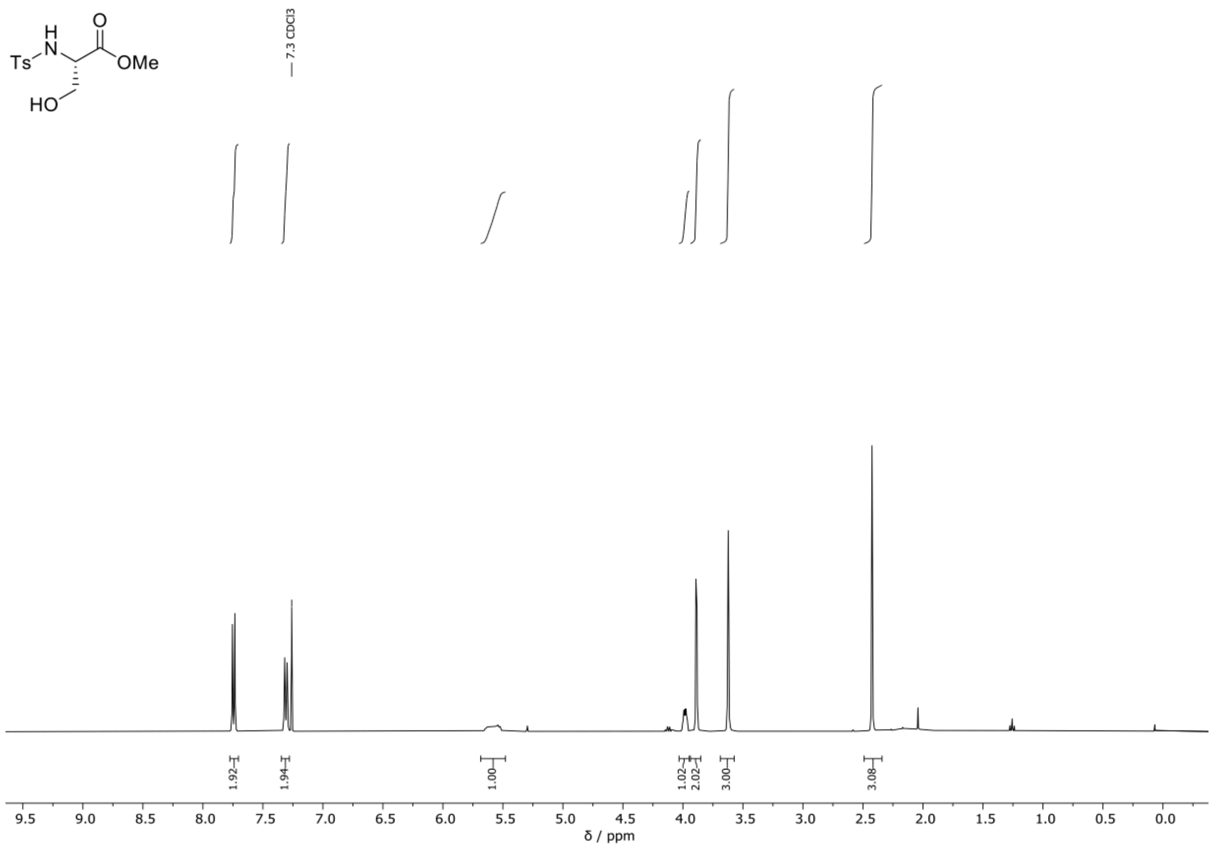
H
N
Ts
O
OMe
HO
7.3 CDCl3
1.92
1.94
1.00
1.02
2.02
3.00
3.08
9.5
9.0
8.5
8.0
7.5
7.0
6.5
6.0
5.5
5.0
4.5
4.0
3.5
3.0
2.5
2.0
1.5
1.0
0.5
0.0
δ / ppm

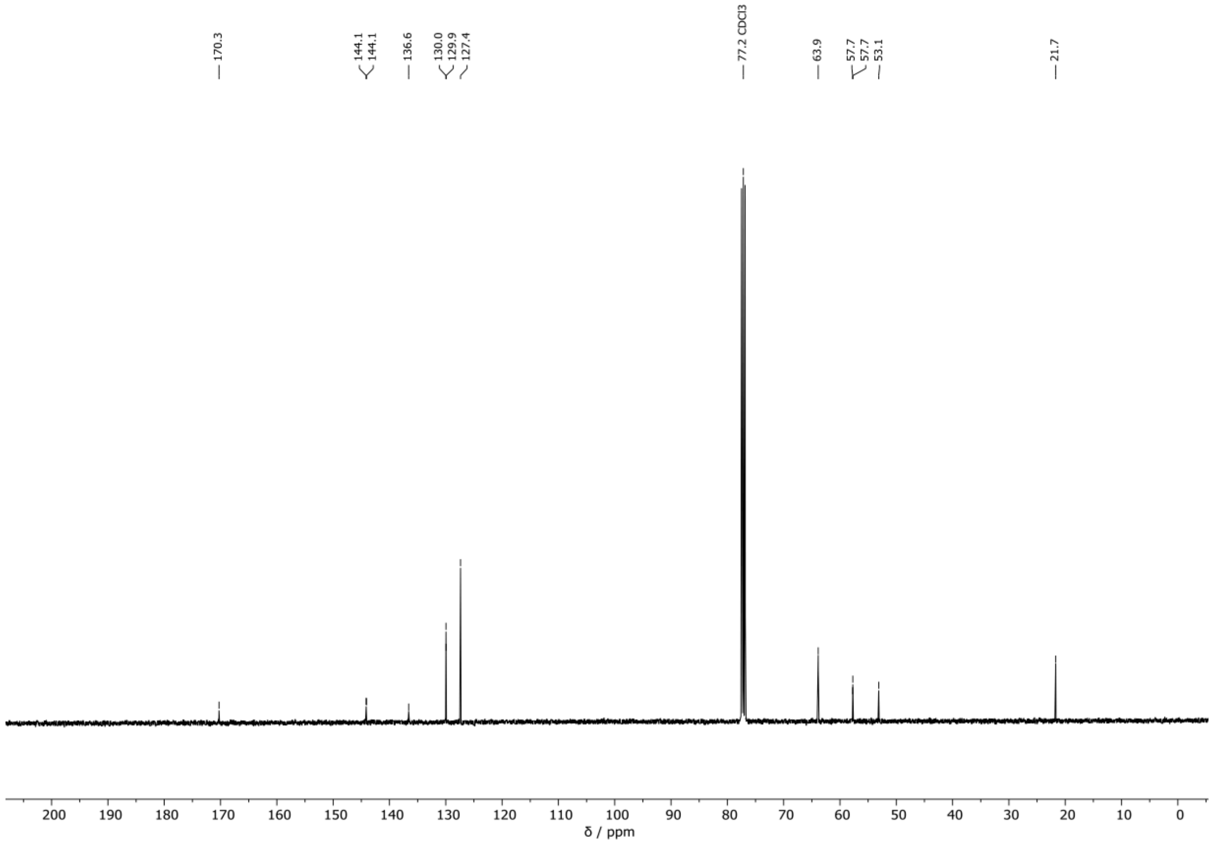
170.3
144.1
144.1
136.6
130.0
129.9
127.4
77.2 CDCl3
63.9
57.7
57.7
53.1
21.7
200
190
180
170
160
150
140
130
120
110
100
90
80
70
60
50
40
30
20
10
0
δ / ppm

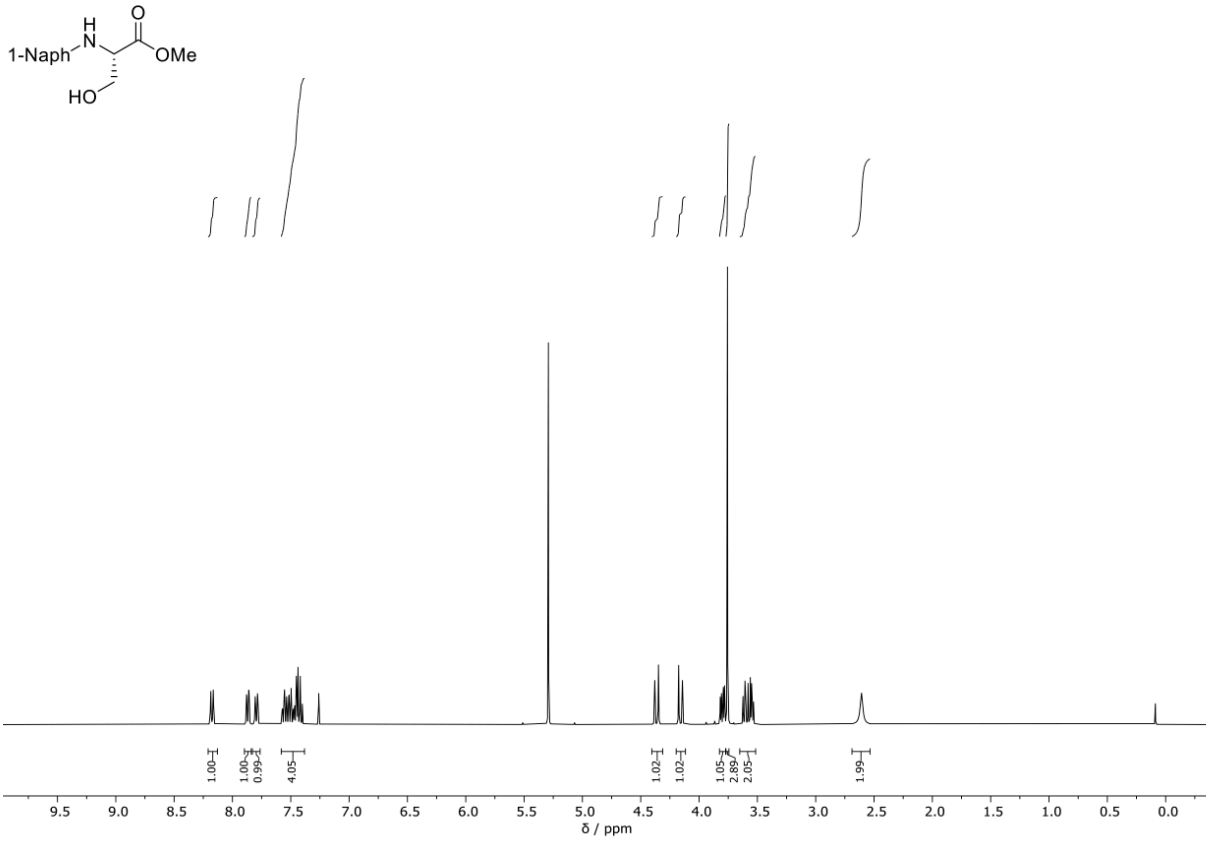
H
N
O
1-Naph
OMe
HO
1.00
1.00
0.99
4.05
1.02
1.02
1.05
2.89
2.05
1.99
9.5
9.0
8.5
8.0
7.5
7.0
6.5
6.0
5.5
5.0
4.5
4.0
3.5
3.0
2.5
2.0
1.5
1.0
0.5
0.0
δ / ppm

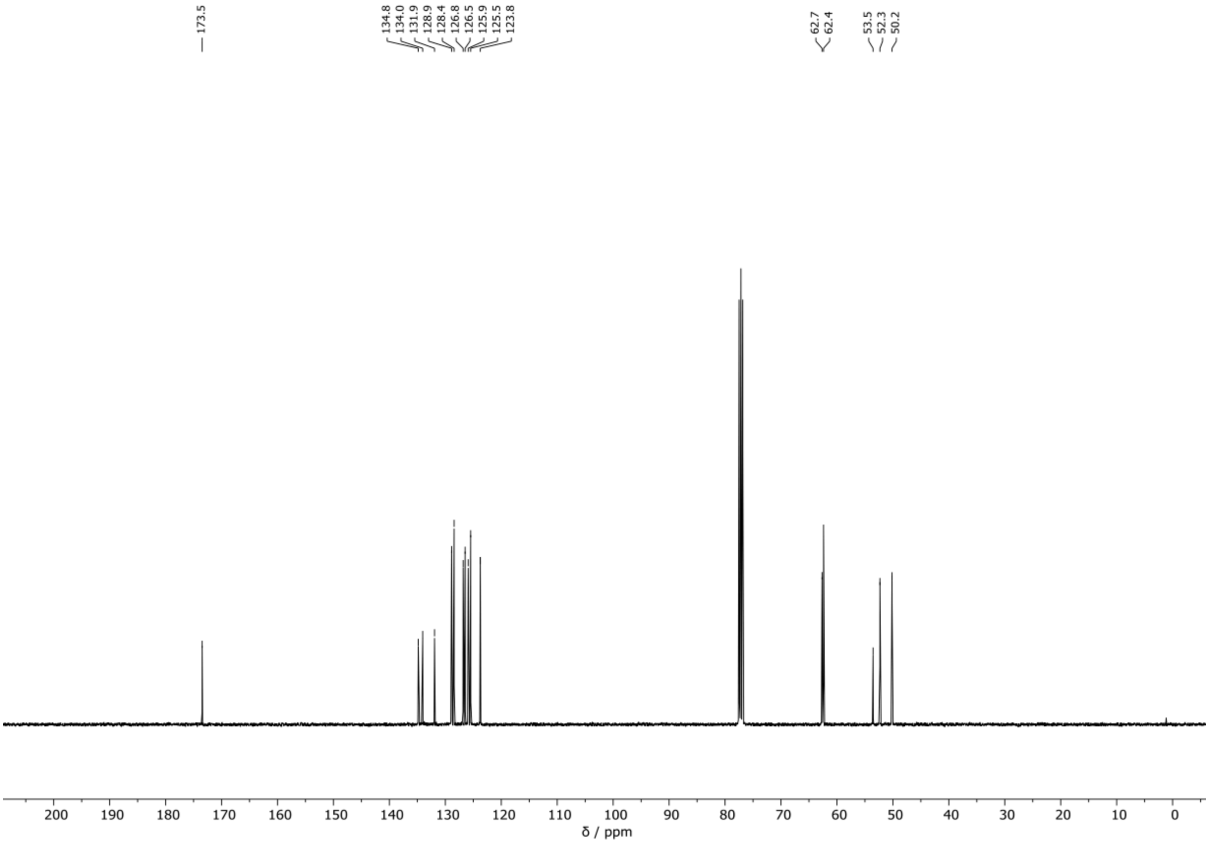
173.5
134.8
134.0
131.9
128.9
128.4
126.8
126.5
125.9
125.5
123.8
62.7
62.4
53.5
52.3
50.2
200
190
180
170
160
150
140
130
120
110
100
90
80
70
60
50
40
30
20
10
0
δ / ppm

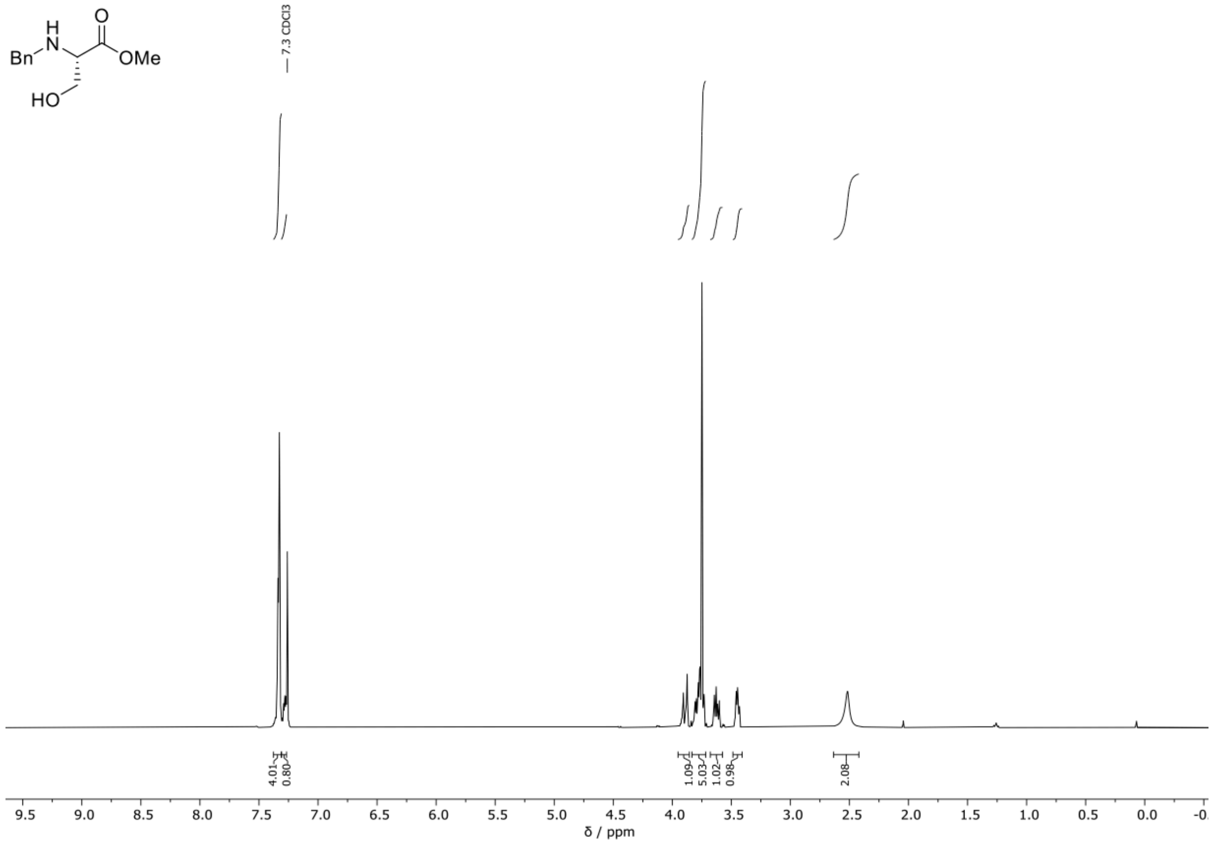
H
N
Bn
O
OMe
HO
7.3 CDCl3
4.01
0.80
1.09
5.03
1.02
0.98
2.08
9.5 9.0 8.5 8.0 7.5 7.0 6.5 6.0 5.5 5.0 4.5 4.0 3.5 3.0 2.5 2.0 1.5 1.0 0.5 0.0 -0.
δ / ppm

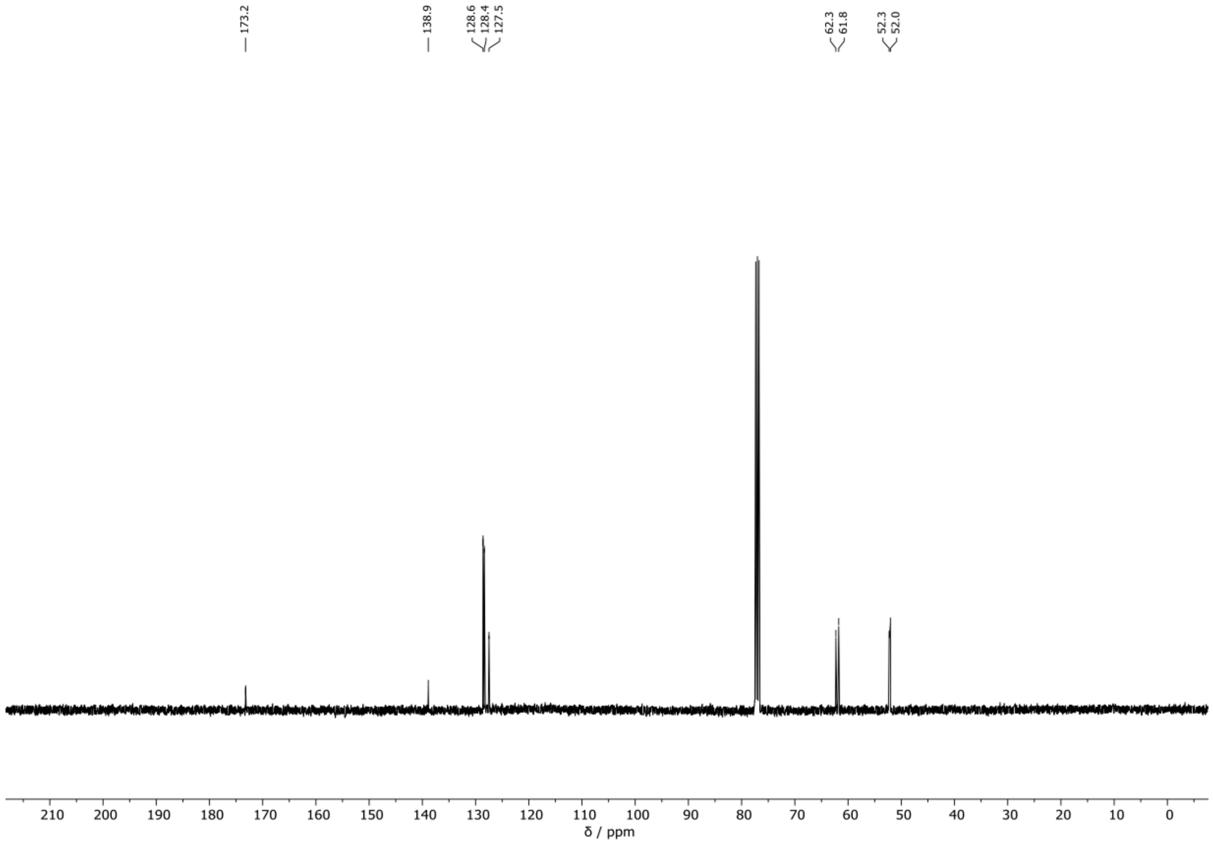
173.2
138.9
128.6
128.4
127.5
62.3
61.8
52.3
52.0
210 200 190 180 170 160 150 140 130 120 110 100 90 80 70 60 50 40 30 20 10 0
δ / ppm

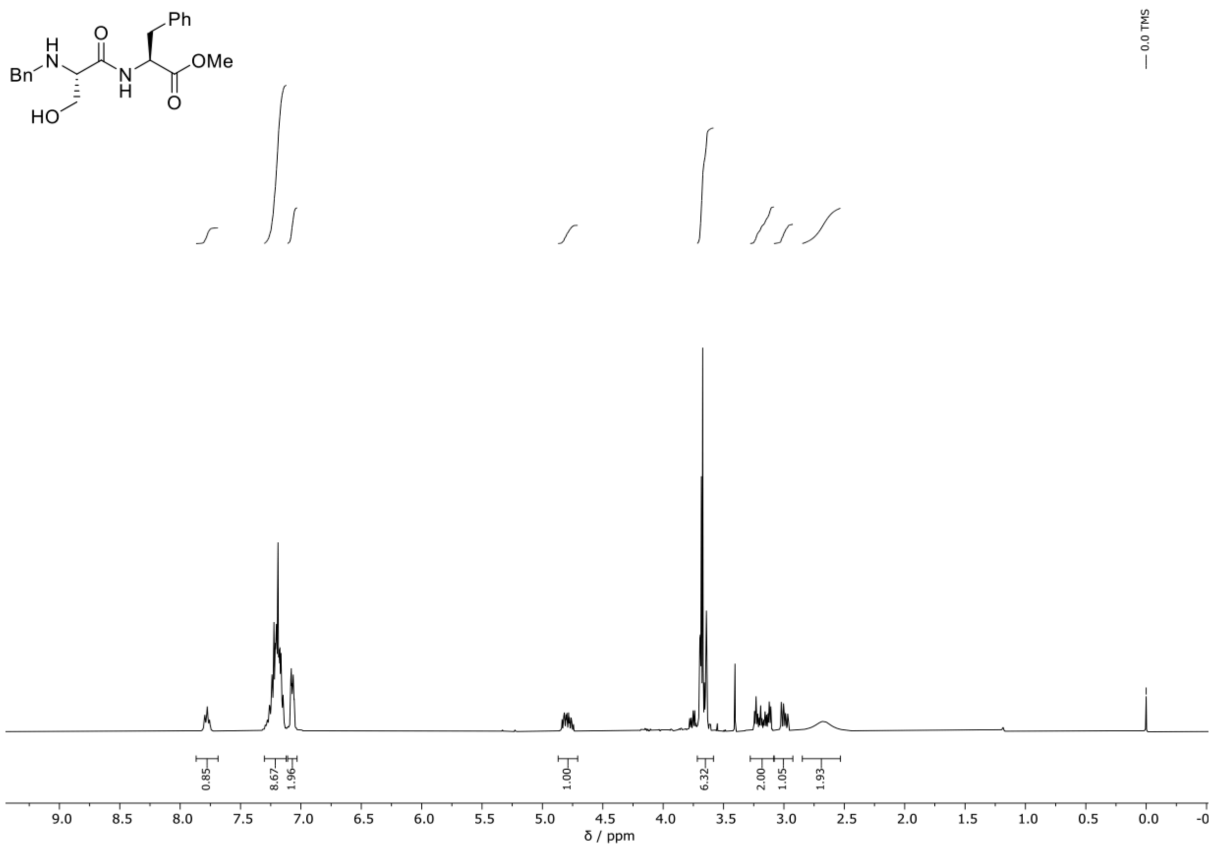
Ph
H
N
Bn
O
OMe
N
H
O
HO
— 0.0 TMS
0.85
8.67
1.96
1.00
6.32
2.00
1.05
1.93
9.0
8.5
8.0
7.5
7.0
6.5
6.0
5.5
5.0
4.5
4.0
3.5
3.0
2.5
2.0
1.5
1.0
0.5
0.0
δ / ppm

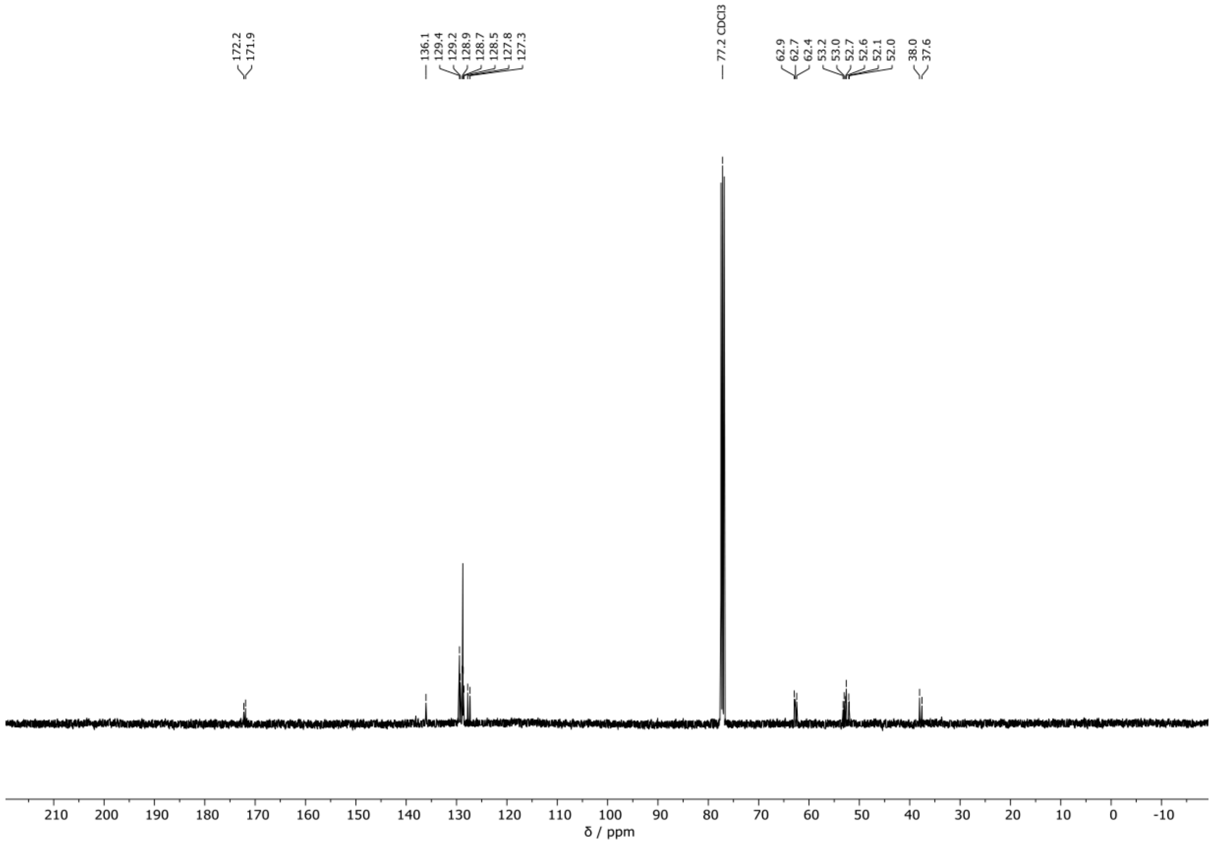
172.2
171.9
136.1
129.4
129.2
128.9
128.7
128.5
127.8
127.3
77.2 CDCl3
62.9
62.7
62.4
53.2
53.0
52.7
52.6
52.1
52.0
38.0
37.6
210
200
190
180
170
160
150
140
130
120
110
100
90
80
70
60
50
40
30
20
10
0
-10
δ / ppm

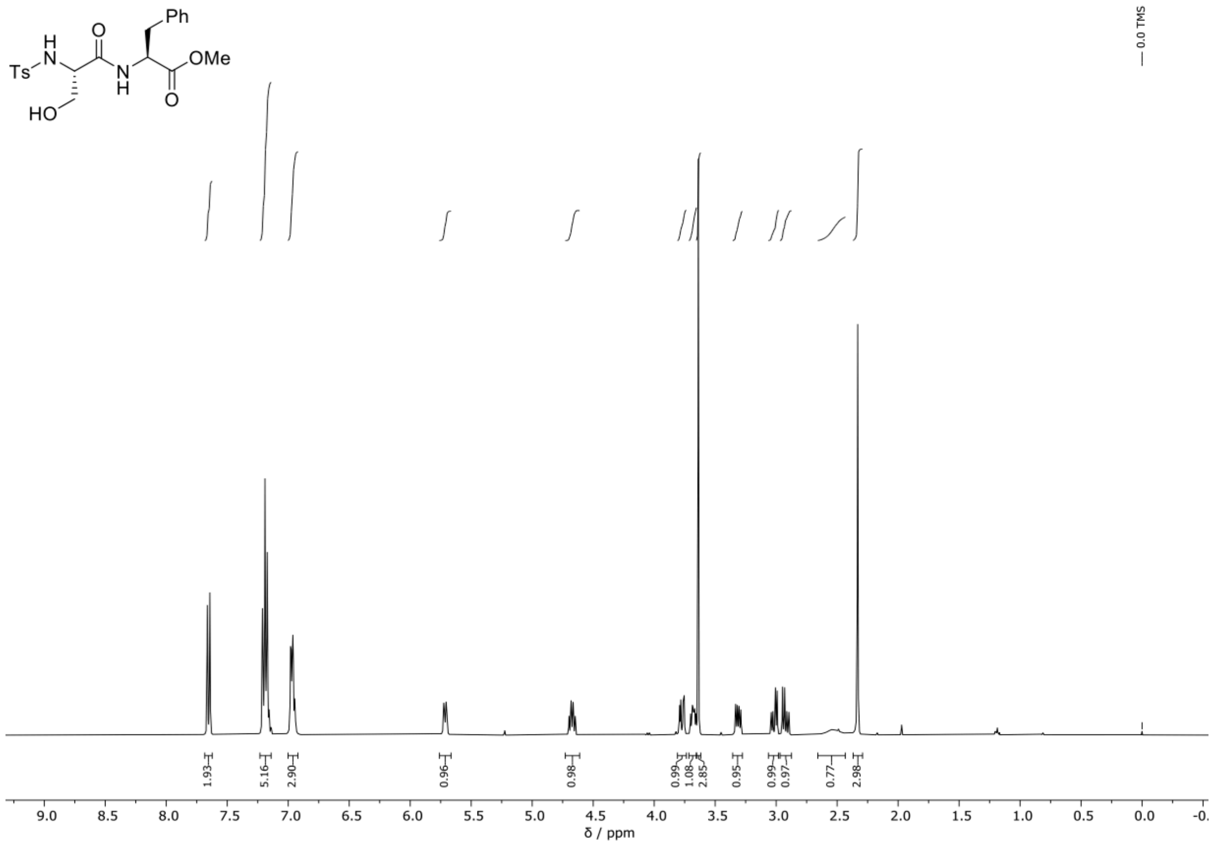
Ts
H
N
O
N
H
Ph
OMe
O
HO
— 0.0 TMS
1.93
5.16
2.90
0.96
0.98
0.99
1.08
2.85
0.95
0.99
0.97
0.77
2.98
9.0
8.5
8.0
7.5
7.0
6.5
6.0
5.5
5.0
4.5
4.0
3.5
3.0
2.5
2.0
1.5
1.0
0.5
0.0
δ / ppm

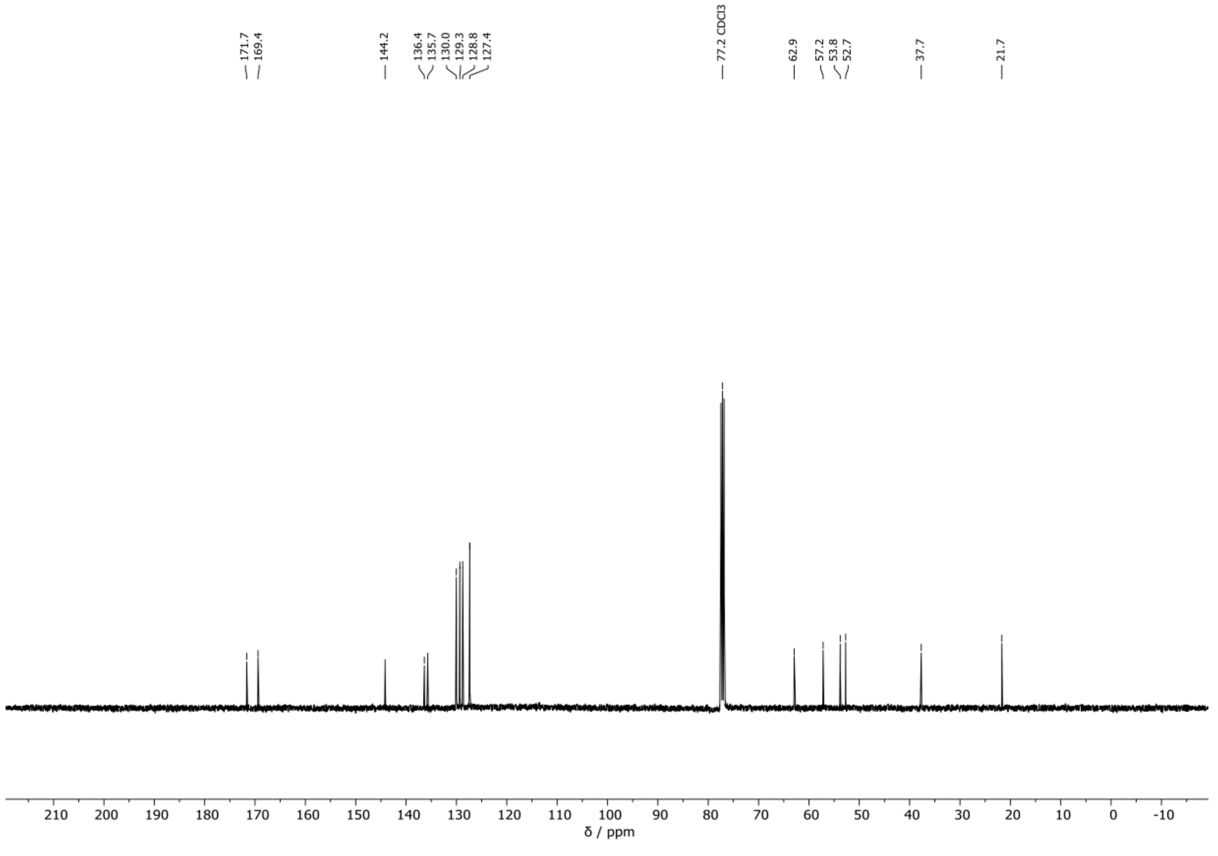
171.7
169.4
144.2
136.4
135.7
130.0
129.3
128.8
127.4
77.2 CDCl3
62.9
57.2
53.8
52.7
37.7
21.7
210
200
190
180
170
160
150
140
130
120
110
100
90
80
70
60
50
40
30
20
10
0
-10
δ / ppm

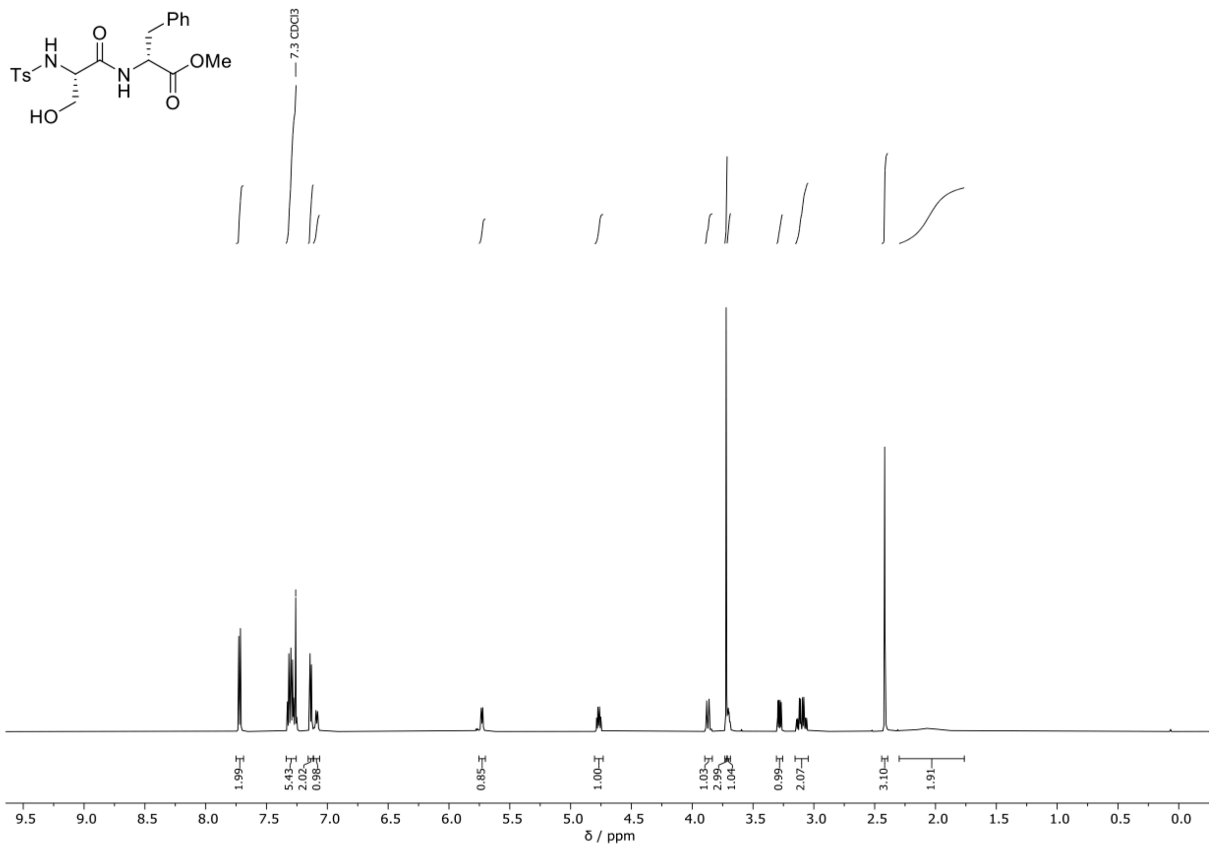
Ts
H
N
O
N
H
Ph
OMe
O
HO
7.3 CDCl3
1.99
5.43
2.02
0.98
0.85
1.00
1.03
2.99
1.04
0.99
2.07
3.10
1.91
9.5
9.0
8.5
8.0
7.5
7.0
6.5
6.0
5.5
5.0
4.5
4.0
3.5
3.0
2.5
2.0
1.5
1.0
0.5
0.0
δ / ppm

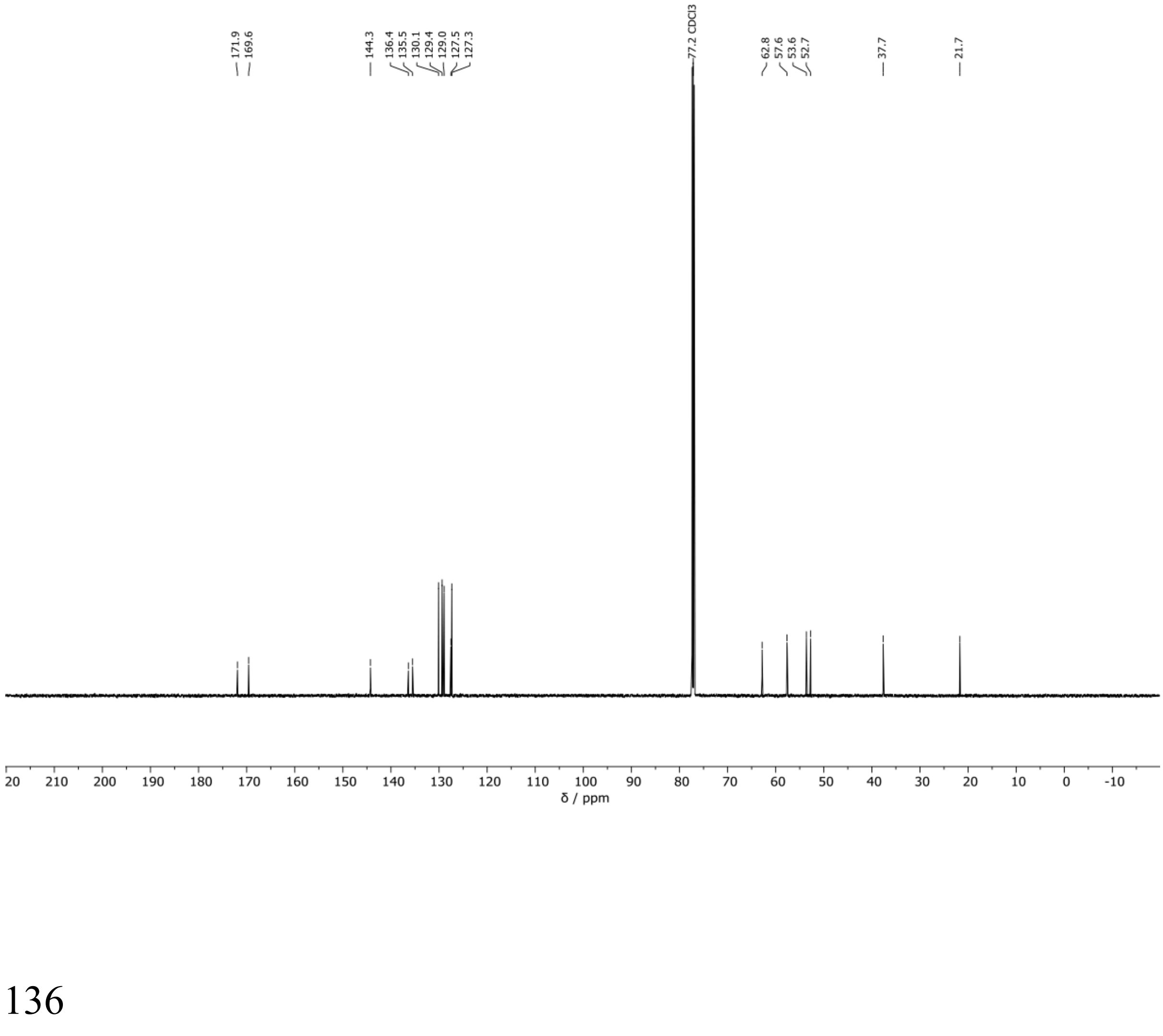
171.9
169.6
144.3
136.4
135.5
130.1
129.4
129.0
127.5
127.3
77.2 CDCl3
62.8
57.6
53.6
52.7
37.7
21.7
20
210
200
190
180
170
160
150
140
130
120
110
100
90
80
70
60
50
40
30
20
10
0
-10
δ / ppm

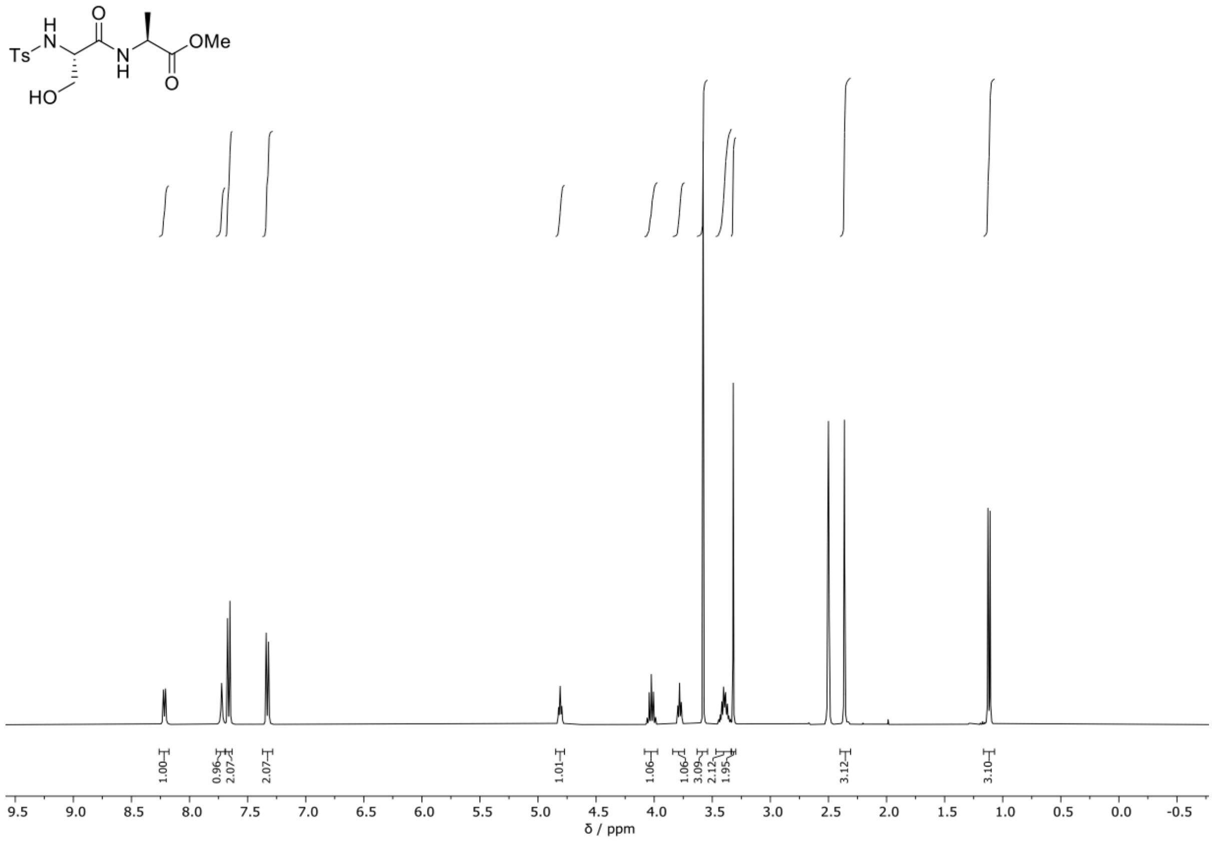
Ts
H
N
O
N
H
OMe
O
HO
1.00
0.96
2.07
2.07
1.01
1.06
1.06
3.09
2.12
1.95
3.12
3.10
9.5
9.0
8.5
8.0
7.5
7.0
6.5
6.0
5.5
5.0
4.5
4.0
3.5
3.0
2.5
2.0
1.5
1.0
0.5
0.0
-0.5
δ / ppm

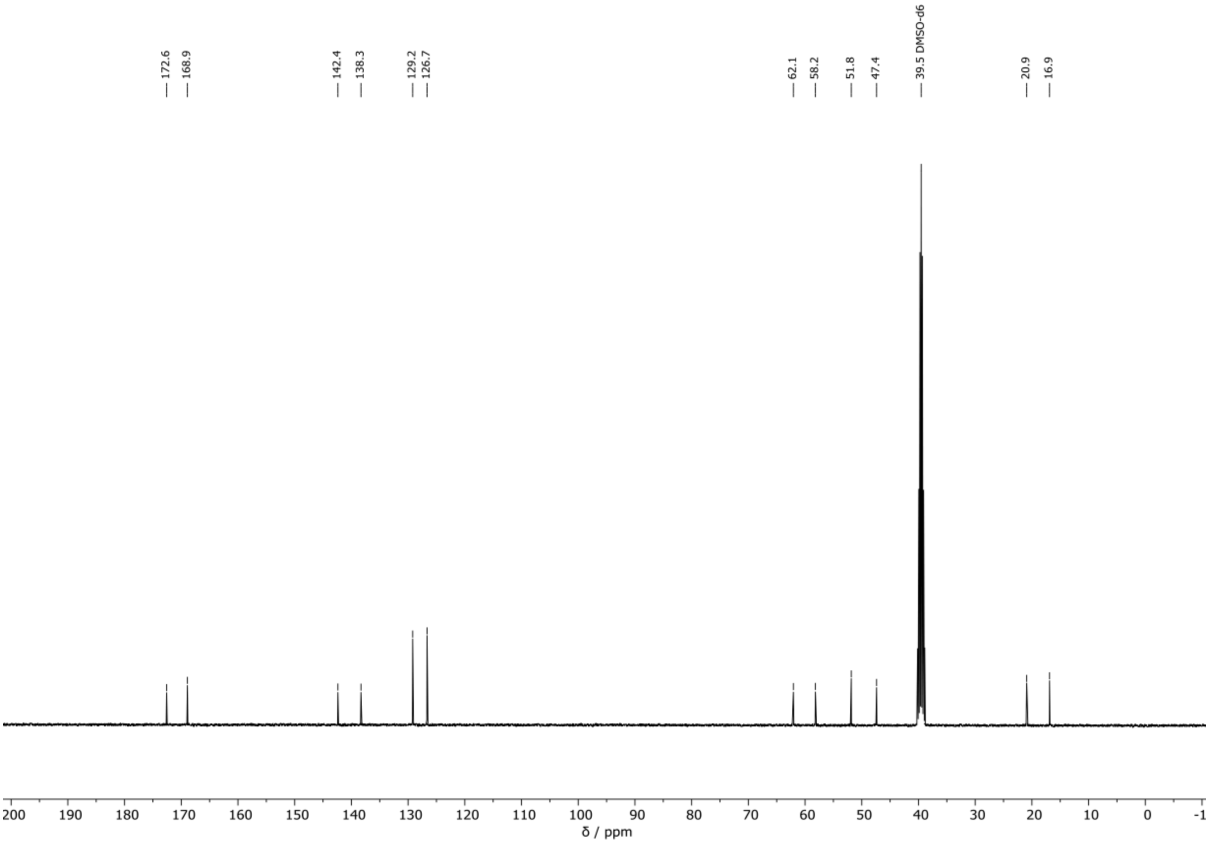
172.6
168.9
142.4
138.3
129.2
126.7
62.1
58.2
51.8
47.4
39.5 DMSO-d6
20.9
16.9
200
190
180
170
160
150
140
130
120
110
100
90
80
70
60
50
40
30
20
10
0
-1
δ / ppm

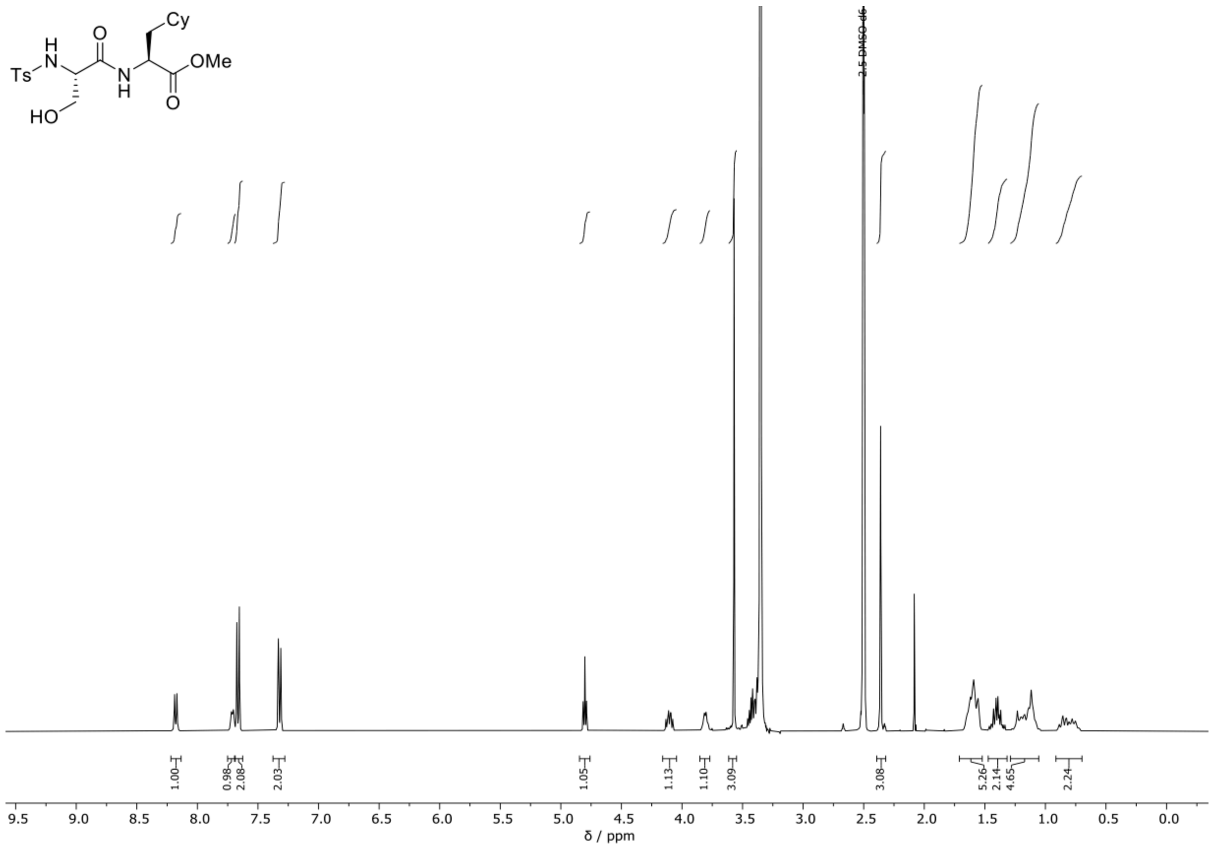
Ts
H
N
O
N
H
Cy
OMe
O
HO
2.5 DMSO-d6
1.00
0.98
2.08
2.03
1.05
1.13
1.10
3.09
3.08
5.26
2.14
4.65
2.24
9.5
9.0
8.5
8.0
7.5
7.0
6.5
6.0
5.5
5.0
4.5
4.0
3.5
3.0
2.5
2.0
1.5
1.0
0.5
0.0
δ / ppm

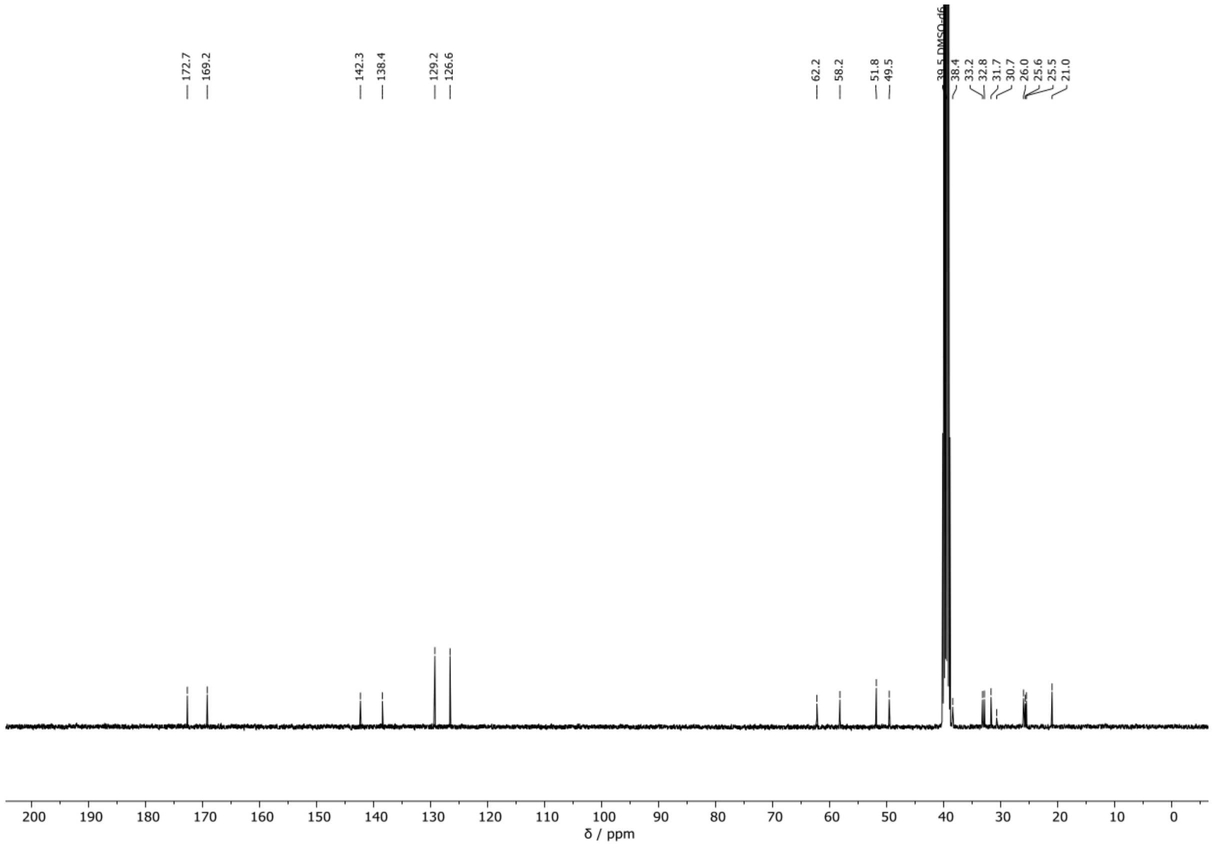
172.7
169.2
142.3
138.4
129.2
126.6
62.2
58.2
51.8
49.5
39.5 DMSO-d6
38.4
33.2
32.8
31.7
30.7
26.0
25.6
25.5
21.0
200
190
180
170
160
150
140
130
120
110
100
90
80
70
60
50
40
30
20
10
0
δ / ppm

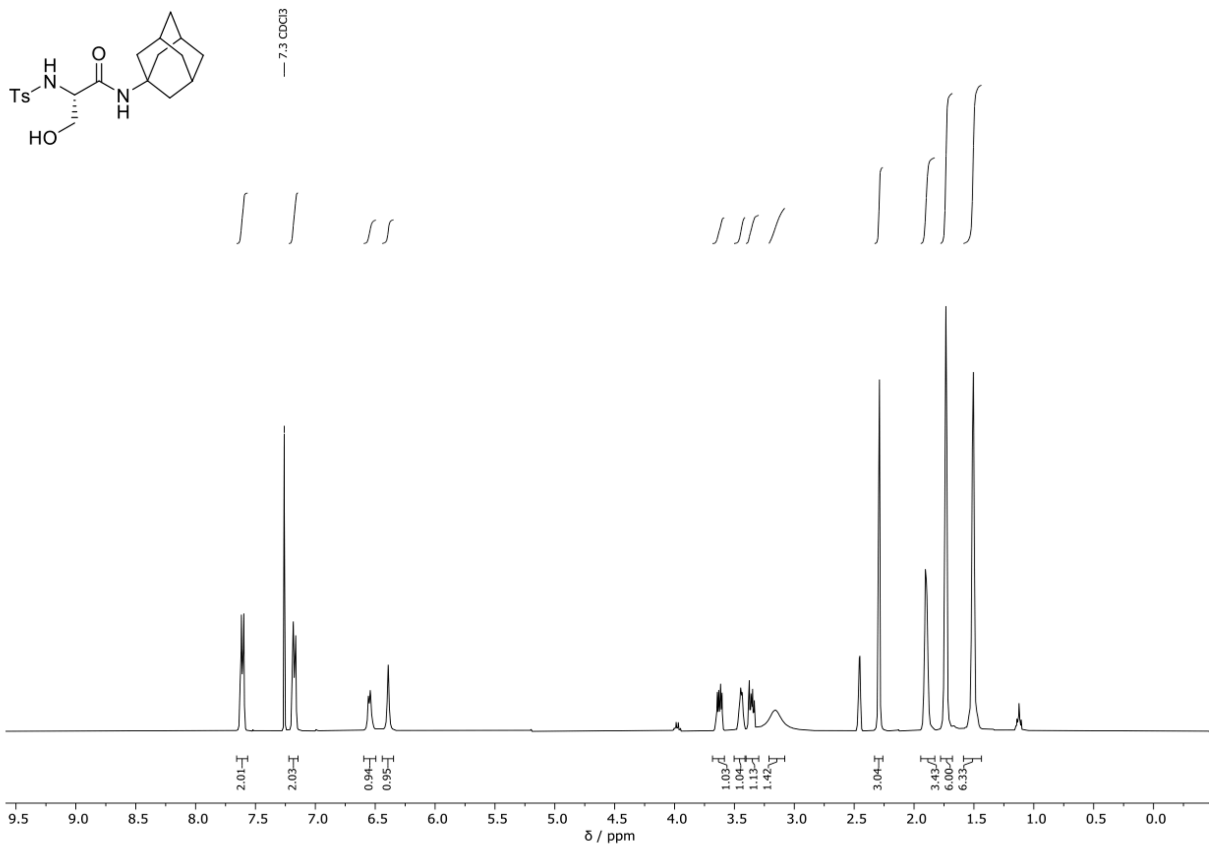
Ts
N
H
O
N
H
HO
— 7.3 CDCl3
2.01
2.03
0.94
0.95
1.03
1.04
1.13
1.42
3.04
3.43
6.00
6.33
9.5
9.0
8.5
8.0
7.5
7.0
6.5
6.0
5.5
5.0
4.5
4.0
3.5
3.0
2.5
2.0
1.5
1.0
0.5
0.0
δ / ppm

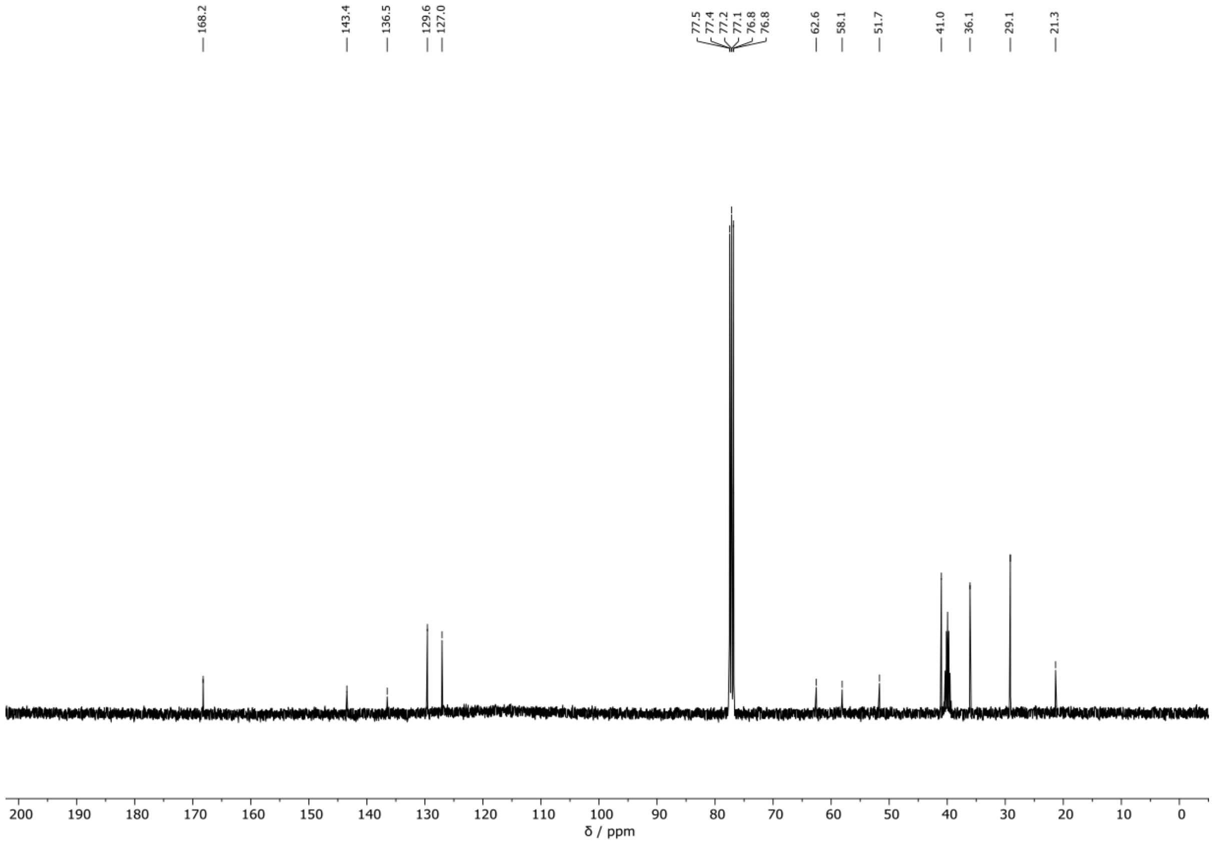
168.2
143.4
136.5
129.6
127.0
77.5
77.4
77.2
77.1
76.8
76.8
62.6
58.1
51.7
41.0
36.1
29.1
21.3
200
190
180
170
160
150
140
130
120
110
100
90
80
70
60
50
40
30
20
10
0
δ / ppm

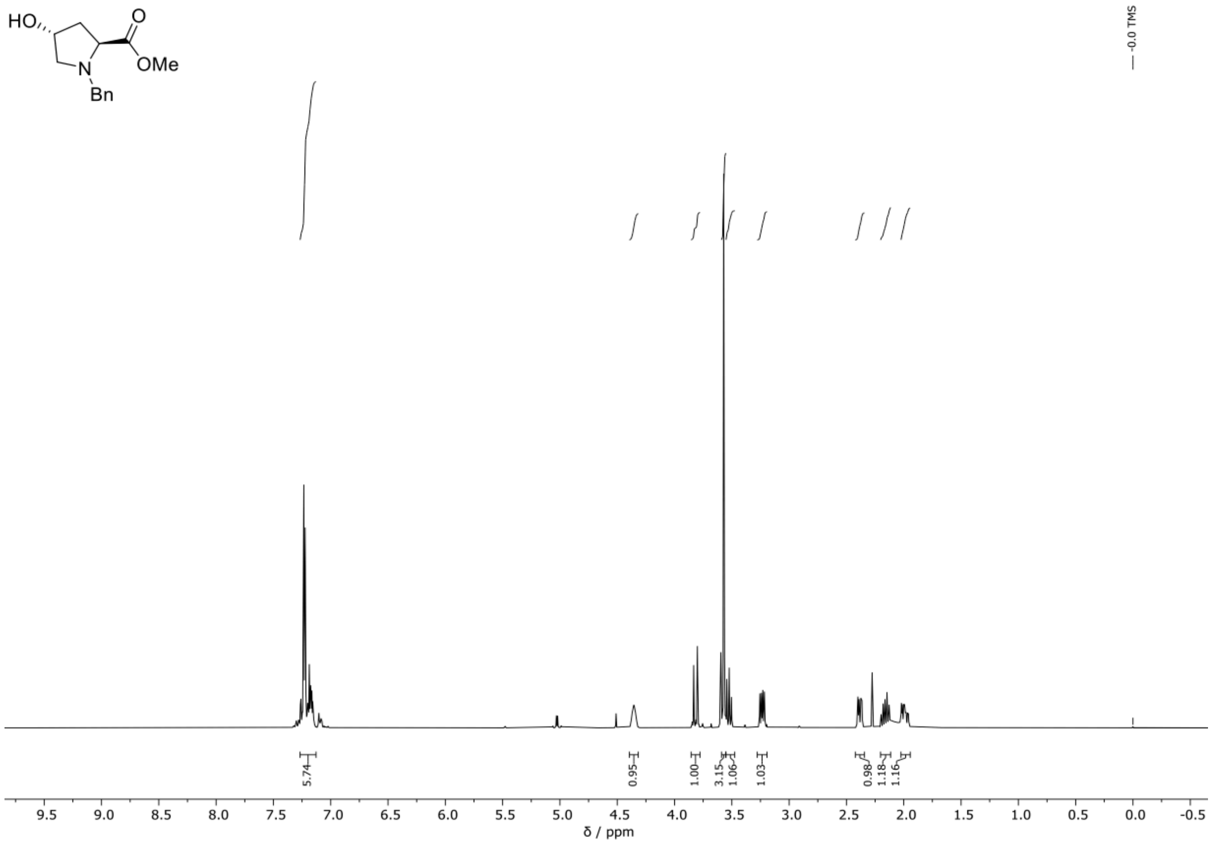
HO
O
OMe
N
Bn
-0.0 TMS
5.74
0.95
1.00
3.15
1.06
1.03
0.98
1.18
1.16
9.5
9.0
8.5
8.0
7.5
7.0
6.5
6.0
5.5
5.0
4.5
4.0
3.5
3.0
2.5
2.0
1.5
1.0
0.5
0.0
-0.5
δ / ppm

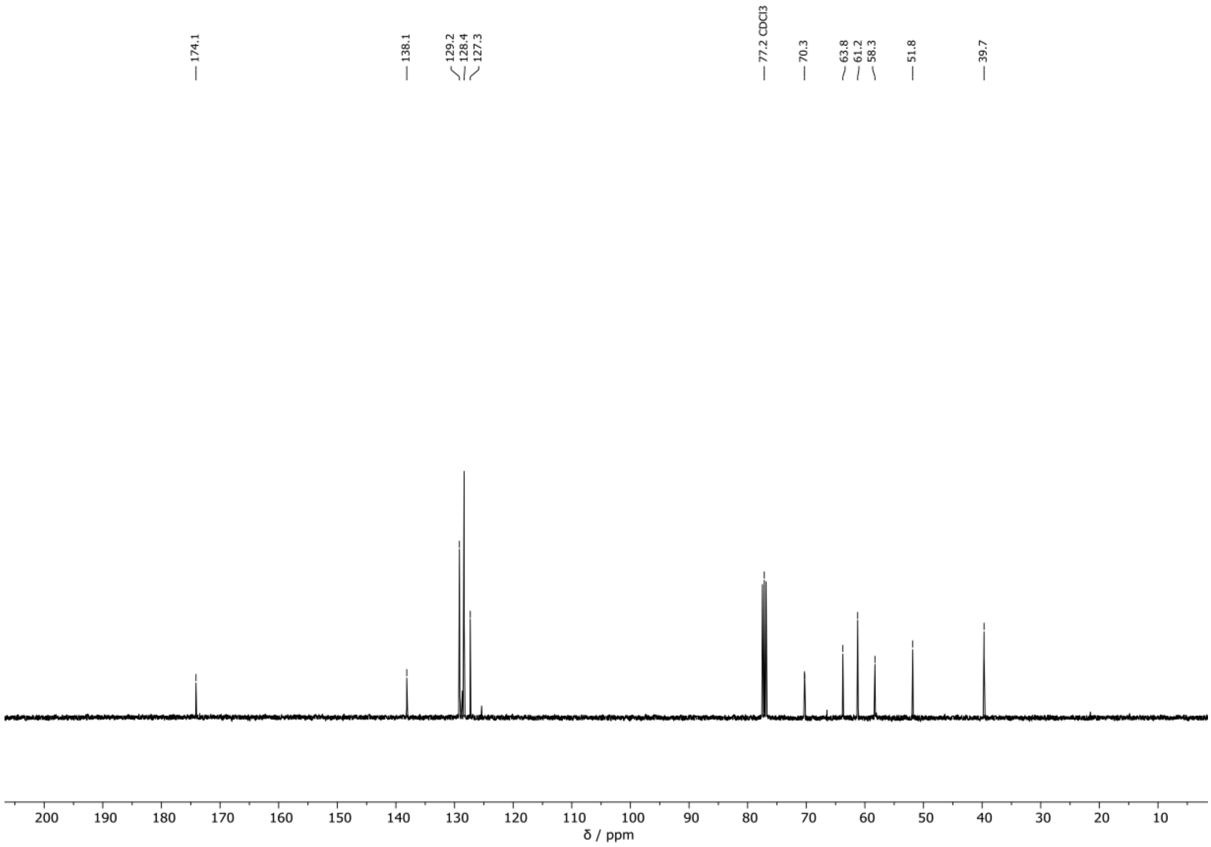
174.1
138.1
129.2
128.4
127.3
77.2 CDCl3
70.3
63.8
61.2
58.3
51.8
39.7
200
190
180
170
160
150
140
130
120
110
100
90
80
70
60
50
40
30
20
10
δ / ppm

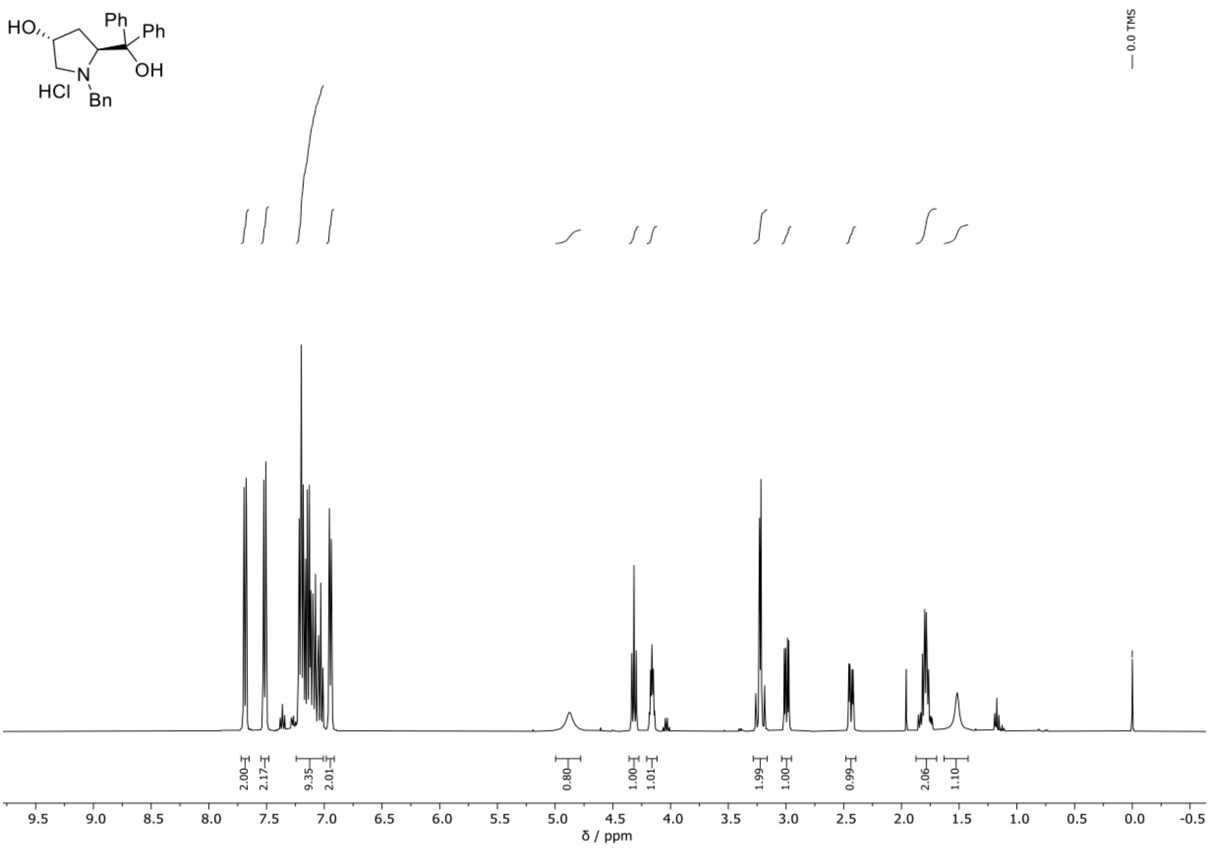
HO
Ph
Ph
OH
N
HCl
Bn
0.0 TMS
2.00
2.17
9.35
2.01
0.80
1.00
1.01
1.99
1.00
0.99
2.06
1.10
9.5
9.0
8.5
8.0
7.5
7.0
6.5
6.0
5.5
5.0
4.5
4.0
3.5
3.0
2.5
2.0
1.5
1.0
0.5
0.0
-0.5
δ / ppm

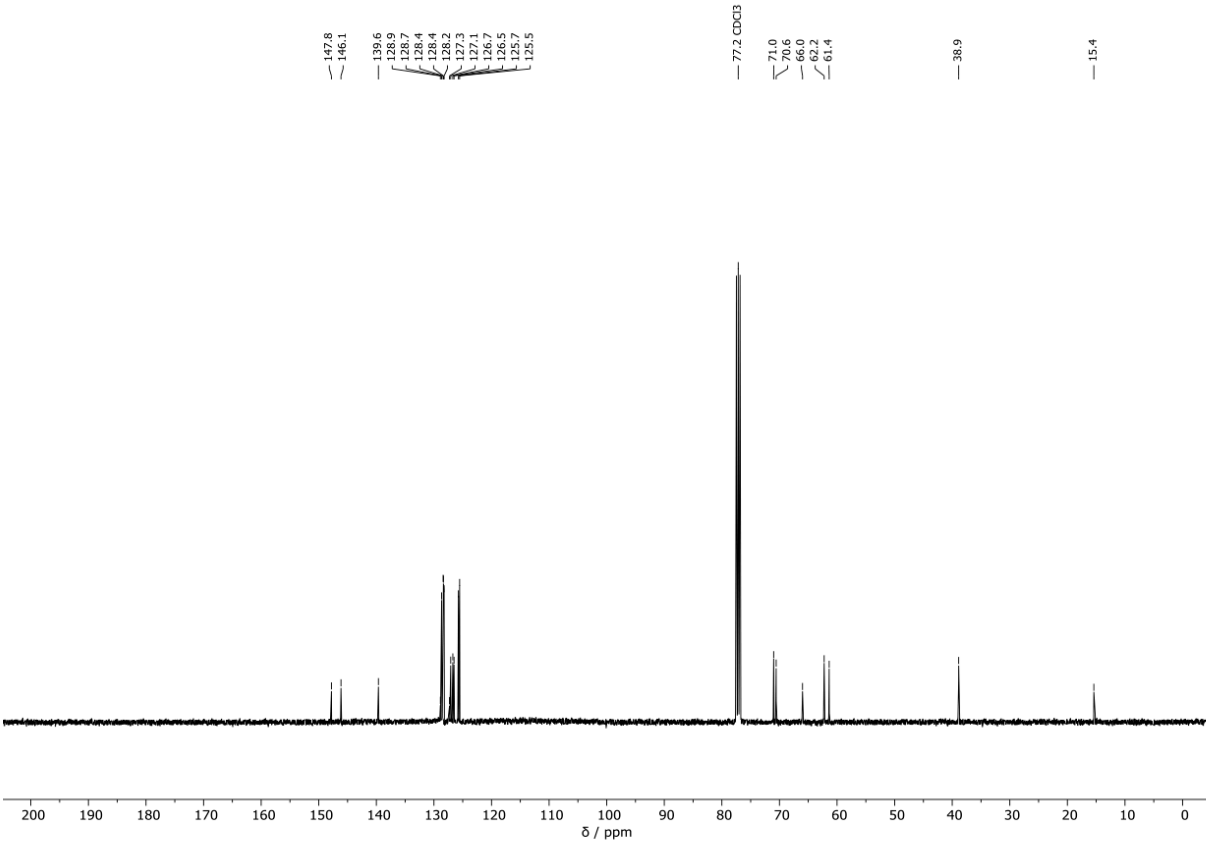
147.8
146.1
139.6
128.9
128.7
128.4
128.4
128.2
127.3
127.1
126.7
126.5
125.7
125.5
77.2 CDCl3
71.0
70.6
66.0
62.2
61.4
38.9
15.4
200
190
180
170
160
150
140
130
120
110
100
90
80
70
60
50
40
30
20
10
0
δ / ppm

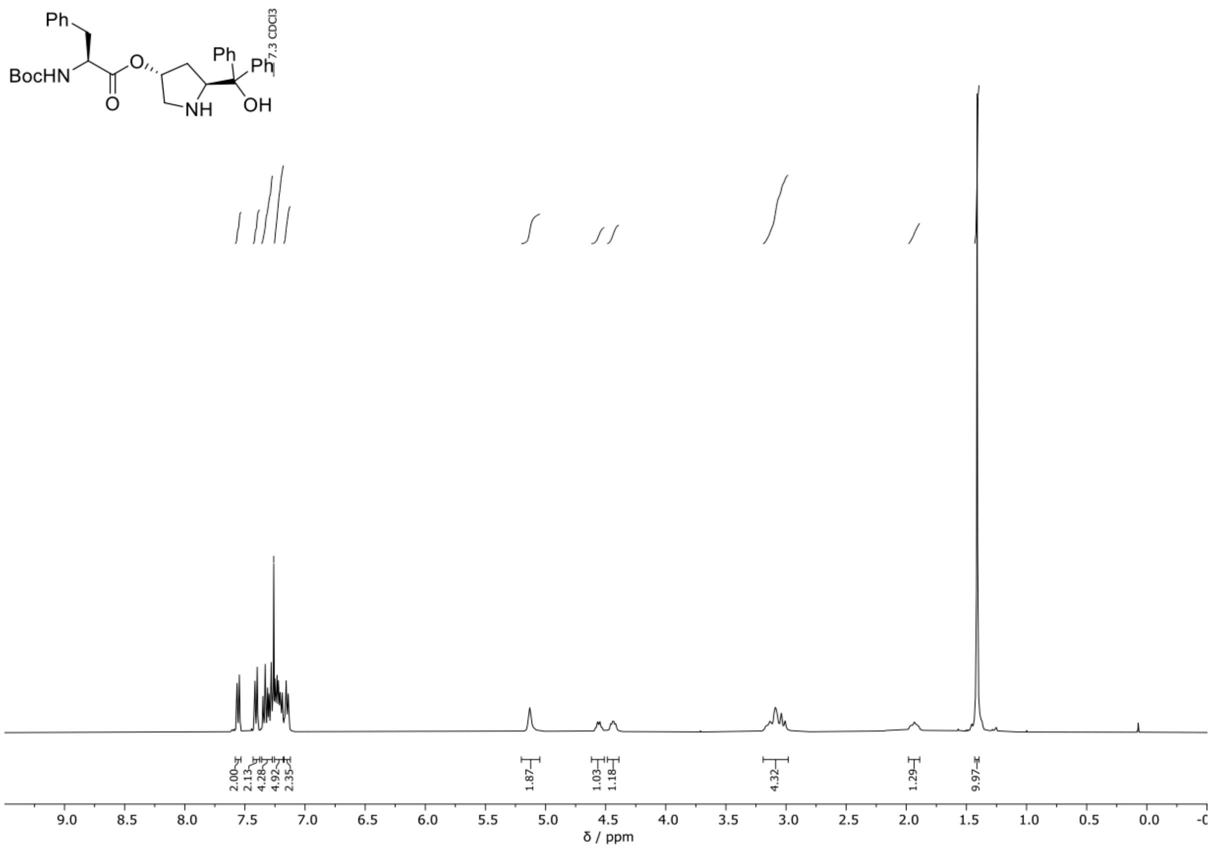
Ph
BocHN
O
O
NH
Ph
Ph
OH
7.3 CDCl3
2.00
2.13
4.28
4.92
2.35
1.87
1.03
1.18
4.32
1.29
9.97
9.0 8.5 8.0 7.5 7.0 6.5 6.0 5.5 5.0 4.5 4.0 3.5 3.0 2.5 2.0 1.5 1.0 0.5 0.0
δ / ppm

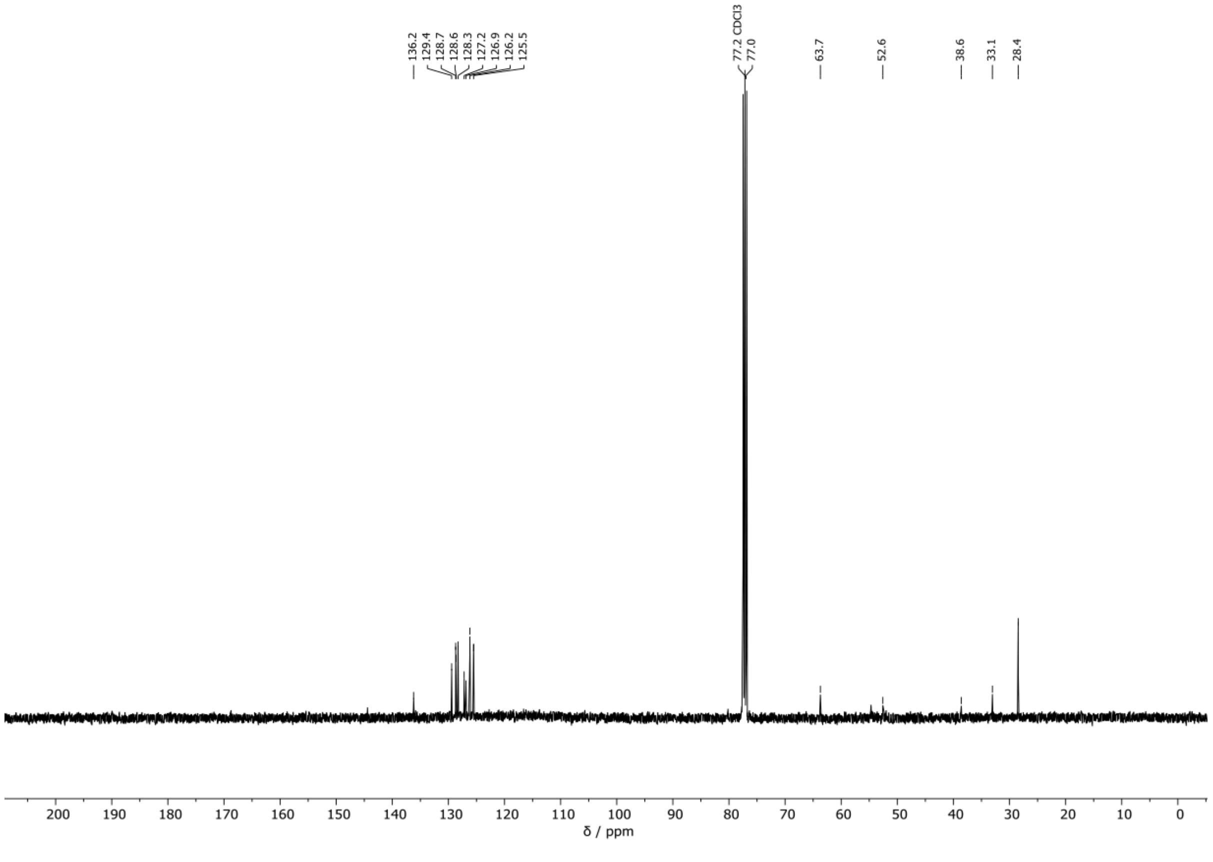
136.2
129.4
128.7
128.6
128.3
127.2
126.9
126.2
125.5
77.2 CDCl3
77.0
63.7
52.6
38.6
33.1
28.4
200 190 180 170 160 150 140 130 120 110 100 90 80 70 60 50 40 30 20 10 0
δ / ppm

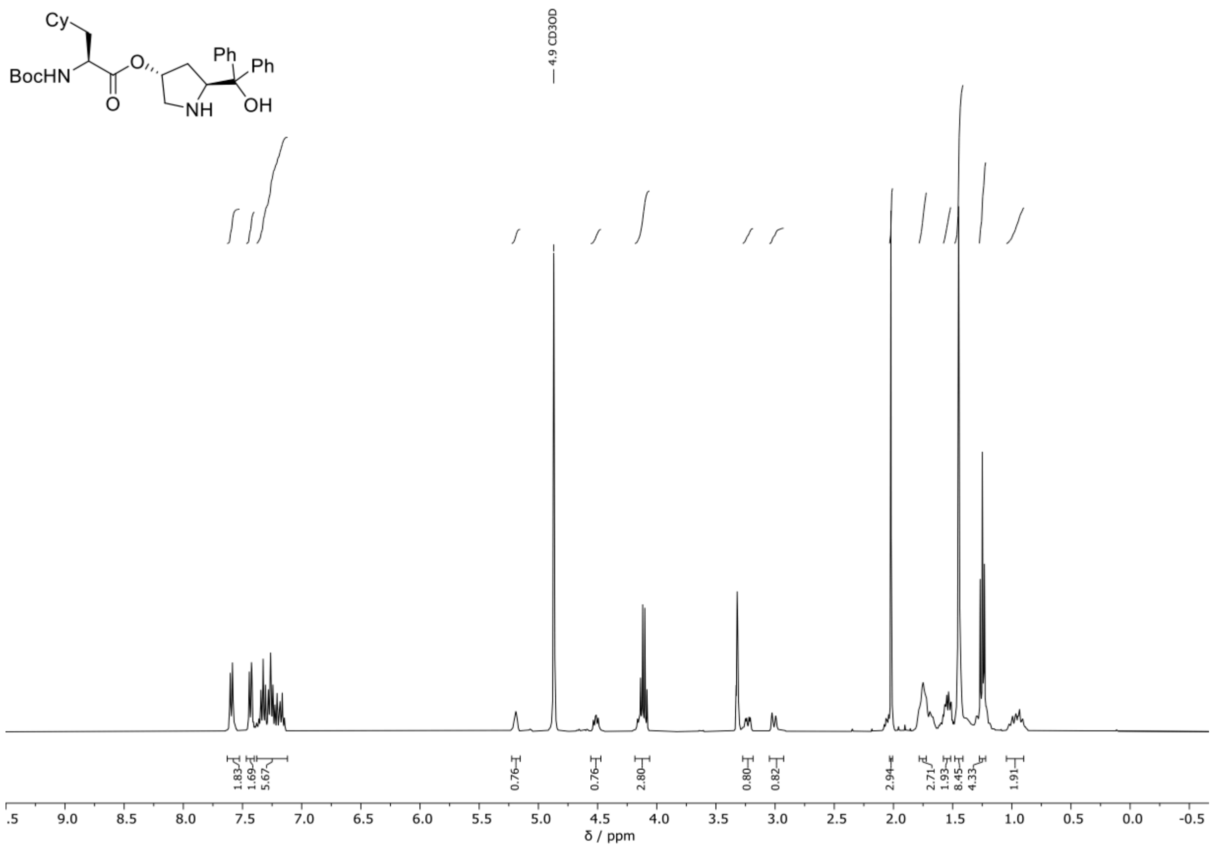
Cy
BocHN
O
O
NH
Ph
Ph
OH
4.9 CD3OD
1.83
1.69
5.67
0.76
0.76
2.80
0.80
0.82
2.94
2.71
1.93
8.45
4.33
1.91
.5
9.0
8.5
8.0
7.5
7.0
6.5
6.0
5.5
5.0
4.5
4.0
3.5
3.0
2.5
2.0
1.5
1.0
0.5
0.0
-0.5
δ / ppm

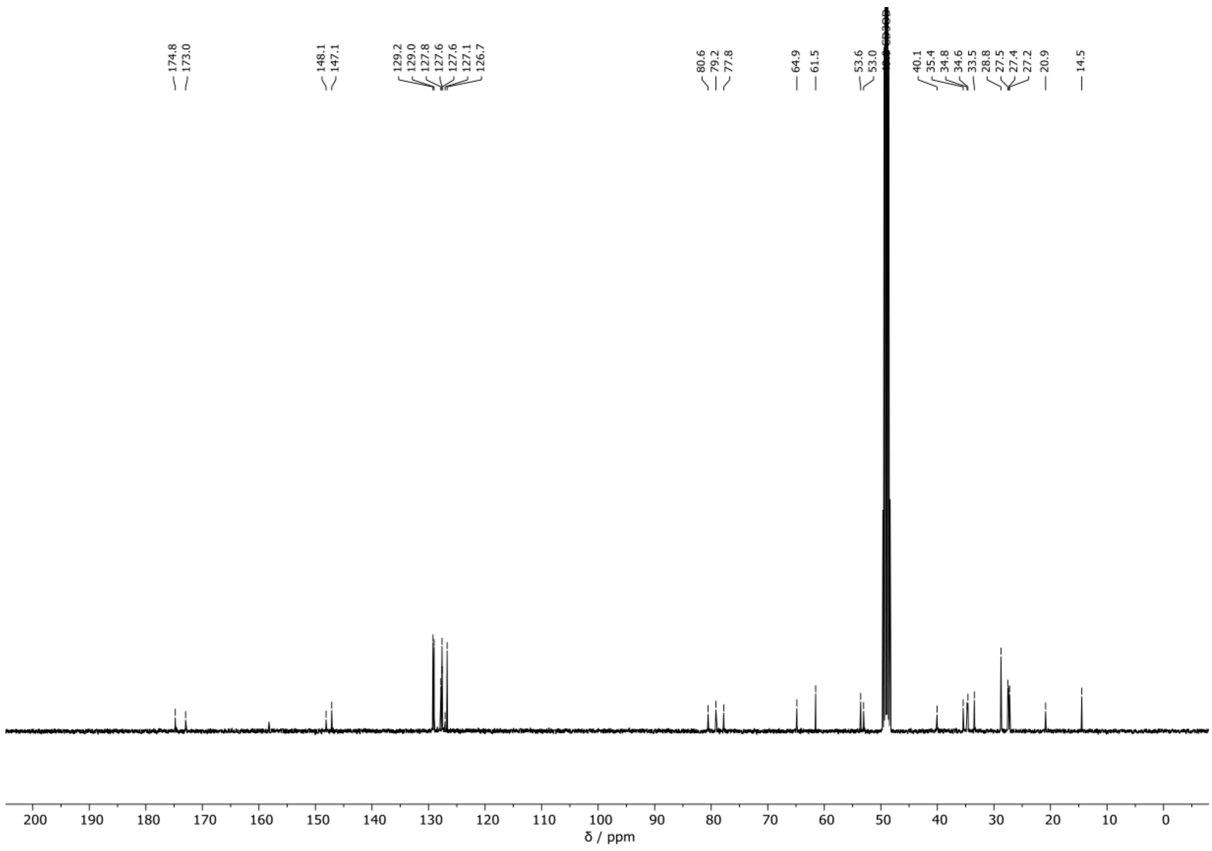
174.8
173.0
148.1
147.1
129.2
129.0
127.8
127.6
127.6
127.1
126.7
80.6
79.2
77.8
64.9
61.5
53.6
53.0
CD3OD
40.1
35.4
34.8
34.6
33.5
28.8
27.5
27.4
27.2
20.9
14.5
200
190
180
170
160
150
140
130
120
110
100
90
80
70
60
50
40
30
20
10
0
δ / ppm

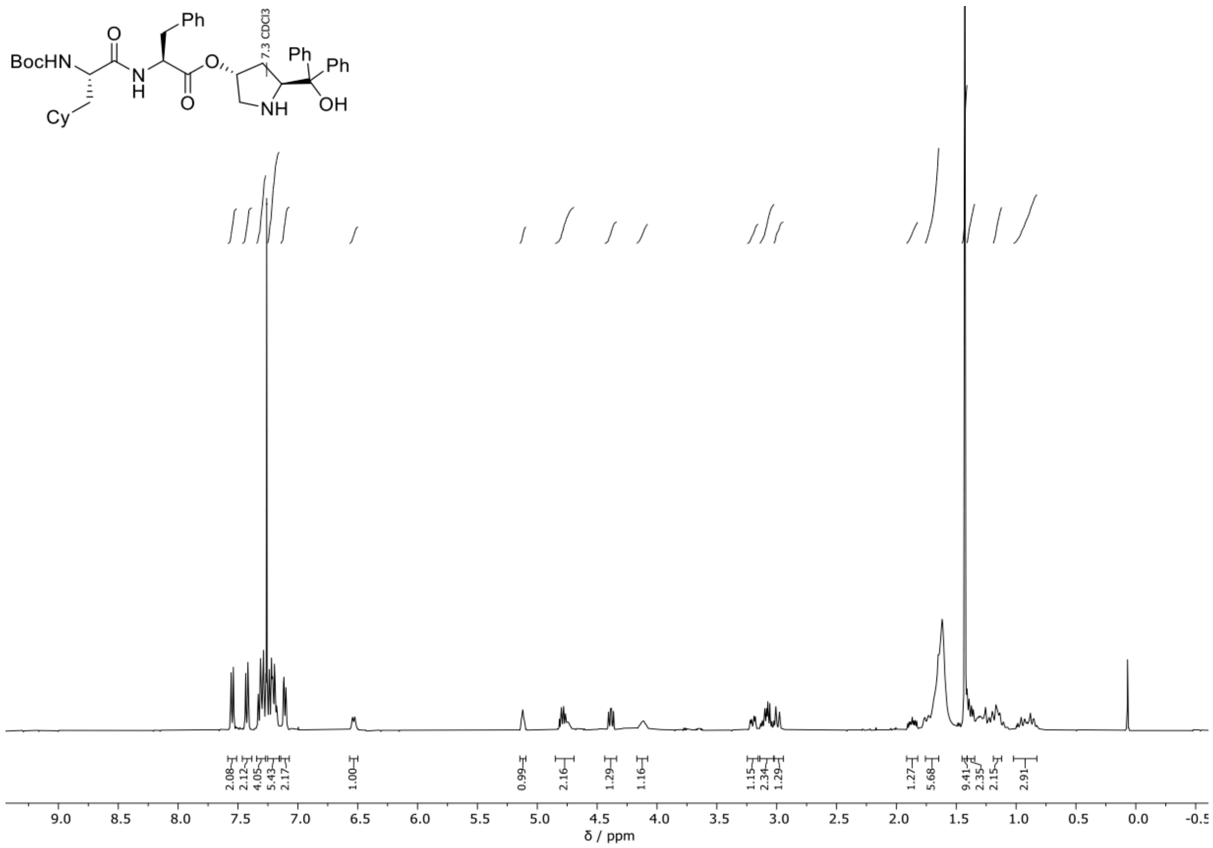
BocHN
Cy
O
N
H
Ph
O
O
NH
Ph
Ph
OH
7.3 CDCl3
2.08
2.12
4.05
5.43
2.17
1.00
0.99
2.16
1.29
1.16
1.15
2.34
1.29
1.27
5.68
9.41
2.35
2.15
2.91
9.0
8.5
8.0
7.5
7.0
6.5
6.0
5.5
5.0
4.5
4.0
3.5
3.0
2.5
2.0
1.5
1.0
0.5
0.0
-0.5
δ / ppm

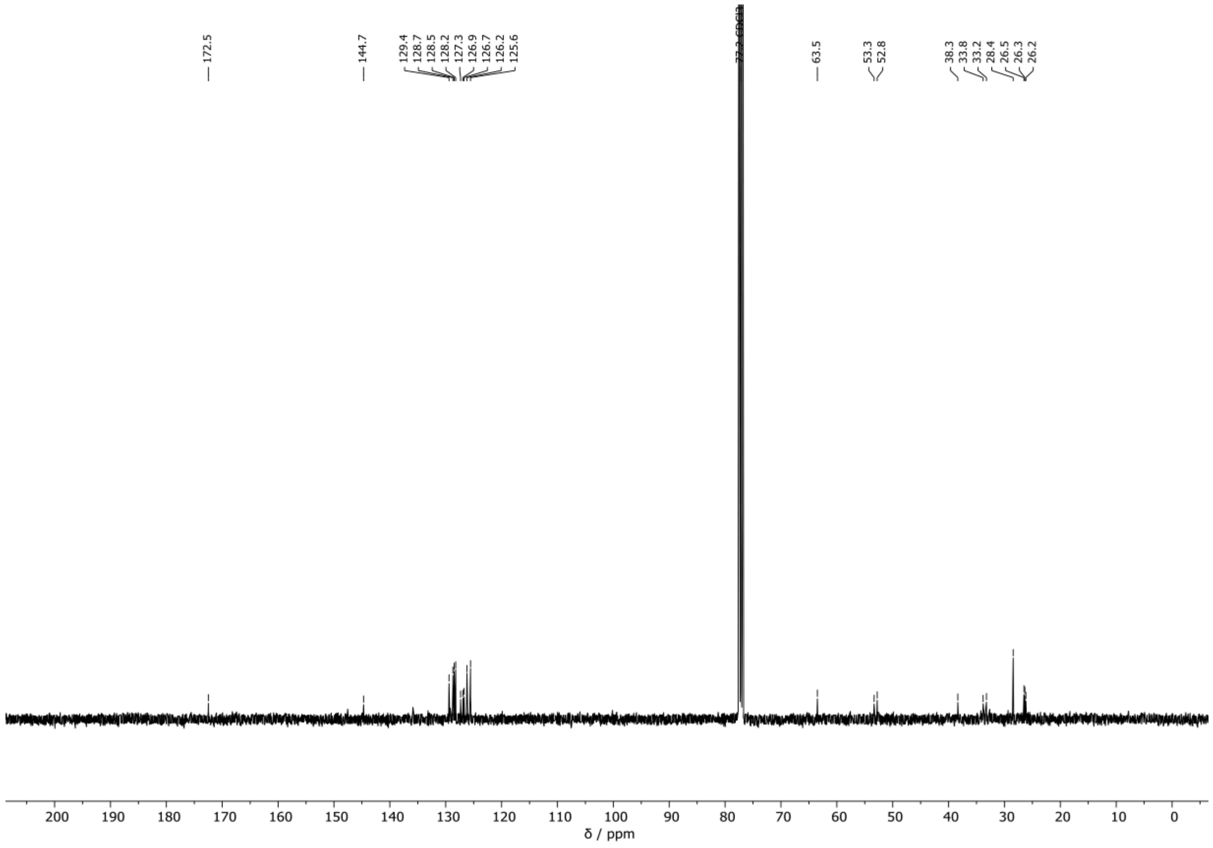
172.5
144.7
129.4
128.7
128.5
128.2
127.3
126.9
126.7
126.2
125.6
77.2 CDCl3
63.5
53.3
52.8
38.3
33.8
33.2
28.4
26.5
26.3
26.2
200
190
180
170
160
150
140
130
120
110
100
90
80
70
60
50
40
30
20
10
0
δ / ppm

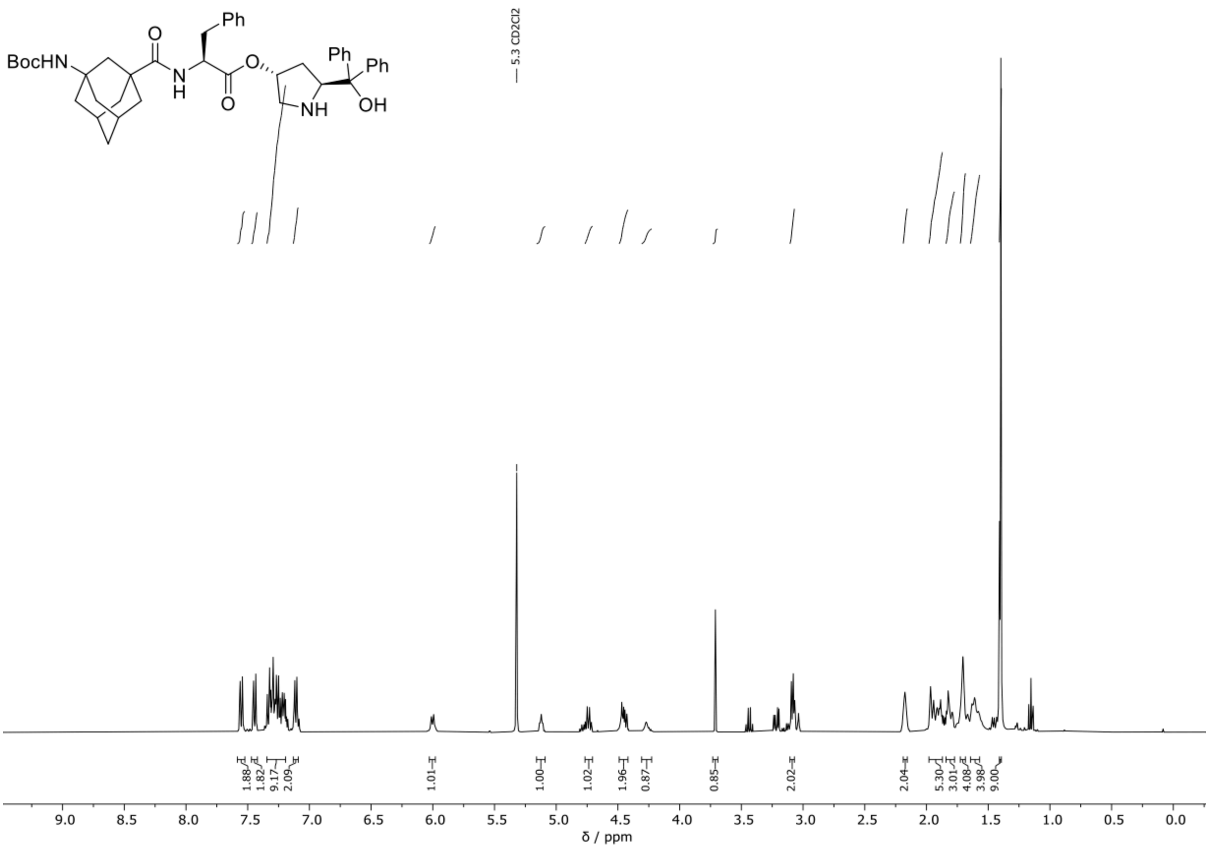
BocHN
O
N
H
Ph
O
O
Ph
Ph
NH
OH
5.3 CD2Cl2
1.88
1.82
9.17
2.09
1.01
1.00
1.02
1.96
0.87
0.85
2.02
2.04
5.30
3.01
4.08
3.98
9.00
9.0
8.5
8.0
7.5
7.0
6.5
6.0
5.5
5.0
4.5
4.0
3.5
3.0
2.5
2.0
1.5
1.0
0.5
0.0
δ / ppm

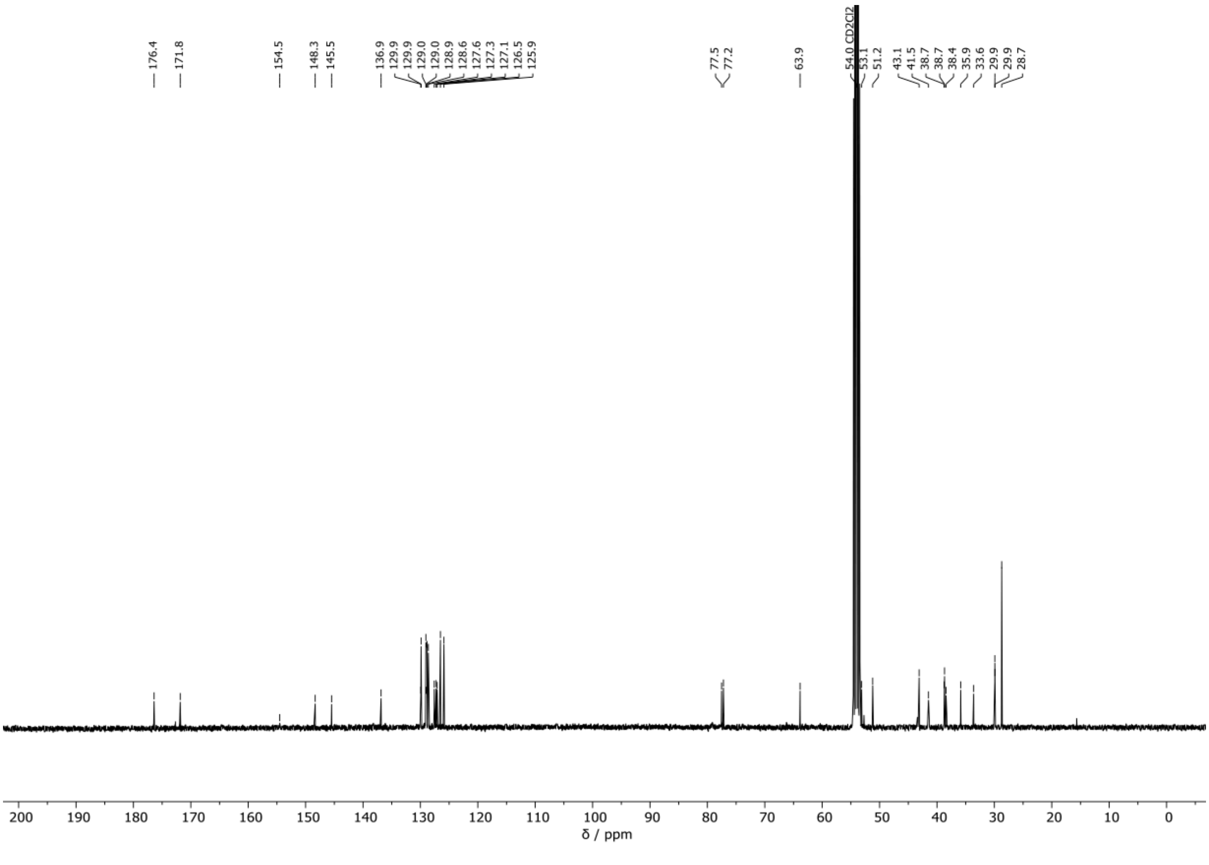
176.4
171.8
154.5
148.3
145.5
136.9
129.9
129.9
129.0
129.0
128.9
128.6
127.6
127.3
127.1
126.5
125.9
77.5
77.2
63.9
54.0 CD2Cl2
53.1
51.2
43.1
41.5
38.7
38.7
38.4
35.9
33.6
29.9
29.9
28.7
200
190
180
170
160
150
140
130
120
110
100
90
80
70
60
50
40
30
20
10
0
δ / ppm

6. References

[1] H. Wennemers, *Chem. Commun.* **2011**, *47*, 12036–12041.

[2] E. A. C. Davie, S. M. Mennen, Y. Xu, S. J. Miller, *Chem. Rev.* **2007**, *107*, 5759–5812.

[3] C. E. Müller, D. Zell, R. Hrdina, R. C. Wende, L. Wanka, S. M. M. Schuler, P. R. Schreiner, *J. Org. Chem.* **2013**, *78*, 8465–8484.

[4] A. J. Metrano, A. J. Chinn, C. R. Shugrue, E. A. Stone, B. Kim, S. J. Miller, *Chem. Rev.* **2020**, *120*, 11479–11615.

[5] B. R. Sculimbrene, S. J. Miller, *J. Am. Chem. Soc.* **2001**, *123*, 10125–10126.

[6] K. W. Fiori, A. L. A. Puchlopek, S. J. Miller, *Nat. Chem.* **2009**, *1*, 630–634.

[7] S. Mukherjee, J. W. Yang, S. Hoffmann, B. List, *Chem. Rev.* **2007**, *107*, 5471–5569.

[8] C. Hofmann, S. M. M. Schuler, R. C. Wende, P. R. Schreiner, *Chem. Commun.* **2014**, *50*, 1221–1223.

[9] C. Hofmann, J. M. Schümann, P. R. Schreiner, *J. Org. Chem.* **2015**, *80*, 1972–1978.

[10] R. Hrdina, C. E. Müller, R. C. Wende, L. Wanka, P. R. Schreiner, *Chem. Commun.* **2012**, *48*, 2498–2500.

[11] G. Peris, S. J. Miller, *Org. Lett.* **2008**, *10*, 3049–3052.

[12] K. Akagawa, K. Kudo, *Adv. Synth. Catal.* **2011**, *353*, 843–847.

[13] S. R. Gilbertson, S. E. Collibee, A. Agarkov, *J. Am. Chem. Soc.* **2000**, *122*, 6522–6523.

[14] B. V. Popp, Z. T. Ball, *J. Am. Chem. Soc.* **2010**, *132*, 6660–6662.

[15] I. B. Sivaev, V. I. Bregadze, *Coord. Chem. Rev.* **2014**, *270–271*, 75–88.

[16] E. J. Corey, R. K. Bakshi, S. Shibata, C. P. Chen, V. K. Singh, *J. Am. Chem. Soc.* **1987**, *109*, 7925–7926.

[17] E. J. Corey, R. K. Bakshi, S. Shibata, *J. Am. Chem. Soc.* **1987**, *109*, 5551–5553.

[18] Y. Kawanami, S. Murao, T. Ohga, N. Kobayashi, *Tetrahedron* **2003**, *59*, 8411–8414.

[19] K. Ishihara, S. Kondo, H. Yamamoto, *J. Org. Chem.* **2000**, *65*, 9125–9128.

[20] E. J. Corey, T. P. Loh, *J. Am. Chem. Soc.* **1991**, *113*, 8966–8967.

[21] T. Harada, C. Inui, *J. Org. Chem.* **2006**, *71*, 1277–1279.

[22] E. J. Corey, T. Shibata, T. W. Lee, *J. Am. Chem. Soc.* **2002**, *124*, 3808–3809.

[23] D. H. Ryu, E. J. Corey, *J. Am. Chem. Soc.* **2003**, *125*, 6388–6390.

[24] K. Futatsugi, H. Yamamoto, *Angew. Chem. Int. Ed.* **2005**, *44*, 1484–1487.

[25] K. Mahender Reddy, E. Bhimireddy, B. Thirupathi, S. Breitler, S. Yu, E. J. Corey, *J. Am. Chem. Soc.* **2016**, *138*, 2443–2453.

[26] K. Ishihara, S. Kondo, H. Yamamoto, *Synlett* **1999**, *1999*, 1283–1285.

[27] S. Grimme, J. Antony, S. Ehrlich, H. Krieg, *J. Chem. Phys.* **2010**, *132*, 154104.

[28] S. Grimme, S. Ehrlich, L. Goerigk, *J. Comput. Chem.* **2011**, *32*, 1456–1465.

[29] C. Bannwarth, S. Ehlert, S. Grimme, *J. Chem. Theory Comput.* **2019**, *15*, 1652–1671.

[30] S. Danishefsky, T. Kitahara, *J. Am. Chem. Soc.* **1974**, *96*, 7807–7808.

[31] S. Danishefsky, T. Kitahara, C. F. Yan, J. Morris, *J. Am. Chem. Soc.* **1979**, *101*, 6996–7000.

[32] E. J. Corey, C. L. Cywin, T. D. Roper, *Tetrahedron Lett.* **1992**, *33*, 6907–6910.

[33] F. W. Lichtenthaler, S. Nishiyama, P. Jarglis, *Angew. Chem. Int. Ed.* **1979**, *91*, 1001–1002.

[34] D. C. Harrowven, J. C. Hannam, *Tetrahedron Lett.* **1998**, *39*, 9573–9574.

[35] C. Zhao, J. Wang, *Adv. Synth. Catal.* **2019**, *361*, 1668–1672.

[36] E. J. Corey, R. K. Bakshi, S. Shibata, *J. Am. Chem. Soc.* **1987**, *109*, 5551–5553.

[37] O. V Maltsev, A. S. Kucherenko, S. G. Zlotin, *Eur. J. Org. Chem.* **2009**, *2009*, 5134–5137.

[38] M. S. Chauhan, S. Singh, *J. Mol. Catal. A Chem.* **2015**, *398*, 184–189.

[39] R. Baltzly, *J. Org. Chem.* **1976**, *41*, 920–928.

[40] Xu, Wei, Zhang, *J. Org. Chem.* **2003**, *68*, 10146–10151.

[41] G. B. Stone, *Tetrahedron Asymmetry* **1994**, *5*, 465–472.

[42] A. F. Zahrt, N. I. Rinehart, S. E. Denmark, *Eur. J. Org. Chem.* **2021**, *2021*, 2343–2354.

[43] R. C. Wende, P. R. Schreiner, *Green Chem.* **2012**, *14*, 1821–1849.

[44] P. Eisenberger, C. M. Crudden, *Dalt. Trans.* **2017**, *46*, 4874–4887.

[45] T. S. De Vries, A. Prokofjevs, E. Vedejs, *Chem. Rev.* **2012**, *112*, 4246–4282.

[46] C. R. Shugrue, S. J. Miller, *Chem. Rev.* **2017**, *117*, 11894–11951.

[47] D. Niedek, F. R. Erb, C. Topp, A. Seitz, R. C. Wende, A. K. Eckhardt, J. Kind, D. Herold, C. M. Thiele, P. R. Schreiner, *J. Org. Chem.* **2020**, *85*, 1835–1846.

[48] A. Seitz, R. C. Wende, E. Roesner, D. Niedek, C. Topp, A. C. Colgan, E. M. McGarrigle, P. R. Schreiner, *J. Org. Chem.* **2021**, *86*, 3907–3922.

[49] J. Li, S. Grosslight, S. J. Miller, M. S. Sigman, F. D. Toste, *ACS Catal.* **2019**, *9*, 9794–9799.

[50] M. W. Giuliano, S. J. Miller, *Site-Selective Catalysis*, Springer, Cham, **2015**, pp. 157–201.

[51] C. Palomo, M. Oiarbide, J. M. García, *Chem. Soc. Rev.* **2012**, *41*, 4150.

[52] A. P. G. Macabeo, F. P. A. Martinez, T. Kurtán, L. Tóth, A. Mándi, S. Schmidt, J. Heilmann, G. J. D. Alejandro, M. Knorn, H. M. Dahse, S.G. Franzblau, *J. Nat. Prod.* **2014**, *77*, 2711–2715.

[53] Y. Fu, P. Wu, J. Xue, X. Wei, *J. Nat. Prod.* **2014**, *77*, 1791–1799.

[54] K. Nakamura, S. I. Kondo, Y. Kawai, K. Hida, K. Kitano, A. Ohno, *Tetrahedron Asymmetry* **1996**, *7*, 409–412.

[55] T. Koike, K. Murata, T. Ikariya, *Org. Lett.* **2000**, *2*, 3833–3836.

[56] W. Adam, M. T. Díaz, R. T. Fell, C. R. Saha-Möller, *Tetrahedron Asymmetry* **1996**, *7*, 2207–2210.

[57] C. E. Müller, L. Wanka, K. Jewell, P. R. Schreiner, *Angew. Chem. Int. Ed.* **2008**, *47*, 6180–6183.

[58] K. Chapman, M. Holmes, J. Seckl, *Physiol. Rev.* **2013**, *93*, 1139–1206.

[59] K. A. Ahrendt, C. J. Borths, D. W. C. MacMillan, *J. Am. Chem. Soc.* **2000**, *122*, 4243–4244.

[60] G. E. Keck, X.-Y. Y. Li, D. Krishnamurthy, *J. Org. Chem.* **1995**, *60*, 5998–5999.

Chapter 3 London Dispersion Interactions Rather than Steric Hindrance Determine the Enantioselectivity of the Corey-Bakshi-Shibata Reduction

Christian Eschmann, Lijuan Song, and Peter R. Schreiner, *Angew. Chem. Int. Ed.* **2021**, *60*, 4823–4832

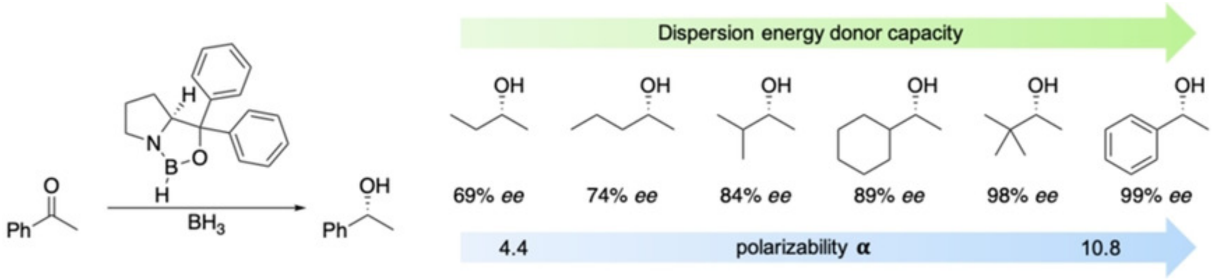

Abstract : The well-known Corey–Bakshi–Shibata (CBS) reduction is a powerful method for the asymmetric synthesis of alcohols from prochiral ketones, often featuring high yields and excellent selectivities. While steric repulsion has been regarded as the key director of the observed high enantiose- lectivity for many years, we show that London dispersion (LD) interactions are at least as important for enantiodiscrimination. We exemplify this through a combination of detailed computa- tional and experimental studies for a series of modified CBS catalysts equipped with dispersion energy donors (DEDs) in the catalysts and the substrates. Our results demonstrate that attractive LD interactions between the catalyst and the substrate, rather than steric repulsion, determine the selectivity. As a key outcome of our study, we were able to improve the catalyst design for some challenging CBS reductions.

1. Introduction

1.1. The CBS Reduction

The detailed understanding of reaction mechanisms and the origin of enantioselectivity is essential for successful catalyst design. Enantioselectivity imparted by chiral, small- molecule catalysts is rationalized typically by preferential steric destabilization derived from the repulsive part of the van der Waals (vdW) potential because it can be readily understood and taught with hard-sphere classical mechanics models. In contrast, London Dispersion (LD), the attractive part of the vdW potential,[1] is often neglected in mechanistic considerations and for catalyst design.[2] However, for a de- tailed understanding of a given catalytic system, all interactions must be considered, even though we are just learning how to conceptualize this for reaction planning.[3] Fortunately, modern computational techniques like dispersion corrected density functional theory (DFT) now allow a detailed analysis of all factors contributing to transition state stabilization for a much better understanding of catalyst design.[4] Here we chose the Corey-Bakshi-Shibata (CBS) reduction, which is a versatile method for the enantioselective reduction of prochiral ketones by oxazaborolidines (OXB), achieving high selectivities and yields[5] to demonstrated that all steric factors, attraction and repulsion, have to be taken into account to arrive at a balanced description of the mechanism and to design new, more selective catalysts.

Corey‘s widely accepted mechanistic model bases stereo- selection exclusively on steric repulsion between the boron substituent **R** on the catalyst and the large $\mathbf{R_L}$ and small $\mathbf{R_S}$ substituents of the ketone in a six-membered boat-like transition state (Scheme 1).[5f,6] With this model, one can qualitatively predict the enantiofacial discrimination of numerous substrates. However, this model of steric destabilization does not offer a satisfying explanation for the selectivity and reactivity of some substrates. For example, the reduction of trichloroacetophenone predominantly generates the (*R*)-enantiomer.[6a] This implies that the large phenyl group (R_L) faces the boron substituent in the favored transition state, which is in contrast to Corey‘s standard model depicted in Scheme 1. In the reduction of cyclopropyl isopropyl ketone (1-cyclopropyl-2-methylpropan-1-one) one would assume poor selectivity, because both substituents are similar in steric size. Nonetheless, the reduction delivers the (*R*)-enantiomer with a selectivity of 91% *ee*.[5f] Similarly, a high *ee* (81%) was also found for *p*-methoxy-*p*’-nitro-benzophenone with two groups of similar size.[5f] In these two cases, the cyclopropyl substituent and the *p*-methoxyphenyl group act as R_L, respectively, thereby demonstrating that other factors must also play an important role in the transition state structure. Furthermore, despite bearing bulky groups, there are substrates that do not deliver high selectivity, e.g., unbranched aliphatic ketones.[7]

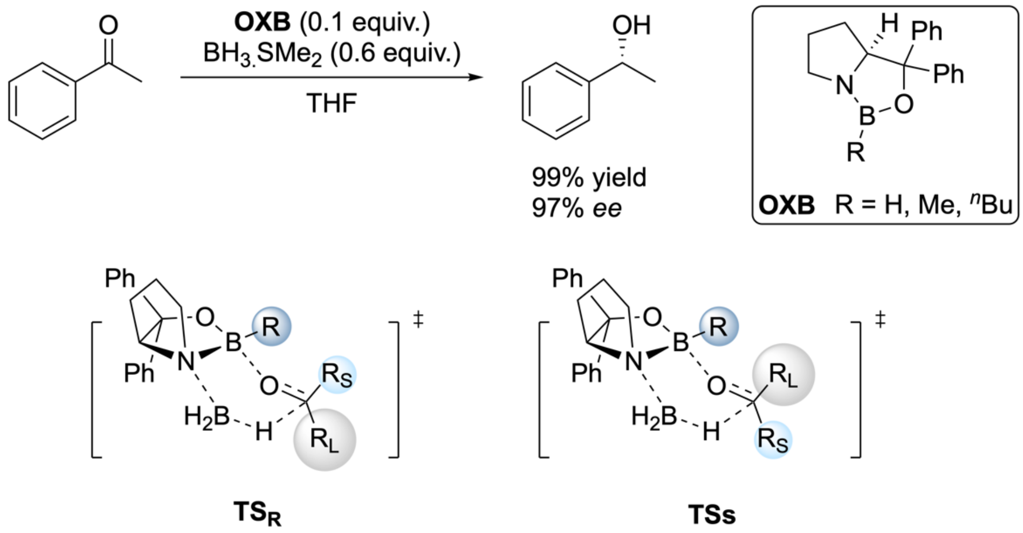

Scheme 1 CBS reduction of acetophenone and proposed transition structures for hydride transfer, favoring the (*R*)-product on the basis of minimizing the steric repulsion between "**R**" and "$\mathbf{R_L}$".

There are several reports on the stereoselection of the CBS reduction trying to shed light on the origin of its enantioselectivity. In 1993 Liotta *et al.* used the MNDO semiempirical approach to suggest that the reduction is more likely to occur *via* a chair-like transition state. In addition, the carbinol phenyl substituents of the catalyst are required to lie parallel to the $\mathbf{R_L}$ substituent to minimize steric repulsion.[8] Meyer *et al.* investigated the role of steric repulsion in the transition structures of the reduction by determining kinetic isotope effects (KIE), as the C-D bond is effectively shorter than the C-H bond, resulting in inverse ^{2}H KIEs for reactions in which steric repulsion increases in the transition structure.[9] They concluded that Corey's steric reasoning is too simplistic, because in the reduction of acetophenone the chair-like transition state prevails, with the boron substituent only playing a minor role.[10] In a recent theoretical study, Lachtar *et al.* suggested that the origin of the enantioselectivity for the oxazaborolidine catalyzed reduction of ketimines can be traced back to noncovalent interactions in the preferred transition structure.[11] However, by replacing the phenyl groups of the catalyst by hydrogens, they used a computationally reduced model that neglects major parts of these key noncovalent interactions. Furthermore, their B3LYP/6-31G(d,p) computations do not include dispersion corrections.

Herein, we aim at bringing together experimental and computational studies geared towards understanding a reaction whose stereochemical outcome was classically interpreted as being derived solely on the basis of steric repulsion. We demonstrate that a more detailed and hence more powerful mechanistic reasoning emerges when all interactions are taken into account and we gauge the role of attractive LD stabilization in this particular reaction.

2. Results and Discussion

This section is organized in three parts. First, a comprehensive computational investigation of the various noncovalent interactions (NCI) in the transition structures provides a contemporary view of the origin of the enantioselectivity in the CBS reduction. Then we show how these insights help in the design of new catalysts to improve enantioselectivity, especially for some challenging substrates. Finally, we provide an experimental validation of our improved understanding of catalyst design.

2.1. Reconsidering Steric Effects

None of the previously reported computational mechanistic studies include LD corrections,[8–12] which are needed to strike a proper balance between repulsive and attractive noncovalent interactions. As this is the very concept of an "equilibrium structure", we set out to determine the role LD plays in the CBS reduction. We first computed the reaction pathway for the reduction of acetophenone using a comparison of B3LYP vs. B3LYP-D3(BJ) with appropriate basis sets and solvent inclusion (see Computational Details below); the difference should provide a good estimate of the role dispersion plays (Fig. 1). A detailed potential energy surface (PES) of the complete reaction pathway and higher-level single-point energy computations with DLPNO-CCSD- (T)[13] (domain-based local pair natural orbital CCSD(T)) for the key step are provided in the Supporting Information (Supporting Information, Fig. S1).

In this simplified PES, we start with the catalyst, the reducing agent, and acetophenone as reference **1**. The hydride transfer determining enantioselectivity occurs *via* two diastereomeric transition structures. If LD is not taken into account (color-coded in gray), the transition structures **TS1'$_{\mathbf{S}}$** and **TS1'$_{\mathbf{R}}$** are found to be very high in free energy exhibiting barriers of 29.8 kcal mol^{-1} and 31.7 kcal mol^{-1}, respectively. These energy barriers are too high for such a fast reaction at 25 °C. After inclusion of LD (color-coded in black), the relative energies of the transition structures **TS1$_{\mathbf{R}}$** and **TS1$_{\mathbf{S}}$** are notably lower with barriers of only 13.7 kcal mol^{-1} and 15.7 kcal mol^{-1}, respectively, which is much more reasonable for a catalyzed reaction that proceeds quickly at room temperature. The calculated enantioselectivity of the reduction, which is expressed in the energy difference between the transition structures ($\Delta\Delta G^{\ddagger}$) for hydride transfer, is –2.0 kcal mol^{-1} and thereby consistent with previously published experimental results (–2.2 kcal mol^{-1}).[5b] We computed the transition structures in solvent within the limitations of an SCRF model. The energy difference of **TS1$_{\mathbf{R}}$** and **TS1$_{\mathbf{S}}$** in gas phase is 4.0 kcal mol^{-1}, while it is 2.0 kcal mol^{-1} in THF. As expected, the LD interactions are attenuated by the interaction with the solvent but, more importantly, they do not vanish. Catalyst regeneration and release of the boronate 7 is exergonic by –15.1 kcal mol^{-1}. For comparison, we also added DLPNO-CCSD(T)/cc-pVTZ single-point energies on the DFT-optimized geometries (and ZPVE corrections) of **TS1$_{\mathbf{S}}$** and **TS1$_{\mathbf{R}}$**, which are 7.7 kcal mol^{-1} and 10.8 kcal mol^{-1}, respectively. This indicates that the dispersion-corrected energy barrier is more reasonable and that more complete inclusion of electron correlation effects emphasize the importance of LD.

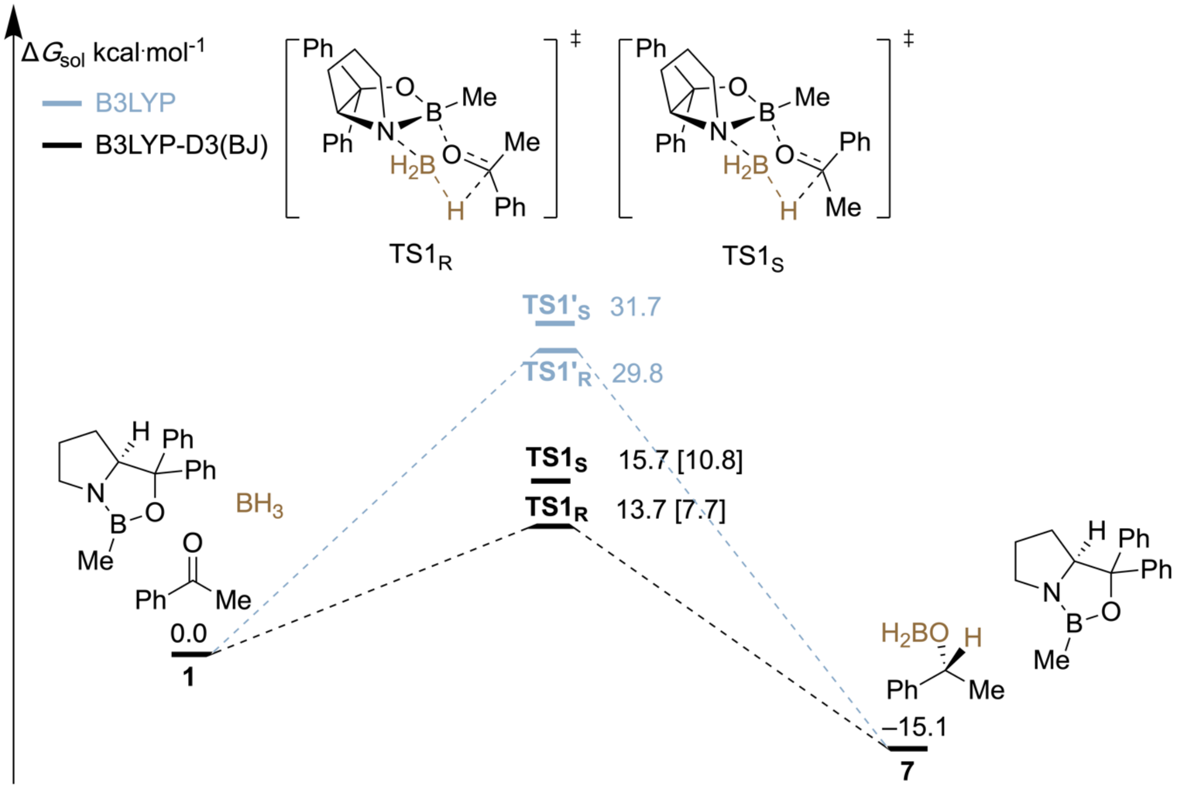

Figure 1 Potential energy surface displaying the free energies ($\Delta G_{\mathrm{sol}}^{275}$) of the CBS pathway with (black) and without dispersion (gray) corrections at 2 °C (for a more detailed PES, see the Supporting Information, Fig. S2). Level of theory: B3LYP-D3(BJ)/6–311+G(d,p)-SMD(THF)//B3LYP-D3(BJ)/6–311G(d,p). The free energies in brackets are based on electronic DLPNO-CCSD(T)/cc-pVTZ single-point energy (corrected for ZPVE).

A closer look at the geometries of the transition structures **TS1$_\mathrm{R}$** and **TS1$_\mathrm{S}$** reveals chair-like conformations (Fig. 2), which are 3.8 kcal mol^{-1} lower in energy, than the corresponding boat-like conformations suggested by Corey (Supporting Information, Fig. S1). Thereby, the catalyst binds to the ketone at the lone pair facing the small substituent (**R$_\mathrm{S}$**) *anti* to the electron-rich substituent as it is also described in Corey's model. NCI plots indicate some differences of the noncovalent interactions between catalyst and substrate in the two transition structure conformations.[14] Contrary to Corey's model no steric destabilization (repulsion is color-coded red in the NCI plot) by hydrogen-hydrogen contacts can be found in less favored **TS1$_\mathrm{S}$**. In fact, the bond distances of around 2.5 Å in the preferred transition structure **TS1$_\mathrm{R}$** lead to stabilizing $\sigma - \pi$ LD interactions[15] between acetophenone and the phenyl groups of the catalyst, as visualized by the green areas in the NCI plot. Additionally, the methyl substituent of the substrate interacts favorably with the boron substituent of the catalyst. In the less favored transition structure **TS1$_\mathrm{S}$** the long distance between substituents of substrate and catalyst prevent optimal interactions. These computations suggest LD interactions to be important for enantiodiscrimination. We additionally employed LD potential maps developed by Pollice and Chen to visualize these LD interactions (Supporting Information, Fig. S2).[16] These confirm the conclusions drawn from the qualitative NCI analysis.

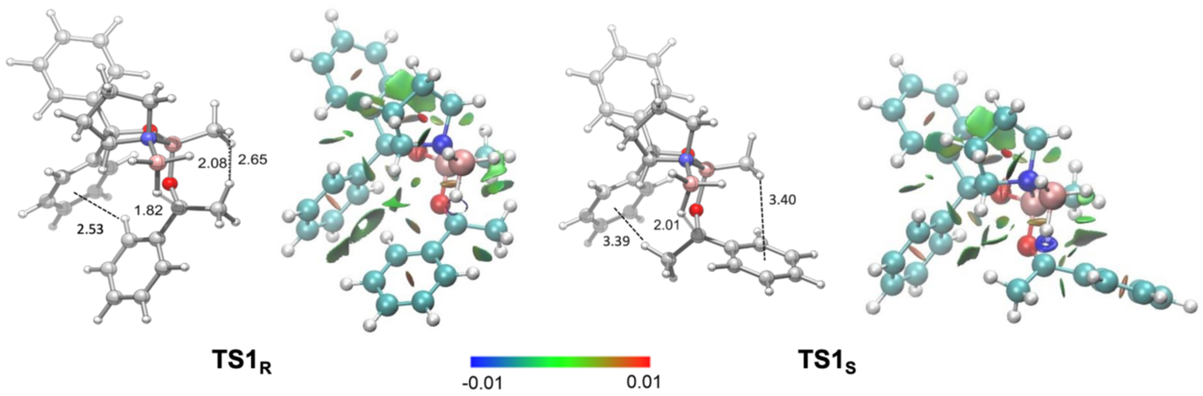

Figure 2 Selectivity determining transition structures for hydride transfer in the CBS-reduction of acetophenone with (*S*)-1-methyl-3,3-diphenylhexahydropyrrolo[1,2-*c*][1,3,2]oxazaborole as the catalyst. Selected bond distances in Å and noncovalent interaction (NCI) plots (s=0.5 a.u., –0.01 < r < +0.01 a.u.). Color code: repulsion (red), strong attraction (blue), weak noncovalent interactions (green). The transition structures were optimized at B3LYP-D3(BJ)/6–311G(d,p).

To examine the general effect of LD interactions on the enantioselectivity, three literature examples with various substrates and catalysts were also studied (Tab. 1). In the reduction of cyclohexyl methyl ketone (1-cyclohexylethanone, entry 2) the moderate enantioselectivity (85% *ee*) is likely due to decreased LD interactions of the cyclohexyl with the phenyl group of the catalyst.[5a] Similarly, replacing the phenyl substituents with a spirocyclopentyl group in the catalyst leads to diminished enantioselectivity of 67% *ee*.[17] This implies that the LD interactions of the phenyl groups in the catalyst are crucial for enantioselectivity. Note that the selectivities obtained from our LD corrected computations (B3LYP-D3(BJ)) are in better agreement with the experimental *ee* values (Tab. 1) than the uncorrected values.[5a,17]

Table 1 Activation free energy (at the temperature of the experiment) differences in kcal mol^{-1}: experiment vs. theory. Level of theory: B3LYP-D3(BJ)/6–311+G(d,p)-SMD//B3LYP-D3(BJ)/6–311G(d,p).

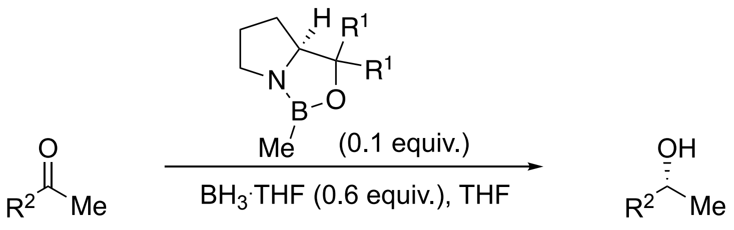

R^1/catalyst structure	R^2	config *ee* (%)	$\Delta\Delta G^{\ddagger}_{exp}$	$\Delta\Delta G^{\ddagger}_{sol}$ (without D3)	$\Delta\Delta G^{\ddagger}_{sol}$ (with D3)
Ph	Ph	*R* 97	2.2 (2 °C)	1.9	2.0
Ph	Cy	*R* 85	1.3 (–10 °C)	0.9	1.1
-(CH$_2$)$_4$-	Ph	*R* 67	1.0 (23 °C)	2.4	1.2

SAPT0 (Symmetry Adapted Perturbation Theory) was employed to analyze the different energetic contributions of the interactions between substrate and catalyst in the transition structures (Fig. 3).[18] The components include electrostatics, exchange, induction, and LD energies. The electrostatic term arises from the large Coulomb interactions between the Lewis acid and Lewis base sites (carbonyl and boryl as well as amino and boryl groups). In the transition structures, electrostatics and induction dominate the interactions but they are counterbalanced by a large exchange term (i.e., Pauli repulsion), indicating significant steric repulsion. However, the larger exchange energy in favored **TS1$_{\mathbf{R}}$** disagrees with Corey's model, in which the larger exchange term should favor **TS1$_{\mathbf{S}}$**. Therefore, the selectivity is not determined by steric repulsion (alone). Although LD is a small part of the total interaction energy, it decisively contributes. The LD energy preference for **TS1$_{\mathbf{R}}$** is 5.9 kcal mol^{-1}, which is in good agreement with the experimentally observed high selectivity.[5a,b] Thus, our computational results strongly suggest that LD interactions between catalyst and substrate also determine the enantioselectivity.

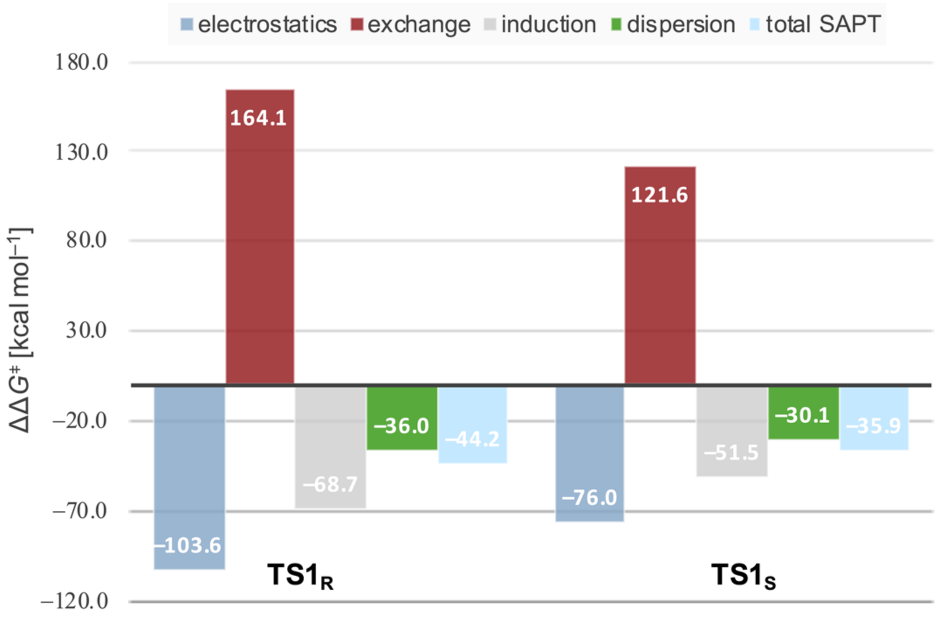

Figure 3 SAPT0 analysis of the transition structures **TS1$_{\mathbf{R}}$** and **TS1$_{\mathbf{S}}$** in the CBS reduction of acetophenone. Level of theory: SAPT0/jun-cc- pvdz. For a plot of relative energies and more information, see the Supporting Information.

2.2. Improving Catalyst Design with Dispersion Energy Donors

Based on our new understanding of the origin of enantioselectivity in the CBS reduction, we hypothesized that higher enantioselectivity can be achieved by modifying the catalyst with dispersion energy donors (DEDs)[2c,15b] that enable favorable substrate-catalyst interactions through increasing polarizability. The catalyst modifications involve on the one hand the boron substituent and the carbinol substituents on the other.

First, we investigated the effect of the substituent at boron (Tab. 2); DEDs including ^{i}Pr, ^{t}Bu, Cy, CH$_2$Cy, *c*-C$_5$H$_9$ were employed. In the reduction of cyclohexyl ketone LD interactions are the highest using CH$_2$Cy with a $\Delta\Delta G^{\ddagger}$ of 3.5 kcal mol^{-1} (entry 1). As expected for large and highly polarizable groups, Cy and ^{t}Bu should also deliver significant enantiodiscrimination (entries 2 and 4). For *tert*-butyl methyl ketone, only the ^{t}Bu and Me substituents show high selectivity (entries 8 and 9). However, our experimental results demonstrate that the selectivity does not change much as compared to the original catalyst when using CH$_2$Cy and Cy groups (Supporting Information, Fig. S3). This implies that the interactions between substrate and the substituent at boron on the catalyst only have a subtle effect on the enantioselectivity.

Table 2 The energy difference between the transition structures for hydride transfer for computed substrates and catalysts at 25 °C. Level of theory: B3LYP-D3(BJ)/6-311+G(d,p)-SMD// B3LYP-D3(BJ)/6-311G(d,p).

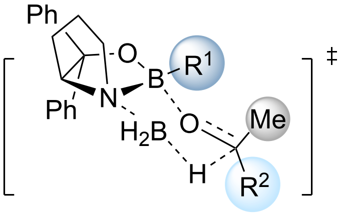

TS1$_R$

Entry	R^1	R^2	$\Delta\Delta G^{\ddagger}_{sol}$ (without D3)	$\Delta\Delta G^{\ddagger}_{sol}$ (with D3)
1	CH$_2$Cy	Cy	1.0	3.5
2	Cy	Cy	–0.4	2.3
3	*c*-C$_5$H$_9$	Cy	–2.2	–0.2
4	^{t}Bu	Cy	0.1	2.0
5	^{i}Pr	Cy	1.2	0.9
6	Cy	^{t}Bu	–0.5	–1.1
7	*c*-C$_5$H$_9$	^{t}Bu	–0.3	0.1
8	^{t}Bu	^{t}Bu	1.7	2.3
9	Me	^{t}Bu	4.1	4.2

The variation of carbinol substituents of the catalyst leads to much larger changes of enantioselectivity. Replacing the phenyl groups with aliphatic DEDs, e.g., Me, ^{i}Pr, and ^{n}Bu show comparable or even reduced selectivity relative to the original catalyst with its unsubstituted phenyl groups.[6b]

The introduction of DEDs in the meta-positions of the aryl groups of the catalyst results in comparably high or even slightly higher enantioselectivities relative to the original catalyst in the reduction of acetophenone (Fig. 4).

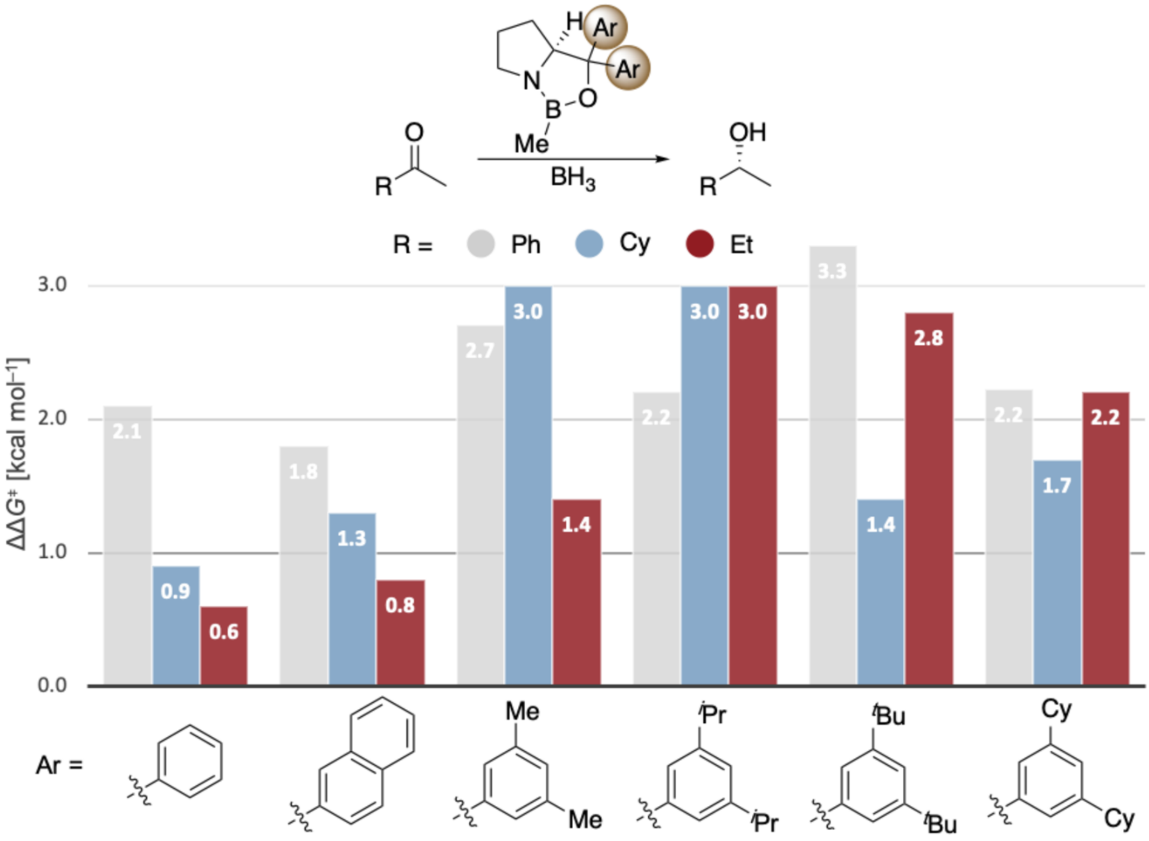

Figure 4 Computed enantioselectivities (expressed through $\Delta\Delta G^{\ddagger}$) in the reduction of acetophenone, cyclohexyl methyl ketone, and 2-butanone using different Ar groups on the catalyst at 25 °C. Level of theory: B3LYP-D3(BJ)/6-311+G(d,p)-SMD// B3LYP-D3(BJ)/6-311G(d,p).

The intermolecular stabilization by all-*meta* substitution in dispersion-driven systems has been demonstrated recently, e.g., in the stabilization of molecular dimers[19] and in the catalytic hydroamination of olefins.[3d] Here we also find that DEDs in *meta*-aryl positions provide additional attractive interactions with, e.g., the ethyl substituent of 2-butanone, as indicated in the NCI plots (Fig. 5). Again, more stabilizing interactions (–2.8 kcal mol^{-1}) between aryl groups on the catalyst and the ethyl group in the substrate are found in the preferred **TS$_R$**.

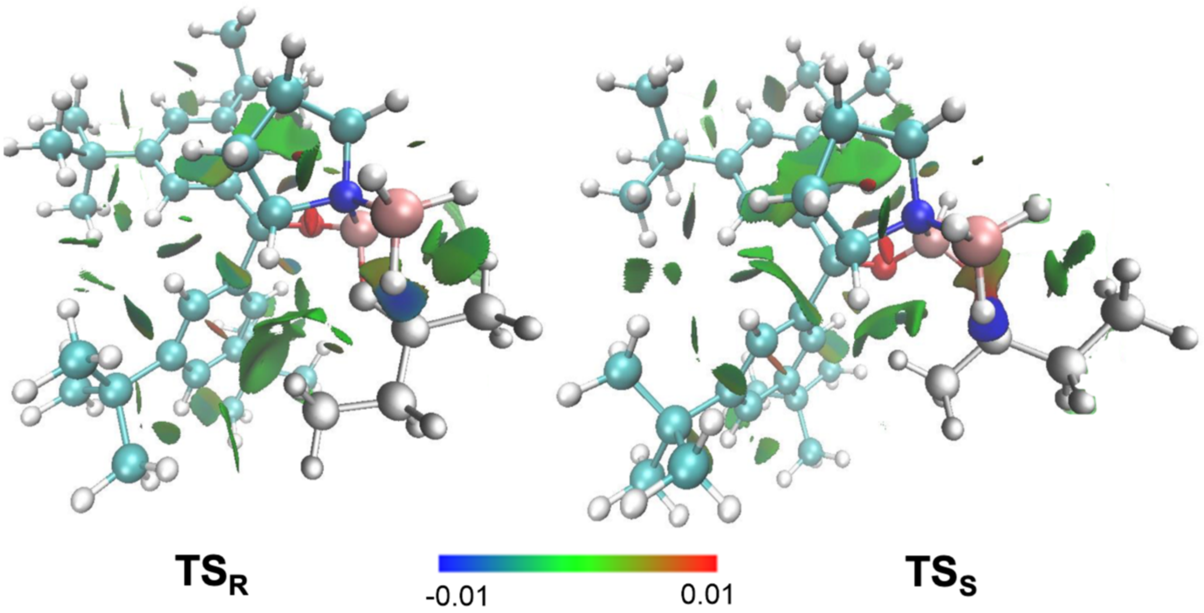

Figure 5 NCI plots (s = 0.5 a.u., –0.01 < r < +0.01 a.u.) of the transition structures in the reduction of 2-butanone using 3,5-^{t}Bu$_2$Ph as carbinol substituent on the catalyst. Color code: repulsion (red), strong attraction (blue), weak noncovalent interactions (green). The transition structures were optimized at B3LYP-D3(BJ)/6-311G(d,p).

To explore the general potential of aryl-substituted catalysts computationally, the 3,5-^{t}Bu$_2$Ph catalyst was computed in the reduction of various substrates (Fig. 6). The modified catalyst shows comparable or improved enantioselectivity, especially for substrates yielding low enantioselectivity with the original catalyst, e.g., 2-butanone and cyclohexyl methyl ketone. For 2-butanone, $\Delta\Delta G^{\ddagger}$ improves from 0.6 to 2.8 kcal mol^{-1}, implying a theoretical change in *ee* from 47% to 98%.

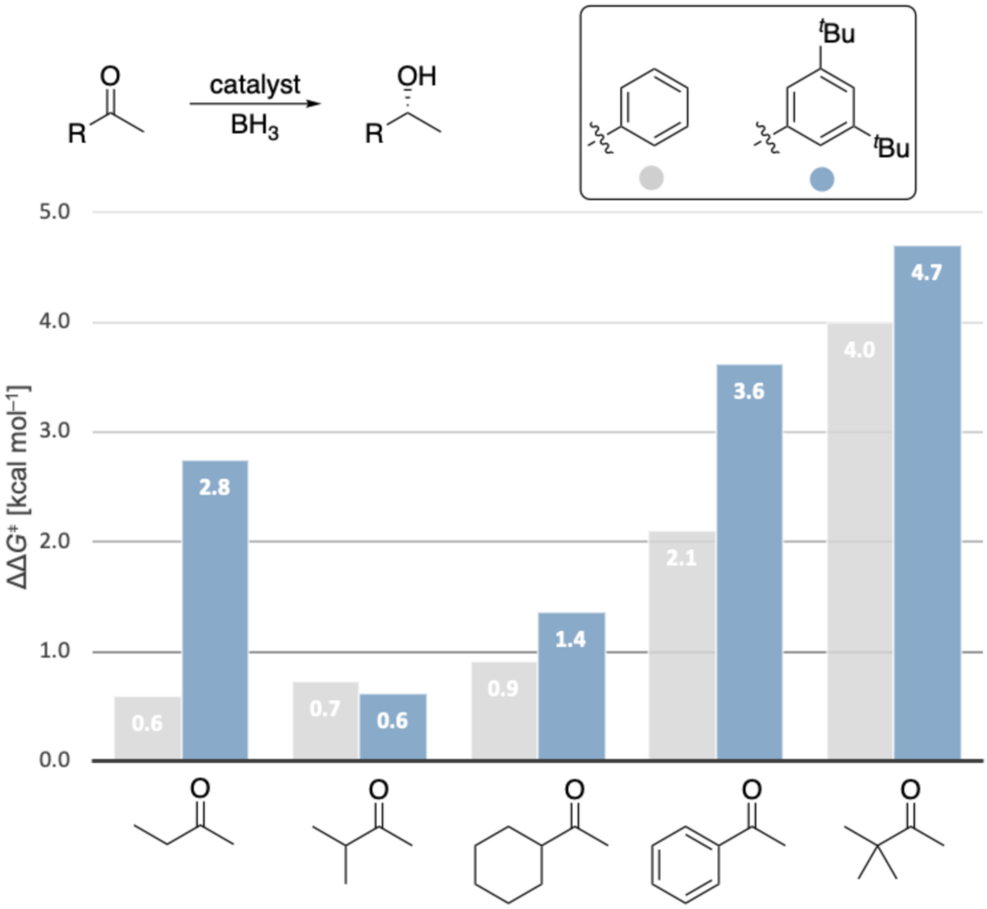

Figure 6 Computed enantioselectivities (expressed as $\Delta\Delta G^{\ddagger}$ values) for the reduction of various ketones employing the 3,5- ^{t}Bu$_2$Ph catalyst compared to the original CBS catalyst at 25 °C. Level of theory: B3LYP-D3(BJ)/6-311G+(d,p)-SMD// B3LYP-D3(BJ)/6-311G(d,p).

2.3. Experimental Validation

To examine our computational predictions, we performed an experimental validation employing various catalysts and substrates. We started with comparing the effects of changing the substituents in the catalyst at the carbinol and boron positions. We compared the original CBS catalyst to three modified versions in the reduction of three ketones bearing aromatic, branched or unbranched alkyl substituents. We employed Corey‘s standard protocol using 10 mol% of catalyst, 1.1 equivalents of reducing agent in THF at 50 °C for 1.5 h (Fig. 7).[6b] We chose slightly elevated temperatures, as for borane reductions there is an increase in selectivity with increasing temperature up to 30–50 °C (Supporting Information, Tab. S2).[20] This resulted in nearly quantitative yields. As expected, by changing the carbinol substituent of the catalyst from hydrogen to phenyl, the selectivity increases.

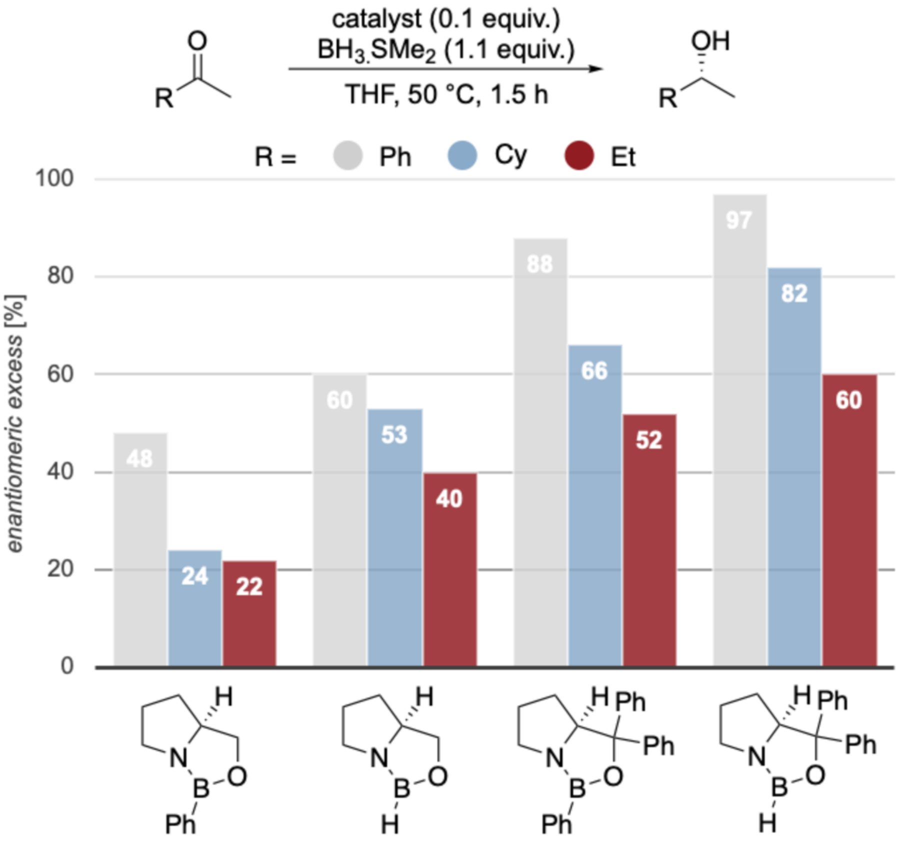

Figure 7 Reduction of prochiral ketones employing modified CBS catalysts.

These initial findings support our proposal that the carbinol substituents are key for enantiofacial discrimination due to LD interactions with the substrate. Furthermore, when replacing the hydrogen at boron with a phenyl group, we observe a decrease in enantioselectivity. This disagrees with the steric repulsion hypothesis, where (*R*)-selectivity should improve with increasing steric size of the substituent at boron.[6b] Consistent with our computations (Figures 2 and 3), we relate this to stabilizing LD interactions between substrate and the phenyl group at boron in less favored $\mathbf{TS}_S$ (Fig. 2). This does not exclude the notion that catalysts bearing a phenyl group at boron are probably weaker Lewis acids and less effective, and the lower selectivity might also be a result of a more prominent unselective background reaction.

Next, we experimentally probed the computationally predicted effects of the carbinol substituents shown in Figure 4. We employed catalysts with aryl groups bearing additional DEDs to check whether the LD interactions increase and thereby increase enantioselectivity (Figures 8 and 9). In all cases, at 50 °C after 1.5 h the reduction results in near quantitative yields. In the reduction of cyclohexyl methyl ketone all modified catalysts achieve higher selectivities due to additional LD stabilizations. As LD through the *meta*-substituent seems to be maximized at methyl already, we decided to test the 4-OMe-3,5-Me$_2$Ph and 4-OMe-3,5-^{t}Bu$_2$Ph catalysts that should be even more polarizable due to electron donation from the methoxy group. Indeed, the best selectivities were achieved with the 3,5-Me$_2$Ph- and 4-OMe-3,5-Me$_2$Ph catalysts. The selectivities with 3,5-^{i}Pr$_2$Ph, 3,5-^{t}Bu$_2$Ph and 4-OMe-3,5-^{t}Bu$_2$Ph are slightly lower, as the substituents are getting too bulky for cyclohexyl ketone; the results are similar for the reduction of 2-heptanone. While the overall selectivity is lower due to entropic penalty of the linear alkyl chain,[21] we observed the best selectivities with 3,5-Me_2Ph and 4-OMe-3,5-Me_2Ph. These experimental results fit the qualitative expectation from our improved model and confirm our computations of Figure 4, as the 3,5-Me_2Ph catalyst was the also the best computed catalyst for cyclohexyl ketone.

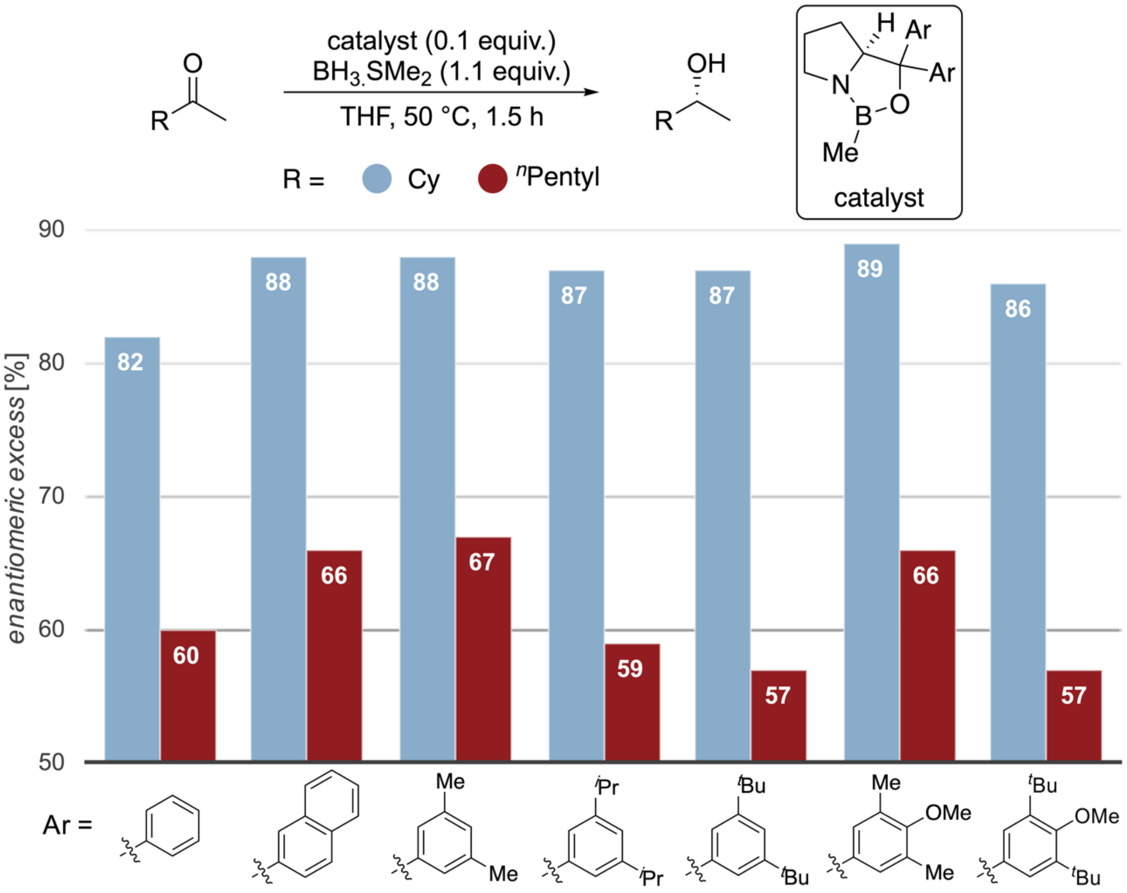

Figure 8 CBS Reductions employing modified catalysts with DEDs in the catalyst's carbinol position.

Importantly, in the challenging reductions of smaller *n*-alkyl ketones, we achieve a steady increase in selectivity from 60% up to 72% *ee* for 2-butanone and 64% up to 74% *ee* for 2-pentanone by increasing DEDs and adding further electron-donor groups (4-OMe-3,5-Me_2Ph, 4-OMe-3,5-$^tBu_2Ph$) to the catalyst (Fig. 9). These results also fit qualitatively to the computations of Figures 4 and 5, as computations suggest the 3,5-$^iPr_2Ph$ and 3,5-$^tBu_2Ph$ derivatives to be the best performing catalysts (the 4-OMe-3,5-Me_2Ph, 4-OMe-3,5-$^tBu_2Ph$ catalysts have not been computed). Note that all newly designed catalysts show improvement over Corey's original catalyst.

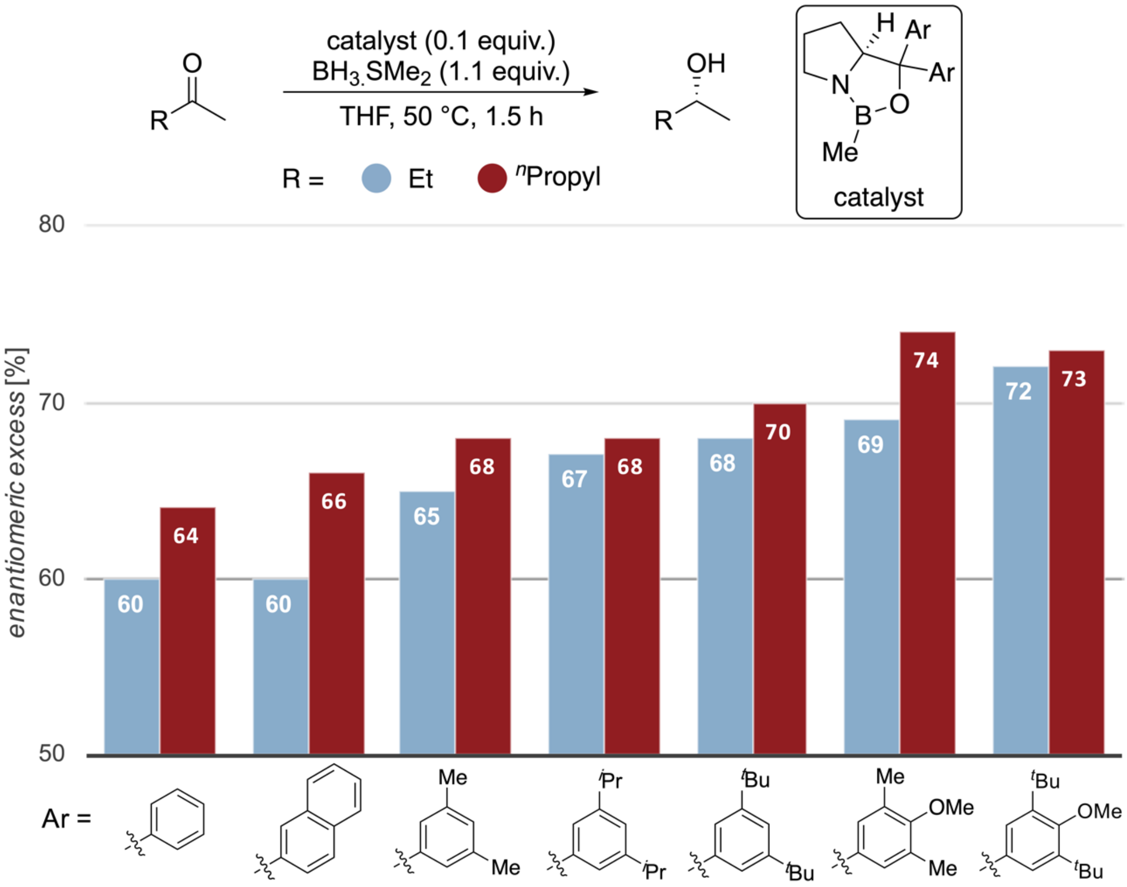

Figure 9 CBS reductions employing modified catalysts with DEDs in the catalyst's carbinol position for challenging substrates. Corey's original catalyst is the first entry (Ar = phenyl).

The trend of increasing selectivities in the experiments is consistent with our computational results but the absolute selectivities differ. While computations suggest an increase of selectivity of up to 98% *ee* by introducing DEDs, the experimentally observed improvement is more moderate. There may be several reasons for this. First, the mechanism is more complex than accounted for in the computations. Second, the reduction features also a non-negligible background reaction with BH_3, which could have a larger impact on the modified catalysts, as the activity of these is lower compared to the original catalyst, because the EDG in the carbinol position reduces the Lewis acidity at boron.[22] Third, the computations are not accurate enough as compared to highest level *ab initio* computations. This is certainly true but we are pleased to see trends with predictability leading to improved catalyst performance, in particular, for the most challenging of substrates.

In order to also provide some counter examples, we included catalysts with 3,5-$(CF_3)_2$Ph and C_6F_5 carbinol substituents and found that the fluorinated catalysts are much less selective (Fig. 10), despite their high steric demand and significant activation of the boron Lewis acid. These results are in accord with the computed values (Supporting Information, Tab. S1) and suggest weakened LD interactions between the fluorinated aryl groups and the substrates, as we decrease attractive $\sigma - \pi$ interactions through the strongly electron withdrawing fluorine substituents.[15c,23]

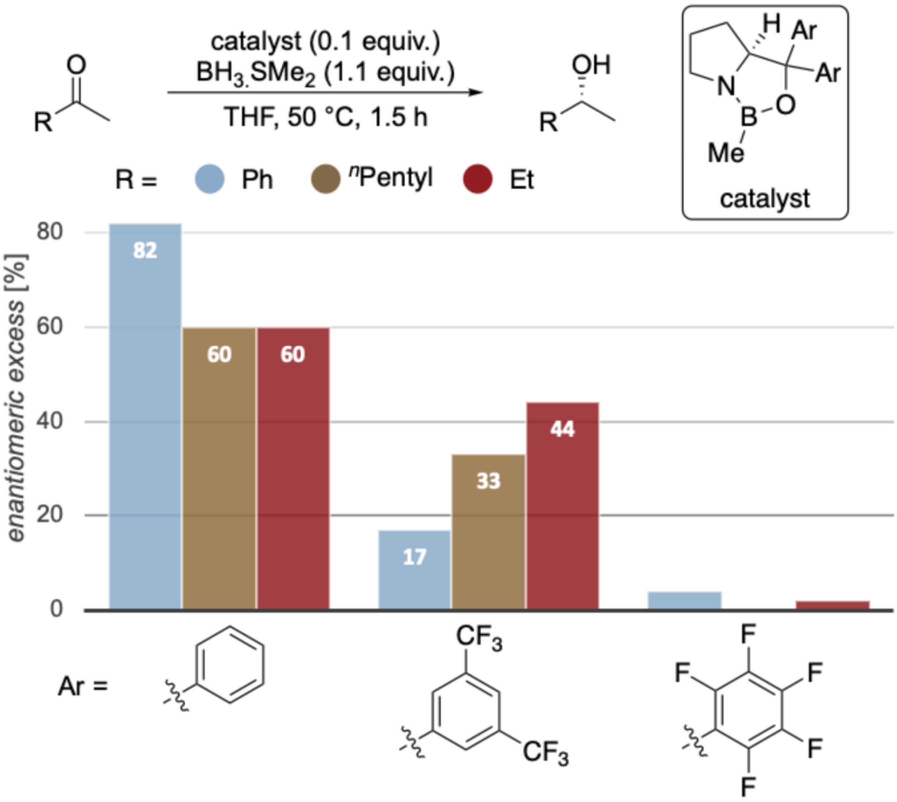

Figure 10 Reductions employing phenyl-substituted and fluorinated catalysts relative to Corey's original catalyst (Ar = phenyl).

Moreover, this is consistent with the reduction of special substrates like pentafluorobenzophenone and *p*-methoxy-*p*'-nitro-benzophenone (Tab. 3). In all cases, the enantiomer maximizing the attractive $\sigma - \pi$ interactions in the TS is favored. Also, the $\sigma - \pi$ interaction of a C_6F_5 substituent to a phenyl ring is lower than the $\sigma - \pi$ of two phenyl groups (entry 1).[15c] For *p*-methoxy-*p*'-nitro-benzophenone the electron-rich aryl group (4-OMe-C_6H_4) provides the stronger interaction with the catalyst (entries 2 and 3). In the case of cyclopropyl isopropyl ketone (entry 4), the catalyst interacts with the more π-electron rich cyclopropyl substituent favoring the *R* enantiomer. With trichloroacetophenone (entries 5 and 6), the more attractive $\sigma - \pi$ interaction results in *R* selectivity, as chloromethanes strongly interact with aryl rings due to LD (Supporting Information, Tab. S4).[23a]

Table 3 Reductions employing some challenging ketones. For further details, see the Supporting Information.

Entry	R^1	R^2	cat. Ar	config[a] *ee* (%)
1	Ph	C_6F_5	Ph	*S* 92
2	4-OMe-C_6H_4	4-NO_2-C_6H_4	Ph	*R* 56
3	4-OMe-C_6H_4	4-NO_2-C_6H_4	4-OMe-3,5-Me_2Ph	*R* 62
4	*c*-Pr	^{i}Pr	Ph	*R* 91[b]
5	CCl_3	Ph	Ph	*R* 27

6	CCl_3	Ph	4-OMe-3,5-Me_2Ph	*R* 45

[a] Abs. configuration is based upon measurement of rotation and comparison with literature or computed values (Supporting Information). [b] Reaction as reported by Corey *et al.* with 15 mol% of catalyst and catecholborane as reducing agent at −78 °C.[5f]

Figure 11 summarizes the results for the reductions of a variety of ketones with our best modified catalyst. These data also indicate that enantioselectivities increase with the computed polarizabilities per volume α/V, resulting in a higher interaction energy of the substituent with the catalyst (Fig. 12).[15a]

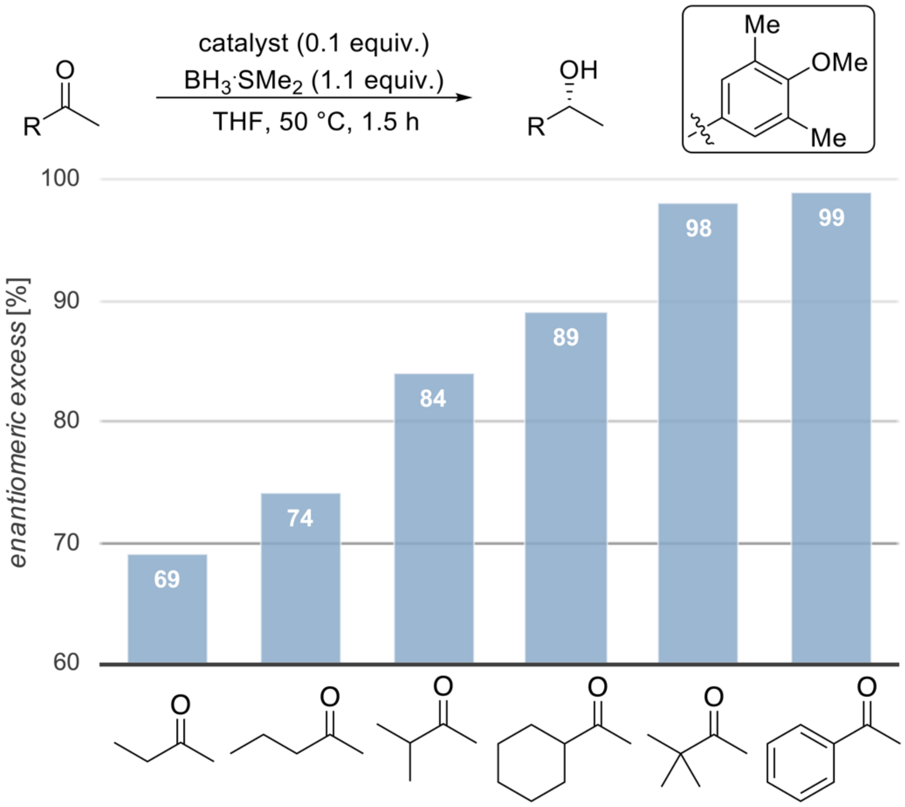

Figure 11 Reductions of various substrates employing our new modified CBS catalyst.

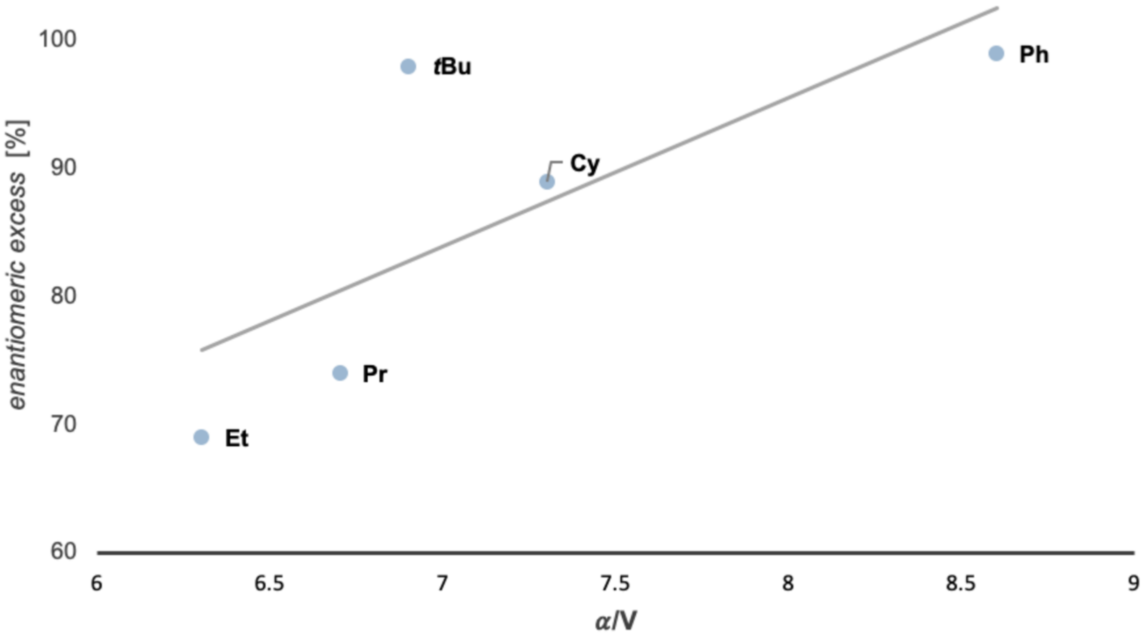

Figure 12 Increasing polarizability per Volume α/V of the substrates typically leads to higher enantio-selectivites in the reduction with a given catalyst (here: 4-OMe-3,5-Me_2Ph). Computed values of polarizability (α) and volume (V) of the corresponding substituent. Level of theory: PBE0/aug-cc-pVDZ//B3LYP-D3(BJ)/6-311G(d,p).[24]

These findings are confirmed by a competitive rate analysis in the reduction of 2-pentanone and *tert*-butyl methyl ketone in the same reaction flask (Fig. 13). After the given reaction times, we took a small sample of the reaction mixture, quenched it in citric acid, and analyzed the conversion after work up. We chose *tert*-butyl methyl ketone and 2-pentanone, as they are reduced with quite different selectivities (Fig. 11). While *tert*-butyl methyl ketone is reduced in excellent selectivity, the reaction should proceed slowly because the neopentyl position is traditionally viewed as highly sterically encumbered, thereby hampering the attack of nucleophiles.[25] Remarkably, the consumption of *tert*-butyl methyl ketone occurs at a higher reaction rate than that of 2-pentanone. Computations show that the complex of the catalyst with *tert*-butyl methyl ketone has a similar energy as that with 2-pentanone (Supporting Information, Fig. S6). This implies that electrostatic interactions with catalyst are similar, and electronic effects are not significant. We conclude that stabilizing LD interactions in the TS are at work because the rate of the sterically more demanding substrate is higher.

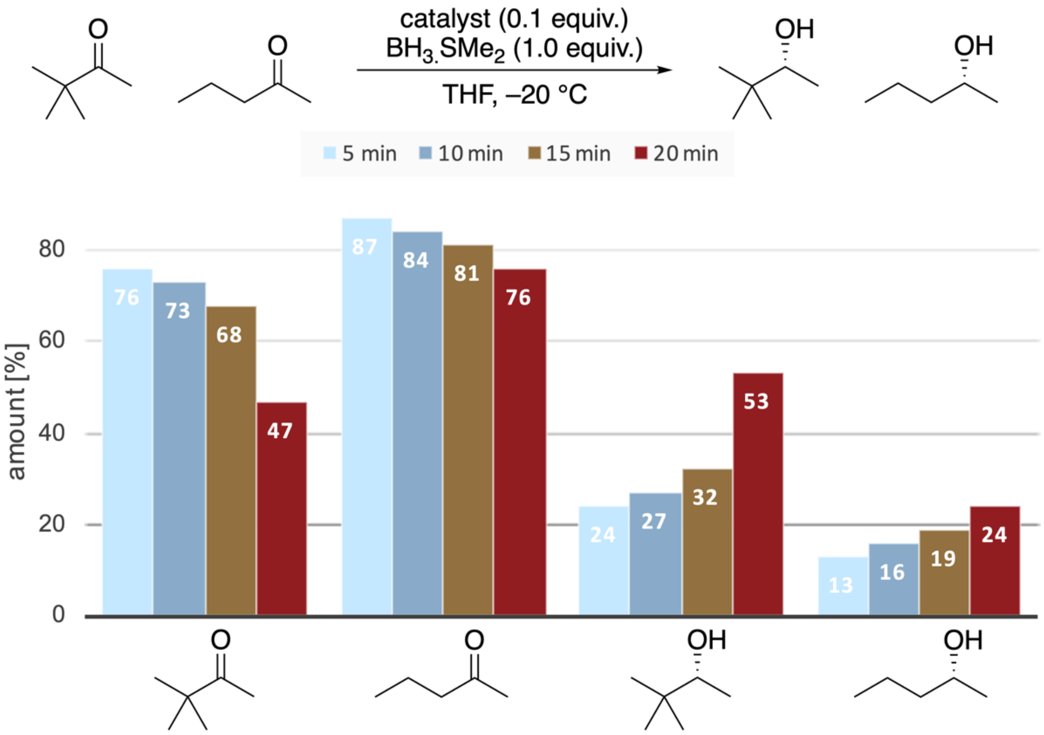

Figure 13 Ketone-to-alcohol ratios in the competitive reduction of *tert*-butyl ketone and 2-pentanone after the given reaction times.

3. Conclusion

We present a combined computational and experimental exploration of the origin of the enantioselectivities in CBS reductions. Contrary to the current hypothesis that makes steric repulsion solely responsible for enantioselection, our computations reveal the presence of stabilizing noncovalent interactions in the hydride transfer transition structure. NCI plots qualitatively aided in visualizing these intermolecular interactions particularly between the substrate and the phenyl substituents of the catalyst. A quantitative SAPT analysis suggests that LD interactions tip the balance in favor of attractive noncovalent steric interactions to achieve high enantioselectivity.

Catalysts bearing DEDs in the *meta*-positions of the aryl groups increase the enantioselectivity for different substrates, as confirmed computationally and experimentally. More polarizable substrates lead to stronger LD interactions with the catalyst and therefore to higher enantioselectivities as well as faster reaction rates. If steric repulsion were the chief selector, the rates would diminish with increasing selectivity - the opposite is the case. Even though the overall positive effect on enantioselectivity through the addition of DEDs is moderate, it provides strong evidence that the success of the CBS reduction is due to an excellent balance of attractive and repulsive steric interactions, with LD interactions being key to rationalizing the experimental findings. Our study therefore emphasizes that attractive LD interactions can and should be used as a modern catalyst design principle.

4. Computational Methods

All computations were performed with the Gaussian16 or ORCA[26] program suite. Geometries were optimized with dispersion corrections [DFT-D3[4a](BJ)[4b]] and without dispersion corrections in conjunction with the B3LYP functional combining a 6-311G(d,p) basis set. Vibrational frequencies were computed for each optimized structure to verify the stationary structures as minima or saddle points. Solvent effects were included by single-point energy computations with the SMD model[27] at the same level as for the optimized geometry. Higher level single-point energies were computed by the domain-based local pair natural orbital CCSD(T) (labeled DLPNO-CCSD(T)) method with a cc-pVTZ basis set. The SAPT analysis was performed at the SAPT0/jun-cc- pvdz level of theory on the optimized geometries[28] utilizing the PSI4 code.[29] Conformational analyses were performed using xtb (version 5.8) employing GFN2-xTB by simulated annealing molecular dynamics (MD) simulations in the gas phase.[30] All energies discussed are Gibbs free relative energies at 298.15 K and 1 atm in kcal mol^{-1} unless noted otherwise. Effects of zero-point vibrational energy (ZPVE) corrections are included.

5. Acknowledgements

We acknowledge financial support from the DFG within the priority program SPP 1807 “Control of London Dispersion Interactions in Molecular Chemistry” (SCHR 597/28-2). This work was also supported by the Alexander von Humboldt Foundation (Fellowship to L.J.S.). We thank Jan M. Schümann (Justus Liebig University Giessen) for valuable discussions and Olga Reshetylova (Igor Sikorsky Kyiv Polytechnic Institute) for synthetic contributions. We acknowledge Heike Hausmann (Justus Liebig University Giessen) for support with NMR spectroscopy and Dennis Gerbig (Justus Liebig University Giessen) for maintaining the computer server cluster. Open access funding enabled and organized by Projekt DEAL.

6. References

[1] J. N. Israelachvili, *Intermolecular and surface forces*, Academic Press, London, **1991**.

[2] a) R. Eisenschitz, F. London, *Z. Phys*. **1930**, *60*, 491 – 527; b) F. London, *Z. Phys*. **1930**, *63*, 245–279; c)J.P. Wagner, P.R. Schreiner, *Angew. Chem. Int. Ed.* **2015**, *54*, 12274–12296; *Angew. Chem.* **2015**, *127*, 12446–12471.

[3] a) R. C. Wende, A. Seitz, D. Niedek, S. M. M. Schuler, C. Hofmann, J. Becker, P. R. Schreiner, *Angew. Chem. Int. Ed.* **2016**, *55*, 2719–2723 ; *Angew. Chem*. **2016**, *128*, 2769–2773 ; b) E. Prochµzkovµ, A. Kolmer, J. Ilgen, M. Schwab, L. Kaltschnee, M. Fredersdorf, V. Schmidts, R. C. Wende, P. R. Schreiner, C. M. Thiele, *Angew. Chem. Int. Ed*. **2016**, *55*, 15754–15759; *Angew. Chem*. **2016**, *128*, 15986–15991; c) A. J. Neel, M. J. Hilton, M. S. Sigman, F. D. Toste, *Nature* **2017**, *543*, 637–646 ; d) G. Lu, R. Y. Liu, Y. Yang, C. Fang, D. S. Lambrecht, S. L. Buchwald, P. Liu, *J. Am. Chem. Soc*. **2017**, *139*, 16548–16555; e) J. Miró, T. Gensch, M. Ellwart, S.-J. Han, H.-H. Lin, M. S. Sigman, F. D. Toste, *J. Am. Chem. Soc*. **2020**, *142*, 6390–6399 ; f) T. Deb, R. M. Franzini, *Synlett* **2020**, *31*, 938–944.

[4] a) S. Grimme, J. Antony, S. Ehrlich, H. Krieg, *J. Chem. Phys.* **2010**, *132*, 154104; b)S. Grimme, S. Ehrlich, L. Goerigk, *J. Comput. Chem*. **2011**, *32*, 1456–1465 ; c) S. Grimme, A. Hansen, J. G. Brandenburg, C. Bannwarth, *Chem. Rev*. **2016**, *116*, 5105–5154.

[5] a) E. J. Corey, R. K. Bakshi, S. Shibata, C. P. Chen,V. K. Singh, *J. Am. Chem. Soc*. **1987**, *109*, 7925–7926; b) E. J. Corey, R. K. Bakshi, S. Shibata, *J. Am. Chem. Soc.* **1987**, *109*, 5551–5553 ; c) E. J. Corey, S. Shibata, R. K. Bakshi, *J. Org. Chem*. **1988**, *53*, 2861–2863 ; d) E. J. Corey, J. O. Link, *Tetrahedron Lett*. **1989**, *30*, 6275–6278 ; e) E. J. Corey, R. K. Bakshi, *Tetrahedron Lett.* **1990**, *31*, 611–614; f) E. J. Corey, C. J. Helal, *Tetrahedron Lett.* **1995**, *36*, 9153–9156.

[6] a) E. J. Corey, J. O. Link, R. K. Bakshi, *Tetrahedron Lett*. **1992**, *33*, 7107–7110 ; b) E. J. Corey, C. J. Helal, *Angew. Chem. Int. Ed.* **1998**, *37*, 1986–2012 ; *Angew. Chem.* **1998**, *110*, 2092–2118.

[7] B. T. Cho, D.-J. Kim, *Bull. Korean Chem. Soc*. **2004**, *25*, 1385–1391.

[8] D. K. Jones, D. C. Liotta, I. Shinkai, D. J. Mathre, *J. Org. Chem*. **1993**, *58*, 799–801.

[9] a) M. P. Meyer, *Org. Lett.* **2009**, *11*, 4338–4341; b) T. Giagou, M. P. Meyer, *Chem. Eur. J.* **2010**, *16*, 10616–10628.

[10] H. Zhu, D. J. O'Leary, M. P. Meyer, *Angew. Chem. Int. Ed*. **2012**, *51*, 11890–11893 ; *Angew. Chem.* **2012**, *124*, 12060–12063.

[11] Z. Lachtar, A. Khorief Nacereddine, A. Djerourou, *Struct. Chem*. **2020**, *31*, 253–261.

[12] a) V. Nevalainen, *Tetrahedron: Asymmetry* **1991**, *2*, 429–435; b) V. Nevalainen, *Tetrahedron: Asymmetry* **1991**, *2*, 827–842; c) V. Nevalainen, *Tetrahedron : Asymmetry* **1991**, *2*, 63–74 ; d) V. Nevalainen, *Tetrahedron: Asymmetry* **1992**, *3*, 933–945; e) V. Nevalainen, *Tetrahedron : Asymmetry* **1992**, *3*, 921–932 ; f) L. P. Linney, C. R. Self, I. H. Williams, *J. Chem. Soc. Chem. Commun*. **1994**, 1651–1652.

[13] a) C. Riplinger, F. Neese, *J. Chem. Phys*. **2013**, *138*, 034106; b) C. Riplinger, B. Sandhoefer, A. Hansen, F. Neese, J. Chem. Phys. **2013**, *139*, 134101.

[14] J. Contreras-García, E. R. Johnson, S. Keinan, R. Chaudret, J. P. Piquemal, D. N. Beratan, W. Yang, J. *Chem. Theory Comput*. **2011**, *7*, 625–632.

[15] a) A. Fujii, H. Hayashi, J. W. Park, T. Kazama, N. Mikami, S. Tsuzuki, Phys. *Chem. Chem. Phys*. **2011**, *13*, 14131–14141; b) S. Grimme, R. Huenerbein, S. Ehrlich, *ChemPhysChem* **2011**, *12*, 1258–1261; c) J. W. G. Bloom, R. K. Raju, S. E. Wheeler, *J. Chem. Theory Comput.* **2012**, *8*, 3167–3174.

[16] R. Pollice, P. Chen, *Angew. Chem. Int. Ed.* **2019**, *58*, 9758–9769 ; *Angew. Chem.* **2019**, *131*, 9860–9871.

[17] A. S. Demir, I. Mecitoglu, C. Tanyeli, V. Gülbeyaz, *Tetrahedron: Asymmetry* **1996**, *7*, 3359–3364.

[18] A. J. Misquitta, R. Podeszwa, B. Jeziorski, K. Szalewicz, *J. Chem. Phys*. **2005**, *123*, 214103.

[19] a) B. Kahr, D. Van Engen, K. Mislow, *J. Am. Chem. Soc*. **1986**, *108*, 8305–8307; b) S. Rösel, C. Balestrieri, P. R. Schreiner, *Chem. Sci.* **2017**, *8*, 405–410 ; c) A. C. N. Kwamen, M. Schlottmann, D. Van Craen, E. Isaak, J. Baums, L. Shen, A. Massomi, C. Räuber, B. P. Joseph, G. Raabe, C. Göb, I. M. Oppel, R. Puttreddy, J. S. Ward, K. Rissanen, R. Fröhlich, M. Albrecht, *Chem. Eur. J.* **2020**, *26*, 1396–1405.

[20] G. B. Stone, *Tetrahedron: Asymmetry* **1994**, *5*, 465–472.

[21] a) D. Van Craen, W. H. Rath, M. Huth, L. Kemp, C. Räuber, J. M. Wollschläger, C. A. Schalley, A. Valkonen, K. Rissanen, M. Albrecht, *J. Am. Chem. Soc*. **2017**, *139*, 16959–16966 ; b) M. Strauss, H. A. Wegner, *Angew. Chem. Int. Ed*. **2019**, *58*, 18552–18556 ; *Angew. Chem.* **2019**, *131*, 18724–18729.

[22] I. A. Kieffer, N. R. Treich, J. L. Fernandez, Z. M. Heiden, *Dalton Trans*. **2018**, *47*, 3985–3991.

[23] a) S. Tsuzuki, K. Honda, T. Uchimaru, M. Mikami, K. Tanabe, *J. Phys. Chem. A* **2002**, *106*, 4423–4428; b) M. C. Sherman, M. R. Ams, K. D. Jordan, *J. Phys. Chem. A* **2016**, *120*, 9292–9298.

[24] C. Adamo, M. Cossi, G. Scalmani, V. Barone, *Chem. Phys. Lett*. **1999**, *307*, 265–271.

[25] W. Gerrard, A. Nechvatal, *Nature* **1947**, *159*, 812–813.

[26] F. Neese, *WIREs Comput. Mol. Sci*. **2012**, *2*, 73–78.

[27] A. V. Marenich, C. J. Cramer, D. G. Truhlar, *J. Phys. Chem. B* **2009**, *113*, 6378–6396.

[28] E. Papajak, J. Zheng, X. Xu, H. R. Leverentz, D. G. Truhlar, *J. Chem. Theory Comput*. **2011**, *7*, 3027–3034.

[29] R. M. Parrish, L. A. Burns, D. G. A. Smith, A. C. Simmonett, A. E. DePrince, E. G. Hohenstein, U. Bozkaya, A. Y. Sokolov, R. Di Remigio, R. M. Richard, J. F. Gonthier, A. M. James, H. R. McAlexander, A. Kumar, M. Saitow, X. Wang, B. P. Pritchard, P. Verma, H. F. Schaefer, K. Patkowski, R. A. King, E. F. Valeev, F. A. Evangelista, J. M. Turney, T. D. Crawford, C. D. Sherrill, *J. Chem. Theory Comput.* **2017**, *13*, 3185–3197.

[30] C. Bannwarth, S. Ehlert, S. Grimme, *J. Chem. Theory Comput*. **2019**, 15, 1652–1671.

7. Supporting Information

7.1. General Information

Unless otherwise noted, chemicals were purchased from Acros Organics, TCI, Alfa Aesar, Lancaster, Merck, or Fluka at the highest purity grade available and were used without further purification. All solvents were distilled prior to use. Toluene, THF, and CH_2Cl_2, were distilled from appropriate drying agents prior to use and stored under argon atmosphere. All catalytic reactions were carried out under an argon atmosphere employing oven- and flame-dried glassware. Column chromatography was conducted using Merck silica gel 60 (0.040 – 0.063 mm).

7.2. Analytical Methods

Thin Layer Chromatography (TLC) was performed on silica coated plates (*Merck*, silica 60 F254) with detection by UV-light (λ = 254 nm) and/or by staining with a cerium ammonium molybdate solution [CAM] and developed by heating.

CAM-staining solution: cerium sulfate tetrahydrate (1.00 g), ammonium molybdate (25.0 g), and concentrated sulfuric acid (25.0 mL) in water (250 mL).

Nuclear Magnetic Resonance (NMR) spectra were recorded at room temperature either on a *Bruker* AV-400 or a *Bruker* AV-400HD. ^1H NMR spectra were referenced to the residual proton signal of $CDCl_3$ (δ = 7.26 ppm). ^{13}C NMR spectra were referenced to the ^{13}C-D triplet of $CDCl_3$ (δ = 77.2 ppm). The following abbreviations for single multiplicities were used: *br* = broad, s = singlet, d = doublet, t = triplet, q = quartet, quint = quintet, sept = septet.

High resolution mass spectrometry (HRMS) was performed employing either a Bruker MicrOToF or a Bruker Impact II using methanol solutions of the respective compounds.

Chiral Gas Chromatography (GC): Enantioselectivities were determined by chiral stationary phase GC analyses on Hewlett Packard 5890 or 6890 gas chromatographs, respectively.

7.3. Potential Energy Hypersurface

We computed the reaction pathway for the reduction of acetophenone using a comparison of B3LYP/6-311G(d,p) and B3LYP-D3(BJ)/6-311G(d,p) (Fig. S1) to estimate the dispersion correction. ΔG_{298K} values are discussed unless noted otherwise. The conformational analysis was performed manually. There are four conformations in the hydride transfer step, regarding the direction of the coordinated oxygen lone pair (chair-like vs. boat-like) and the geometry (*R* vs *S*) as in Figure S2. The chair-like transition state with the oxygen lone pair *anti* to the larger group (Ph) is favored. In addition, for those substrates or catalysts with more than one conformation, a conformational search was carried out using xtb employing GFN2-xTB with simulated annealing molecular dynamics (MD) simulations.

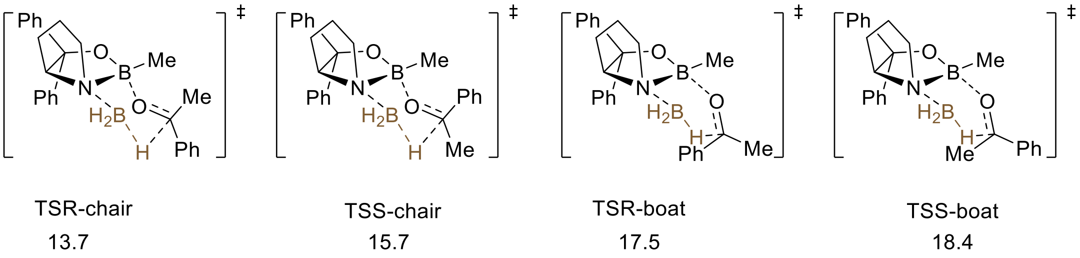

TSR-chair 13.7

TSS-chair 15.7

TSR-boat 17.5

TSS-boat 18.4

Figure S1 Conformations for the hydride transfer step.

Oxazaborolidine, BH_3, and acetophenone were used as reference point **1** at 0.0 kcal mol^{-1}. Coordination of one solvent molecule (THF) would form complex **1’**, which is higher in free energy. Initial coordination of BH_3 to the oxazaborolidine leads to a 5.5 kcal mol^{-1} more stable complex **2**. Coordination of the ketone to give complex **3** is endergonic and exhibits an energy barrier of 15.0 kcal mol^{-1}. Here a solvent molecule (THF) competes with acetophenone to form **2’**. The subsequent hydride transfer is the most important step in the reaction, which determines enantioselectivity. Without dispersion correction **TS1’**$_{\mathbf{S}}$ and **TS1’**$_{\mathbf{R}}$ are found to be very high in energy exhibiting relative energies of 29.8 kcal mol^{-1} and 31.7 kcal mol^{-1} respectively, related to the starting point **1**. These energy barriers seem to be too high for such a fast catalyzed reaction at temperatures of 298 K. Including dispersion correction, the relative energies of all intermediates and transition structures decrease, presenting larger stabilizing intermolecular interactions. Especially the transition structures **TS1**$_{\mathbf{R}}$ and **TS1**$_{\mathbf{S}}$ are notably lower in energy with barriers of 13.7 kcal mol^{-1} and 15.7 kcal mol^{-1} respectively, which seem much more reasonable for a catalyzed reaction. The calculated enantioselectivity of the reduction, which is expressed in the energy difference between the transition structures ($\Delta\Delta G^{\ddagger}$) of the hydride transfer, is −2.0 kcal mol^{-1} and thereby consistent with previously published experimental results (−2.2 kcal mol^{-1}).[1] After the hydride transfer, intermediate **4R** with an open ring structure forms. There are two possible pathways for product release **7** and catalyst regeneration. The direct release *via* **TS2**$_{\mathbf{R}}$ towards **5R** is less preferred (+3.5 kcal mol^{-1}) than *via* **TS3**$_{\mathbf{R}}$ by addition of an additional equivalent of borane to **6R**.

When employing DLPNO-CCSD(T)/cc-pVTZ to compute the electronic energies of **TS1$_S$** and **TS1$_R$**, the free energies (corrected for ZPVE) of the TS are 7.7 kcal mol^{-1} and 10.8 kcal mol^{-1}, respectively. This indicates the dispersion-corrected energy barrier is more reasonable and that more complete inclusion of electron correlation effects emphasize the importance of LD even more.

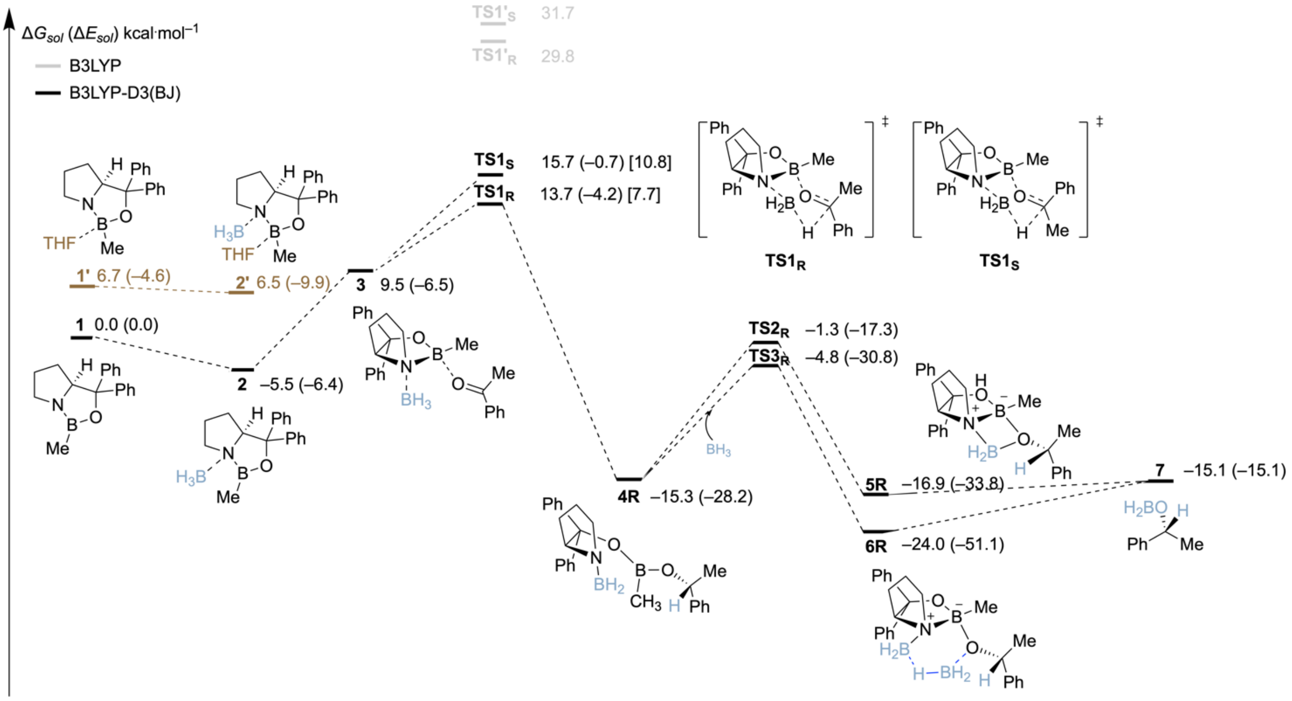
ΔG_sol (ΔE_sol) kcal·mol⁻¹
B3LYP
B3LYP-D3(BJ)
TS1'S 31.7
TS1'R 29.8
TS1S 15.7 (–0.7) [10.8]
TS1R 13.7 (–4.2) [7.7]
TS1R
TS1S
1' 6.7 (–4.6)
2' 6.5 (–9.9)
3 9.5 (–6.5)
1 0.0 (0.0)
2 –5.5 (–6.4)
TS2R –1.3 (–17.3)
TS3R –4.8 (–30.8)
BH3
4R –15.3 (–28.2)
5R –16.9 (–33.8)
6R –24.0 (–51.1)
7 –15.1 (–15.1)
THF
H3B
Ph
Me
H2BO

Figure S2 Potential energy surface containing free energies ($\Delta G_{\text{sol}}^{275}$) electronic energies ($\Delta E_{\text{sol}}$ in parentheses) of the CBS pathway with and without dispersion corrections. Level of theory: B3LYP-D3(BJ)/6-311+G(d,p)-SMD(THF)// B3LYP-D3(BJ)/6-311G(d,p). The free energies in brackets are based on electronic DLPNO-CCSD(T)/cc-pVTZ single-point energy (corrected for ZPVE).

7.4. Symmetry-Adapted Perturbation Theory (SAPT0)

SAPT(0) analysis was employed to determine the noncovalent interaction energies of the transition structures. The structures for SAPT0 were optimized at B3LYP-D3(BJ)/6-311G(d,p). Then the SAPT module of the PSI4 code was employed in conjunction with a jun-cc-pvdz basis set.

Table S1 SAPT0 analysis of the TS of the CBS reduction of acetophenone.

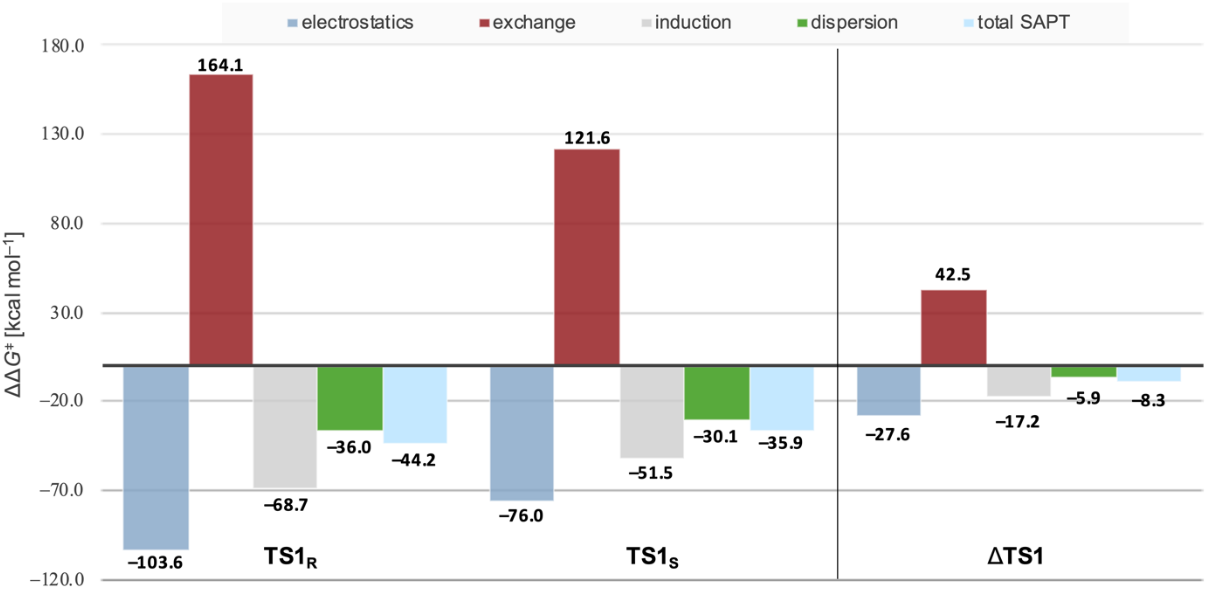

	TS1$_{R}$	**TS1$_{S}$**	**ΔTS1$_{R}$**
electrostatics	−103.6	−76.0	−27.6
exchange	164.1	121.6	42.5
induction	−68.7	−51.5	−17.2
dispersion	−36.0	−30.1	−5.9
total SAPT	−44.2	−35.9	−8.3

All energies are provided in kcal mol^{-1}

7.5. London Dispersion Maps

Besides NCI plots (Fig. 2) we used recent developed LD potential maps by Pollice and Chen to directly visualize LD interactions.[2] Attractive LD interactions are indicated with red areas, which are observed intermolecularly between catalyst and substrate. Larger red areas, indicating stronger LD interactions can be observed in the favored **TS1$_R$** between the phenyl group of the catalyst and the phenyl group of the substrate (Fig. S3). These computations qualitatively confirm the NCI plots (Fig. 2) and the SAPT analysis (Fig. 3) and also suggest that LD interactions are important for enantiodiscrimination.

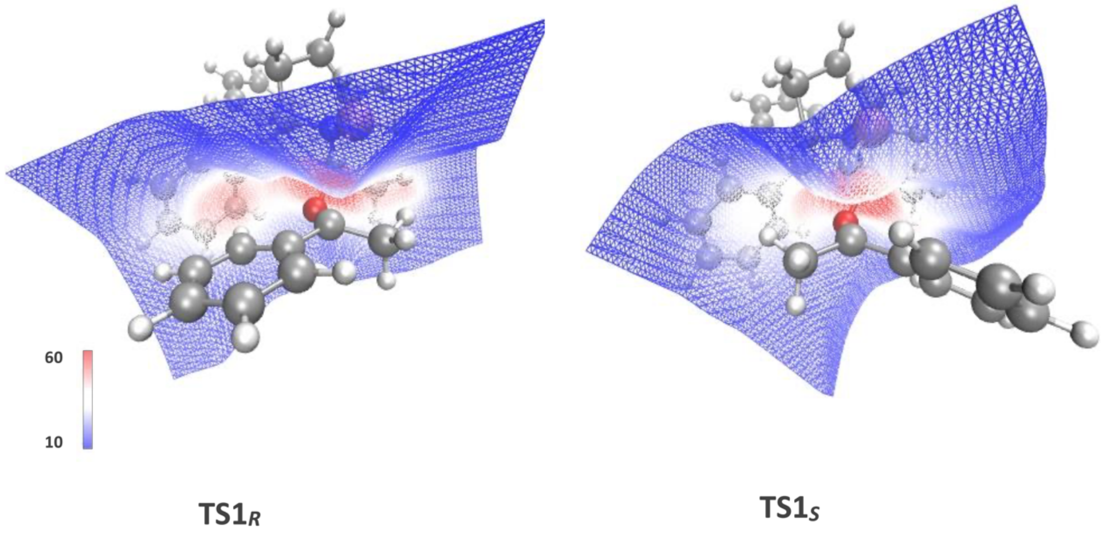

Figure S3 London dispersion maps (values are in kcal$^{0.5}$ mol$^{-0.5}$) of the transition structures **TS1$_R$** and **TS1$_S$** in the reduction of acetophenone. Red areas show more stabilizing LD interactions.

7.6. General Procedure for the OXB Catalyzed Reduction

The respective amino alcohol as catalyst precursor (0.040 mmol, 0.1 equiv.) was placed in a flame dried Schlenk tube under Ar. Anhydrous solvent (1 mL) and $BH_3 \cdot SMe_2$ (0.440 mmol, 1.1 equiv.) were added and the reaction was stirred at 50 °C for 30 min. A solution of the ketone (0.400 mmol, 1.0 equiv. in 0.5 mL THF) was added *via* a syringe pump within 30 min. The reaction mixture was stirred for another 60 min at 50 °C. The reaction was quenched by addition of 6.0 mL citric acid [0.5 M] and the mixture was extracted with EtOAc (3 × 5 mL). The combined organic layers were washed with brine, dried over Na_2SO_4, filtered, and the solvent was carefully removed under reduced pressure. Alcohols whose enantiomers could not be separated by chiral GC, were directly derivatized either by addition of Ac_2O (0.042 mL, 0.440 mmol, 1.1 equiv.), DMAP (0.005 g, 0.044 mmol, 0.1 equiv.), and Et_3N (0.041 mL, 0.440 mmol, 1.1 equiv.) or benzoyl chloride (0.051 mL, 0.440 mmol, 1.1 equiv.).

7.7. Experimental Evaluation of Reaction Conditions

We started our investigation employing the 3,5-*t*Bu$_2$Ph catalyst in the reduction of 2-butanone (Tab. S2). In all cases, at 50 °C after 1.5 h the reduction resulted in near quantitative yields. We chose a slightly elevated temperature, because the boron reduction often proceeds with better enantioselectivity at higher temperatures (entries 1 and 2).[3] We could not improve the enantioselectivity by changing the solvent to PhMe or CH_2Cl_2 (entries 3 and 4) or by lowering the concentration (entry 5). Furthermore, there was no difference in selectivity when using $BH_3 \cdot THF$ instead of $BH_3 \cdot SMe_2$ (entries 2 and 6). The best selectivity was achieved when adding the ketone slowly *via* a syringe pump to the reducing mixture (entries 2, 7, and 8).

Table S2 Investigation of the reaction conditions.

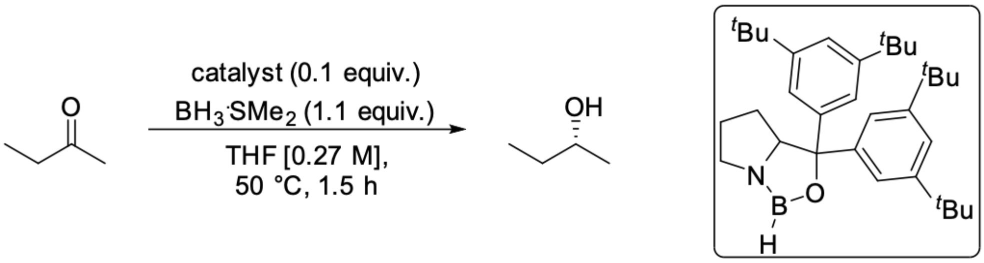

Entry	Solvent	*ee* [%]
1[a]	THF	53
2	THF	67
3	PhMe	67
4	CH_2Cl_2	42
5[b]	THF	64
6[c]	THF	67
7[d]	THF	60
8[e]	THF	44

[a] Reaction performed at 0 °C; [b] THF [0.1] M; [c] $BH_3 \cdot THF$ used as reducing agent; [d] Without syringe pump; [e] $BH_3 \cdot SMe_2$ added *via* syringe pump.

7.8. Experimental Evaluation of the Boron Substituent

We investigated the effect of the substituent at boron computationally (Tab. 2) and experimentally (Fig. S4). Computations suggest that in the reduction of cyclohexyl methyl ketone LD interactions can be increased using Cy or CH_2Cy with selectivities ($\Delta\Delta G^{\ddagger}$) of 2.3 kcal mol^{-1} and 3.5 kcal mol^{-1} respectively (Tab. 2 entries 1 and 2). We synthesized the corresponding oxazaborolidines *in situ via* azeotropic distillation following a common literature protocol with a Dean-Stark trap.[4] We employed the catalysts in the reduction of three different ketones. The results show that the selectivity does not change much as compared to the original catalyst when using CH_2Cy and Cy groups (Fig. S4). This implies that the interactions between substrate and the substituent at boron on the catalyst only have a subtle effect on the enantioselectivity.

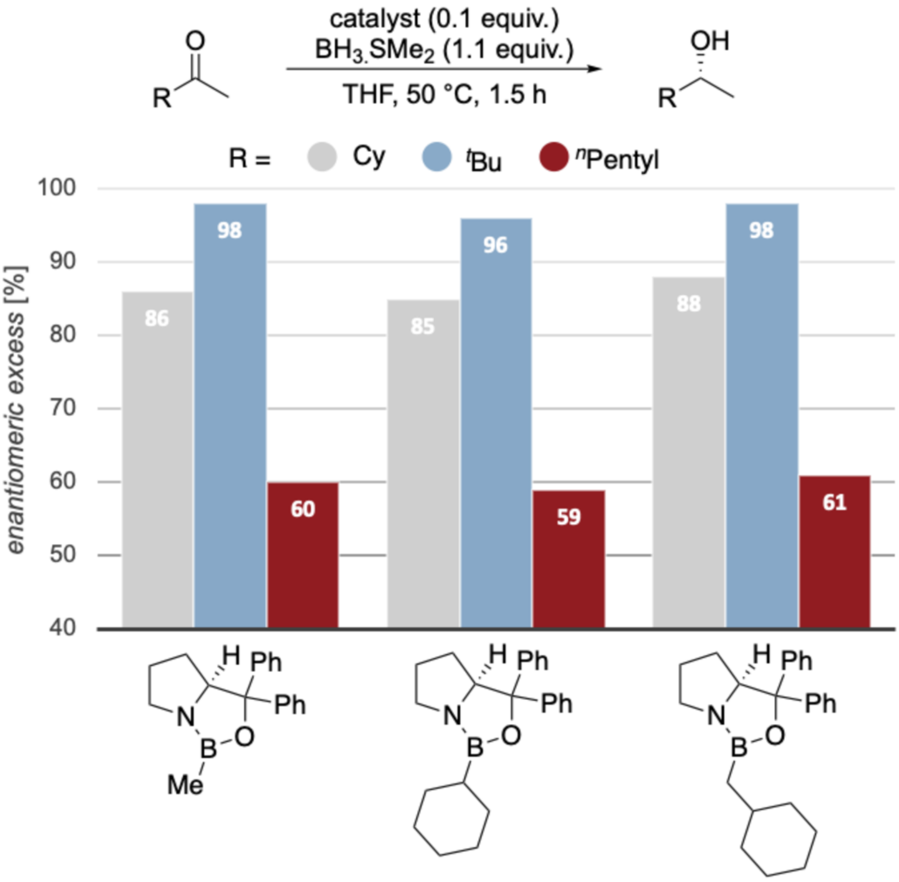

Figure S4 Reductions employing modified CBS catalysts with different boron substituents.

7.9. Computational Evaluation of Fluorinated Catalysts

We also employed catalysts with 3,5-$(CF_3)_2Ph$ and C_6F_5 carbinol substituents and found experimentally that the fluorinated catalysts are less selective (Fig. 10). These results are in accord with computed values (Tab. S2), as attractive $\sigma - \pi$ interactions decrease through strongly electron withdrawing fluorine substituents.[5]

Table S2 Calculated enantioselectivities ($\Delta\Delta G^{\ddagger}_{\mathrm{sol}}$) in the reduction of 2-butanone employing fluorinated catalysts. Level of theory: B3LYP-D3(BJ)/6-311G(d,p).

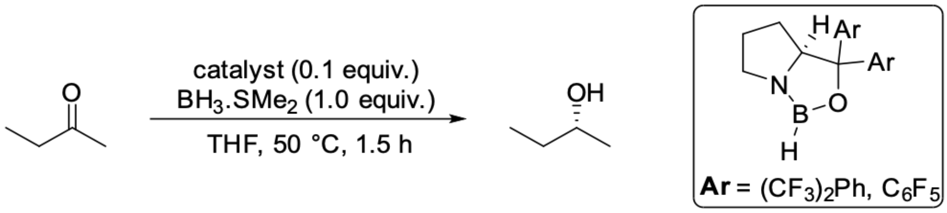

Entry	Catalyst	$\Delta\Delta G^{\ddagger}_{sol}$ (with D3)
1	CF_3	0.2
2	C_5F_6	0.3

$\Delta\Delta G^{\ddagger}_{\mathrm{sol}} = \Delta\Delta G^{\ddagger}_{\mathrm{sol}}(\mathrm{TS_S}) - \Delta\Delta G^{\ddagger}_{\mathrm{sol}}(\mathrm{TS_R})$, at reaction temp.; (kcal mol^{-1})

7.10. Evaluation of Special Substrates

In the reduction of pentafluorobenzophenone we achieved 92% *ee* for the (*S*) enantiomer (Fig. S5). This is consistent with our results for the fluorinated catalysts (Tab S2) as we still have attractive T-shaped $\sigma - \pi$ interactions between the phenyl of substrate and catalyst. Accordingly the $\sigma - \pi$ interaction of a C_6F_5 substituent to a phenyl is meant to be lower than the $\sigma - \pi$ of two phenyl groups.[5b] The bulky and electron deficient pentafluorophenyl takes the position of the former Me group, which is in contrast to the traditional model based on steric repulsion.

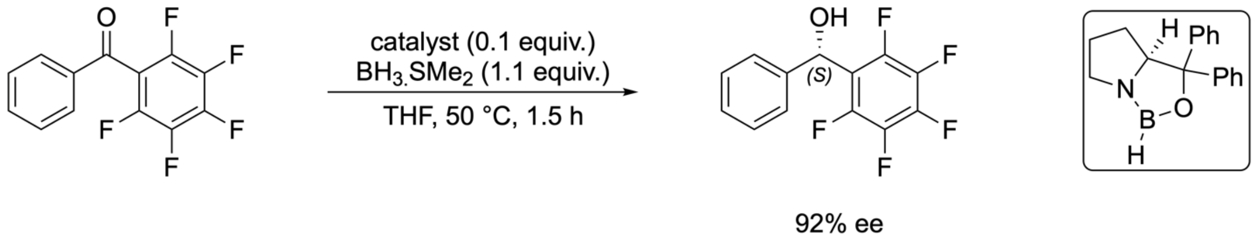

Figure S5 Reduction of pentafluorobenzophenone.

The reduction of *p*-methoxy-*p'*-nitrobenzophenone yielded the (*R*) enantiomer in moderate selectivities (Tab S3). The electron enriched aryl group (4-OMe-C_6H_4) provides the higher interaction with the catalyst. These results are consistent with the reduction of pentafluorobenzophenone as both electron deficient aryl groups (pentafluorophenyl, *p'*-nitrophenyl) point away from the catalysts' phenyl groups because of a weakened noncovalent interaction.

Table S3 Reduction of *p*-methoxy-*p'*-nitrobenzophenone

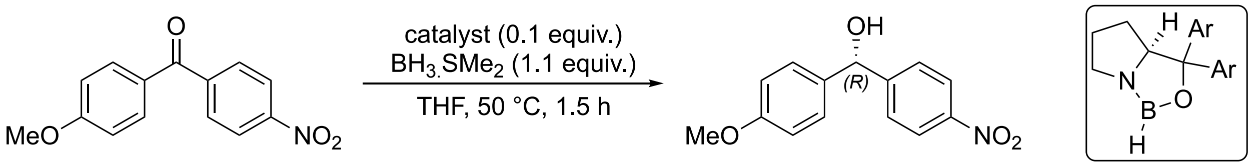

Entry	Catalyst Ar	*ee* [%]
1	Ph	(*R*) 56
2	4-OMe-3,5-Me_2Ph	(*R*) 62

In the reduction of trichloroacetophenone employing catecholborane as reducing agent at –78 °C Corey achieved predominantly the (*R*) enantiomer.[6] Comparing this to acetophenone, the geometries of the **TS1$_R$** and **TS1$_S$** (Fig. 2) are swapped, as for stereochemistry the trichloromethyl has the higher priority than phenyl. When using the standard conditions with $BH_3 \cdot SMe_2$ we also obtained the (*R*) enantiomer but with lower selectivity (Tab. S4 entry 1). With the modified version of the CBS catalyst (entry 3), the selectivity increased to 45% *ee*. Our computations suggest a preference for the (*R*) enantiomer (entry 2), because of stabilizing interactions between the trichloromethyl group with the *π*-system of the catalyst, originating from London dispersion (LD).[5c]

Table S4 Reduction of 2,2,2-Trichloro-1-phenylethanone

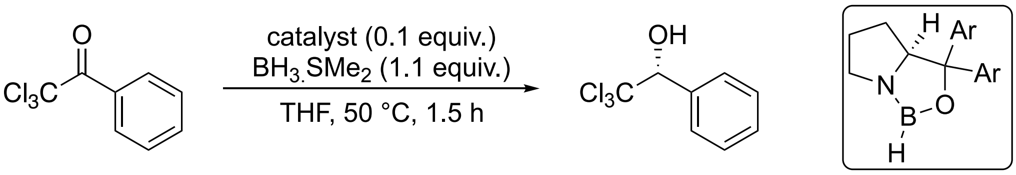

Entry	Catalyst Ar	*ee* [%]
1	Ph	(*R*) 27

2	Ph[a]	(*R*) 18
3	4-OMe-3,5-Me$_2$Ph	(*R*) 45

[a] Selectivity computed at B3LYP-D3(BJ)/6-311G(d,p)

7.11. Supplementary Computations to the Competitive Reduction

In a competitive experiment we observed that ^{t}Bu methyl ketone is reduced faster than 2-pentanone (Fig 13). We conclude that stabilizing interactions in the TS are responsible for that rate difference, because reduction at the neopentyl position of ^{t}Bu ketone should proceed with a lower rate. The ^{t}Bu ketone is more electron-rich, so it may form a stronger interaction with the catalyst. However, our computations show that the two catalyst-ketone complexes have very similar binding energies. This implies that differential electronic effects are not significant. As ^{t}Bu ketone is also reduced with higher selectivity (Fig. 11) and possesses a higher polarizability per Volume α/V (Fig. 12), we conclude that stabilizing LD interactions in the TS must be responsible for these observations.

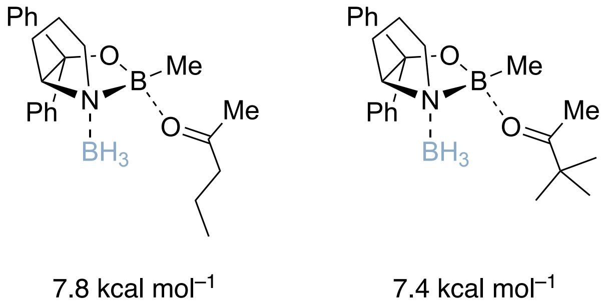

Figure S6 Computed energies of the complex structures. Level of theory: B3LYP-D3(BJ)/6-311G(d,p).

Furthermore, the SAPT analysis of the transition structures suggests, that the ^{t}Bu ketone has higher dispersion energy than 2-pentanone, therefor leading to a lower total SAPT.

Table S5 Computed energies of the complex structures. Level of theory: B3LYP-D3(BJ)/6-311G(d,p).

Transition structures	Electrostatics	Exchange	Induction	Dispersion	Total SAPT
2-pentanone TS$_R$	−94.3	142.8	−60.7	−30.8	−43.0
^{t}Bu ketone TS$_R$	−97.1	147.7	−62.4	−32.5	−44.2

All energies are provided in kcal mol^{-1}; Level of theory: SAPT0/jun-cc-pvdz.

7.12. Synthetic Procedures and Analytical Data

7.12.1. GC Analytics of Alcohols

2-Butanol

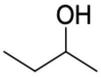

Enantioselectivity was determined by investigation of the benzoylated alcohol *via* chiral stationary phase GC employing a 30 m FS-Hydrodex β-6TBDM column (Macherey Nagel).

T (Injector + Detector) = 250 °C

Splitflow = 80 mL min^{-1}

Precolumn pressure = 0.8 bar

Conditions: 100 °C – 140 °C, 2 °C min^{-1}

Retention Times: (*R*) = 14.3 min; (*S*) = 14.5 min

2-Pentanol

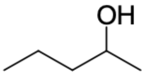

Enantioselectivity was determined by investigation of the benzoylated alcohol *via* chiral stationary phase GC employing a 30 m FS-Hydrodex β-6TBDM column (Macherey Nagel).

T (Injector + Detector) = 250 °C

Splitflow = 80 mL min^{-1}

Precolumn pressure = 0.8 bar

Conditions: 80 °C, 10 min; 80 – 120 °C, 0.5 °C min^{-1}

Retention Times: (*R*) = 63.2 min; (*S*) = 64.0 min

2-Heptanol

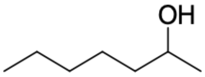

Enantioselectivity was determined by investigation of the acylated alcohol *via* chiral stationary phase GC employing a 30 m FS-Hydrodex β-6TBDM column (Macherey Nagel).

T (Injector + Detector) = 250 °C

Splitflow = 80 mL min^{-1}

Precolumn pressure = 0.8 bar

Conditions: 100 °C – 120 °C, 2 °C min^{-1}

Retention Times: (*R*) = 4.2 min; (*S*) = 4.4 min

3-Methyl-2-butanol

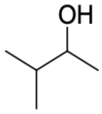

Enantioselectivity was determined *via* chiral stationary phase GC employing a 30 m FS-Hydrodex β-6TBDM column (Macherey Nagel).

T (Injector + Detector) = 250 °C

Splitflow = 80 mL min^{-1}

Precolumn pressure = 0.8 bar

Conditions: 80 °C, 10 min

Retention Times: (*R*) = 5.8 min; (*S*) = 6.1 min

3,3-Dimethyl-2-butanol

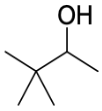

Enantioselectivity was determined *via* chiral stationary phase GC employing a 30 m FS-Hydrodex β-6TBDM column (Macherey Nagel).

T (Injector + Detector) = 250 °C

Splitflow = 80 mL min^{-1}

Precolumn pressure = 0.8 bar

Conditions: 60 °C, 10 min

Retention Times: (*R*) = 5.3 min; (*S*) = 5.5 min

1-Cyclohexylethanol

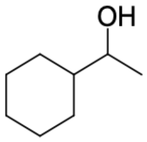

Enantioselectivity was determined *via* chiral stationary phase GC employing a 30 m FS-Hydrodex β-TBDAc column (Macherey Nagel).

T (Injector + Detector) = 250 °C

Splitflow = 80 mL min^{-1}

Precolumn pressure = 0.8 bar

Conditions: 80 °C, 20 min; 80 – 120 °C, 2 °C min^{-1}

Retention Times: (*R*) = 26.9 min; (*S*) = 27.4 min

1-Phenylethanol

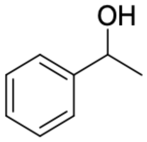

Enantioselectivity was determined *via* chiral stationary phase GC employing a 30 m FS-Hydrodex β-6TBDM column (Macherey Nagel).

T (Injector + Detector) = 250 °C

Splitflow = 80 mL min^{-1}

Precolumn pressure = 0.8 bar

Conditions: 100 °C, 20 min

Retention Times: (*R*) = 10.8 min; (*S*) = 11.2 min

2,2,2-Trichloro-1-phenylethanol

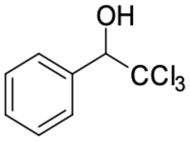

Enantioselectivity was determined by investigation of the acylated alcohol *via* chiral stationary phase GC employing a 30 m FS-Hydrodex β-6TBDM column (Macherey Nagel).

T (Injector + Detector) = 250 °C

Splitflow = 80 mL min^{-1}

Precolumn pressure = 0.8 bar

Conditions: 100 °C – 190 °C, 2 °C min^{-1}

Retention Times: (*R*) = 26.5 min; (*S*) = 26.7 min

$[\alpha]_D^{24}$ = −18.4 ([0.77 M] in $CHCl_3$) 40% *ee (R)* (lit.[7] $[\alpha]_D^{20}$ = −27.0 ([1.0 M] in EtOH) 56% *ee* (*R*))

Computed value with Boltzmann weighted conformers:

(*R*) $[\alpha]_D^{25}$ = −56.4 (in $CHCl_3$) [B3LYP/6-311G(d,p)]

2,3,4,5,6-Pentafluoro-α-phenylbenzenemethanol

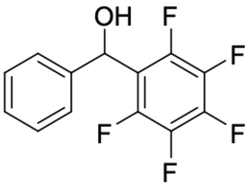

Enantioselectivity was determined *via* chiral stationary phase HPLC employing a Chiralpak IC column (Daicel).

Detector (UV/VIS) = 254 nm

Flow = 1.0 mL min^{-1}

Eluent ^{n}hexane (97%), ^{i}PrOH (3%)

Retention Times: (*R*) = 5.3 min; (*S*) = 6.0 min

$[\alpha]_D^{20}$ = −42.2 ([0.78 M] in $CHCl_3$) 92% *ee* (*S*) (lit.[8] $[\alpha]_D^{20}$ = −45.0 ([1.90 M] in $CHCl_3$) 99% *ee* (*S*))

Computed value with Boltzmann weighted conformers

(*S*) $[\alpha]_D^{25}$ = −42.6 (in $CHCl_3$) [B3LYP/6-311G(d,p)]

4-Methoxyphenyl-4-nitrophenylmethanol

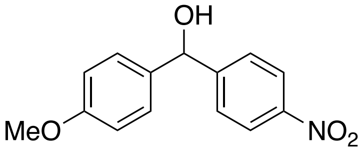

Enantioselectivity was determined *via* chiral stationary phase HPLC employing a Chiralpak IA column (Daicel).

Detector (UV/VIS) = 270 nm

Flow = 1.0 mL min^{-1}

Eluent ^{n}hexane (75%), EtOAc (25%)

Retention Times: (*S*) = 9.5 min; (*R*) = 11.2 min

$[\alpha]_D^{24}$ = +48.5 ([0.50 M] in EtOH) 62% *ee* (*R*) (lit.[8] $[\alpha]_D^{20}$ = +43.1 ([1.14 M] in $CHCl_3$) 79% *ee* (*R*))

7.12.2. Synthesis of Substrates

2,3,4,5,6-Pentafluoro-α-phenylbenzenemethanol

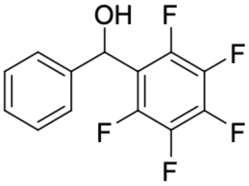

To a solution of pentafluoroiodobenzene (3.29 g, 11.2 mmol, 1.0 equiv.) in dry Et_2O under Ar at −78 °C, ^{n}BuLi in hexane [1.6 M] (7.00 mL, 11.2 mmol, 1.0 equiv.) was added dropwise. After stirring at −78 °C for 2 h benzaldehyde (1.13 mL, 11.2 mmol, 1.0 equiv.) was added and the solution was stirred at −78 °C for 3 h. Saturated NH_4Cl solution was added and the mixture was extracted with EtOAc (3 × 70 mL). The combined organic layers were washed with brine, dried over Na_2SO_4, filtered, and the solvent was removed under reduced pressure, to yield 2,3,4,5,6-Pentafluoro-α-phenylbenzenemethanol as colorless oil (2.71 g, 9.88 mmol, 89%). The product was used without further purification.

^{1}H NMR (400 MHz, $CDCl_3$): δ/ppm = 7.43 – 7.29 (m, 5H), 6.25 (s, 1H), 2.64 (s, 1H).

^{13}C NMR (101 MHz, $CDCl_3$): δ/ppm = 146.0 (m, CF), 143.5 (m, CF), 142.4 (m, CF), 140.7 (C), 139.0 (m, CF), 136.6 (m, CF), 128.9 (CH), 128.5 (CH), 125.5 (CH), 67.8 (CHOH).

The NMR spectra are in accordance with those reported in the literature.[8]

2,3,4,5,6-Pentafluorobenzophenone

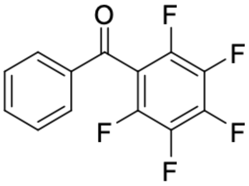

To a solution of 2,3,4,5,6-Pentafluoro-α-phenylbenzenemethanol (1.00 g, 3.65 mmol, 1.00 equiv.) in 10 mL CH_2Cl_2 was added pyridinium chlorochromate (PCC) (1.18 g, 5.47 mmol, 1.50 equiv.). The suspension was stirred at r.t. for 2 h, then filtered through a pad of Celite and washed with small portions of Et_2O. The solvent was removed under reduced pressure and the crude product was purified by column chromatography (silica, Hex/EtOAc = 40/1), to yield 2,3,4,5,6-Pentafluorobenzophenone as a colorless oil (0.721 g, 2.65 mmol, 73%).

***R*$_{f}$** = 0.21 (Hex:EtOAc /40:1) [UV, CAM].

^{1}H NMR (400 MHz, $CDCl_3$): δ/ppm = 7.85 (dd, *J* = 8.3, 1.3 Hz, 2H), 7.72 – 7.65 (m, 1H), 7.57 – 7.49 (m, 2H).

^{13}C NMR (101 MHz, $CDCl_3$): δ/ppm = 185.4 (C), 145.2 (m, CF), 143.9 (m, CF), 142.7 (m, CF), 139.1 (m, CF), 136.1 (C), 135.2 (CH), 129.9 (CH), 129.2 (CH).

HRMS (ESI): calcd for $C_{13}H_5F_5O$ $[M+H]^+$: 273.0333; found: 273.0334

The NMR spectra are in accordance with those reported in the literature.[9]

2,2,2-Trichloro-1-phenylethanone

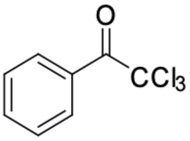

A solution of TCCA (9.30 g, 40.0 mmol, 2.0 equiv.) and acetophenone (2.36 g, 20.0 mmol, 1.0 equiv.) in 40 mL acetic acid was refluxed for 5 hr. After cooling, the precipitate was filtered and washed with acetic acid, the filtrate was diluted with water, and the mixture extracted with 4 x 40 mL pentane. The pentane solution was washed with brine and dried over Na_2SO_4. After filtration, the pentane was removed under reduced pressure and the residue purified by column chromatography (silica, Hex/EtOAc = 1/0 → 40/1), to yield 2,2,2-Trichloro-1-phenylethanone as a colorless liquid (3.89 g, 17.4 mmol, 87%).

***R*~f~** = 0.20 (Hex) [UV].

^{1}H NMR (400 MHz, $CDCl_3$): δ/ppm = 8.28 – 8.25 (m, 2H), 7.68 – 7.62 (m, 1H), 7.53 – 7.47 (m, 2H).

^{13}C NMR (101 MHz, $CDCl_3$): δ/ppm = 181.4 (C), 134.4 (CH), 131.7 (CH), 129.3 (C), 128.6 (CH), 95.6 (C).

The NMR spectra are in accordance with those reported in the literature.[10]

7.12.3. Miscellaneous

4-Bromo-2,6-diisopropylaniline

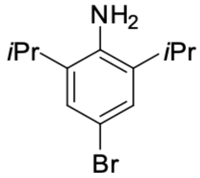

A solution of Br_2 (2.1 ml, 41.0 mmol, 1.05 equiv.) in CH_2Cl_2/MeOH (100 ml, 1/1) was added to a stirring solution of 2,6-diisopropylaniline (7.4 ml, 39.0 mmol, 1.0 equiv.) in CH_2Cl_2/MeOH (200 mL, 1/1) at r.t. over 2 h. The red solution was stirred for 24 h. The solvents were evaporated, and the resultant red solid was washed with PE 35-70 and further recrystallized from CH_2Cl_2/PE 35-70 to yield a colorless crystalline solid. 100 mL of CH_2Cl_2 were added and the organic phase was washed three times with small portions of 2 M aqueous sodium hydroxide solution and with brine. The organic phase was dried over Na_2SO_4, filtered and the solvent was removed under reduced pressure to yield the title compound as a colorless liquid (9.98 g, 38.9 mmol, 95%).

^{1}H NMR (400 MHz, $CDCl_3$): δ/ppm = 7.11 (s, 2H), 3.71 (s, 2H), 2.88 (hept, *J* = 6.8 Hz, 2H), 1.25 (d, *J* = 6.8 Hz, 12H).

^{13}C NMR (101 MHz, $CDCl_3$): δ/ppm = 139.4 (C), 134.8 (C), 125.9 (CH), 111.3 (C), 28.2 (CH), 22.4 (CH_3).

The NMR spectra are in accordance with those reported in the literature.[11]

1-Bromo-3,5-diisopropylbenzene

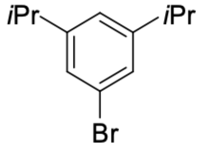

Sodium nitrite (4.45 g, 64.5 mmol, 2.50 equiv.) was added in portions to a suspension of 4-Bromo-2,6-diisopropylaniline (6.6 g, 26.0 mmol, 1.00 equiv.) in HCl [2 M] (70 mL) at –5 °C. The reaction was allowed to react for 10 min at –5 °C and then 50% H_3PO_2 (30 mL, 258 mmol, 10.0 equiv.) was added. The reaction mixture was left at 4 °C for 24 h and then at room temperature for 24 h. The aqueous layer was extracted with Et_2O (3 × 100 mL). The combined organic layers were dried over Na_2SO_4, filtered and the solvent was removed under reduced pressure to yield 1-Bromo-3,5-diisopropylbenzene as a light red liquid (6.08 g, 36.9 mmol, 97%).

***R*f** = 0.35 (Hex:EtOAc / 3:1) [UV, CAM].

^{1}H NMR (400 MHz, $CDCl_3$): δ/ppm = 7.18 (d, *J* = 1.5 Hz, 2H), 7.00 – 6.96 (m, 1H), 2.85 (hept, *J* = 6.9 Hz, 2H), 1.23 (d, *J* = 6.9 Hz, 12H).

^{13}C NMR (101 MHz, $CDCl_3$): δ/ppm = 151.2 (C), 127.0 (CH), 123.9 (CH), 122.5 (C), 34.2 (CH), 24.0 (CH_3).

HRMS (ESI): calcd for $C_{12}H_{18}Br$ $[M+H]^+$: 241.0586; found: 241.0584.

The NMR spectra are in accordance with those reported in the literature.[12]

7.12.4. Synthesis of Catalyst Precursors

General Procedure 1: Grignard Addition to Benzylprolinesters

To a suspension of magnesium (2.50 equiv.) in anhydrous THF under Ar was added a crystal of iodine and stirred at room temperature for 30 min. Then 5% of the solution of aryl bromide (2.50 equiv.) in THF was added and the reaction mixture was warmed to 50 °C. As soon as the color changed from brown to pale yellow, the remaining solution of aryl bromide was added dropwise *via* an addition funnel (0.1 mL min^{-1}). The reaction mixture was refluxed for 1 h and then cooled to 0 °C.

To the arylmagnesium bromide suspension, a solution of (*S*)-methyl-1-benzylpyrrolidin-2-carboxylate (1.00 equiv.) in THF was added dropwise (0.1 mL min^{-1}). The reaction mixture was stirred for the appropriate amount of time, monitored by TLC analysis. At 0 °C, saturated NH_4Cl solution was added to quench the reaction. The mixture was then extracted three times with ethyl acetate. The combined organic layers were washed with brine, dried over Na_2SO_4, filtered, and the solvent was removed under reduced pressure. The crude product was purified by column chromatography.

General Procedure 2: Hydrogenolysis of Benzyl Group

The benzyl-protected prolinol was dissolved in methanol and palladium on charcoal (10–20 wt%) was added. The reaction flask was purged with hydrogen gas. After stirring 24 h at room temperature the reaction mixture was filtered through a pad of Celite and washed with small portions of methanol. The solvent was removed under reduced pressure, and the residue was dissolved in EtOAc and washed with 2 M aqueous sodium hydroxide solution (3 × 50 mL) and with brine, dried over Na_2SO_4, filtered, and the solvent was removed under reduced pressure. The crude product was purified by column chromatography.

(*S*)-Methyl-1-benzylpyrroldine-2-carboxylate

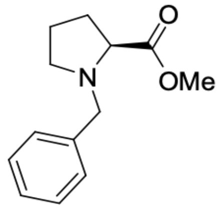

Esterification: To a solution of L-proline (5.00 g, 43.4 mmol, 1.00 equiv.) in methanol (40 mL, 1 M) at 0 °C was added dropwise thionyl chloride (7.87 mL, 109 mmol, 2.50 equiv.) and stirred for 20 h at room temperature. Methanol was removed under reduced pressure and toluene (50 mL) was added and removed under reduced pressure three times. The crude material was used without further purification for the next step

Benzylation: The crude material was dissolved in dichloromethane (40 mL, 1 M) and D*i*PEA (14.0 mL, 109 mmol, 2.50 equiv.) was added. The formed precipitate was filtered and washed with small portions of CH_2Cl_2. The solvent was removed under reduced pressure and the residue was suspended in Et_2O (50 mL), cooled to 0 °C and benzyl bromide (5.67 mL, 47.8 mmol, 1.10 equiv.) was slowly added dropwise. After stirring for 24 h at room temperature the reaction mixture was filtered, washed with small portions of Et_2O, and the solvent was removed under reduced pressure. After column chromatography (silica, Hex/EtOAc = 3/1), (*S*)-methyl-1-benzylpyrrolidin-2-carboxylate (8.1 g, 36.9 mmol, 95%) was obtained as an orange oil.

***R*f** = 0.35 (Hex:EtOAc / 3:1) [CAM].

^{1}H NMR (400 MHz, $CDCl_3$): δ/ppm = 7.28 – 7.11 (m, 5H), 3.80 (d, *J* = 12.8 Hz, 1H), 3.55 (s, 3H), 3.49 (d, *J* = 12.8, 1.4 Hz, 1H), 3.17 (dd, *J* = 8.9, 6.2 Hz, 1H), 2.96 (td, *J* = 8.6, 2.6 Hz, 1H), 2.35 – 2.27 (m, 1H), 2.11 – 1.98 (m, 1H), 1.94 – 1.74 (m, 2H), 1.74 – 1.63 (m, 1H).

^{13}C NMR (101 MHz, $CDCl_3$): δ/ppm = 174.5 (C), 138.3 (C), 129.2 (CH), 128.2 (CH), 127.1 (CH), 65.3 (CH), 58.7 (CH_2), 53.3 (CH_2), 51.7 (CH_3), 29.4 (CH_2), 23.9 (CH_2).

The NMR spectra are in accordance with those reported in the literature.[13]

(*S*)-(1-Benzylpyrrolidin-2-yl)diphenylmethanol

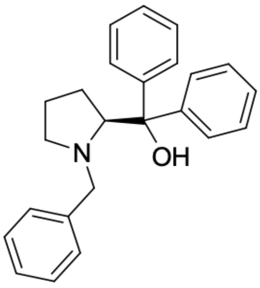

Using GP1, (*S*)-Methyl-1-benzylpyrrolidin-2-carboxylate (0.750 g, 3.42 mmol, 1.00 equiv.) was converted with bromobenzene (0.895 mL, 1.34 g, 8.55 mmol, 2.50 equiv.) and magnesium (0.208 g, 8.55 mmol, 2.50 equiv.) in 20 h at room temperature. After column chromatography (silica, Hex/EtOAc = 1/0 → 9/1), (*S*)-(1-benzylpyrrolidin- 2-yl)bis(3,5-dimethyl-phenyl)methanol (1.09 g, 3.18 mmol, 93%) was obtained as an orange foam and directly used in the next step.

***R*f** = 0.45 (Hex:EtOAc / 1:1) [UV, CAM].

(*S*)-Diphenyl)(pyrrolidin-2-yl)methanol

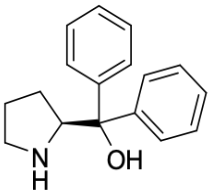

Using GP2, (*S*)-(1-Benzylpyrrolidin-2-yl)diphenylmethanol (1.09 g, 3.18 mmol, 1.00 equiv.) was converted with palladium on charcoal (0.674 g, 10 wt%, 0.20 equiv.) under hydrogen atmosphere in 24 h. After column chromatography (silica, Hex/EtOAc = 1/0 → 9/1) (*S*)-Diphenyl)(pyrrolidin-2-yl)methanol (0.699 g, 2.76 mmol, 87%) was obtained as a pale yellow solid.

***R*f** = 0.11 (Hex:EtOAc / 1:1) [UV, CAM].

^{1}H NMR (400 MHz, $CDCl_3$): δ/ppm = 7.61 – 7.55 (m, 2H), 7.51 – 7.46 (m, 2H), 7.33 – 7.24 (m, 5H), 7.20 – 7.13 (m, 2H), 4.29 (t, *J* = 7.6 Hz, 1H), 3.05 – 2.89 (m, 2H), 1.80 – 1.51 (m, 4H).

^{13}C NMR (101 MHz, $CDCl_3$): δ/ppm = 148.0 (C), 145.4 (C), 128.4 (CH), 128.1 (CH), 126.7 (CH), 126.5 (CH), 126.0 (CH), 125.6 (CH), 77.3 (COH), 64.7 (CH), 46.9 (CH_2), 26.5 (CH_2), 25.6 (CH_2).

HRMS (ESI): calcd for $C_{17}H_{20}NO$ $[M+H]^+$: 254.1539; found: 254.1540

The NMR spectra are in accordance with those reported in the literature.[14]

(*S*)-(1-Benzylpyrrolidin-2-yl)bis(3,5-dimethylphenyl)methanol

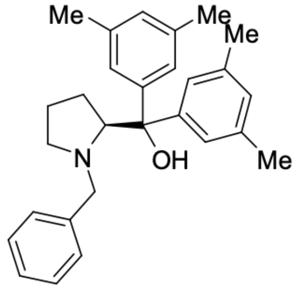

Using GP1, (*S*)-Methyl-1-benzylpyrrolidin-2-carboxylate (2.66 g, 12.1 mmol, 1.00 equiv.) was converted with 1-Bromo-3,5-dimethylbenzene (4.19 mL, 5.61 g, 30.33 mmol, 2.50 equiv.) and magnesium (0.737 g, 30.33 mmol, 2.50 equiv.) in 20 h at room temperature. After column chromatography (silica, Hex/EtOAc = 1/0 → 10/1), (*S*)-(1-benzylpyrrolidin- 2-yl)bis(3,5-dimethylphenyl)methanol (3.23 g, 8.13 mmol, 67%) was obtained as an orange oil.

R

R_f = 0.30 (Hex:EtOAc / 10:1) [UV, CAM].

^{1}H NMR (400 MHz, $CDCl_3$): δ/ppm = 7.31 – 7.28 (m, 2H), 7.25 – 7.16 (m, 5H), 7.09 – 7.02 (m, 2H), 6.80 (s, 1H), 6.71 (s, 1H), 4.77 (s, 1H), 3.89 (dd, *J* = 9.5, 4.5 Hz, 1H), 3.18 – 2.97 (m, 2H), 2.95 – 2.88 (m, 1H), 2.30 (s, 6H), 2.25 (s, 6H), 2.17 (s, 2H), 2.04 – 1.87 (m, 1H), 1.83 – 1.71 (m, 1H).

^{13}C NMR (101 MHz, $CDCl_3$): δ/ppm = 148.0 (C), 146.6 (C), 140.1 (C), 137.5 (C), 137.4 (C), 128.8 (CH), 128.2 (CH), 128.2 (CH), 128.0 (CH), 126.9 (CH), 123.7 (CH), 123.6 (CH), 78.2 (COH), 70.9 (CH), 60.8 (CH_2), 55.8 (CH_2), 30.0 (CH_2), 24.5 (CH_2), 21.8 (CH_3), 21.7 (CH_3).

HRMS (ESI): calcd for $C_{28}H_{34}NO$ $[M+H]^+$: 400.2635; found: 400.2638.

The NMR spectra are in accordance with those reported in the literature.[13]

(*S*)-Bis(3,5-dimethylphenyl)(pyrrolidin-2-yl)methanol

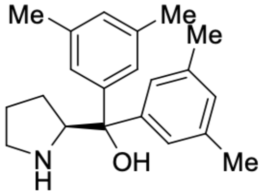

Using GP2, (*S*)-(1-Benzylpyrrolidin-2-yl)diphenylmethanol (3.23 g, 8.13 mmol, 1.00 equiv.) was converted with palladium on charcoal (1.72 g, 10 wt%, 0.20 equiv.) under hydrogen atmosphere in 24 h. After column chromatography (silica, Hex/EtOAc = 1/0 → 10/1) (*S*)-Diphenyl)(pyrrolidin-2-yl)methanol (2.31 g, 7.46 mmol, 92%) was obtained as a pale yellow solid.

***R*f** = 0.21 (Hex:EtOAc / 10:1) [UV, CAM].

^{1}H NMR (400 MHz, $CDCl_3$): δ/ppm = 7.18 (s, 2H), 7.10 (s, 2H), 6.80 (s, 2H), 4.23 (t, *J* = 7.7 Hz, 1H), 3.05 – 2.97 (m, 1H), 2.97 – 2.89 (m, 1H), 2.28 (d, *J* = 5.1 Hz, 12H), 1.79 – 1.67 (m, 2H), 1.67 – 1.53 (m, 2H).

^{13}C NMR (101 MHz, $CDCl_3$): δ/ppm = 148.2 (C), 145.4 (C), 137.7 (C), 137.4 (C), 128.3 (CH), 128.2 (CH), 123.8 (CH), 123.4 (CH), 77.4 (COH), 64.7 (CH), 46.87 (CH_2), 26.4 (CH_2), 25.6 (CH_2), 21.7 (CH_3).

HRMS (ESI): calcd for $C_{21}H_{28}NO$ $[M+H]^+$: 310.2165; found: 310.2168.

The NMR spectra are in accordance with those reported in the literature.[13]

(*S*)-(1-Benzylpyrrolidin-2-yl)bis(3,5-diisopropylphenyl)methanol

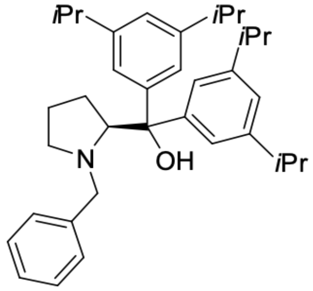

Using GP1, (*S*)-Methyl-1-benzylpyrrolidin-2-carboxylate (0.848 g, 3,87 mmol, 1.00 equiv.) was converted with 1-Bromo-3,5-diisopropylbenzene (2.33 g, 9.68 mmol, 2.50 equiv.) and magnesium (0.235 g, 9.68 mmol, 2.50 equiv.) in 20 h at room temperature. After column chromatography (silica, Hex/EtOAc = 10/1), (*S*)-(1-Benzylpyrrolidin-2-yl)bis(3,5-diisopropylphenyl)methanol (0.603 g, 1.18 mmol, 31%) was obtained as a colorless foam.

***R*f** = 0.20 (Hex:EtOAc / 10:1) [UV, CAM].

^{1}H NMR (600 MHz, $CDCl_3$): δ/ppm 7.49 (d, *J* = 1.6 Hz, 2H), 7.31 (d, *J* = 1.7 Hz, 2H), 7.25 – 7.17 (m, 3H), 7.05 – 7.01 (m, 2H), 6.90 – 6.79 (m, 2H), 4.88 (s, 1H), 4.00 (dd, *J* = 9.4, 4.8 Hz, 1H), 3.13 (dd, *J* = 125.9, 12.6 Hz, 2H), 2.96 – 2.82 (m, 5H), 2.38 (td, *J* = 9.5, 6.6 Hz, 1H), 1.97 – 1.88 (m, 1H), 1.78 – 1.53 (m, 3H), 1.26 (d, *J* = 6.9, 1.1 Hz, 12H), 1.21 (d, *J* = 7.0 Hz, 12H).

^{13}C NMR (151 MHz, $CDCl_3$): δ/ppm = 148.4 (C), 148.2 (C), 148.2 (C), 146.7, 140.3, 128.8 (CH), 128.1 (CH), 126.8 (C), 122.8 (C), 122.3 (C), 121.5 (CH), 121.2 (CH), 78.3 (COH), 71.6 (CH), 60.6 (CH_2), 55.8 (CH_2), 34.5 (CH), 34.4 (CH), 29.8 (CH_2), 24.4 (CH_3), 24.3 (CH_3), 24.2 (CH_3), 24.1 (CH_3).

HRMS (ESI): calcd for $C_{36}H_{50}NO$ $[M+H]^+$: 512.3887; found: 512.3884.

(*S*)-Bis(3,5-diisopropylphenyl)(pyrrolidin-2-yl)methanol

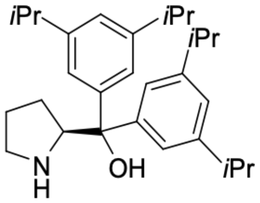

Using GP2, (*S*)-(1-benzylpyrrolidin-2-yl)bis(3,5-diisopropylphenyl)methanol (0.603 g, 1.18 mmol, 1.00 equiv.) was converted with palladium on charcoal (0.232 g, 10 wt%, 0.20 equiv.) under hydrogen atmosphere in 24 h. After column chromatography (silica, Hex/EtOAc = 3/1) (*S*)-bis(3,5-diisopropylphenyl)(pyrrolidin-2-yl)methanol (0.294 g, 0.697 mmol, 59%) was obtained as a colorless solid.

***R*f** = 0.15 (Hex:EtOAc / 3:1) [UV, CAM].

^{1}H NMR (400 MHz, $CDCl_3$): δ/ppm = 7.28 (d, *J* = 1.6 Hz, 2H), 7.20 (d, *J* = 1.7 Hz, 2H), 6.87 (dt, *J* = 6.2, 1.8 Hz, 2H), 4.24 (t, *J* = 7.7 Hz, 1H), 3.05 – 2.91 (m, 2H), 2.86 (dq, *J* = 13.3, 6.8 Hz, 4H), 1.79 – 1.52 (m, 5H), 1.25 – 1.17 (m, 24H).

^{13}C NMR (101 MHz, $CDCl_3$): δ/ppm = 148.5 (C), 148.1 (C), 145.4 (C), 122.5 (CH), 122.5 (CH), 121.7 (CH), 121.3 (CH), 77.4 (COH), 65.4 (CH), 46.9 (CH_2), 34.4 (CH), 26.5 (CH_2), 25.6 (CH_2), 24.5 (CH_3), 24.3 (CH_3), 24.2 (CH_3), 24.1 (CH_3).

HRMS (ESI): calcd for $C_{29}H_{44}NO$ $[M+H]^+$: 421.3417; found: 421.3415.

(*S*)-(1-Benzylpyrrolidin-2-yl)bis(3,5-di-^{t}buylphenyl)methanol

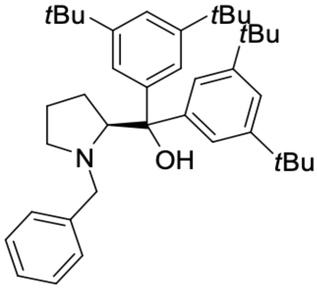

Using GP1, (*S*)-methyl-1-benzylpyrrolidin-2-carboxylate (0.700 g, 3.19 mmol, 1.00 equiv.) was converted with 1-bromo-3,5-di-^{t}butylbenzene (2.15 g, 7.98 mmol, 2.50 equiv.) and magnesium (0.194 g, 7.98 mmol, 2.50 equiv.) in 20 h at room temperature. After column chromatography (silica, Hex/EtOAc = 1/0 → 20/1), (*S*)-(1-benzylpyrrolidin-2-yl)bis(3,5-di-^{t}buylphenyl)methanol (1.06 g, 1.88 mmol, 59%) was obtained as a colorless foam.

***R*f** = 0.20 (Hex:EtOAc / 20:1) [UV, CAM].

^{1}H NMR (400 MHz, $CDCl_3$): δ/ppm = 7.61 (d, *J* = 1.8 Hz, 2H), 7.42 (d, *J* = 1.8 Hz, 2H), 7.17 – 7.03 (m, 5H), 6.96 – 6.86 (m, 2H), 5.12 (s, 2H), 3.94 (dd, *J* = 9.3, 4.7 Hz, 1H), 3.12 (d, *J* = 12.6 Hz, 1H), 2.92 (d, *J* = 12.7 Hz, 1H), 2.88 – 2.80 (m, 1H), 2.28 (td, *J* = 9.2, 6.9 Hz, 1H), 1.88 – 1.72 (m, 1H), 1.69 – 1.47 (m, 3H), 1.23 (d, *J* = 18.1 Hz, 36H).

^{13}C NMR (101 MHz, $CDCl_3$): δ/ppm = 150.1 (C), 149.9 (C), 147.6 (C), 146.1 (C), 140.3 (C), 128.7 (CH), 128.1 (CH), 126.8 (CH), 120.3 (CH), 119.9 (CH), 119.8 (CH), 78.4 (COH), 71.9 (CH), 60.5 (CH_2), 55.8 (CH_2), 53.5 (CH_2), 35.1 (C), 35.0 (C), 31.8 (CH_3), 31.7 (CH_3), 29.8 (CH_3), 24.3 (CH_2).

HRMS (ESI): calcd for $C_{40}H_{57}NONa$ $[M+Na]^+$: 590.4332; found: 590.4335.

(*S*)-Bis(3,5-di-^{t}butylphenyl)(pyrrolidin-2-yl)methanol

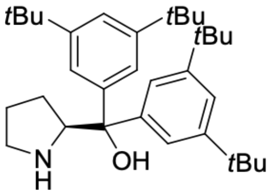

Using GP2, (*S*)-(1-benzylpyrrolidin-2-yl)bis(3,5-di^{t}buylphenyl)methanol (1.06 g, 1.88 mmol, 1.00 equiv.) was converted with palladium on charcoal (0.397 g, 10 wt%, 0.20 equiv.) under hydrogen atmosphere in 24 h. After column chromatography (silica, Hex/EtOAc 3/1) (*S*)-bis(3,5-di-^{t}butylphenyl)(pyrrolidin-2-yl)methanol (0.794 g, 1.66 mmol, 89%) was obtained as a colorless solid.

***R*f** = 0.18 (Hex:EtOAc / 3:1) [UV, CAM].

^{1}H NMR (400 MHz, CD_2Cl_2): δ/ppm = 7.50 (d, *J* = 1.8 Hz, 2H), 7.39 (d, *J* = 1.8 Hz, 2H), 7.26 (t, *J* = 1.8 Hz, 1H), 7.22 (t, *J* = 1.8 Hz, 1H), 4.44 (t, *J* = 7.8 Hz, 1H), 2.85 (s, 2H), 1.78 – 1.67 (m, 2H), 1.65 – 1.54 (m, 2H), 1.30 (d, *J* = 9.2 Hz, 36H).

^{13}C NMR (101 MHz, CD_2Cl_2): δ/ppm = 151.1 (C), 150.7 (C), 145.3 (C), 121.3 (CH), 120.7 (CH), 120.2 (CH), 120.0 (CH), 78.2 (COH), 65.9 (CH), 47.3 (CH_2), 35.4 (C), 31.9 (CH_3), 31.8 (CH_3), 27.0 (CH_2), 26.0 (CH_2).

HRMS (ESI): calcd for $C_{33}H_{53}NO$ $[M+H]^+$: 478.4044; found: 478.4044.

The NMR spectra are in accordance with those reported in the literature.[15]

(*S*)-(1-Benzylpyrrolidin-2-yl)bis(3,5-dimethyl-4-Methoxy-phenyl)methanol

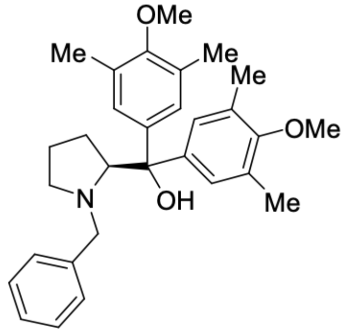

Using GP1, (*S*)-methyl-1-benzylpyrrolidin-2-carboxylate (2.00 g, 9.66 mmol, 1.00 equiv.) was converted with 1-bromo-3,5-dimethyl-4-methoxybenzene (6.50 g, 24.15 mmol, 2.50 equiv.) and magnesium (0.587 g, 24.15 mmol, 2.50 equiv.) in 20 h at room temperature. After column chromatography (silica, Hex/EtOAc = 10/1), (*S*)-(1-benzylpyrrolidin-2-yl)bis(3,5-dimethyl-4-Methoxy-phenyl)methanol (1.50 g, 3.26 mmol, 34%) was obtained as a colorless oil.

***R*f** = 0.16 (Hex:EtOAc / 10:1) [UV, CAM].

^{1}H NMR (400 MHz, $CDCl_3$): δ/ppm = 7.31 – 7.15 (m, 7H), 7.05 – 7.00 (m, 2H), 4.71 (s, 1H), 3.83 (dd, *J* = 9.5, 4.4 Hz, 1H), 3.68 (s, 3H), 3.58 (s, 3H), 3.08 (dd, 2H), 2.96 – 2.90 (m, 1H), 2.35 (td, *J* = 9.3, 7.3 Hz, 1H), 2.27 (s, 6H), 2.21 (s, 6H), 2.01 – 1.87 (m, 1H), 1.81 – 1.69 (m, 1H), 1.67 – 1.54 (m, 2H).

^{13}C NMR (101 MHz, $CDCl_3$): δ/ppm = 155.5 (C), 155.4 (C), 143.2 (C), 141.9 (C), 140.1 (C), 130.2 (CH), 130.2 (CH), 128.7 (CH), 128.2 (CH), 126.9 (CH), 126.3 (CH), 126.2 (CH), 77.7 (COH), 71.1 (CH), 60.8 (CH_2), 59.8 (CH_3), 59.7 (CH_3), 55.9 (CH_2), 30.0 (CH_2), 24.5 (CH_2), 16.6 (CH_3), 16.5 (CH_3).

HRMS (ESI): calcd for $C_{30}H_{38}NO_3$ $[M+H]^+$: 460.2846; found: 460.2848.

(*S*)-Bis(3,5-dimethyl-4-Methoxy-phenyl)(pyrrolidin-2-yl)methanol

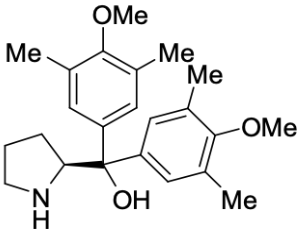

Using GP2, (*S*)-(1-Benzylpyrrolidin-2-yl)bis(3,5-dimethyl-4-Methoxy-phenyl)methanol (1.37 g, 2.98 mmol, 1.00 equiv.) was converted with palladium on charcoal (0.632 g, 10 wt%, 0.20 equiv.) under hydrogen atmosphere in 24 h. After column chromatography (silica, Hex/EtOAc = 1/1 → 0/1) (*S*)-Bis(3,5-dimethyl-4-Methoxy-phenyl)(pyrrolidin-2-yl)methanol (0.717 g, 1.94 mmol, 65%) was obtained as a light orange solid.

***R*f** = 0.11 (Hex:EtOAc / 1:1) [UV, CAM].

^{1}H NMR (400 MHz, CD_2Cl_2): δ/ppm = 7.19 (s, 2H), 7.11 (s, 2H), 4.23 (t, *J* = 7.7 Hz, 1H), 3.66 (d, *J* = 1.5 Hz, 6H), 3.02 – 2.88 (m, 2H), 2.24 (d, *J* = 5.5 Hz, 12H), 1.71 (p, *J* = 7.1 Hz, 2H), 1.60 – 1.51 (m, 2H).

^{13}C NMR (101 MHz, CD_2Cl_2): δ/ppm = 156.0 (C), 155.9 (C), 144.1 (C), 141.6 (C), 130.9 (C), 130.6 (C), 126.6 (CH), 126.2 (CH), 76.9 (COH), 64.9 (CH), 60.0 (CH_3), 47.3 (CH_2), 26.7 (CH_2), 26.1 (CH_2), 16.7 (CH_3), 16.6 (CH_3).

HRMS (ESI): calcd for $C_{23}H_{32}NO_3$ $[M+H]^+$: 370.2378; found: 370.2379.

The NMR spectra are in accordance with those reported in the literature.[15]

(*S*)-Bis(3,5-di-^{t}butyl-4-Methoxy-phenyl)(pyrrolidin-2-yl)methanol

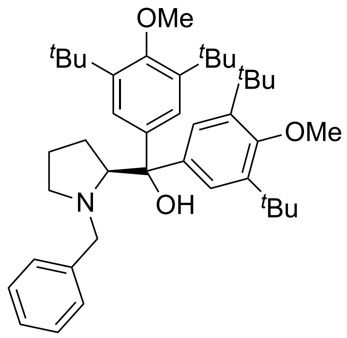

Using GP1, (*S*)-methyl-1-benzylpyrrolidin-2-carboxylate (0.750 g, 3.42 mmol, 1.00 equiv.) was converted with 1-bromo-3,5-di-^{t}butyl-4-methoxybenzene (2.56 g, 8.55 mmol, 2.50 equiv.) and magnesium (0.208 g, 8.55 mmol, 2.50 equiv.) in 20 h at room temperature. After column chromatography (silica, CH_2Cl_2), (*S*)-bis(3,5-di-^{t}butyl-4-Methoxy-phenyl)(pyrrolidin-2-yl)methanol (1.65 g, 2.63 mmol, 77%) was obtained as an orange oil, which was directly used in the next step.

***R*~f~** = 0.3 (CH_2Cl_2) [UV, CAM].

(*S*)-Bis(3,5-di-^{t}butyl-4-Methoxy-phenyl)(pyrrolidin-2-yl)methanol

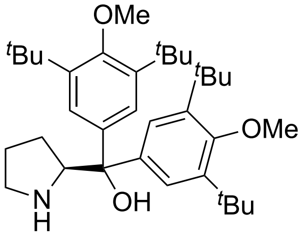

Using GP2, (*S*)-(1-benzylpyrrolidin-2-yl)bis(3,5-di-^{t}butyl-4-Methoxy-phenyl)methanol (0.661 g, 1.05 mmol, 1.00 equiv.) was converted with palladium on charcoal (0.223 g, 10 wt%, 0.20 equiv.) under hydrogen atmosphere in 24 h. After column chromatography (silica, CH_2Cl_2/MeOH = 40/1) (*S*)-bis(3,5-di-^{t}butyl-4-methoxy-phenyl)(pyrrolidin-2-yl)methanol (0.298 g, 0.554 mmol, 53%) was obtained as a colorless solid.

$\boldsymbol{R}_\mathbf{f}$ = 0.10 (CH_2Cl_2:MeOH / 40:1) [UV, CAM].

^{1}H NMR (400 MHz, $CDCl_3$): δ/ppm = 7.37 (s, 2H), 7.24 (s, 2H), 4.23 – 4.11 (m, 1H), 3.56 (d, *J* = 8.1 Hz, 6H), 2.83 – 2.71 (m, 2H), 1.69 – 1.58 (m, 3H), 1.53 – 1.42 (m, 1H), 1.34 (s, 18H), 1.31 (s, 18H), 1.21 – 1.14 (m, 1H).

^{13}C NMR (101 MHz, $CDCl_3$): δ/ppm = 158.2 (C), 157.8 (C), 143.0 (C), 142.6 (C), 139.0 (C), 124.3 (CH), 124.0 (CH), 77.4 (COH), 65.7 (CH), 64.2 (CH_3), 46.8 (CH_2), 36.0 (CH_3), 32.3 (CH_3), 26.7 (CH_2), 25.4 (CH_2).

HRMS (ESI): calcd for $C_{35}H_{56}NO_3$ $[M+H]^+$: 538.4255; found: 538.4252.

The NMR spectra are in accordance with those reported in the literature.[16]

(*S*)-(1-Benzylpyrrolidin-2-yl)dinaphthylmethanol

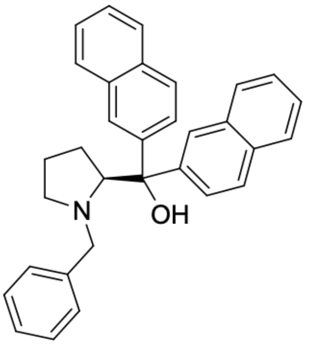

Using GP1, (*S*)-methyl-1-benzylpyrrolidin-2-carboxylate (2.12 g, 9.66 mmol, 1.00 equiv.) was converted with 2-bromonaphthalene (5.00 g, 24.15 mmol, 2.50 equiv.) and magnesium (0.587 g, 24.15 mmol, 2.50 equiv.) in 20 h at room temperature. After column chromatography (silica, Hex/EtOAc = 80/1 → 10/1), (*S*)-(1-benzylpyrrolidin-2-yl)dinaphthyl-methanol (1.85 g, 4.78 mmol, 49%) was obtained as a colorless solid.

***R*$_f$** = 0.19 (Hex:EtOAc / 40:1) [UV, CAM].

^{1}H NMR (400 MHz, CDCl$_3$): δ/ppm = 8.34 (s, 1H), 8.11 (s, 1H), 7.89 – 7.66 (m, 8H), 7.52 – 7.29 (m, 4H), 7.19 (s, 3H), 7.03 – 6.95 (m, 2H), 5.25 (s, 1H), 4.24 (dd, *J* = 9.4, 4.8 Hz, 1H), 3.18 (dd, *J* = 89.1, 12.6 Hz, 2H), 2.97 (d, *J* = 18.5 Hz, 1H), 2.48 – 2.37 (m, 1H), 2.02 (s, 1H), 1.90 (s, 1H), 1.64 (s, 2H).

^{13}C NMR (101 MHz, CDCl$_3$): δ/ppm = 145.4 (C), 144.0 (C), 139.6 (C), 133.4 (C), 133.4 (C), 132.2 (C), 128.7 (CH), 128.4 (CH), 128.3 (CH), 128.2 (CH), 128.0 (CH), 127.9 (CH), 127.6 (CH), 127.6 (CH), 127.0 (CH), 126.2 (CH), 126.0 (CH), 125.8 (CH), 125.8 (CH), 124.6 (CH), 124.5 (CH), 124.3 (CH), 124.1 (CH), 78.5 (COH), 70.2 (CH), 60.7 (CH$_2$), 55.7 (CH$_2$), 30.1 (CH$_2$), 24.3 (CH$_2$).

HRMS (ESI): calcd for $C_{32}H_{30}NO$ [M+H]$^+$: 444.2322; found: 444.2322.

(*S*)-Dinaphthalenyl-2-pyrrolidinemethanol

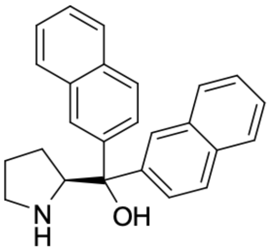

Using GP2, (*S*)-(1-benzylpyrrolidin-2-yl)dinaphthylmethanol (1.85 g, 4.78 mmol, 1.00 equiv.) was converted with palladium on charcoal (0.883 g, 10 wt%, 0.20 equiv.) under hydrogen atmosphere in 24 h. After column chromatography (silica, Hex/EtOAc = 1/1) (*S*)-bis(3,5-dimethyl-4-methoxy-phenyl)(pyrrolidin-2-yl)methanol (0.665 g, 1.88 mmol, 39%) was obtained as a colorless solid.

***R*f** = 0.19 (Hex:EtOAc / 1:1) [UV, CAM].

^{1}H NMR (400 MHz, $CDCl_3$): δ/ppm = 8.16 (d, *J* = 1.8 Hz, 2H), 7.91 (td, *J* = 8.1, 1.5 Hz, 2H), 7.83 – 7.69 (m, 5H), 7.63 (dd, *J* = 8.6, 1.8 Hz, 1H), 7.55 – 7.41 (m, 4H), 4.53 (t, *J* = 7.1 Hz, 1H), 3.12 – 2.91 (m, 2H), 1.86 – 1.71 (m, 3H), 1.69 – 1.58 (m, 1H).

^{13}C NMR (101 MHz, $CDCl_3$): δ/ppm = 145.4 (C), 142.7 (C), 133.3 (C), 133.2 (C), 132.4 (C), 132.3 (C), 128.4 (CH), 128.3 (CH), 128.2 (CH), 127.8 (CH), 127.6 (CH), 126.1 (CH), 126.0 (CH), 125.9 (CH), 125.7 (CH), 125.4 (CH), 124.5 (CH), 124.1 (CH), 123.9 (CH), 77.6 (COH), 64.1 (CH), 46.9 (CH_2), 26.6 (CH_2), 25.7 (CH_2).

HRMS (ESI): calcd for $C_{25}H_{24}NO$ $[M+H]^+$: 354.1853; found: 354.1854.

The NMR spectra are in accordance with those reported in the literature.[14]

(*S*)-(1-Benzylpyrrolidin-2-yl)bis(3,5-bistrifluoromethylphenyl)methanol

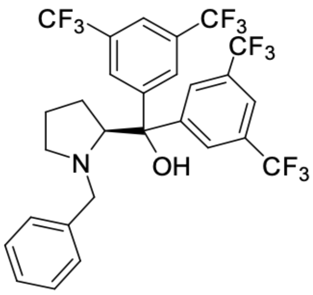

Using GP1, (*S*)-methyl-1-benzylpyrrolidin-2-carboxylate (0.500 g, 2.28 mmol, 1.00 equiv.) was converted with 1-bromo-3,5-bis(trifluoromethyl)benzene (1.67 g, 5.70 mmol, 2.50 equiv.) and magnesium (0.139 g, 5.70 mmol, 2.50 equiv.) in 20 h at room temperature. After column chromatography (silica, Hex/EtOAc = 80/1 → 10/1), (*S*)-(1-benzylpyrrolidin-2-yl)dinaphthyl-methanol (0.688 g, 1.12 mmol, 49%) was obtained as a colorless solid, which was directly used in the next step.

***R*f** = 0.25 (Hex:EtOAc / 10:1) [UV, CAM]

(*S*)-Bis(3,5-bistrifluoromethylphenyl)(pyrrolidin-2-yl)methanol

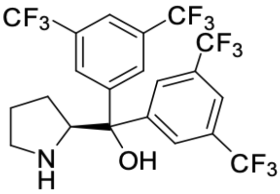

Using GP2, (*S*)-(1-benzylpyrrolidin-2-yl)bis(3,5-bistrifluoromethylphenyl)methanol (0.688 g, 1.12 mmol, 1.00 equiv.) was converted with palladium on charcoal (0.237 g, 10 wt%, 0.20 equiv.) under hydrogen atmosphere in 24 h. After column chromatography (silica, Hex/EtOAc = 10/1) (*S*)-bis(3,5-dimethyl-4-methoxy-phenyl)(pyrrolidin-2-yl)methanol (0.546 g, 1.04 mmol, 93%) was obtained as a colorless solid.

***R*f** = 0.20 (Hex:EtOAc / 5:1) [UV, CAM].

^{1}H NMR (400 MHz, $CDCl_3$): δ/ppm = 8.05 (s, 2H), 7.96 (s, 2H), 7.76 (d, *J* = 4.4 Hz, 2H), 5.06 (dd, *J* = 8.7, 4.2 Hz, 0H), 4.35 (t, *J* = 7.7 Hz, 1H), 3.12 – 3.00 (m, 2H), 1.87 – 1.72 (m, 2H), 1.66 – 1.46 (m, 2H).

^{13}C NMR (101 MHz, $CDCl_3$): δ/ppm = 149.6 (C), 147.1 (C), 132.1 (qd, *J* = 33.4, 25.5 Hz, C), 127.4 (CH), 126.0 (dd, *J* = 37.7, 4.0 Hz, C), 124.7 (CH), 121.6 (dt, *J* = 19.3, 3.8 Hz), 119.3 (CH), 76.8 (COH), 65.0 (CH), 47.9 (CH_2), 27.9 (CH_2), 25.2 (CH_2).

HRMS (ESI): calcd for $C_{21}H_{16}F_{12}NO$ $[M+H]^+$: 526.1035; found: 526.1036.

The NMR spectra are in accordance with those reported in the literature.[17]

(*S*)-(1-Benzylpyrrolidin-2-yl)dipentafluorophenylmethanol

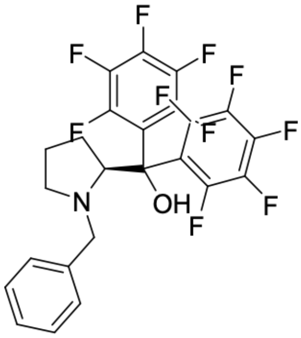

To a solution of pentafluoroiodobenzene (1.37 mL, 10.3 mmol, 3.0 equiv.) in 25 mL dry Et_2O under Ar at −78 °C, ^{n}BuLi in hexane [1.6 M] (6.00 mL, 9.6 mmol, 2.80 equiv.) was added dropwise. After stirring at −78 °C for 2 h (*S*)-methyl-1-benzylpyrrolidin-2-carboxylate (0.670 mL, 3.43 mmol, 1.0 equiv.) were added and the solution was stirred at −78 °C for 3 h. Saturated NH_4Cl solution was added and the mixture was extracted with EtOAc (3 × 70 mL). The combined organic layers were washed with brine, dried over Na_2SO_4, filtered, and the solvent was removed under reduced pressure. After column chromatography (silica, Hex/EtOAc = 10/1) (*S*)-(1-benzylpyrrolidin-2-yl)dipentafluoro-phenylmethanol was obtained as a colorless solid (1.02 g, 1.95 mmol, 57%).

R

R_f = 0.49 (Hex:EtOAc / 10:1) [UV, CAM].

^{1}H NMR (400 MHz, $CDCl_3$): δ/ppm = 7.38 – 7.16 (m, 3H), 7.15 – 7.08 (m, 2H), 4.90 (s, 1H), 4.06 – 3.98 (m, 1H), 3.30 (dd, *J* = 88.6, 13.1 Hz, 2H), 3.05 (dt, *J* = 8.8, 3.5 Hz, 1H), 2.45 – 2.33 (m, 1H), 2.33 – 2.19 (m, 1H), 2.02 – 1.91 (m, 1H), 1.81 – 1.67 (m, 2H).

^{13}C NMR (101 MHz, $CDCl_3$): δ/ppm = 146.3 (d, *J* = 53.2 Hz, CF), 144.0 (d, *J* = 51.3 Hz, CF), 142.3 (m, CF), 139.2 (m, CF), 136.7 (m, CF), 128.7 (CH), 128.0 (CH), 127.5 (CH), 118.5 (m, C), 116.7 (m, C), 80.0 (COH), 70.2 (CH), 62.3 (CH_2), 56.5 (CH_2), 30.1 (CH_2), 25.4 (CH_2).

HRMS (ESI): calcd for $C_{24}H_{16}F_{10}NO$ $[M+H]^+$: 524.1065; found: 524.1064.

(*S*)-Dipentafluorophenyl(pyrrolidin-2-yl)methanol

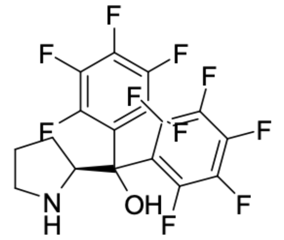

Using GP2, (*S*)-(1-Benzylpyrrolidin-2-yl)dipentafluorophenylmethanol (1.02 g, 1.95 mmol, 1.00 equiv.) was converted with palladium on charcoal (0.413 g, 10 wt%, 0.20 equiv.) under hydrogen atmosphere in 24 h. After column chromatography (silica, Hex/EtOAc = 40/1) and further crystallization from *ⁿ*heptane (*S*)-Dipentafluorophenyl(pyrrolidin-2-yl)methanol (0.507 g, 1.17 mmol, 60%) was obtained as a colorless solid.

$\boldsymbol{R}_\mathbf{f}$ = 0.22 (Hex:EtOAc / 40:1) [UV, CAM].

^{1}H NMR (400 MHz, $CDCl_3$): δ/ppm = 4.16 (t, *J* = 7.1 Hz, 1H), 3.62 – 3.50 (m, 1H), 3.26 – 3.15 (m, 1H), 2.93 (s, 1H), 2.29 – 1.92 (m, 4H).

^{13}C NMR (101 MHz, $CDCl_3$): δ/ppm = 146.0 (m, CF), 145.2 (m, CF), 144.3 (m, CF), 143.5 (m, CF), 141.8 (m, CF), 137.1 (m, CF), 136.4 (m, CF), 135.9 (m, CF), 134.8 (m, CF), 133.3 (m, CF), 117.9 (m, C), 117.0 (m, C), 80.1 (COH), 78.9 (CH), 52.2 (CH_2), 26.9 (CH_2), 24.7 (CH_2).

HRMS (ESI): calcd for $C_{17}H_{10}F_{10}NO$ $[M+H]^+$: 434.0597; found: 434.0599.

(*S*)-Prolinol

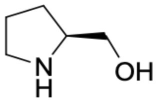

To a suspension of $LiAlH_4$ (0.850 g, 22.4 mmol, 1.6 equiv.) in dry THF was added (*S*)-proline (1.61 g, 14.0 mmol, 1.0 equiv.) in small portions. After refluxing for 2 h, the reaction was stopped by careful addition of potassium hydroxide solution (0.4 g in 1.6 mL dest. H_2O). The mixture was then refluxed for 15 min and the hot solution was filtered. The precipitate was refluxed with THF for an additional hour and filtered once more. The combined filtrates were concentrated under reduced pressure and used without further purification in quantitative yield (1.41 g, 14.0 mmol, 99%).

^{1}H NMR (400 MHz, $CDCl_3$): δ/ppm = 3.61 – 3.50 (m, 1H), 3.39 – 3.28 (m, 2H), 3.09 (s, 2H), 3.01 – 2.85 (m, 2H), 1.90 – 1.63 (m, 3H), 1.50 – 1.37 (m, 1H).

^{13}C NMR (101 MHz, $CDCl_3$): δ/ppm = 64.6 (CH_2OH), 59.7 (CH), 46.4 (CH_2), 27.7 (CH_2), 26.1 (CH_2).

HRMS (ESI): calcd for $C_5H_{11}NO$ $[M+H]^+$: 102.0919; found: 102.0915.

The NMR spectra are in accordance with those reported in the literature.[18]

8. NMR Spectra

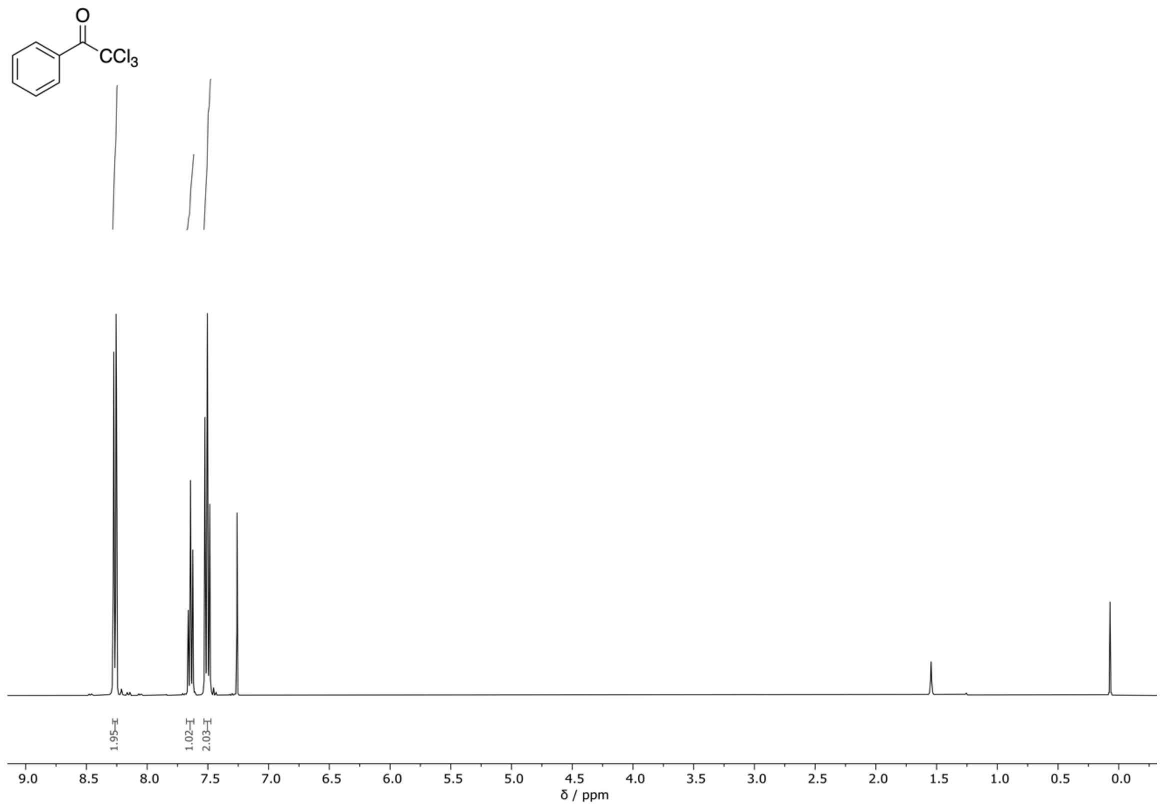

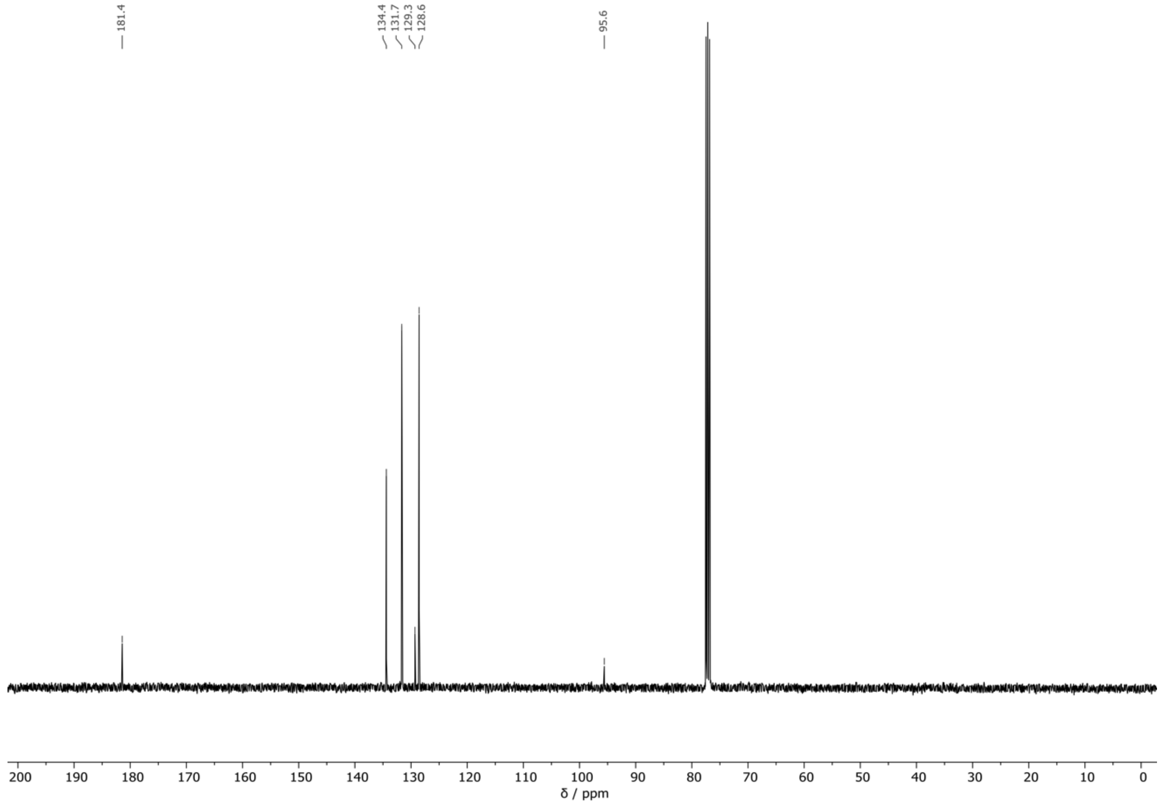

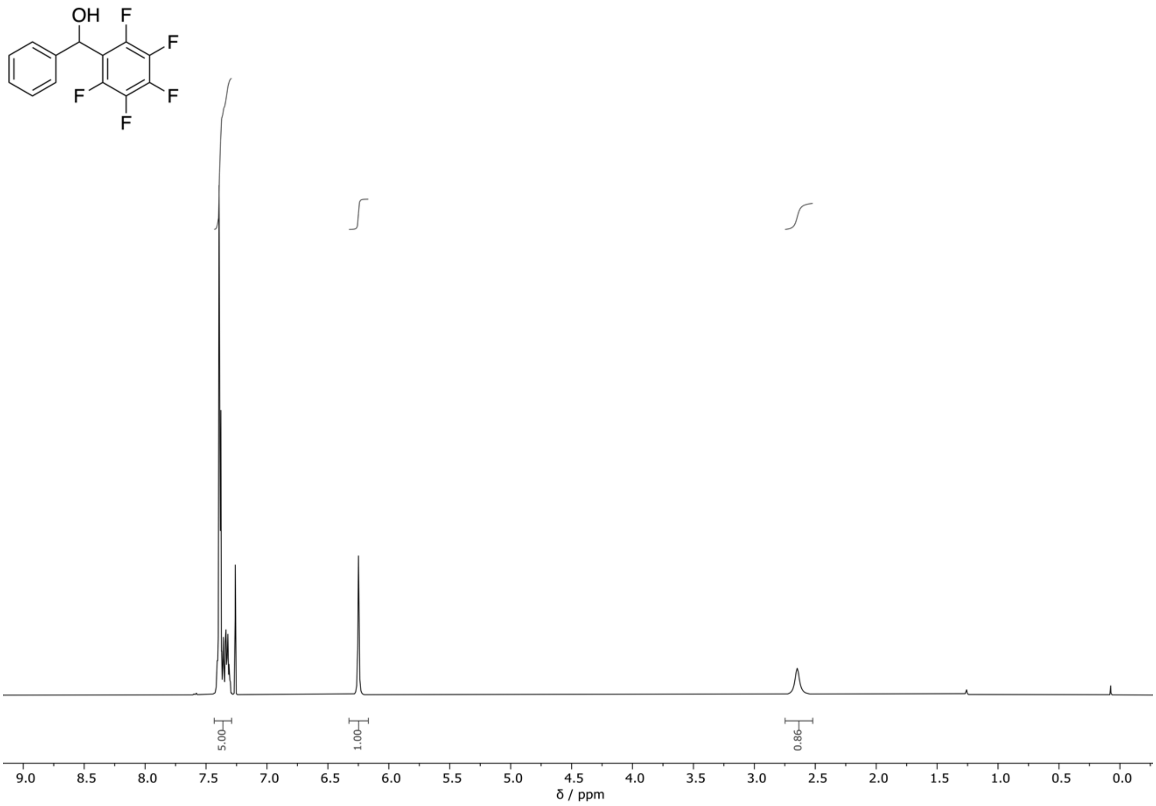
OH
F
F
F
F
F
5.00
1.00
0.86
9.0 8.5 8.0 7.5 7.0 6.5 6.0 5.5 5.0 4.5 4.0 3.5 3.0 2.5 2.0 1.5 1.0 0.5 0.0
δ / ppm

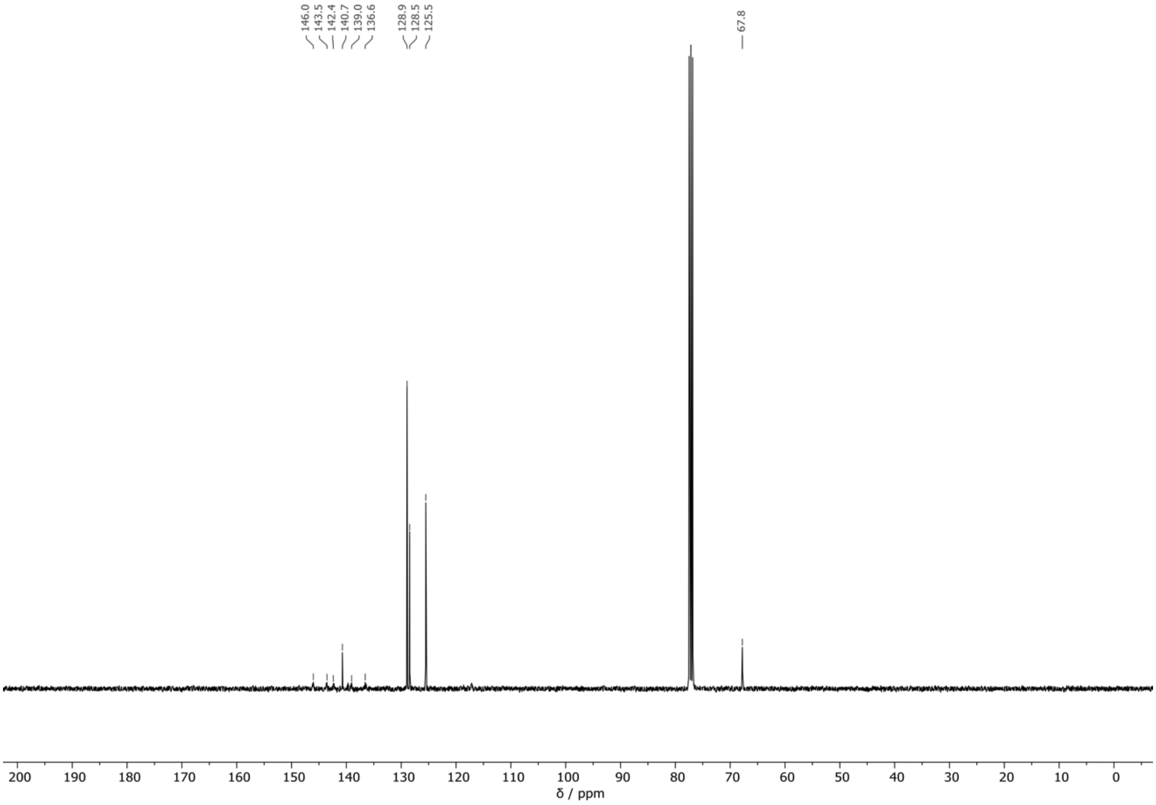
146.0
143.5
142.4
140.7
139.0
136.6
128.9
128.5
125.5
67.8
200 190 180 170 160 150 140 130 120 110 100 90 80 70 60 50 40 30 20 10 0
δ / ppm

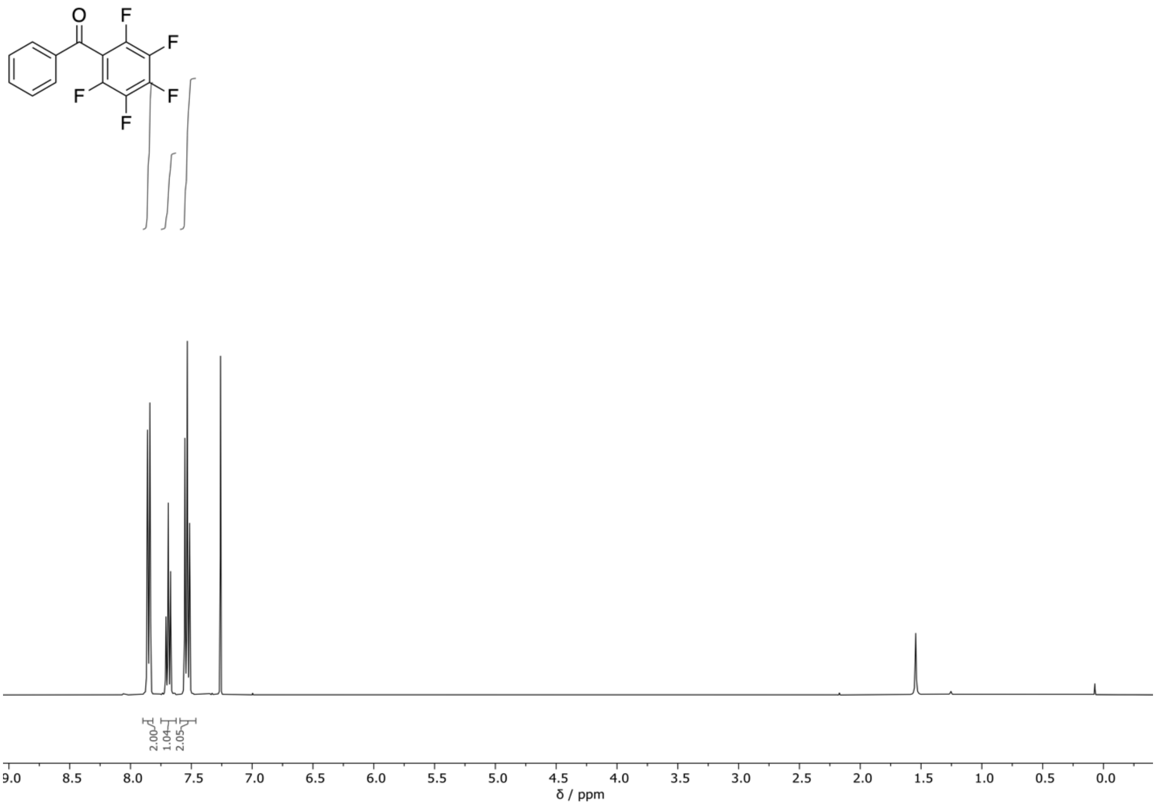
O
F
F
F
F
F
2.00
1.04
2.05
9.0
8.5
8.0
7.5
7.0
6.5
6.0
5.5
5.0
4.5
4.0
3.5
3.0
2.5
2.0
1.5
1.0
0.5
0.0
δ / ppm

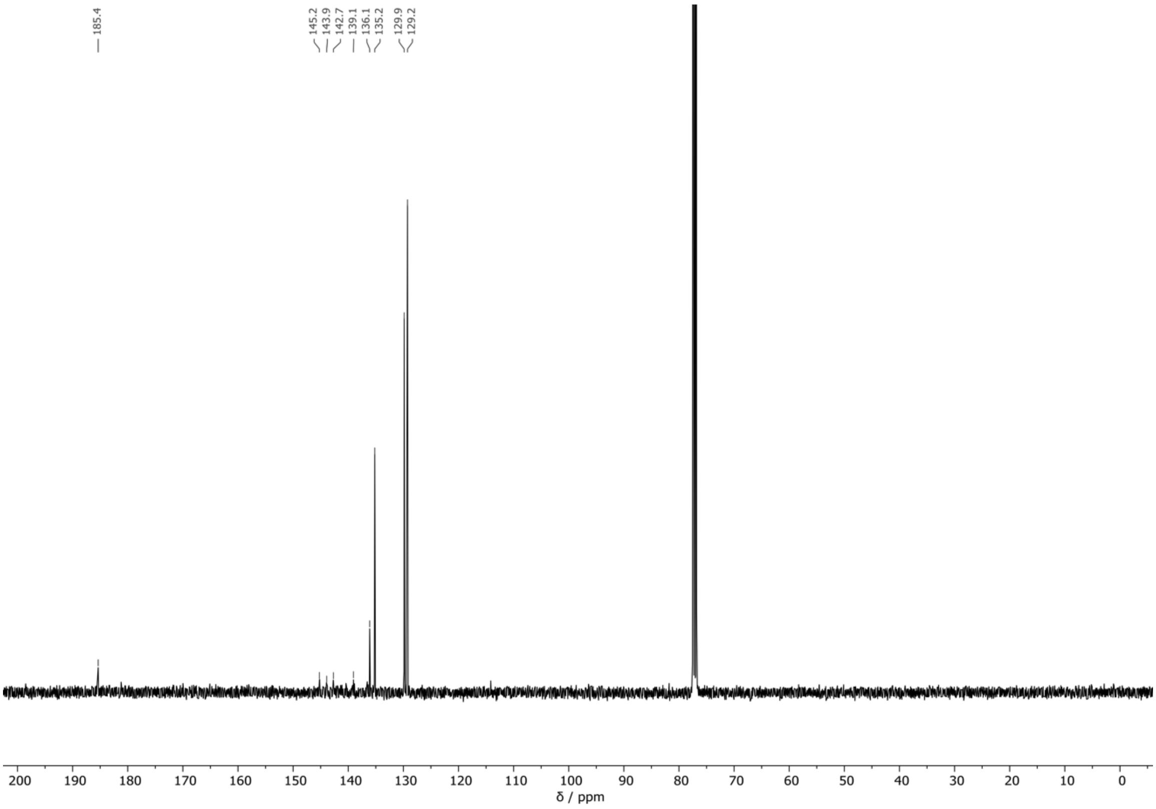
185.4
145.2
143.9
142.7
139.1
136.1
135.2
129.9
129.2
200
190
180
170
160
150
140
130
120
110
100
90
80
70
60
50
40
30
20
10
0
δ / ppm

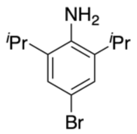
NH2
iPr
iPr
Br

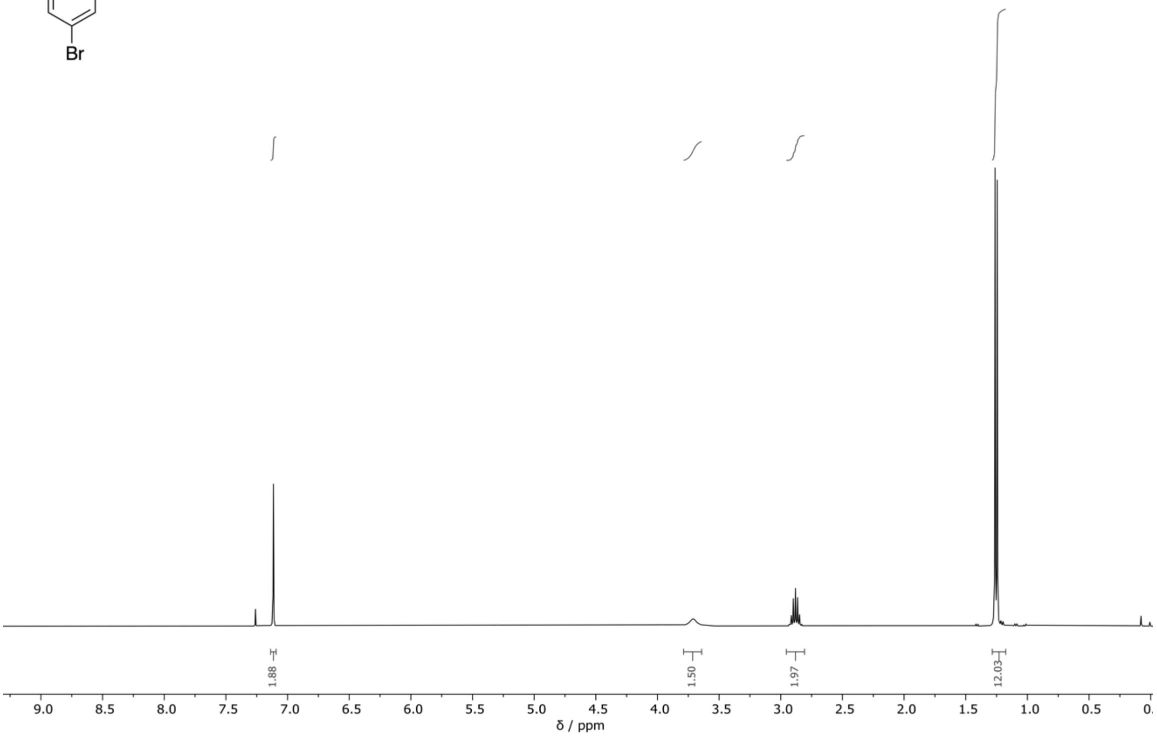
1.88
1.50
1.97
12.03
9.0 8.5 8.0 7.5 7.0 6.5 6.0 5.5 5.0 4.5 4.0 3.5 3.0 2.5 2.0 1.5 1.0 0.5 0.
δ / ppm

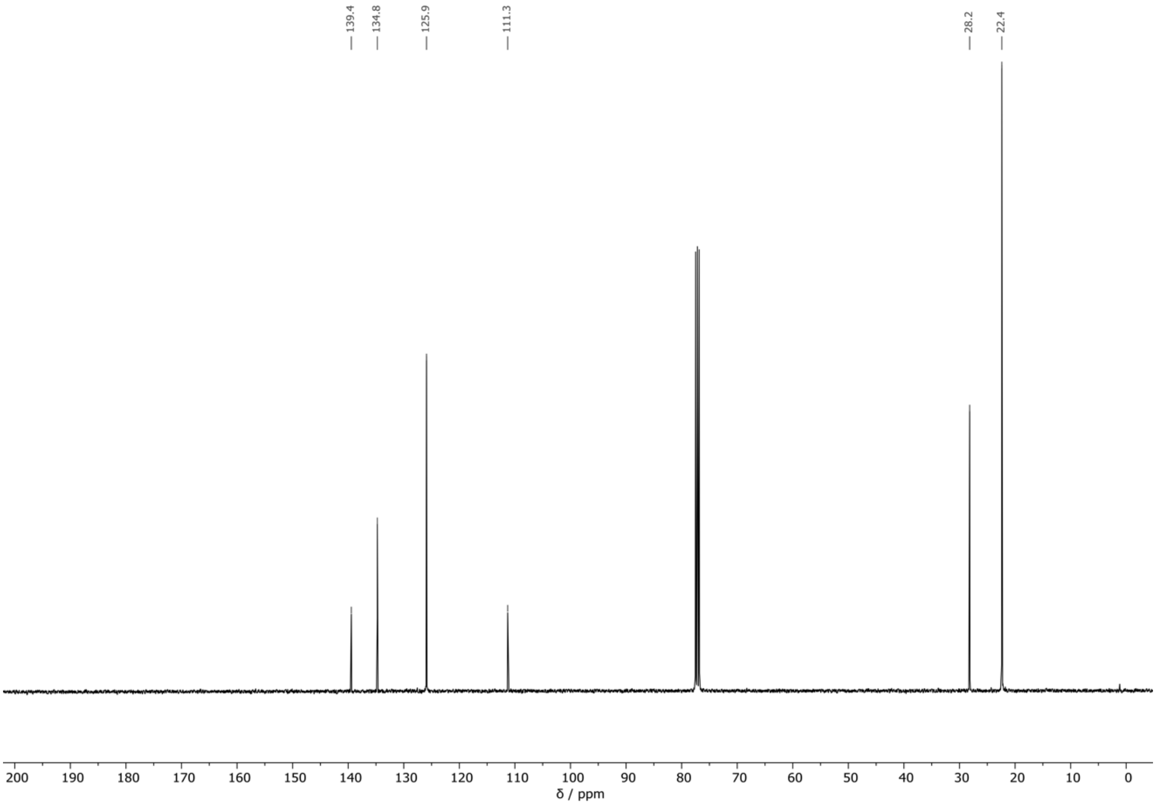
139.4
134.8
125.9
111.3
28.2
22.4
200 190 180 170 160 150 140 130 120 110 100 90 80 70 60 50 40 30 20 10 0
δ / ppm

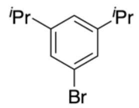

ⁱPr
ⁱPr
Br

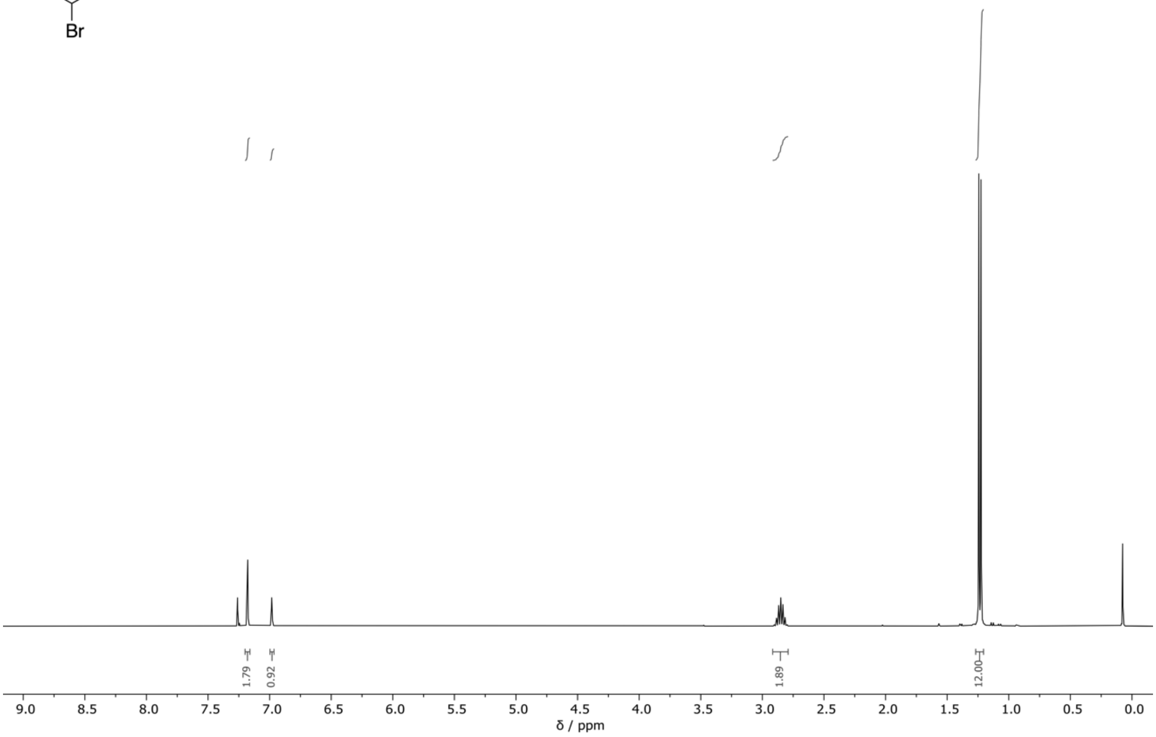

1.79
0.92
1.89
12.00
9.0
8.5
8.0
7.5
7.0
6.5
6.0
5.5
5.0
4.5
4.0
3.5
3.0
2.5
2.0
1.5
1.0
0.5
0.0
δ / ppm

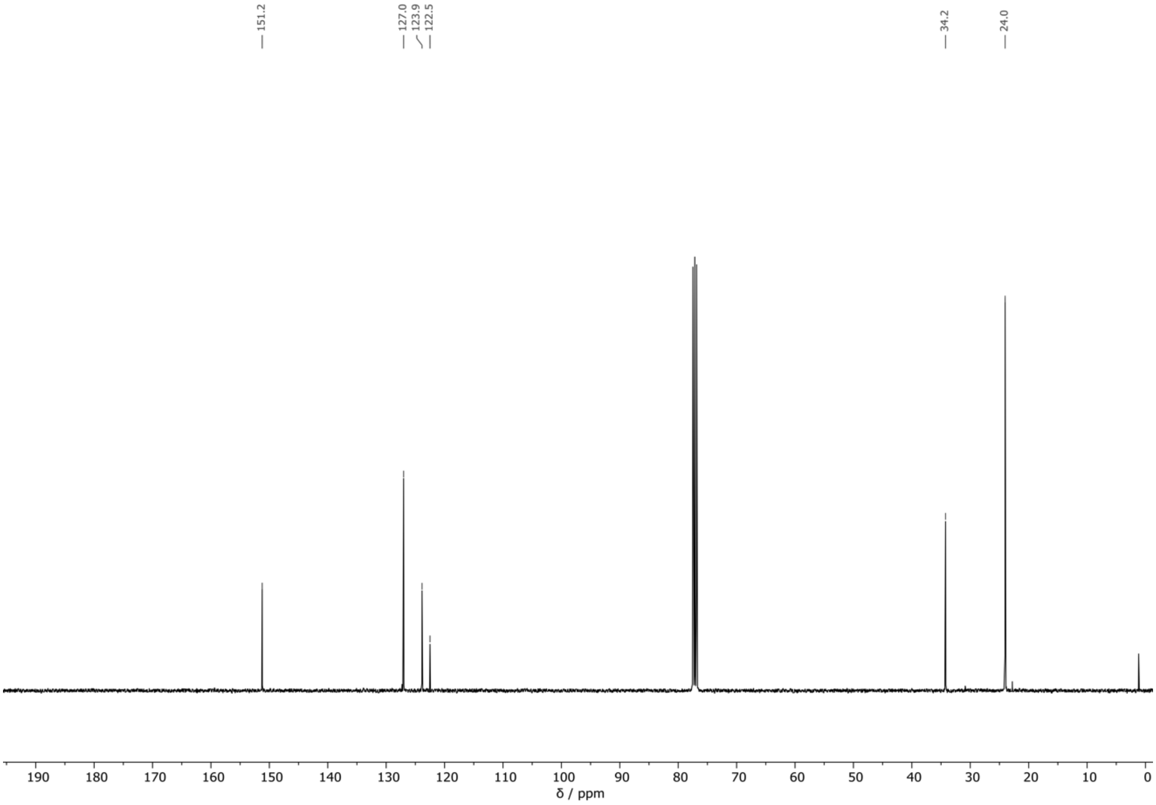

151.2
127.0
123.9
122.5
34.2
24.0
190
180
170
160
150
140
130
120
110
100
90
80
70
60
50
40
30
20
10
0
δ / ppm

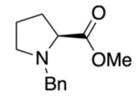
O
OMe
N
Bn

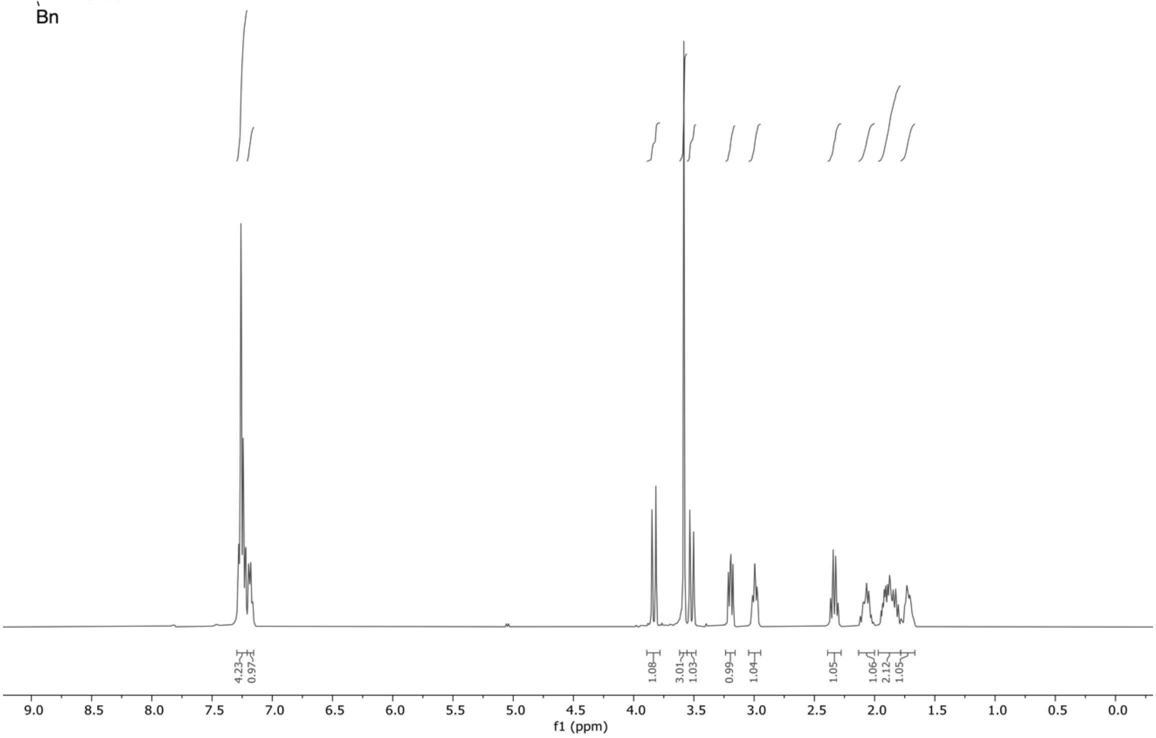
4.23
0.97
1.08
3.01
1.03
0.99
1.04
1.05
1.06
2.12
1.05
9.0
8.5
8.0
7.5
7.0
6.5
6.0
5.5
5.0
4.5
4.0
3.5
3.0
2.5
2.0
1.5
1.0
0.5
0.0
f1 (ppm)

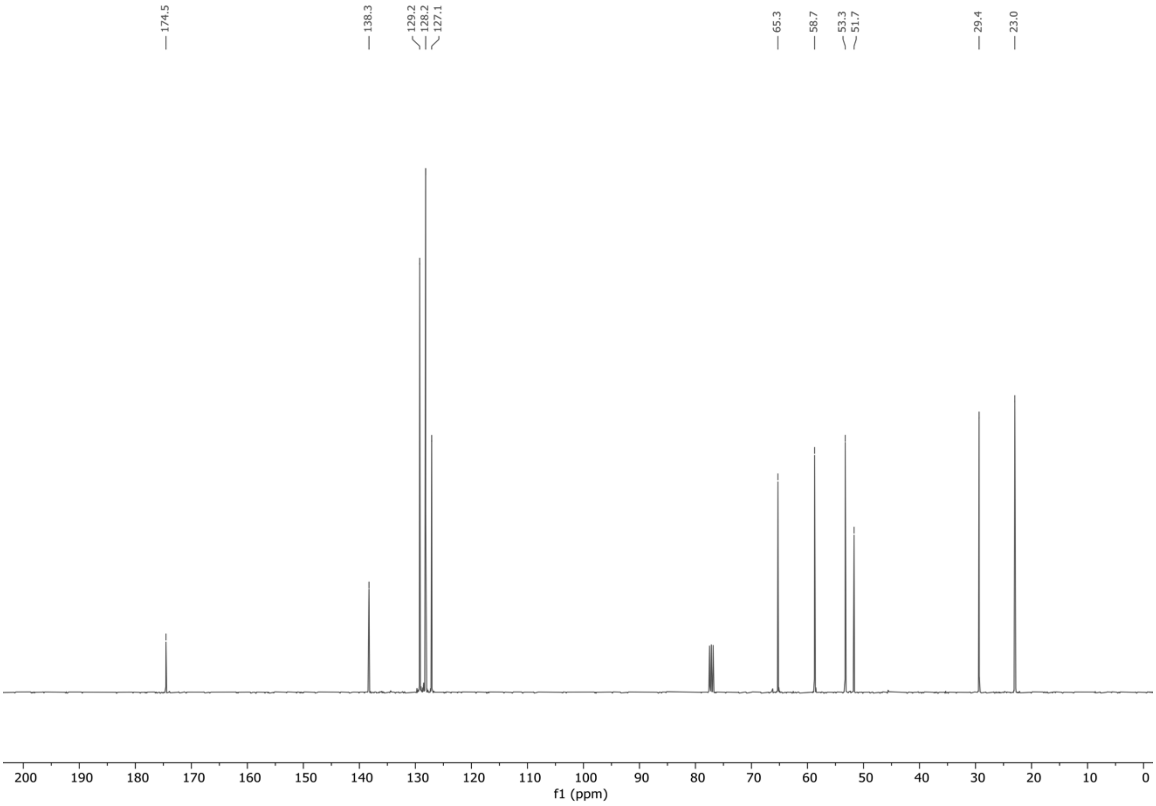
174.5
138.3
129.2
128.2
127.1
65.3
58.7
53.3
51.7
29.4
23.0
200
190
180
170
160
150
140
130
120
110
100
90
80
70
60
50
40
30
20
10
0
f1 (ppm)

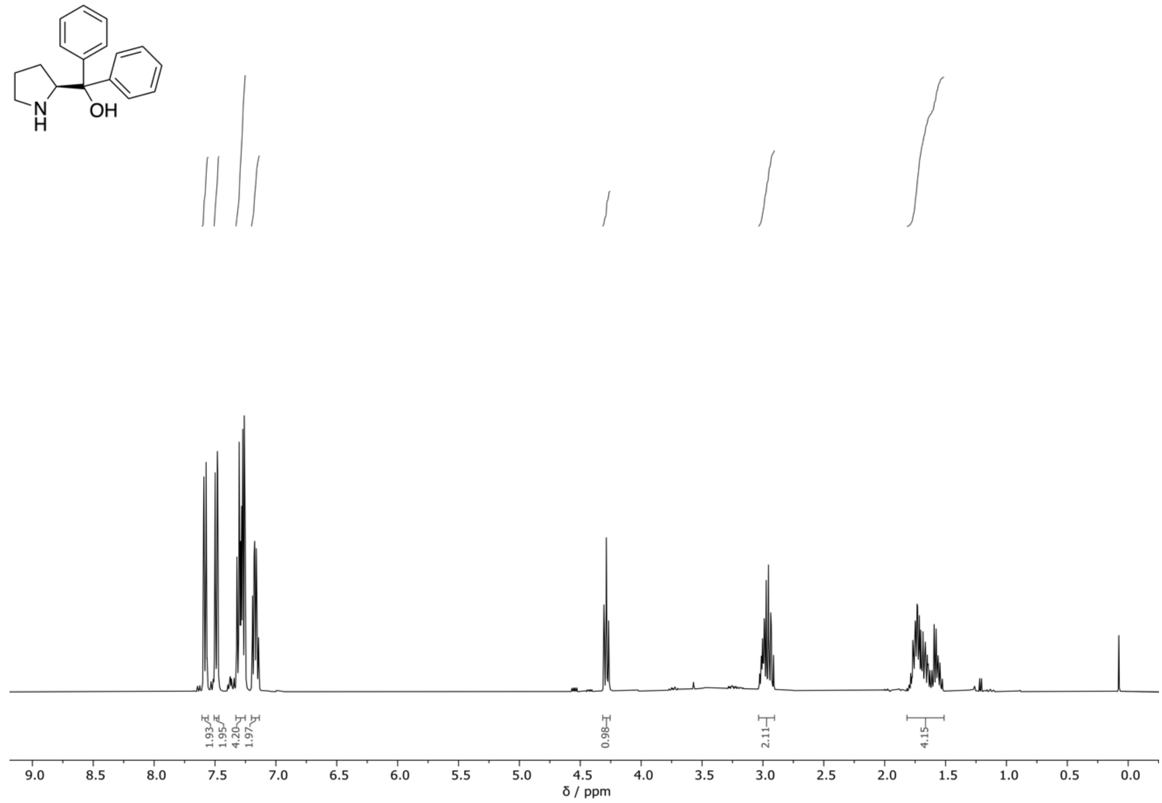
N
H
OH
1.93
1.95
4.20
1.97
0.98
2.11
4.15
9.0
8.5
8.0
7.5
7.0
6.5
6.0
5.5
5.0
4.5
4.0
3.5
3.0
2.5
2.0
1.5
1.0
0.5
0.0
δ / ppm

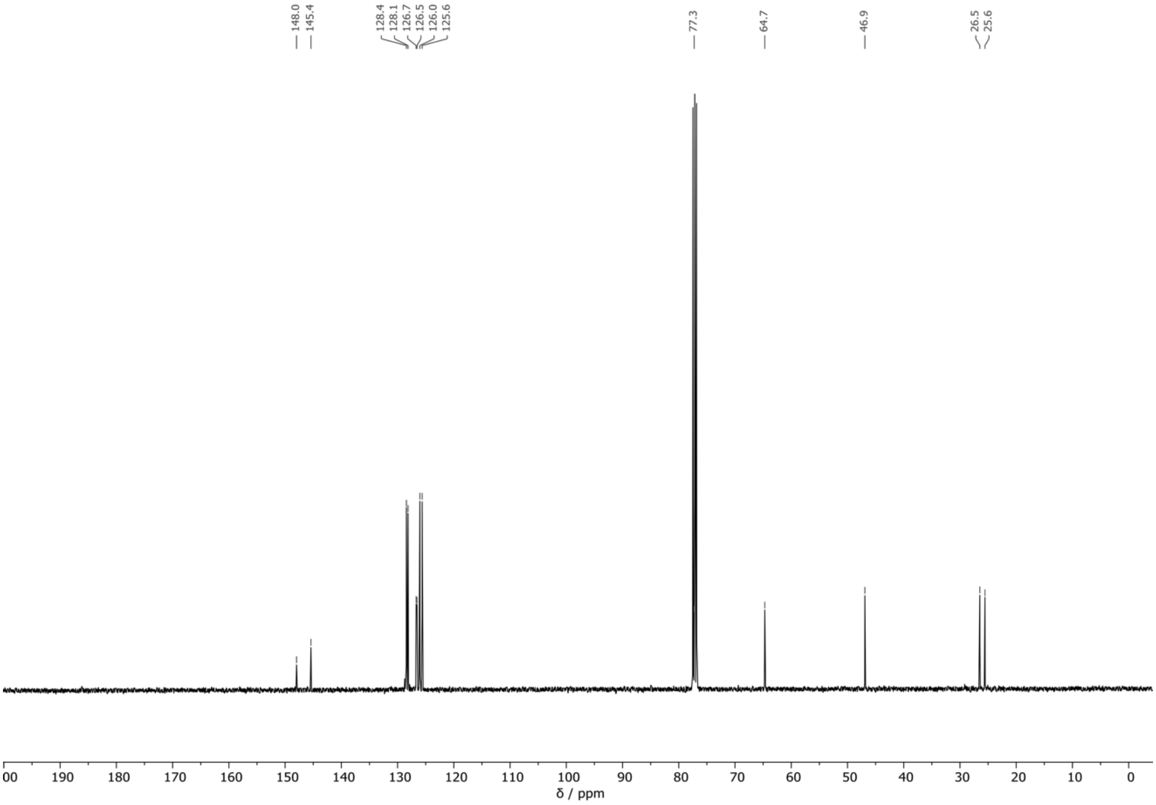
148.0
145.4
128.4
128.1
126.7
126.5
126.0
125.6
77.3
64.7
46.9
26.5
25.6
00
190
180
170
160
150
140
130
120
110
100
90
80
70
60
50
40
30
20
10
0
δ / ppm

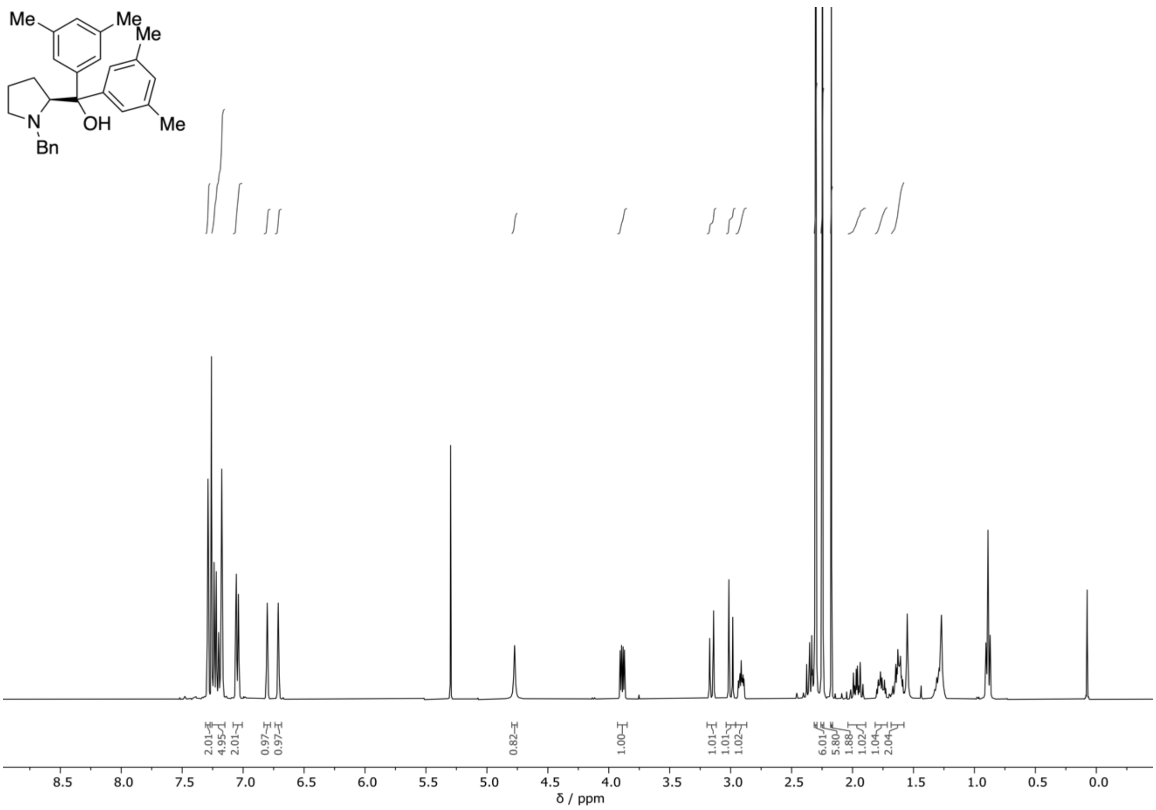
Me
Me
Me
Me
N
Bn
OH
2.01
4.95
2.01
0.97
0.97
0.82
1.00
1.01
1.01
1.02
6.01
5.80
1.88
1.02
1.04
2.04
8.5
8.0
7.5
7.0
6.5
6.0
5.5
5.0
4.5
4.0
3.5
3.0
2.5
2.0
1.5
1.0
0.5
0.0
δ / ppm

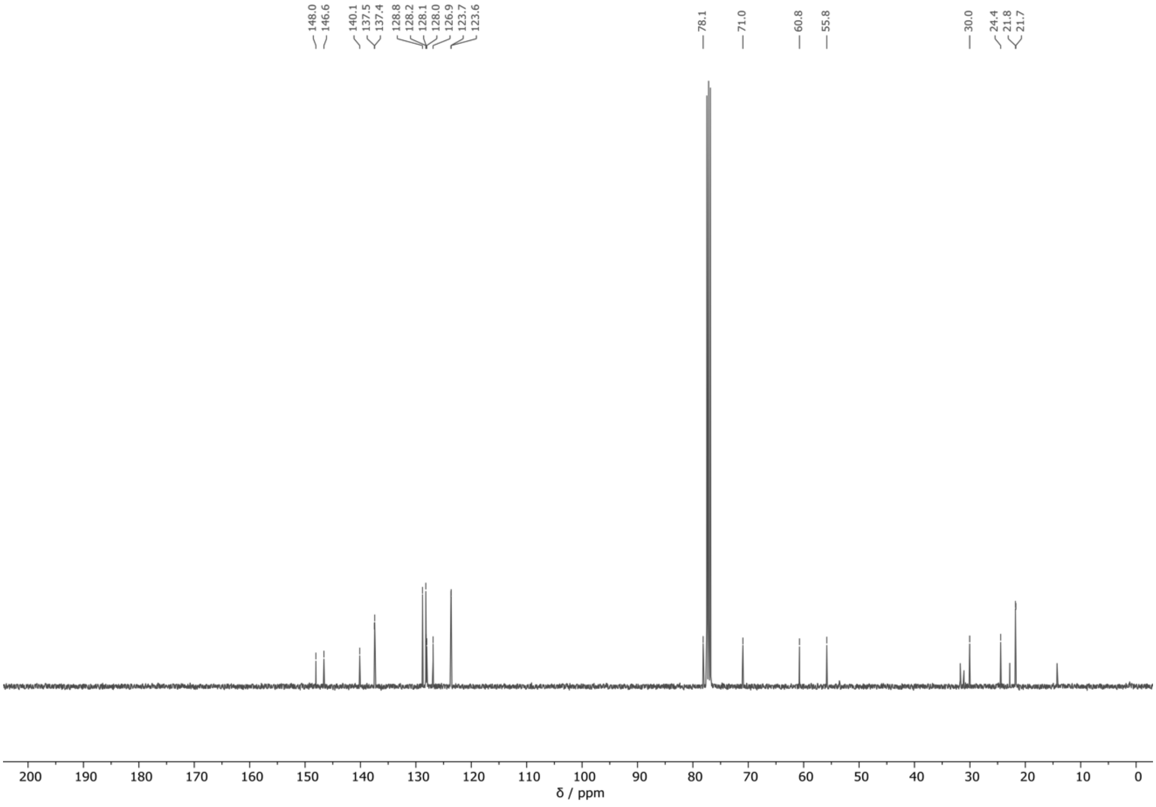
148.0
146.6
140.1
137.5
137.4
128.8
128.2
128.1
128.0
126.9
123.7
123.6
78.1
71.0
60.8
55.8
30.0
24.4
21.8
21.7
200
190
180
170
160
150
140
130
120
110
100
90
80
70
60
50
40
30
20
10
0
δ / ppm

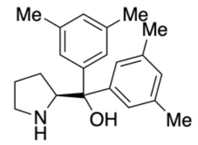
Me
Me
Me
Me
N
H
OH

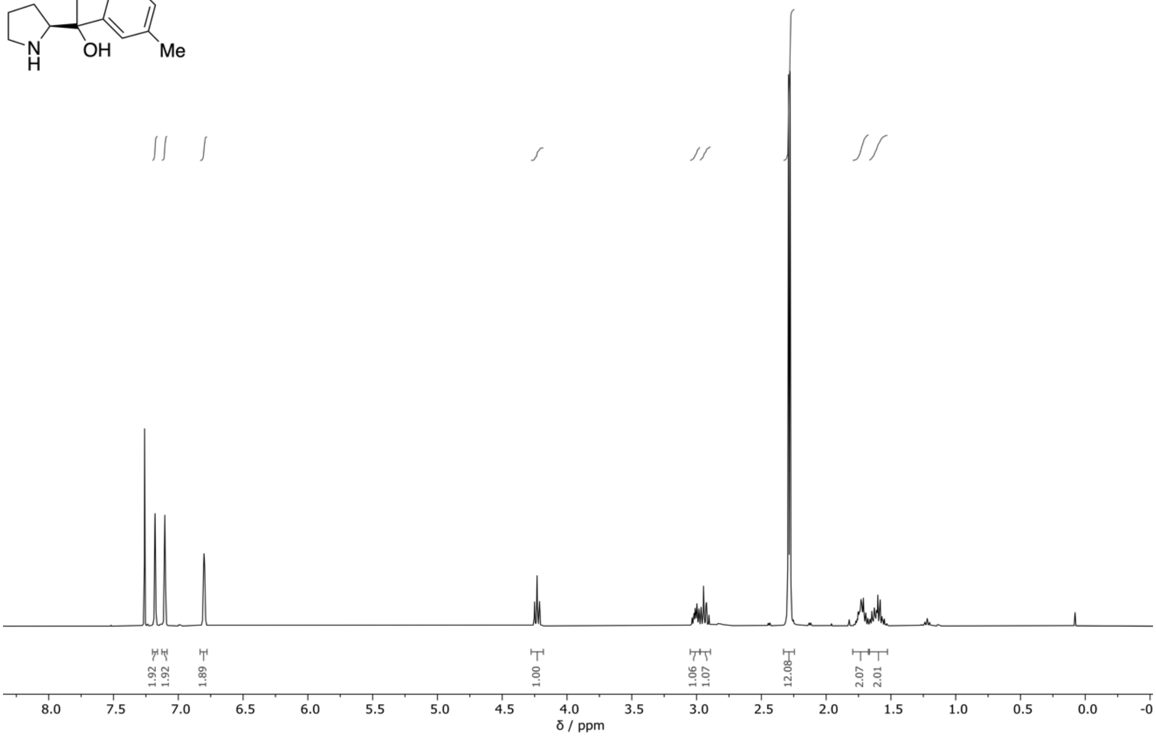
1.92
1.92
1.89
1.00
1.06
1.07
12.08
2.07
2.01
8.0
7.5
7.0
6.5
6.0
5.5
5.0
4.5
4.0
3.5
3.0
2.5
2.0
1.5
1.0
0.5
0.0
-0
δ / ppm

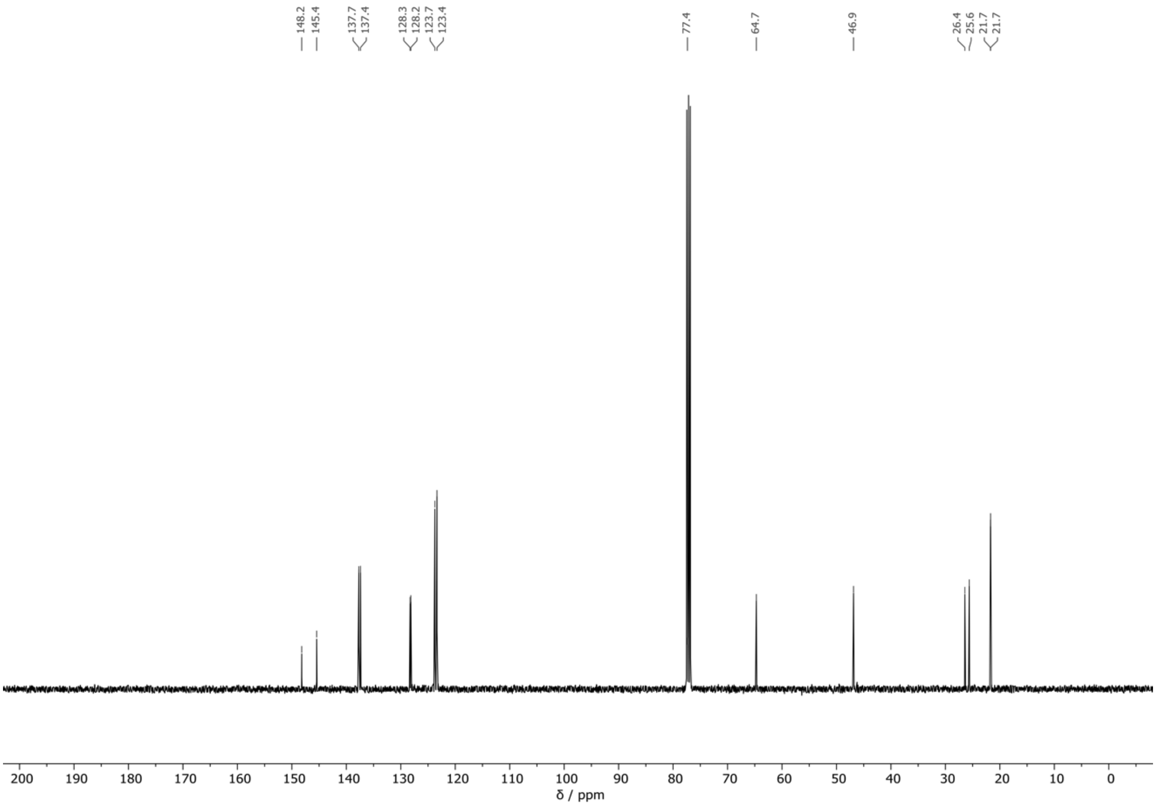
148.2
145.4
137.7
137.4
128.3
128.2
123.7
123.4
77.4
64.7
46.9
26.4
25.6
21.7
21.7
200
190
180
170
160
150
140
130
120
110
100
90
80
70
60
50
40
30
20
10
0
δ / ppm

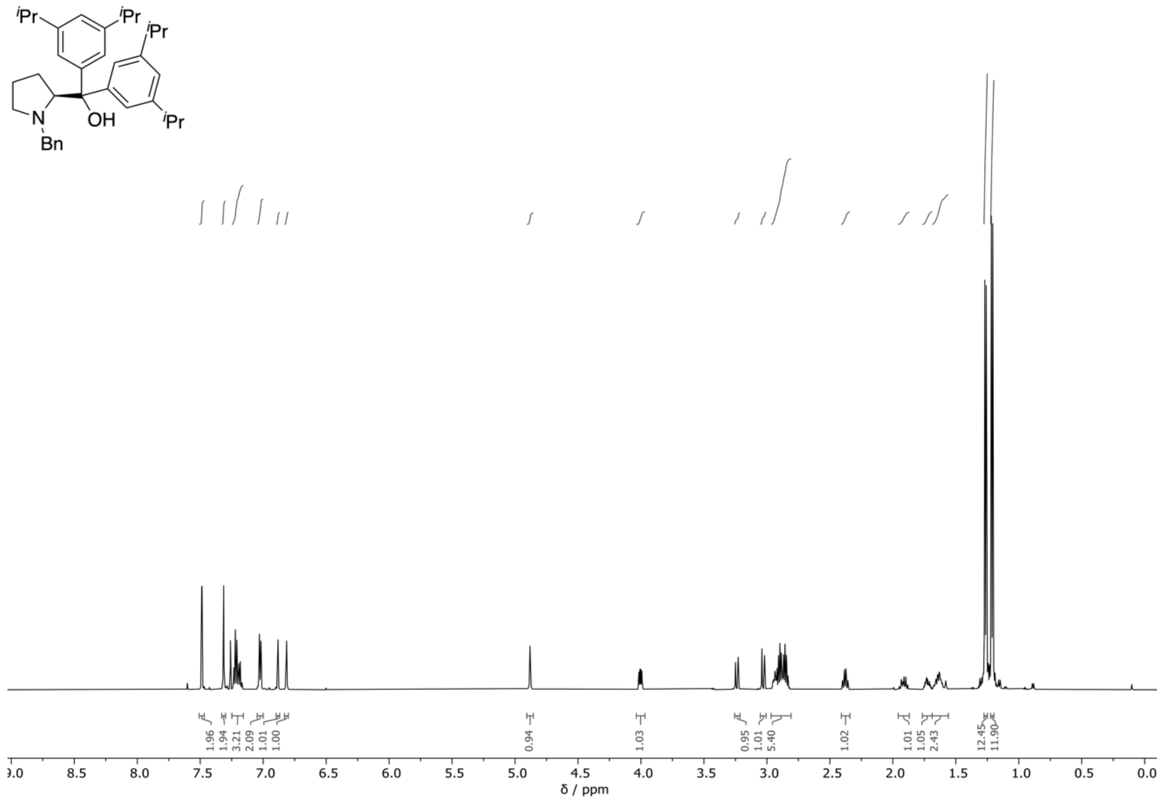

^{i}Pr
^{i}Pr
^{i}Pr
^{i}Pr
N
Bn
OH
1.96
1.94
3.21
2.09
1.01
1.00
0.94
1.03
0.95
1.01
5.40
1.02
1.01
1.05
2.43
12.45
11.90
9.0
8.5
8.0
7.5
7.0
6.5
6.0
5.5
5.0
4.5
4.0
3.5
3.0
2.5
2.0
1.5
1.0
0.5
0.0
δ / ppm

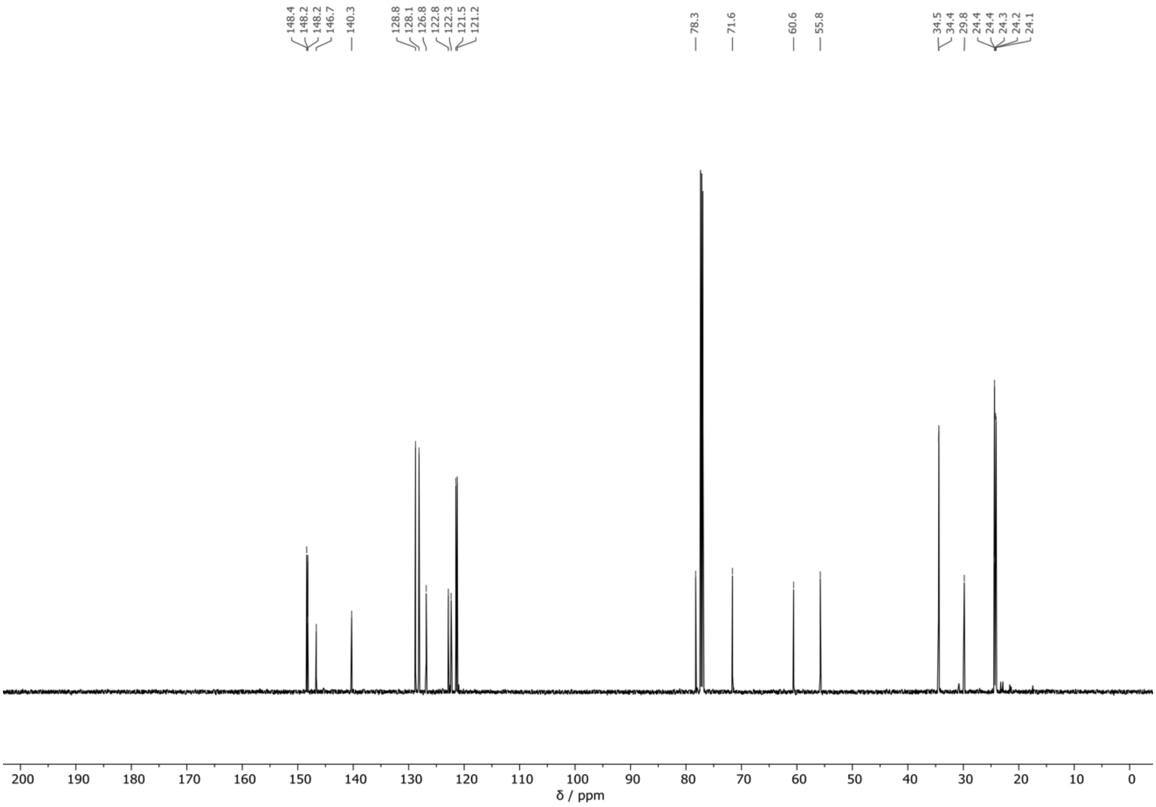

148.4
148.2
148.2
146.7
140.3
128.8
128.1
126.8
122.8
122.3
121.5
121.2
78.3
71.6
60.6
55.8
34.5
34.4
29.8
24.4
24.4
24.3
24.2
24.1
200
190
180
170
160
150
140
130
120
110
100
90
80
70
60
50
40
30
20
10
0
δ / ppm

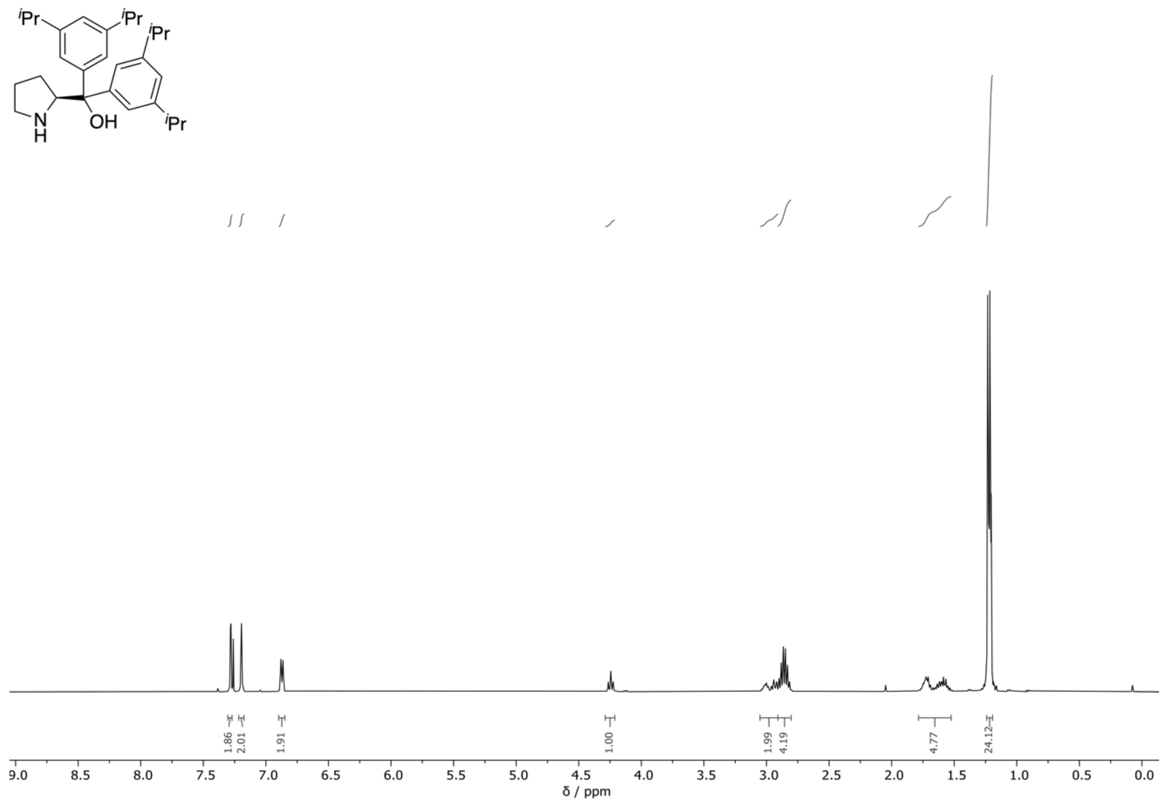

^{i}Pr
^{i}Pr
^{i}Pr
^{i}Pr
N
H
OH
1.86
2.01
1.91
1.00
1.99
4.19
4.77
24.12
9.0
8.5
8.0
7.5
7.0
6.5
6.0
5.5
5.0
4.5
4.0
3.5
3.0
2.5
2.0
1.5
1.0
0.5
0.0
δ / ppm

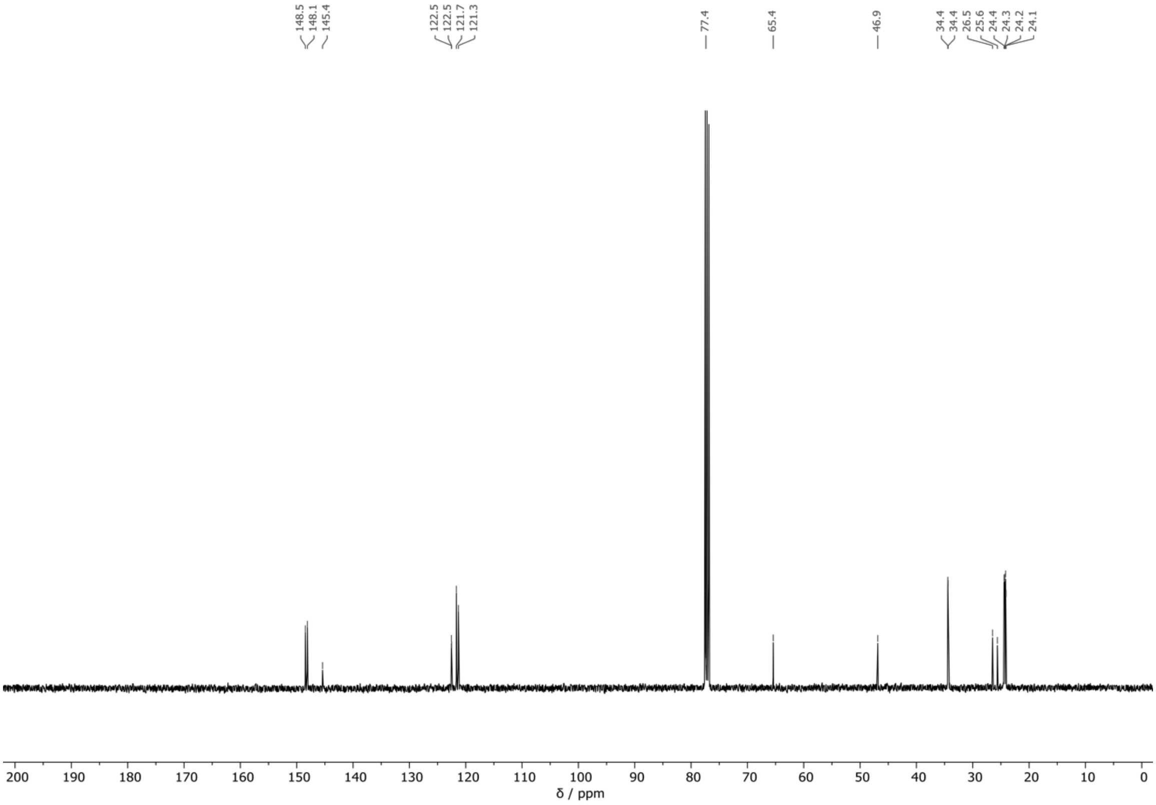

148.5
148.1
145.4
122.5
122.5
121.7
121.3
77.4
65.4
46.9
34.4
34.4
26.5
25.6
24.4
24.3
24.2
24.1
200
190
180
170
160
150
140
130
120
110
100
90
80
70
60
50
40
30
20
10
0
δ / ppm

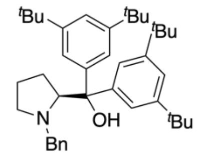

^{t}Bu
^{t}Bu
^{t}Bu
^{t}Bu
N
OH
Bn

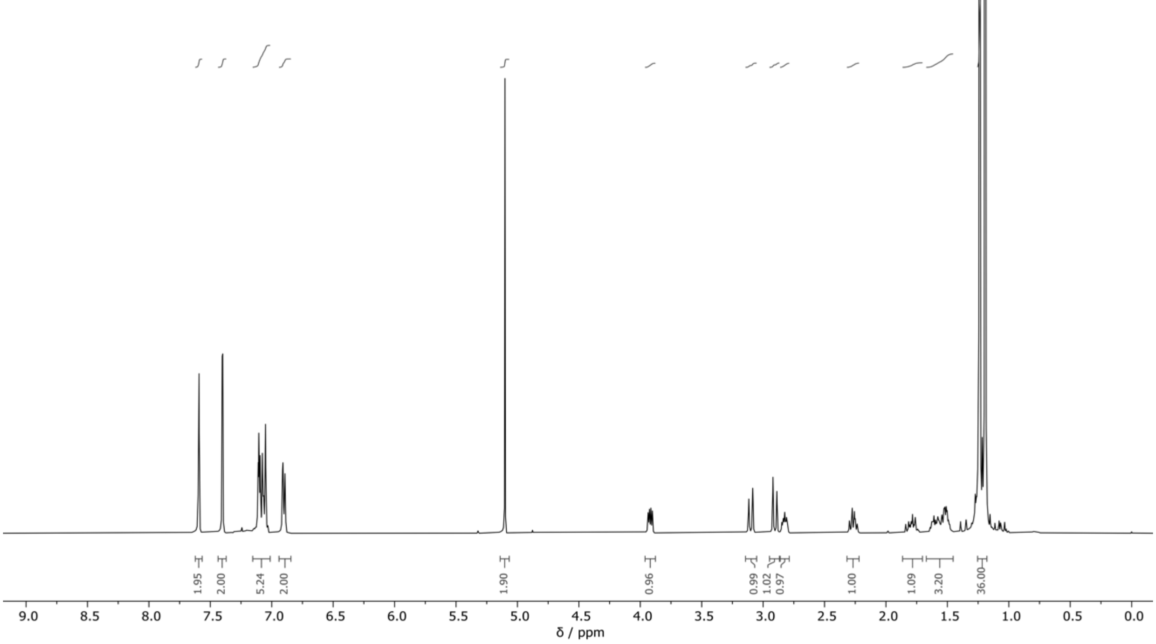

1.95
2.00
5.24
2.00
1.90
0.96
0.99
1.02
0.97
1.00
1.09
3.20
36.00
9.0
8.5
8.0
7.5
7.0
6.5
6.0
5.5
5.0
4.5
4.0
3.5
3.0
2.5
2.0
1.5
1.0
0.5
0.0
δ / ppm

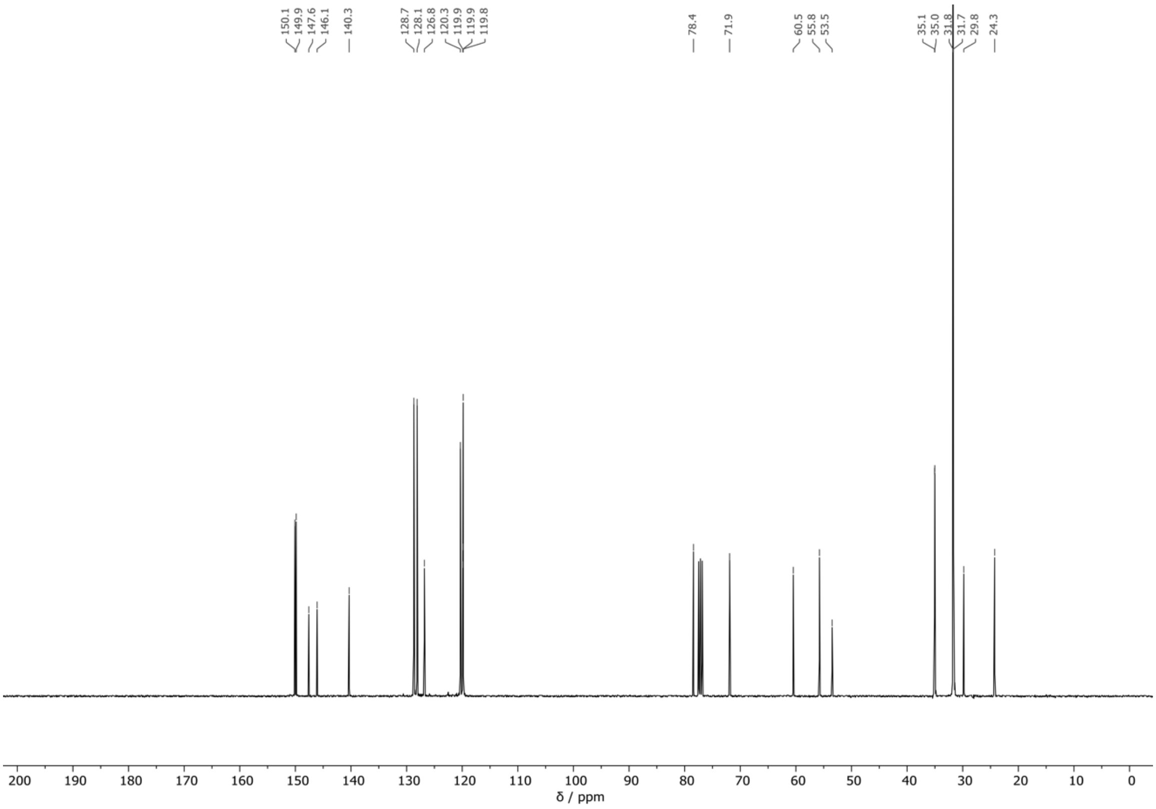

150.1
149.9
147.6
146.1
140.3
128.7
128.1
126.8
120.3
119.9
119.9
119.8
78.4
71.9
60.5
55.8
53.5
35.1
35.0
31.8
31.7
29.8
24.3
200
190
180
170
160
150
140
130
120
110
100
90
80
70
60
50
40
30
20
10
0
δ / ppm

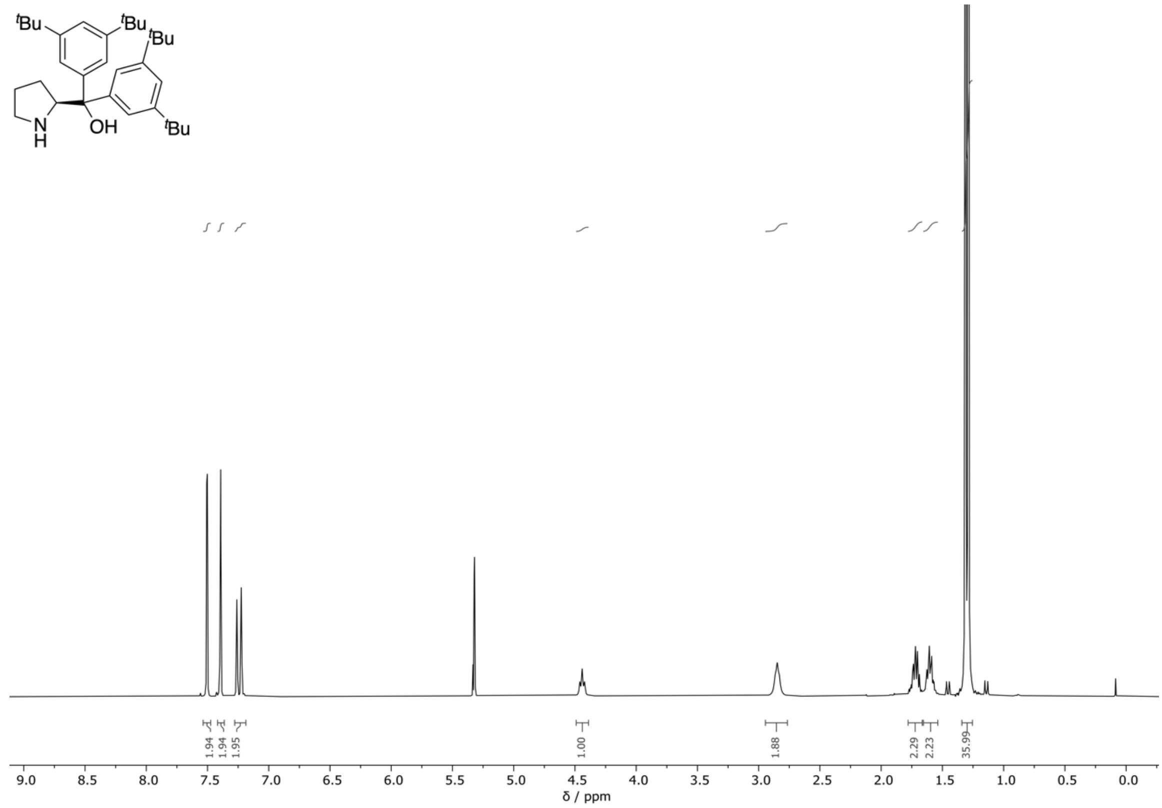

^{t}Bu
^{t}Bu
^{t}Bu
^{t}Bu
N
H
OH
1.94
1.94
1.95
1.00
1.88
2.29
2.23
35.99
9.0
8.5
8.0
7.5
7.0
6.5
6.0
5.5
5.0
4.5
4.0
3.5
3.0
2.5
2.0
1.5
1.0
0.5
0.0
δ / ppm

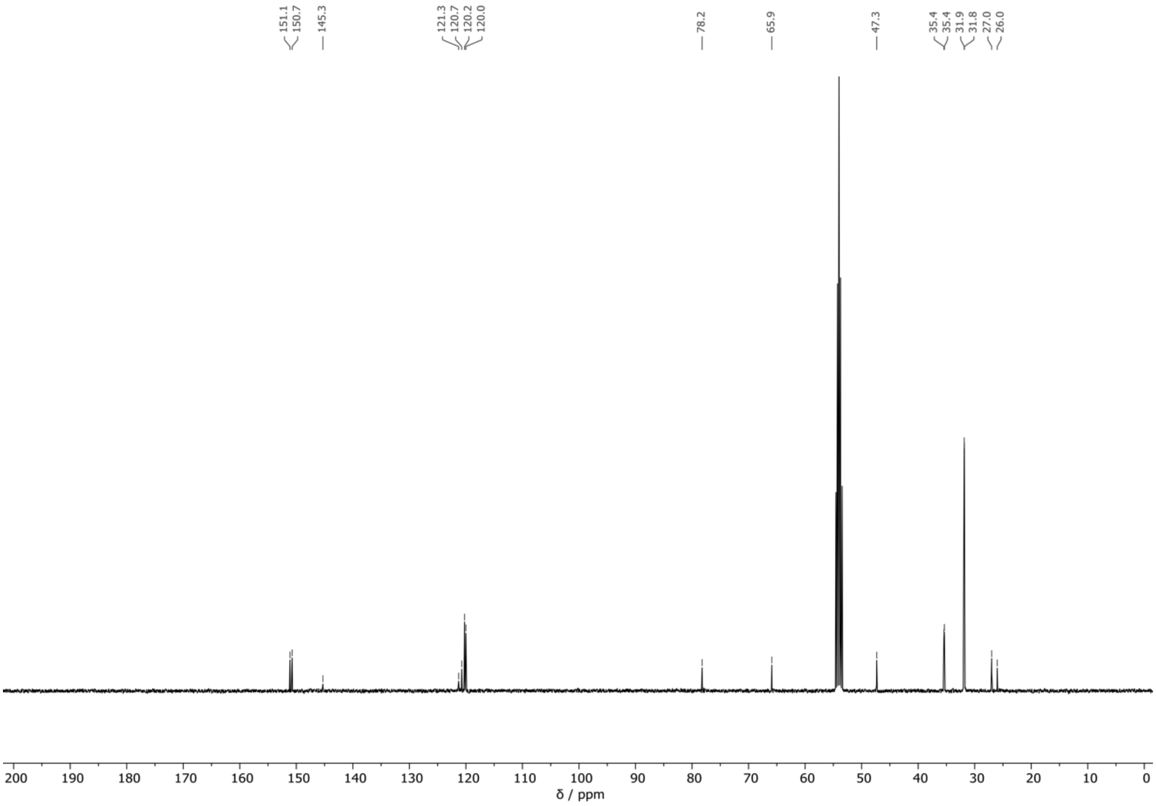

151.1
150.7
145.3
121.3
120.7
120.2
120.0
78.2
65.9
47.3
35.4
35.4
31.9
31.8
27.0
26.0
200
190
180
170
160
150
140
130
120
110
100
90
80
70
60
50
40
30
20
10
0
δ / ppm

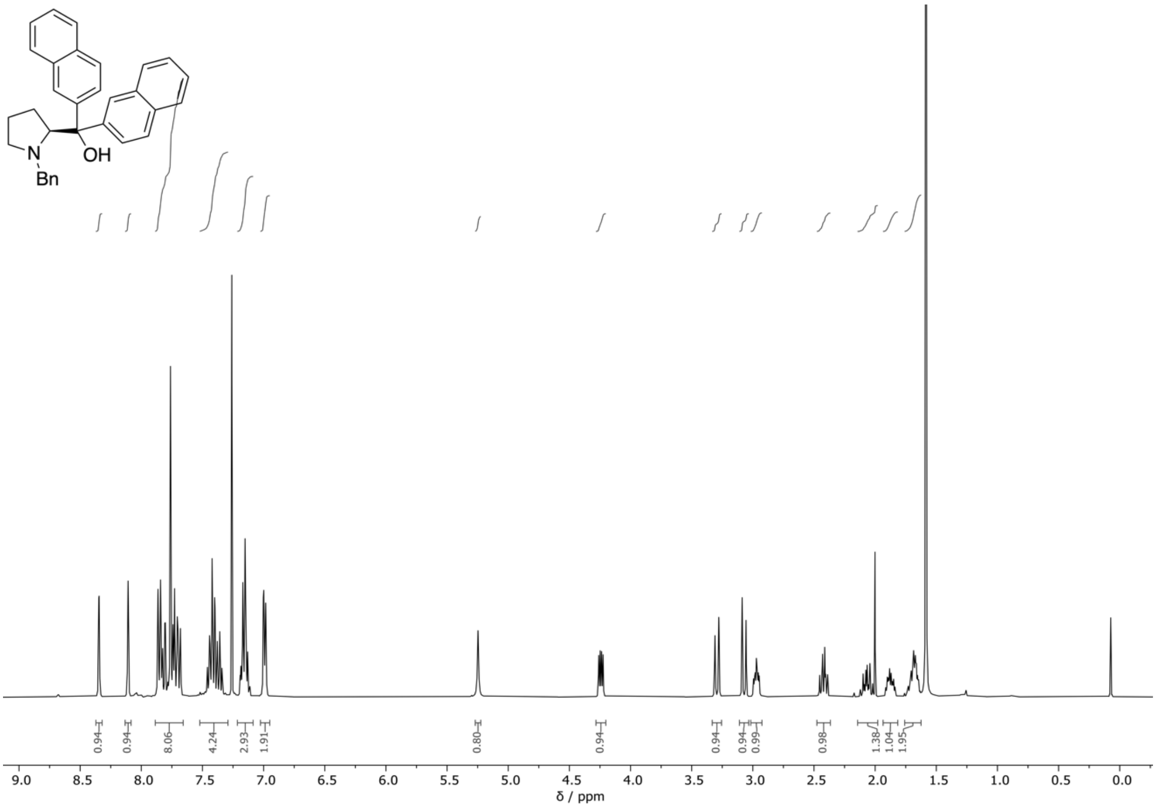
N
OH
Bn
0.94
0.94
8.06
4.24
2.93
1.91
0.80
0.94
0.94
0.94
0.99
0.98
1.38
1.04
1.95
9.0 8.5 8.0 7.5 7.0 6.5 6.0 5.5 5.0 4.5 4.0 3.5 3.0 2.5 2.0 1.5 1.0 0.5 0.0
δ / ppm

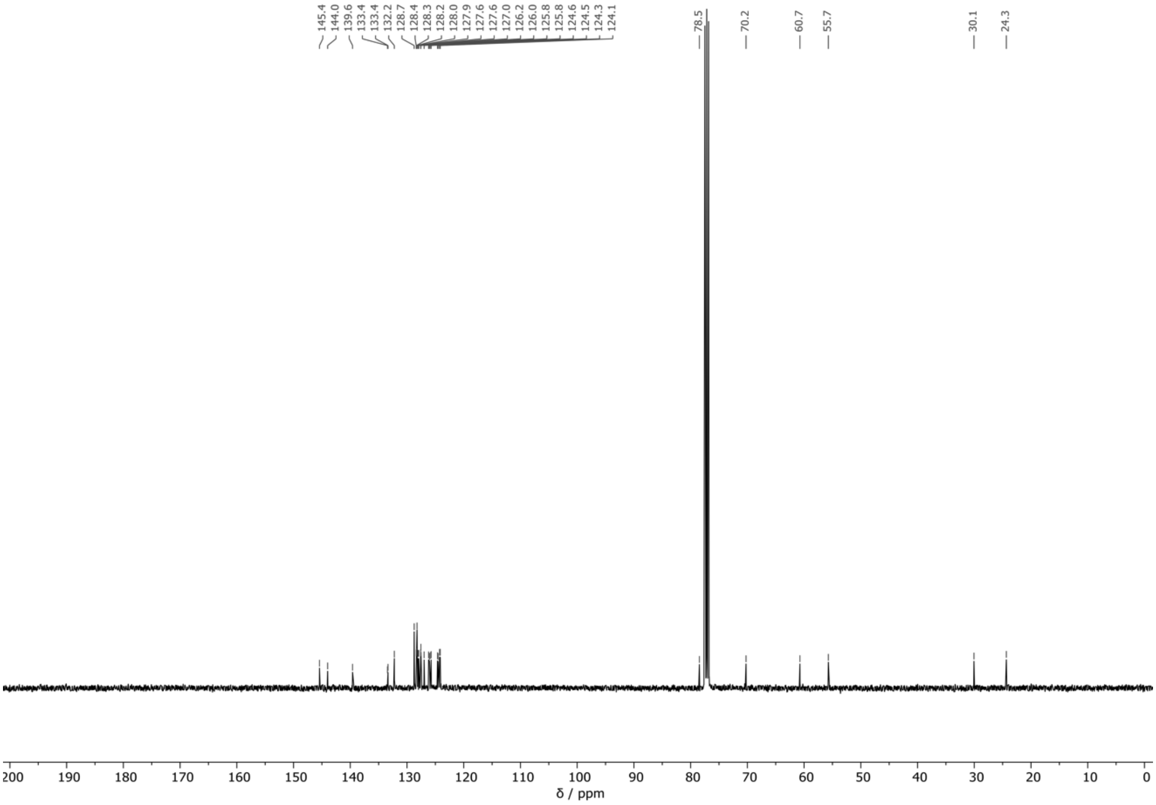
145.4
144.0
139.6
133.4
133.4
132.2
128.7
128.4
128.3
128.2
128.0
127.9
127.6
127.6
127.0
126.2
126.0
125.8
124.6
124.5
124.3
124.1
78.5
70.2
60.7
55.7
30.1
24.3
200 190 180 170 160 150 140 130 120 110 100 90 80 70 60 50 40 30 20 10 0
δ / ppm

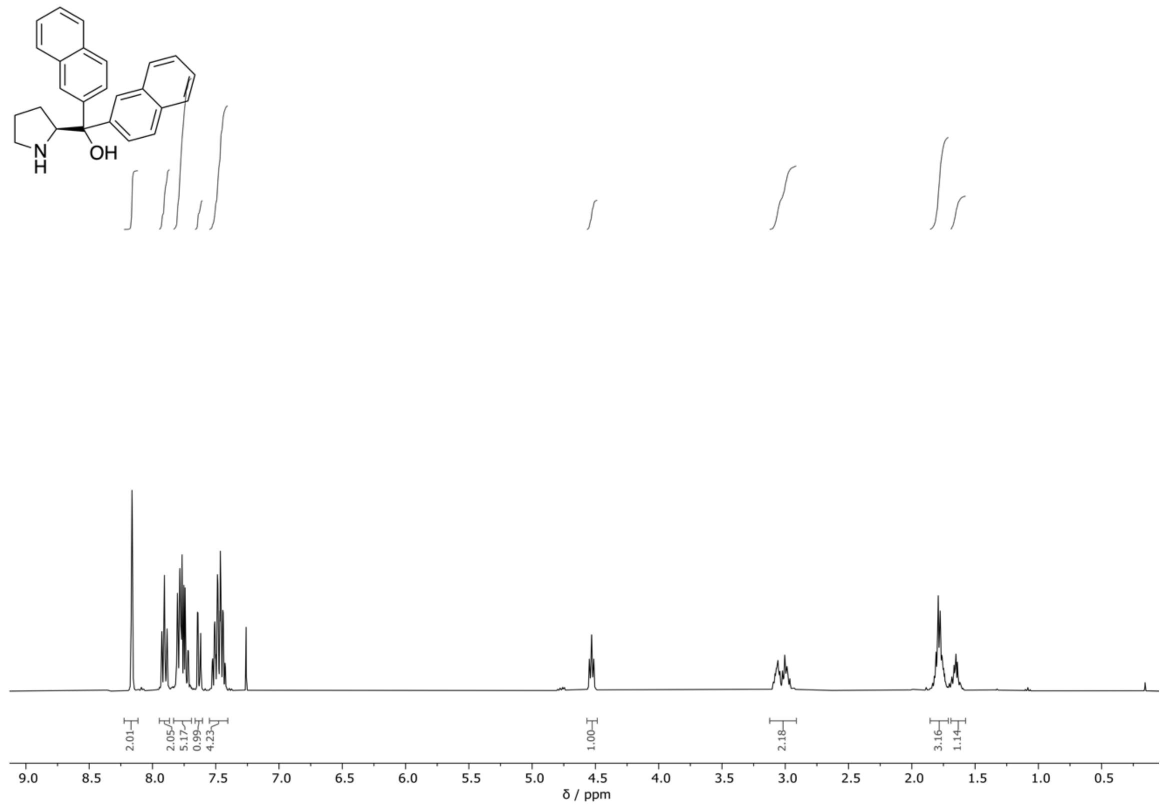
N
H
OH
2.01
2.05
5.17
0.99
4.23
1.00
2.18
3.16
1.14
9.0
8.5
8.0
7.5
7.0
6.5
6.0
5.5
5.0
4.5
4.0
3.5
3.0
2.5
2.0
1.5
1.0
0.5
δ / ppm

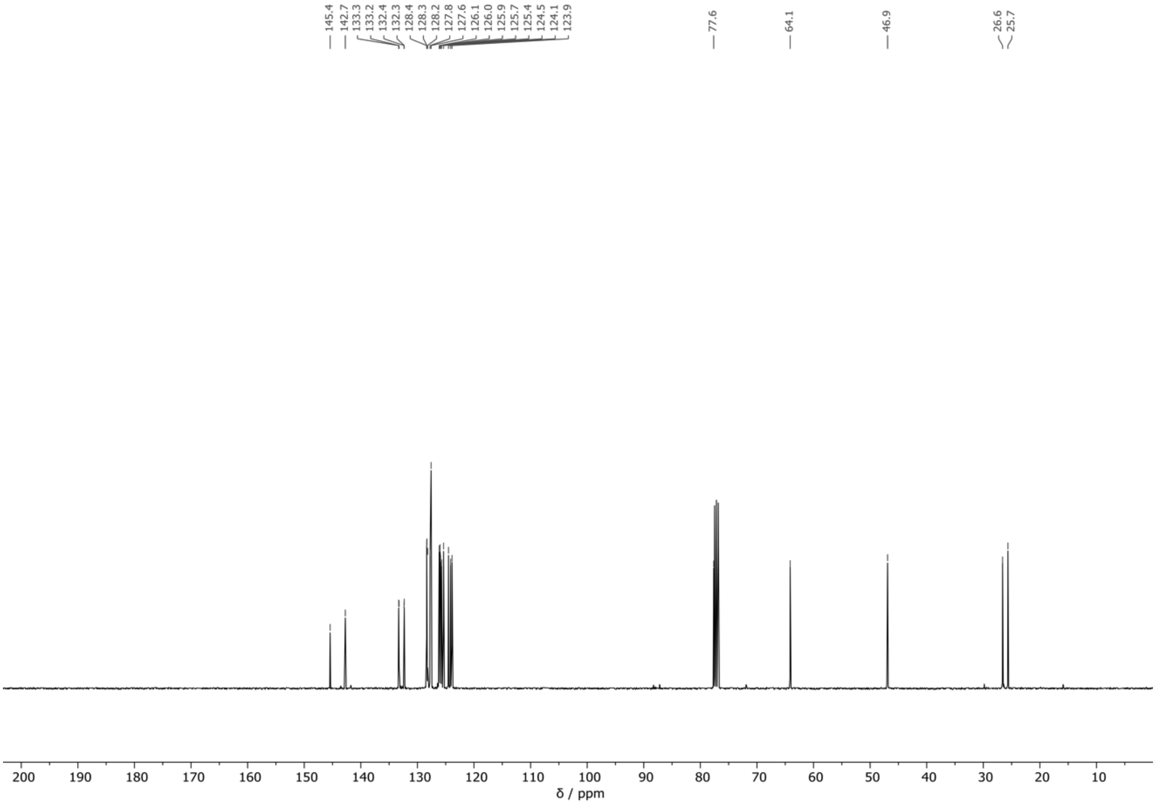
145.4
142.7
133.3
133.2
132.4
132.3
128.4
128.3
128.2
127.8
127.6
126.1
126.0
125.9
125.7
125.4
124.5
124.1
123.9
77.6
64.1
46.9
26.6
25.7
200
190
180
170
160
150
140
130
120
110
100
90
80
70
60
50
40
30
20
10
δ / ppm

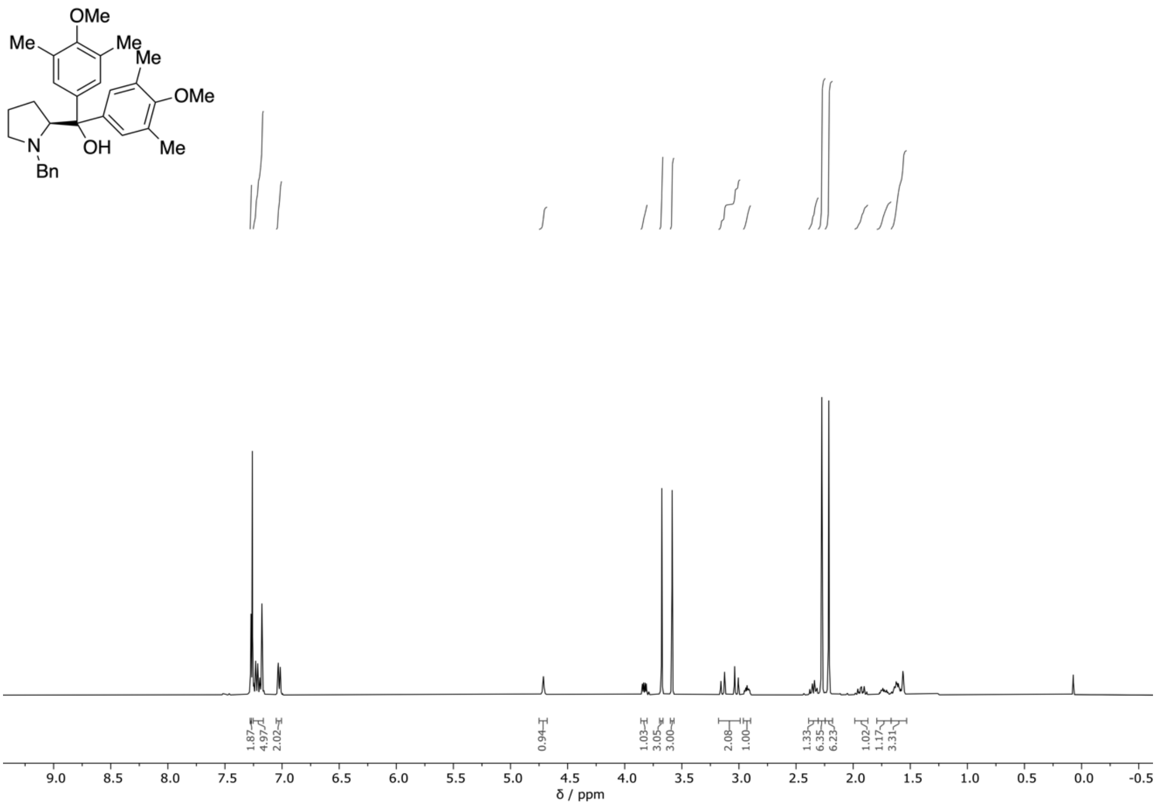
OMe
Me
Me
Me
OMe
Me
N
Bn
OH
1.87
4.97
2.02
0.94
1.03
3.05
3.00
2.08
1.00
1.33
6.35
6.23
1.02
1.17
3.31
9.0 8.5 8.0 7.5 7.0 6.5 6.0 5.5 5.0 4.5 4.0 3.5 3.0 2.5 2.0 1.5 1.0 0.5 0.0 -0.5
δ / ppm

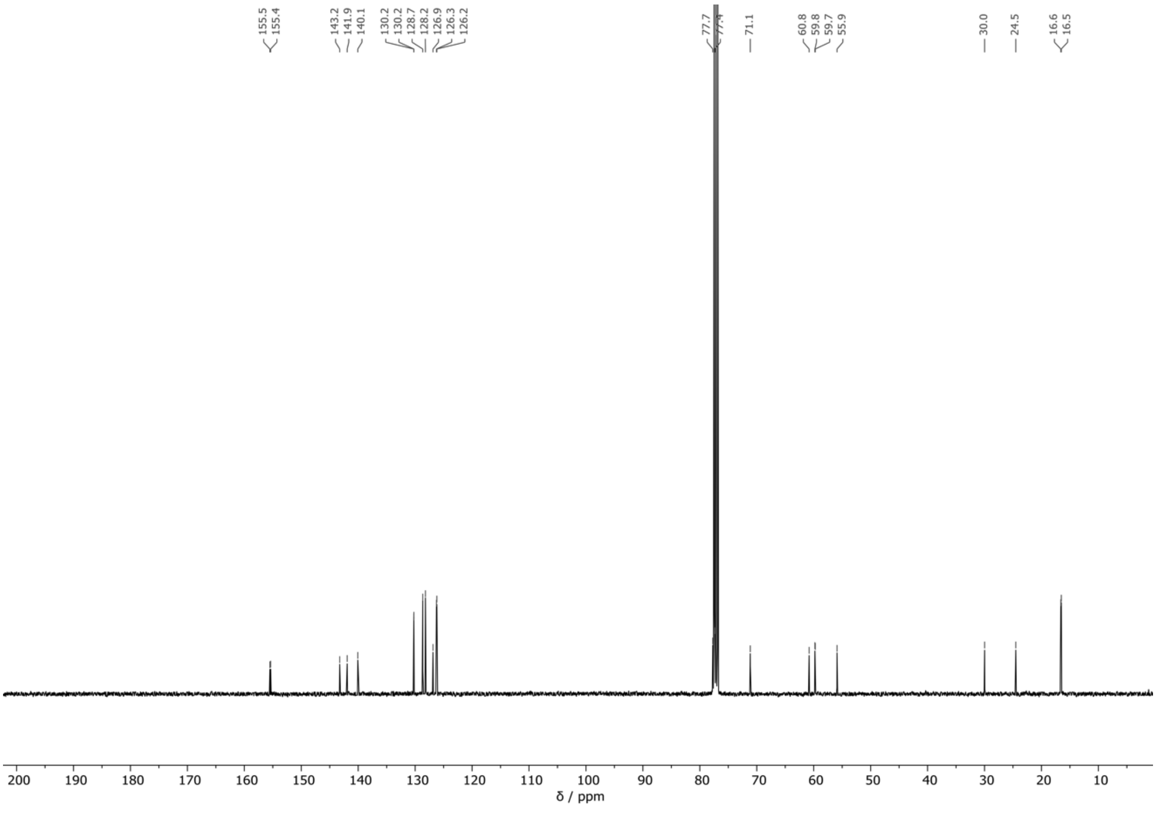
155.5
155.4
143.2
141.9
140.1
130.2
130.2
128.7
128.2
126.9
126.3
126.2
77.7
77.4
71.1
60.8
59.8
59.7
55.9
30.0
24.5
16.6
16.5
200 190 180 170 160 150 140 130 120 110 100 90 80 70 60 50 40 30 20 10
δ / ppm

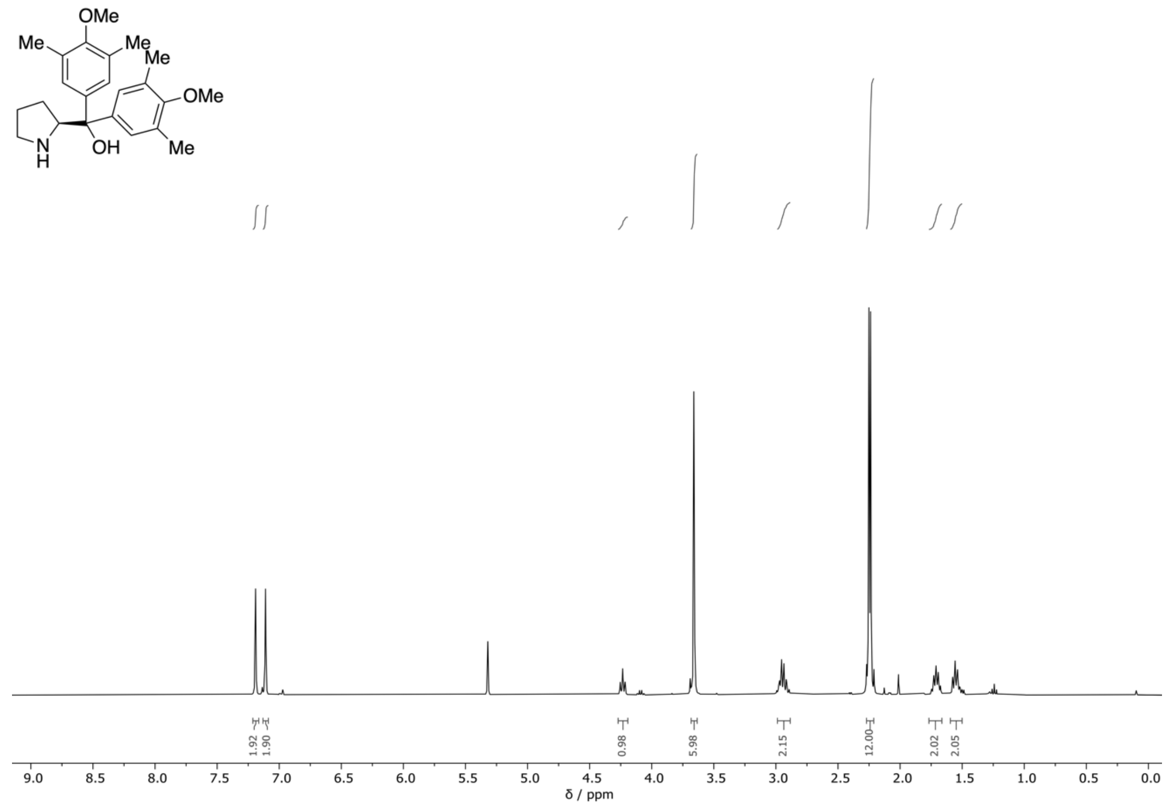
OMe
Me
Me
Me
OMe
Me
N
H
OH
1.92
1.90
0.98
5.98
2.15
12.00
2.02
2.05
9.0
8.5
8.0
7.5
7.0
6.5
6.0
5.5
5.0
4.5
4.0
3.5
3.0
2.5
2.0
1.5
1.0
0.5
0.0
δ / ppm

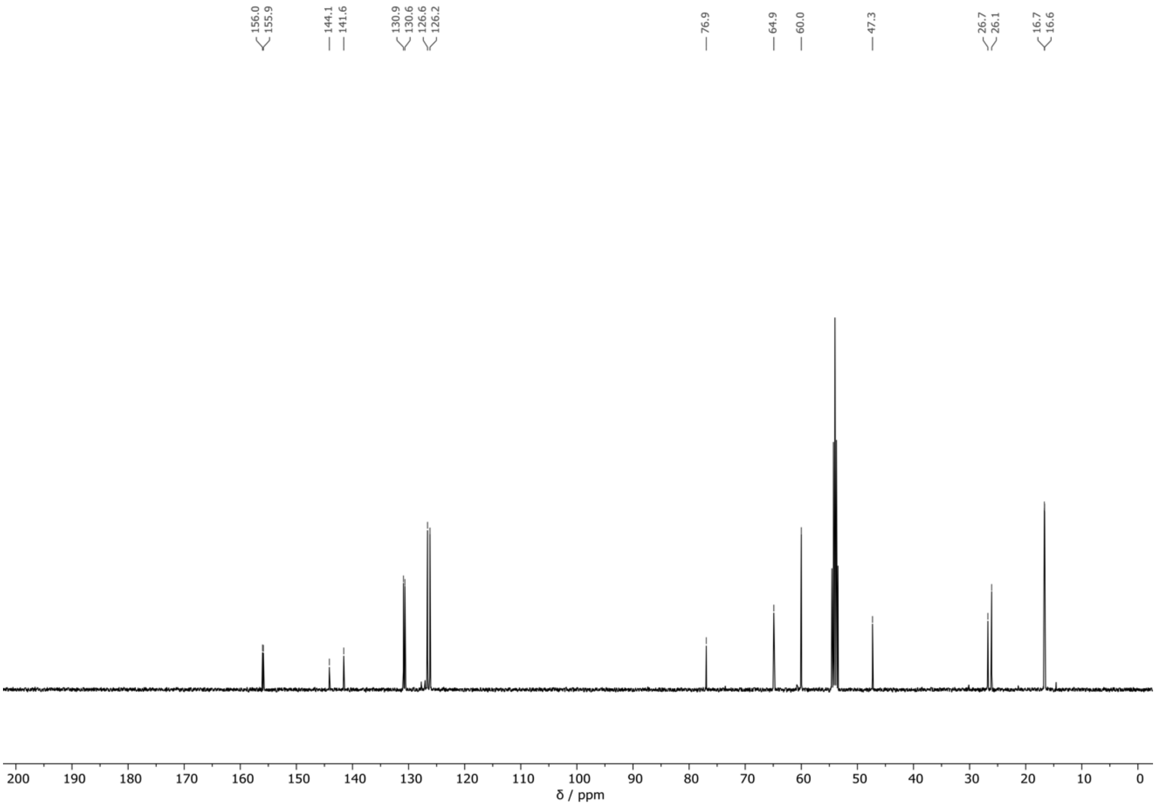
156.0
155.9
144.1
141.6
130.9
130.6
126.6
126.2
76.9
64.9
60.0
47.3
26.7
26.1
16.7
16.6
200
190
180
170
160
150
140
130
120
110
100
90
80
70
60
50
40
30
20
10
0
δ / ppm

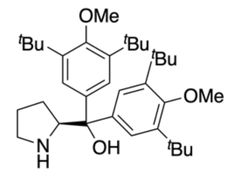
OMe
^{t}Bu
^{t}Bu
^{t}Bu
OMe
^{t}Bu
N
H
OH

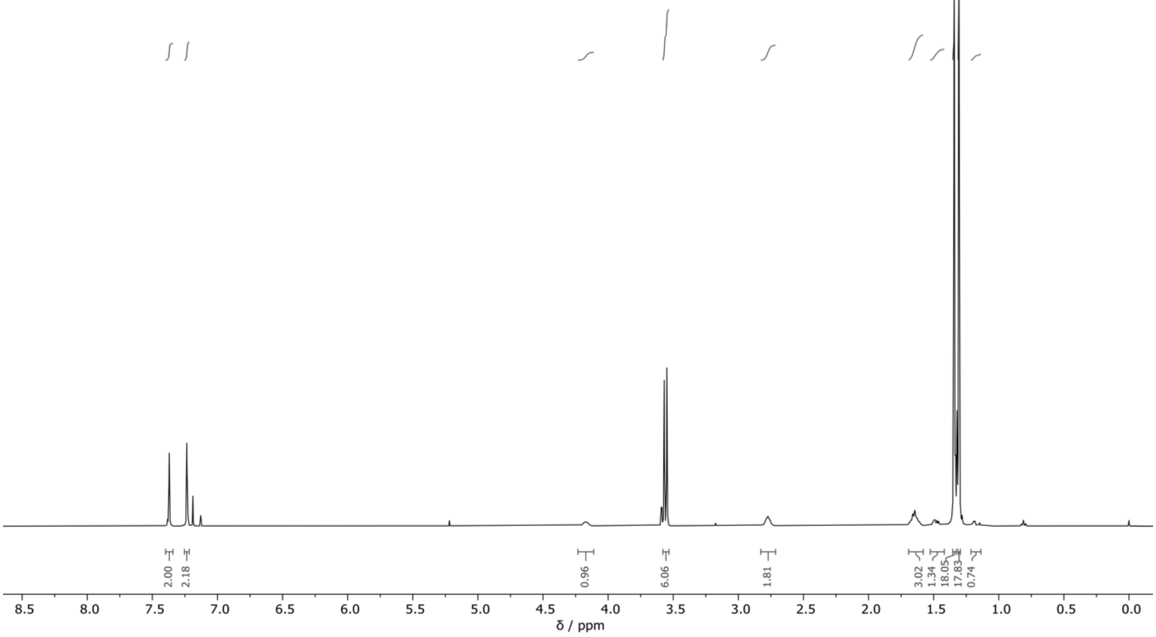
2.00
2.18
0.96
6.06
1.81
3.02
1.34
18.05
17.83
0.74
8.5
8.0
7.5
7.0
6.5
6.0
5.5
5.0
4.5
4.0
3.5
3.0
2.5
2.0
1.5
1.0
0.5
0.0
δ / ppm

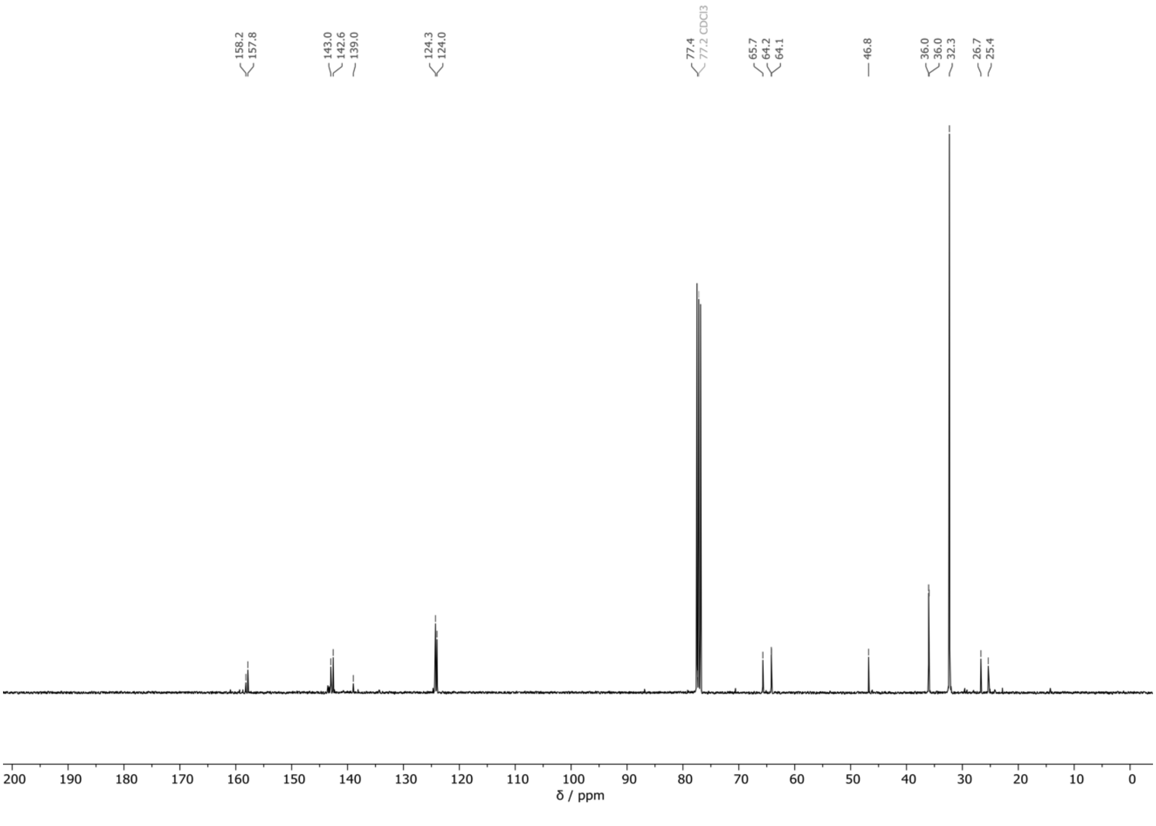
158.2
157.8
143.0
142.6
139.0
124.3
124.0
77.4
77.2 CDCl3
65.7
64.2
64.1
46.8
36.0
36.0
32.3
26.7
25.4
200
190
180
170
160
150
140
130
120
110
100
90
80
70
60
50
40
30
20
10
0
δ / ppm

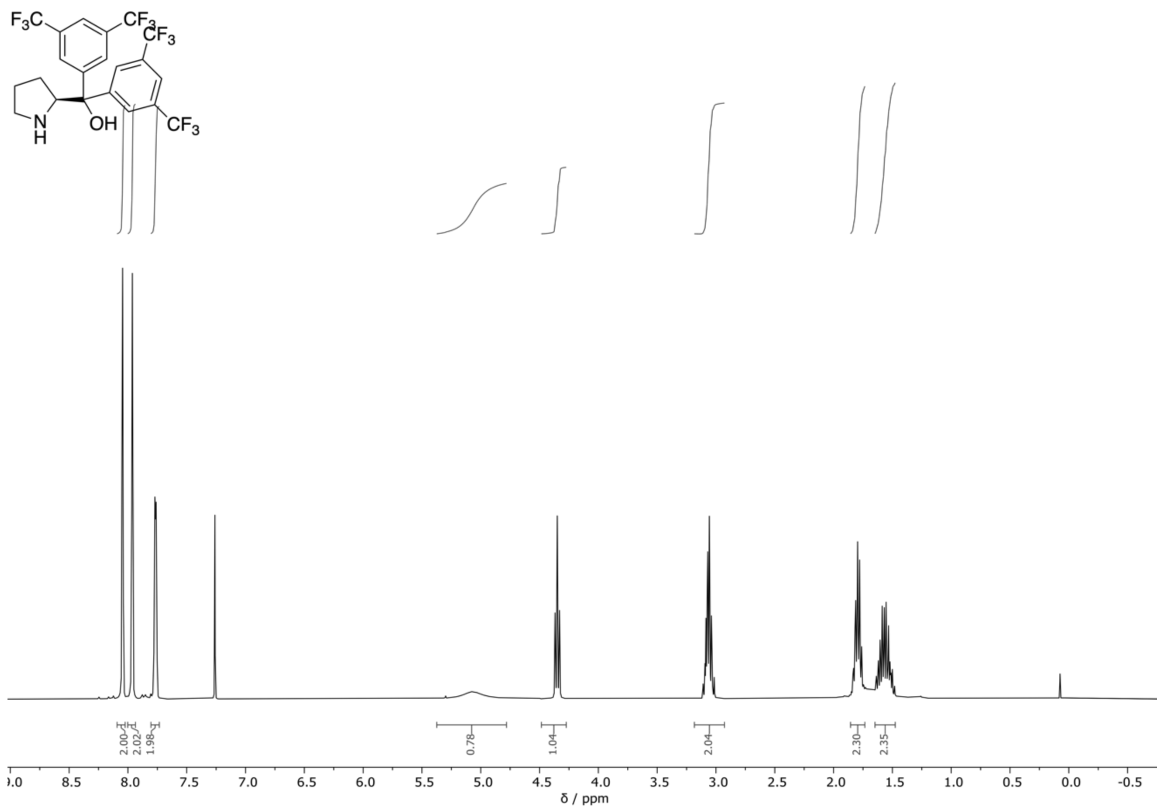
F₃C
CF₃
CF₃
N
H
OH
CF₃
2.00
2.02
1.98
0.78
1.04
2.04
2.30
2.35
.0
8.5
8.0
7.5
7.0
6.5
6.0
5.5
5.0
4.5
4.0
3.5
3.0
2.5
2.0
1.5
1.0
0.5
0.0
-0.5
δ / ppm

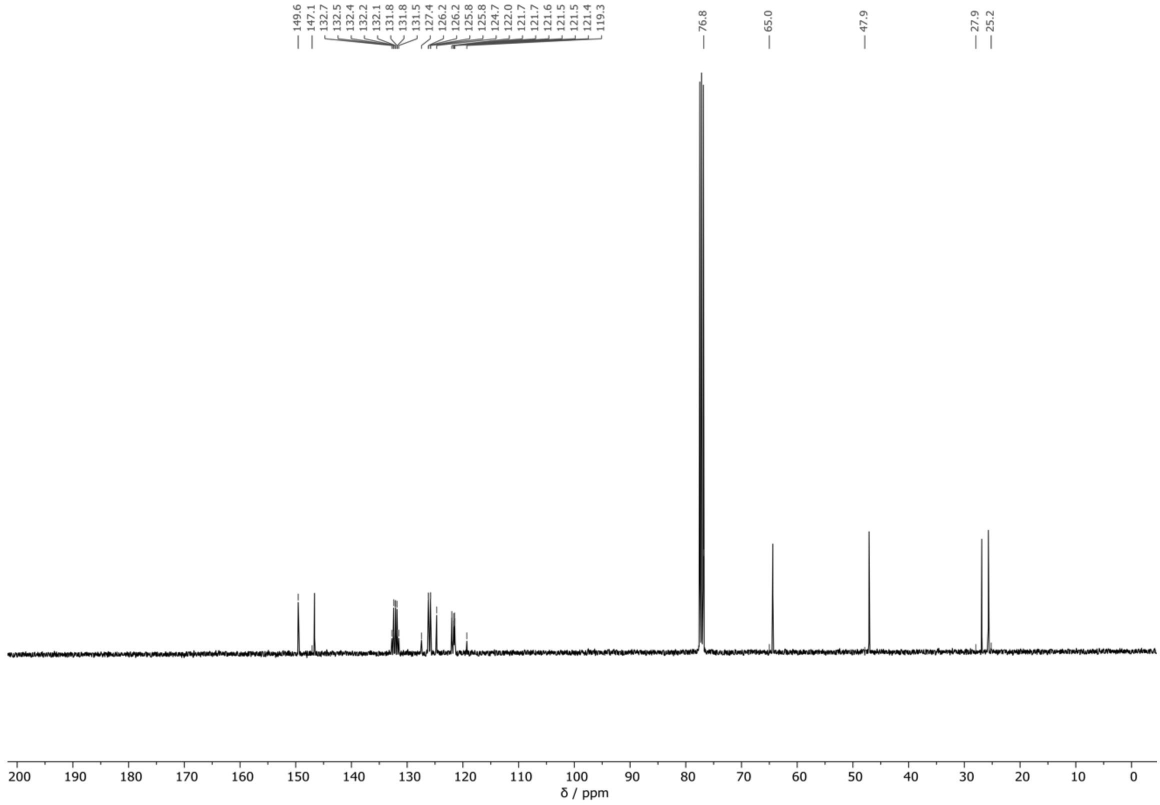
149.6
147.1
132.7
132.5
132.4
132.2
132.1
131.8
131.8
131.5
127.4
126.2
126.2
125.8
125.8
124.7
122.0
121.7
121.7
121.6
121.5
121.5
121.4
119.3
76.8
65.0
47.9
27.9
25.2
200
190
180
170
160
150
140
130
120
110
100
90
80
70
60
50
40
30
20
10
0
δ / ppm

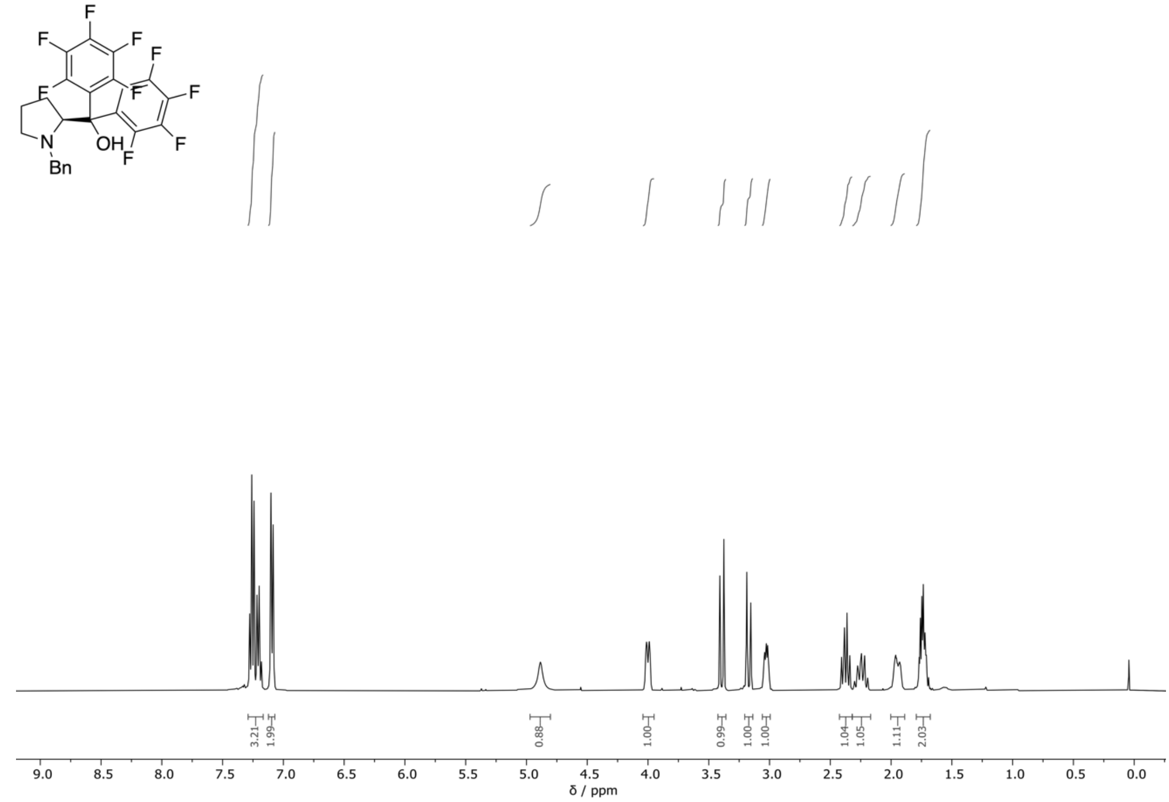
F
F
F
F
F
F
F
F
F
F
N
OH
Bn
3.21
1.99
0.88
1.00
0.99
1.00
1.00
1.04
1.05
1.11
2.03
9.0
8.5
8.0
7.5
7.0
6.5
6.0
5.5
5.0
4.5
4.0
3.5
3.0
2.5
2.0
1.5
1.0
0.5
0.0
δ / ppm

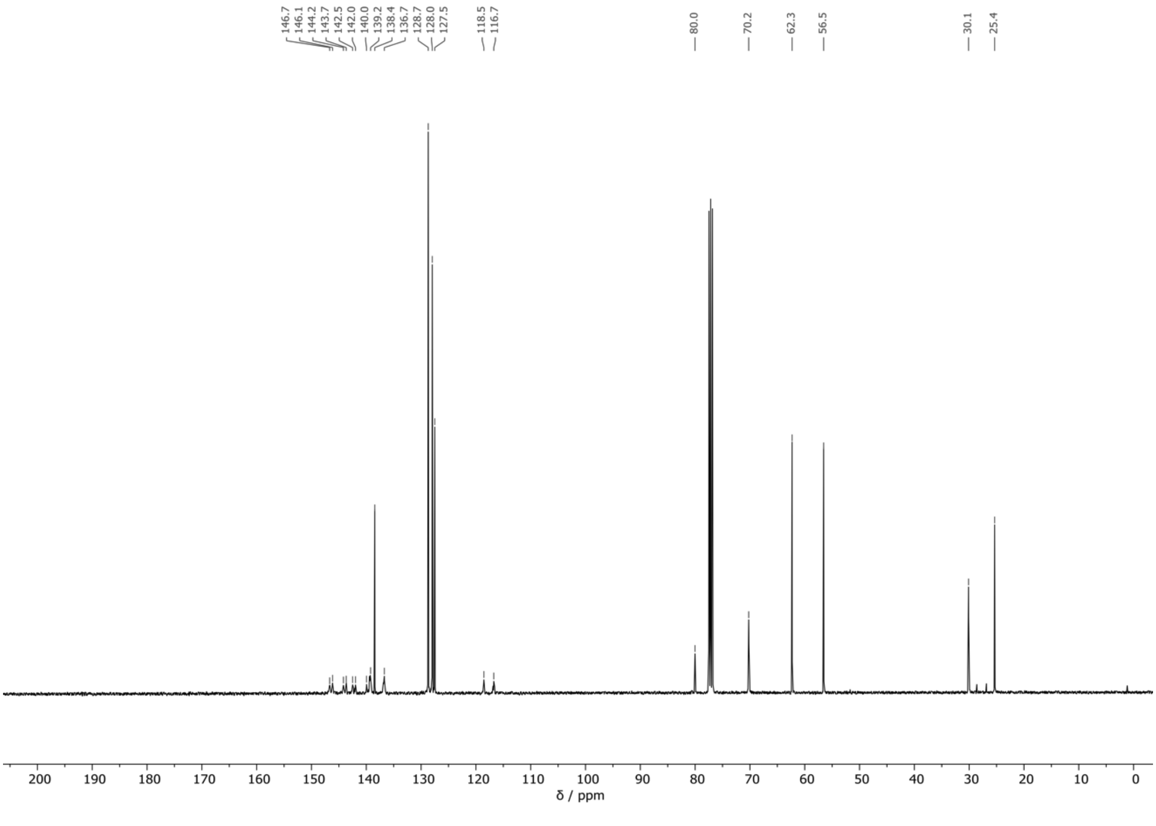
146.7
146.1
144.2
143.7
142.5
142.0
140.0
139.2
138.4
136.7
128.7
128.0
127.5
118.5
116.7
80.0
70.2
62.3
56.5
30.1
25.4
200
190
180
170
160
150
140
130
120
110
100
90
80
70
60
50
40
30
20
10
0
δ / ppm

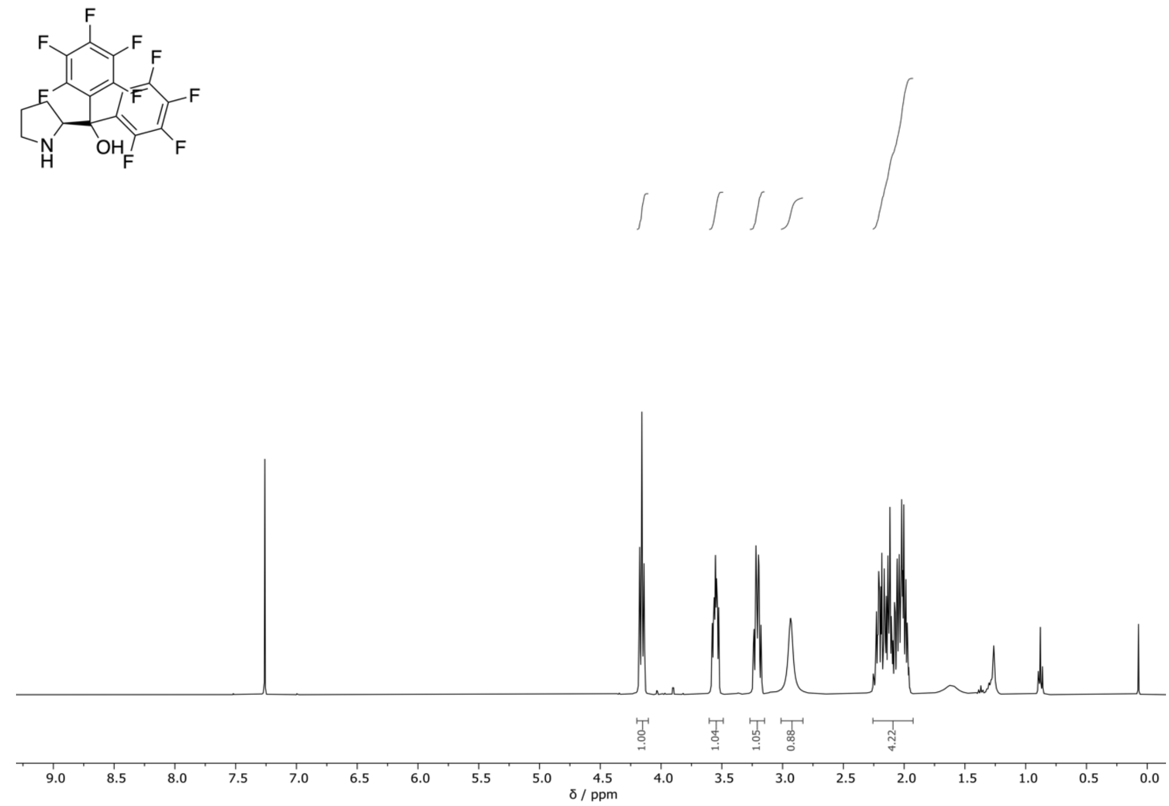
F
F
F
F
F
F
F
F
F
F
N
H
OH
1.00
1.04
1.05
0.88
4.22
9.0 8.5 8.0 7.5 7.0 6.5 6.0 5.5 5.0 4.5 4.0 3.5 3.0 2.5 2.0 1.5 1.0 0.5 0.0
δ / ppm

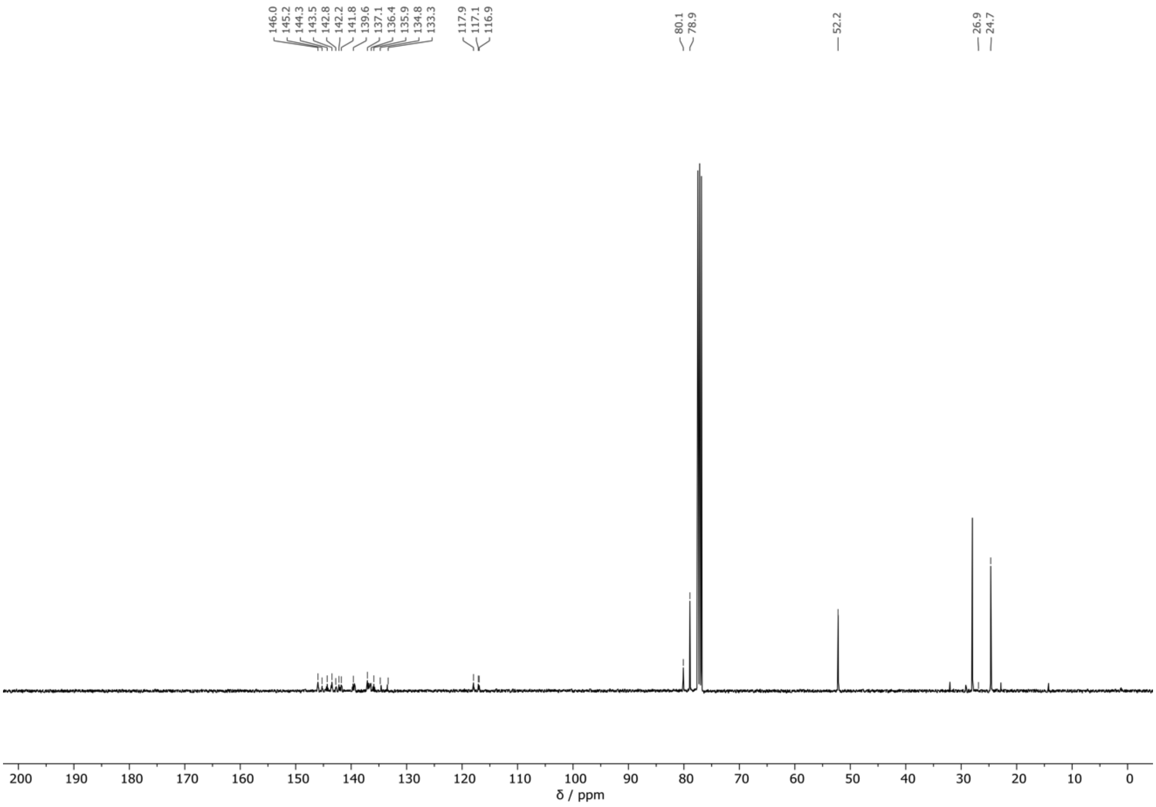
146.0
145.2
144.3
143.5
142.8
142.2
141.8
139.6
137.1
136.4
135.9
134.8
133.3
117.9
117.1
116.9
80.1
78.9
52.2
26.9
24.7
200 190 180 170 160 150 140 130 120 110 100 90 80 70 60 50 40 30 20 10 0
δ / ppm

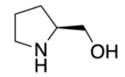
N
H
OH

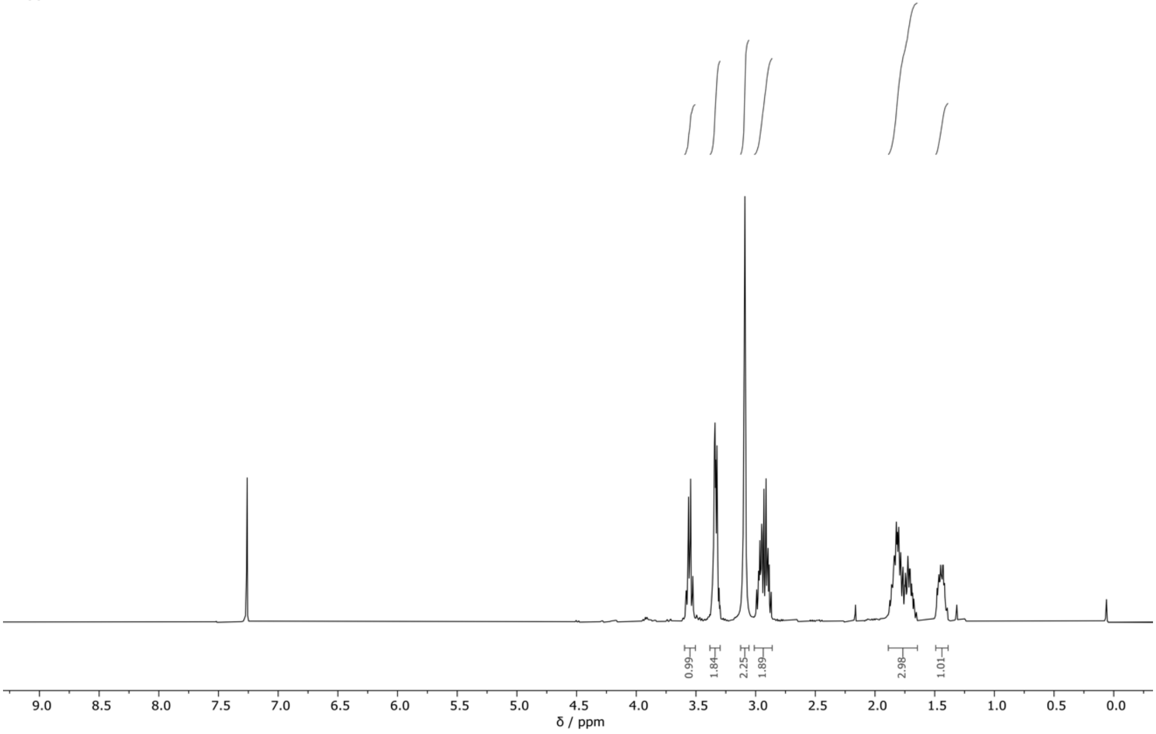
0.99
1.84
2.25
1.89
2.98
1.01
9.0
8.5
8.0
7.5
7.0
6.5
6.0
5.5
5.0
4.5
4.0
3.5
3.0
2.5
2.0
1.5
1.0
0.5
0.0
δ / ppm

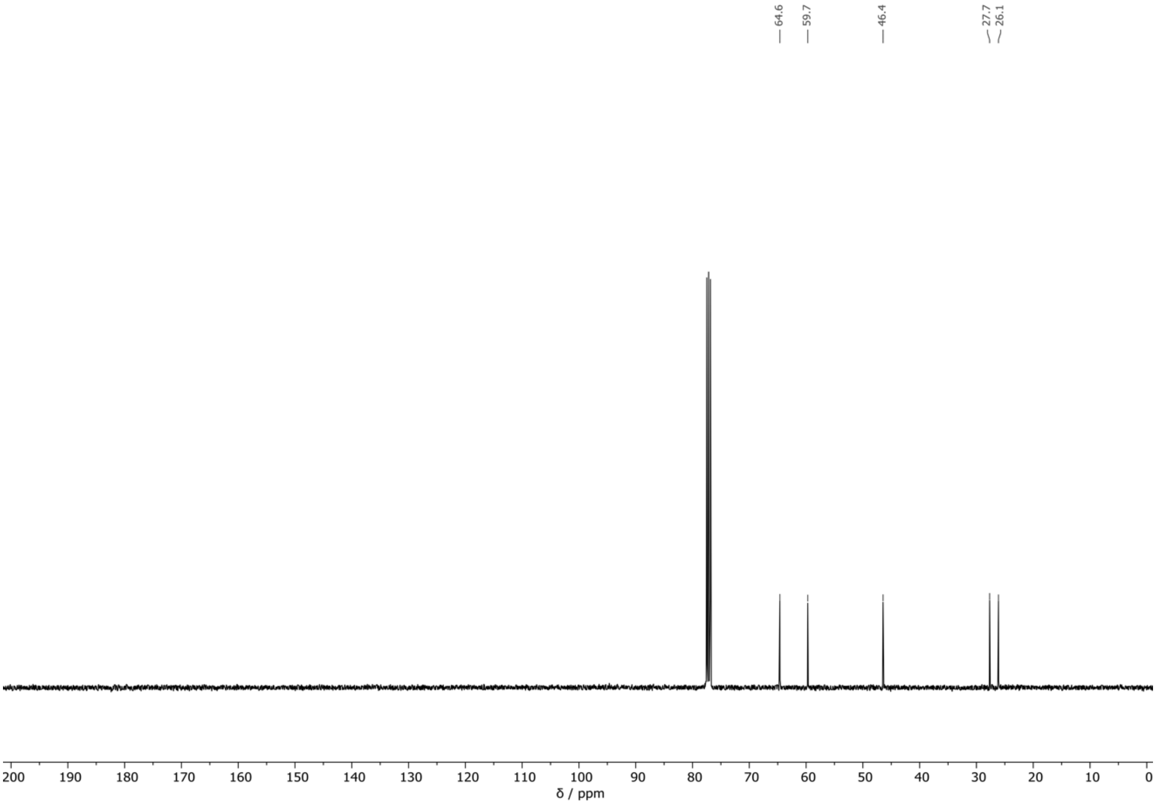
64.6
59.7
46.4
27.7
26.1
200
190
180
170
160
150
140
130
120
110
100
90
80
70
60
50
40
30
20
10
0
δ / ppm

9. References

[1] E. J. Corey, C. J. Helal, *Angew. Chem. Int. Ed.* **1998**, *37*, 1986-2012.

[2] R. Pollice, P. Chen, *Angew. Chem. Int. Ed.* **2019**, *58*, 9758-9769.

[3] G. B. Stone, *Tetrahedron: Asymmetry* **1994**, *5*, 465-472.

[4] a) E. J. Corey, R. K. Bakshi, S. Shibata, C. P. Chen, V. K. Singh, *J. Am. Chem. Soc.* **1987**, *109*, 7925-7926; b) E. J. Corey, R. K. Bakshi, S. Shibata, *J. Am. Chem. Soc.* **1987**, *109*, 5551-5553; c) E. J. Corey, J. O. Link, *Tetrahedron Lett.* **1989**, *30*, 6275-6278.

[5] a) M. C. Sherman, M. R. Ams, K. D. Jordan, *J. Phys. Chem. A* **2016**, *120*, 9292-9298; b) J. W. G. Bloom, R. K. Raju, S. E. Wheeler, *J. Chem. Theory. Comput.* **2012**, *8*, 3167-3174; c) S. Tsuzuki, K. Honda, T. Uchimaru, M. Mikami, K. Tanabe, *J. Phys. Chem. A* **2002**, *106*, 4423-4428.

[6] E. J. Corey, J. O. Link, R. K. Bakshi, *Tetrahedron Lett.* **1992**, *33*, 7107-7110.

[7] M. P. Gamble, A. R. C. Smith, M. Wills, *J. Org. Chem.* **1998**, *63*, 6068-6071.

[8] T. Touge, H. Nara, M. Fujiwhara, Y. Kayaki, T. Ikariya, *J. Am. Chem. Soc.* **2016**, *138*, 10084-10087.

[9] A. C. Albéniz, P. Espinet, R. Manrique, A. Pérez-Mateo, *Angew. Chem. Int. Ed.* **2002**, *41*, 2363-2366.

[10] G. A. Hiegel, K. B. Peyton, *Synth. Commun.* **1985**, *15*, 385-392.

[11] A. L.-F. Chow, M.-H. So, W. Lu, N. Zhu, C.-M. Che, *Chem. Asian J.* **2011**, *6*, 544-553.

[12] V. Diemer, H. Chaumeil, A. Defoin, A. Fort, A. Boeglin, C. Carré, *Eur. J. Org. Chem.* **2006**, *2006*, 2727-2738.

[13] S. Poplata, T. Bach, *J. Am. Chem. Soc.* **2018**, *140*, 3228-3231.

[14] D. J. Mathre, T. K. Jones, L. C. Xavier, T. J. Blacklock, R. A. Reamer, J. J. Mohan, E. T. T. Jones, K. Hoogsteen, M. W. Baum, E. J. J. Grabowski, *J. Org. Chem.* **1991**, *56*, 751-762.

[15] A. Lattanzi, A. Russo, *Tetrahedron* **2006**, *62*, 12264-12269.

[16] Y.-k. Liu, C. Ma, K. Jiang, T.-Y. Liu, Y.-C. Chen, *Org. Lett.* **2009**, *11*, 2848-2851.

[17] C. Ó Dálaigh, S. J. Connon, *J. Org. Chem.* **2007**, *72*, 7066-7069.

[18] D. Enders, P. Fey, H. Kipphardt, *Org. Prep. Proced. Int.* **1985**, *17*, 1-9.

Part 2

Lewis Acid Enhancement in the House-Meinwald Rearrangement of Epoxides

1. Introduction

1.1. The House Meinwald Rearrangement of Epoxides

Due to their polarity and ring tension, epoxides are endowed with a versatile and high reactivity. They can undergo manifold transformations with electrophiles, nucleophiles, acids, bases, reducing, and sometimes also oxidizing reagents like CO_2 to yield carbonates.[1] Moreover, epoxides can also rearrange to aldehydes or ketones in a House-Meinwald rearrangement (HMR). The initial investigations of epoxide rearrangements of stilbene oxide (**1**) to aldehyde **2** or ketone **3** were described by House in 1955. He reported that depending on the Lewis acid, *trans*-stilbene oxide (**1a**) provides either aldehyde **2** or ketone **3** (Scheme 1a), whereas *cis*-stilbene oxide (**1b**) only rearranges to aldehyde **2** (Scheme 1b). House concluded that the reaction must proceed *via* the corresponding zwitterions **4a** and **4b**, but he had no explanation for the selectivity.[2]

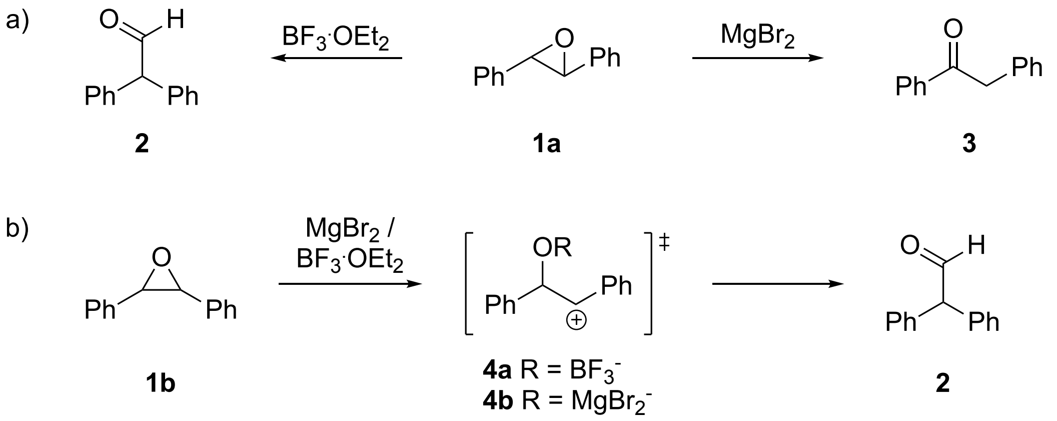

Scheme 1 Rearrangement of stilbene oxide (**1**) to either aldehyde **2** or ketone **3**, depending on the Lewis acid and stereochemistry of the epoxide.[2]

In an additional report, House and Wasson further described the influence of the solvent. Depending on the solvent, the $BF_3·OEt_2$ mediated rearrangement of α-β-epoxy ketone **5** provides either fluoroalcohol **6** (diethyl ether) or the corresponding diketone **7** (benzene) (Scheme 2). Thereby the formation of **7** can only occur if an intermediate analogous to **4a** (Fig. 1) is formed, in which the rearrangement of the acyl group then takes place.[3]

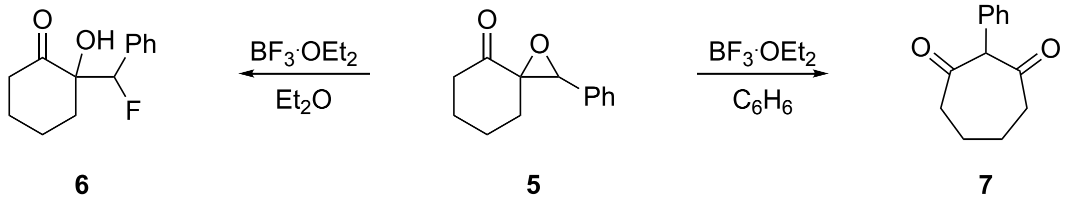

Scheme 2 Rearrangement of α-β-epoxy ketone **5** to fluoroalcohol **6** or diketone **7**, depending on the solvent.[3]

The group of Meinwald reported in 1963 that treatment of [2.2.1]-heptadiene (**8**) with peracetic acid does not provide the desired epoxide **9**, but rather aldehyde **10**. They postulated a mechanism in which the intermediately formed epoxide **9** is protonated by acetic acid, resulting in an equilibrium of cations **11a** and **11b**, which rearrange in a 1,3-alkyl shift to aldehyde **10**.[4] Later, Meinwald *et al.* were able to prove their postulated mechanism, demonstrating that after epoxidation of **8** with *m*CPBA, the addition of dilute sulfuric acid leads to the rearrangement product **10** (Scheme 3).[5]

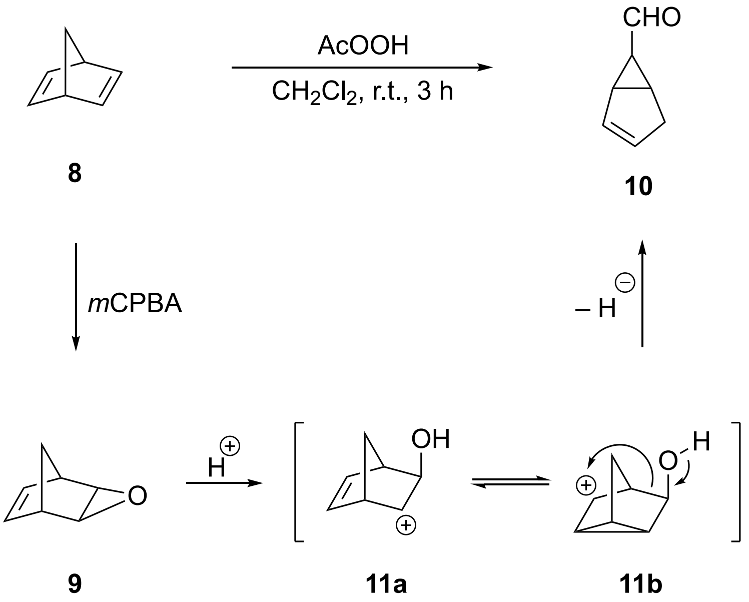

Scheme 3 Rearrangement of [2.2.1]-heptadiene (**8**) to aldehyde **10** with either peracetic acid or *m*CPBA and diluted sulfuric acid.[4,5]

A lot of effort was made to further elucidate the mechanism of the HMR. Initial quantum mechanical studies by Bock, George, and Glusker suggested that for oxirane the proton-catalyzed rearrangement proceeds in a concerted manner, whereas for the analogous fluoroxirane they calculated a mechanism with a stable carbonium ion.[6] Coxon *et al.* further demonstrated with the help of quantum mechanical calculations and isotope labelling experiments that the BF_3-catalyzed HMR of methylpropene oxide (**12**) and 2,3,3-trimethyl-1,2-epoxybutane (**12b**) proceeds *via* a multistep process involving zwitterionic intermediate **14**.[7–9] The formation of the corresponding fluorohydrin **13** was regarded as a competitive reaction with a dead-end (Scheme 4).

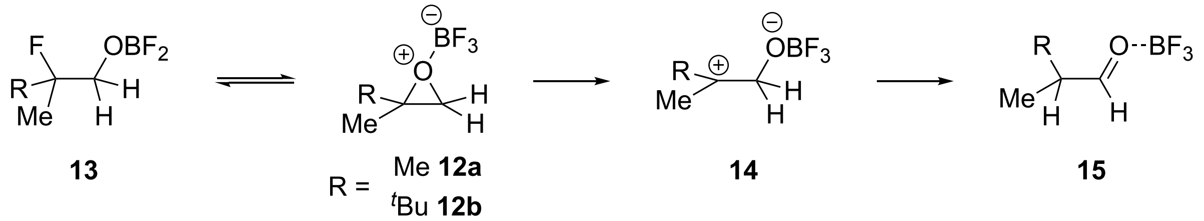

Scheme 4 Proposed mechanism of the BF_3 catalyzed HMR by Coxon *et al.*.

In 2014, the group of Salvatella performed a detailed theoretical study of the BF_3-catalyzed HMR utilizing M06-2X/6-311++G(d,p) in dichloromethane by using the polarizable continuum model (PCM). The quantum mechanical calculations did not reveal a general mechanism, but showed that the main part of the activation barrier is caused by the C-O bond cleavage. Furthermore, the moderate activation barriers could be assigned to the stabilization of the intermediate in polar media with a high dipole moment. Moreover, Salvatella concluded that there are at least “three phases” during the HMR: epoxide opening, bond rotation, and hydrogen or alkyl group shift.[10]

Since various epoxides are easily accessible, the HMR is often used in organic synthesis for the preparation of various bioactive natural products.[11–14] The chemoselectivity of the rearrangement depends on the catalyst used. Metal complexes of Pd,[15,16] Bi,[17,18] Ir,[19] In,[20] V,[21] Er,[22] Fe,[23–25] and Cu[26,27] predominantly catalyze a hydrogen shift, while complexes of B,[28] Al,[29,30] and Cr[31,32] favor an alkyl shift. An exception are lithium salts with which Rickborn and Gerkin observed rearrangements of cyclohexene oxides dependent on the counterion. While LiBr mainly forms the corresponding cyclopentylcarbaldehyde, $LiClO_4$ provides predominantly the cyclic ketone. The selectivity was explained by the fact that the reaction with LiBr proceeds *via* a halohydrin intermediate, while the rearrangement with $LiClO_4$ proceeds *via* a carbanion.[33,34]

In 2011, Schreiner *et al.* reported the stereospecific 1,2-rearrangement of enantiomerically enriched trisubstituted epoxides **16** to chiral quaternary aromatic carbaldehydes **17**. As a catalyst they used an *in situ* generated complex **18** of Schreiner’s thiourea[35] and $SiCl_4$ (Scheme 5).[36] Catalyst complex **18** facilitates a chemoselective alkyl shift to the corresponding aldehydes. Moreover, an increase in the enantiomeric purity of the starting materials as well as the products was observed. The authors therefore assumed a mechanism similar to that of a kinetic resolution. However, a catalyst controlled enantioselective version with an analogous chiral thiourea-$SiCl_4$ complex has not been reported, yet.

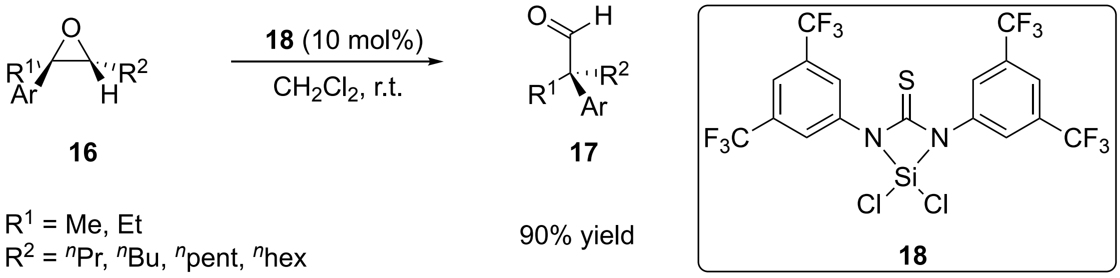

Scheme 5 Chemoselective and stereospecific HMR of epoxides **16** to aldehydes **17** catalyzed by thiourea-$SiCl_4$ complex **18**.[36]

The first catalyst-controlled enantioselective rearrangement of disubstituted epoxides was reported by Zhuang and Du who used chiral phosphoric acids (CPAs) and *N*-phosphoramides (NPAs) as catalysts. With NPA **21** the rearrangements of epoxides **19** provide aldehydes **20** in moderate yields but only low selectivities (Scheme 6a). Further, the rearrangement of trisubstituted epoxide **22** does not provide any of the desired rearrangement products, but solely allyl alcohol **23** (Scheme 6b).[37]

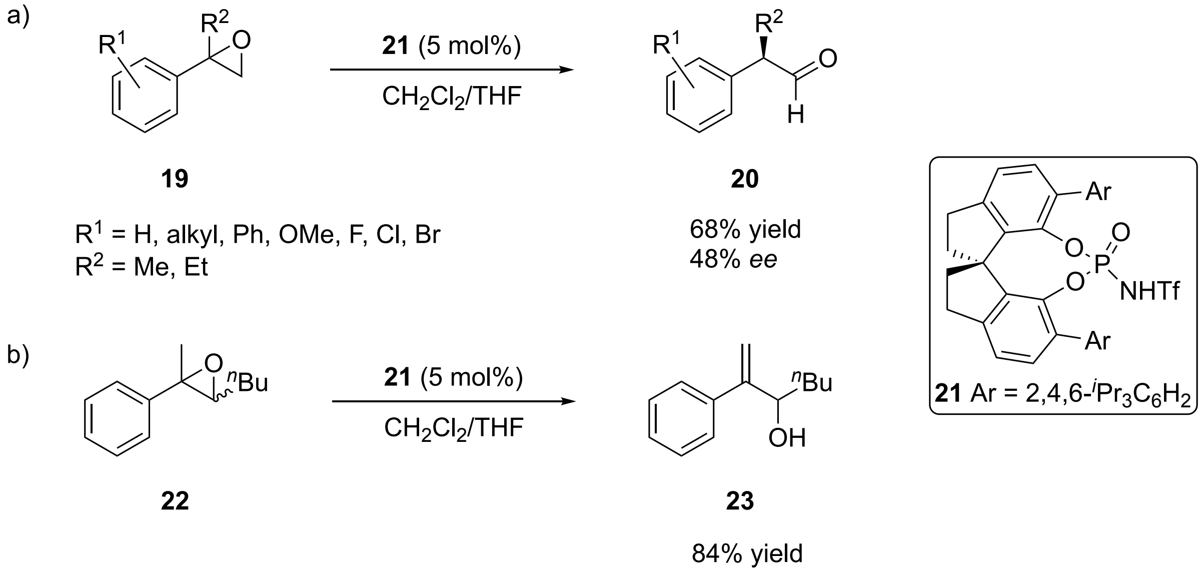
a)
19
R1 = H, alkyl, Ph, OMe, F, Cl, Br
R2 = Me, Et
21 (5 mol%)
CH2Cl2/THF
20
68% yield
48% ee
b)
22
21 (5 mol%)
CH2Cl2/THF
23
84% yield
21 Ar = 2,4,6-iPr3C6H2

Scheme 6 a) Enantioselective HMR of disubstituted epoxides **19** to chiral aldehydes **20**. b) Rearrangement of trisubstituted epoxide **22** only provides allyl alcohol **23**.[37]

Wu, Wang, and Zhu recently achieved the catalytic enantioselective HMR of tetrasubstituted diaryl-epoxides **68** to 2,2-diarylcyclohexanones **69**. NPA **26** as catalyst provides very good yields and enantioselectivities (Scheme 7).[38]

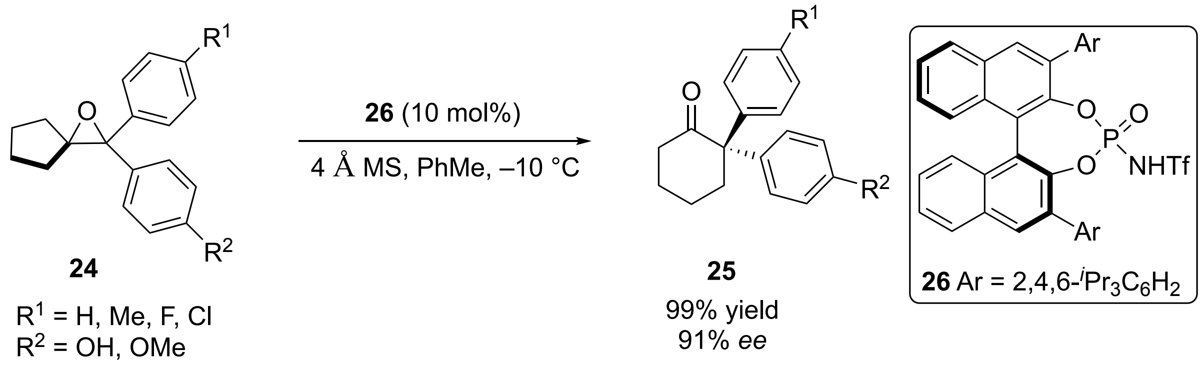
24
R1 = H, Me, F, Cl
R2 = OH, OMe
26 (10 mol%)
4 Å MS, PhMe, –10 °C
25
99% yield
91% ee
26 Ar = 2,4,6-iPr3C6H2

Scheme 7 NPA **26** catalyzed enantioselective HMR of tetrasubstituted diarylepoxides **24** to 2,2-diarylcyclohexanones **25**.[38]

Almost simultaneously, Ma, Miao, and Sun reported the enantioselective rearrangement to cyclic and acyclic ketones **28** from tetrasubstituted epoxides **27**. They also employed chiral CPA **29** or NPA **30** as catalysts, achieving excellent yields and selectivities (Scheme 8). In their proposed mechanism the epoxide is opened to a benzylic cation with subsequent semipinacol-type alkyl shift. Thereby the enantioselectivity is determined either by the chiral counterion or hydrogen bonding.[39] This proposed mechanism is generally consistent with the assumptions made by Salvatella *et al.* and Coxon. In both publications, a possible hydrogen shift as competing reaction was avoided by employing only tetrasubstituted epoxides. Furthermore, epoxides with two aryl groups were used in each case, to stabilize the intermediate cation. The effective enantioselective HMR of di- and trisubstituted epoxides in high selectivities, as well as the HMR of tetrasubstituted epoxides with only one aryl group therefore remain challenging.

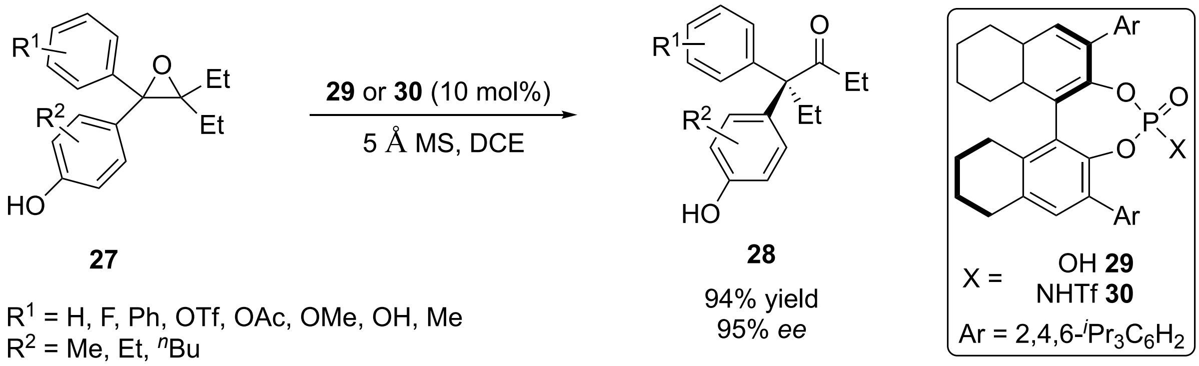
R1
R2
HO
O
Et
Et
27
R1 = H, F, Ph, OTf, OAc, OMe, OH, Me
R2 = Me, Et, nBu
29 or 30 (10 mol%)
5 Å MS, DCE
O
Et
Et
28
94% yield
95% ee
Ar
O
P
O
X
Ar
X = OH 29
NHTf 30
Ar = 2,4,6-iPr3C6H2

Scheme 8 CPA **29** or NPA **30** catalyzed enantioselective HMR of tetrasubstituted diarylepoxides **27** to ketones **28**.[39]

1.2. Lewis Acid Enhancement

BINOL derivatives and thioureas are well established hydrogen bond donors (HBD) in organic synthesis and catalysis. In addition to their direct use as HBD catalysts for the activation of substrates, thiourea and BINOL derivatives also allow the activation of transition metals and other Lewis acids such as silicon triflates or halides by complexation or anion binding. Transition metal complexes with BINOL ligands have been known since the 1980s. Initially, Yamamoto reported Al- and Zn-BINOL complexes in the asymmetric En-reaction.[40,41]. The extension to Ti as metal resulted in considerable improvements in activity and stereoselectivity and enabled the use of catalytic amounts of **33** in the En-reaction of disubstituted olefins **31** and esters **32** (Scheme 9).[42] These BINOL-Ti complexes also possess a high selectivity in allylations, Diels-Alder, and hetero-Diels-Alder reactions.[43–45]

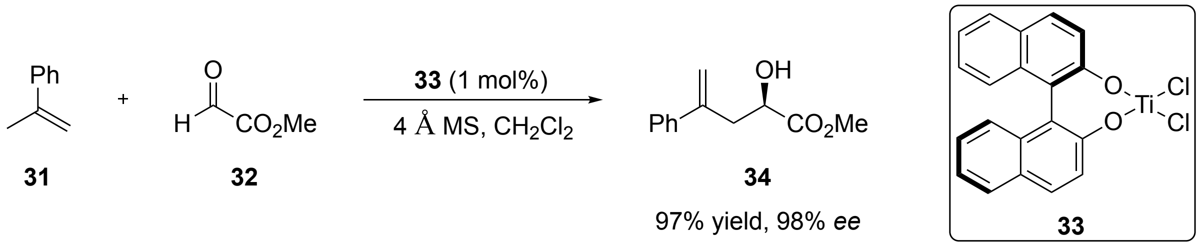
Ph
+
O
H
CO2Me
31
32
33 (1 mol%)
4 Å MS, CH2Cl2
OH
Ph
CO2Me
34
97% yield, 98% ee
O
Ti
Cl
O
Cl
33

Scheme 9 BINOL-Ti complex **33** catalyzed asymmetric En-reaction to **34**.[42]

The application of thioureas as ligands was demonstrated by the group of Schreiner. The complexation of the electron withdrawing Schreiner thiourea to $SiCl_4$ leads to a highly Lewis acidic complex for the HMR of epoxides (Scheme 5).[36] Inspired by nature's anion recognition, HBD also enable anion binding to generate chiral ion-pairs, which can act as highly reactive Lewis acid complexes.[46] In 2017, Jacobsen reported the enantioselective [4+3] cycloaddition of oxyallyl cation precursor **35** with furan derivatives **36**, catalyzed by a combination of squaramide **37** and silyl triflates. He suggested that the intrinsic Lewis acidity of silyl triflates is enhanced by the formation of a charge-separated complex, which then effectively promotes the [4+3] cycloaddition *via* formation of an oxyallyl cation intermediate.[47]

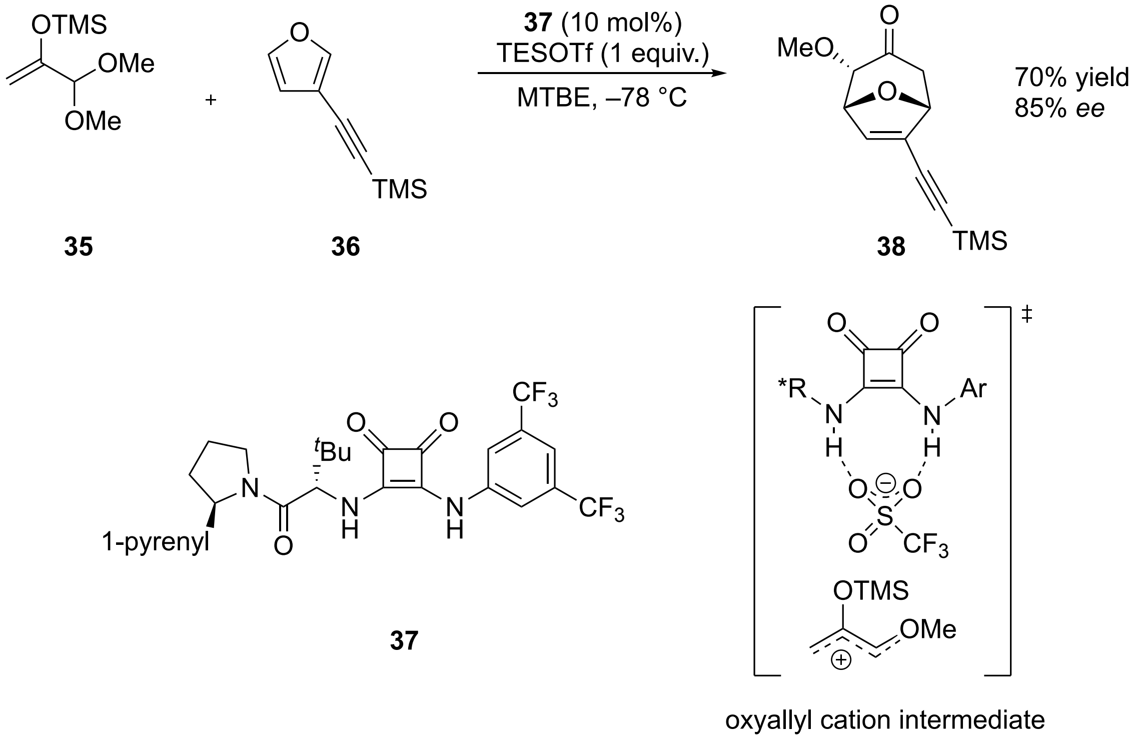

Scheme 10 a) Enantioselective [4+3] cycloaddition catalyzed by squaramide **37** and TESOTf. b) Anion binding leads to a charge separated complex, which activates **35** *via* an oxyallyl cation intermediate.[47]

2. Motivation

Although CPAs and NPAs have been successfully employed in the enantioselective HMR, the epoxide scope remains rather limited. Mainly tetrasubstituted epoxides bearing two aryl groups are successfully employed in catalyst controlled enantioselective rearrangements.[39] The enantioselective HMR of racemic disubstituted epoxides still proceeds with only poor yield and enantioselectivity, respectively. Moreover, the rearrangements of trisubstituted epoxides provide difficulties with chemoselectivity between the competing hydrogen and alkyl shift, when CPAs are employed as catalyst.[37] Therefore, di- and trisubstituted epoxides are limited to the stereospecific rearrangement of already enantioenriched epoxides, as reported by Schreiner in 2011.[36]

In order to broaden the epoxide scope for the enantioselective HMR, new activating strategies and chiral catalysts have to be applied. While achiral metal-based Lewis acids have proven to effectively catalyze the HMR of various epoxides, complexation with thioureas and BINOLs as ligands may enhance the Lewis acidity and, moreover, provide a chiral backbone. Building on the work of the Schreiner group, we aimed to combine the concept of Lewis acid enhancement with thioureas or BINOLs to establish an effective catalyst system for the HMR. Therefore, we investigated the combination of several readily available Lewis acids with achiral and chiral ureas, thioureas, squaramides, and BINOLs in the rearrangement of racemic epoxides.

3. Results

3.1. Thiourea Assisted Lewis Acids in the HMR

3.1.1. Synthesis of Epoxides

We commenced our study with the synthesis of substrates for the HMR. Starting from readily available acetophenone derivatives **39**, we synthesized trisubstituted olefins **40a** and **40b** *via* a literature known Wittig olefination with *n*-BuLi and triphenylbutylphosphonium bromide (Scheme 11).[36]

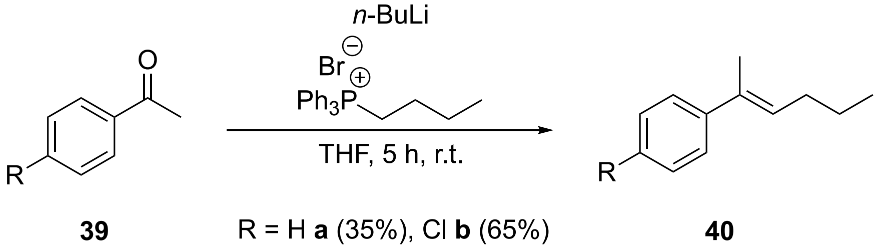

Scheme 11 Synthesis of olefins *via* Wittig reaction with triphenylbutylphosphonium bromide.

Afterwards, the alkenes were converted to the corresponding epoxides in a Prileschajew epoxidation with *m*CPBA (Scheme 12).[48] Alternatively, the epoxidation was also performed with H_2O_2 and catalytic amounts of trifluoroacetophenone. With both methods, epoxides **42**, **43a**, and **43b** were isolated with high purity, but only moderate yield.

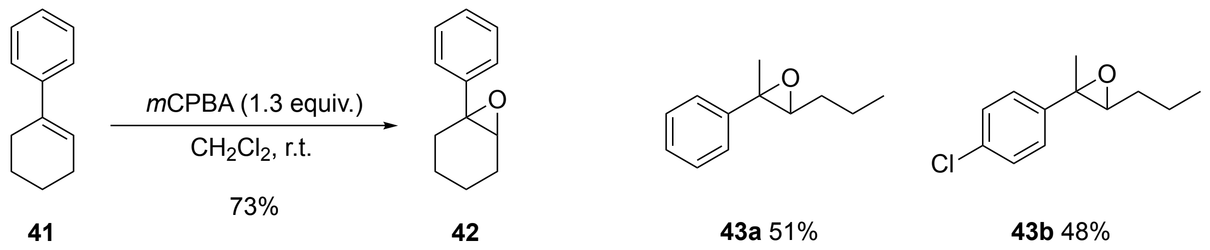
mCPBA (1.3 equiv.)
CH2Cl2, r.t.
73%
O
Cl
41
42
43a 51%
43b 48%

Scheme 12 Prileschajew epoxidation of olefins.

3.1.2. Synthesis of Thioureas and Thiosquaramides

While a wide range of achiral ureas and thioureas already was available in the working group, squaric acids, thiosquaramides, and chiral derivatives first had to be synthesized. Starting from (*R*,*R*)-1,2-diaminocyclohexane (**44**) the corresponding tosylate salt was obtained in a condensation reaction with phthalic anhydride. The tosylate salt then was directly converted to the protected amide **45** by treatment with aqueous $NaHCO_3$.[49] Subsequent Eschweiler-Clarke methylation with formalin and formic acid afforded tertiary amine **46** in high purity.[50] Afterwards, the phthalimide was cleaved with hydrazine to yield amine **47** (Scheme 13). Contrary to literature reports, we did not obtain product **47** in sufficient purity by just precipitating the by-product phthalhydrazide with diethyl ether. Therefore, we purified the free amine by column chromatography, which resulted in lower yield compared to the literature.[51] With the amine **47** in hand, we synthesized Takemoto's bifunctional chiral thiourea **49** in high yield by addition of 3,5-bis-(trifluoromethyl) phenyl isocyanate **48** (Scheme 14).[52]

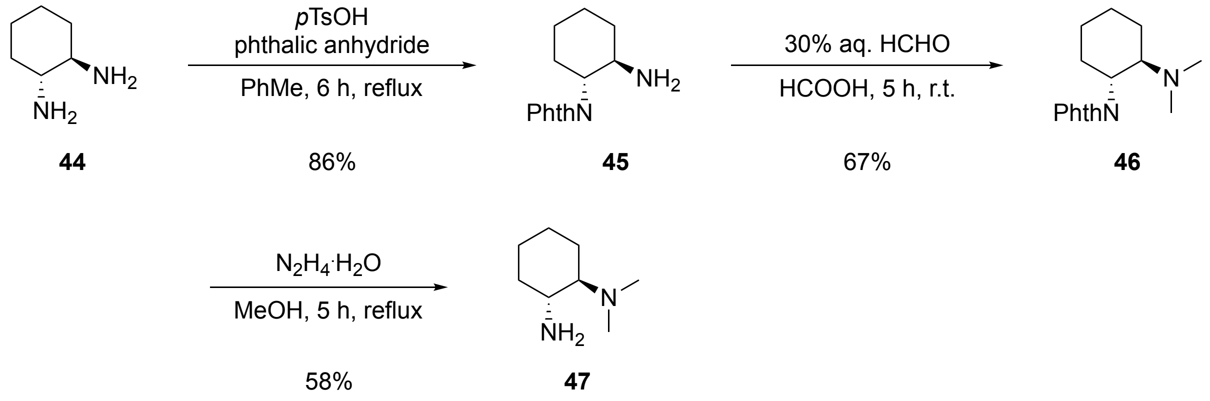
NH2
NH2
pTsOH
phthalic anhydride
PhMe, 6 h, reflux
86%
NH2
PhthN
30% aq. HCHO
HCOOH, 5 h, r.t.
67%
N
PhthN
N2H4·H2O
MeOH, 5 h, reflux
58%
N
NH2
44
45
46
47

Scheme 13 Synthesis route to tertiary amine **47**.

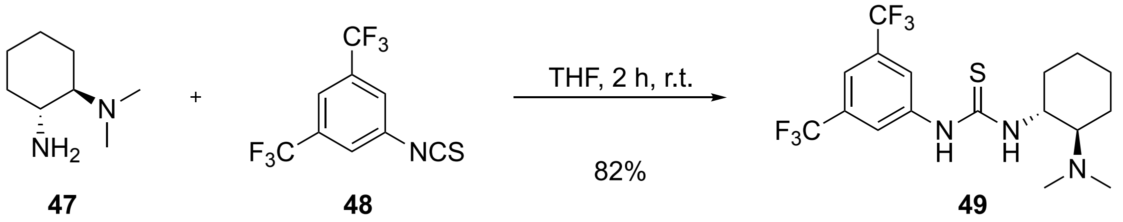

Scheme 14 Synthesis of Takemoto's thiourea **49**.

For the synthesis of squaramide **52**, we performed a substitution reaction of the commercially available squaric acid ester **50** with 3,5-bis(trifluoromethyl)phenylaniline (**51**). The long reaction time resulted from the low nucleophilicity of the electron-poor aniline **51** (Scheme 15).[53]

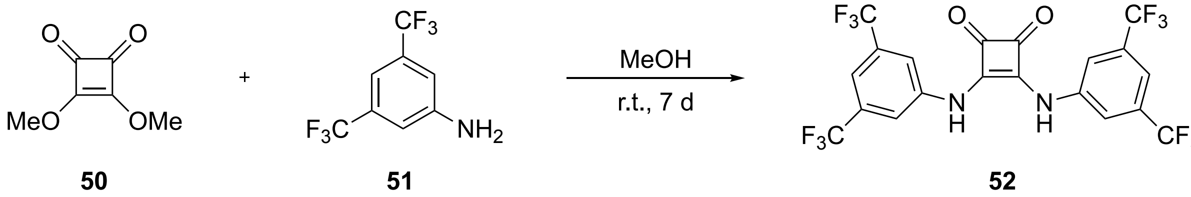

Scheme 15 Synthesis of squaramide **52** by substitution of ester **50**.

Subsequently, we attempted to synthesize the corresponding thiosquaramide **53** with phosphorous sulfide (P_4S_{10}) by the method of Jolliffe and Gale.[54] Certainly, the reaction resulted in a complex mixture and neither product nor starting material could be reisolated. We also utilized Lawesson's reagent as a further carbonyl thionation reagent, but again failed to isolate the desired product **53**.[55]

In early 2018, Rawal published the synthesis of **53** starting from squaric acid **54**.[56] Using his procedure, **54** was reacted with an excess of cyclopentanol in an azeotropic distillation to give the squaric acid ester **55** in 74% yield. Ester **55** was then thionated with Lawesson's reagent to give the corresponding thioester **56** in 49% yield. Rawal reported that the corresponding thioesters are not stable in solution, which explains the moderate yield.[56] In the final step, a substitution of **56** with an excess of 3,5-bis(trifluoromethyl)phenylaniline (**51**) provided thiosquaramide **53**. Since aniline **51** is extremely electron deficient, the reaction time was extended to six days and the product was then precipitated with *n*-hexane (Scheme 16).

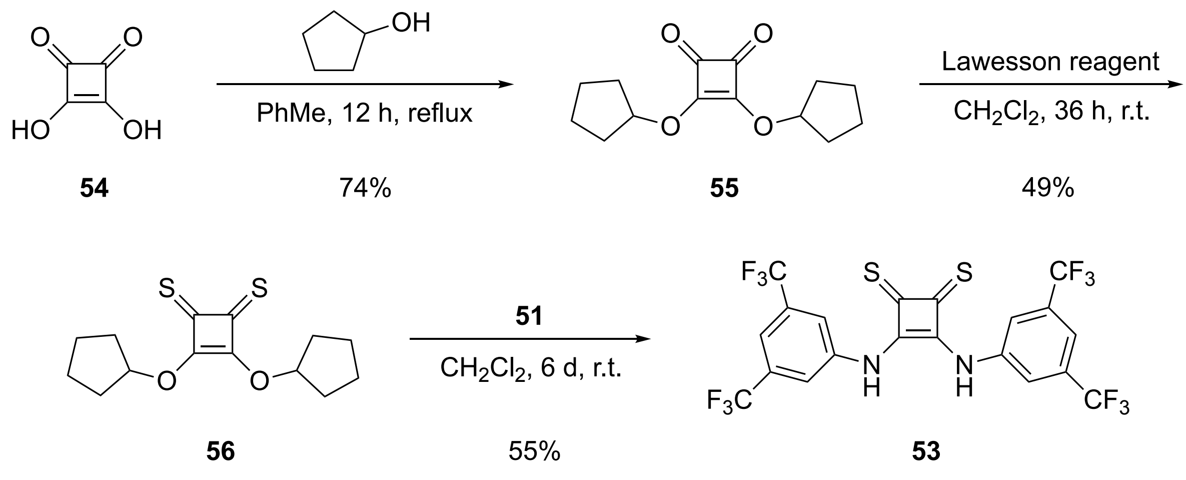

Scheme 16 Synthesis route to thiosquaramide **53**.[56]

To synthesize an asymmetric thiosquaramide catalyst, a sub-stoichiometric amount of the aniline **51** was added portionwise to **55** in order to synthesize the mono-thiosquaramide **57**. During the purification by column chromatography, we noticed a decomposition over time of the crude product, since after some time the fractions became dark in color. As a result, we added aniline **51** in one portion and performed the column chromatographic purification immediately afterwards. In this way, we isolated 40% of **57** and 10% of the by-product **53**. Afterwards, we substituted **57** with an excess of amine **47** to yield the chiral thiosquaramide **58** (Scheme 17). Purification *via* column chromatography turned out to be challenging because of high polarity and similar R_f values of **57**, **58**, and degradation products. Therefore, we attempted the precipitation of the hydrochloride salt of **58** in *n*-hexane.[56] However, filtration of the suspension provided insufficient purity of **58**.

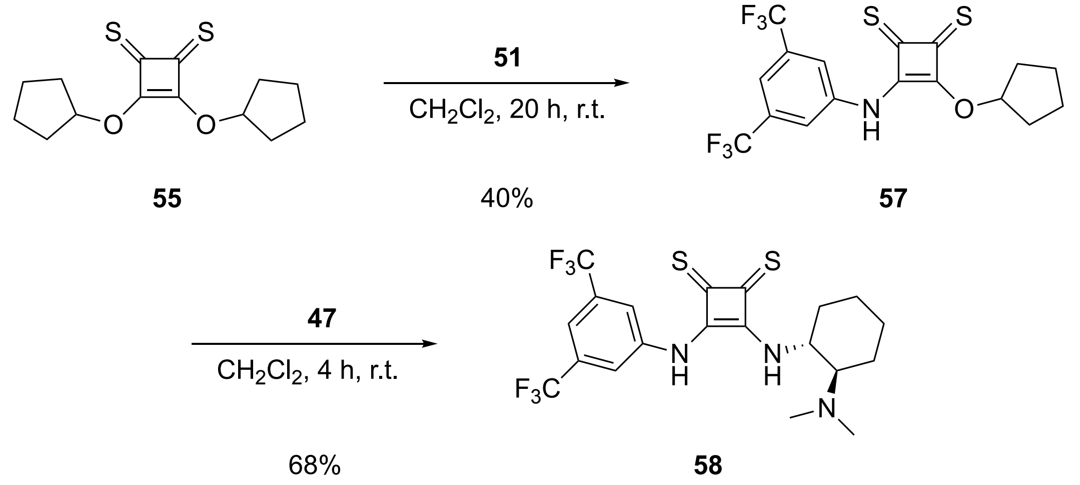

Scheme 17 Synthesis of chiral thiosquaramide **58**.

3.1.3. Screening of Lewis Acids in the HMR

In the following, various achiral Lewis acids were tested in the HMR (Tab. 1). Epoxide **42** was used as test epoxide, since the corresponding rearrangement products are described and characterized in the literature.[20,36] Catalytic activity in the epoxide rearrangement to aldehyde **59** was only observed with $TiCl_4$ (entry 3), $InCl_3$ (entry 5), and $AlCl_3$ (entry 8). While $AlCl_3$ provided the highest yield of the aldehyde, in all three cases the formation of the corresponding ketone **60** and small amounts of α-chloroalcohol **61** were also observed.

Table 1 Screening of various Lewis acids in the HMR of test epoxide **42**.

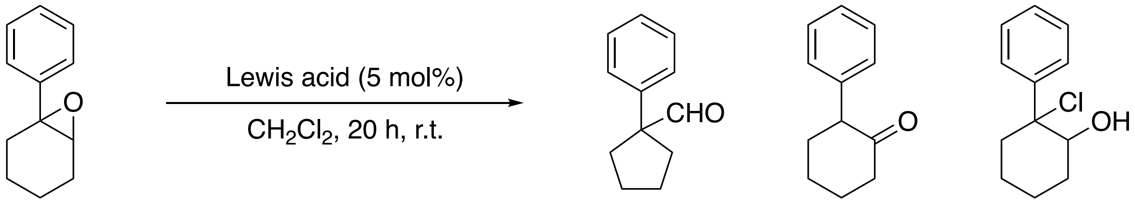

42 **59** **60** **61**

Entry	Lewis acid	42 [%][a]	59 [%][a]	60 [%][a]	61 [%][a]
1	$SiCl_4$	99	0	0	0
2	$PhBCl_2$	99	0	0	0
3	$TiCl_4$	7	26	7	n.d.[b]
4	$Ti(OPr)_4$	85	5	<1	0
5	$InCl_3$	0	22	9	13
6	$LaCl_3$	85	<1	2	2
7	$Co(acac)_3$	97	0	0	0
8	$AlCl_3$	0	78	8	4
9	$Al(acac)_3$	99	0	0	0
10	$MnAc_2$	99	0	0	0
11	$SmCl_3 \cdot 6\ H_2O$	99	0	0	0

[a] Conversion and product ratios were determined *via* ^1H NMR spectroscopy with *p*-nitrobenzaldehyde as internal standard; [b] Conversion could not be determined, as the signals were overlapping.

Analogous to the work of Hrdina and Schreiner, the metal-thiourea complexes were prepared *in situ* by complexation of Schreiner's thiourea **62** with a Lewis acid and subsequently employed in the HMR of epoxide **42** (Tab. 2). In addition to D*i*PEA, also NaH was used to investigate the influence of the base on the reactivity. We successfully reproduced Schreiner's results with $SiCl_4$ (entry 1). Again, we observed formation of aldehyde **59** only when using $InCl_3$ (entry 7), $TiCl_4$ (entries 2 and 5), or $AlCl_4$ (entry 12). Noticeably, with the metal-thiourea complexes, the yields of the aldehyde were higher compared to the Lewis acids alone. In addition, the formation of by-products **60** and **61** was reduced, which clearly demonstrates the influence of thiourea **62**. The highest yields were obtained with $AlCl_3$ (94%, entry 12) and $TiCl_4$ (84%, entry 5) as Lewis acid and NaH as the base. Furthermore, it was observed that D*i*PEA in combination with $TiCl_4$ (16%, entry 2) or $SiCl_4$ in combination with NaH (3%, entry 13) gave significantly lower yields in comparison with the combination of the corresponding other bases. This means that the base has a considerable influence on the reactivity and provides specific Lewis acid / base pairs.

Table 2 Schreiner's thiourea **62** in combination with various Lewis acids in the HMR of epoxide **42**.

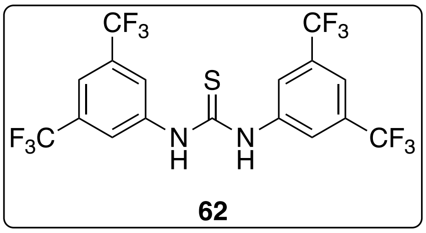

62

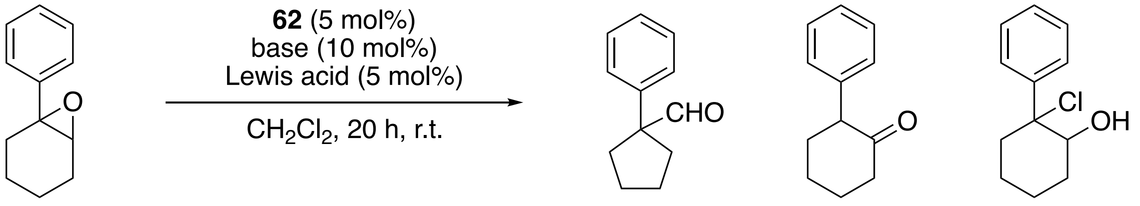

42 **59** **60** **61**

Entry	Lewis acid	Base	**42** [%][a]	**59** [%][a]	**60** [%][a]	**61** [%][a]
1	$SiCl_4$	D*i*PEA	4	68	<1	8
2	$TiCl_4$	D*i*PEA	43	16	6	14
3	Ti(O*i*Pr)$_4$	D*i*PEA	99	0	0	0
4	$SnCl_4$	D*i*PEA	95	<1	<1	<1
5	$TiCl_4$	NaH	0	84	8	2
6	$NiCl_2$	NaH	97	0	0	0
7	$InCl_3$	NaH	65	11	<1	3
8	$LaCl_3$	NaH	96	0	0	0
9	Co(acac)$_3$	NaH	99	0	0	0
10	Al(acac)$_3$	NaH	99	0	0	0
11	$SmCl_3 \cdot 6\ H_2O$	NaH	96	0	0	<1
12	$AlCl_3$	NaH	2	94	<1	<1
13	$SiCl_4$	NaH	47	3	0	10

[a] Conversion and product ratios were determined *via* ^{1}H NMR spectroscopy with *p*-nitrobenzaldehyde as internal standard.

Since the background reaction of $AlCl_3$ itself was already high (Tab. 1, entry 8), $TiCl_4$ was preferably used as Lewis acid and further bases were investigated with regard to their reactivity (Tab. 3). Using LiH, *n*-BuLi, or LiHMDS provided lower conversion (entry 3-5) than NaH, from which an influence of the corresponding cation could be determined. In addition, two approaches with non-dry solvents were carried out to investigate the influence of traces of water on the reaction (entries 6 and 7). We observed that the yield decreased by about half and that the water content of the reaction should therefore be kept as low as possible. We also tested shorter reaction times in order to be able to estimate the reaction kinetics (entries 8-10). On the one hand, the reaction was almost complete after 200 min (entry 9) and, on the other hand we observed a significantly slower reaction rate when using $TiCl_4$ and **62** without additional base (entry 10). These first encouraging results clearly demonstrate the influence of the thiourea **42** and indicate a base mediated complexation with $TiCl_4$.

Table 3 Influence of various bases in the HMR of **42** catalyzed by a complex of thiourea **62** and $TiCl_4$.

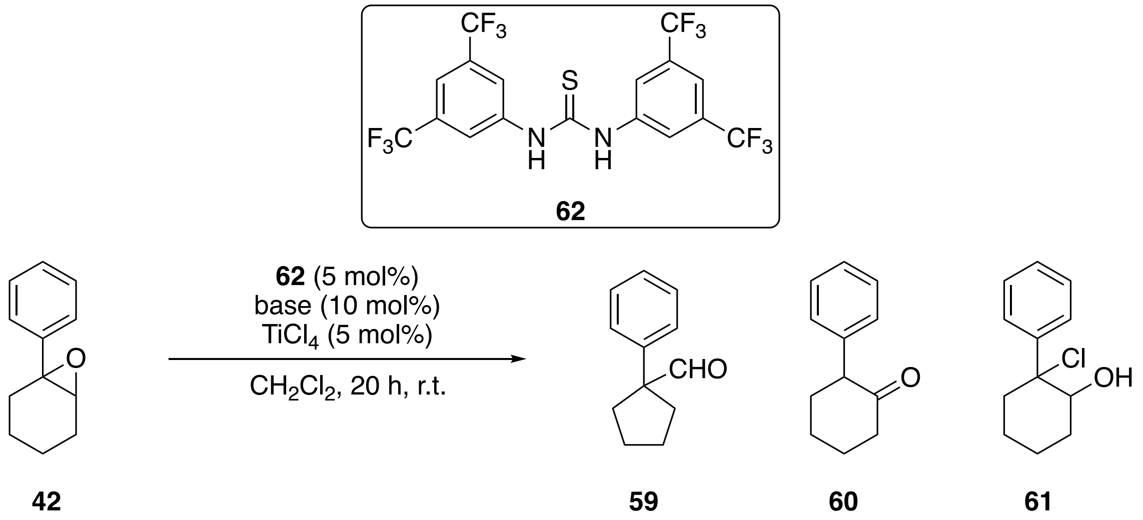

Entry	Base	42 [%][a]	59 [%][a]	60 [%][a]	61 [%][a]
1	D*i*PEA	45	16	6	14
2	NaH	0	84	8	3
3	*n*-BuLi	0	49	17	15
4	LiHMDS	52	6	3	10
5	LiH	0	34	11	5
6[b]	NaH	0	49	16	8
7[b]	–	0	48	15	10
8[c]	NaH	0	53	7	2
9[d]	NaH	0	70	8	3
10[d]	–	45	15	3	5

[a] Conversion and product ratios were determined *via* ^1H NMR spectroscopy with *p*-nitrobenzaldehyde as internal standard; [b] "wet" CH_2Cl_2 was used; [c] 50 min reaction time; [d] 200 min reaction time

3.1.4. Catalyst Characterization

The structure of the silicon thiourea catalyst **18** (Scheme 5) has been proven by Schreiner and Hrdina by means of NMR spectroscopy and high resolution mass spectrometry (MS). In order to elucidate the structure of our catalyst based on $TiCl_4$, we envisaged to crystallize the catalyst for a subsequent single-crystal X-ray diffraction analysis. Although no syntheses are known in the literature for crystallizations of titanium-thiourea complexes, Lavoie described and characterized structurally similar complexes **63**-**65** (Fig. 1).[57]

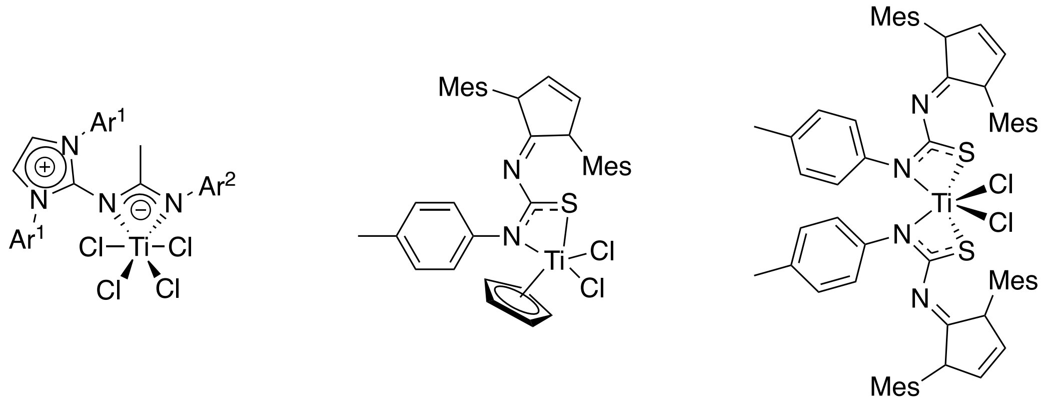

63 **64** **65**

Figure 1 Synthesized and characterized titanium complexes by Lavoie.[57]

Based on this work, various crystallization approaches were carried out. Therefore, the complex was prepared analogously to the *in situ* generation for catalysis. Crystallization attempts in dichloromethane, dichloroethane, benzene, and acetonitrile as coordinating solvent failed and provided no single crystals. The typical red color, which is described in the literature as an indication of six-coordinate titanium complexes, was observed in all approaches. However, the color changed after longer crystallization times due to possible hydrolysis of the complex by trace amounts of moisture that could have entered the reaction apparatus.

Following the crystallization experiments, various NMR experiments were carried out in order to clarify the binding of the thiourea to $TiCl_4$. In the work of Schreiner and Hrdina, the structure of silicon-thiourea complex **18** has been proven by ^4J-coupling of silicon to the *ortho* protons of the thiourea.[36] However, titanium is a quadrupolar nucleus and does not show ^4J-coupling to the *ortho* protons.[58] Nonetheless, we considered several assumptions for the NMR characterization. Coordination of thiourea **62** to titanium can occur either *via* both nitrogen atoms **66a** or *via* one nitrogen and the sulfur **66b**, though the number of chloride substituents remains unclear (Fig. 2). Taking into account the HSAB principle, we assumed that the coordination of the hard titanium species rather occurs *via* both nitrogen atoms, which are "harder" compared to sulfur. This assumption is also supported by the Marcus theory to rationalize ambident reactivity.[59] The corresponding structure **66a** would result in only six signals due to its symmetry in the ^{13}C NMR spectrum, whereas eleven signals are expected for structure **66b** because the two aryl groups differ electronically. One aromatic is conjugated to the imine while the amine substituent of the other aromatic coordinates the titanium. Furthermore, only one signal should be observed in the ^{19}F NMR spectrum of **66a** and two signals for **66b**, which in turn can be explained by asymmetry.

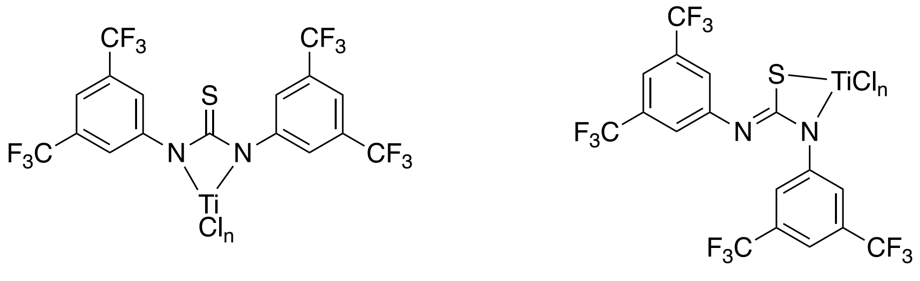

66a **66b**

Figure 2 Possible structures **66a** und **66b** of the Ti-thiourea-complex.

The titanium-thiourea complex was prepared in anhydrous CD_2Cl_2 and transferred to a flame dried NMR tube and covered with Ar. An additional $TiCl_4$ sample of the same concentration was used for the external calibration of the titanium measurement, and the corresponding signal could be clearly observed. In contrast, no titanium signal was observed in the ^{47,49}Ti NMR spectrum of the thiourea-Ti complex sample (Fig. 3). This may be due to the decrease of sensitivity of titanium as the size of the complex increases. As described in the literature, NMR signals of organo-titanium compounds are often not detected.[58] Furthermore, the absence of Ti-signals also means that there is no longer any unbound $TiCl_4$ present and thus a complexation must have taken place.

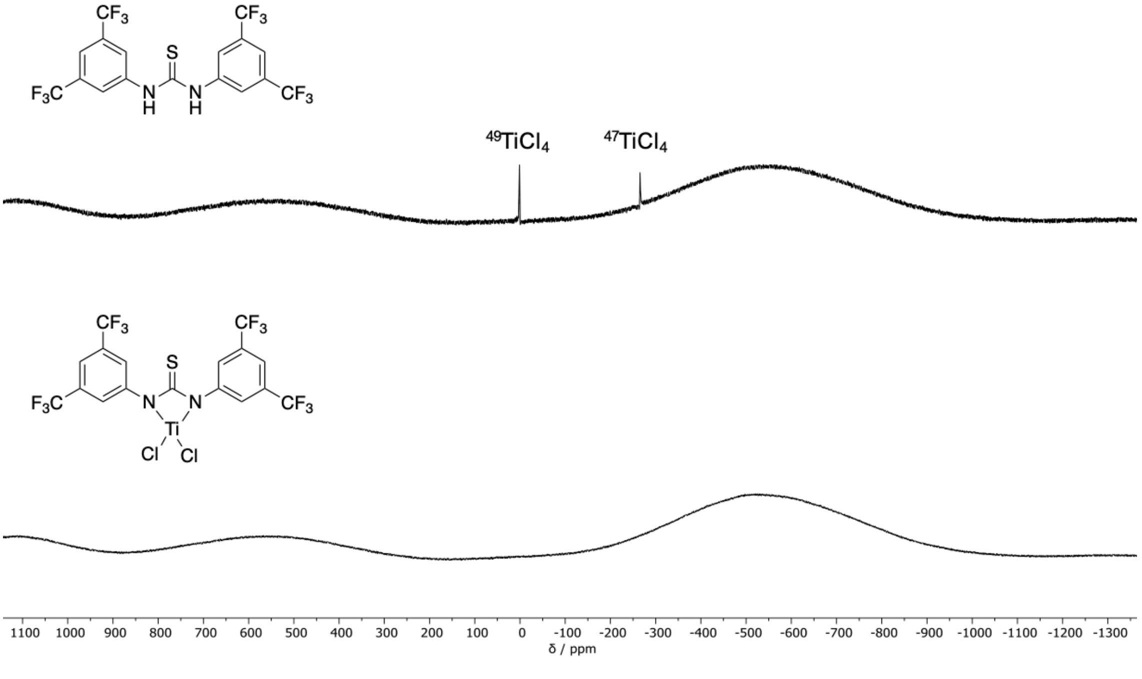

Figure 3 ^{47,49}Ti NMR spectra of **62** (at the top). The signal at 0 ppm and –267 ppm correspond to the external calibration with $^{49}TiCl_4$ and $^{47}TiCl_4$, respectively. ^{47,49}Ti NMR spectra of Ti-thiourea complex (at the bottom).

The ^{19}F NMR spectrum showed one signal, which was slightly shifted compared to the signal of thiourea **62** (0.01 ppm). This indicates that the binding to the titanium very likely takes place according to structure **66a**, since with this coordination, only one peak can be observed and the influence of the fluorine atoms should be weak. We also observed two additional signals with significantly lower intensity, which indicate a low proportion of **66b** which, however, appears to be negligible (Fig. 4).

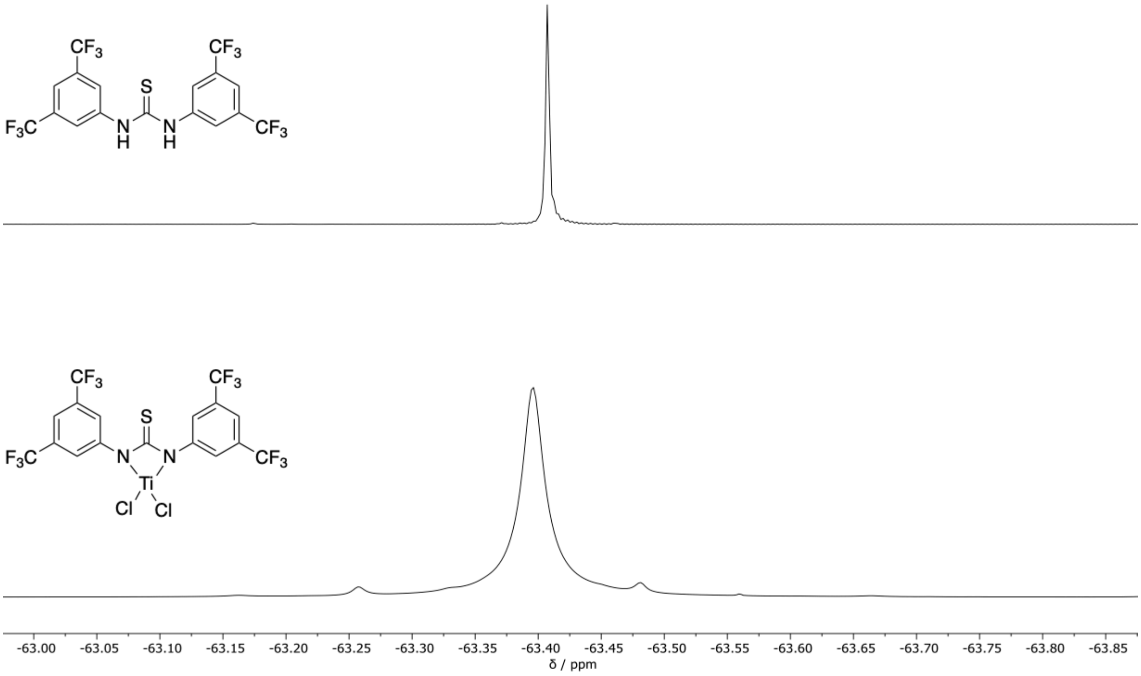

Figure 4 ^{19}F NMR spectra of **62** (at the top) and the Ti-thiourea complex (at the bottom).

On the basis of the ^{13}C NMR spectra, the complex structure **66a** could be confirmed, since the signals also indicate symmetrical coordination (Fig. 5). While we observed an appreciable upfield shift of the corresponding thiocarbonyl – the meta-carbons shifted downfield. Although the quartet signals of the CF_3 groups in the complex are somewhat overlaid by the *para* and *ortho* signals, they remained almost unchanged, which explains the minor difference of shifts in the previous ^{19}F NMR spectrum.

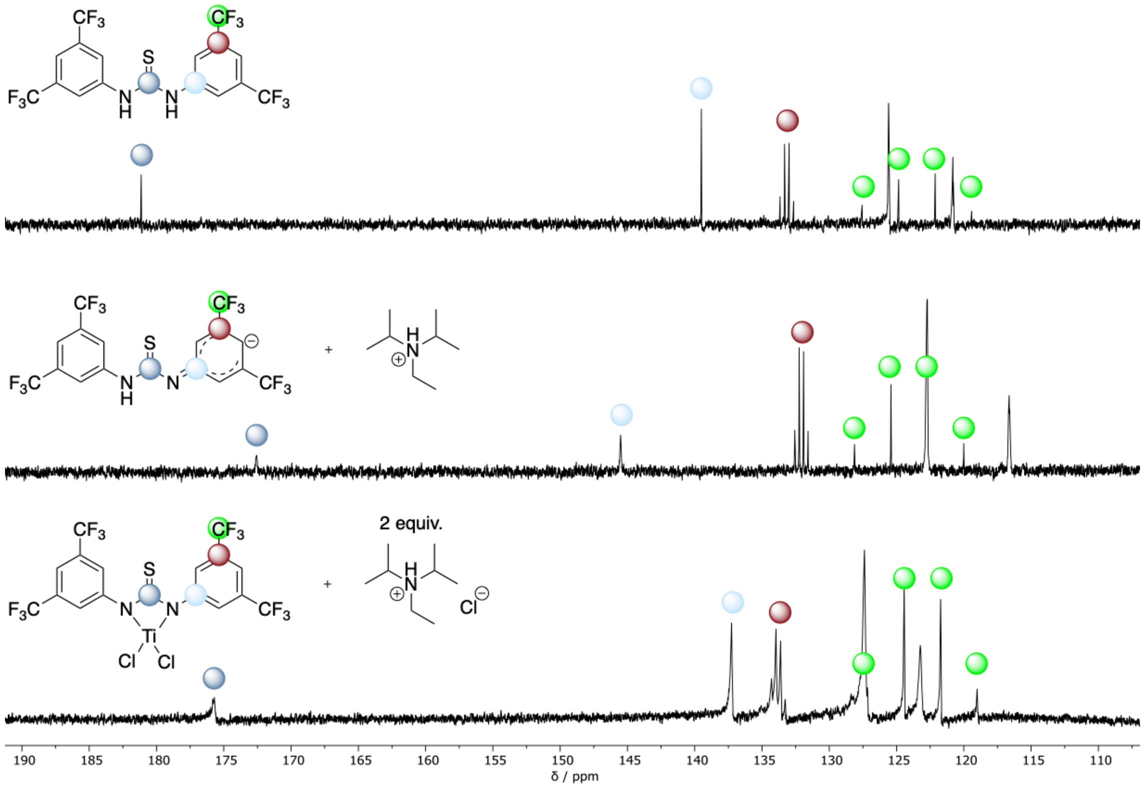

Figure 5 ^{13}C NMR spectra of **62** and of the Ti-thiourea complex in CD_2Cl_2.

Based on the NMR spectra we conclude that the Ti-thiourea complex formation occurs in symmetrical coordination (**66a**), in accordance with the results by Schreiner and Hrdina for Si-thiourea complex **18**.

Manners reported in 2013, that for Ti(III) complexes, no ^{1}H- and ^{13}C spectroscopy resonances can be observed.[60] Because we clearly observed resonances, we assume that either two or four chloride ligands must be present in complex **66a**. In order to determine the number of chloride ligands the complex was studied by high resolution mass spectrometry. Together with the Institute for Analytical Chemistry, we carried out several MS and fragmentation experiments.

Schreiner and Hrdina were able to unambiguously detect species **18** in their MS experiments.[36] However, in both negative and positive mode, we predominantly observed the m/z signal associated of **62**. Moreover, checking for the isotope pattern of titanium no corresponding signals were observed. (Fig. 6). This could be due to hydrolysis of the complex during the injection or an excessively high ionization energy that may lead to fragmentation of the complex during ionization.

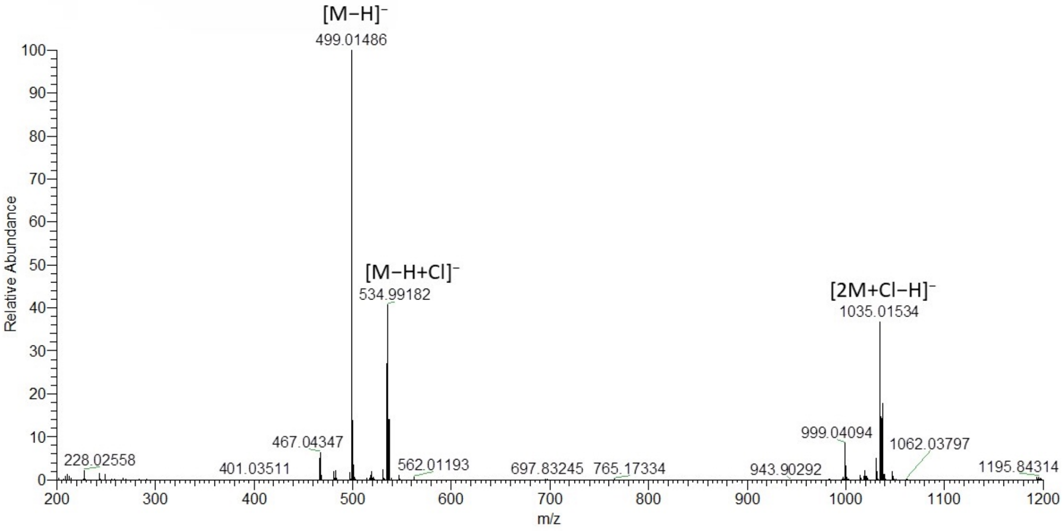

Figure 6 FT-ICR spectra in negative mode of the *in situ* formed Ti-thiourea-complex **66a**.

We also performed DFT calculations to further characterize the catalyst structure. Figure 7 shows the optimized geometry of the thiourea-Ti complex **66a** at the B3LYP/6-31+G(d,p) level of theory. A four-membered ring with slightly twisted phenyl substituents was identified as energetic minimum. The natural bond orbital (NBO) analysis suggested similarities to the thiourea-Si complex **18**.[36] Both structures can be viewed as internal salts.

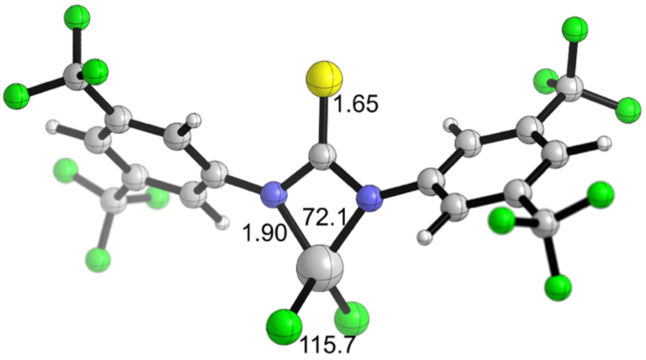

T1·SiCl$_2$ **18**		T1·TiCl$_2$ **66a**	
atom	**NBO Charge**	**atom**	**NBO Charge**
S	−0.032	S	−0.037
C (C=S)	0.233	C (C=S)	0.199
N	−0.863	N	−0.623
Si	1.782	Ti	0.995
Cl	−0.302	Cl	−0.166

Figure 7 B3LYP/6-31+G(d,p)-optimized structure of **66a** with NBO charges.

3.1.5. Investigating the Thiourea Scope

After catalyst characterization, we tried to enhance the thiourea scope for the titanium complexation in the catalytic HMR. Various titanium-thiourea complexes were generated *in situ* and tested in the rearrangement of epoxide **42** (Tab. 4). Previously optimized conditions were used with NaH as base. All reactions provided aldehyde **59** as predominant product, but ketone **60** and chloroalcohol **61** were always detected as by-products. Comparing the results of thioureas **62**, **67**, **68**, and urea **69**, we observed a dependency on the pK_a value. The more acidic the ligand, the better the yield of aldehyde **59** (Table 4, entries 1-4).[61] This observation is consistent with the results of the thiourea-Si complexes by Hrdina and Schreiner.[36] As a result, we reached the highest yield of 84% with Schreiner's thiourea **62** (entry 4). Although, squaramide **52** and thiosquaramide **53** are even more acidic, they provided much lower yields than their urea or thiourea pendants (entries 5 and 6). One reason could be that the aromatic structure, which is obtained by double deprotonation of the thiosquaramide, is stabilized by mesomerism and thus bears higher electron density, which results in reduced catalytic activity (Fig. 8).[62] Chiral thiourea **49** provided much lower conversion than the achiral thioureas, due to the decreased acidity of the N-H protons (entry 7).

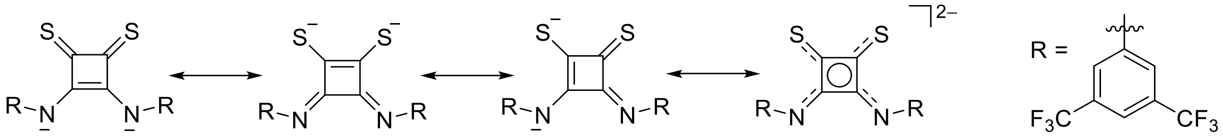

Figure 8 Mesomeric stabilization of doubly deprotonated thiosquaramide.

Table 4 Impact of different thioureas with $TiCl_4$ in the HMR of epoxide **42**.

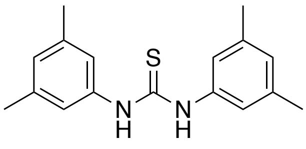

67

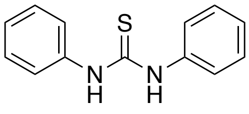

68

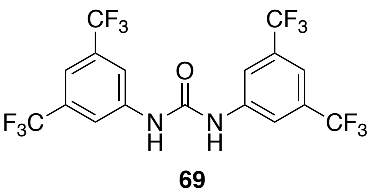

69

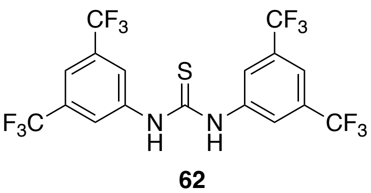

62

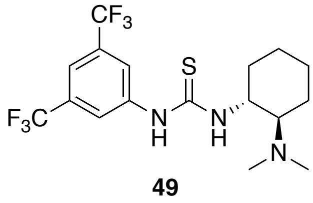

49

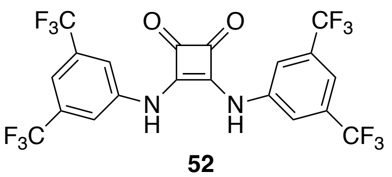

52

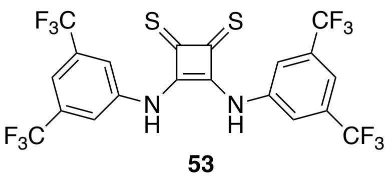

53

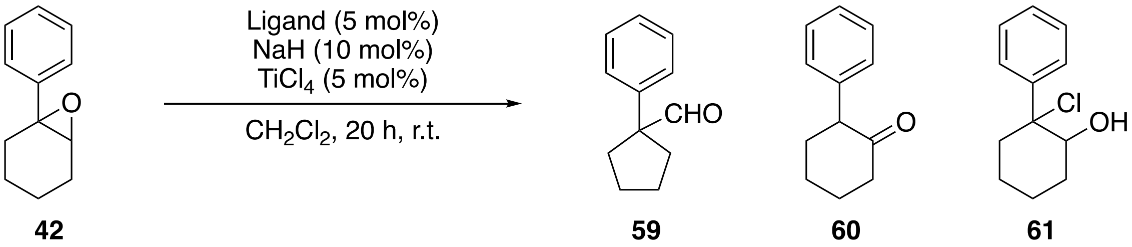

Entry	Ligand	59 [%][a]	60 [%][a]	61 [%][a]
1	**67**	29	4	3
2	**68**	45	5	4
3	**69**	59	4	6
4	**62**	84	8	3
5	**52**	5	2	1
6	**53**	44	3	2
7	**49**	23	2	4

[a] Conversion and product ratios were determined *via* ^{1}H NMR spectroscopy with *p*-nitrobenzaldehyde as internal standard.

Since chiral ligand **49** only provided poor yield, we did not try further chiral catalysts, but rather focused on Schreiner's thiourea **62** as our best working ligand. We extended the substrates to epoxides **43a** and **43b** with various solvents and at different reaction temperatures. Both epoxides showed a slight background reaction, which, however, appeared to be negligible (Table 5, entries 1 and 2). As expected, yields for the chlorinated epoxide **43b** were lower, which can be explained by the lower electron density in the benzylic position.[36] Generally, both epoxides performed worse in the rearrangement to the aldehyde than epoxide **42**. Although the epoxides were usually completely converted, larger proportions of by-products, such as ketone or chloroalcohol, formed. When we performed the reactions in THF or toluene, we obtained only low yields of the aldehyde (entries 7 and 8), whereas in chlorinated solvents the rearrangement generally performed better. Furthermore, the yields could be increased with a catalyst loading of 10 mol% (entries 11 and 12). Analogous to epoxide **42**, only small amounts of rearrangement product were obtained when squaramide **52** was used as ligand (entries 9 and 10). Almost no rearrangements occurred at −10 °C, even after 42 h (entries 13-15). Based on these results, the most promising reaction conditions were determined to be with 10 mol% of catalyst **62** in CH_2Cl_2 at room temperature.

Table 5 HMR of trisubstituted epoxides **43a** and **b** catalyzed by thiourea-Ti complexes.

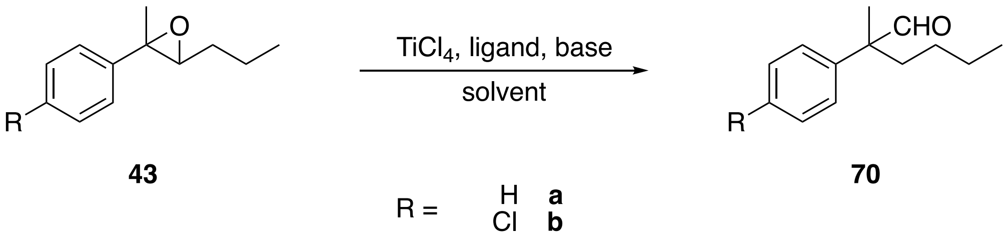

Entry	**R**	**Ligand**	**Solvent**	**T [°C]**	***t* [h]**	**Conversion [%]**[a]
1	H	-	CH_2Cl_2	r.t.	20	16
2	Cl	-	CH_2Cl_2	r.t.	20	<1
3	H	**62** 5 mol%	CH_2Cl_2	r.t.	20	43
4	Cl	**62** 5 mol%	CH_2Cl_2	r.t.	20	28
5	H	**62** 5 mol%	Toluene	r.t.	20	5
6	Cl	**62** 5 mol%	Toluene	r.t.	20	15
7	H	**62** 5 mol%	THF	r.t.	20	8
8	Cl	**62** 5 mol%	THF	r.t.	20	<1
9	H	**52** 5 mol%	CH_2Cl_2	r.t.	20	17
10	Cl	**52** 5 mol%	CH_2Cl_2	r.t.	20	6
11	Cl	**62** 10 mol%	CH_2Cl_2	r.t.	20	35
12	Cl	**62** 10 mol%	$C_2H_4Cl_2$	r.t.	20	33
13	H	**62** 10 mol%	CH_2Cl_2	−10 °C	42	15
14	Cl	**62** 10 mol%	CH_2Cl_2	−10 °C	42	<1
15	Cl	**62** 10 mol%	$C_2H_4Cl_2$	−10 °C	42	<1

[a] Conversion was determined *via* ^{1}H NMR spectroscopy with *p*-nitrobenzaldehyde as internal standard.

3.1.6. Application of the HMR

Finally, we aimed to employ the established Ti-thiourea complex in the rearrangement of biscyclohexyl epoxide (**72**). The catalytic rearrangement of **72** by an alkyl shift would provide a quaternary spiro ketone, which is difficult to access by other methods. Therefore, we synthesized olefine **71** by a McMurry coupling of cyclohexanone.[63] The subsequent Prileschajew epoxidation provided epoxide **72** in 25% yield (Scheme 18).

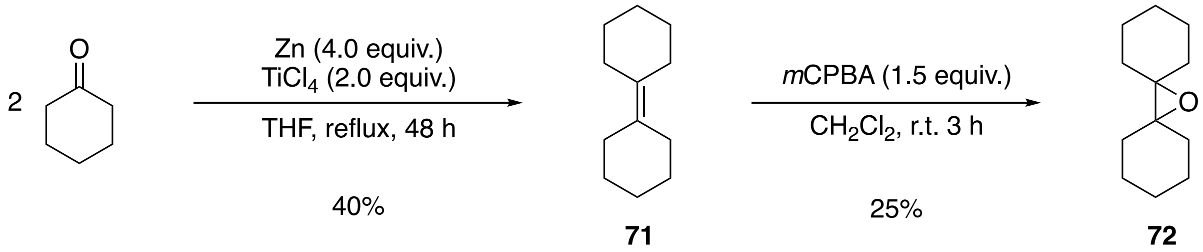

Scheme 18 Synthesis of epoxide **72** *via* McMurry coupling of cyclohexanone followed by Prileschajew epoxidation.

We employed epoxide **72** in the HMR under the previous reaction conditions with thiourea **62** as our best working ligand and additionally Takemoto's thiourea **49** as chiral ligand (Tab. 6). Unfortunately, with both catalysts we obtained inferior yields at room temperature (entries 1 and 2). A slight increase of yield could be achieved at elevated temperatures even when chiral thiourea **49** was used (entries 3 and 4). However, we were not able to separate the enantiomers by stationary phase GC or HPLC to check for stereoselectivity.

Table 6 Meinwald rearrangement of epoxide **72** to quaternary spiro ketone **73**.

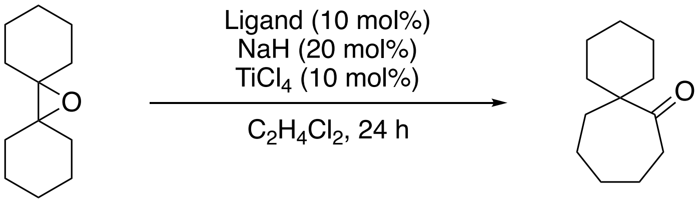

72 **73**

Entry	Ligand	T [°C]	Yield [%][a]
1	**62**	r.t.	8
2	**49**	r.t.	6
3	**62**	45 °C	17
4	**49**	45 °C	15

[a] Yield of isolated product.

In summary, we established a Lewis acid enhancement protocol by complexation of $TiCl_4$ to thioureas. The complexes showed catalytic activity in the HMR of several epoxides. However, in our test reactions, the conversion to the desired aldehyde as rearrangement product was generally low. Especially asymmetric thiourea **49** provided only poor yields, therefore an efficient asymmetric rearrangement did not seem to be achievable. Thus, we did not pursue the complexation of thioureas any longer but rather envisaged the complexation with chiral BINOL derivatives.

3.2. BINOL Assisted Lewis Acids in the HMR

With the thiourea-silicon complex developed in the Schreiner group, trisubstituted epoxides can be transformed into quaternary aldehydes in a stereospecific rearrangement (Scheme 5).[36] However, the use of asymmetric thioureas and the use of alkylsilanes instead of $SiCl_4$ only provides low yields in the rearrangement. Consequently, we investigated the use of other Lewis acids, such as $TiCl_4$ in combination with thioureas or (thio)-squaramides. Although the combination of Schreiner's thiourea **62** and $TiCl_4$ provided high yields in the rearrangement of epoxide **42**, the HMR of trisubstituted epoxides **43a** and **43b** only provided low yields of the desired aldehyde and moreover the formation of undesired by-products. Furthermore, we encountered similar difficulties as with the use of thioureas and $SiCl_4$. Except for **62**, no other thiourea, squaramide or thiosquaramide was able to convince in the HMR with $TiCl_4$. A catalyst-controlled enantioselective HMR is therefore hardly possible with this strategy.

Due to the known *in situ* formation of BINOL-Ti complexes and their reported catalytic activity in various reactions, we investigated whether BINOL-Ti complexes can be employed for an enantioselective HMR of epoxides.[42–45]

3.2.1. BINOL Ti Complex

As proof of concept, we tested the catalytic activity of readily available unsubstituted (*R*)-BINOL (**74**) in a combination with $Ti(O^iPr)_4$ in the rearrangement of epoxide **42**. The BINOL-Ti complexes were prepared *in situ*, with the resulting ^iPrOH being trapped by 4 Å MS (Tab. 7). First, possible background reactions with (*R*)-BINOL (**(*R*)-74**) or $Ti(O^iPr)_4$, as well as the combination of $Ti(O^iPr)_4$ and 4 Å MS were investigated. While (*R*)-BINOL (**(*R*)-74**) or $Ti(O^iPr)_4$ did not catalyze the rearrangement to aldehyde **59** even after 66 h (Table 7, entries 1 and 2), the combination with 4 Å MS in CH_2Cl_2 led to a very low background reaction, which however was considered to be negligible (entry 3). In the non-polar solvent toluene, this background reaction practically did not take place (entry 4), which can be explained by the well-known formation of $Ti(O^iPr)_4$ monomers in non-polar solvents, so that an exchange of an isopropoxide ligand with the epoxide for catalysis is not possible. With the (*R*)-BINOL-Ti complex, the rearrangement selectively provided aldehyde **59** in 65% yield (entry 5). Because this promising result clearly indicates the activation of $Ti(O^iPr)_4$ by BINOL we were encouraged to test also various substituted BINOL derivatives, as the substitution pattern may tune both activity and selectivity of BINOL catalysts.[64]

Table 7 HMR of epoxide **42** catalyzed by Ti(O^{i}Pr)$_4$ and in combination with (*R*)-BINOL ((***R***)**-74**).

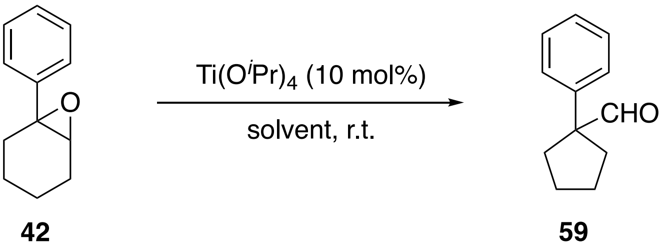
Ti(O^{i}Pr)$_4$ (10 mol%)
solvent, r.t.
O
CHO
42
59

Entry	(*R*)-BINOL	Molecular sieve	Solvent	*t* [h]	42 [%][a]	59 [%][a]
1[b]	10 mol%	-	CH_2Cl_2	66	99	<1
2	-	-	CH_2Cl_2	66	97	<1
3	-	4 Å MS	CH_2Cl_2	66	73	13
4	-	4 Å MS	Toluene	66	97	<1
5	10 mol%	4 Å MS	CH_2Cl_2	22	<1	65

[a] Conversion was determined *via* ^{1}H NMR spectroscopy with *p*-nitrobenzaldehyde as internal standard; [b] reaction without Ti(O^{i}Pr)$_4$.

3.2.2. Synthesis of Substituted BINOL Ligands

For the synthesis of substituted BINOL derivatives, we started from readily available unsubstituted (*R*)-BINOL ((***R***)**-74**) by protection of the hydroxy groups. Methylation using methyl iodide afforded (*R*)-2,2'-dimethoxy-1,1'-binapthtyl ((***R***)**-75**) in quantitative yield.[65] In order to halogenate (***R***)**-75** in both 3-positions, we performed a directed *ortho* lithiation with *n*-BuLi in combination with tetramethylethylenediamine (TMEDA) followed by addition of iodine to achieve the double iodinated product (***R***)**-76** in 77% yield.[66,67] The subsequent Kumada reaction with freshly prepared 2,4,6-triisopropylphenyl Grignard reagent afforded the coupling product (***R***)**-77a** in 46% yield.[66] Afterwards methyl ether deprotection by treatment with boron tribromide afforded BINOL derivative (***R***)**-78a** in an overall yield of 31% over four steps after hydrolysis (Scheme 19).

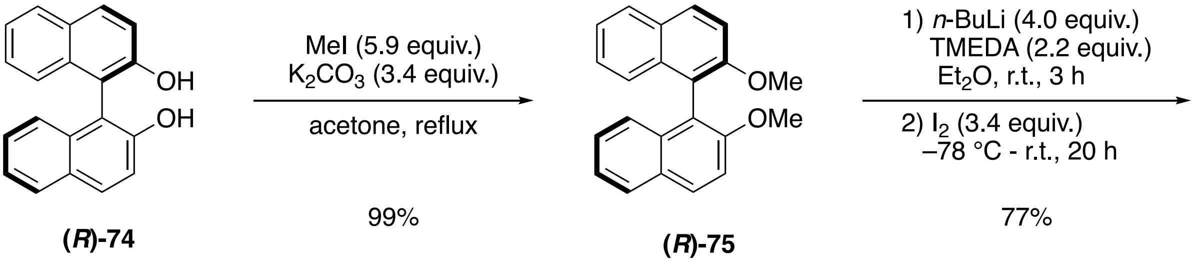
OH
OH
(R)-74
MeI (5.9 equiv.)
K$_2$CO$_3$ (3.4 equiv.)
acetone, reflux
99%
OMe
OMe
(R)-75
1) n-BuLi (4.0 equiv.)
TMEDA (2.2 equiv.)
Et$_2$O, r.t., 3 h
2) I$_2$ (3.4 equiv.)
−78 °C - r.t., 20 h
77%

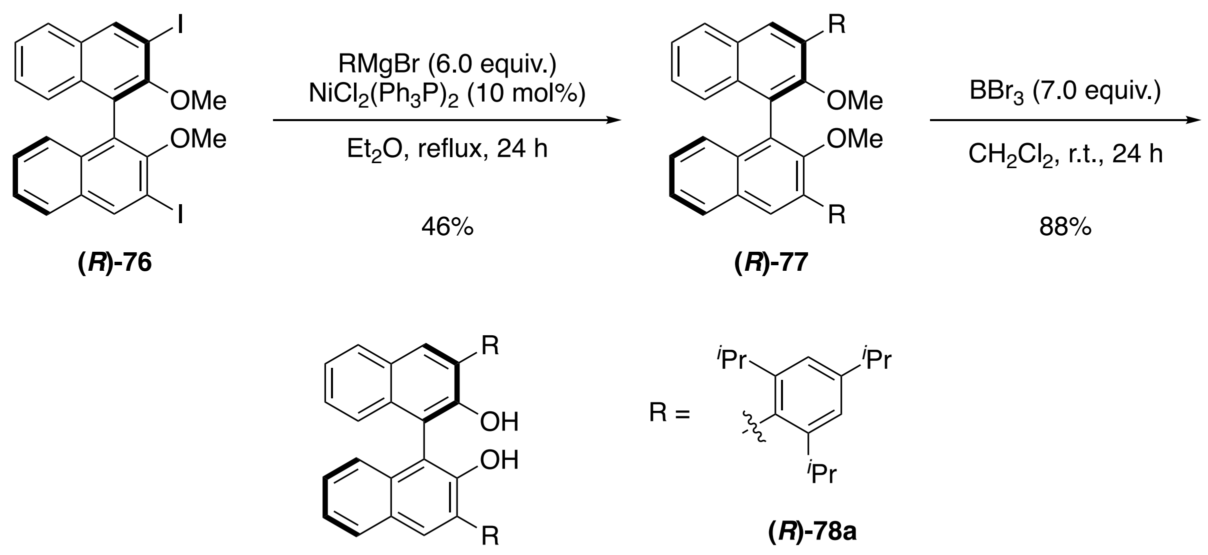
I
OMe
OMe
I
(R)-76
RMgBr (6.0 equiv.)
NiCl2(Ph3P)2 (10 mol%)
Et2O, reflux, 24 h
46%
R
OMe
OMe
R
(R)-77
BBr3 (7.0 equiv.)
CH2Cl2, r.t., 24 h
88%
R
OH
OH
R
R =
iPr
iPr
iPr
(R)-78a

Scheme 19 Synthesis of (*R*)-BINOL derivative **78a** *via* Kumada coupling.[65–67]

Since the Kumada coupling only proceeded in 46% yield, we decided to synthesize further BINOL derivatives *via* Suzuki coupling.[68] Therefore, after *ortho* lithiation of **(*R*)-75** we added triethyl borate with subsequent hydrolysis to achieve the corresponding diboronic acid **(*R*)-79** in high yield. Then the 3,5-bis(trifluoromethyl)phenyl and 1-naphthyl groups were introduced from the corresponding bromides in Suzuki couplings, in which the crude products were directly deprotected by treatment with BBr_3. In this way, **(*R*)-78b** was obtained in four steps with an overall yield of 74% and **(*R*)-78c** with 77% (Scheme 20).

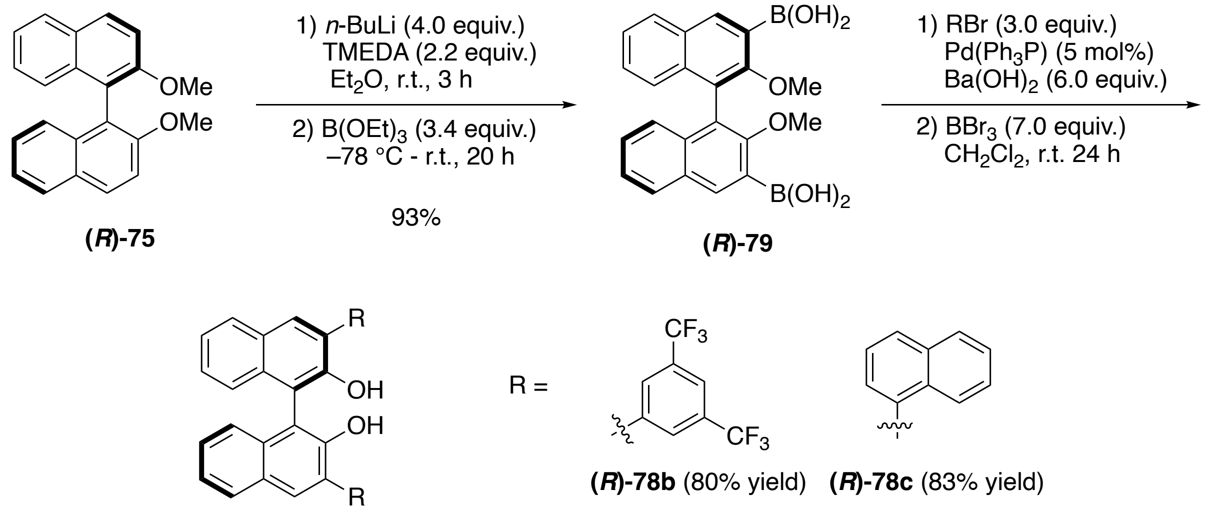
OMe
OMe
(R)-75
1) n-BuLi (4.0 equiv.)
TMEDA (2.2 equiv.)
Et2O, r.t., 3 h
2) B(OEt)3 (3.4 equiv.)
–78 °C - r.t., 20 h
93%
B(OH)2
OMe
OMe
B(OH)2
(R)-79
1) RBr (3.0 equiv.)
Pd(Ph3P) (5 mol%)
Ba(OH)2 (6.0 equiv.)
2) BBr3 (7.0 equiv.)
CH2Cl2, r.t. 24 h
R
OH
OH
R
R =
CF3
CF3
(R)-78b (80% yield)
(R)-78c (83% yield)

Scheme 20 Synthesis of (*R*)-BINOL derivatives **78b** and **78c** *via* Suzuki coupling.[65–68]

For an easier and more practicable hydroxy protection/deprotection without the need for Schlenk conditions, we changed to the methoxymethyl protecting group (MOM). The MOM protecting group was introduced by bromomethyl methyl ether after deprotonation of (*R*)-BINOL (**(*R*)-74**) with NaH, whereby **(*R*)-80** was obtained in 93% yield.[66] In contrast to the previous aryl residues, the perfluorophenyl group was attached directly after *ortho* lithiation of **(*R*)-80** by substitution with perfluorobenzene.[69] The disubstituted product **(*R*)-81** was isolated in 57% yield. Acidic cleavage of the acetal provided the desired BINOL derivative **(*R*)-78d** in an overall yield of 48% (Scheme 21).

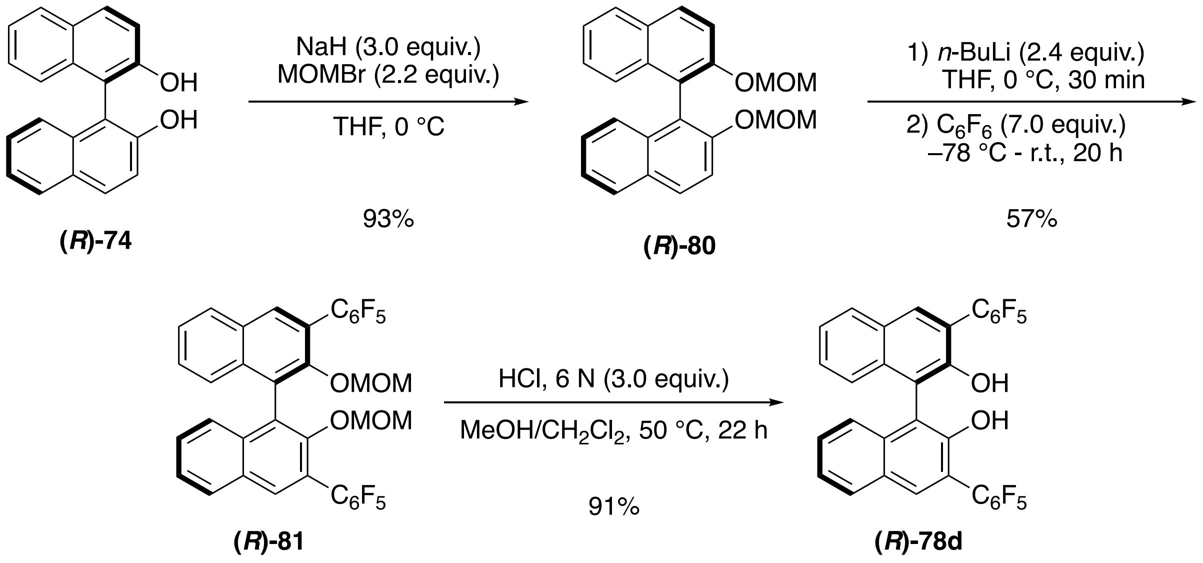
OH
OH
(R)-74
NaH (3.0 equiv.)
MOMBr (2.2 equiv.)
THF, 0 °C
93%
OMOM
OMOM
(R)-80
1) n-BuLi (2.4 equiv.)
THF, 0 °C, 30 min
2) C6F6 (7.0 equiv.)
–78 °C - r.t., 20 h
57%
C6F5
OMOM
OMOM
C6F5
(R)-81
HCl, 6 N (3.0 equiv.)
MeOH/CH2Cl2, 50 °C, 22 h
91%
C6F5
OH
OH
C6F5
(R)-78d

Scheme 21 Synthesis of (*R*)-BINOL derivative **78d**.[69]

In addition to the disubstituted derivatives, we also tested a monosubstituted BINOL derivative in the titanium catalyzed HMR. For monosubstitution in the 3-position, we performed the *ortho* lithiation with reduced equivalents of *n*-BuLi and TMEDA, again followed by addition of $B(OEt)_3$ and hydrolysis to the boronic acid **(*R*)-82**.[70] The reduced equivalents of *n*-BuLi and TMEDA as well as a challenging chromatographic separation of disubstituted product led to only 28% yield. Nonetheless, the 3,5-bis(trifluoromethyl)phenyl group was attached in a Suzuki coupling followed by acidic acetal cleavage to provide monosubstituted catalyst **(*R*)-83** in an overall yield of 23% over four steps (Scheme 22).

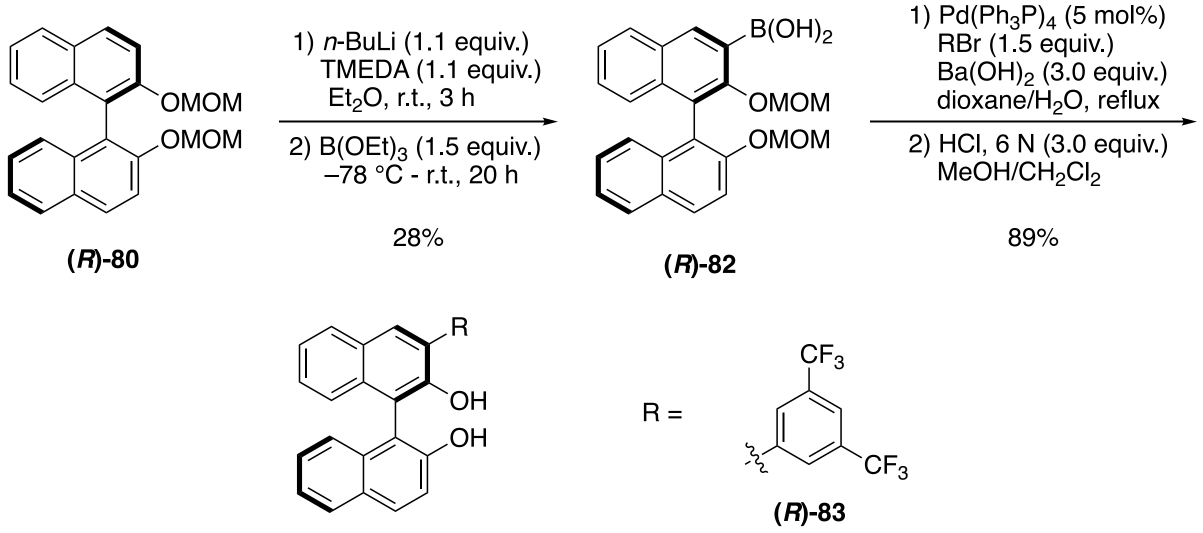
OMOM
OMOM
(R)-80
1) n-BuLi (1.1 equiv.)
TMEDA (1.1 equiv.)
Et2O, r.t., 3 h
2) B(OEt)3 (1.5 equiv.)
–78 °C - r.t., 20 h
28%
B(OH)2
OMOM
OMOM
(R)-82
1) Pd(Ph3P)4 (5 mol%)
RBr (1.5 equiv.)
Ba(OH)2 (3.0 equiv.)
dioxane/H2O, reflux
2) HCl, 6 N (3.0 equiv.)
MeOH/CH2Cl2
89%
R
OH
OH
R =
CF3
CF3
(R)-83

Scheme 22 Synthesis of monosubstituted (*R*)-BINOL derivative **(*R*)-83**.[70]

3.2.3. Catalytic HMR

With the substituted BINOL ligands in hand, we compared their catalytic activity in the HMR of epoxide **42** employing 10 mol% of ligand, 10 mol% of $Ti(O^iPr)_4$, and 4 Å MS in CH_2Cl_2 (Tab. 8). While the combination of $Ti(O^iPr)_4$ and unsubstituted (*R*)-BINOL (**(*R*)-74**) catalyzed the rearrangement in 65% conversion after 22 h (entry 1), disubstituted BINOL derivatives generally provided low conversion. Ligand **(*R*)-78a** provided almost no reaction after 22 h (entry 2). The use of other solvents also did not result in higher conversion (entries 3 and 4) and after 68 h still only low conversion to aldehyde **59** was detected (entry 5). Disubstituted ligands **(*R*)-78b** and **(*R*)-78c** gave equally poor results even after 68-80 h reaction time (entries 6 and 7). Only the perfluorophenyl substituted derivative **(*R*)-78d** showed a noticeable catalytic activity with 33% conversion after 68 h (entry 8). This indicates that disubstitution greatly reduces the catalytic activity of the BINOL-Ti complexes in the HMR. Surprisingly, the monosubstituted ligand **(*R*)-83** selectively catalyzed the rearrangement to aldehyde **59** in high conversion after 22 h (entry 9).

Table 8 HMR of epoxide **42** catalyzed by various BINOL-Ti complexes.

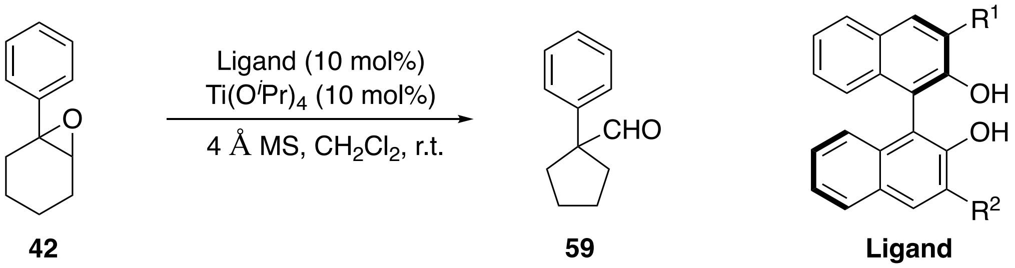

Entry	Ligand	R^1	R^2	*t* [h]	**42** [%][a]	**59** [%][a]
1	**(*R*)-74**	H	H	22	<1	65
2	**(*R*)-78a**	$2,4,6\text{-}(^iPr)_3Ph$	$2,4,6\text{-}(^iPr)_3Ph$	22	90	<1
3[b]	**(*R*)-78a**	$2,4,6\text{-}(^iPr)_3Ph$	$2,4,6\text{-}(^iPr)_3Ph$	22	94	<1
4[c]	**(*R*)-78a**	$2,4,6\text{-}(^iPr)_3Ph$	$2,4,6\text{-}(^iPr)_3Ph$	22	88	10
5	**(*R*)-78a**	$2,4,6\text{-}(^iPr)_3Ph$	$2,4,6\text{-}(^iPr)_3Ph$	68	63	24
6	**(*R*)-78b**	1-naphthyl	1-naphthyl	80	71	8
7	**(*R*)-78c**	$3,5\text{-}(CF_3)_2Ph$	$3,5\text{-}(CF_3)_2Ph$	68	65	12
8	**(*R*)-78d**	C_6F_5	C_6F_5	68	45	33
9	**(*R*)-83**	$3,5\text{-}(CF_3)_2Ph$	H	22	<1	85

[a] Conversion was determined *via* ^{1}H NMR spectroscopy with *p*-nitrobenzaldehyde as internal standard; [b] reaction was performed in THF; [c] reaction was performed in toluene.

Next we employed the BINOL catalysts in the rearrangement of trisubstituted epoxide **43a** again employing 10 mol% of ligand, 10 mol% of $Ti(O^iPr)_4$, and 4 Å MS in CH_2Cl_2 (Tab. 9). After 22 h, unsubstituted (*R*)-BINOL (**(*R*)-74**) catalyzed the rearrangement to aldehyde **70a** only in low conversion (entry 1). Surprisingly, we observed *ee* for the aldehyde **70a** as well as of the remaining substrate epoxide **43a**. Because the epoxides were synthesized in a racemic fashion using *m*CPBA, this may indicate a kinetic resolution. To our delight, unsubstituted (*R*)-BINOL **(*R*)-74** provided a high selectivity factor (*s* factor) of 16 for the (*S*)-enantiomer after 68 h reaction time (entry 2). Similar to our previous results, the disubstituted BINOL derivatives **(*R*)-78a-78c** showed no catalytic activity even after long reaction times (entries 5-7). Only disubstituted **(*R*)-78d** turned out to catalyze the rearrangement, but with very low conversion. In contrast, monosubstituted BINOL **(*R*)-83** provided the best conversion after 24 h, but with a lower selectivity than unsubstituted BINOL **(*R*)-74** (entry 9). Importantly, in contrast to unsubstituted (*R*)-BINOL **(*R*)-74**, disubstituted and monosubstituted derivatives catalyzed the kinetic resolution to the (*R*)-enantiomer of the aldehyde. This clearly demonstrates the effect of BINOL substitution and gives an indication of possible NCIs, which here probably represent a balance between steric repulsion and London dispersion interactions.

Table 9 Kinetic resolution of epoxide **43a** catalyzed by BINOL-Ti complexes.

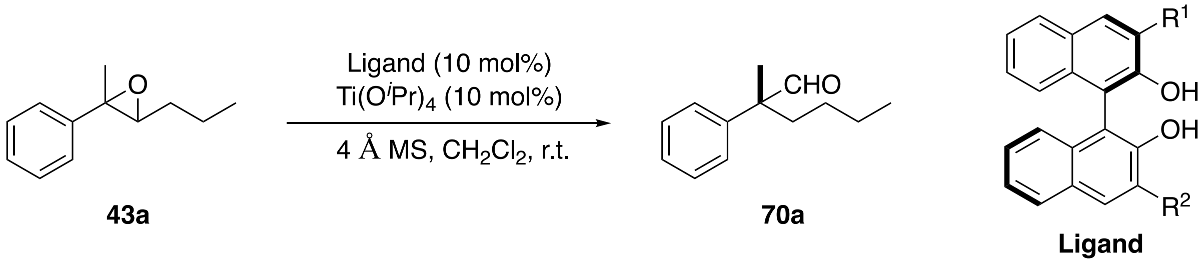

Entry	Ligand	R^1	R^2	*t* [h]	Conversion [%][a]	*ee* product [%][b]	*s* factor[c]
1	**(*R*)-74**	H	H	22	10	(*S*) 36	2
2	**(*R*)-74**	H	H	68	45	(*S*) 78	16
5	**(*R*)-78a**	2,4,6-(^{i}Pr)$_3$Ph	2,4,6-(^{i}Pr)$_3$Ph	22	<1	-	-
6	**(*R*)-78b**	1-naphthyl	1-naphthyl	68	<1	-	-
7	**(*R*)-78c**	3,5-(CF$_3$)$_2$Ph	3,5-(CF$_3$)$_2$Ph	68	<1	-	-
8	**(*R*)-78d**	C$_6$F$_5$	C$_6$F$_5$	24	3	(*R*) 18	1
9	**(*R*)-83**	3,5-(CF$_3$)$_2$Ph	H	24	42	(*R*) 12	1

[a] Conversion was determined *via* ^{1}H NMR spectroscopy with *p*-nitrobenzaldehyde as internal standard; [b] enantioselectivities were determined *via* chiral stationary phase GC; [c] selectivity factors (*s* factors) were determined following the procedure of Kagan and Fiaud.[71]

However, it should be noted that a proper calculation of the *s* factor is only possible if the kinetic resolution is first-order in substrate for the selectivity-determining step and therefore the *s* factor should be independent of conversion.[72] Comparing Table 9 entries 1 and 2, the *s* factor differs greatly by time and conversion. Moreover, with increasing conversion, the enantioselectivity of the product also increases. This is contrary to a first-order kinetic resolution, in which the enantioselectivity of the product should decrease with increasing conversion. Hence, this reaction is not a pure kinetic resolution first-order in substrate. In line with Schreiners proposed mechanism of two epoxides coordinating to the Lewis acid,[36] our results rather suggest that the catalyst activity is influenced in the course of the reaction, resulting in a more complex rate law.[72] We conclude, that for this specific case the calculation of the *s* factor may be misleading and incorrect. Thus we rather focus on conversion and product enantioselectivity.

The rearrangement of cyclic epoxide **42** always provided better conversion than epoxide **43a**, so we envisaged a kinetic resolution of a cyclic epoxide. As the rearrangement of **42** to aldehyde **59** is achiral, we synthesized substituted prochiral epoxide **86** by a simple Grignard reaction followed by Prileschajew epoxidation starting from commercially available 4,4-dimethylcyclohexanone **84** (Scheme 23). A HMR of epoxide **86** would provide the chiral aldehyde.

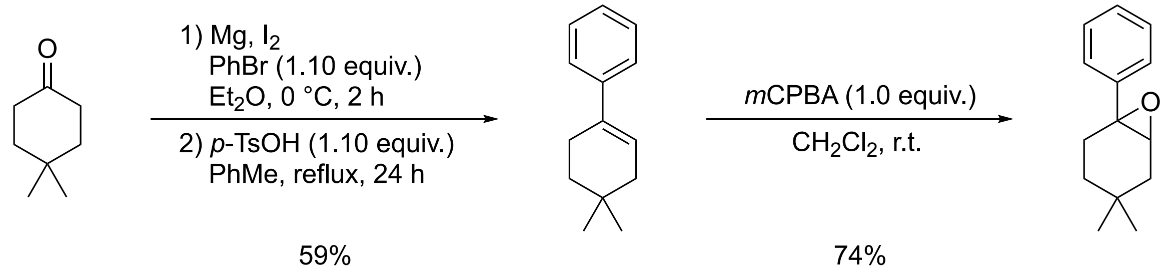

84 **85** **86**

Scheme 23 Grignard reaction followed by dehydration and Prileschajew epoxidation to afford cyclic, disubstituted epoxide **86**.

We employed epoxide **86** in the catalyzed HMR under previously used reaction conditions (Tab. 10). In fact, we were able to observe a kinetic resolution, too. Using unsubstituted (*R*)-BINOL (**(*R*)-74**), the (*R*)-enantiomer of aldehyde **87** formed with 56% conversion and 41% *ee* (entry 1). Disubstituted BINOL **(*R*)-78d** performed the rearrangement in a lower conversion, but with a comparable selectivity of 50% *ee* for the (*S*)-enantiomer (entry 2). Monosubstituted derivative **(*R*)-83** provided good conversion, but low selectivity for the (*S*)-enantiomer (entry 3). These results are consistent with the results obtained with **43a** (Tab. 10). In both cases the disubstituted BINOL derivatives provided only low conversion but good selectivities, whereas monosubstituted BINOL **(*R*)-83** facilitated the HMR in good conversion but low selectivities. The overall best results were achieved with unsubstituted BINOL **(*R*)-74** affording both, good conversion and selectivity.

Table 10 Kinetic resolution of epoxide **86** catalyzed by BINOL-Ti complexes

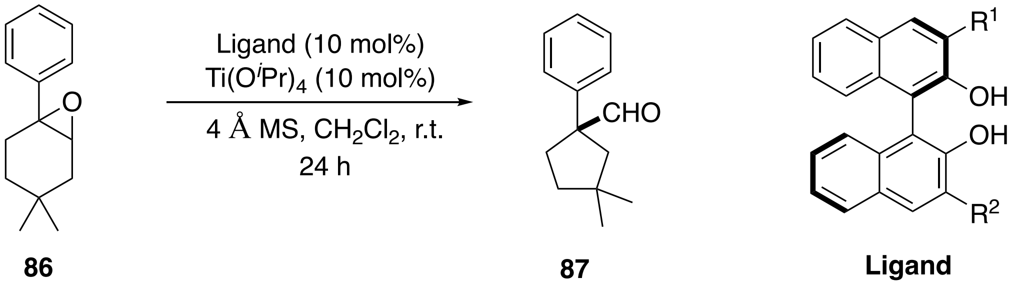

Entry	Ligand	R^1	R^2	Conversion [%][a]	*ee* product [%][b]
1	**(*R*)-74**	H	H	56	(*R*) 41
2	**(*R*)-78d**	C_6F_5	C_6F_5	28	(*S*) 50
3	**(*R*)-83**	3,5-$(CF_3)_2$Ph	H	55	(*S*) 8

[a] Conversion was determined *via* ^{1}H NMR spectroscopy with *p*-nitrobenzaldehyde as internal standard; [b] enantioselectivities were determined *via* chiral stationary phase GC;

4. Summary & Outlook

In this work, we investigated the concept of Lewis acid enhancement of various Lewis acids with thiourea as well as BINOL ligands for the application in the rearrangement of epoxides. Therefore we took up previous work by the group of Schreiner, which utilized a combination of thiourea **62** with $SiCl_4$ for a stereospecific HMR.[36] A screening of **62** with various Lewis acids determined $TiCl_4$ as a potent combination for complex formation, which we have proven by NMR studies. The **62-Ti** complex showed catalytic activity in the rearrangement of epoxide **42** (Scheme 24). However, substituting **62** with other thioureas, ureas, squaramides, or thiosquaramides resulted in very low conversion. For ureas and thioureas we observed a dependency of catalytic activity on pK_a, whereas squaramides and thiosquaramides generally performed worse, probably because of their aromatic nature after deprotonation.[62] This confirms the superior catalytic enhancement by **62**, but makes the use of other achiral and even chiral ligands less desirable.

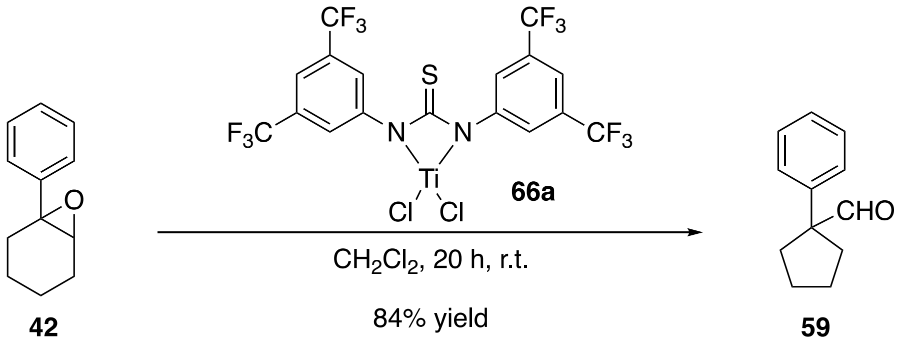

Scheme 24 HMR of epoxide **42** catalyzed by thiourea-Ti complex **66a**.

As a possible application we described the synthetic route to biscyclohexyl epoxide **72**, which was employed in the rearrangement to spiro ketone **73** (Scheme 25). These ketones are difficult to access using other methods. Utilizing thiourea-Ti complexes, we were able to synthesize spiro ketone **73**, but just in low yield. For future experiments, an optimization of reaction conditions *via* a Design of Experiments (DoE) approach is necessary. Some parameters such as different bases, solvents, and temperatures have already been tested. Since higher temperatures and solvents with a high dipole moment seemed to give better yields, the use of dichloroethane (b.p. 82 °C), 1,1,2,2-tetrachloroethane (b.p. 147 °C), chlorobenzene (b.p. 131 °C), *o*-dichlorobenzene (b.p. 179 °C), α,α,α-trifluorotoluene (b.p. 102 °C), and benzonitrile (b.p.: 191 °C) should be investigated first.

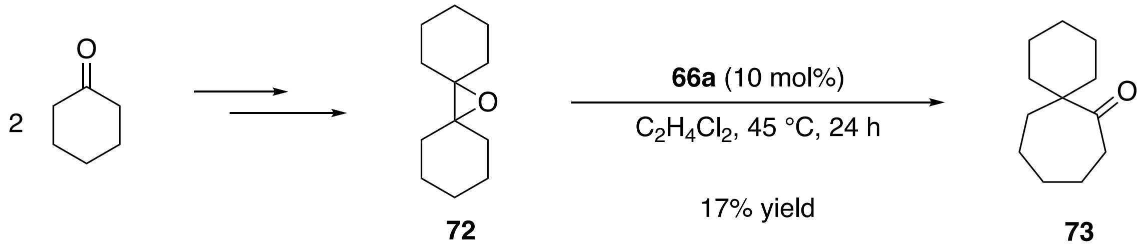

Scheme 25 Synthesis of biscyclohexyl epoxide **72** and catalytic HMR to spiro ketone **73**.

Because Takemoto's chiral thiourea **49** did not lead to promising results in the Lewis acid enhanced epoxide rearrangement, we further investigated the combination of titanium Lewis acids in combination with chiral BINOL ligands. Therefore, we employed various chiral BINOL ligands with $Ti(O^iPr)_4$ in the HMR of several epoxides. Surprisingly, in the rearrangement of epoxides **43a** and **86** we observed a kinetic resolution (Scheme 26). As there are no reports about a kinetic resolution in epoxide rearrangements up to date, this is a new and important finding that should be further pursued. In accordance with the previous results of the Schreiner group[36] our results suggest that this kinetic resolution does not obey a first-order in substrate but a more complex rate law.[72] Therefore, the calculation of the *s* factor can be incorrect and the specification of the enantioselectivity should be preferred. While unsubstituted (*R*)-BINOL ((***R*)-74**) delivered overall good results in the kinetic resolution, disubstituted BINOL derivative **(*R*)-78d** provided good selectivity but only traces of product. In contrast, monosubstituted BINOL derivative **(*R*)-83** performed the rearrangements in good yields, but low selectivity. Moreover, the substituted (*R*)-BINOL derivatives catalyzed the kinetic resolution to the opposite enantiomer than unsubstituted (*R*)-BINOL, which indicates the influence of NCIs for selectivity in the rearrangement.

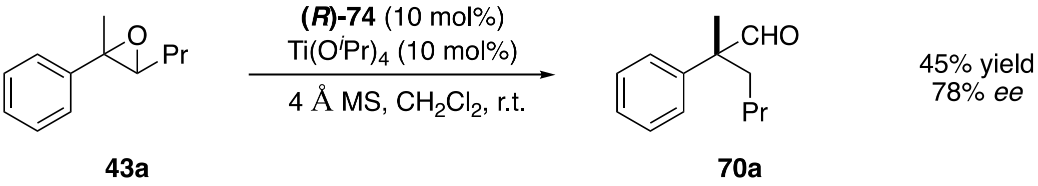

Scheme 26 Kinetic resolution of epoxide **43a** catalyzed by BINOL-Ti complexes.

These results are a good starting point for a DoE to maximize yield and selectivity. Therefore, the unsubstituted and disubstituted BINOL derivatives should be used preferentially, while monosubstituted derivatives are negligible because of the unpromising selectivity. Afterwards, the substrate scope should be extended. Epoxide **43a** was synthesized *via* a Wittig route, so other derivatives are easily accessible by changing the starting materials, many of which are commercially available.

The group of Gschwind recently investigated structural effects and noncovalent interactions in Brønsted acid catalysis of 3,3′-substituted BINOL derived phosphoric acids, using in depth NMR spectroscopy studies in conjunction with quantum mechanical computations.[73–75] To elucidate possible interactions which lead to the difference in selectivity in our epoxide rearrangement, a cooperation with the Gschwind group could be considered.

5. Experimental Section

5.1. General Information

Unless otherwise noted, chemicals were purchased from Acros Organics, TCI, Alfa Aesar, Lancaster, Merck, or Fluka at the highest purity grade available and were used without further purification. All solvents were distilled prior to use. Toluene, THF, and CH_2Cl_2, were distilled from appropriate drying agents prior to use and stored under argon atmosphere. All catalytic reactions were carried out under an argon atmosphere employing oven- and flame-dried glassware. Column chromatography was conducted using Merck silica gel 60 (0.040 – 0.063 mm).

5.2. Analytical Methods

Thin Layer Chromatography (TLC) was performed on silica coated plates (*Merck*, silica 60 F254) with detection by UV-light ($\lambda = 254$ nm) and/or by staining with a cerium ammonium molybdate solution [CAM] and developed by heating.

CAM-staining solution: cerium sulfate tetrahydrate (1.00 g), ammonium molybdate (25.0 g), and concentrated sulfuric acid (25.0 mL) in water (250 mL).

Nuclear Magnetic Resonance (NMR) spectra were recorded at room temperature either on a *Bruker* AV-400 or a *Bruker* AV-400HD. ^{1}H NMR spectra were referenced to the residual proton signal of $CDCl_3$ ($\delta = 7.26$ ppm). ^{13}C NMR spectra were referenced to the ^{13}C-D triplet of $CDCl_3$ ($\delta = 77.2$ ppm). The following abbreviations for single multiplicities were used: *br* = broad, s = singlet, d = doublet, t = triplet, q = quartet, quint = quintet, sept = septet.

High resolution mass spectrometry (HRMS) was performed employing either a Bruker MicrOToF or a Bruker Impact II using methanol solutions of the respective compounds.

Chiral Gas Chromatography (GC): Enantioselectivities were determined by chiral stationary phase GC analyses on Hewlett Packard 5890 or 6890 gas chromatographs, respectively.

5.3. Standards for Catalysis

GC analytics of chiral aldehydes

α-Butyl-α-methylbenzeneacetaldehyde (70a)

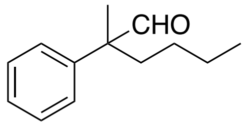

Enantioselectivity was determined *via* chiral stationary phase GC employing a 30 m FS-Hydrodex γ-TBDAc column (Macherey Nagel).

T (Injector + Detector) = 250 °C

Splitflow = 80 mL min^{-1}

Precolumn pressure = 0.8 bar

Conditions: 100 – 190 °C, 2 °C min^{-1}

Retention Times: (*R*) = 19.1 min; (*S*) = 19.3 min

1-Phenyl-3,3-dimethylcyclopentanecarboxaldehyde (87)

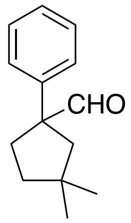

Enantioselectivity was determined *via* chiral stationary phase GC employing a 30 m FS-Hydrodex γ-DIMOM column (Macherey Nagel).

T (Injector + Detector) = 250 °C

Splitflow = 80 mL min^{-1}

Precolumn pressure = 0.8 bar

Conditions: 100 – 170 °C, 1 °C min^{-1}

Retention Times: (*R*) = 44.1 min; (*S*) = 44.5 min

5.4. General Procedures

GP1: Methyl deprotection

A 1 M BBr_3 solution in CH_2Cl_2 was added dropwise to a solution of a methyl-protected BINOL in anhydrous CH_2Cl_2, which was cooled using an ice bath. The solution was warmed to room temperature and stirred for 24 h. Afterwards the mixture was cooled to 0 °C and dist. H_2O was added and the organic phase was separated. The aqueous phase was extracted with CH_2Cl_2 (3×) and the combined organic phases were washed with brine, dried over Na_2SO_4, filtered, and the solvent was removed under reduced pressure. The crude product was purified *via* column chromatography.

GP2: Suzuki-Coupling

The boronic acid, $Ba(OH)_2$, and the aryl bromide were dispersed in dioxane/water (3/1) and degassed for 30 minutes with Ar. After the addition of $Pd(PPh_3)_4$, the reaction mixture was refluxed for 20 h. The reaction mixture was cooled to room temperature and 1 M HCl solution was added. The organic phase was separated and the aqueous phase was extracted with CH_2Cl_2 (3×). The combined organic phases were dried over Na_2SO_4, filtered, and the solvent was removed under reduced pressure.

GP3: Methoxymethyl deprotection

To a solution of the MOM ether in CH_2Cl_2/MeOH (5/1) 3.0 equiv. of a 6 M aqueous HCl solution was added. The reaction mixture was refluxed until full conversion was achieved, which was monitored by TLC. The reaction mixture was then cooled to 0 °C and sat. $NaHCO_3$ solution was added. The separated aqueous phase was extracted with CH_2Cl_2 (3×) and the combined organic phases were dried over Na_2SO_4, filtered, and the solvent was removed under reduced pressure. The crude product was purified *via* column chromatography.

GP4: Wittig-Reaction

To a cooled solution of triphenylbutylphosphonium bromide in anhydrous THF was added a 2.5 M *n*-BuLi solution and stirred for 30 min at 0 °C. The corresponding ketone in THF was slowly added to the reaction mixture. After stirring for 3 h at room temperature, sat. NH_4Cl solution and Et_2O were slowly added. The organic phase was separated and washed several times with brine. The combined organic phases were dried over $MgSO_4$, filtered, and the solvent was removed under reduced pressure. The crude product was purified *via* column chromatography.

GP5: Prileschajew epoxidation of alkenes

To a 0 °C cooled solution of the alkene in CH_2Cl_2 was added *m*CPBA. The reaction mixture was stirred at room temperature for 3 h. Then the reaction was quenched by the addition of sat. $NaHCO_3$ solution. The organic phase was separated and washed three times with sat. $NaHCO_3$ solution. The combined organic phases were dried with Na_2SO_4, filtered, and the solvent was removed under reduced pressure. The crude product was purified by column chromatography.

GP6: McMurry-Coupling

To a suspension of zinc powder in THF $TiCl_4$ was slowly added and the solution was subsequently refluxed for 2 h. Then the ketone dissolved in THF was added to the reaction and the resulting mixture was refluxed for 2 days. The reaction was quenched by the addition of sat. NH_4Cl solution and the aqueous phase was separated and extracted EtOAc (3×). The combined organic phases were washed with brine, dried over $MgSO_4$, filtered, and the solvent was removed under reduced pressure. The crude product was purified *via* column chromatography.

GP7: Catalytic HMR employing Thioureas and $TiCl_4$

A flame dried Schlenk flask was loaded with 0.1 mmol thiourea and 0.2 mmol base in 4 mL solvent under Ar and stirred for 15 min. After the addition of 0.1 mL of a 1 M $TiCl_4$ solution (1 M in CH_2Cl_2), the mixture was stirred for a further 15 min and 1 mmol of epoxide was added. After 20 h 5 mL of sat. $NaHCO_3$ solution were added and the aqueous phase was extracted with CH_2Cl_2 (5×5 mL) and the combined organic phases were dried over $MgSO_4$, filtered, and the solvent was removed under reduced pressure. The conversion was determined *via* ^1H NMR spectroscopy with 10 mol% *p*-nitrobenzaldehyde as internal standard.

GP8: Catalytic HMR employing BINOL derivatives and $Ti(^iOPr)_4$

A flame dried Schlenk flask was loaded with 4 Å MS, $Ti(O^iPr)_4$ and the BINOL derivative dissolved in 0.5 mL of solvent under Ar. The reaction mixture was stirred at room temperature for 1 h. Then 0.25 mmol of starting material and 0.5 mL of solvent were added and the reaction was stirred at the appropriate temperature under Ar. To quench the reaction, 1 mL of sat. $NaHCO_3$ solution was added, the aqueous phase was extracted with CH_2Cl_2 (4×) and the combined organic phases were dried over MgSO4, filtered and the solvent was removed under reduced pressure. The conversion was determined *via* ^1H NMR spectroscopy with 10 mol% *p*-nitrobenzaldehyde as internal standard.

5.5. Synthesis of Thioureas, Squaramides and Thiosquaramides

_N,N′_-Bis[3,5-bis(trifluoromethyl)phenyl]thiourea (69)

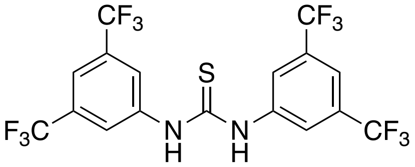

3,5-bistrifluoromethyl)aniline (3.10 g, 13.5 mmol) and Et_3N (2.00 mL, 15.0 mmol) were dissolved in 100 mL THF and cooled to 0 °C. Subsequently thiophosgene (0.98 mL, 13 mmol) was added and the reaction mixture was stirred at room temperature for 66 h. The solvent was removed under reduced pressure and 50 mL of dist. H_2O were added. The aqueous phase was extracted three times with 20 mL Et_2O. The combined organic phases were washed with brine, dried with Na_2SO_4, filtered, and the solvent was removed under reduced pressure. The crude product was recrystallized twice from chloroform to yield **69** as colorless amorphous solid (3.40 g, 6.78 mmol, 50%).

^{1}H NMR (400 MHz, MeOD): δ/ppm = 8.21 (s, 4H), 7.72 (s, 2H).

^{13}C NMR (101 MHz, MeOD): δ/ppm = 182.6, 142.6, 132.8 (q), 128.7, 126.0, 124.8 (q), 123.3, 120.6, 118.8 (q), 114.5.

The NMR spectra are in accordance with those reported in the literature.[35]

2-[(1*R*,2*R*)-2-Aminocyclohexyl]-1*H*-isoindole-1,3(2*H*)-dione (45)

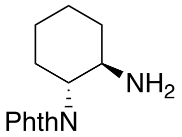

(1*R*,2*R*)-diaminocyclohexane (6.97 g, 61.2 mmol, 1.0 equiv.) and phthalic anhydride (9.43 g, 63.7 mmol, 1.0 equiv.) were added to a solution of *p*-TsOH (11.1 g, 64.3 mmol, 1.1 equiv.) in 300 mL of toluene and refluxed for 12 h in a Soxhlet extractor filled with CaH_2 and sand. The solvent was then removed under reduced pressure and the residue was diluted with 300 mL CH_2Cl_2 and 200 mL of sat. $NaHCO_3$ solution and stirred for 2 h at room temperature. Subsequently, the organic phase was separated and the aqueous phase was extracted four times with 40 mL CH_2Cl_2. The combined organic phases were washed with brine, dried with $MgSO_4$, and the solvent was removed under reduced pressure. After column chromatography (CH_2Cl_2/MeOH = 20/1), the product **45** (12.9 g, 52.7 mmol, 86%) was obtained as a colorless solid.

***R*f** = 0.30 (CH_2Cl_2:MeOH / 20:1)

^{1}H NMR (400 MHz, $CDCl_3$): δ/ppm = 7.82 (dd, 2H, *J* = 5.4, 3.1 Hz), 7.70 (dd, 2H, *J* = 5.4, 3.1 Hz), 3.71 (ddd, 1H, *J* = 12.4, 3.9, 3.41 Hz), 3.41 (td, 1H, *J* = 10.9, 4.1 Hz), 2.19 (qd, 1H, *J* = 12.5, 3.6 Hz), 2.04 (m, 1H), 1.85-1.73 (m, 3H), 1.50-1.29 (m, 2H), 1.27-1.13 (m, 3H).

^{13}C NMR (101 MHz, $CDCl_3$): δ/ppm = 168.9, 134.0, 132.1, 123.3, 58.8, 51.0, 36.9, 29.5 25.8, 25.3.

The NMR spectra are in accordance with those reported in the literature.[51]

2-[(1*R*,2*R*)-2-(Dimethylamino)cyclohexyl]-1*H*-isoindole-1,3(2*H*)-dione (46)

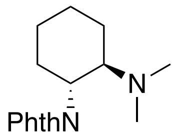

A solution of 2-[(1*R*,2*R*)-2-aminocyclohexyl]-1*H*-isoindole-1,3(2*H*)-dione (**45**) (3.42 g, 14.0 mmol, 1.0 equiv.), in 37% formaldehyde (2.6 mL, 31 mmol, 2.2 equiv.) and 8 mL formic acid was refluxed for 5 h. Subsequently, the solvent was removed under reduced pressure and 20 mL CH_2Cl_2 were added. The organic phase was washed with sat. $NaHCO_3$ solution (4×50 mL), dried with Na_2SO_4, filtered, and the solvent was removed under reduced pressure. The product **46** (2.55 g, 9.40 mmol, 67%) was obtained as a yellow oil.

^{1}H NMR (400 MHz, $CDCl_3$): δ/ppm = 7.80 (dd, 2H, *J* = 5.4, 3.0 Hz), 7.67 (dd, 2H, *J* = 5.4, 3.0 Hz), 4.11 (td, 1H, *J* = 11.6, 3.9 Hz), 3.38-3.25 (m, 1H), 2.28-2.05 (m, 7H), 2.00-1.90 (m, 1H), 1.89-1.75 (m, 3H), 1.42-1.10 (m, 3H).

^{13}**C NMR** (101 MHz, CDCl$_3$): δ/ppm = 168.9, 133.7, 132.4, 123.1, 62.3, 52.4, 40.4, 30.4, 25.9, 25.2, 23.0.

The NMR spectra are in accordance with those reported in the literature.[51]

(1*R*,2*R*)-*N*,*N*-Dimethyl-1,2-cyclohexanediamine (47)

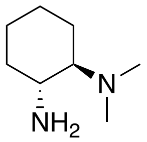

2-[(1*R*,2*R*)-2-(Dimethylamino)cyclohexyl]-1*H*-isoindole-1,3(2*H*)-dione (**46**) (3.82 g, 14.0 mmol, 1.0 equiv.) and $N_2H_4 \cdot H_2O$ (2.00 mL, 44 mmol, 3.1 equiv.) were dissolved in 100 mL MeOH and refluxed for 5 h. After cooling the solution, 10 mL Et$_2$O was added to the reaction mixture and the resulting phthalhydrazide was filtered off. The solvent was removed under reduced pressure and after column chromatography (CH$_2$Cl$_2$/MeOH = 10/1) the product **47** (1.16 g, 8.13 mmol, 58%) was obtained as a yellow oil.

***R*f** = 0.10 (CH$_2$Cl$_2$:MeOH / 10:1)

^{1}**H NMR** (400 MHz, CDCl$_3$): δ/ppm = 2.62-2.55 (m, 1H), 2.42-2.33 (m, 2H), 2.47-2.43 (m, 6H), 2.10-2.01 (m, 1H), 2.01-1.93 (m, 1H), 1.8-1.72 (m, 2H), 1.70-1.63 (m, 1H), 1.26-1.01 (m, 4H).

^{13}**C NMR** (101 MHz, CDCl3): δ/ppm = 67.1, 51.6, 40.3, 32.3, 25.1, 24.7, 21.2.

The NMR spectra are in accordance with those reported in the literature.[51]

N-[3,5-Bis(trifluoromethyl)phenyl]-*N′*-[(1*R*,2*R*)-2-(dimethylamino)cyclohexyl]thiourea (49)

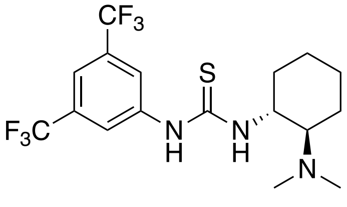

To a solution of amine **47** (0.080 g, 0.56 mmol, 1.0 equiv.) in 2 mL anhydrous THF was added 3,5-Bis(triflouormethyl)phenylisothiocyanate (0.175 g, 0.645 mmol, 1.1 equiv.) and the reaction mixture was stirred at room temperature for 2 h. The solvent was removed under reduced pressure and the crude reaction mixture was purified by column chromatography (CH$_2$Cl$_2$/MeOH = 15/1 → 9/1) to yield the product **49** (0.190 g, 0.460 mmol, 82%) as colorless solid.

***R*$_f$** = 0.25 (CH_2Cl_2:MeOH / 7:1)

^{1}H NMR (400 MHz, DMSO-d$_6$): δ = 10.02 (brs, 1H), 8.26-8.19 (m, 1H), 8.17 (s, 1H), 7.68 (brs, 1H), 4.17-4.05 (m, 1H), 2.60.2.51 (m, 2H), 2.29-2.13 (m, 1H), 2.23 (s, 6H), 1.89-1.81 (m, 1H), 1.78 – 1.71 (m, 1H), 1.68-1.61 (m, 1H), 1.27 – 1.07 (m, 4H) ppm.

^{13}C NMR (101 MHz, DMSO-d$_6$): δ/ppm = 187.7, 141.9, 130.4 (q, *J* = 32.4 Hz), 123.3, (q, *J* = 272.9 Hz), 121.0, 115.4, 65.0, 55.2, 40.2, 31.6, 24.6, 24.5, 21.1.

^{19}F NMR (377 MHz, DMSO-d$_6$): δ/ppm = 61.6.

The NMR spectra are in accordance with those reported in the literature.[43]

3,4-Bis-(cyclopentyloxy)-cyclobut-3-en-1,2-dione (55)

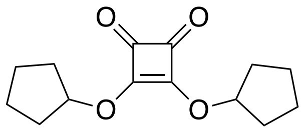

A solution of squaric acid (4.56 g, 40.0 mmol, 1 equiv.) and cyclopentanol (24.0 mL, 260 mmol, 6.5 equiv.) in 150 mL toluene was refluxed for 12 h in a Soxhlet extractor filled with CaH_2 und sand. Afterwards the solvent was removed under reduced pressure and the reaction mixture was purified *via* column chromatography (CH_2Cl_2 → CH_2Cl_2/MeOH = 50/1) to yield the product **55** (7.40 g, 29.6 mmol, 74%) as colorless solid, which was crystallized from a sat. solution in CH_2Cl_2.

***R*$_f$** = 0.25 (CH_2Cl_2:MeOH / 100:1)

^{1}H NMR (200 MHz, $CDCl_3$): δ/ppm = 5.58-5.48 (m, 2H), 2.08-1.87 (m, 8H), 1.85-1.85 (m, 8H).

The ^{1}H NMR spectrum is in accordance with literature data.[49]

3,4-Bis-(cyclopentyloxy)-cyclobut-3-en-1,2-dithion (56)

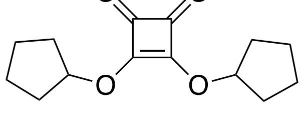

To a solution of Lawesson's reagent (11.9 g, 29.3 mmol, 1.05 equiv.) in anhydrous CH_2Cl_2 was added 3,4-Bis-(cyclopentyloxy)-cyclobut-3-en-1,2-dione (**55**) (6.95 g, 27.8 mmol, 1.0 equiv.) and the reaction mixture was stirred at room temperature for 36 h. Afterwards, the solvent was removed under reduced pressure and the crude mixture was purified *via* column chromatography (n-Hex/CH_2Cl_2 = 1/1) to yield the product **56** (3.84 g, 13.6 mmol, 49%) as orange solid.

***R*f** = 0.2 (n-Hex:CH_2Cl_2 / 1:1)

^{1}H NMR (400 MHz, $CDCl_3$): δ/ppm = 6.05 (p, J = 4.0 Hz, 2H), 2.05-1.97 (m, 8H), 1.90-1.80 (m, 4H), 1.75-1.65 (m, 4H).

^{13}C NMR (101 MHz, $CDCl_3$): δ/ppm = 218.7, 186.2, 88.8, 34.3, 23.9.

The NMR spectra are in accordance with those reported in the literature.[49]

3,4-Bis[[3,5-bis(trifluoromethyl)phenyl]amino]-3-cyclobutene-1,2-dithione (53)

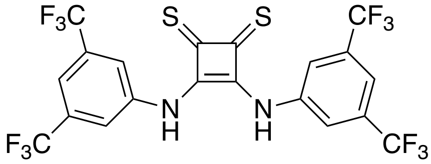

A solution of 1,2-dithione **56** (1.04 g, 3.67 mmol, 1.0 equiv.) and 3,5-bis(trifluoromethyl)aniline (3.48 g, 15.2 mmol, 4.1 equiv.) in 11 mL anhydrous CH_2Cl_2 was stirred at room temperature for 6 days. Afterwards hexane (3 mL) was added and the precipitate was filtered to yield the product **53** (1.15 g, 2.02 mmol, 55%) as yellow solid.

^{1}H NMR (400 MHz, CD_3CN): δ/ppm = 9.14 (brs, 2H), 7.69 (s, 4H), 7.62 (s, 2 H).

^{13}C NMR (101 MHz, CD_3CN): δ/ppm = 213.2, 170.2, 139.8, 132.8 (q, J = 33.9 Hz), 123.9 (q, J = 272.2 Hz), 123.2, 119.9.

^{19}F NMR (377 MHz, $CDCl_3$): δ = 63.8 ppm.

The NMR spectra are in accordance with those reported in the literature.[49]

3,4-Bis[[3,5-bis(trifluoromethyl)phenyl]amino]-3-cyclobutene-1,2-dione (52)

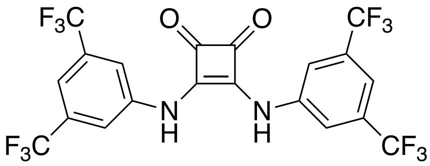

A solution of 3,4-bis-(dimethoxy)-cyclobut-3-en-1,2-dione (1.01 g, 7.08 mmol, 1 equiv.) and 3,5-bis(trifluoromethyl)aniline (3.72, 16.2 mmol, 2.3 equiv.) in 50 mL MeOH were stirred at room temperature for 7 days. Afterwards, the precipitate was filtered and washed with 100 mL

MeOH. After drying under reduced pressure, the product **52** (3.71 g, 6.92 mmol, 99%) was obtained as light yellow solid.

^{1}H NMR (400 MHz, DMSO-d$_6$): δ/ppm = 12.21 (brs, 2H), 8.49 (s, 4H), 7.82 (s, 2 H).

Because of insufficient solubility, we were not able to obtain a suitable ^{13}C NMR spectrum.

5.6. Synthesis of BINOLs

(1*R*)-2,2′-Dimethoxy-1,1′-binaphthalene ((*R*)-75)

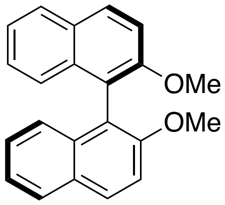

In a flame dried flask, a suspension of (*R*)-BINOL (**(*R*)-74**) (8.90 g, 0.0311 mol, 1.00 equiv.), MeI (9.70 mL, 0.156 mol, 5.01 equiv.), and K_2CO_3 (14.6 g, 0.106 mol, 3.40 equiv.) in 280 mL of anhydrous acetone was refluxed. After determining the end of the reaction by TLC control, the reaction mixture was cooled to room temperature. The volatile components were then removed under reduced pressure and the resulting colorless solid was diluted with 200 mL CH_2Cl_2 and washed with 100 mL dist. H_2O. The aqueous phase was extracted with CH_2Cl_2 3 × 50 mL) and the combined organic phases were dried over MgSO4, filtered, and the solvent was removed under reduced pressure to yield the product (**(*R*)-75**) (9.81 g, 0.0311 mol, 99%) as colorless solid.

^{1}H NMR (400 MHz, $CDCl_3$): δ/ppm = 7.98 (d, J = 9.0 Hz, 2H), 7.87 (d, J = 8.1 Hz, 2H), 7.47 (d, J = 9.0 Hz, 2 H), 7.35 – 7.30 (m, 2 H), 7.24 – 7.19 (m, 2 H), 7.13 (d, J = 8.1 Hz, 2 H), 3.77 (s, 6 H).

^{13}C NMR (101 MHz, $CDCl_3$): δ/ppm = 155.1, 134.2, 129.5, 129.4, 128.1, 126.4, 125.4, 123.6, 119.8, 114.4, 57.1.

The NMR spectra are in accordance with those reported in the literature.[65]

(1*R*)-2-Methoxy-2′-(methoxymethoxy)-1,1′-binaphthalene ((*R*)-80)

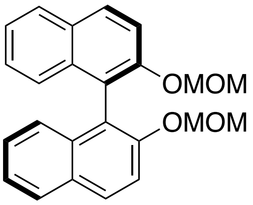

In a flame dried flask, NaH (2.29 g, 90.6 mmol, 3.08 equiv.) was suspended in 80 ml anhydrous THF under Ar and cooled to 0 °C. (*R*)-BINOL (**(*R*)-74**) (8.43 g, 29.4 mmol, 1.00 equiv.) in 60 ml anhydrous THF was added dropwise to the suspension. The mixture was first stirred at 0 °C for 1 h and then warmed to room temperature. Methoxymethyl bromide (6.00 mL, 73.9 mmol, 2.51 equiv.) was added dropwise *via* a syringe and the suspension was stirred at 0 °C. After determining the end of the reaction by TLC control, 50 mL sat. NH_4Cl solution were added. The aqueous phase was extracted with CH_2Cl_2 (4 × 50 mL) and the combined organic phases were dried over $MgSO_4$, filtered, and the solvent was removed under reduced pressure to yield the product (**(*R*)-80**) (10.3 g, 27.4 mmol, 93%) as colorless solid.

^{1}H NMR (400 MHz, $CDCl_3$): δ/ppm = 7.95 (d, *J* = 9.0 Hz, 2 H), 7.88 (d, *J* = 8.2 Hz, 2 H), 7.58 (d, *J* = 9.0 Hz, 2 H), 7.37 – 7,32 (m, 2 H), 7.25 – 7.20 (m, 2 H), 7.16 (d, *J* = 8.4 HZ, 2 H), 5.09 (d, *J* = 6.8 Hz, 2), 4.98 (d, *J* = 6.8 Hz, 2 H), 3.15 (s, 6 H).

^{13}C NMR (101 MHz, $CDCl_3$): δ/ppm = 152.8, 134.2, 130.2, 129.5, 128.0, 126.4, 125.7, 124.2, 121.5, 117.5, 95.4, 56.0.

The NMR spectra are in accordance with those reported in the literature.[66]

(1*R*)-3,3′-Diiodo-2,2′-dimethoxy-1,1′-binaphthalene ((*R*)-76)

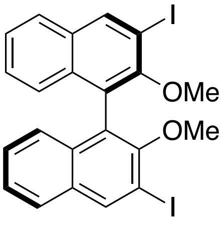

In a flame dried flask was added TMEDA (3.30 mL, 22.0 mmol, 2.20 equiv.) in 160 mL anhydrous Et_2O under Ar. A 1.60 M *n*-BuLi in hexane (25.0 mL, 40.0 mmol, 4.00 equiv.) was added and the mixture was stirred at room temperature for 20 min. Then (1*R*)-2,2′-dimethoxy-1,1′-binaphthalene (**(*R*)-75**) (3.14 g, 10.0 mmol, 1.00 equiv.) was added and the suspension was stirred at room temperature for 3 h. The mixture was cooled to –90 °C and a solution of I_2 (8.67 g , 34.2 mmol, 3.41 equiv.) in 70 ml anhydrous THF was added dropwise. The reaction mixture was warmed to room temperature and stirred for further 20 h. The reaction was quenched with half-sat. $Na_2S_2O_3$ solution and stirred for 1 h. The aqueous phase was extracted with Et_2O (5 × 80 mL) and the combined organic phases were dried over $MgSO_4$, filtered, and the solvent was removed under reduced pressure. After purification *via* column chromatography (*n*-Hex/toluene = 4/1), the product (4.36 g, 76.9 mmol, 77%) (**(*R*)-76**) was obtained as colorless solid.

^{1}H NMR (400 MHz, $CDCl_3$): δ/ppm = 8.54 (s, 2 H), 7.79 (d, *J* = 8.2 Hz, 2 H), 7.44 – 7.38 (m, 2 H), 7.30 – 7.24 (m, 2 H), 7.07 (d, *J* = 8.5 Hz, 2 H), 3.42 (s, 6 H).

^{13}C NMR (101 MHz, $CDCl_3$): δ/ppm = 154.6, 140.0, 134.0, 132.3, 127.2, 127.1, 125.9, 125.8, 125.5, 92.5, 61.3.

The NMR spectra are in accordance with those reported in the literature.[66]

(1*R*)-2,2′-Dimethoxy-3,3′-bis[2,4,6-tris(1-methylethyl)phenyl]-1,1′-binaphthalene ((*R*)-77)

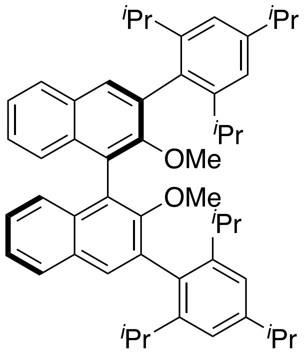

Preparation of the Grignard solution: In a flame dried flask under Ar were placed Mg turnings (1.75 g, 72.1 mmol, 12.0 equiv.) and I_2 in 10 mL anhydrous Et_2O. A solution of 2,4,6-triisopropylphenyl bromide (9.10 ml, 36.3 mmol, 6.00 equiv.) in 47 ml of anhydrous Et_2O was then added dropwise. The reaction mixture was stirred under reflux until only traces of magnesium were present.

Kumada coupling: The freshly prepared Grignard solution was added dropwise to a suspension of (1*R*)-3,3′-diiodo-2,2′-dimethoxy-1,1′-binaphthalene (**(*R*)-76**) (3.41 g, 6.02 mmol, 1.00 equiv.) and $NiCl_2(PPh_3)_2$ (0.394 g, 0.603 mmol, 0.100 equiv.) in 37 mL anhydrous Et_2O. The resulting solution was refluxed for 20 h. To quench the reaction, 50 ml of 1 M HCl solution were added. The aqueous phase was extracted three times with CH_2Cl_2 (3 × 50 mL) and the combined organic phases were dried over Na_2SO_4, filtered, and the solvent was removed under reduced pressure. After purification *via* column chromatography (*n*-Hex/EtOAc = 100/1) the product (**(*R*)-77**) (1.99 g, 2.78 mmol, 46%) was obtained as colorless solid.

^{1}H NMR (400 MHz, CD_2Cl_2): δ/ppm = 7.88 (d, *J* = 8.2 Hz, 2 H), 7.44 – 7.39 (m, 2 H), 7.32 – 7.28 (m, 4 H), 7.14 – 7.08 (m, 4 H), 3.12 (s, 6 H), 2.97 (sept, *J* = 6.9 Hz), 2.83 (sept, *J* = 6.8 Hz, 2 H), 2.77 (sept, *J* = 6.8 Hz, 2 H), 1.32 (d, *J* = 6.9 Hz, 12 H), 1.18 (d, *J* = 6.9 Hz, 6 H), 1.17 (d, *J* = 6.9 Hz, 6 H) 1.12 (d, *J* = 6.8 Hz, 6H), 1.10 (d, *J* = 6.8 Hz, 6 H).

^{13}C NMR (101 MHz, CD_2Cl_2): δ/ppm = 155.6, 149.0, 147.7, 147.6, 134.6, 134.4, 134.0, 131.6, 130.9, 128.5, 126.6, 126.1, 125.2, 125.1, 121.3, 60.4, 34.9, 31.6, 31.5, 25.7, 25.5, 24.4, 23.6, 23.5.

The NMR spectra are in accordance with those reported in the literature.[66]

(1*R*)-3,3′-Bis[2,4,6-tris(1-methylethyl)phenyl][1,1′-binaphthalene]-2,2′-diol ((*R*)-78a)

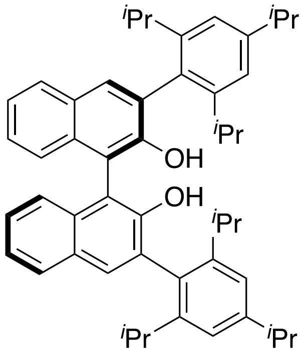

Using GP1**,** (1*R*)-2,2′-Dimethoxy-3,3′-bis[2,4,6-tris(1-methylethyl)phenyl]-1,1′-binaphthalene (**(*R*)-77**) (1.99 g, 2.78 mmol. 1.00 equiv.) was converted with BBr_3 (1.90 mL, 20.0 mmol, 7.20 equiv.). After purification *via* column chromatography (*n*-Hex:EtOAc = 99/1), the product (**(*R*)-78a**) (1.69 g, 2.45 mmol, 88%) was obtained as colorless solid.

$\boldsymbol{R}_\mathbf{f}$ = 0.12 (*n*-Hex)

^{1}H NMR (400 MHz, $CDCl_3$): δ/ppm =7.87 (d, *J* = 8.0 Hz, 2 H), 7.77 (s, 2 H), 7.41 – 7.27 (m, 6 H), 7.16 – 7.11 (m, 2 H), 4.93 (s, 1 H), 2.97 (sept, *J* = 6.9 Hz, 2 H), 2.86 (sept, *J* = 6.8 Hz, 2 H), 2.70 (sept, *J* = 6.8 Hz, 2 H), 1.32 (d, *J* = 6.9 Hz, 12 H), 1.21 (d, *J* = 6.8 Hz, 6 H), 1.12 (d, *J* = 6.9 Hz, 6 H), 1.10 (d, *J* = 6.9 Hz, 6 H), 1.04 (d, *J* = 6.8 Hz, 6 H).

^{13}C NMR (101 MHz, $CDCl_3$): δ/ppm =150.8, 149.3, 147.9, 147.9, 133.6, 130.8, 130.5, 129.3, 129.2, 128.4, 126.8, 124.7, 123.9, 121.4, 121.3, 113.4, 34.5, 31.1, 31.0, 31.0, 24.5, 24.4, 24.2, 24.1, 24.1, 23.9.

HRMS (ESI): calcd for $C_{50}H_{58}O_2$ $[M+Na]^+$: 713.4329 found: 713.4331.

The NMR spectra are in accordance with those reported in the literature.[66]

B,*B*′-[(1*R*)-2,2′-Dimethoxy[1,1′-binaphthalene]-3,3′-diyl]bis[boronic acid] ((*R*)-79)

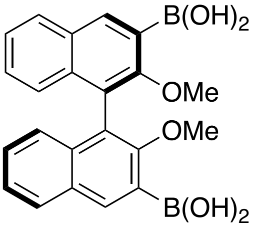

A solution of TMEDA (6.00 mL, 40.0 mmol, 3.07 equiv.) and 2.50 M *n*-BuLi (17.0 mL, 42.5 mmol. 3.26 equiv.) in 170 mL anhydrous Et_2O was stirred at room temperature for 30 min. Then (1*R*)-2,2′-dimethoxy-1,1′-binaphthalene (**(*R*)-75**) (4.10 g, 13.0 mmol, 1.00 equiv.) in 30 mL anhydrous Et_2O was added dropwise. The resulting suspension was stirred at room temperature for further 3 h, before it was cooled to –80 °C. Triethyl borate (16.0 mL, 94.0 mmol, 7.21 equiv.) was added dropwise within 15 min and the reaction was stirred at room temperature for 16 h. Afterwards, 100 mL 1 M HCl solution were added at 0 °C, the phases were separated and the organic phase was washed with 1 M HCl solution (2 × 50 mL) and once with brine (50 mL). The organic phase was then dried over Na_2SO_4, filtered, and the solvent was removed under reduced pressure. The product (**(*R*)-79**) (4.72 g, 11.7 mmol, 90%) was obtained after recrystallization from toluene as colorless crystals.

^{1}H NMR (400 MHz, acetone-d_6): δ/ppm = 8.56 (s, 2 H), 8.04 (d, *J* = 8.1 Hz 2 H), 7.45 (t, *J* = 7.1 Hz, 2 H), 7.33 (t, *J* = 7.4 Hz, 2 H), 7.11 (d, *J* = 7.2 Hz, 2 H), 3.43 (s, 6 H).

^{13}C NMR (101 MHz, acetone-d_6): δ/ppm =160.3, 138.1, 135.6, 130.4, 128.7, 128.0, 127.2, 125.3, 124.7, 60.7.

The NMR spectra are in accordance with those reported in the literature.[66]

(1′*R*)-[1,3′:1′,1″:3″,1‴-Quaternaphthalene]-2′,2″-diol ((*R*)-78c)

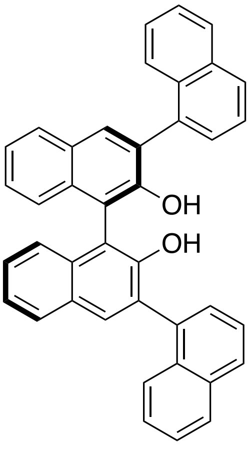

Using GP2 *B*,*B*′-[(1*R*)-2,2′-dimethoxy[1,1′-binaphthalene]-3,3′-diyl]bis[boronic acid] (**(*R*)-79**) (1.85 g, 4.60 mmol, 1.00 equiv.) was treated with $Ba(OH)_2$ (5.05 g, 29.5 mmol, 6.41 equiv.), 1-bromonaphthalene (2.00 mL, 13.7 mmol, 3.11 equiv.), and Pd(PPh_3)$_4$ (0.261 g, 0,226 mmol, 0,05 equiv.) in 60 mL dioxane/H_2O (3:1). Afterwards the crude product was deprotected using GP1 with BBr_3 (3.1 mL, 32.67 mmol, 7.10 equiv.). After purification *via* column chromatography (*n*-Hex/EtOAc = 10/1), the product (**(*R*)-78c**) (2.06 g, 3.82 mmol, 83%) was obtained as colorless solid.

^{1}H NMR (400 MHz, $CDCl_3$): δ/ppm = 8.04 – 8.00 (m, 2 H), 7.99 – 7.89 (m, 6 H), 7.86 – 7.81 (m, 1 H), 7.76 – 7.32 (m,15 H), 5.6 -5.12 (br, 2 H)

^{13}C NMR (101 MHz, $CDCl_3$): δ/ppm = 150.8, 149.3, 147.9, 147.9, 133.6, 130.8, 130.5, 129.3, 129.2, 128.4, 126.8, 124.7, 123.9, 121.4, 121.3, 113.4, 34.5, 31.1, 31.0, 31.0, 24.5, 24.4, 24.2, 24.1, 24.1, 23.9.

HRMS (ESI): calcd for $C_{40}H_{26}O_2$ $[M+Na]^+$: 561.1825 found: 561.1823.

(1*R*)-3,3′-Bis[3,5-bis(trifluoromethyl)phenyl][1,1′-binaphthalene]-2,2′-diol ((*R*)-78b)

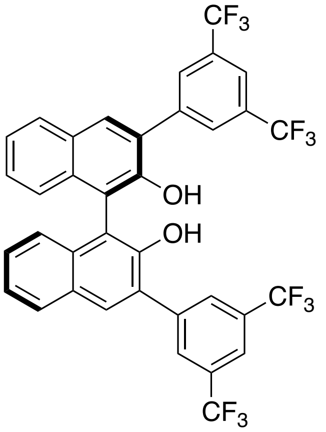

Using GP2, *B*,*B*′-[(1*R*)-2,2′-dimethoxy[1,1′-binaphthalene]-3,3′-diyl]bis[boronic acid] (**(*R*)-79**) (2.01 g, 4.99 mmol, 1.00 equiv.) was treated with Ba(OH)$_2$ (5.52 g, 32.2 mmol, 6.45 equiv.), 3,5-bis(perfluoromethyl)phenylbromide (2.60 mL, 15.4 mmol, 3.08 equiv.), and Pd(PPh_3)$_4$ (0.308 g 0.266 mmol, 0.0533 equiv.) in 65 mL dioxane/H_2O (3:1). Afterwards the crude product was dissolved in 120 mL anhydrous CH_2Cl_2 and deprotected using GP1 with BBr_3 (3.40 mL, 35.8 mmol, 7.18 equiv.) in 35 mL anhydrous CH_2Cl_2. After purification *via* column chromatography (*n*-Hex/EtOAc = 20/1) the product (2.85 g, 4.01 mmol, 80%) (**(*R*)-78b**) was obtained as colorless solid.

***R*$_f$** = 0.31 (*n*-Hex:EtOAc / 20:1)

^{1}H NMR (400 MHz, $CDCl_3$): δ/ppm = 8.24 (s, 4 H), 8.12 (s, 2 H), 8.00 (d, *J* = 7.5 Hz, 2 H), 7.53 – 7.39 (m, 4 H), 7.24 (d, *J* = 8.3 Hz, 2 H), 5.38 (s, 2 H).

^{13}C NMR (101 MHz, $CDCl_3$): δ/ppm = 150.0, 139.6, 133.4, 132.5, 132.2, 131.9, 131.6, 131.3, 130.0, 129.6, 129.1, 128.8, 127.9, 127.6, 125.4, 124.9, 124.1, 122.2, 121.5, 119.5, 111.9.

HRMS (ESI): calcd for $C_{36}H_{18}F_{12}O_2$ $[M+Na]^+$: 733.1007 found: 733.1008

(1*R*)-3,3′-Bis(2,3,4,5,6-pentafluorophenyl)[1,1′-binaphthalene]-2,2′-diol ((*R*)-78d)

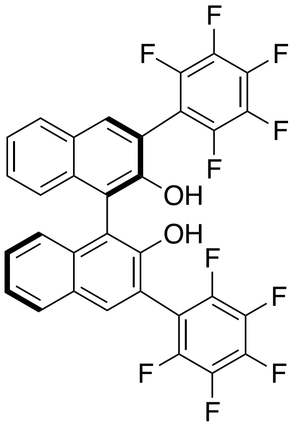

In a flame dried flask under Ar was placed (1*R*)-2-methoxy-2′-(methoxymethoxy)-1,1′-binaphthalene (**(*R*)-80**) (3.74 g, 10.0 mmol, 1.00 equiv.) in 40 mL anhydrous THF. At 0 °C, *n*-BuLi (1.60 M, 15.0 mL, 24.0 mmol, 2.40 equiv.) was added dropwise and the reaction was stirred at 0 °C for 30 min. The suspension was then cooled to –70 °C and hexafluorobenzene (8.10 ml, 70.3 mmol, 7.03 equiv.) was added. The reaction mixture was slowly warmed to room temperature and then stirred for 18 h. Then the reaction was quenched by addition of 100 mL NH_4Cl solution and the aqueous phase was separated and extracted with Et_2O (3 × 100 mL). The combined organic phases were dried over Na_2SO_4, filtered, and the solvent was removed under reduced pressure. The crude product was purified *via* column chromatography (*n*-Hex/EtOAc = 95/5).

Afterwards, the MOM protected product (4.05 g, 5.73 mmol, 1.00 equiv.) was deprotected with 6 M HCl (3.00 mL, 18.0 mmol, 3.14 equiv.) using GP3. After purification *via* column chromatography (*n*-Hex/EtOAc = 95/5) the final product (**(*R*)-78d**) (3.23 g, 5.22 mmol, 52%) was obtained as colorless solid.

***R*~f~** = 0.14 (*n*-Hex:EtOAc / 95:5)

^{1}H NMR (400 MHz, $CDCl_3$): δ/ppm = 8.03 (s, 2 H), 7.97 – 7.93 (m, 2 H), 7.50 – 7.41 (m, 4 H), 7.27 – 7.23 (m, 2 H), 5.34 (s, 2 H).

^{13}C NMR (101 MHz, $CDCl_3$): δ/ppm = 150.5, 146.0, 143.5, 142.5, 139.1, 136.6, 134.2, 133.8, 129.1, 129.1, 129.0, 125.2, 124.2, 115.9, 112.1, 111.6.

HRMS (ESI): calcd for $C_{32}H_{12}F_{10}O_2$ $[M+Na]^+$: 641.0570 found: 641.0572.

(1*R*)-3-[3,5-Bis(trifluoromethyl)phenyl][1,1′-binaphthalene]-2,2′-diol ((*R*)-83)

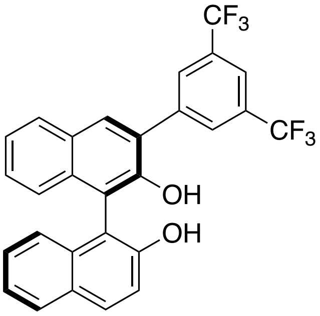

To a solution of TMEDA (2.30 mL, 15.0 mmol, 1.10 equiv.) in 200 mL anhydrous Et_2O was added 1.60 M *n*-BuLi (9.30 mL, 14.9 mmol. 1.09 equiv.) After stirring 30 min at room temperature, (1*R*)-2-methoxy-2′-(methoxymethoxy)-1,1′-binaphthalene (**(*R*)-80**) (5.09 g, 13.6 mmol, 1.00 equiv.) in 30 mL anhydrous Et_2O was added. The resulting suspension was stirred at room temperature for further 3 h, then cooled to –80 °C and triethyl borate (7.00 mL, 41.1 mmol, 3.03 equiv.) was added. The reaction mixture was stirred at room temperature for 16 h, cooled to 0 °C and 100 mL 1 M HCl were added. After 2 h, the organic phase was washed with 1 M HCl (2×50 mL) and brine. The organic phase was dried over Na_2SO_4, filtered, and the solvent was removed under reduced pressure. After purification *via* column chromatography (*n*-Hex/EtOAc = 2/1) the obtained product (**(*R*)-82**) was directly used in the next step.

Using GP2, boronic acid **(*R*)-82** (0.837 g. 2.00 mmol, 1.00 equiv.) was treated with $Ba(OH)_2$ (1.07 g, 6.23 mmol, 3.11 equiv.), 3,5-bis(trifluoromethyl)phenylbromide (1.10 mL, 6.54 mmol, 3.27 equiv.), and $Pd(PPh_3)_4$ (0.116 g, 0.100 mmol, 0.0500 equiv.) in 27 mL 1,4-dioxane/H_2O (3/1). Then the crude product was deprotected with 6 M HCl (1.00 mL, 6.00 mmol, 3.00 equiv.) using GP3. After purification *via* column chromatography (*n*-Hex/EtOAc = 9/1) the final product (**(*R*)-83**) (0.887 g, 1.78 mmol 89%) was obtained as colorless solid.

***R*f** = 0.3 (*n*-Hex:EtOAc / 9:1)

^{1}H NMR (400 MHz, $CDCl_3$): δ/ppm = 8.23 (s, 2 H), 8.08 (s, 1 H), 8.01 (d, *J* = 8.9 Hz, 1 H), 7.98 (d, *J* = 8.0 Hz, 1 H), 7.94 – 7.88 (m,1H), 7.48 – 7.32 (m, 5 H), 7.19 (t, *J* = 7.8 Hz), 5.35 (s, 1H), 5.03 (br, 1 H).

^{13}C NMR (400 MHz, $CDCl_3$): δ/ppm = 153.0, 149.8, 139.9, 133.6, 133.4, 132.1, 132.0, 131.8, 131.5, 130.0, 129.7, 129.5, 128.9, 128.7, 128.5, 128.0, 127.7, 125.1, 125.0, 124.4, 124.1, 122.3, 121.3, 118.0, 112.7, 110.3

HRMS (ESI): calcd for $C_{28}H_{16}F_6O_2$ $[M+Na]^+$: 521.0946 found: 521.0944.

5.7. Synthesis of Epoxides

1-Phenyl-1-cyclohexene oxide (42)

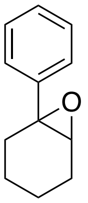

Using GP5, 1-phenyl-1-cyclohexene (2.63 g 16.60 mmol, 1.00 equiv.) was converted with *m*CPBA (70%, 5.34 g, 21.7 mmol, 1.30 equiv.) in 30 mL CH_2Cl_2. After column chromatography (*n*-Hex/EtOAc = 20/1 + 1% Et_3N) the product (**42**) (2.11 g, 12.12 mmol, 73%) was obtained as colorless oil.

***R*~f~** = 0.50 (*n*-Hex:EtOAc / 20:1)

^{1}H NMR (400 MHz, $CDCl_3$): δ/ppm = 7.2-7.31 (m, 4H), 7.27-7.22 (m, 1H), 3.08 (m, 1H), 2.33-2.25 (m, 1H), 2.19-2.08 (m, 1H), 2.04-1.91 (m, 2H), 1.59-1.38 (m, 3H), 1.35-1.25 (m, 1H).

^{13}C NMR (101 MHz, $CDCl_3$): δ/ppm = 142.7, 128.4, 127.3, 125.5, 62.1, 60.4, 29.0, 24.9, 20.3, 19.9.

The NMR spectra are in accordance with those reported in the literature.[36]

(4,4-Dimethyl-1-cyclohexen-1-yl)benzene (85)

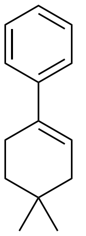

To a suspension of magnesium (0.212 g, 8.72 mmol, 1.10 equiv.) in 20 mL anhydrous Et_2O under Ar was added a crystal of iodine and the mixture was stirred at room temperature for 30 min. Then 5% of a solution of benzyl bromide (0.829 mL, 7.92 mmol, 1.00 equiv.) in 20 mL Et_2O was added and the reaction mixture was stirred under reflux. As soon as the color changed from brown to pale yellow, the remaining solution of benzyl bromide was added dropwise *via* an addition funnel (0.1 mL min^{-1}). The reaction mixture was refluxed for 1 h and then cooled to 0 °C.

To the benzylmagnesium bromide suspension a solution of 4,4-dimethylcyclohexanone (1.08 mL, 7.92 mmol, 1.00 equiv.) in 20 mL Et_2O was added dropwise (0.1 mL min^{-1}). The reaction mixture was stirred under reflux for 2 h. At 0 °C, 20 mL saturated NH_4Cl solution was added to quench the reaction. The mixture was then extracted with EtOAc (3×50 mL). The combined organic layers were washed with brine, dried over Na_2SO_4, filtered, and the solvent was removed under reduced pressure to yield a colorless oil, which was directly used in the next step.

100 mL of toluene and *p*-toluenesulfonic acid (1.50 g, 8.72 mmol, 1.10 equiv.) were added and the reaction mixture was stirred under reflux for 24 h in a Dean-Stark apparatus. The solvent was removed under reduced pressure and 2 M NaOH (5 mL) and 10 mL dist. H_2O were added. The aqueous phase was extracted with EtOAc (3×50 mL) and the combined organic phases were washed with brine, dried over Na_2SO_4, filtered, and the solvent was removed under reduced pressure. The product (**85**) (0.875 g, 4.70 mmol, 59%) was obtained as a light yellow liquid

^{1}H NMR (400 MHz, $CDCl_3$): δ/ppm = 7.43 – 7.38 (m, 2H), 7.34 – 7.28 (m, 2H), 7.24 – 7.19 (m, 1H), 6.07 (hept, *J* = 1.7 Hz, 1H), 2.43 (ddt, *J* = 6.5, 4.0, 2.1 Hz, 2H), 2.01 (dt, *J* = 4.6, 2.5 Hz, 2H), 1.54 (t, *J* = 6.4 Hz, 3H), 0.97 (s, 6H).

^{13}C NMR (101 MHz, $CDCl_3$): δ/ppm = 142.4, 135.2, 128.3, 126.7, 125.1, 123.9, 40.1, 36.0, 28.6, 28.3, 25.2.

The NMR spectra are in accordance with those reported in the literature.[76]

1-Phenyl-4,4-dimethyl-1-cyclohexen oxide (86)

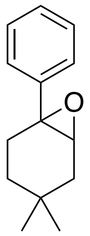

Using GP5, 1-phenyl-4,4-dimethylcyclohexen-1-yl (**85**) (0.875 g 4.70 mmol, 1.00 equiv.) was treated with *m*CPBA (70%, 1.51 g, 6.11 mmol, 1.30 equiv.) in 20 mL CH_2Cl_2. After column chromatography (*n*-Hex/EtOAc = 20/1 + 1% Et_3N) the product (**86**) (0.708 g, 3.50 mmol, 74%) was obtained as colorless oil.

***R*f** = 0.50 (*n*-Hex:EtOAc / 20:1)

^{1}H NMR (400 MHz, $CDCl_3$): δ/ppm = 6.48 – 6.42 (m, 2H), 6.42 – 6.36 (m, 2H), 6.35 – 6.28 (m, 1H), 2.10 (d, *J* = 1.1 Hz, 1H), 1.44 (ddd, *J* = 15.1, 12.3, 5.5 Hz, 1H), 1.13 (dq, *J* = 15.2, 0.9 Hz, 1H), 0.88 – 0.75 (m, 2H), 0.63 – 0.53 (m, 1H), 0.26 (ddt, *J* = 13.3, 5.5, 2.2 Hz, 1H).

^{13}C NMR (101 MHz, $CDCl_3$): δ/ppm = 142.3, 128.4, 127.4, 125.5, 61.0, 60.0, 38.7, 32.3, 31.5, 27.5, 26.6, 25.4.

HRMS (ESI): calcd for $C_{14}H_{18}NaO$ $[M+Na]^+$: 225.1250 found: 225.1251.

(1-Methyl-1-penten-1-yl)benzene (40)

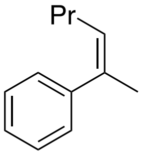

Using GP4, triphenylbutylphosphonium bromide (3.75 g, 25.3 mmol, 1.00 equiv.) was treated with *n*-BuLi (10.5 mL, 26.3 mmol, 1.04 equiv.) and acetophenone (3.75 g, 31.3 mmol, 1.24 equiv.). After purification *via* column chromatography (*n*-Hex/EtOAc = 20/1) the product (**40**) (2.13 g, 13.3 mmol, 53%) was obtained as colorless oil.

E/*Z* ratio = 1:1

^{1}**H NMR** (400 MHz, $CDCl_3$): δ/ppm = δ 7.39 – 7.11 (m, $5H_{Z}$), 7.39 – 7.11 (m, $5H_{E}$), 5.75 (tq, *J* = 7.2, 1.4 Hz, $1H_{Z}$), 5.43 (tq, *J* = 7.3, 1.6 Hz, $1H_{E}$), 2.14 (qd, *J* = 7.3, 1.0 Hz, $2H_{Z}$), 1.99 (s, $3H_{Z}$), 1.99 (s, $3H_{E}$), 1.91 (qd, *J* = 7.3, 1.0 Hz, $2H_{E}$), 1.45 (h, *J* = 7.4 Hz, $2H_{Z}$), 1.32 (h, *J* = 7.4 Hz, $2H_{E}$), 0.93 (t, *J* = 7.4 Hz, $3H_{Z}$), 0.81 (t, *J* = 7.3 Hz, $3H_{E}$).

^{13}**C NMR** (101 MHz, $CDCl_3$): δ/ppm = 144.2, 142.5, 136.2, 134.8, 128.7, 128.3, 128.1, 128.1, 127.9, 126.6, 126.5, 125.7, 31.3, 31.0, 25.7, 23.4, 23.0, 15.9, 14.1, 14.0.

The NMR spectra are in accordance with those reported in the literature.[36]

2-Phenyl-2-hexenoxide (43a)

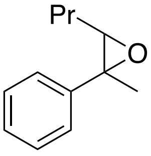

Using GP5, (1-methyl-1-penten-1-yl)benzene (**40**) (2.13 g, 13.3 mmol, 1.00 equiv.) was converted with 70% *m*CPBA (4.37 g, 17.7 mmol, 1.33 equiv.). After purification *via* column chromatography (*n*-Hex/EtOAc = 20/1 + 1% Et_3N) the product (**43a**) (1.36 g, 7.70 mmol, 58%) was obtained as colorless oil.

E/*Z* ratio = 1:5

^{1}**H NMR** (400 MHz, $CDCl_3$): δ/ppm = 7.30 – 7.17 (m, 5H), 2.98 (t, *J* = 6.1 Hz, $1H_{Z}$), 2.75 (t, *J* = 6.1 Hz, $1H_{E}$), 1.59 (s, $3H_{Z}$), 1.59 (s, $3H_{E}$), 1.38 – 1.24 (m, 2H), 1.08 (td, *J* = 7.6, 6.0 Hz, $2H_{Z}$), 0.94 (t, *J* = 7.3 Hz, $2H_{E}$), 0.77 (t, *J* = 7.4 Hz, $3H_{Z}$).

^{13}**C NMR** (101 MHz, $CDCl_3$): δ/ppm = 140.0, 128.1, 127.2, 126.6, 65.7, 62.6, 30.8, 24.8, 19.6, 14.0.

The NMR spectra are in accordance with those reported in the literature.[36]

1-Chlor-4-(1-methyl-1-penten-1-yl)-Benzol (40b)

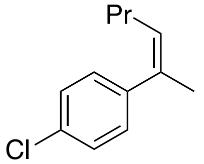

Using GP4, triphenylbutylphosphoniumbromide (14.0 g, 35.0 mmol, 1.0 equiv.) was treated with *n*-BuLi (14.0 mL, 35 .0 mmol, 1.0 equiv.) and *p*-chloroacetophenone (6.18 g, 39.9 mmol, 1.1 equiv.). After purification *via* column chromatography (*n*-Hex/EtOAc = 50/1) the product (**40b**) (4.17 g, 21.4 mmol, 61%) was obtained as colorless oil.

E/*Z* ratio = 1:1

***R*f** = 0.51 (*n*-Hex:EtOAc / 20:1)

^{1}H NMR (400 MHz, CDCl$_3$): δ/ppm = 7.52-7.35 (m, 6H), 7.29-7.21 (m, 2H), 5.91 (tq, 1H, *J* = 7.2, 1.4 Hz), 5.62 (tq, 1H, *J* = 7.3, 1.5 Hz), 2.31 (qd, 2H, *J* = 7.3, 1.0 Hz), 2.18-2.12 (m, 6H), 2.06 (dddd, 2H, *J* = 8.8, 7.5, 6.1, 1.3 Hz), 1.62 (h, 2H, *J* = 7.3 Hz), 1.49 (h, 2H, *J* = 7.4 Hz), 1.10 (t, 3H, *J* = 7.3 Hz), 0.99 (t, 3H, *J* = 7.4 Hz).

^{13}C NMR (101 MHz, CDCl$_3$): δ/ppm = 142.6, 140.8, 135.1, 133.8, 132.3, 132.2, 129.5, 129.3, 128.6, 128.3, 127.0, 77.5, 77.2, 76.8, 31.3, 31.0, 25.6, 23.3, 22.9, 15.9, 14.1, 13.9.

The NMR spectra are in accordance with those reported in the literature.[36]

2-(4-Chlorphenyl)-2-methyl-3-propyl-oxirane (43b)

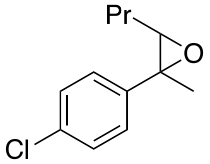

Using GP5, 1-Chlor-4-(1-methyl-1-penten-1-yl)-Benzol (**40b**) (2.20 g, 11.3 mmol, 1.00 equiv.) was reacted with 70% *m*CPBA (3.71 g, 15.0 mmol, 1.33 equiv.). After purification *via* column chromatography (*n*-Hex/EtOAc = 20/1 + 1% Et$_3$N) the product (**43b**) (1.55 g, 7.35 mmol, 65%) was obtained as colorless oil.

***R*f** = 0.45 (*n*-Hex:EtOAc / 20:1 + 1% Et$_3$N)

^{1}H NMR (400 MHz, CDCl$_3$): δ/ppm = 77.29-7.15 (m, 8H), 2.97 (t, 1H, *J* = 6.2 Hz), 2.69 (d, 1H, *J* = 6.2 Hz), 1.72-1.20 (m, 14H), 1.13 – 1.01 (m, 2H), 0.93 (t, 3H, *J* = 7.3 Hz), 0.77 (t, 3H, *J* = 7.4 Hz).

^{13}C NMR (101 MHz, CDCl$_3$): δ/ppm = 142.0, 138.6, 133.1, 133.1, 128.6, 128.3, 128.1, 126.6, 67.0, 65.8, 62.1, 60.1, 31.0, 30.7, 24.5, 19.9, 19.5, 17.8, 14.1, 14.0.

The NMR spectra are in accordance with those reported in the literature.[36]

Bicyclohexylidene (71)

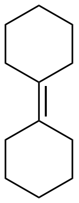

Using GP6, cyclohexanone (2.95 g, 30.1 mmol, 1.00 equiv.) was converted with zink powder 8.02 g, 122 mmol, 4.0 equiv.) and $TiCl_4$ (6.8 mL, 62 mmol, 2.0 equiv.). After purification *via* column chromatography (*n*-Hex) the product (**71**) (0.988 g, 6.01 mmol, 41%) was obtained as colorless oil, which slowly crystalized.

***R*f** = 0.75 (*n*-Hex)

^{1}H NMR (400 MHz, $CDCl_3$): δ/ppm = 2.20-2.13 (m, 8H), 1.66-1.45 (m, 12H).

^{13}C NMR (101 MHz, $CDCl_3$): δ/ppm = 129.6, 30.3, 28.9, 27.5.

Biscyclohexyloxirane (72)

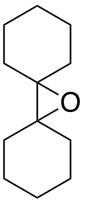

Using GP5, bicyclohexylidene (**71**) (0.988 g, 6.01 mmol, 1.00 equiv.) was reacted with 70% *m*CPBA (2.22 g, 9.02 mmol, 1.50 equiv.). After purification *via* column chromatography (*n*-Hex/EtOAc = 16/1 + 1% Et_3N) the product (**72**) (0.780 g, 4.33 mmol, 72%) was obtained as colorless oil.

***R*f** = 0.30 (*n*-Hex:EtOAc / 80:5 + 1% Et_3N)

^{1}H NMR (400 MHz, $CDCl_3$): δ/ppm = 1.80-1.60 (m, 12H), 1.60-1.47 (m, 8H).

^{13}C NMR (101 MHz, $CDCl_3$): δ/ppm = 67.4, 30.9, 26.1, 25.4.

Spiro[5.6]dodecan-7-one (73)

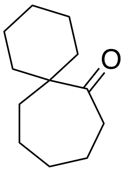

For the synthesis of spiro[5.6]dodecan-7-one**,** biscyclohexyloxirane (**72**) (0.180 g, 1.0 mmol, 1.0 equiv.) was employed in the general procedure for the catalytic Meinwald rearrangement with T1 and $TiCl_4$ in $C_2H_4Cl_2$ at 45 °C. After column chromatography (*n*-Hex/EtOAc = 10/1) the product (**73**) (0.031 g, 0.17 mmol, 17%) was obtained as colorless oil.

***R*f** = 0.22 (*n*-Hex:EtOAc / 10:1)

^{1}H NMR (400 MHz, $CDCl_3$): δ/ppm = 2.51-2.46 (m, 2H), 1.77-1.31 (m, 18H).

^{13}C NMR (101 MHz, $CDCl_3$): δ/ppm = 218.3, 51.0, 39.8, 35.0, 33.5, 30.6, 26.9, 26.1, 24.34, 22.2.

6. Spectra

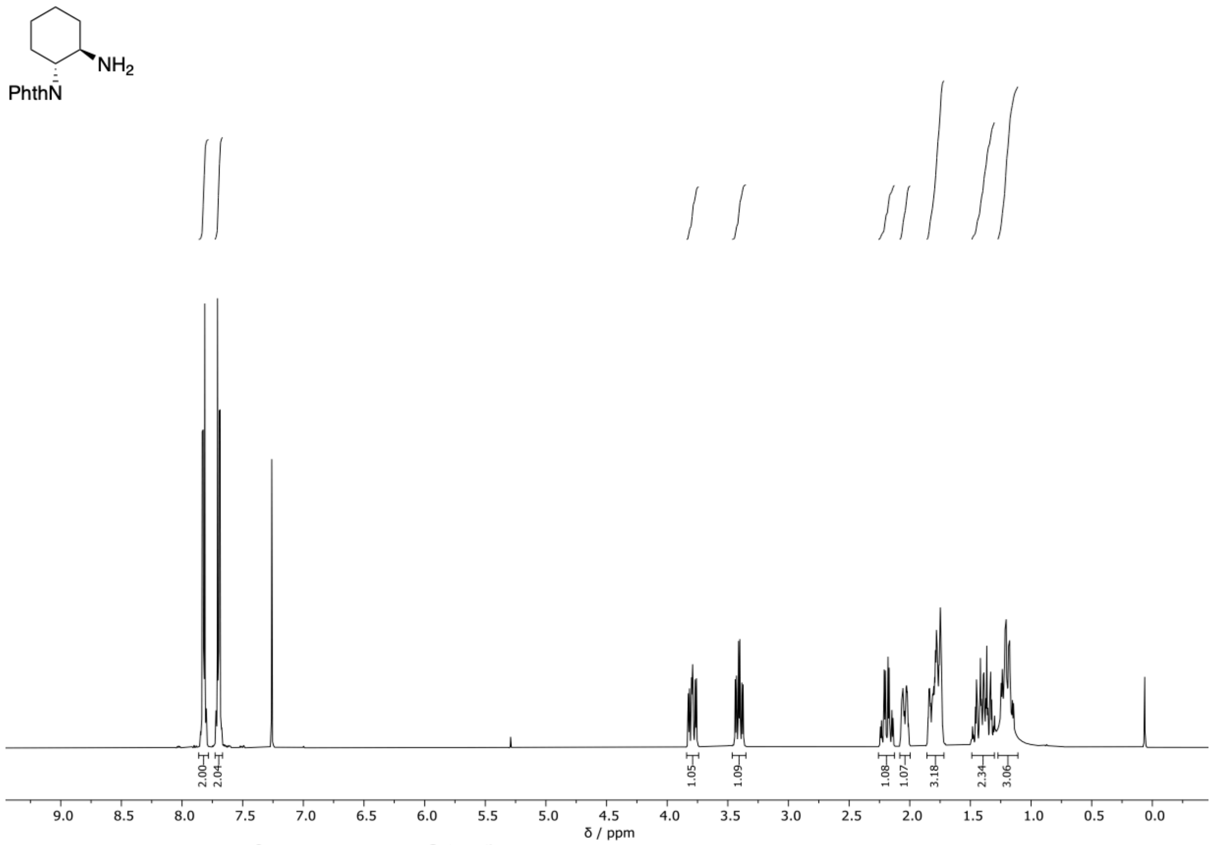
NH2
PhthN
2.00
2.04
1.05
1.09
1.08
1.07
3.18
2.34
3.06
9.0 8.5 8.0 7.5 7.0 6.5 6.0 5.5 5.0 4.5 4.0 3.5 3.0 2.5 2.0 1.5 1.0 0.5 0.0
δ / ppm

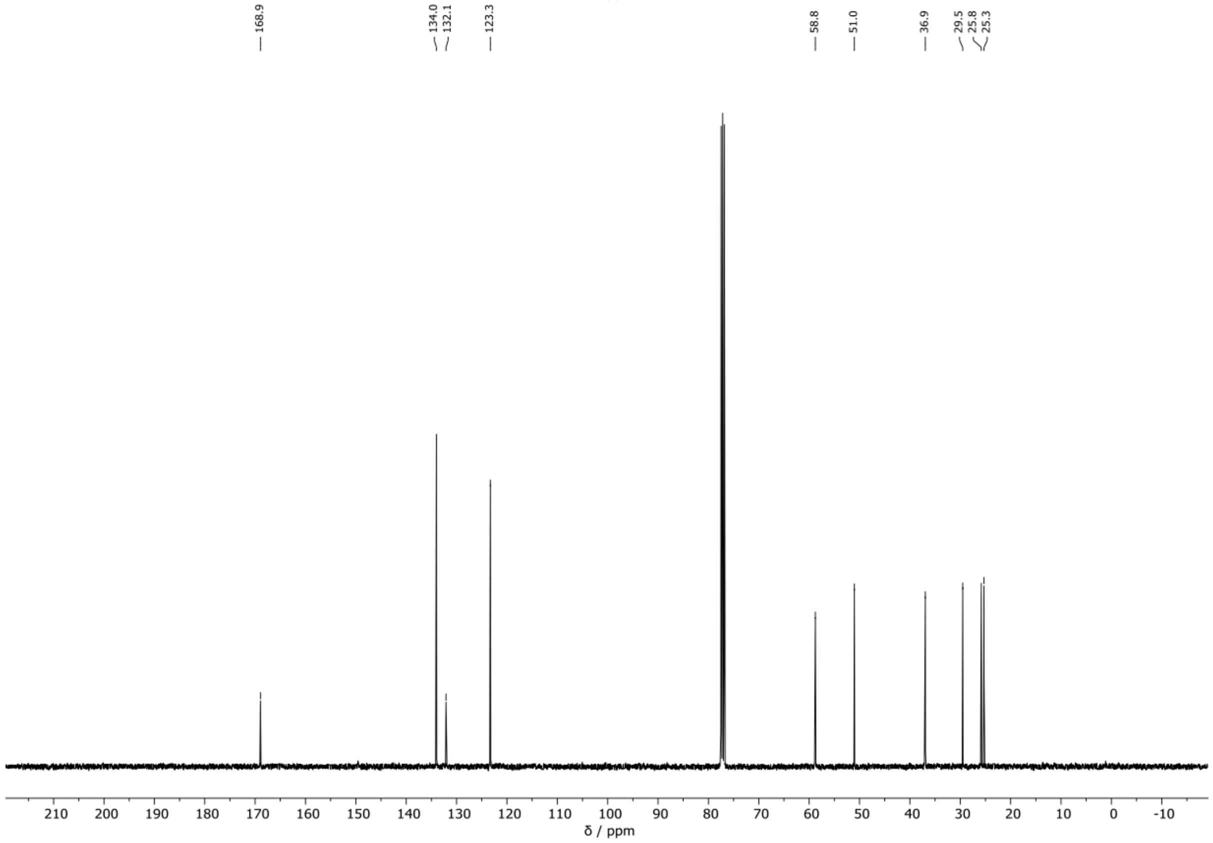
168.9
134.0
132.1
123.3
58.8
51.0
36.9
29.5
25.8
25.3
210 200 190 180 170 160 150 140 130 120 110 100 90 80 70 60 50 40 30 20 10 0 -10
δ / ppm

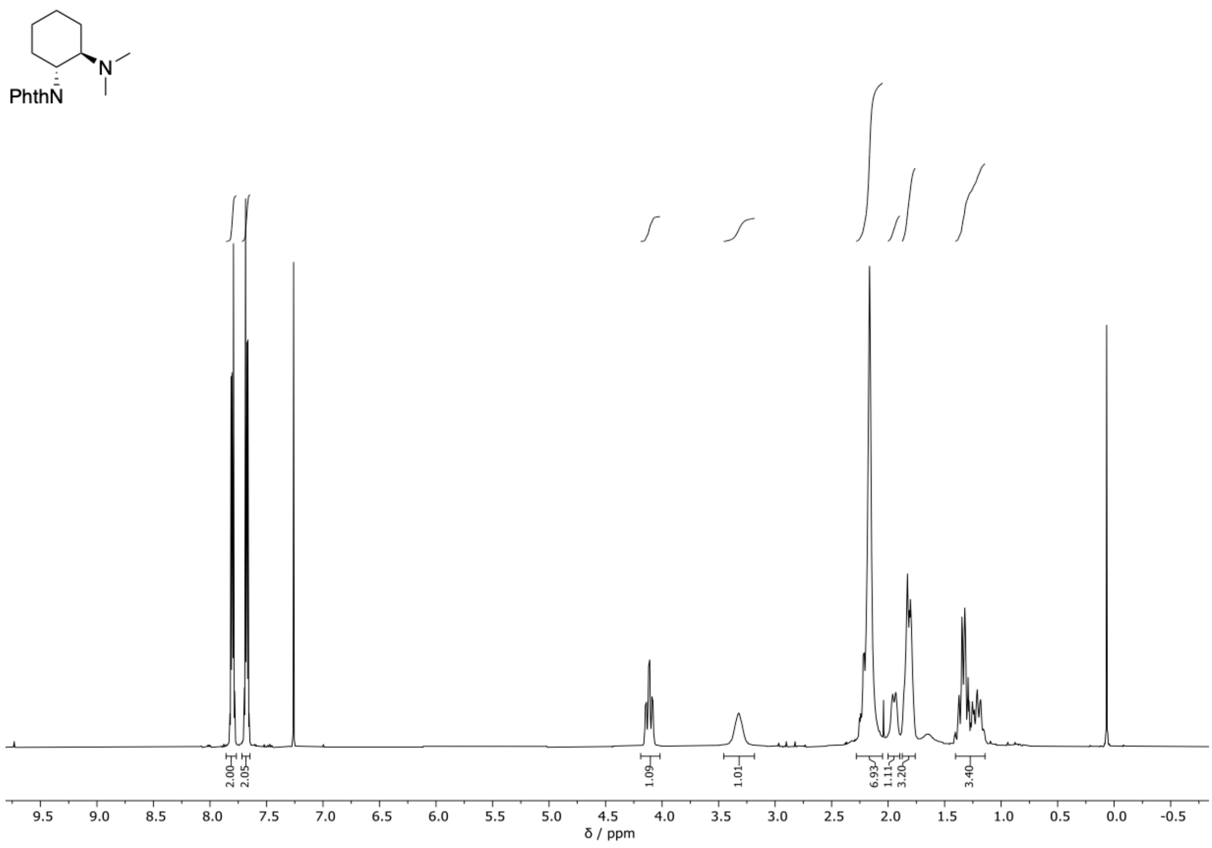
PhthN
N
2.00
2.05
1.09
1.01
6.93
1.11
3.20
3.40
9.5
9.0
8.5
8.0
7.5
7.0
6.5
6.0
5.5
5.0
4.5
4.0
3.5
3.0
2.5
2.0
1.5
1.0
0.5
0.0
-0.5
δ / ppm

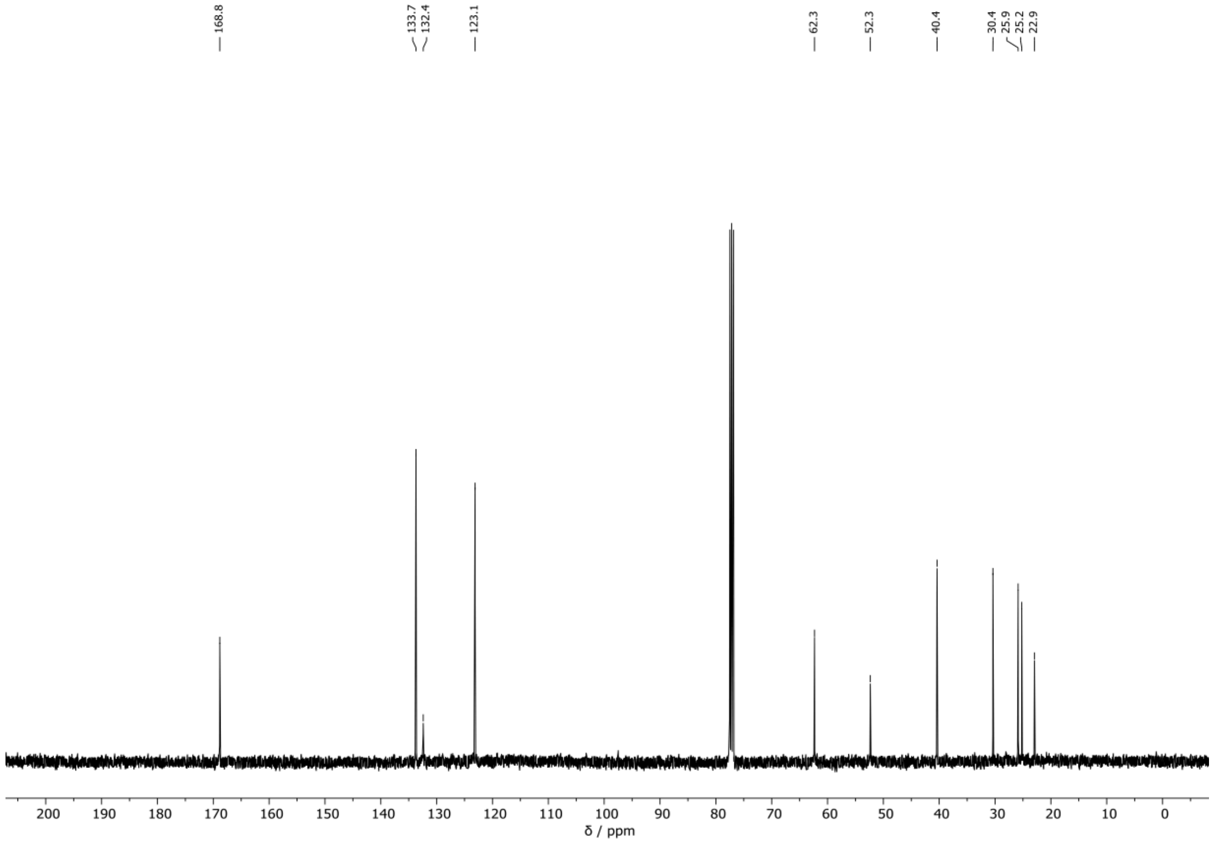
168.8
133.7
132.4
123.1
62.3
52.3
40.4
30.4
25.9
25.2
22.9
200
190
180
170
160
150
140
130
120
110
100
90
80
70
60
50
40
30
20
10
0
δ / ppm

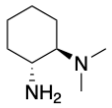
N
NH2

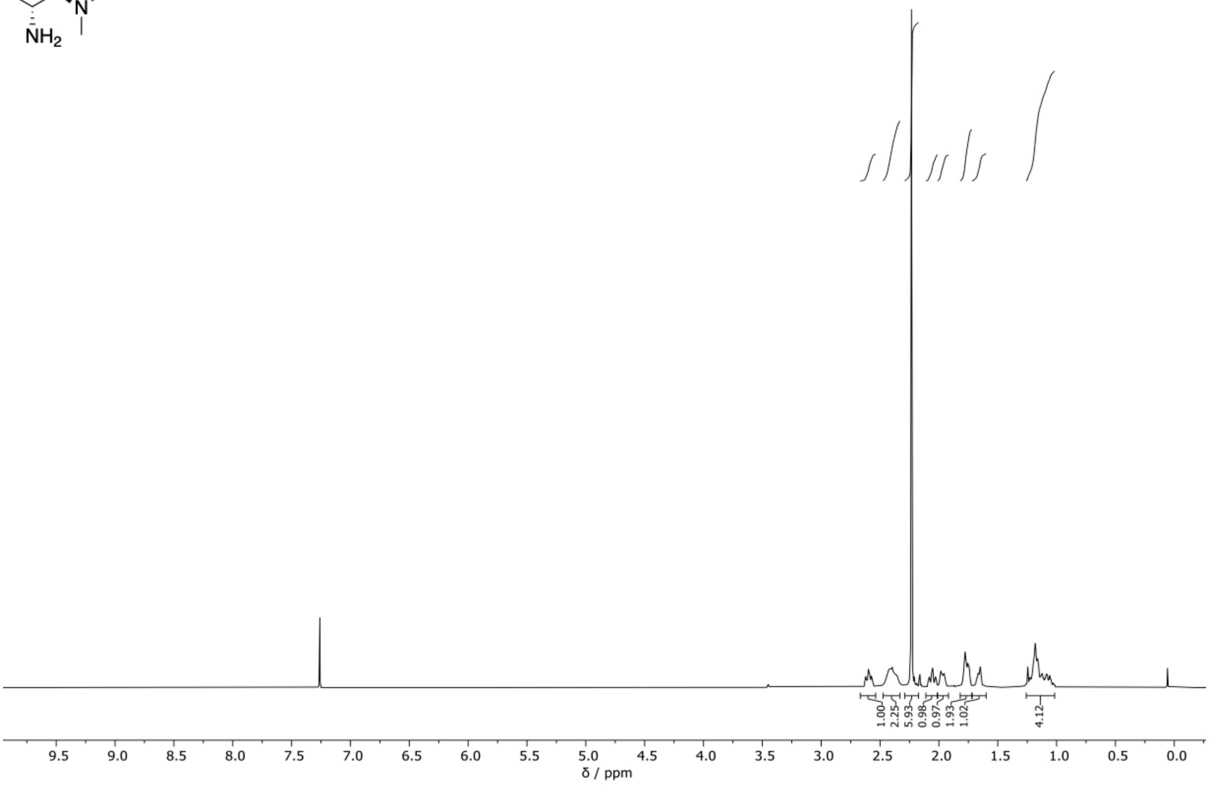
1.00
2.25
5.93
0.98
0.97
1.93
1.02
4.12
9.5
9.0
8.5
8.0
7.5
7.0
6.5
6.0
5.5
5.0
4.5
4.0
3.5
3.0
2.5
2.0
1.5
1.0
0.5
0.0
δ / ppm

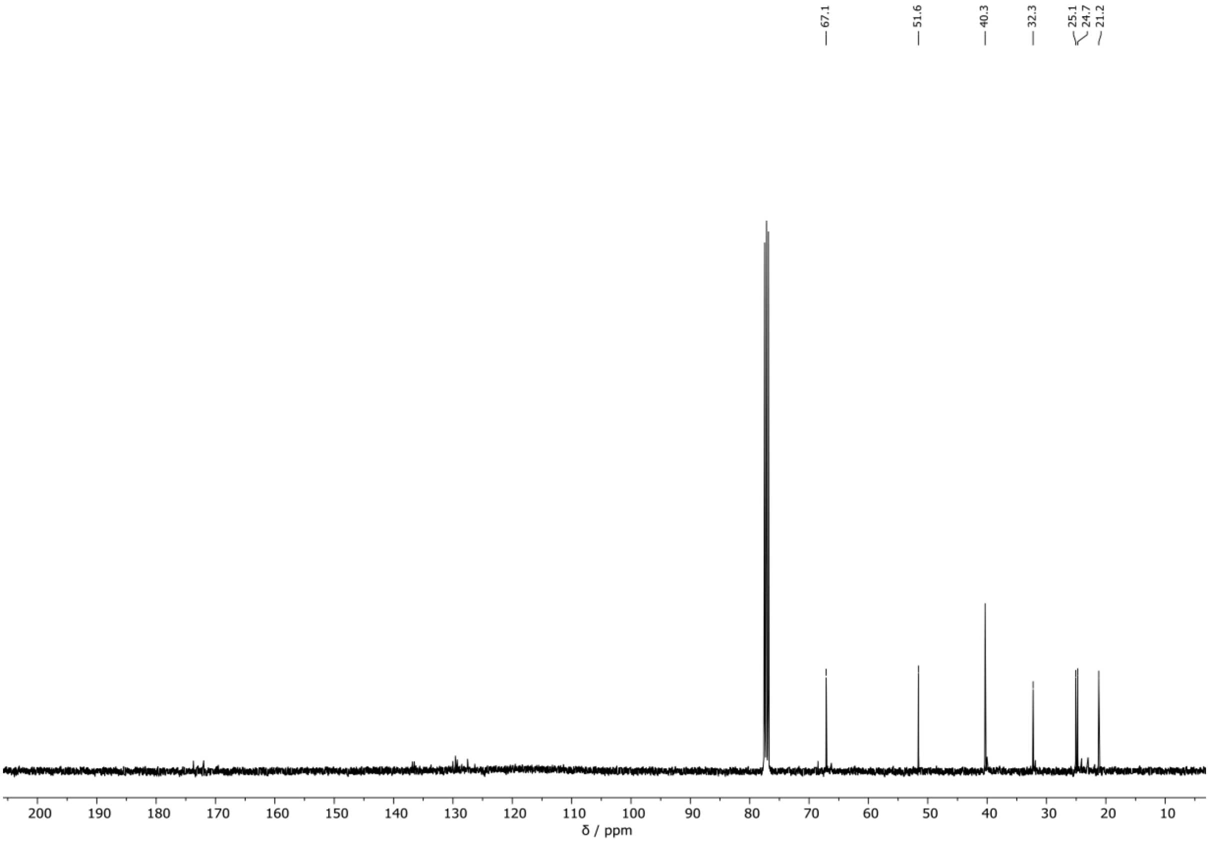
67.1
51.6
40.3
32.3
25.1
24.7
21.2
200
190
180
170
160
150
140
130
120
110
100
90
80
70
60
50
40
30
20
10
δ / ppm

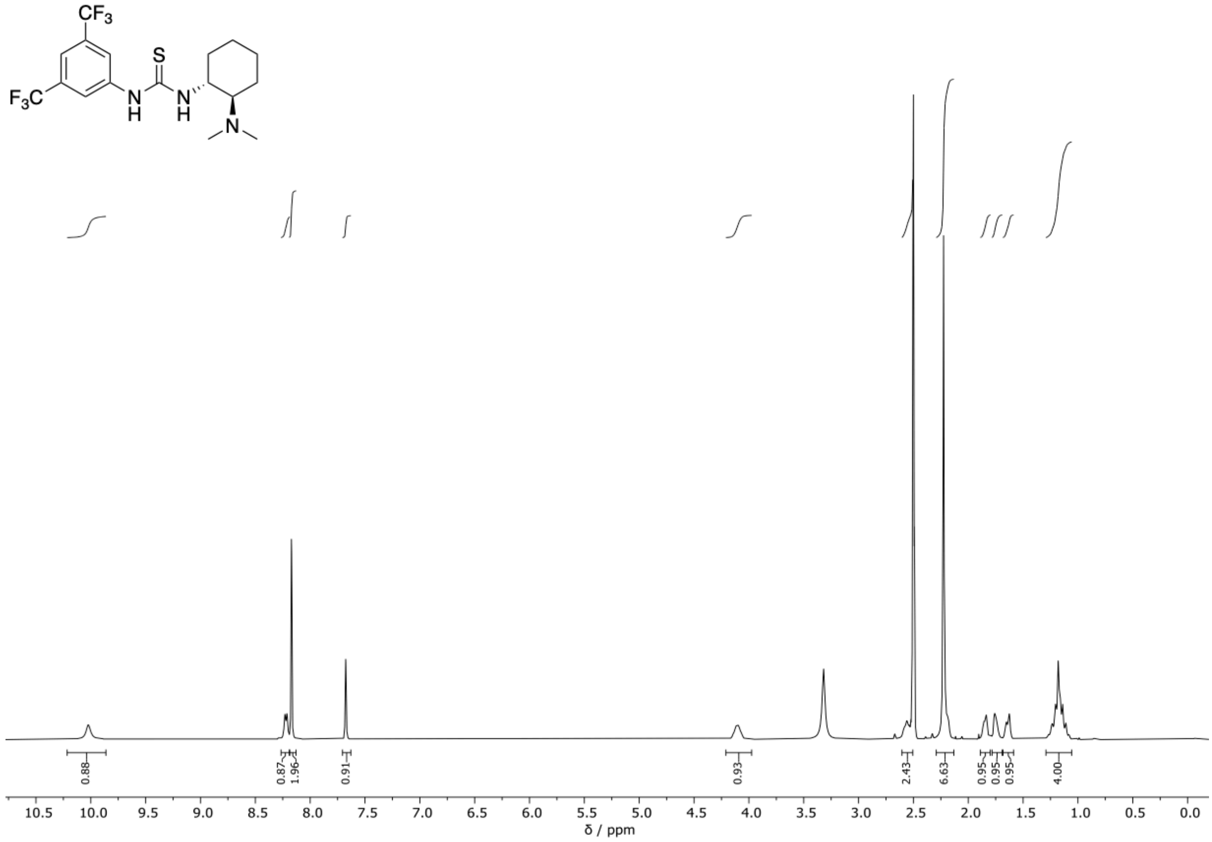
CF3
S
F3C
N
H
N
H
N
0.88
0.87
1.96
0.91
0.93
2.43
6.63
0.95
0.95
0.95
4.00
10.5
10.0
9.5
9.0
8.5
8.0
7.5
7.0
6.5
6.0
5.5
5.0
4.5
4.0
3.5
3.0
2.5
2.0
1.5
1.0
0.5
0.0
δ / ppm

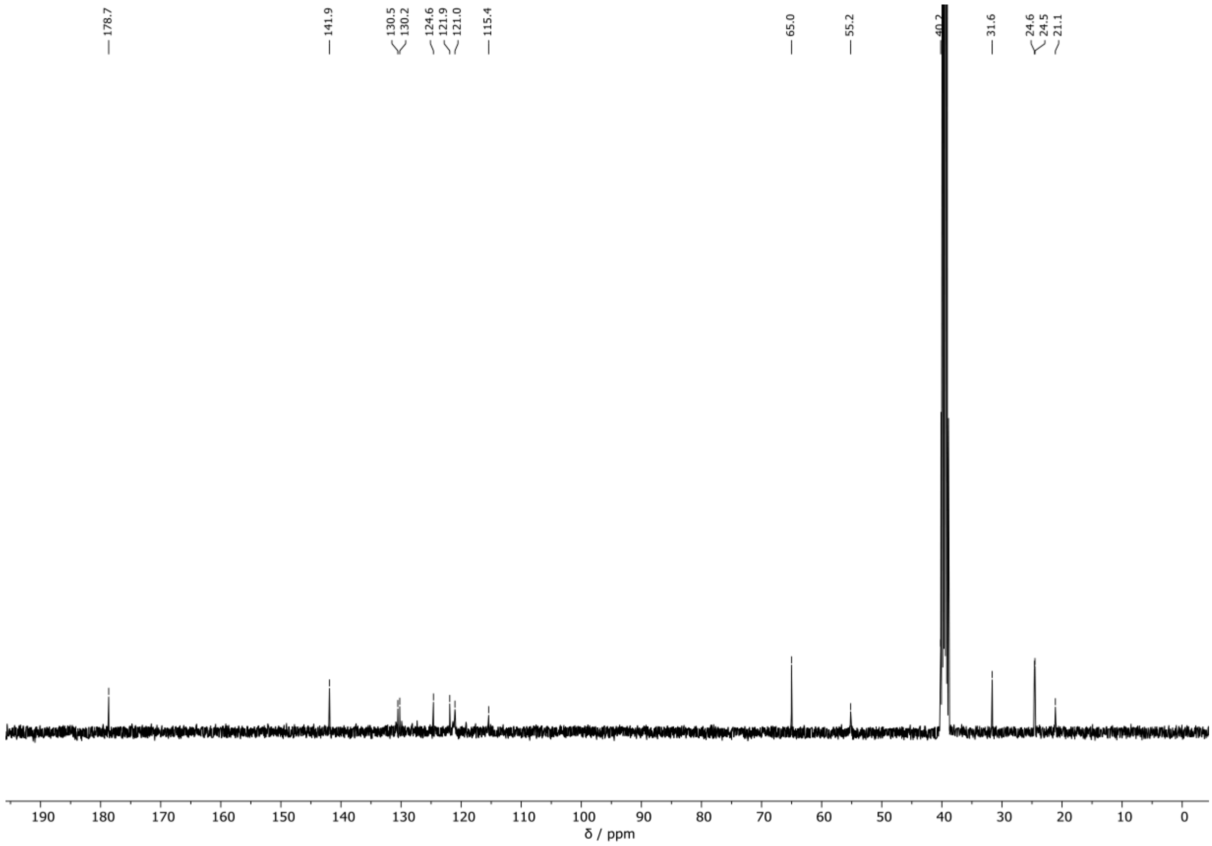
178.7
141.9
130.5
130.2
124.6
121.9
121.0
115.4
65.0
55.2
40.2
31.6
24.6
24.5
21.1
190
180
170
160
150
140
130
120
110
100
90
80
70
60
50
40
30
20
10
0
δ / ppm

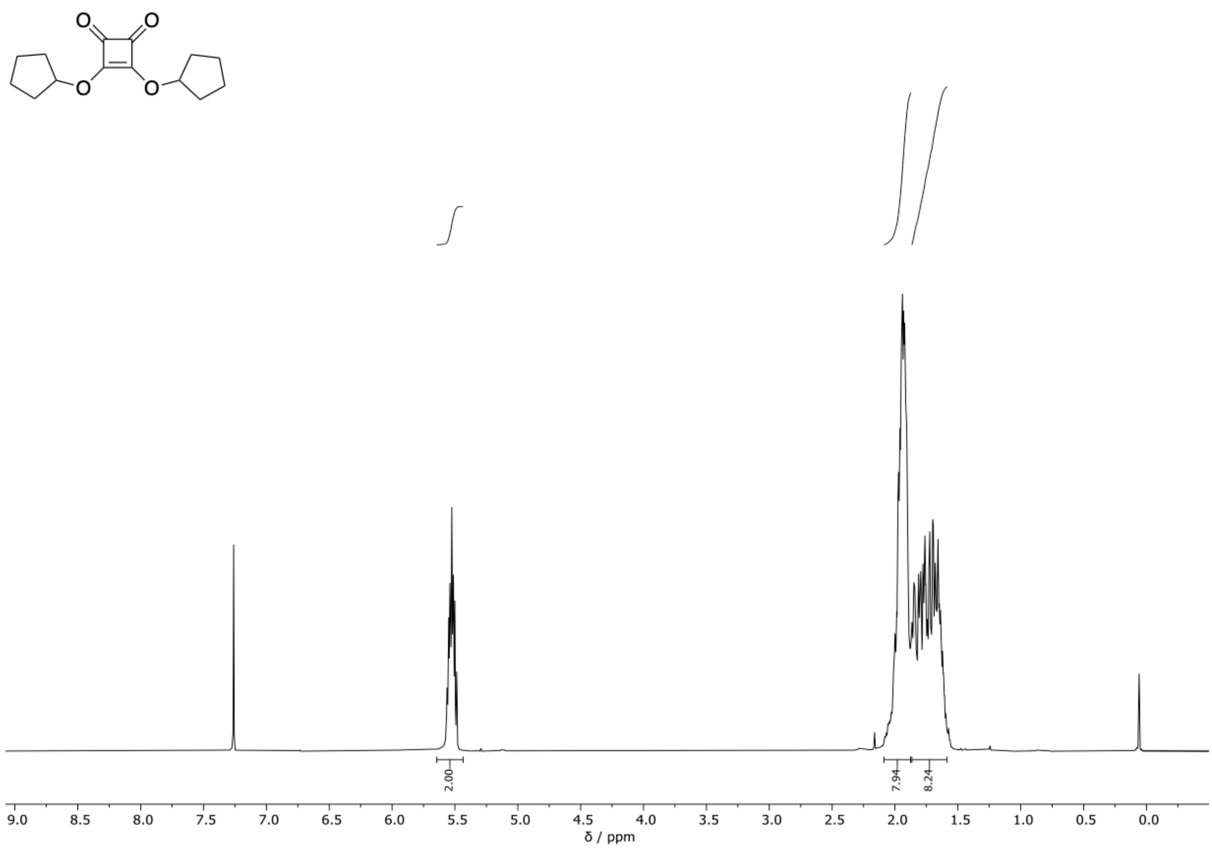
O
O
O
O
2.00
7.94
8.24
9.0
8.5
8.0
7.5
7.0
6.5
6.0
5.5
5.0
4.5
4.0
3.5
3.0
2.5
2.0
1.5
1.0
0.5
0.0
δ / ppm

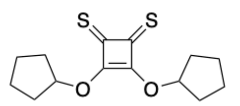
S
S
O
O

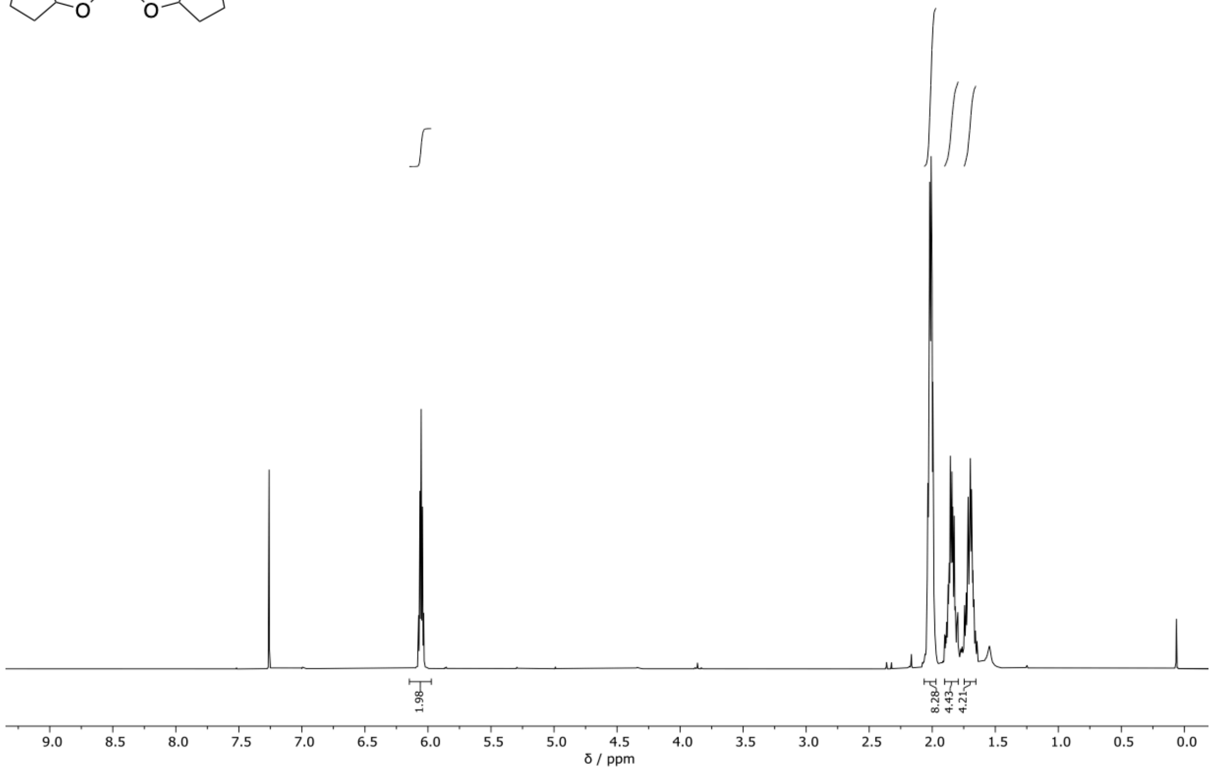
1.98
8.28
4.43
4.21
9.0
8.5
8.0
7.5
7.0
6.5
6.0
5.5
5.0
4.5
4.0
3.5
3.0
2.5
2.0
1.5
1.0
0.5
0.0
δ / ppm

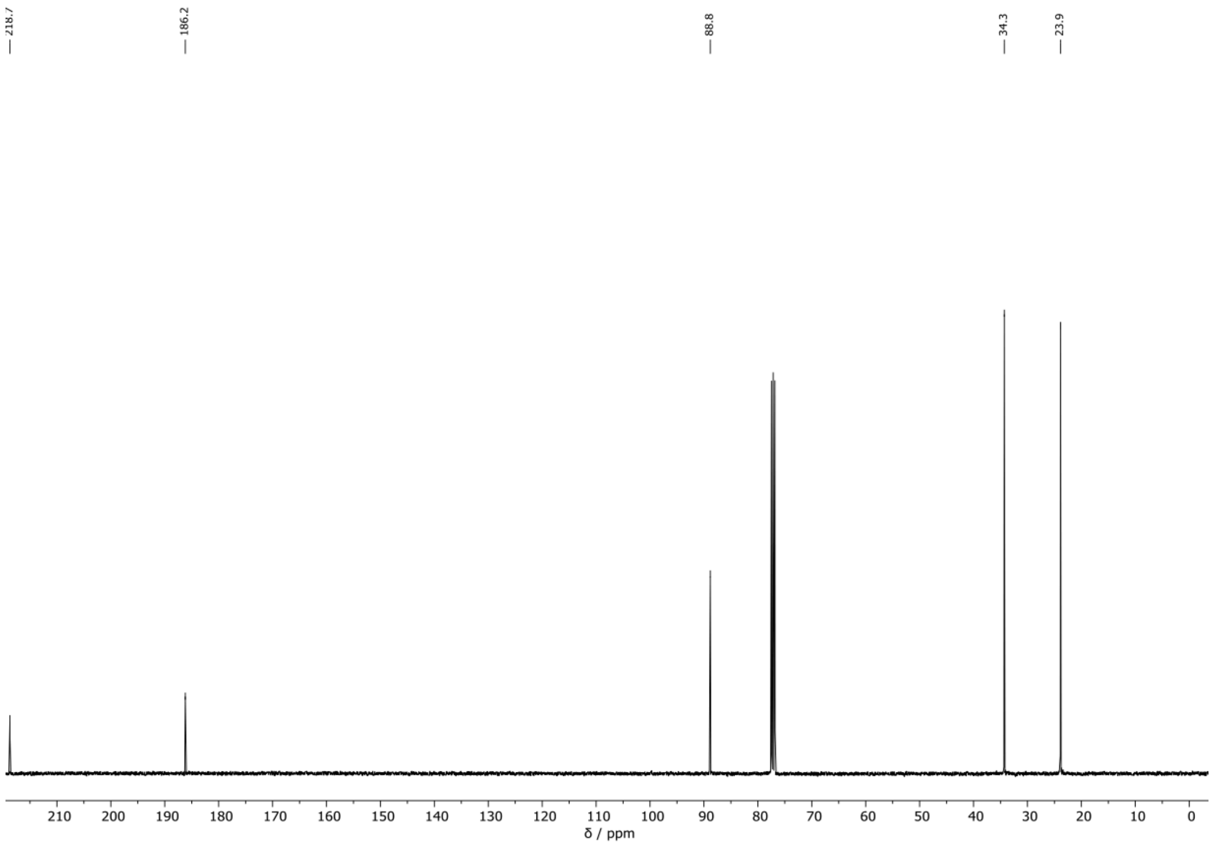
218.7
186.2
88.8
34.3
23.9
210
200
190
180
170
160
150
140
130
120
110
100
90
80
70
60
50
40
30
20
10
0
δ / ppm

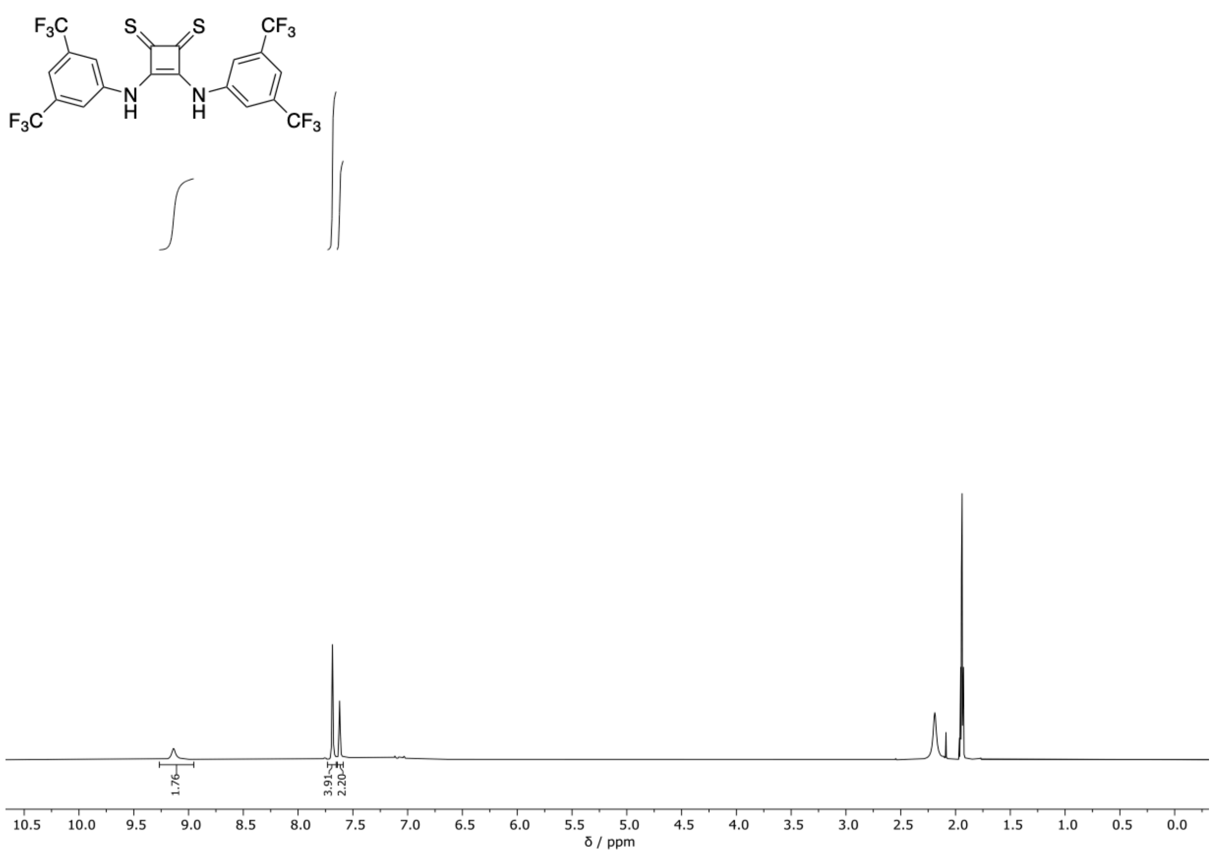
F$_3$C
S
S
CF$_3$
N
H
N
H
F$_3$C
CF$_3$
1.76
3.91
2.20
10.5
10.0
9.5
9.0
8.5
8.0
7.5
7.0
6.5
6.0
5.5
5.0
4.5
4.0
3.5
3.0
2.5
2.0
1.5
1.0
0.5
0.0
δ / ppm

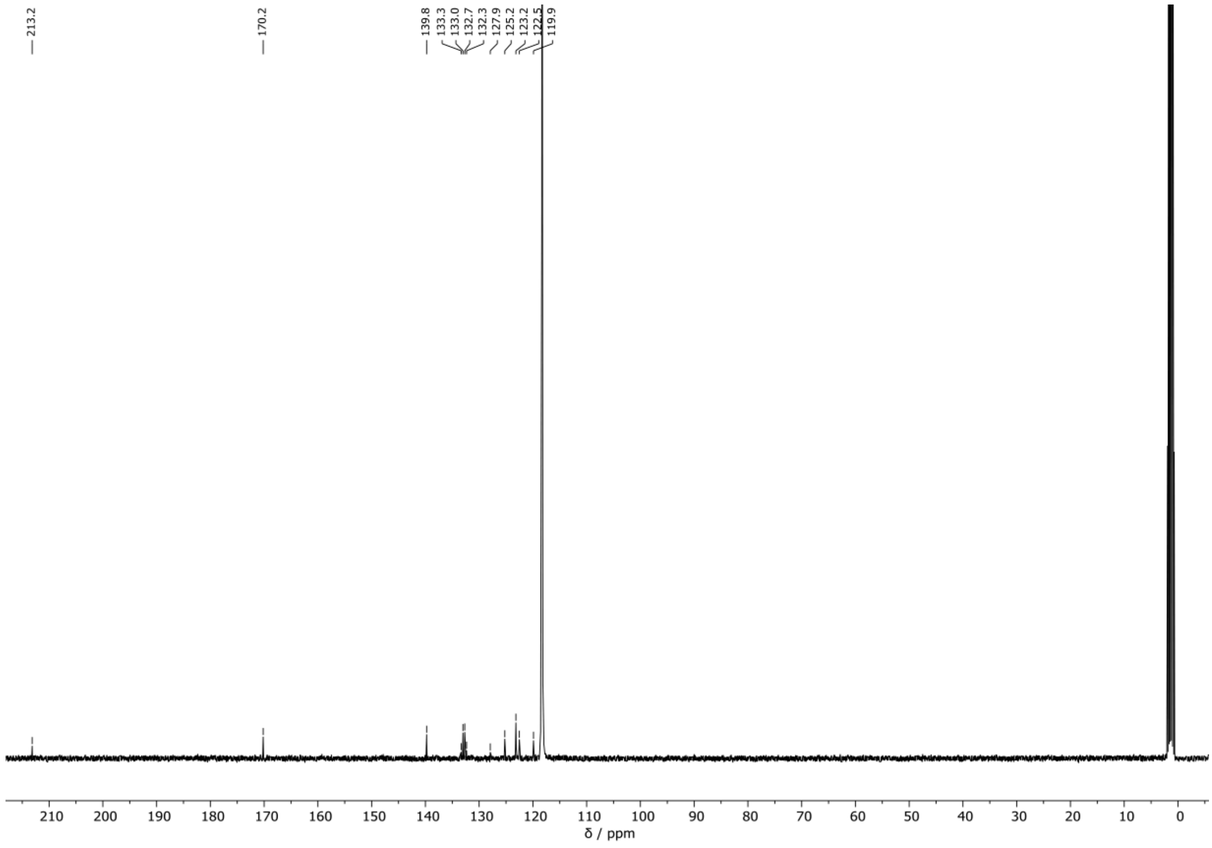
213.2
170.2
139.8
133.3
133.0
132.7
132.3
127.9
125.2
123.2
122.5
119.9
210
200
190
180
170
160
150
140
130
120
110
100
90
80
70
60
50
40
30
20
10
0
δ / ppm

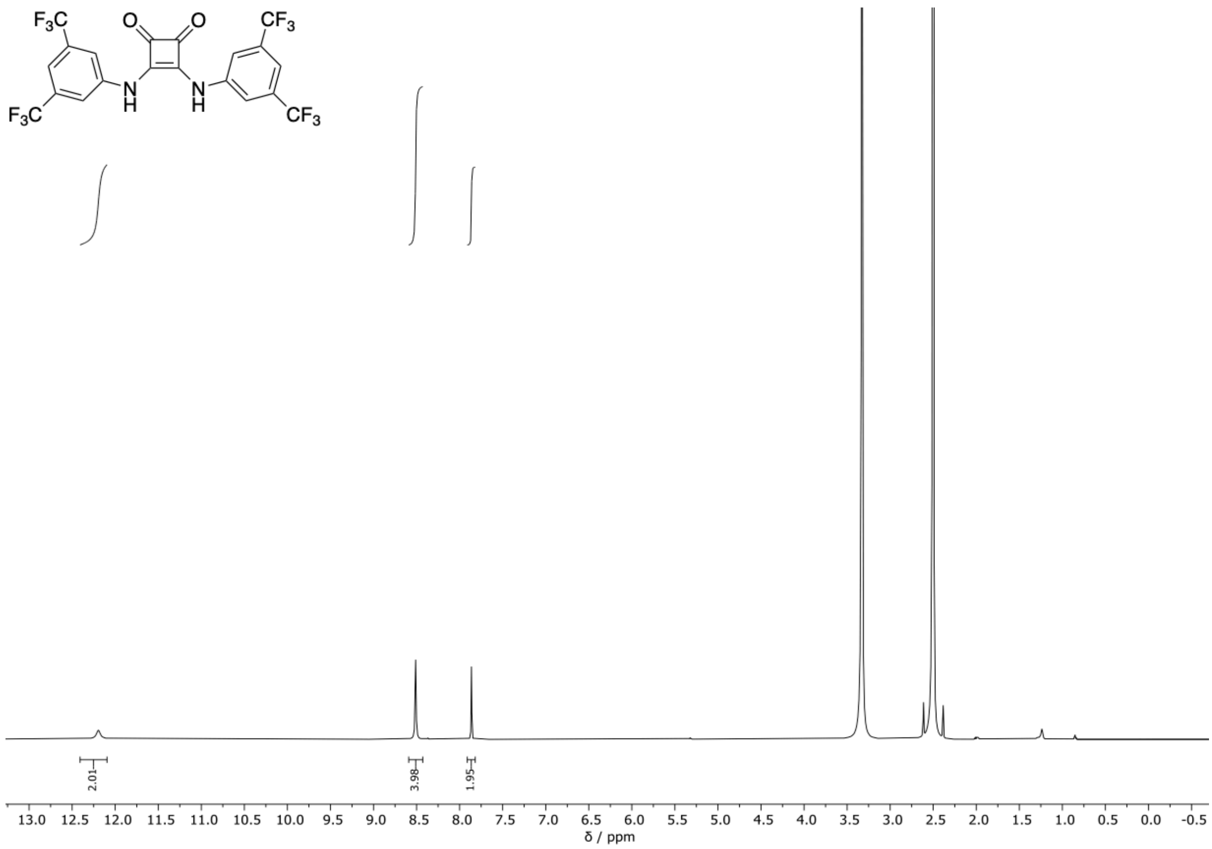
F$_3$C
O
O
CF$_3$
N
H
N
H
F$_3$C
CF$_3$
2.01
3.98
1.95
13.0 12.5 12.0 11.5 11.0 10.5 10.0 9.5 9.0 8.5 8.0 7.5 7.0 6.5 6.0 5.5 5.0 4.5 4.0 3.5 3.0 2.5 2.0 1.5 1.0 0.5 0.0 -0.5
δ / ppm

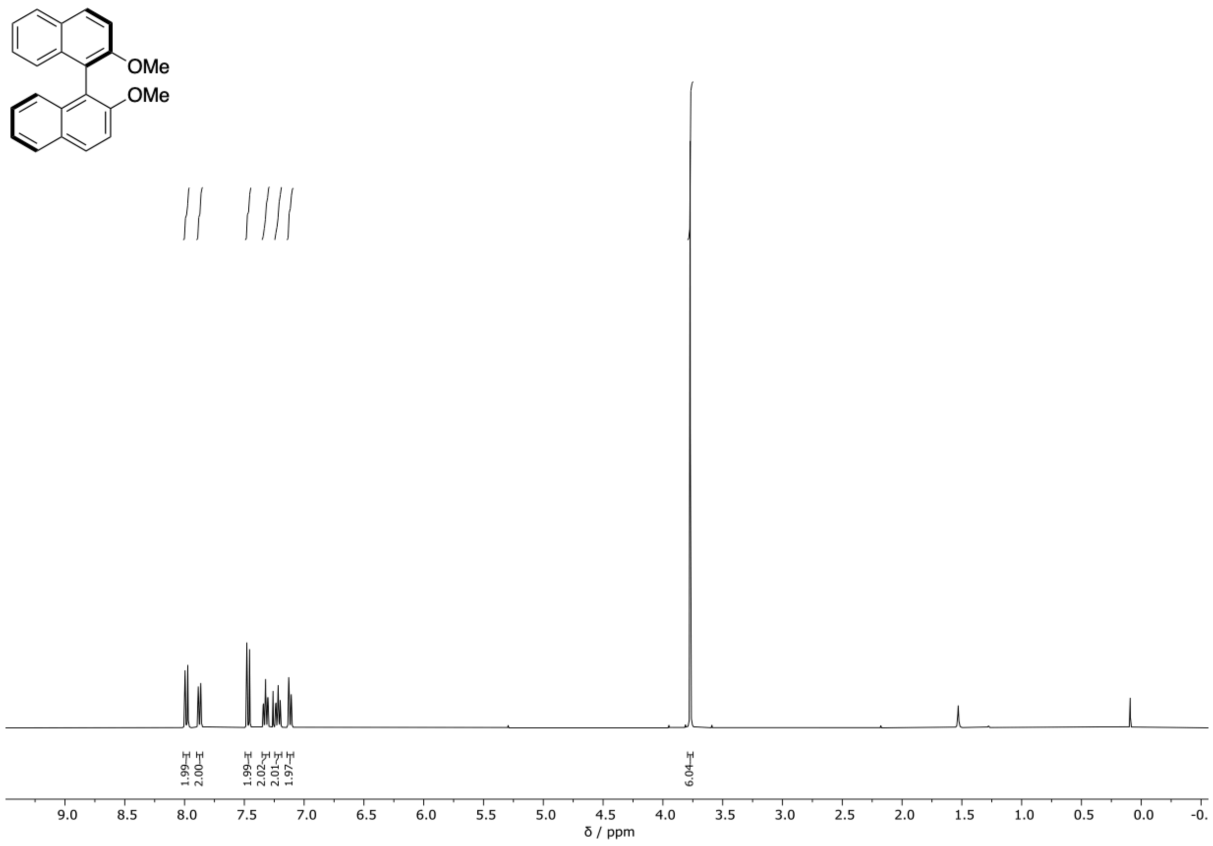
OMe
OMe
1.99
2.00
1.99
2.02
2.01
1.97
6.04
9.0
8.5
8.0
7.5
7.0
6.5
6.0
5.5
5.0
4.5
4.0
3.5
3.0
2.5
2.0
1.5
1.0
0.5
0.0
-0.
δ / ppm

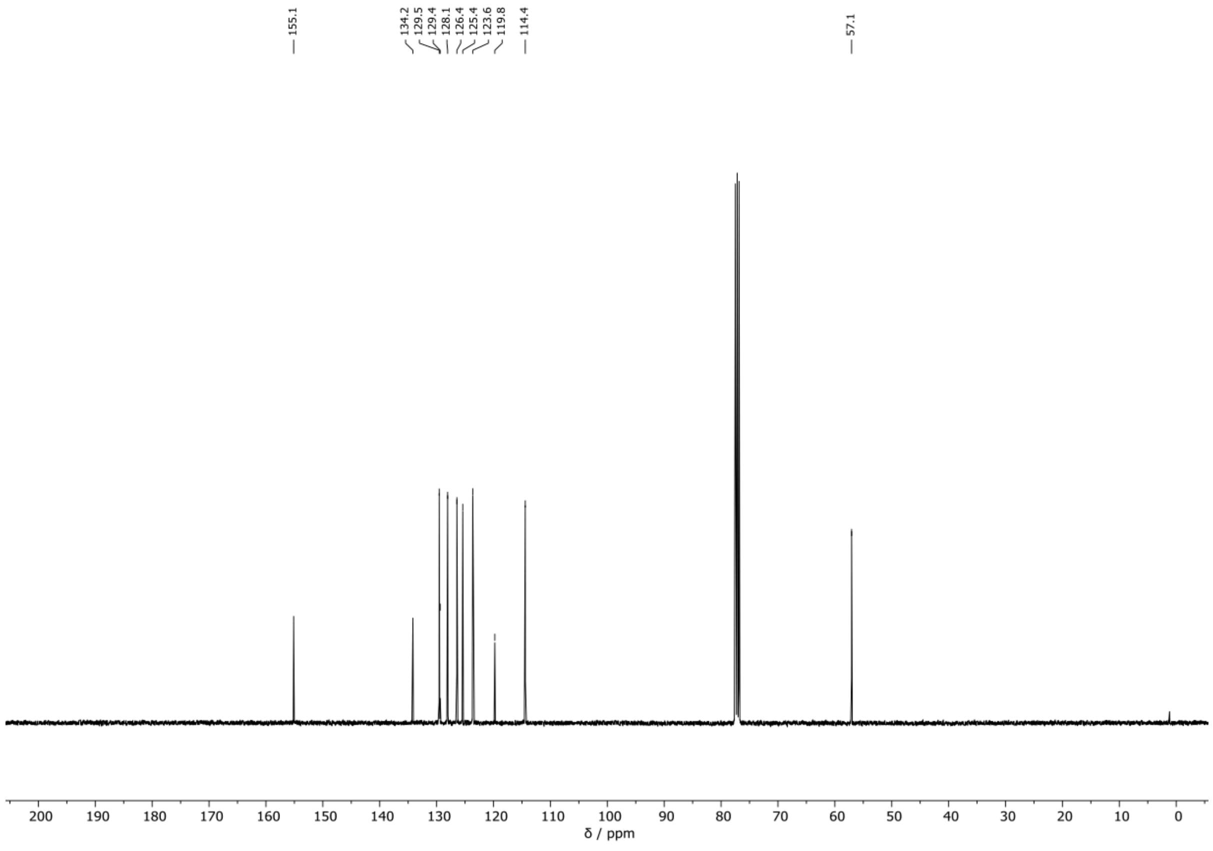
155.1
134.2
129.5
129.4
128.1
126.4
125.4
123.6
119.8
114.4
57.1
200
190
180
170
160
150
140
130
120
110
100
90
80
70
60
50
40
30
20
10
0
δ / ppm

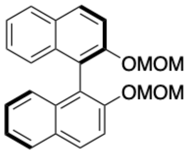
OMOM
OMOM

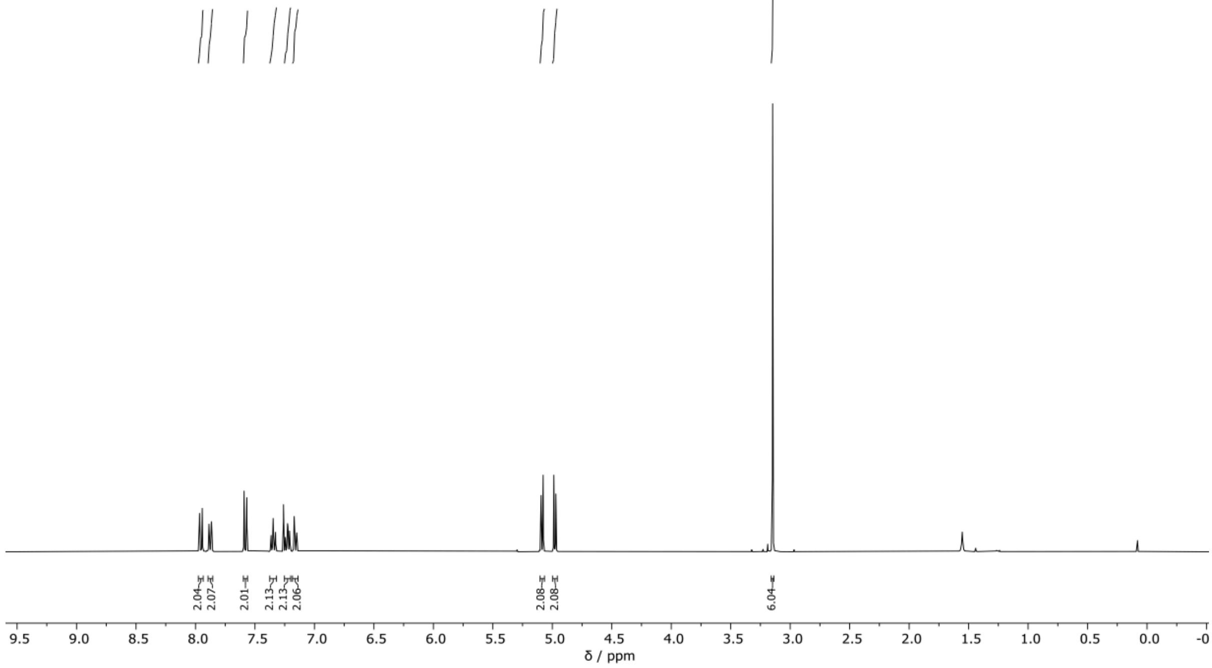
2.04
2.07
2.01
2.13
2.13
2.06
2.08
2.08
6.04
9.5
9.0
8.5
8.0
7.5
7.0
6.5
6.0
5.5
5.0
4.5
4.0
3.5
3.0
2.5
2.0
1.5
1.0
0.5
0.0
-0
δ / ppm

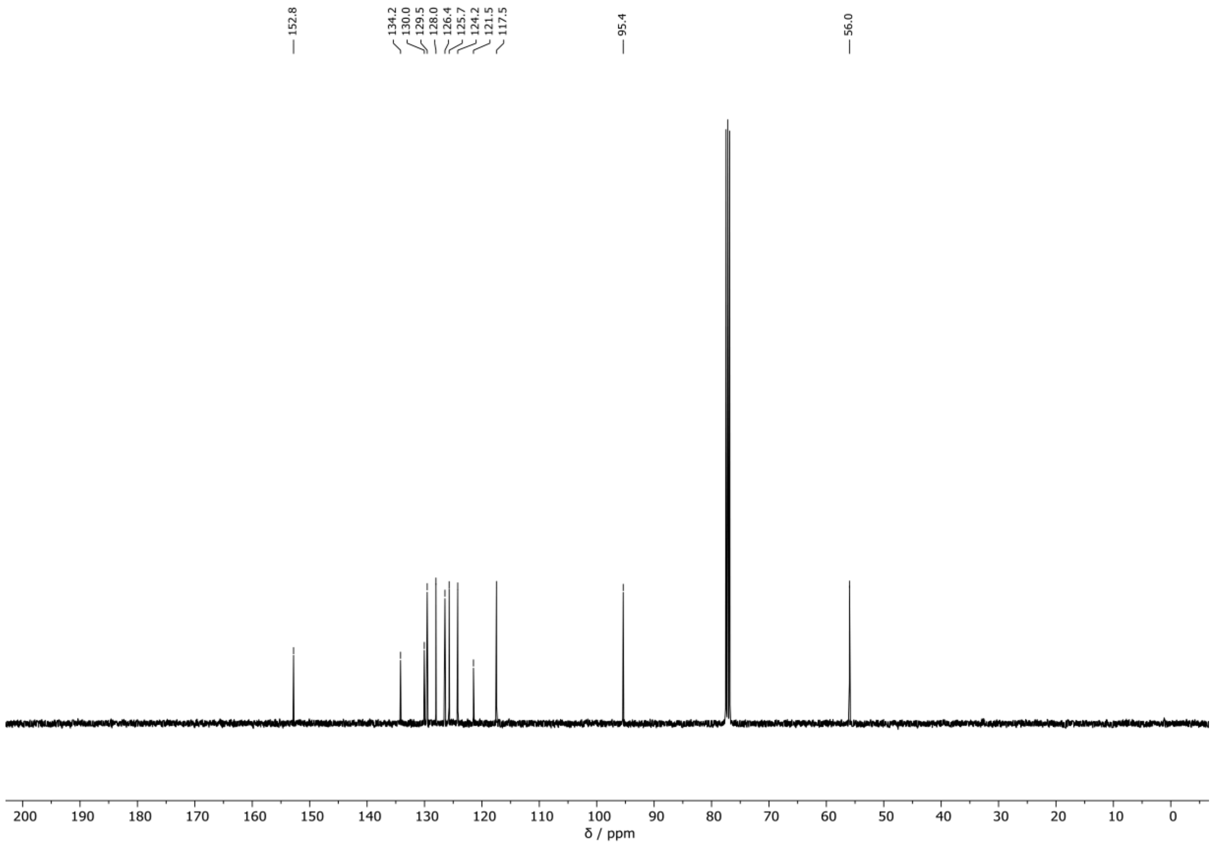
152.8
134.2
130.0
129.5
128.0
126.4
125.7
124.2
121.5
117.5
95.4
56.0
200
190
180
170
160
150
140
130
120
110
100
90
80
70
60
50
40
30
20
10
0
δ / ppm

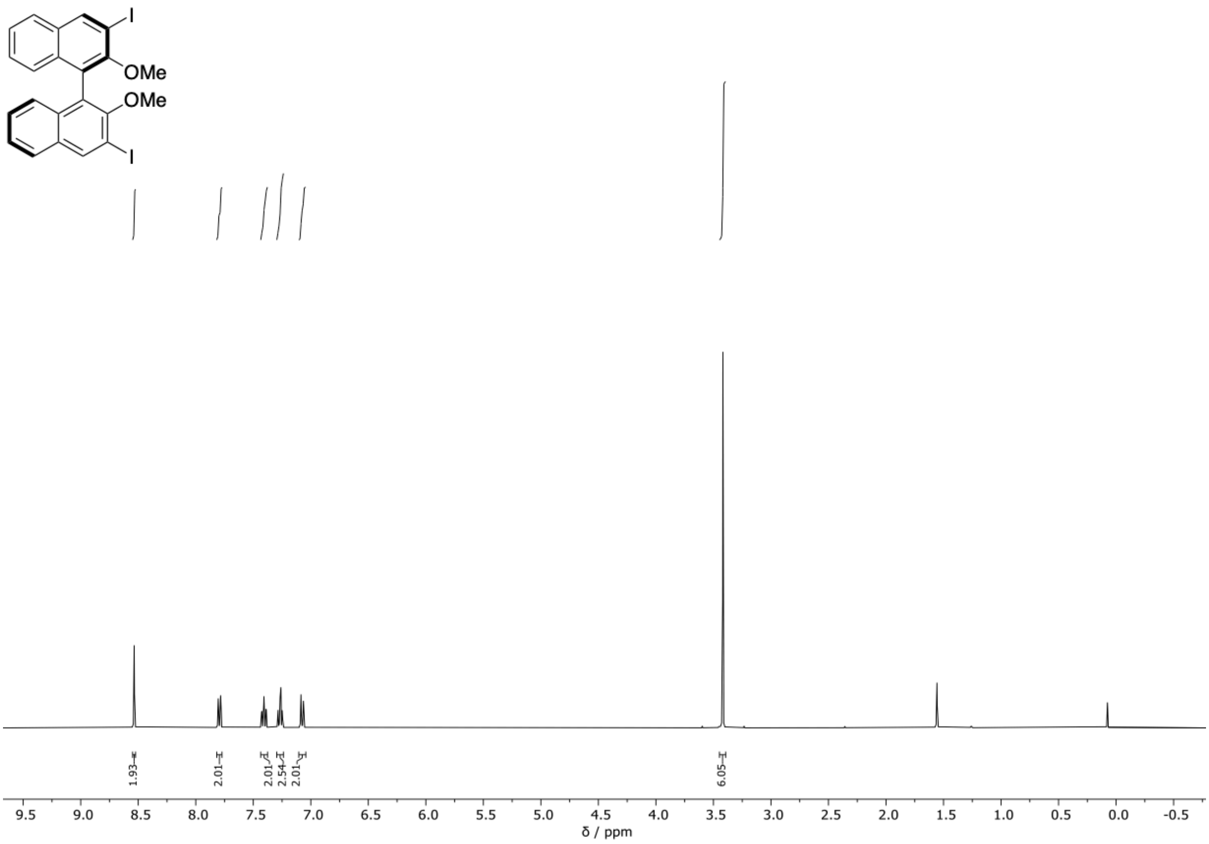
I
OMe
OMe
I
1.93
2.01
2.01
2.54
2.01
6.05
9.5
9.0
8.5
8.0
7.5
7.0
6.5
6.0
5.5
5.0
4.5
4.0
3.5
3.0
2.5
2.0
1.5
1.0
0.5
0.0
-0.5
δ / ppm

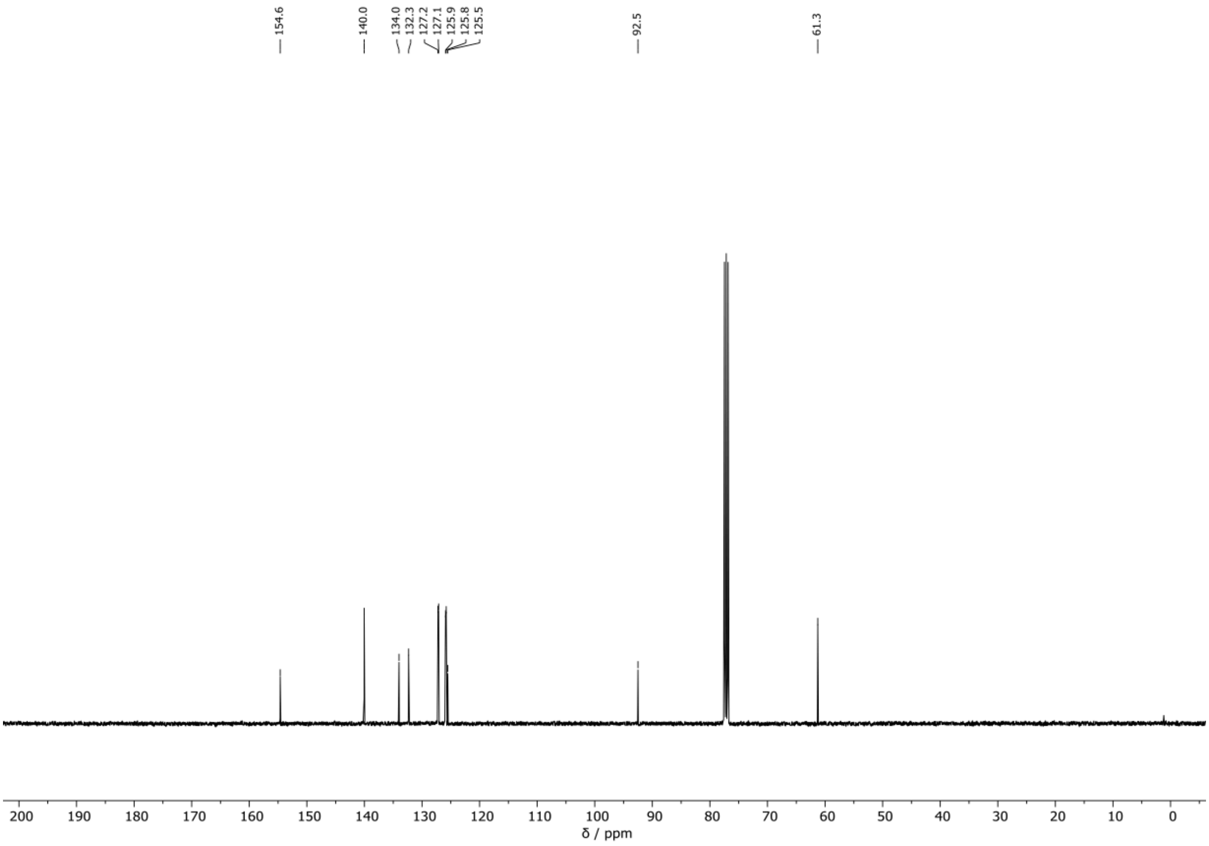
154.6
140.0
134.0
132.3
127.2
127.1
125.9
125.8
125.5
92.5
61.3
200
190
180
170
160
150
140
130
120
110
100
90
80
70
60
50
40
30
20
10
0
δ / ppm

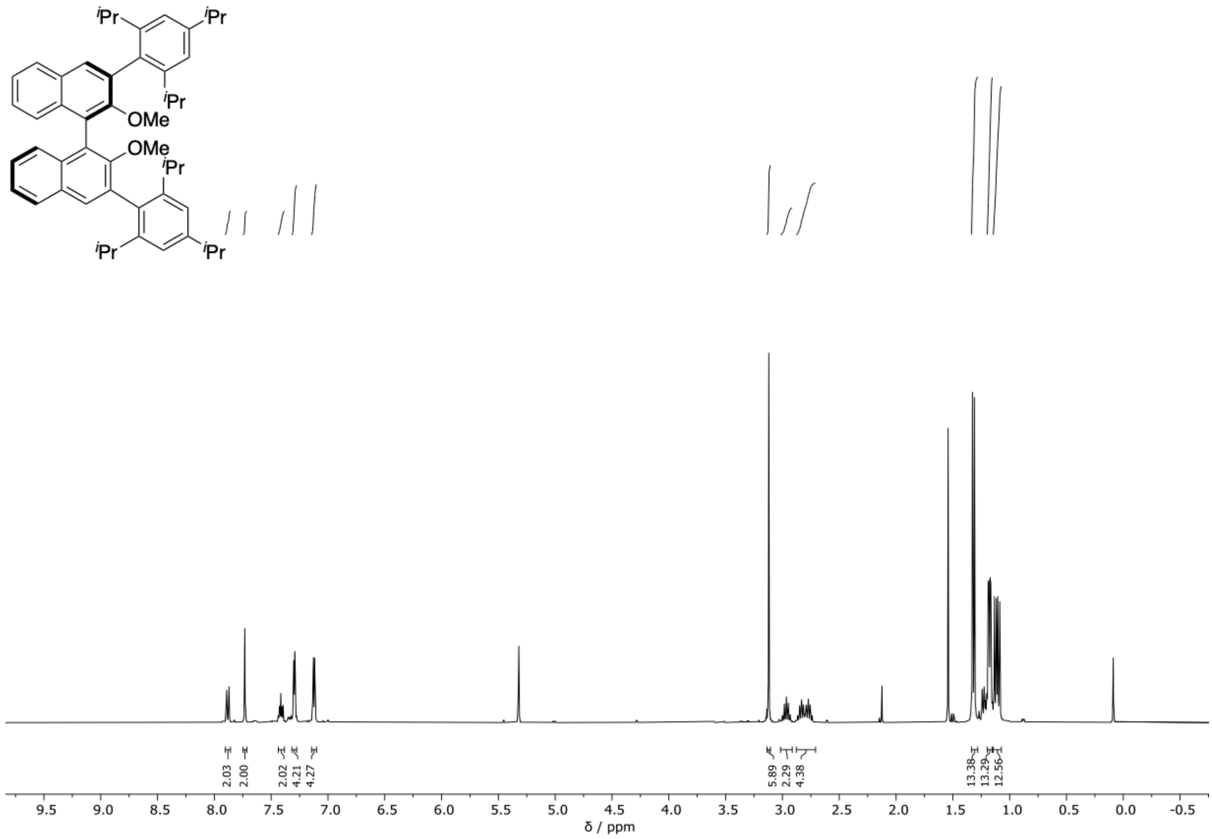
^{i}Pr
^{i}Pr
^{i}Pr
OMe
OMe
^{i}Pr
^{i}Pr
^{i}Pr
2.03
2.00
2.02
4.21
4.27
5.89
2.29
4.38
13.38
13.29
12.56
9.5
9.0
8.5
8.0
7.5
7.0
6.5
6.0
5.5
5.0
4.5
4.0
3.5
3.0
2.5
2.0
1.5
1.0
0.5
0.0
-0.5
δ / ppm

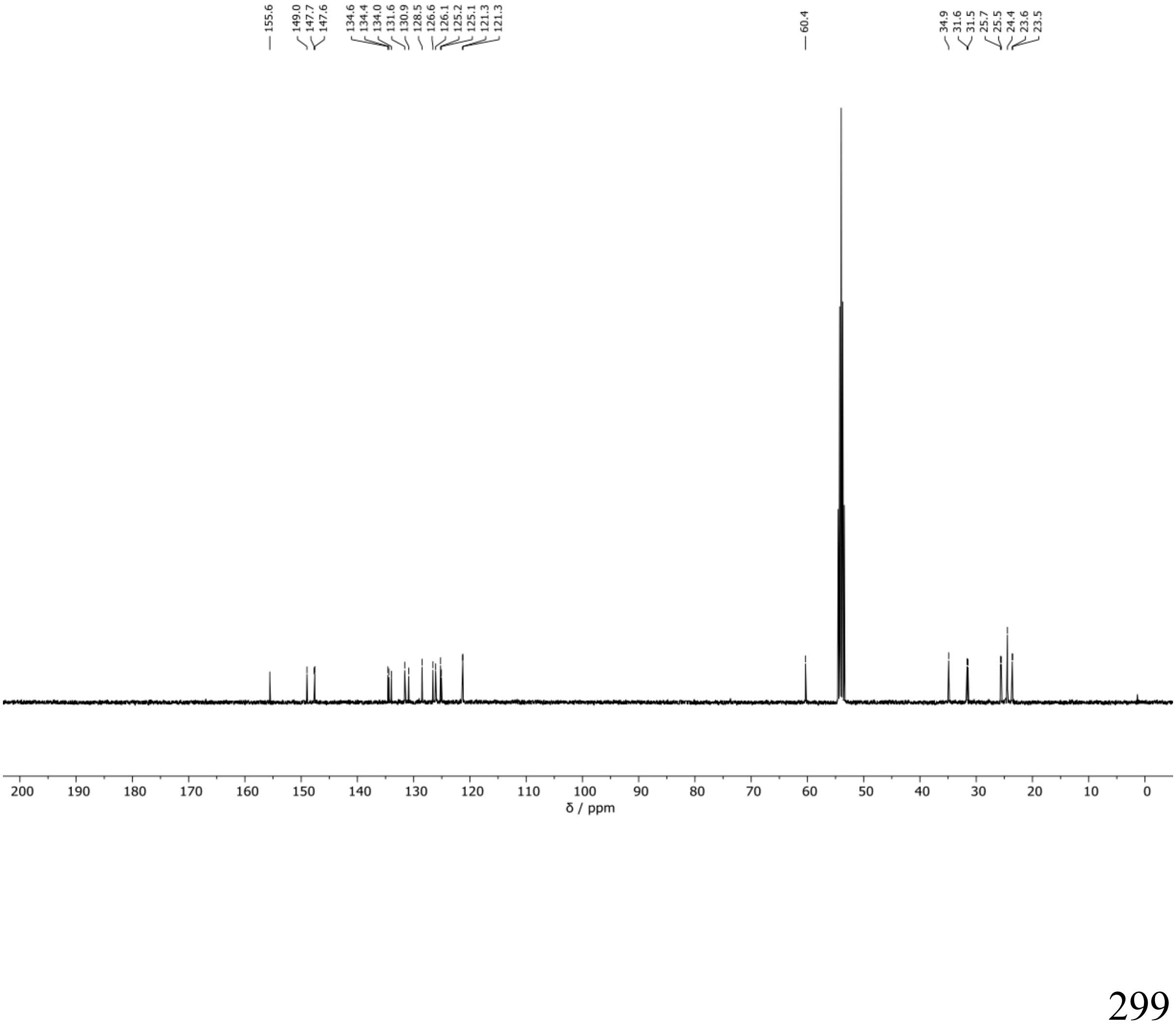
155.6
149.0
147.7
147.6
134.6
134.4
134.0
131.6
130.9
128.5
126.6
126.1
125.2
125.1
121.3
121.3
60.4
34.9
31.6
31.5
25.7
25.5
24.4
23.6
23.5
200
190
180
170
160
150
140
130
120
110
100
90
80
70
60
50
40
30
20
10
0
δ / ppm

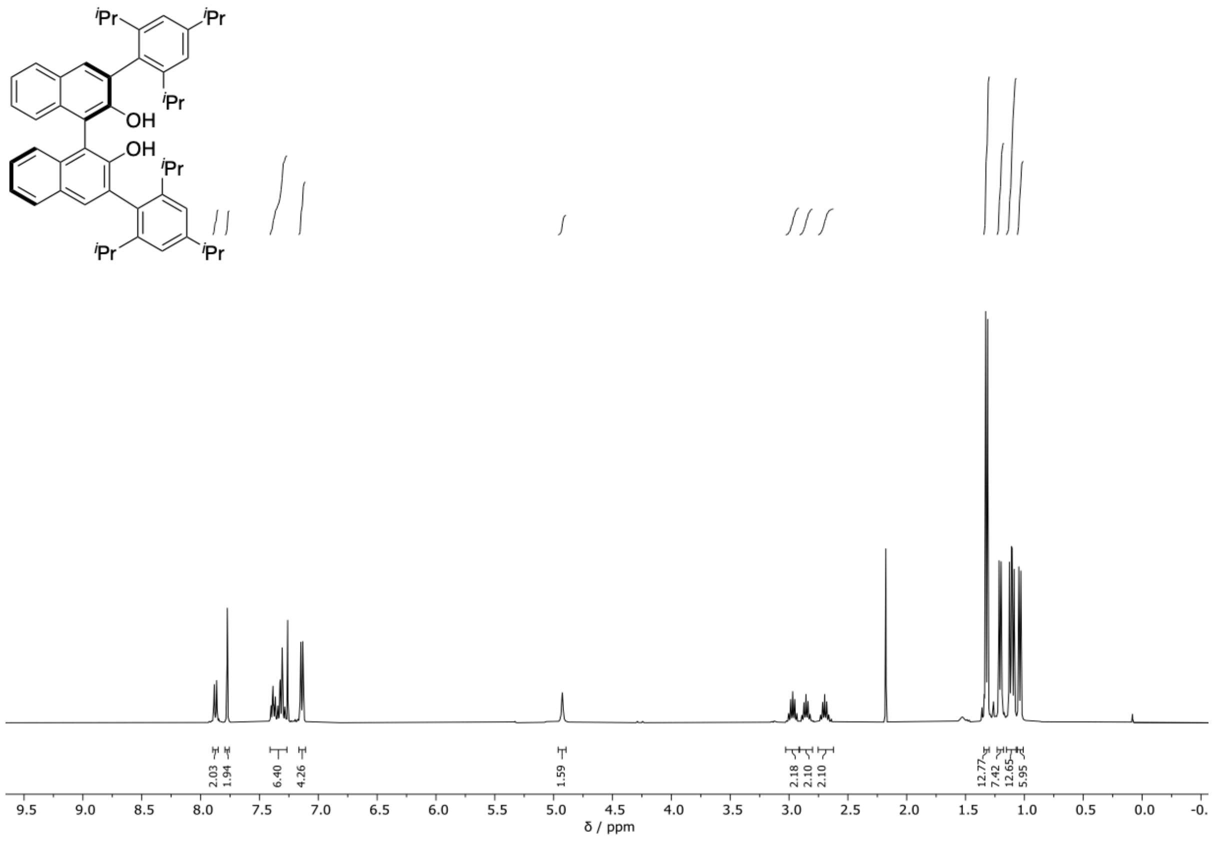

iPr
iPr
iPr
OH
OH
iPr
iPr
iPr
2.03
1.94
6.40
4.26
1.59
2.18
2.10
2.10
12.77
7.42
12.65
5.95
9.5
9.0
8.5
8.0
7.5
7.0
6.5
6.0
5.5
5.0
4.5
4.0
3.5
3.0
2.5
2.0
1.5
1.0
0.5
0.0
-0.
δ / ppm

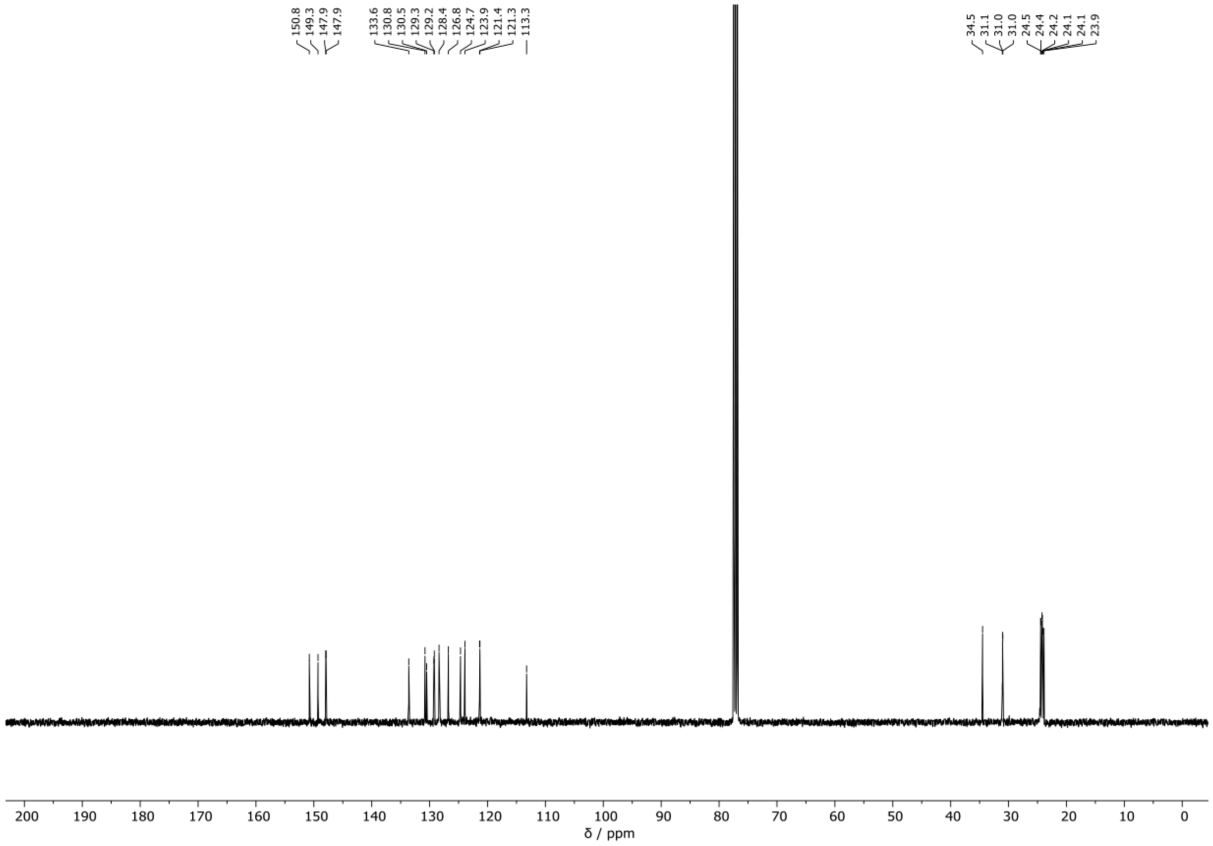

150.8
149.3
147.9
147.9
133.6
130.8
130.5
129.3
129.2
128.4
126.8
124.7
123.9
121.4
121.3
113.3
34.5
31.1
31.0
31.0
24.5
24.4
24.2
24.1
24.1
23.9
200
190
180
170
160
150
140
130
120
110
100
90
80
70
60
50
40
30
20
10
0
δ / ppm

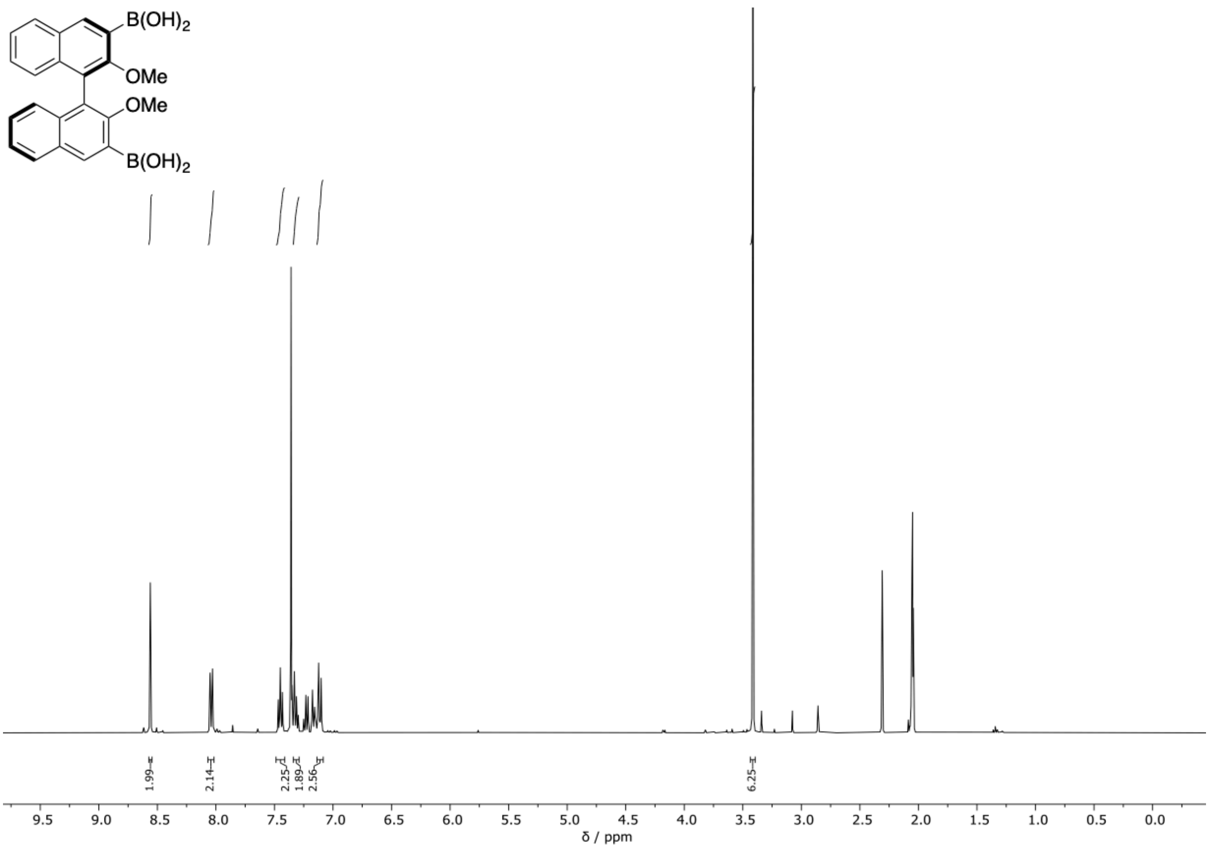
B(OH)2
OMe
OMe
B(OH)2
1.99
2.14
2.25
1.89
2.56
6.25
9.5
9.0
8.5
8.0
7.5
7.0
6.5
6.0
5.5
5.0
4.5
4.0
3.5
3.0
2.5
2.0
1.5
1.0
0.5
0.0
δ / ppm

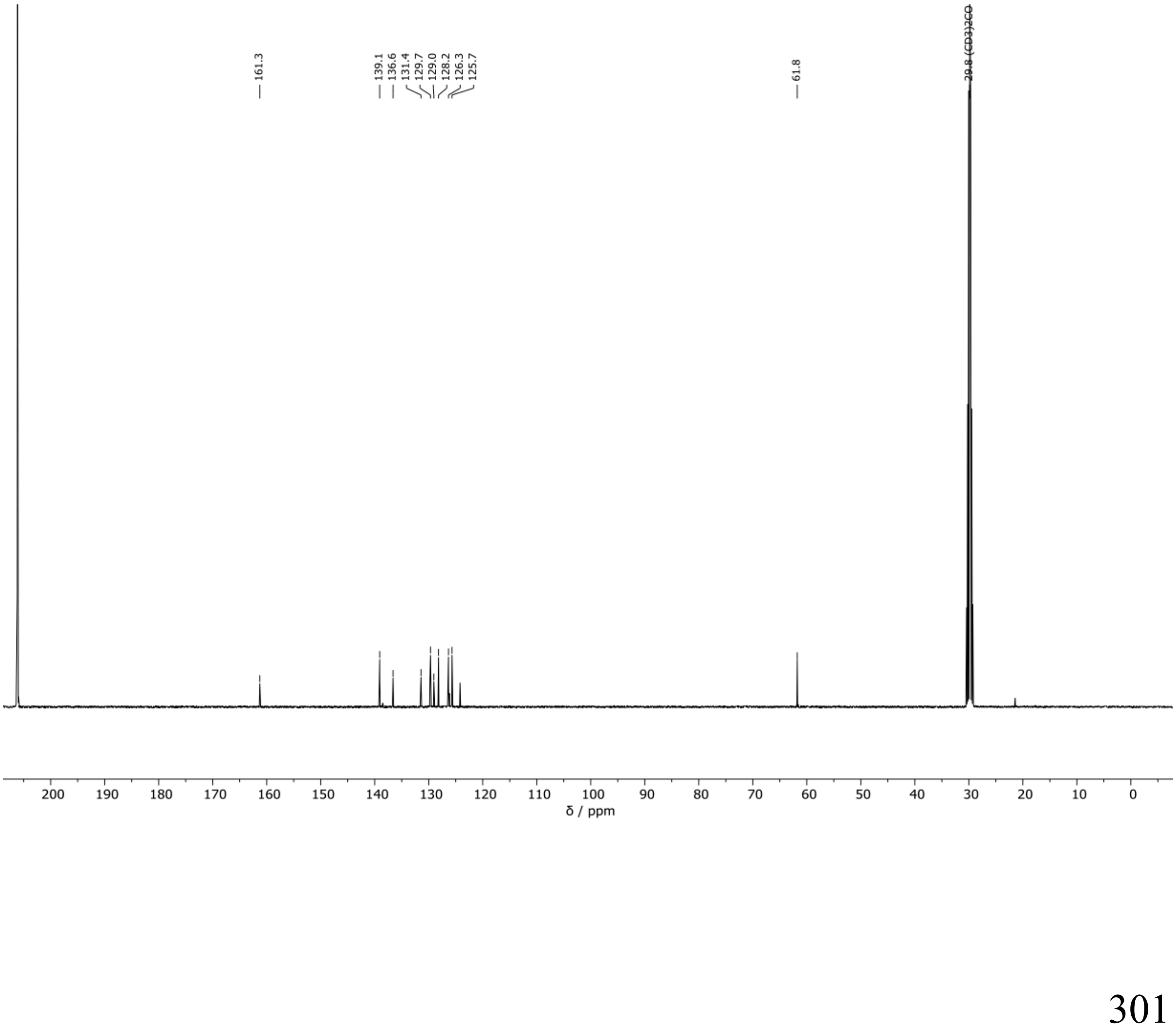
161.3
139.1
136.6
131.4
129.7
129.0
128.2
126.3
125.7
61.8
29.8 (CD3)2CO
200
190
180
170
160
150
140
130
120
110
100
90
80
70
60
50
40
30
20
10
0
δ / ppm

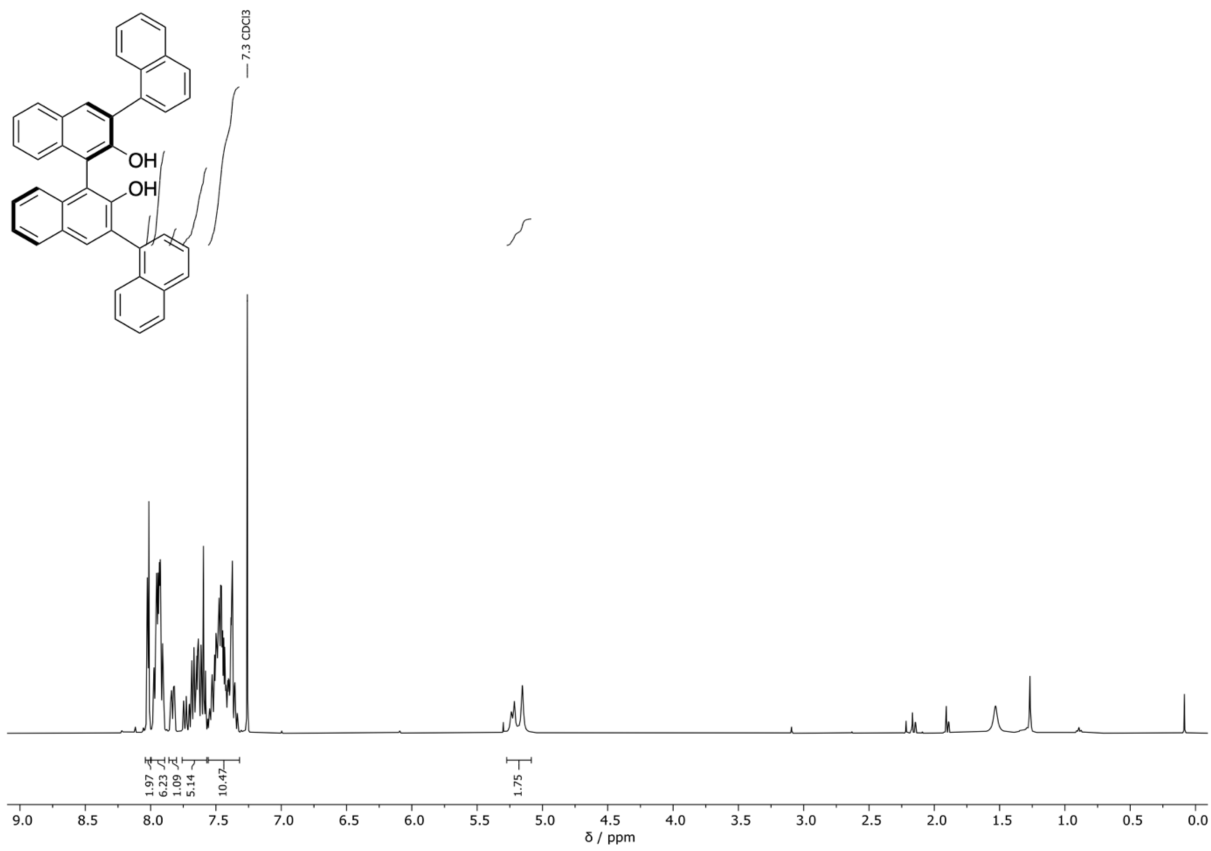
OH
OH
7.3 CDCl3
1.97
6.23
1.09
5.14
10.47
1.75
9.0
8.5
8.0
7.5
7.0
6.5
6.0
5.5
5.0
4.5
4.0
3.5
3.0
2.5
2.0
1.5
1.0
0.5
0.0
δ / ppm

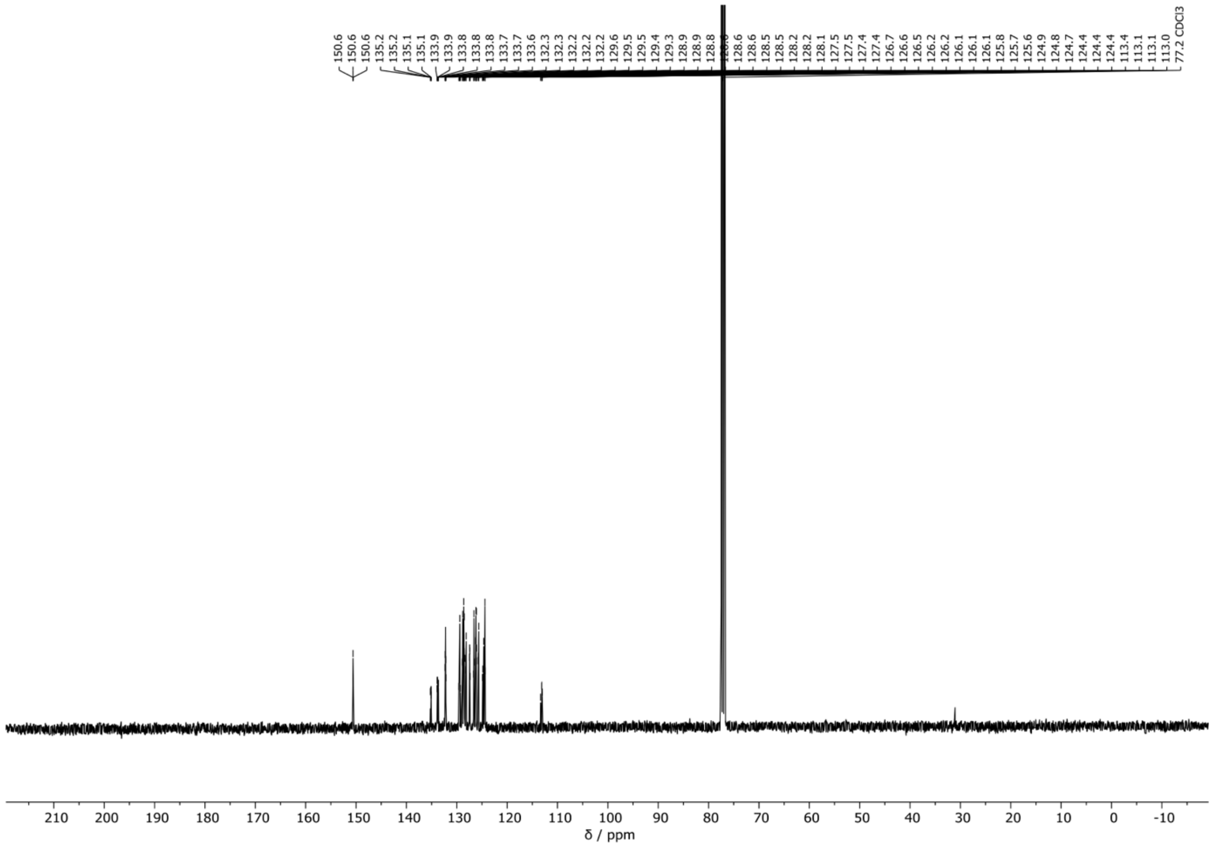
150.6
150.6
150.6
135.2
135.2
135.1
135.1
133.9
133.9
133.8
133.8
133.8
133.7
133.7
133.6
132.3
132.3
132.2
132.2
132.2
129.6
129.5
129.5
129.4
129.3
128.9
128.9
128.8
128.6
128.6
128.5
128.5
128.2
128.2
128.1
127.5
127.5
127.4
127.4
126.7
126.6
126.5
126.2
126.2
126.1
126.1
126.1
125.8
125.7
125.6
124.9
124.8
124.7
124.4
124.4
124.4
113.4
113.1
113.1
113.0
77.2 CDCl3
210
200
190
180
170
160
150
140
130
120
110
100
90
80
70
60
50
40
30
20
10
0
-10
δ / ppm

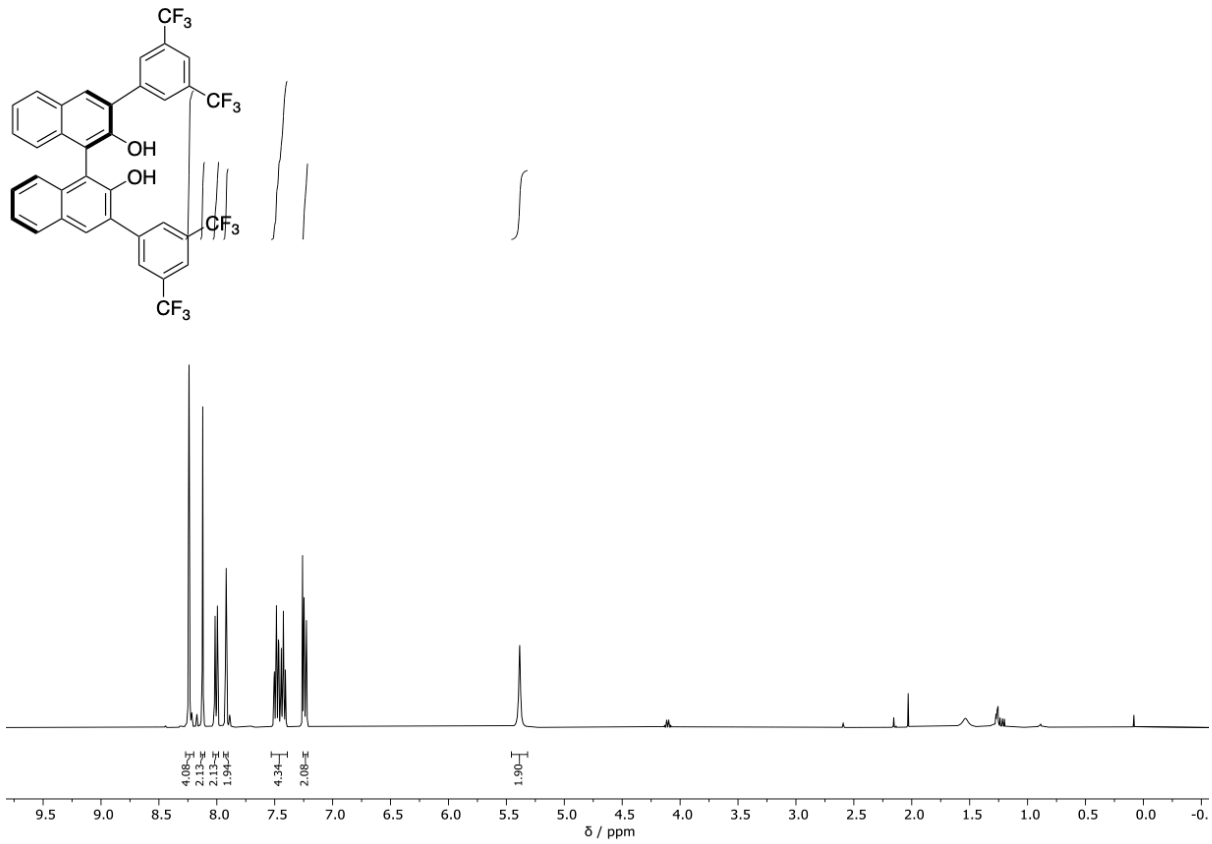
CF$_3$
CF$_3$
OH
OH
CF$_3$
CF$_3$
4.08
2.13
2.13
1.94
4.34
2.08
1.90
9.5
9.0
8.5
8.0
7.5
7.0
6.5
6.0
5.5
5.0
4.5
4.0
3.5
3.0
2.5
2.0
1.5
1.0
0.5
0.0
-0.
δ / ppm

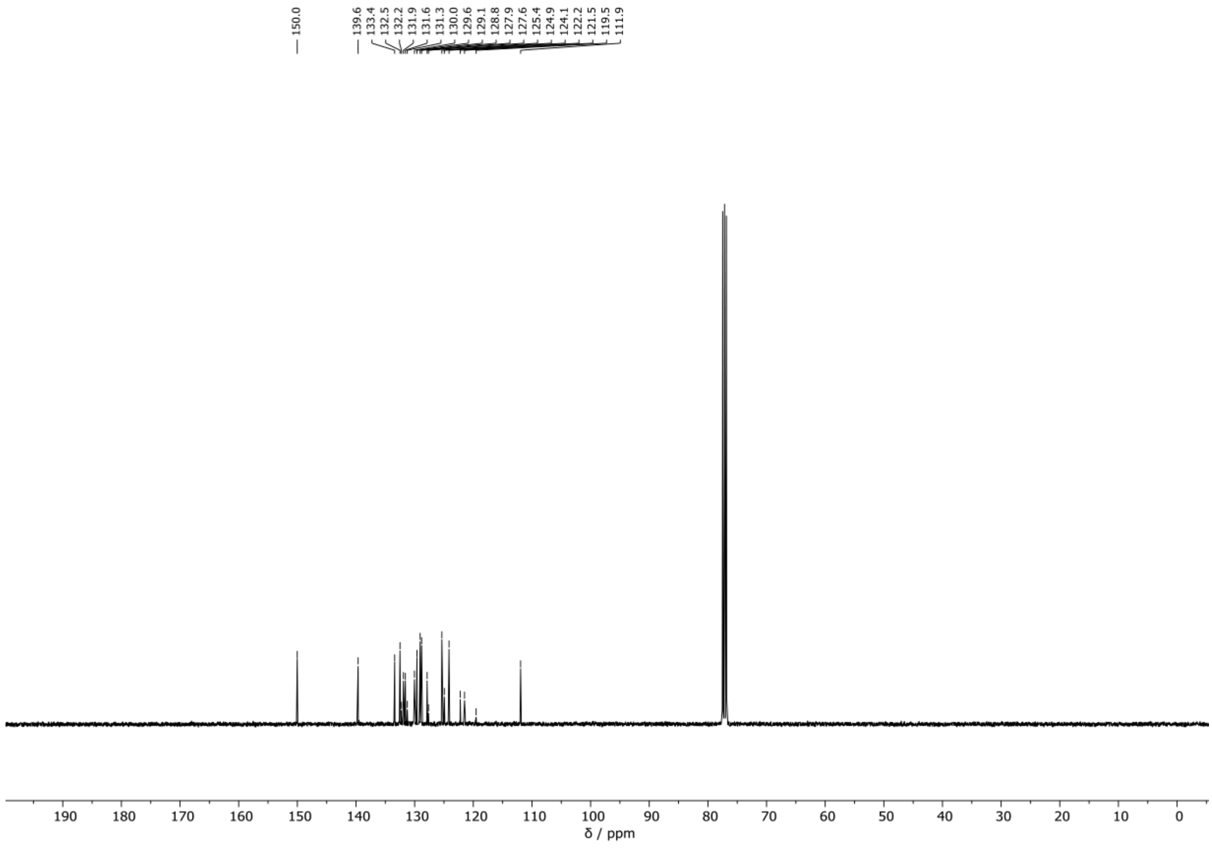
150.0
139.6
133.4
132.5
132.2
131.9
131.6
131.3
130.0
129.6
129.1
128.8
127.9
127.6
125.4
124.9
124.1
122.2
121.5
119.5
111.9
190
180
170
160
150
140
130
120
110
100
90
80
70
60
50
40
30
20
10
0
δ / ppm

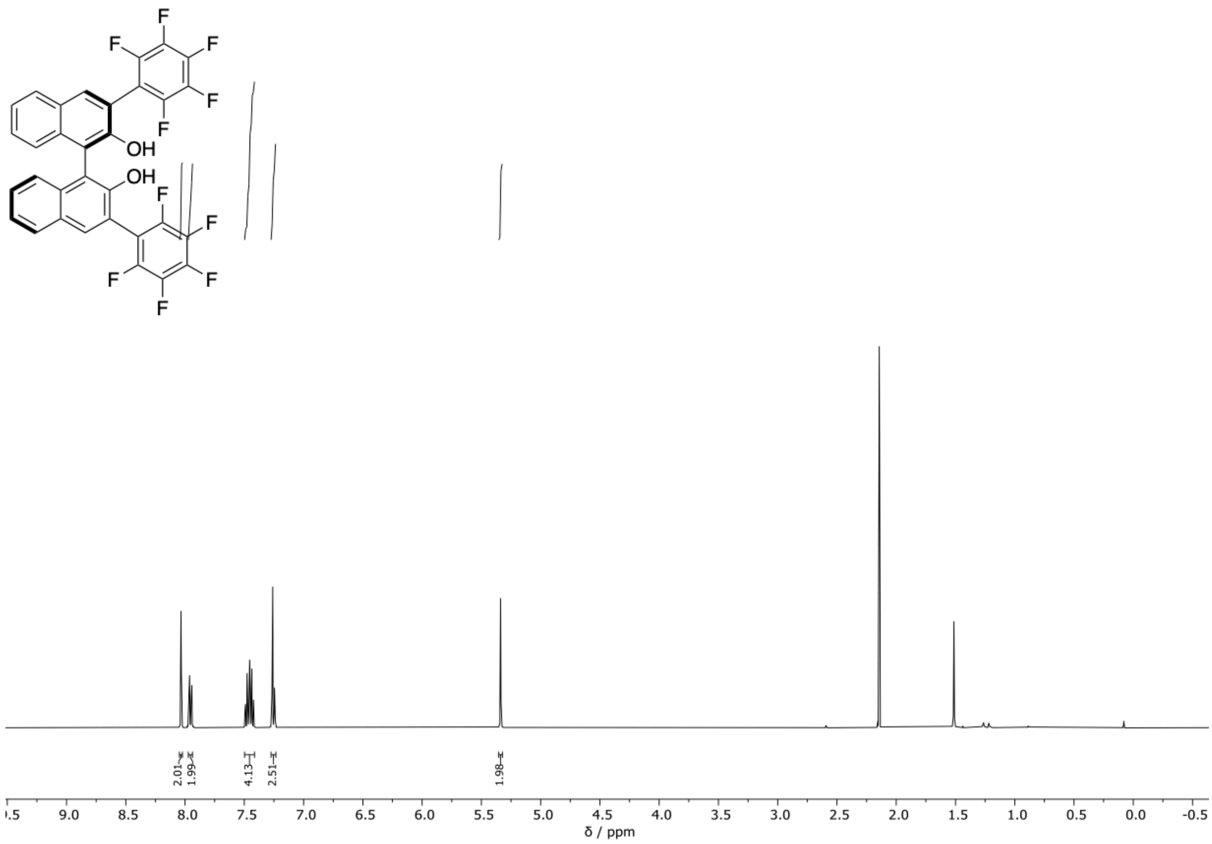
F
F
F
F
F
OH
OH
F
F
F
F
F
2.01
1.99
4.13
2.51
1.98
9.0
8.5
8.0
7.5
7.0
6.5
6.0
5.5
5.0
4.5
4.0
3.5
3.0
2.5
2.0
1.5
1.0
0.5
0.0
-0.5
δ / ppm

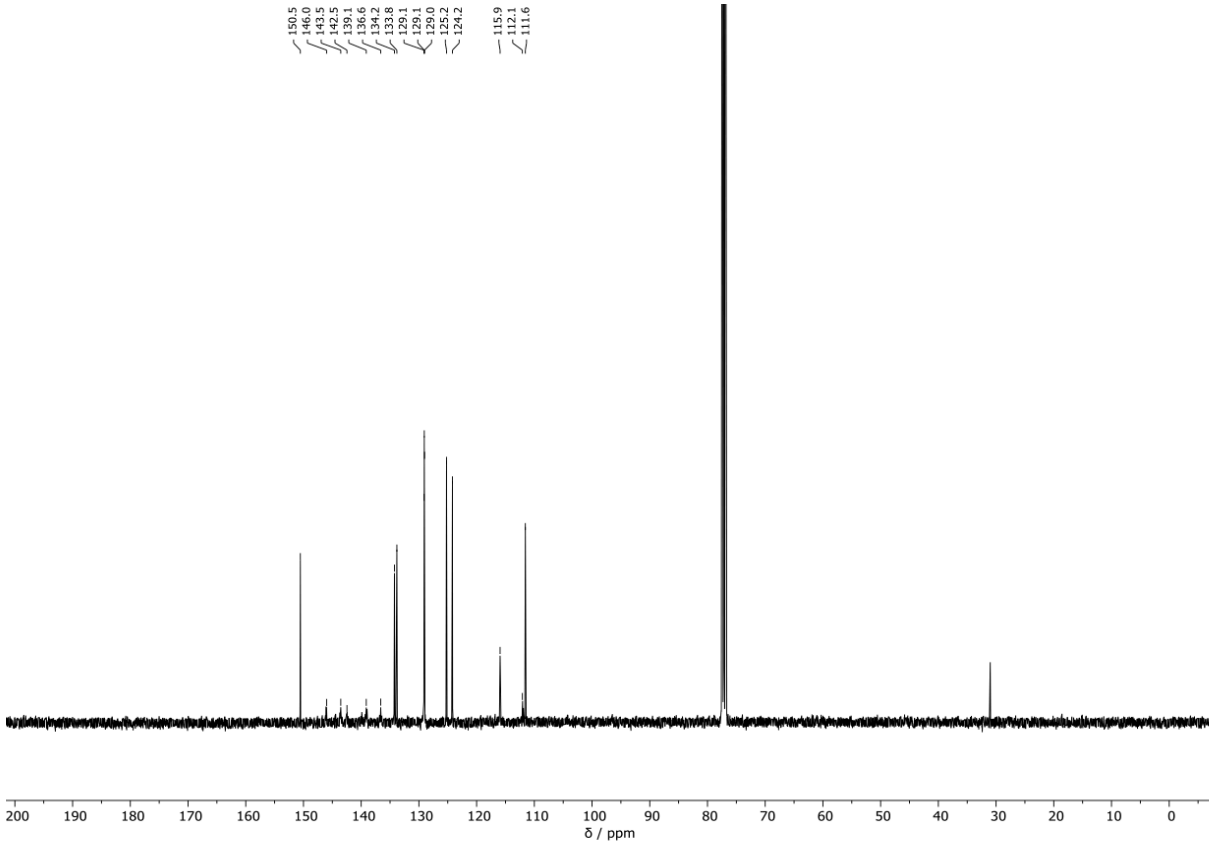
150.5
146.0
143.5
142.5
139.1
136.6
134.2
133.8
129.1
129.1
129.0
125.2
124.2
115.9
112.1
111.6
200
190
180
170
160
150
140
130
120
110
100
90
80
70
60
50
40
30
20
10
0
δ / ppm

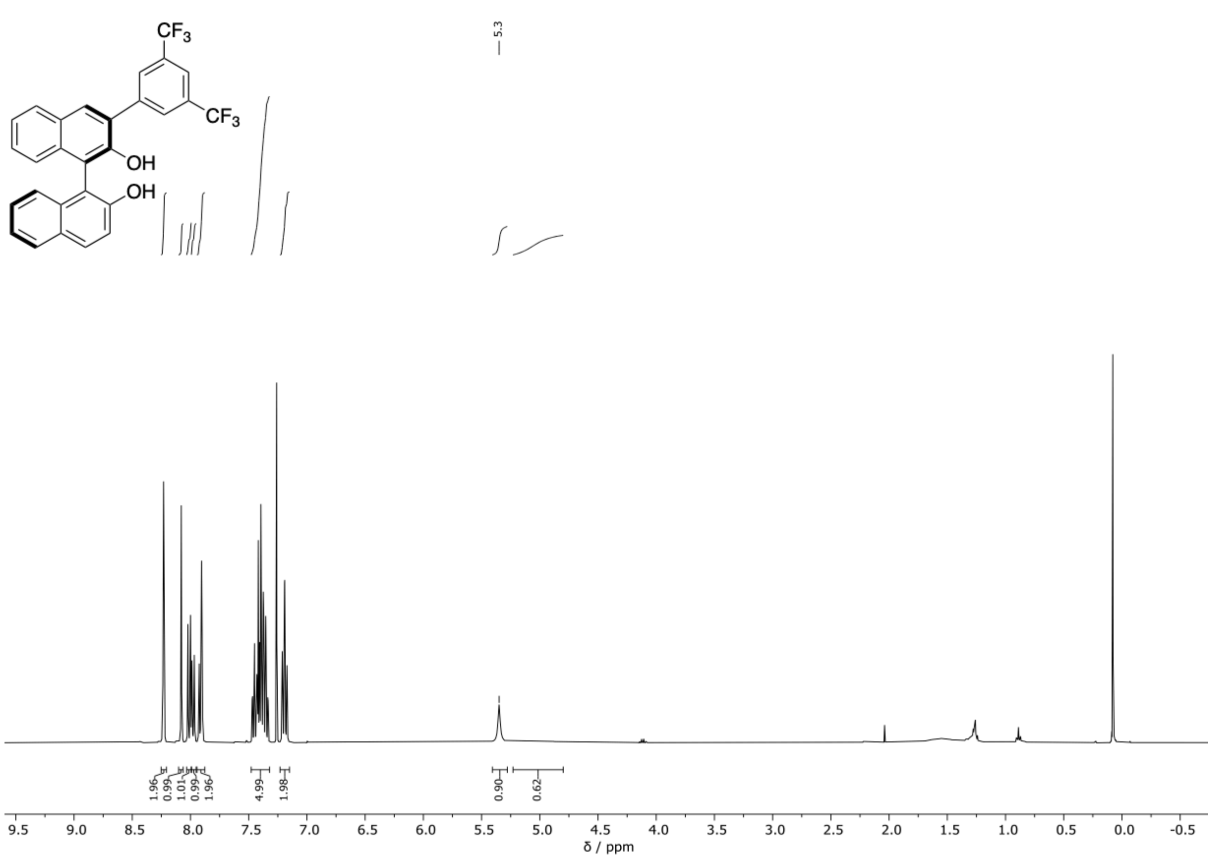
CF3
CF3
OH
OH
5.3
1.96
0.99
1.01
0.99
1.96
4.99
1.98
0.90
0.62
9.5
9.0
8.5
8.0
7.5
7.0
6.5
6.0
5.5
5.0
4.5
4.0
3.5
3.0
2.5
2.0
1.5
1.0
0.5
0.0
-0.5
δ / ppm

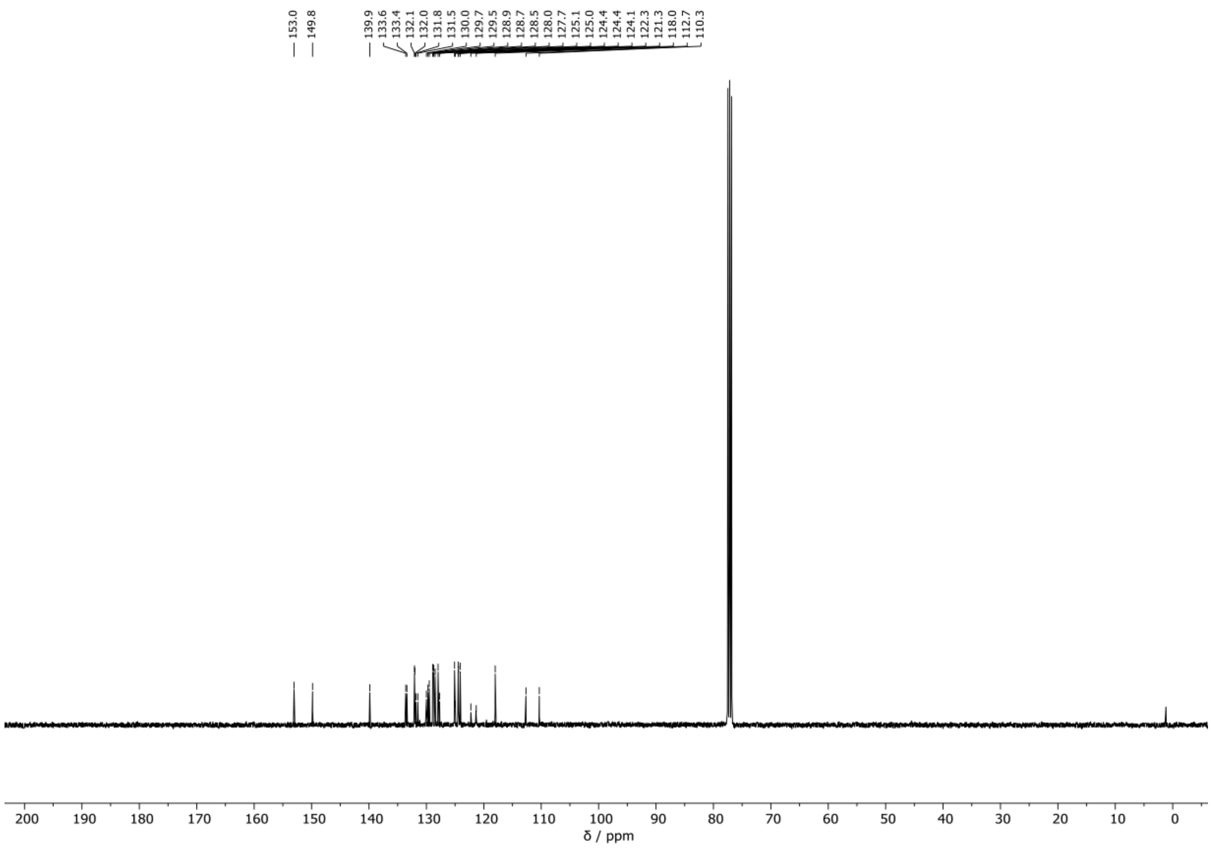
153.0
149.8
139.9
133.6
133.4
132.1
132.0
131.8
131.5
130.0
129.7
129.5
128.9
128.7
128.5
128.0
127.7
125.1
125.0
124.4
124.4
124.1
122.3
121.3
118.0
112.7
110.3
200
190
180
170
160
150
140
130
120
110
100
90
80
70
60
50
40
30
20
10
0
δ / ppm

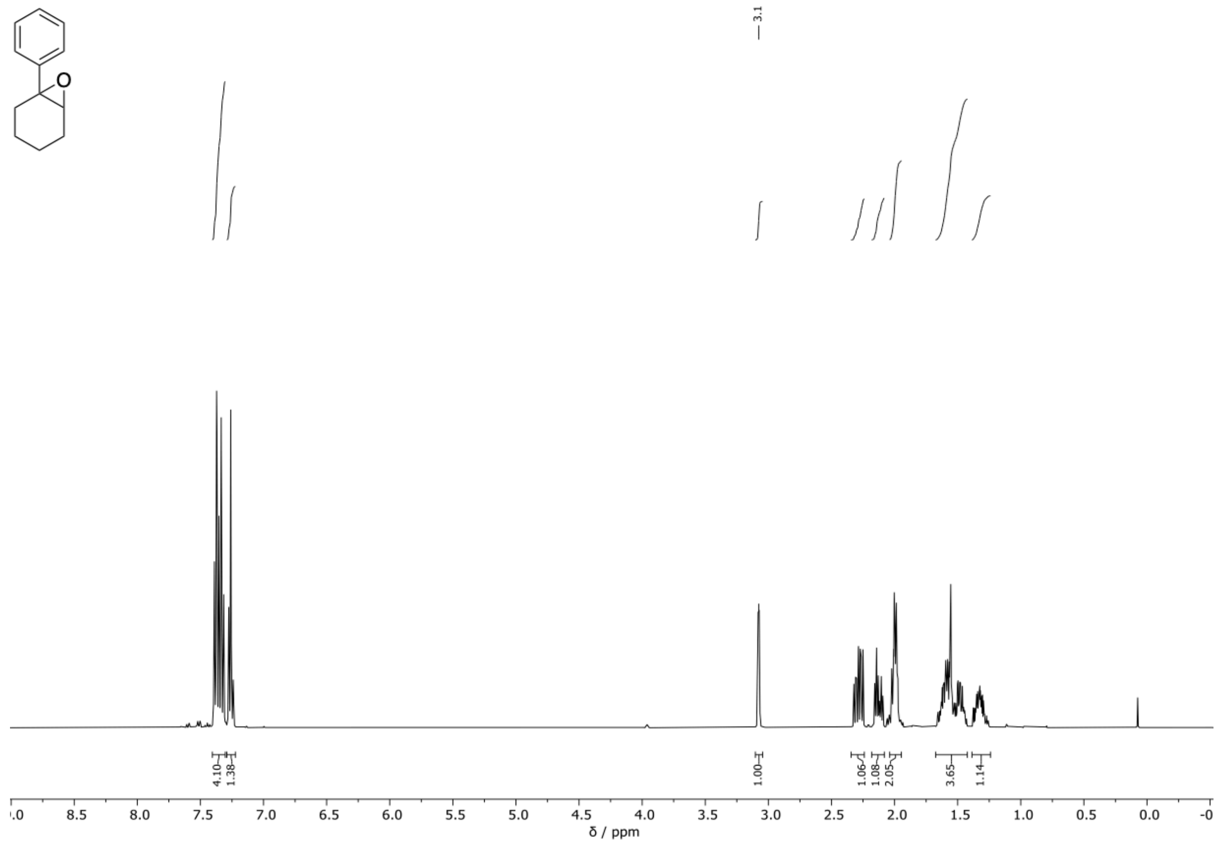
O
3.1
4.10
1.38
1.00
1.06
1.08
2.05
3.65
1.14
9.0 8.5 8.0 7.5 7.0 6.5 6.0 5.5 5.0 4.5 4.0 3.5 3.0 2.5 2.0 1.5 1.0 0.5 0.0 -0
δ / ppm

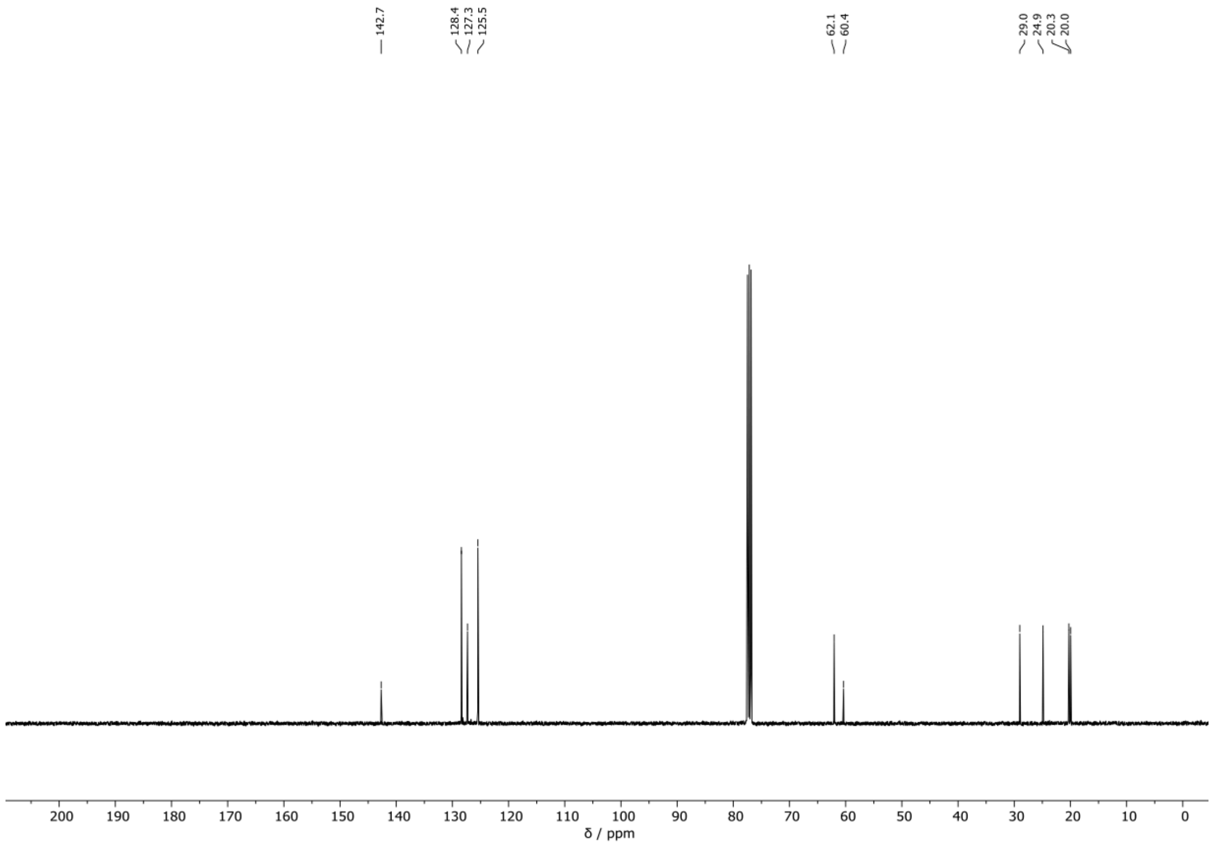
142.7
128.4
127.3
125.5
62.1
60.4
29.0
24.9
20.3
20.0
200 190 180 170 160 150 140 130 120 110 100 90 80 70 60 50 40 30 20 10 0
δ / ppm

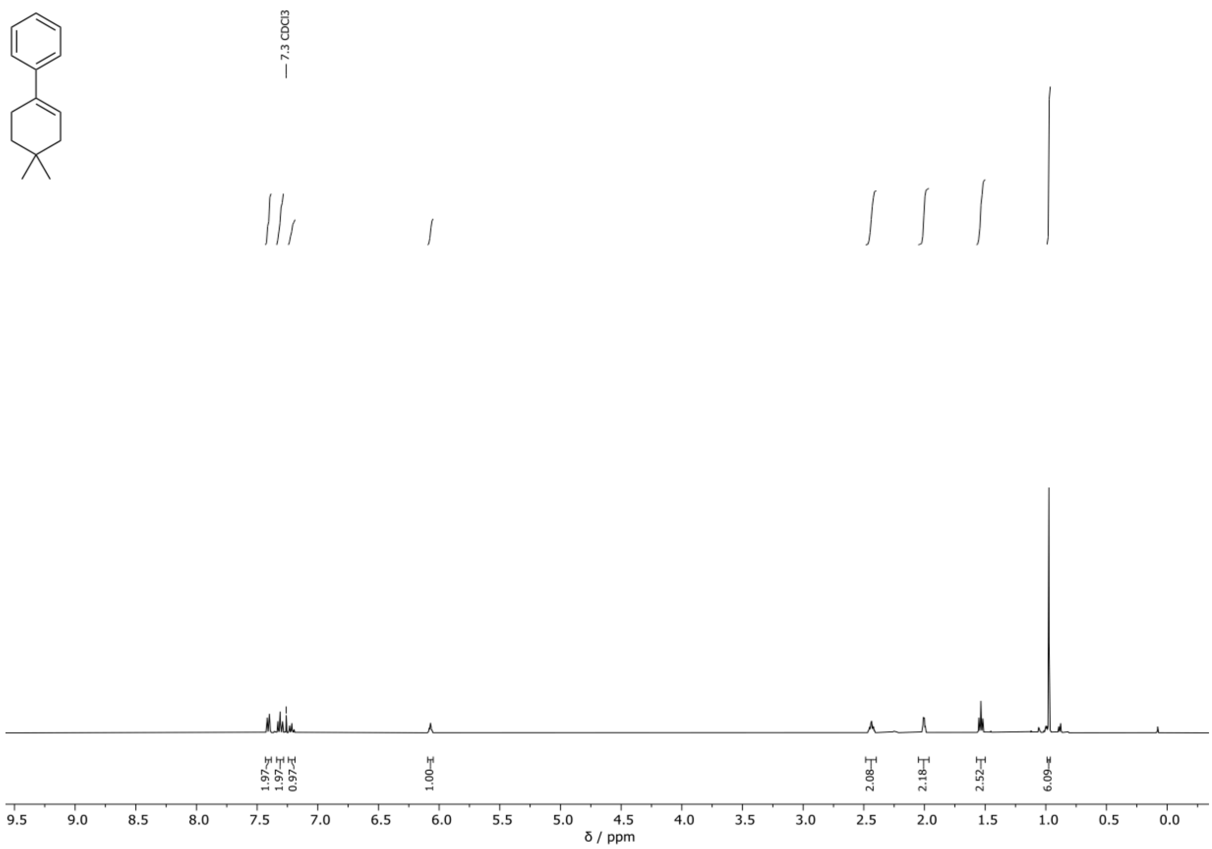
7.3 CDCl3
1.97
1.97
0.97
1.00
2.08
2.18
2.52
6.09
9.5
9.0
8.5
8.0
7.5
7.0
6.5
6.0
5.5
5.0
4.5
4.0
3.5
3.0
2.5
2.0
1.5
1.0
0.5
0.0
δ / ppm

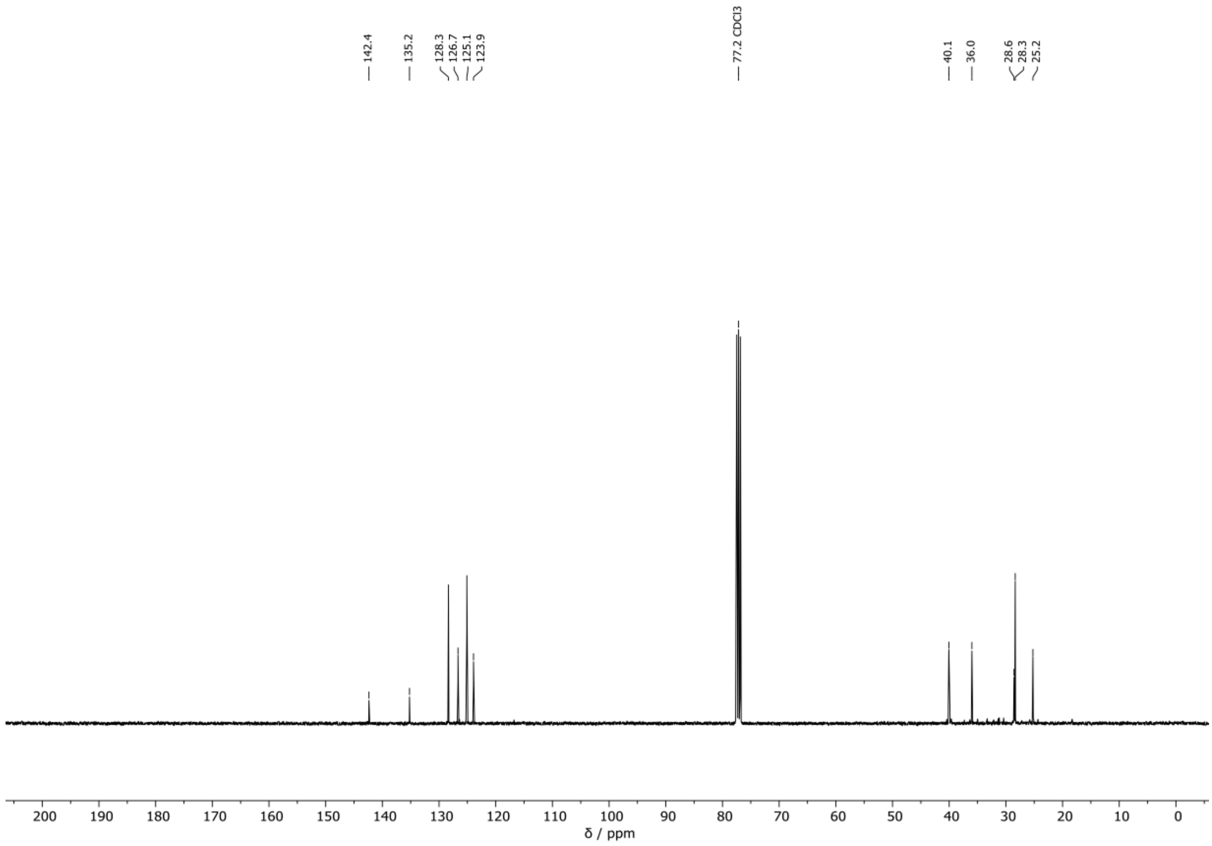
142.4
135.2
128.3
126.7
125.1
123.9
77.2 CDCl3
40.1
36.0
28.6
28.3
25.2
200
190
180
170
160
150
140
130
120
110
100
90
80
70
60
50
40
30
20
10
0
δ / ppm

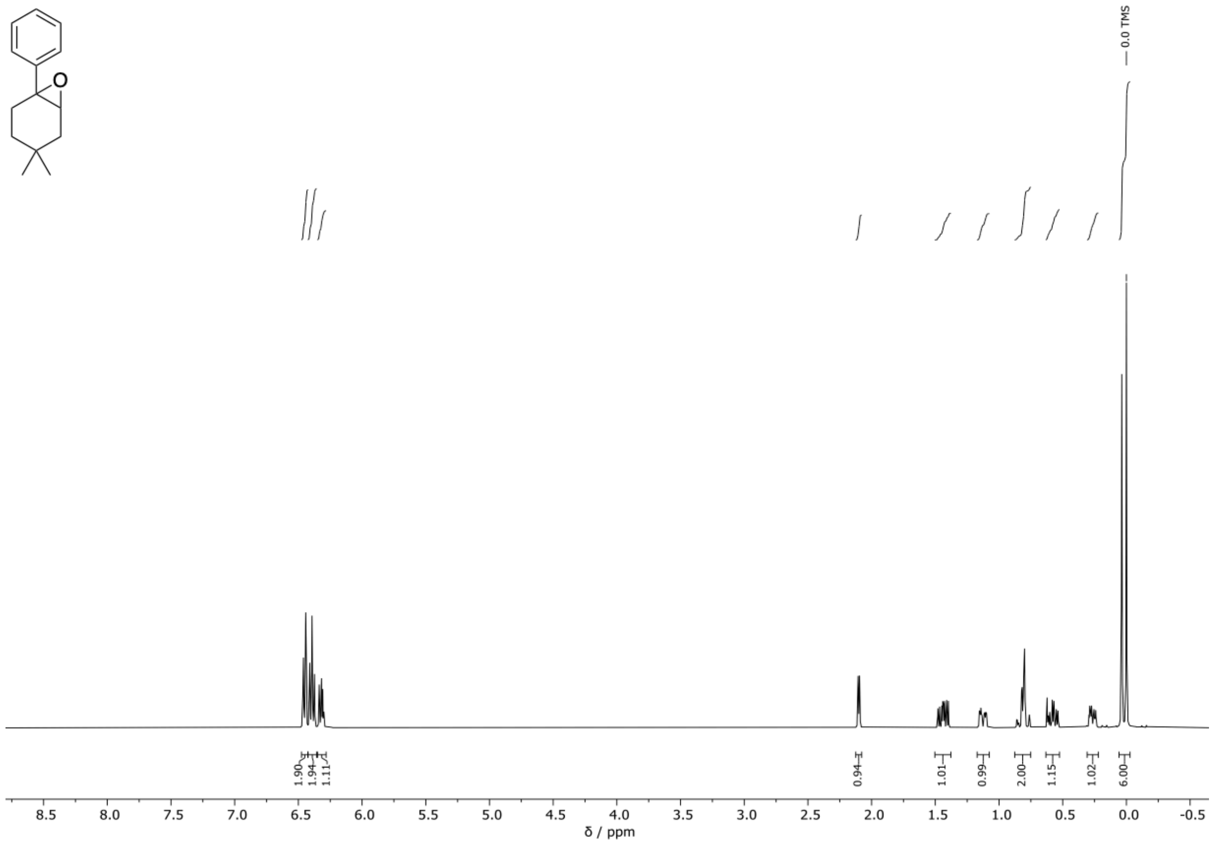
O
0.0 TMS
1.90
1.94
1.11
0.94
1.01
0.99
2.00
1.15
1.02
6.00
8.5
8.0
7.5
7.0
6.5
6.0
5.5
5.0
4.5
4.0
3.5
3.0
2.5
2.0
1.5
1.0
0.5
0.0
-0.5
δ / ppm

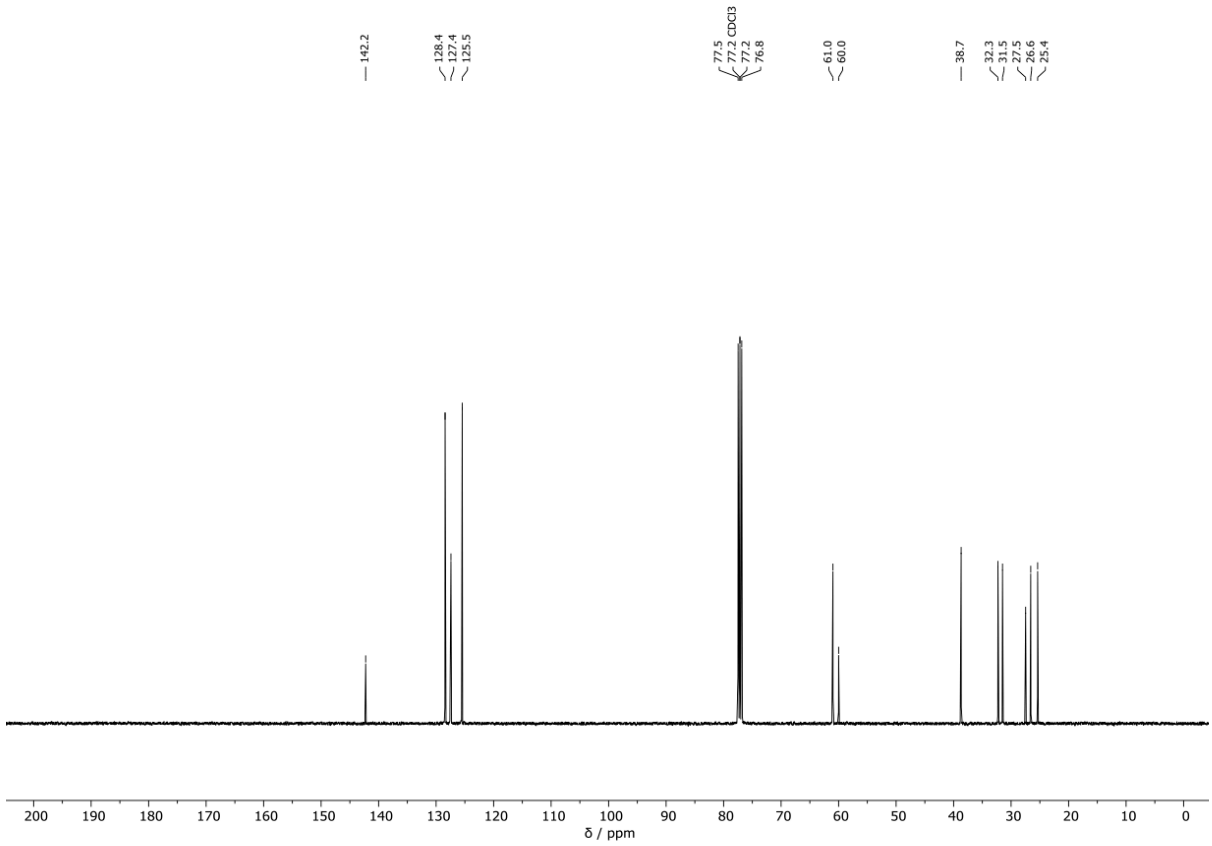
142.2
128.4
127.4
125.5
77.5
77.2 CDCl3
77.2
76.8
61.0
60.0
38.7
32.3
31.5
27.5
26.6
25.4
200
190
180
170
160
150
140
130
120
110
100
90
80
70
60
50
40
30
20
10
0
δ / ppm

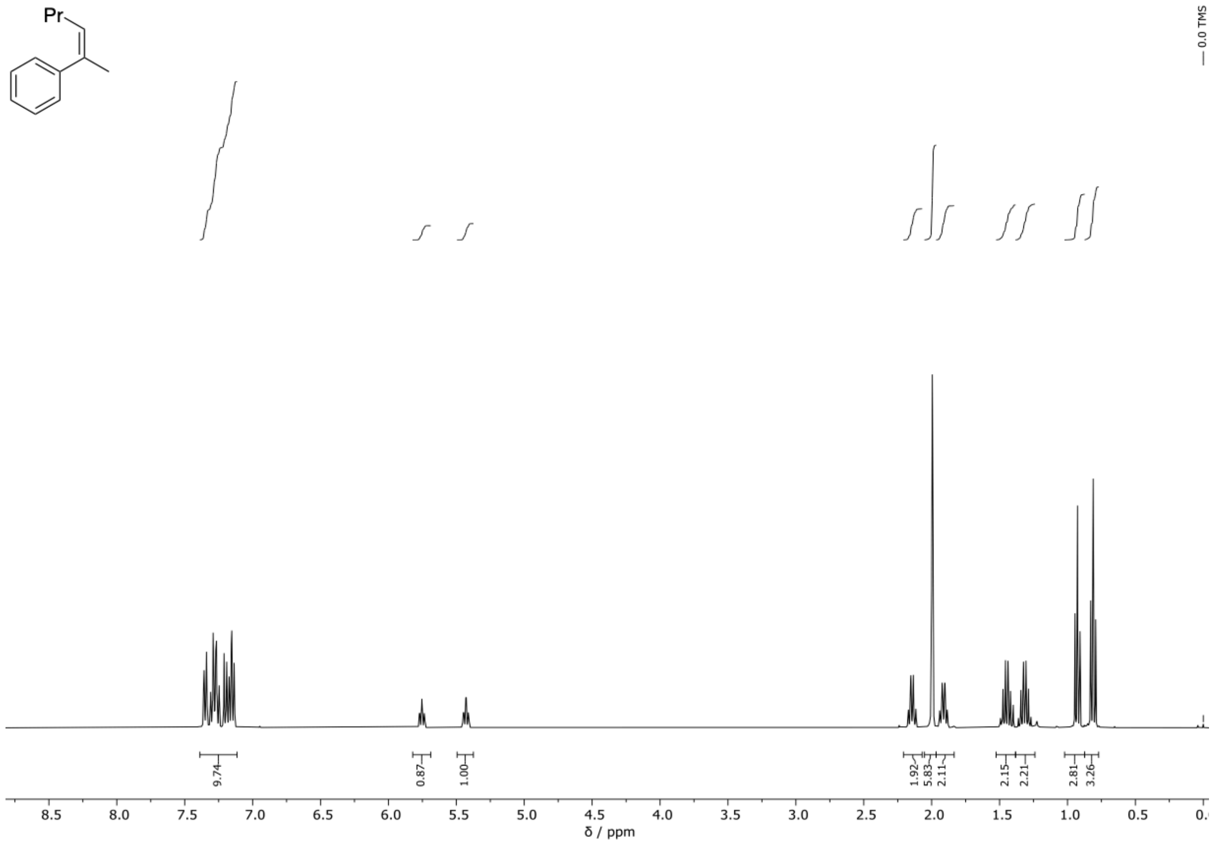
Pr
0.0 TMS
9.74
0.87
1.00
1.92
5.83
2.11
2.15
2.21
2.81
3.26
8.5
8.0
7.5
7.0
6.5
6.0
5.5
5.0
4.5
4.0
3.5
3.0
2.5
2.0
1.5
1.0
0.5
0.
δ / ppm

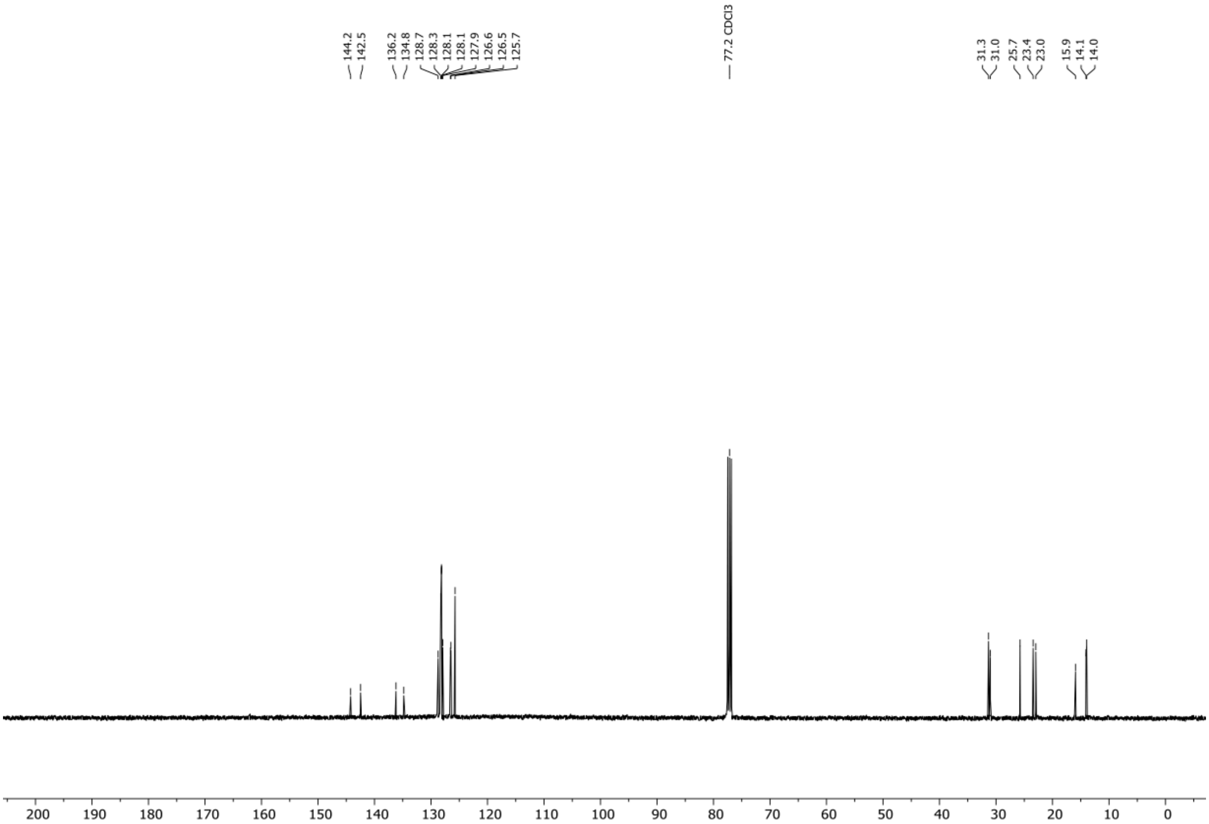
144.2
142.5
136.2
134.8
128.7
128.3
128.1
128.1
127.9
126.6
126.5
125.7
77.2 CDCl3
31.3
31.0
25.7
23.4
23.0
15.9
14.1
14.0
200
190
180
170
160
150
140
130
120
110
100
90
80
70
60
50
40
30
20
10
0
δ / ppm

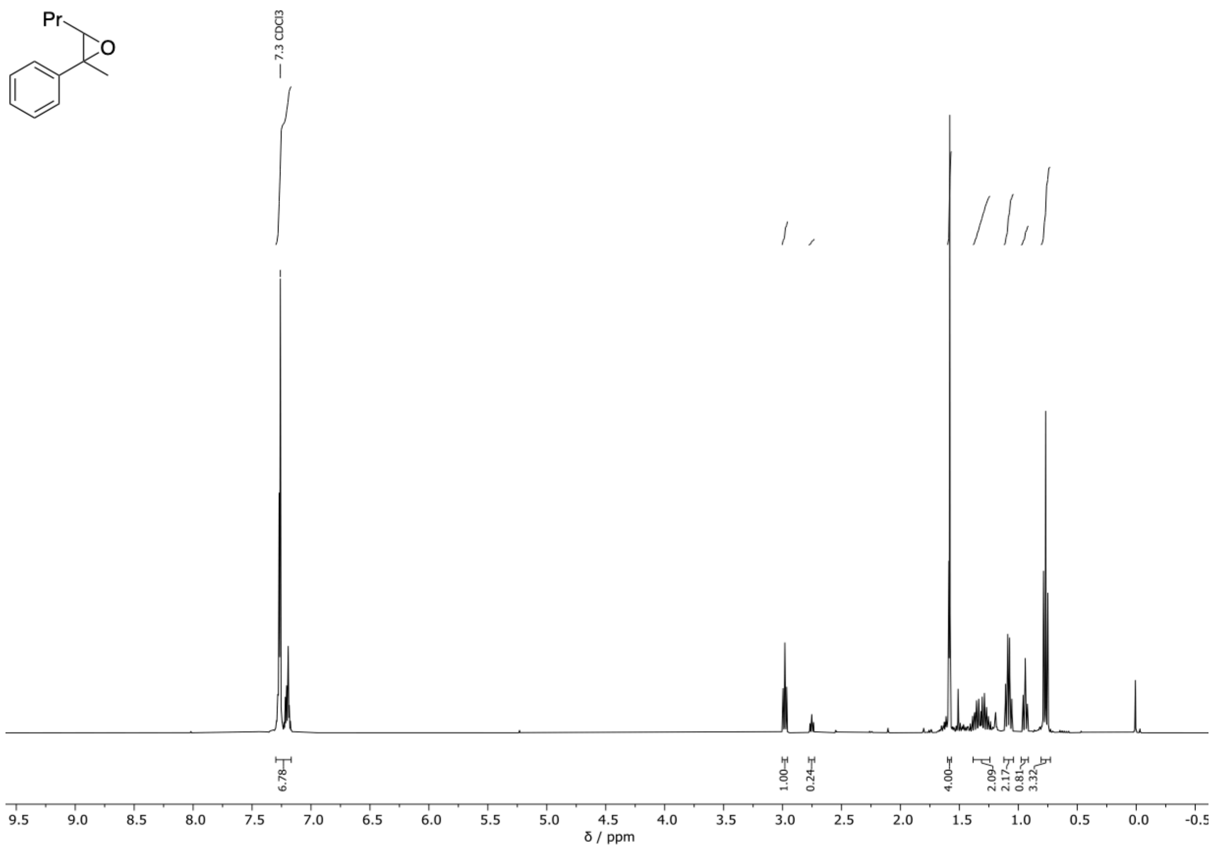
Pr
O
7.3 CDCl3
6.78
1.00
0.24
4.00
2.09
2.17
0.81
3.32
9.5
9.0
8.5
8.0
7.5
7.0
6.5
6.0
5.5
5.0
4.5
4.0
3.5
3.0
2.5
2.0
1.5
1.0
0.5
0.0
-0.5
δ / ppm

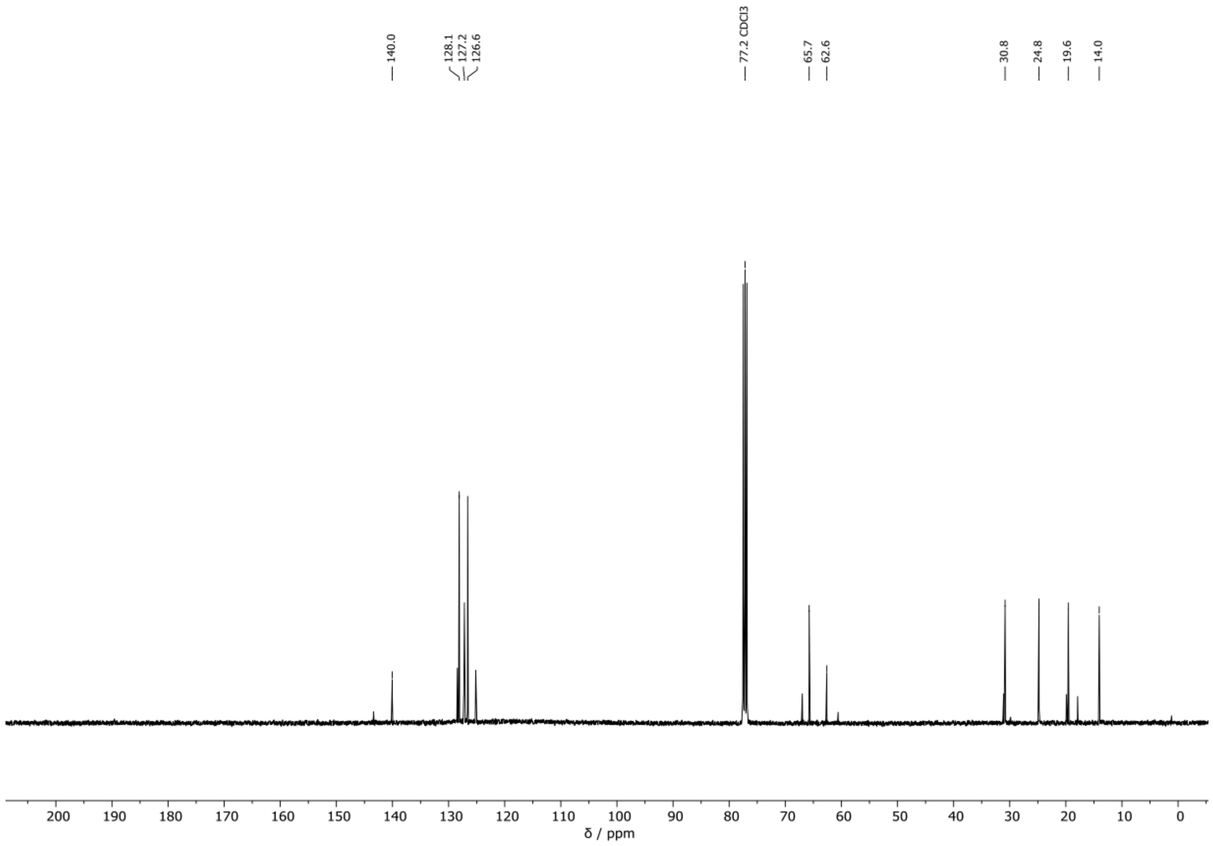
140.0
128.1
127.2
126.6
77.2 CDCl3
65.7
62.6
30.8
24.8
19.6
14.0
200
190
180
170
160
150
140
130
120
110
100
90
80
70
60
50
40
30
20
10
0
δ / ppm

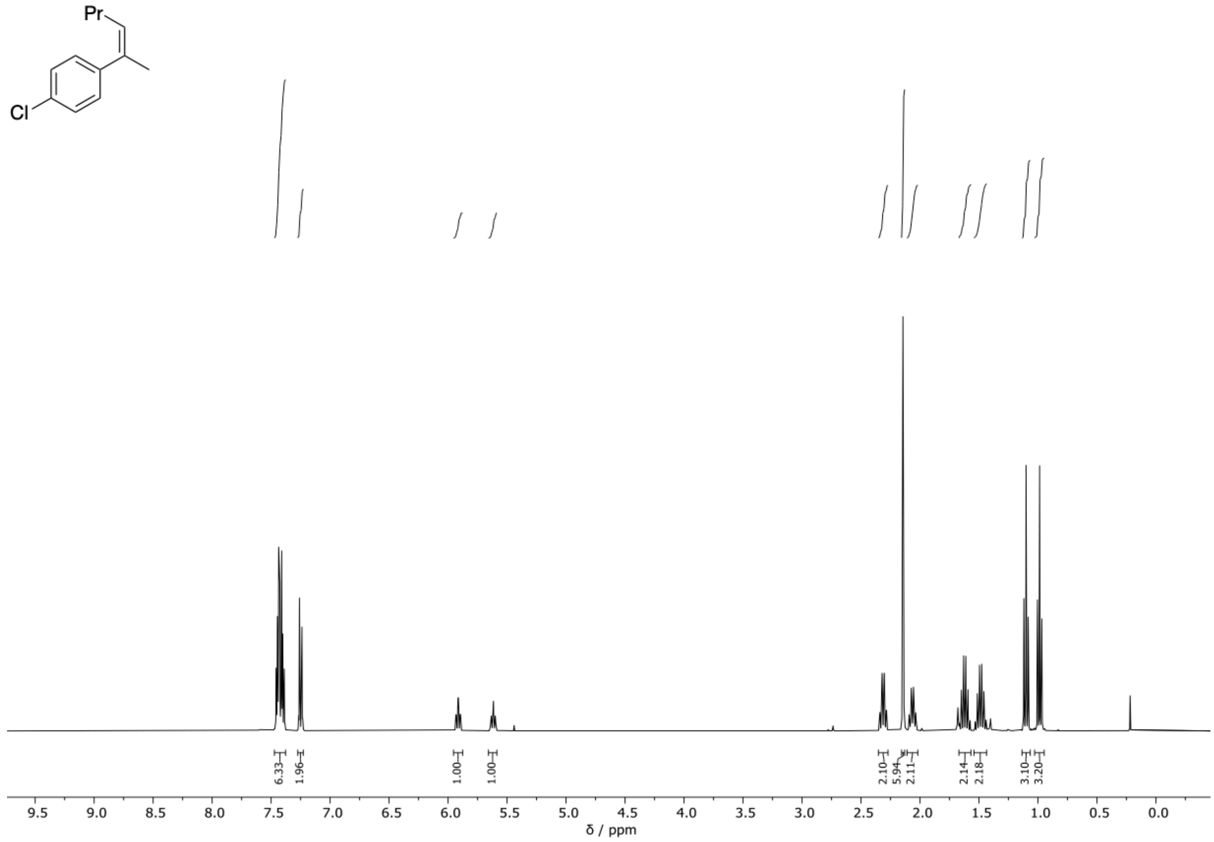
Pr
Cl
6.33
1.96
1.00
1.00
2.10
5.94
2.11
2.14
2.18
3.10
3.20
9.5
9.0
8.5
8.0
7.5
7.0
6.5
6.0
5.5
5.0
4.5
4.0
3.5
3.0
2.5
2.0
1.5
1.0
0.5
0.0
δ / ppm

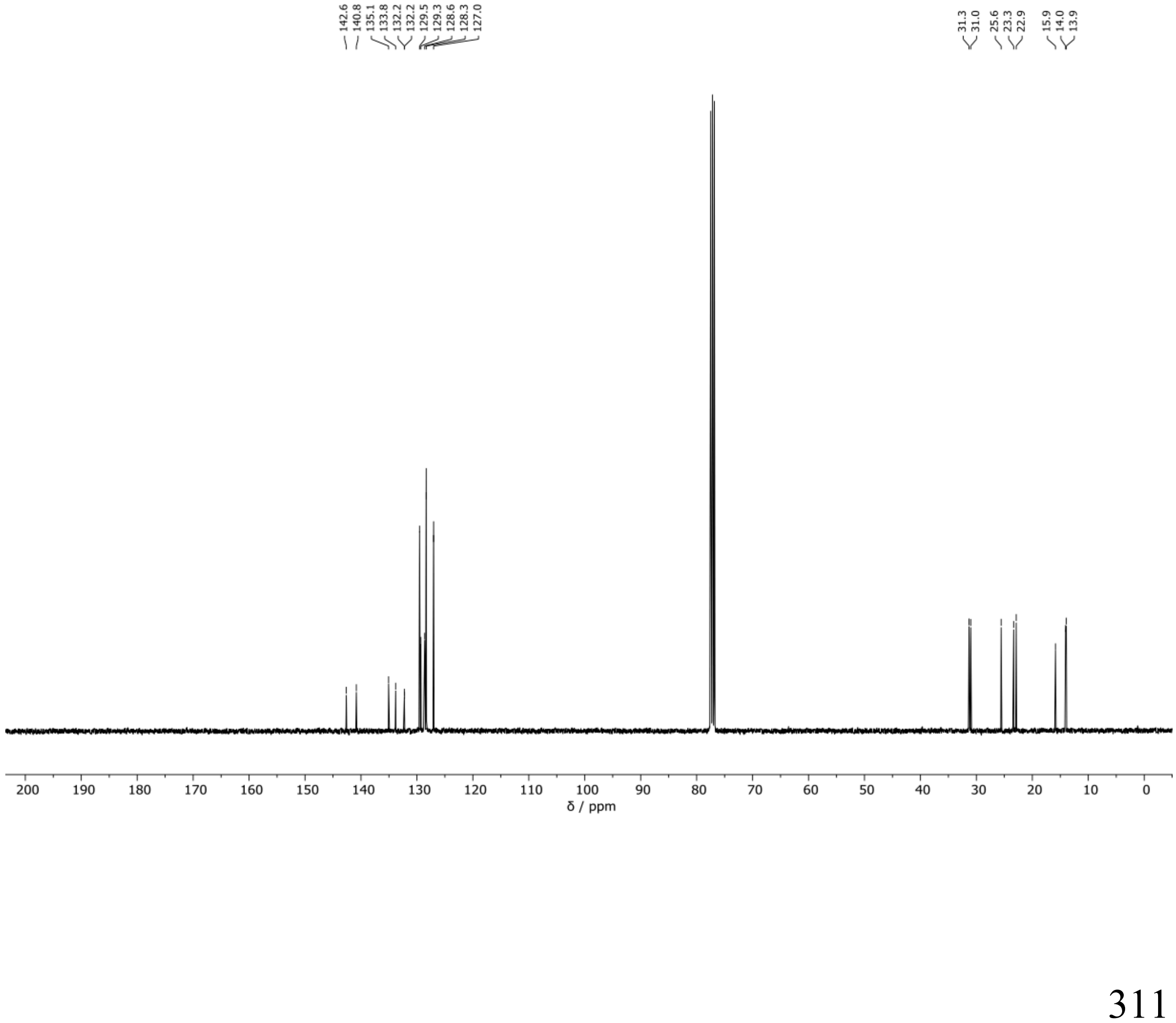
142.6
140.8
135.1
133.8
132.2
132.2
129.5
129.3
128.6
128.3
127.0
31.3
31.0
25.6
23.3
22.9
15.9
14.0
13.9
200
190
180
170
160
150
140
130
120
110
100
90
80
70
60
50
40
30
20
10
0
δ / ppm

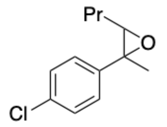
Pr
O
Cl

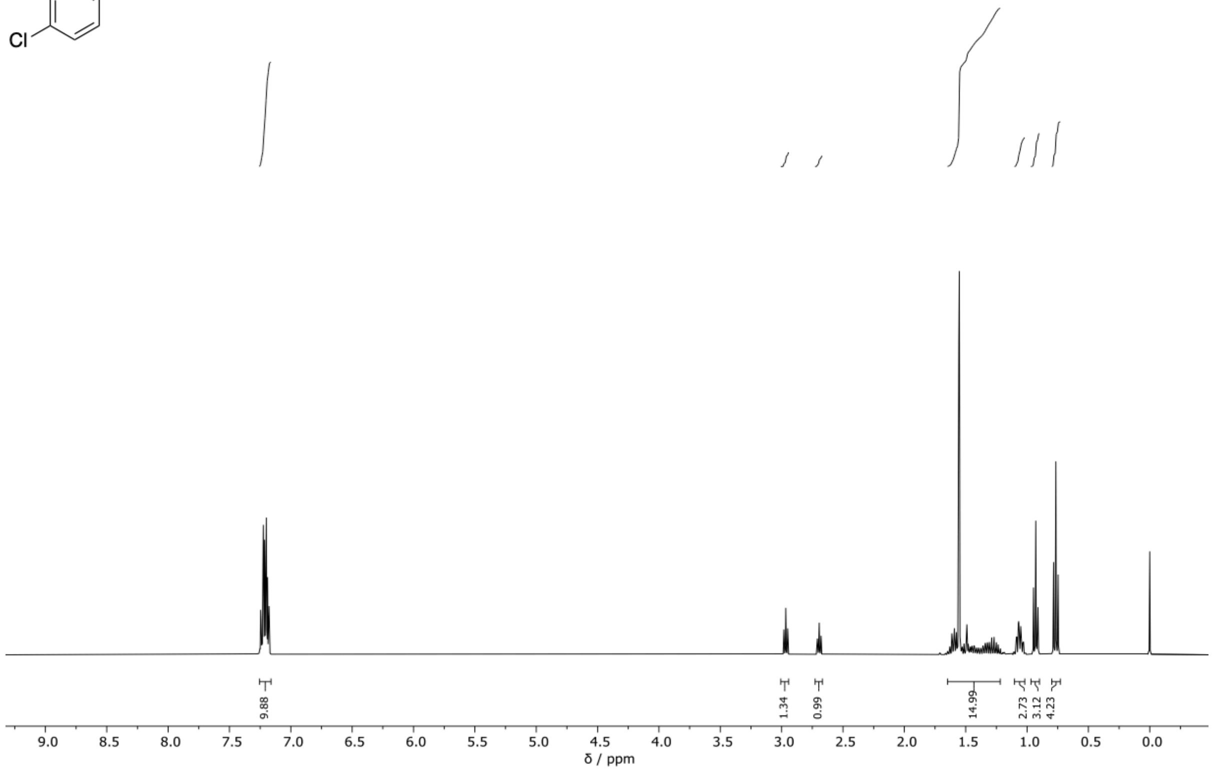
9.88
1.34
0.99
14.99
2.73
3.12
4.23
9.0
8.5
8.0
7.5
7.0
6.5
6.0
5.5
5.0
4.5
4.0
3.5
3.0
2.5
2.0
1.5
1.0
0.5
0.0
δ / ppm

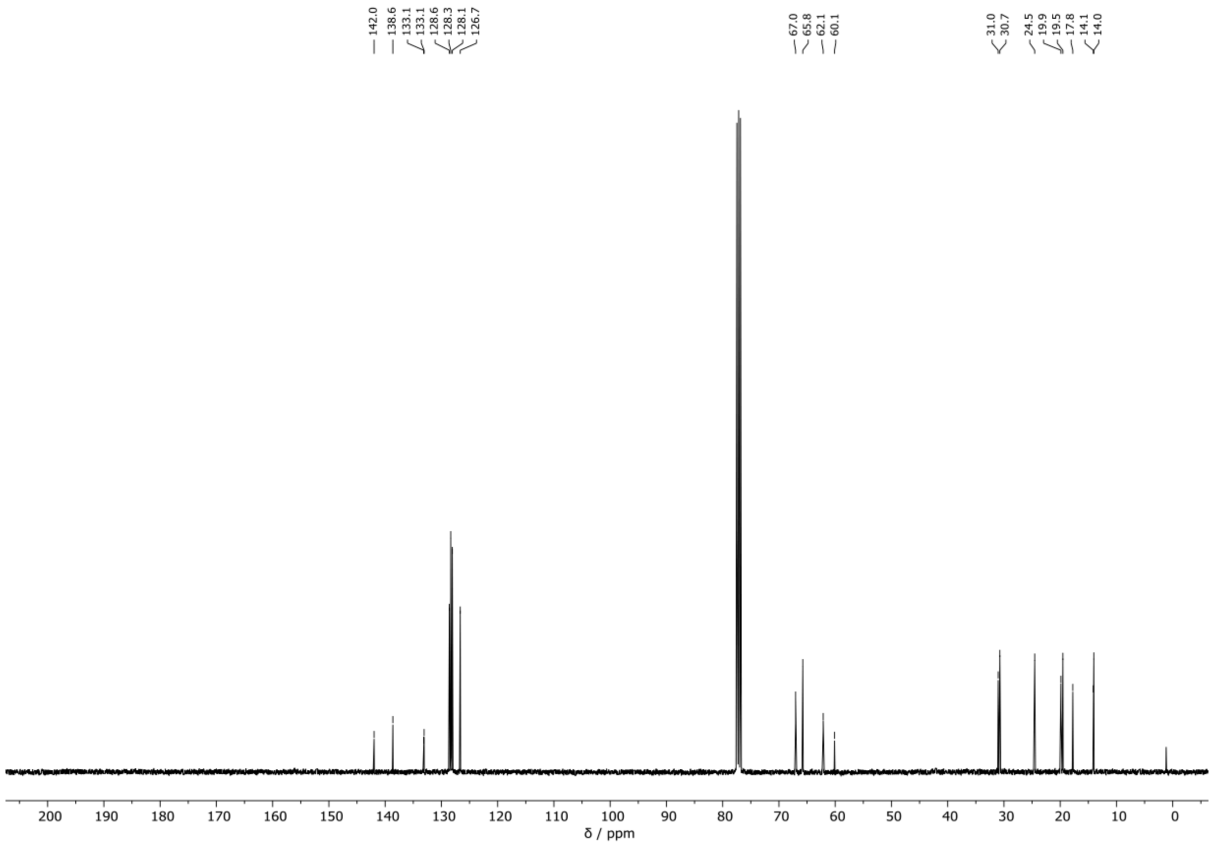
142.0
138.6
133.1
133.1
128.6
128.3
128.1
126.7
67.0
65.8
62.1
60.1
31.0
30.7
24.5
19.9
19.5
17.8
14.1
14.0
200
190
180
170
160
150
140
130
120
110
100
90
80
70
60
50
40
30
20
10
0
δ / ppm

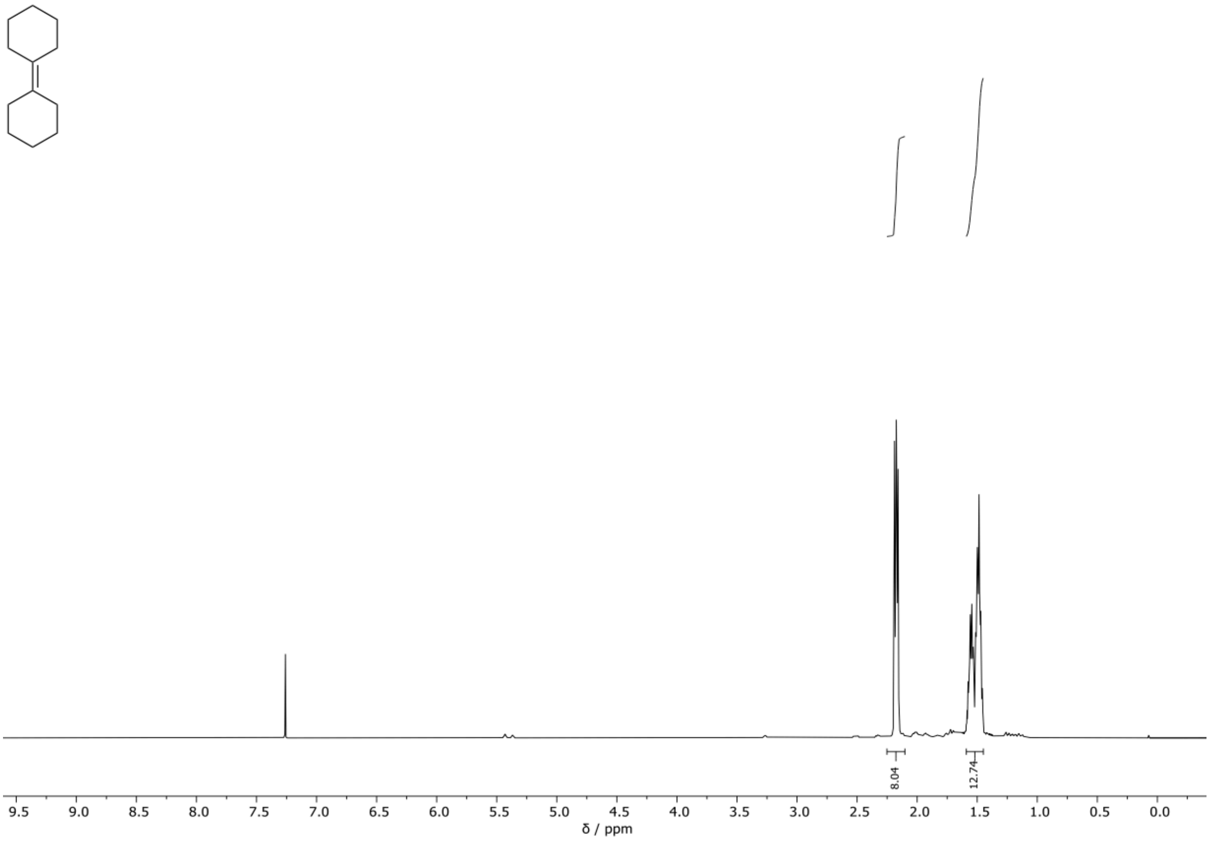
8.04
12.74
9.5
9.0
8.5
8.0
7.5
7.0
6.5
6.0
5.5
5.0
4.5
4.0
3.5
3.0
2.5
2.0
1.5
1.0
0.5
0.0
δ / ppm

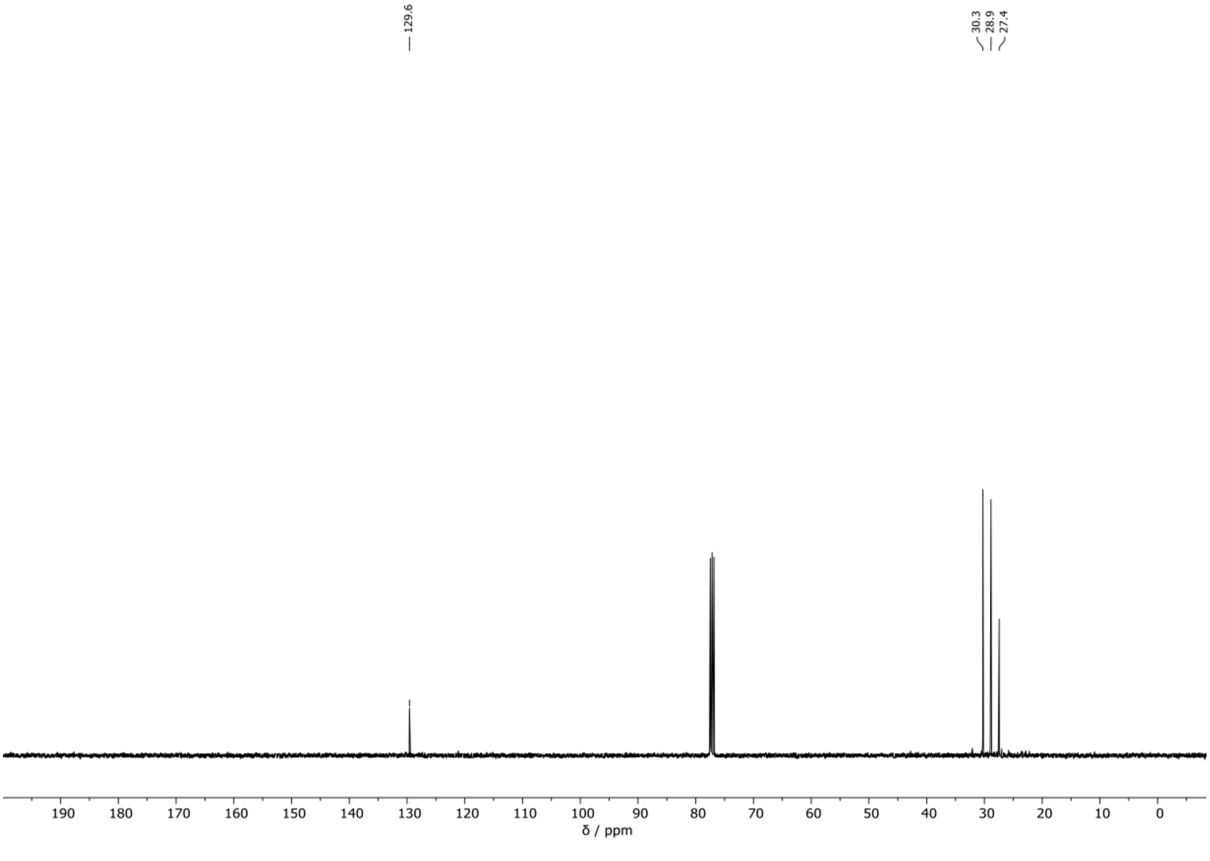
129.6
30.3
28.9
27.4
190
180
170
160
150
140
130
120
110
100
90
80
70
60
50
40
30
20
10
0
δ / ppm

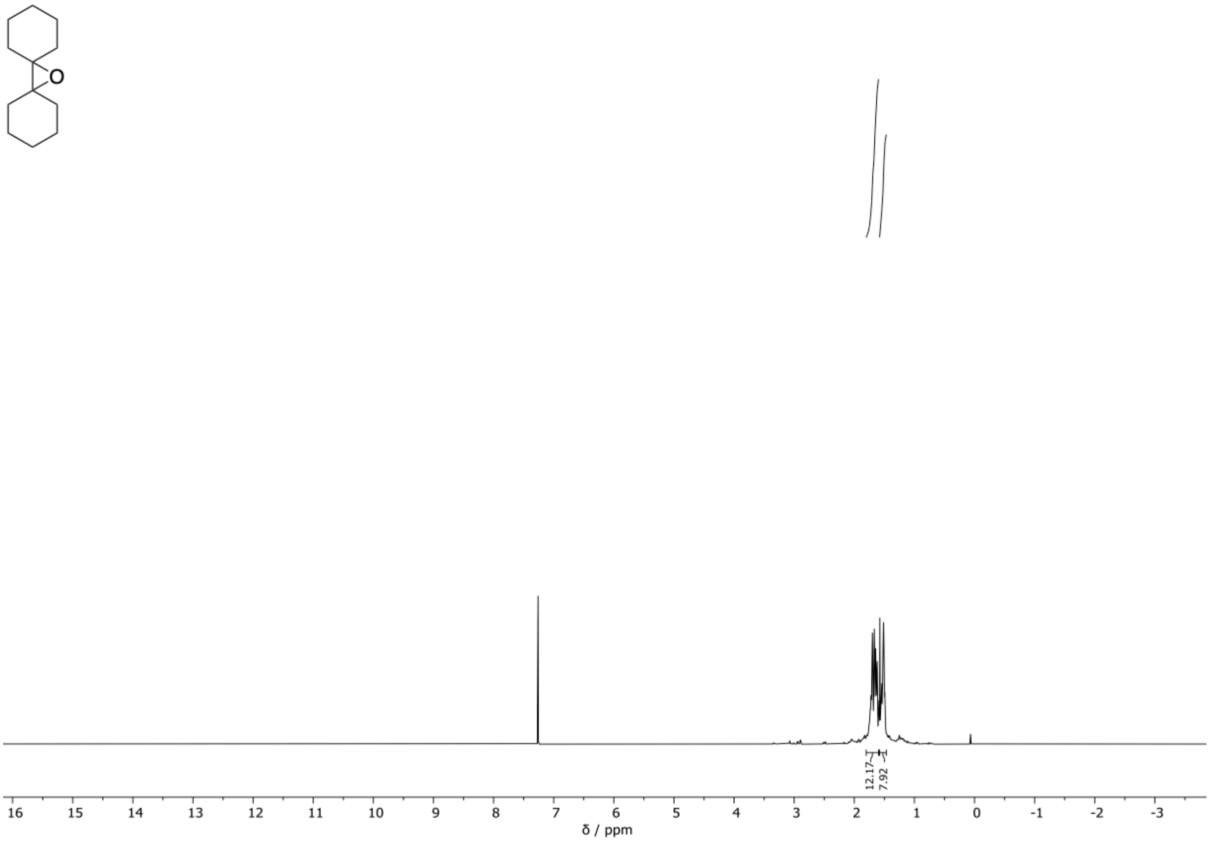
O
12.17
7.92
16
15
14
13
12
11
10
9
8
7
6
5
4
3
2
1
0
-1
-2
-3
δ / ppm

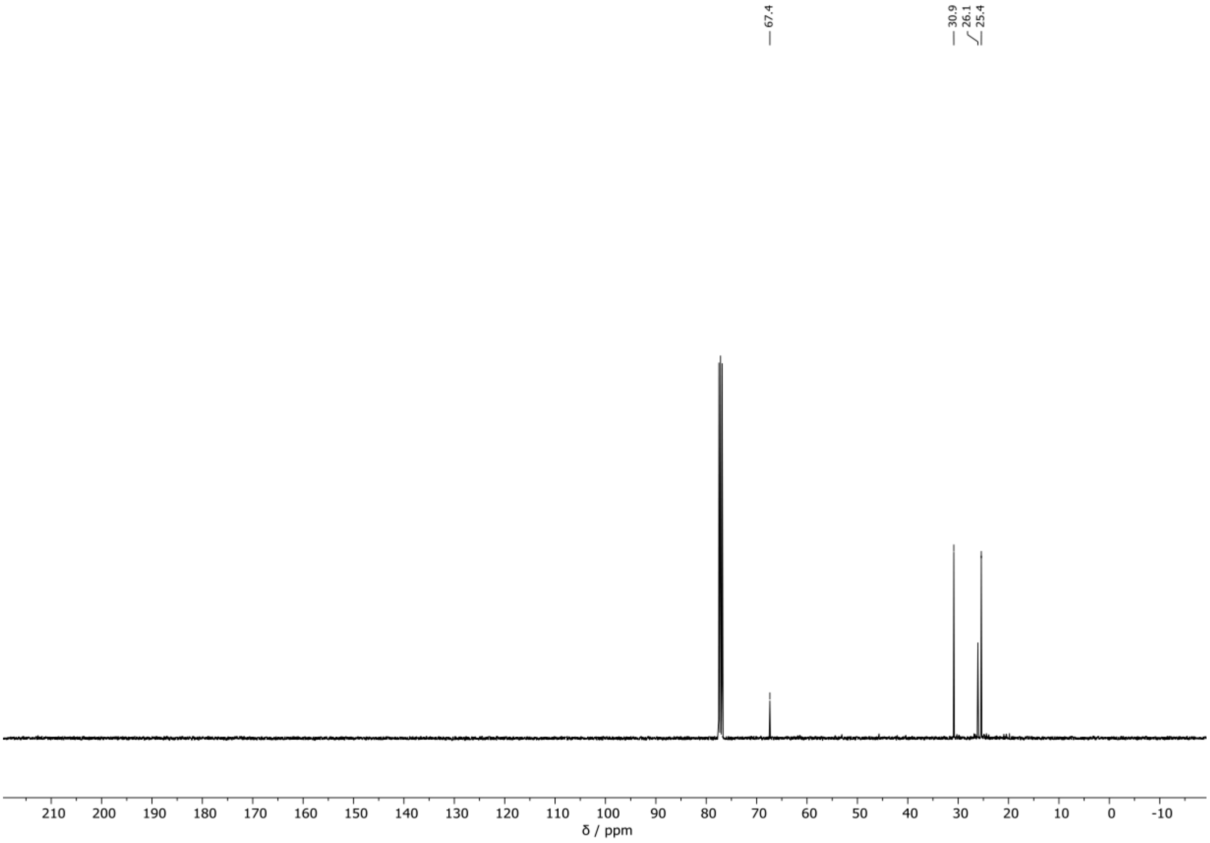
67.4
30.9
26.1
25.4
210
200
190
180
170
160
150
140
130
120
110
100
90
80
70
60
50
40
30
20
10
0
-10
δ / ppm

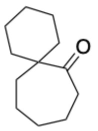
O

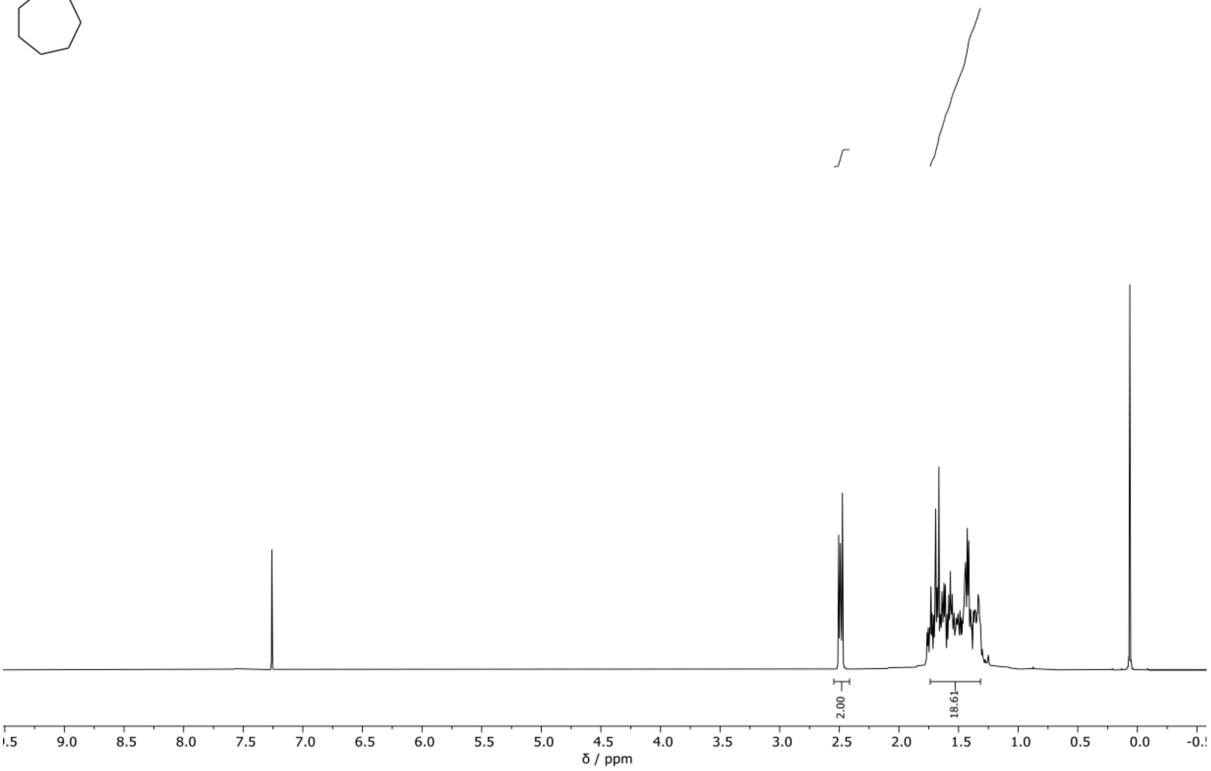
2.00
18.61
.5
9.0
8.5
8.0
7.5
7.0
6.5
6.0
5.5
5.0
4.5
4.0
3.5
3.0
2.5
2.0
1.5
1.0
0.5
0.0
-0.
δ / ppm

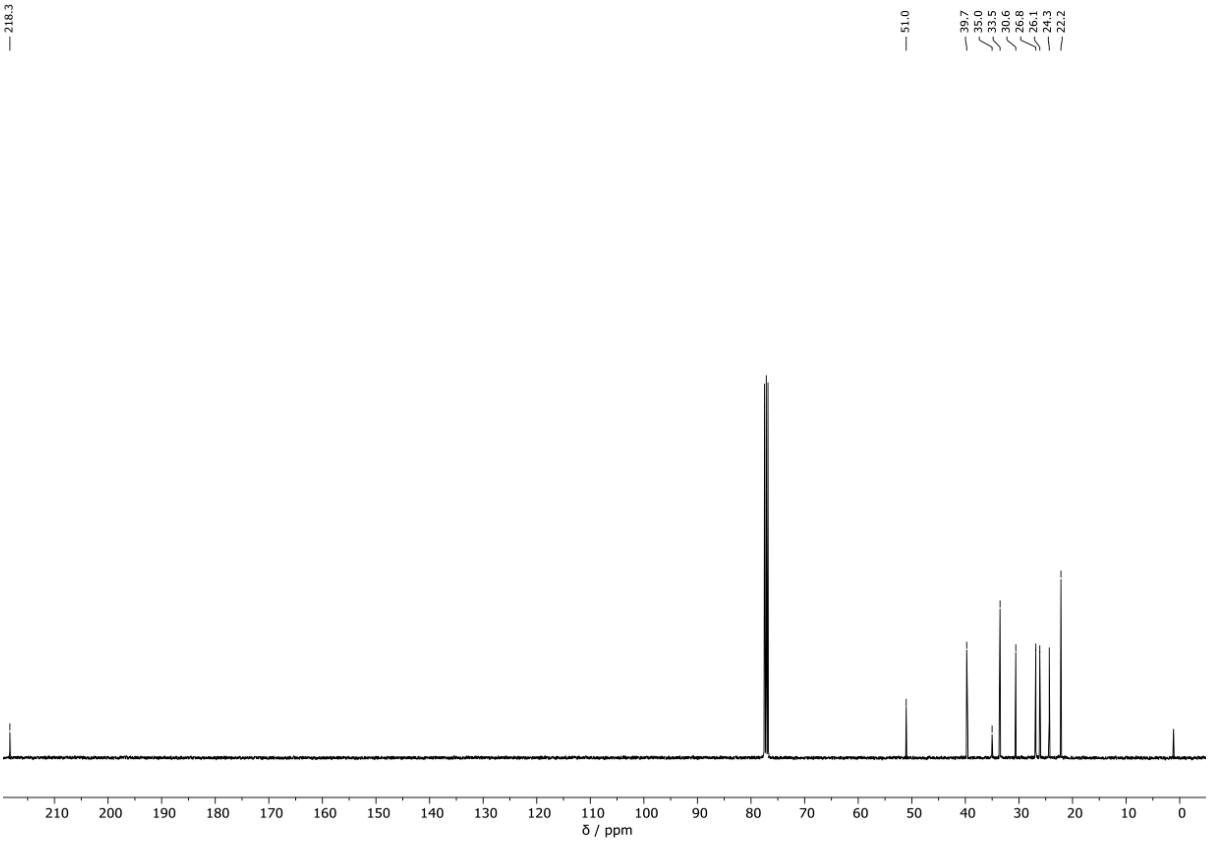
218.3
51.0
39.7
35.0
33.5
30.6
26.8
26.1
24.3
22.2
210
200
190
180
170
160
150
140
130
120
110
100
90
80
70
60
50
40
30
20
10
0
δ / ppm

7. References

[1] C.-Y. Huang, A. G. Doyle, *Chem. Rev.* **2014**, *114*, 8153–8198.
[2] H. O. House, *J. Am. Chem. Soc.* **1955**, *77*, 3070–3075.
[3] H. O. House, R. L. Wasson, *J. Am. Chem. Soc.* **1956**, *78*, 4394–4400.
[4] J. Meinwald, S. S. Labana, M. S. Chadha, *J. Am. Chem. Soc.* **1963**, *85*, 582–585.
[5] J. Meinwald, S. S. Labana, L. L. Labana, G. H. Wahl, *Tetrahedron Lett.* **1965**, *6*, 1789–1793.
[6] C. W. Bock, P. George, J. P. Glusker, *J. Org. Chem.* **1993**, *58*, 5816–5825.
[7] B. Blackett, J. Coxon, M. Hartshorn, K. Richards, *Aust. J. Chem.* **1970**, *23*, 839–840.
[8] J. M. Coxon, A. J. Thorpe, W. B. Smith, *J. Org. Chem.* **1999**, *64*, 9575–9586.
[9] J. M. Coxon, A. J. Thorpe, *J. Org. Chem.* **2000**, *65*, 8421–8429.
[10] J. M. Fraile, J. A. Mayoral, L. Salvatella, *J. Org. Chem.* **2014**, *79*, 5993–5999.
[11] Y. Yamano, M. Ito, *Org. Biomol. Chem.* **2007**, *5*, 3207–3212.
[12] S. Yokoshima, H. Tokuyama, T. Fukuyama, *Angew. Chem. Int. Ed.* **2000**, *39*, 4073–4075.
[13] H. Lin, S. J. Danishefsky, *Angew. Chem. Int. Ed.* **2003**, *42*, 36–51.
[14] M. G. Constantino, P. M. Donate, D. Frederico, T. V. Carvalho, L. E. Cardoso, J. Zukerman-Schpector, *Synth. Commun.* **2000**, *30*, 3327–3340.
[15] S. Kulasegaram, R. J. Kulawiec, *J. Org. Chem.* **1994**, *59*, 7195–7196.
[16] S. Kulasegaram, R. J. Kulawiec, *J. Org. Chem.* **1997**, *62*, 6547–6561.
[17] A. M. Anderson, J. M. Blazek, P. Garg, B. J. Payne, R. S. Mohan, *Tetrahedron Lett.* **2000**, *41*, 1527–1530.
[18] K. A. Bhatia, K. J. Eash, N. M. Leonard, M. C. Oswald, R. S. Mohan, *Tetrahedron Lett.* **2001**, *42*, 8129–8132.
[19] I. Karamé, M. L. Tommasino, M. Lemaire, *Tetrahedron Lett.* **2003**, *44*, 7687–7689.
[20] B. C. Ranu, U. Jana, *J. Org. Chem.* **1998**, *63*, 8212–8216.
[21] F. Martínez, C. del Campo, E. F. Llama, *J. Chem. Soc. Perkin Trans. 1* **2000**, 1749–1751.
[22] A. Procopio, R. Dalpozzo, A. De Nino, M. Nardi, G. Sindona, A. Tagarelli, *Synlett* **2004**, 2633–2635.
[23] K. Suda, K. Baba, S. Nakajima, T. Takanami, *Tetrahedron Lett.* **1999**, *40*, 7243–7246.
[24] K. Suda, K. Baba, S. I. Nakajima, T. Takanami, *Chem. Commun.* **2002**, 2570–2571.
[25] E. Ertürk, M. Göllü, A. S. Demir, *Tetrahedron* **2010**, *66*, 2373–2377.
[26] M. W. C. Robinson, K. S. Pillinger, A. E. Graham, *Tetrahedron Lett.* **2006**, *47*, 5919–5921.
[27] M. W. C. Robinson, K. S. Pillinger, I. Mabbett, D. A. Timms, A. E. Graham, *Tetrahedron* **2010**, *66*, 8377–8382.
[28] K. Ishihara, N. Hanaki, H. Yamamoto, *Synlett* **1995**, 721–722.
[29] K. Maruoka, T. Ooi, H. Yamamoto, *J. Am. Chem. Soc.* **1989**, *111*, 6431–6432.
[30] K. Maruoka, R. Bureau, T. Ooi, H. Yamamoto, *Synlett* **1991**, 491–492.
[31] K. Suda, T. Kikkawa, S. Nakajima, T. Takanami, *J. Am. Chem. Soc.* **2004**, *126*, 9554–9555.
[32] K. Suda, S. Nakajima, Y. Satoh, T. Takanami, *Chem. Commun.* **2009**, 1255–1257.
[33] B. Rickborn, R. M. Gerkin, *J. Am. Chem. Soc.* **1968**, *90*, 4193–4194.
[34] B. Rickborn, R. M. Gerkin, *J. Am. Chem. Soc.* **1971**, *93*, 1693–1700.
[35] P. R. Schreiner, A. Wittkopp, *Org. Lett.* **2002**, *4*, 217–220.
[36] R. Hrdina, C. E. Müller, R. C. Wende, K. M. Lippert, M. Benassi, B. Spengler, P. R. Schreiner, *J. Am. Chem. Soc.* **2011**, *133*, 7624–7627.
[37] M. Zhuang, H. Du, *Org. Biomol. Chem.* **2013**, *11*, 1460–1462.
[38] H. Wu, Q. Wang, J. Zhu, *J. Am. Chem. Soc.* **2019**, *141*, 11372–11377.
[39] D. Ma, C.-B. Miao, J. Sun, *J. Am. Chem. Soc.* **2019**, *141*, 13783–13787.
[40] S. Sakane, K. Maruoka, H. Yamamoto, *Tetrahedron* **1986**, *42*, 2203–2209.
[41] K. Maruoka, Y. Hoshino, T. Shirasaka, H. Yamamoto, *Tetrahedron Lett.* **1988**, *29*, 3967–3970.
[42] K. Mikami, M. Terada, T. Nakai, *J. Am. Chem. Soc.* **1990**, *112*, 3949–3954.
[43] K. Mikami, M. Terada, Y. Motoyama, T. Nakai, *Tetrahedron Asymmetry* **1991**, *2*, 643–646.
[44] J. Long, J. Hu, X. Shen, B. Ji, K. Ding, *J. Am. Chem. Soc.* **2002**, *124*, 10–11.
[45] A. L. Costa, M. G. Piazza, E. Tagliavini, C. Trombini, A. Umani-Ronchi, *J. Am. Chem. Soc.* **1993**, *115*, 7001–7002.
[46] Z. G. Zhang, P. R. Schreiner, *Chem. Soc. Rev.* **2009**, *38*, 1187–1198.
[47] S. M. Banik, A. Levina, A. M. Hyde, E. N. Jacobsen, *Science* **2017**, *358*, 761–764.
[48] N. Prileschajew, *Ber. Dtsch. Chem. Ges.* **1909**, *42*, 4811–4815.
[49] M. Kaik, J. Gawroński, *Tetrahedron Asymmetry* **2003**, *14*, 1559–1563.
[50] W. Eschweiler, *Ber. Dtsch. Chem. Ges.* **1905**, *38*, 880–882.
[51] P. C. Bulman Page, M. M. Farah, B. R. Buckley, Y. Chan, A. J. Blacker, *Synlett* **2016**, *27*, 126–130.
[52] A. Berkessel, B. Seelig, *Synthesis* **2009**, 2113–2115.

[53] A. Rostami, A. Colin, X. Y. Li, M. G. Chudzinski, A. J. Lough, M. S. Taylor, *J. Org. Chem.* **2010**, *75*, 3983–3992.

[54] N. Busschaert, R. B. P. Elmes, D. D. Czech, X. Wu, I. L. Kirby, E. M. Peck, K. D. Hendzel, S. K. Shaw, B. Chan, B. D. Smith, *Chem. Sci.* **2014**, *5*, 3617–3626.

[55] I. Thomsen, K. Clausen, S. Scheibye, S.-O. Lawesson, *Organic Syntheses*, Wiley, Hoboken, **2003**, pp. 158–158.

[56] M. Rombola, V. H. Rawal, *Org. Lett.* **2018**, *20*, 514–517.

[57] M. B. Harkness, E. Alvarado, A. C. Badaj, B. C. Skrela, L. Fan, G. G. Lavoie, *Organometallics* **2013**, *32*, 3309–3321.

[58] S. Berger, W. Bock, C. F. Marth, B. Raguse, M. T. Reetz, *Magn. Reson. Chem.* **1990**, *28*, 559–560.

[59] H. Mayr, M. Breugst, A. R. Ofial, *Angew. Chem. Int. Ed.* **2011**, *50*, 6470–6505.

[60] H. Helten, B. Dutta, J. R. Vance, M. E. Sloan, M. F. Haddow, S. Sproules, D. Collison, G. R. Whittell, G. C. Lloyd-Jones, I. Manners, *Angew. Chem. Int. Ed.* **2013**, *125*, 455–458.

[61] G. Jakab, C. Tancon, Z. Zhang, K. M. Lippert, P. R. Schreiner, *Org. Lett.* **2012**, *14*, 1724–1727.

[62] R. West, H. Y. Niu, *J. Am. Chem. Soc.* **1963**, *85*, 2589–2590.

[63] M. K. J. ter Wiel, R. A. van Delden, A. Meetsma, B. L. Feringa, *J. Am. Chem. Soc.* **2003**, *125*, 15076–15086.

[64] D. Parmar, E. Sugiono, S. Raja, M. Rueping, *Chem. Rev.* **2014**, *114*, 9047–9153.

[65] B. Mechsner, B. Henßen, J. Pietruszka, *Org. Biomol. Chem.* **2018**, *16*, 7674–7681.

[66] F. Romanov-Michailidis, L. Guénée, A. Alexakis, *Angew. Chem. Int. Ed.* **2013**, *125*, 9436–9440.

[67] S. Brenet, C. Minozzi, B. Clarens, L. Amiri, F. Berthiol, *Synthesis* **2015**, *47*, 3859–3873.

[68] L. Qin, P. Wang, Y. Zhang, Z. Ren, X. Zhang, C.-S. Da, *Synlett* **2015**, *27*, 571–574.

[69] N. Momiyama, H. Nishimoto, M. Terada, *Org. Lett.* **2011**, *13*, 2126–2129.

[70] T. Harada, K. Kanda, *Org. Lett.* **2006**, *8*, 3817–3819.

[71] H. B. Kagan, J. C. Fiaud, *Top. Stereochem.* **2007**, *18*, 249–330.

[72] M. D. Greenhalgh, J. E. Taylor, A. D. Smith, *Tetrahedron* **2018**, *74*, 5554–5560.

[73] M. Melikian, J. Gramüller, J. Hioe, J. Greindl, R. M. Gschwind, *Chem. Sci.* **2019**, *10*, 5226–5234.

[74] N. Lokesh, J. Hioe, J. Gramüller, R. M. Gschwind, *J. Am. Chem. Soc.* **2019**, *141*, 16398–16407.

[75] D. Jansen, J. Gramüller, F. Niemeyer, T. Schaller, M. C. Letzel, S. Grimme, H. Zhu, R. M. Gschwind, J. Niemeyer, *Chem. Sci.* **2020**, *11*, 4381–4390.

[76] L. J. Rono, H. G. Yayla, D. Y. Wang, M. F. Armstrong, R. R. Knowles, *J. Am. Chem. Soc.* **2013**, *135*, 17735–17738.

Abbreviations and Acronyms

Ac	acetyl
AC	absolute configuration
aq.	aqueous
Ar	aromatic substituent
asym.	asymmetric
BINOL	1,1’-bi-2,2’-naphthol
BLA	Brønsted acid assisted Lewis acid
Bn	benzyl
Boc	*tert*-butoxycarbonyl
b.p.	boiling point
br	broad
Bu	butyl
Bz	benzoyl
cat.	catalyst
calcd.	calculated
CBS	Corey-Bakshi-Shibata
conv.	conversion
CPA	chiral phosphoric acid
DA	Diels-Alder
D*t*BP	2,6-di*tert*butylpyridine
DFT	density functional theory
d	doublet
dd	doublet of doublet
DCM	dichloromethane
DED	dispersion energy donor
D*i*PEA	diisopropylethylamine
DoE	Design of Experiments
Dosy	diffusion ordered spectroscopy
equiv.	equivalent
EASY-ROESY	efficient adiabatic symmetrized rotating frame Overhauser effect spectroscopy
EDG	electron donating group
ee	enantiomeric excess
Et_3N	triethylamine
EWG	electron withdrawing group
Fmoc	fluorenylmethoxycarbonyl
GC	gas chromatography

HBD	hydrogen bond donor
HMR	House-Meinwald rearrangement
HPLC	high performance liquid chromatography
HRMS	high resolution mass spectroscopy
IDPi	imidodiphosphorimidate
*i*Pr	isopropyl
IR	infrared
KIE	kinetic isotope effect
LD	London dispersion
LED	local energy decomposition
LLA	Lewis acid assisted Lewis acid
m	multiplet
M	molarity [mol L^{-1}]
*m*CPBA	meta chloroperbenzoic acid
Me	methyl
MS	molecular sieve; mass spectroscopy
MTBE	methyl *tert*-butyl ether
MTPA	α-methoxy-α-trifluoromethylphenylacetic acid
MOF	metal organic framework
MOM	methoxy methyl
*n*Bu	*n*-butyl
NBO	natural bond orbital
NCI	noncovalent interaction
NHC	*N*-heterocyclic carbene
NMI	*N*-methylimidazole
NMR	nuclear magnetic resonance
NOE	nuclear Overhauser effect
NPA	*N*-phosphoramide
OXB	oxazaborolidine
PCM	polarizable continuum model
Ph	phenyl
Phthal	phthalimide
Pmh	π-methyl-L-histidine
Pr	propyl
PTC	phase transfer catalyst
quant.	quantitative
RDC	residual dipolar coupling
rt	room temperature
s	singlet
s-factor	selectivity factor

SPPS	solid phase peptide synthesis
t	triplet
*t*Bu	*tert*-butyl
THF	tetrahydrofuran
TLC	thin layer chromatography
Tos	tosyl
TS	transition structure
Tos	tosyl
vdW	van der Waals

Acknowledgements

Nun ist es an der Zeit all den Menschen zu danken, ohne die diese Arbeit niemals möglich gewesen wäre:

Mein herzlicher Dank geht an **Prof. Dr. Peter R. Schreiner, PhD** für die Aufnahme in seine Arbeitsgruppe, die Unterstützung, die exzellenten Arbeitsbedingungen und die gute Zusammenarbeit. Ich habe sehr viel gelernt in den vergangen Jahren!

Ein großes Dankeschön geht an **Lijuan Song, PhD** für die tolle Zusammenarbeit, die vielen Rechnungen und die fachlichen Diskussionen, die letztlich zu einer tollen Publikation führten.

Bei **Dr. Raffael Wende** bedanke ich mich herzlich für die große Unterstützung, die vielen wertvollen Ratschläge und das Korrekturlesen meiner Thesis.

Bei meinen Freunden und Kollegen **Alexander Seitz** und **Jan M. Schümann** danke ich für tolle Stunden im Labor, regelmäßige Kaffeepausen und anregende Diskussionen beim Feierabendbier.

Meinen Studenten **Felix Keul**, **Kai Feuer** und **Friedemann Dreßler** danke ich für den tollen Beitrag, die sie zu dieser Arbeit geleistet haben.

Ein besonderer Dank geht an alle Kolleginnen und Kollegen, die ich in den letzten Jahren kennengelernt habe. Insbesondere möchte ich mich bei **Dr. Dennis Gerbig**, **Dr. Hendrik Quanz, Dr. Dominik Niedek**, **Dr. Jan-Philipp Berndt**, **Cesare Savarino**, **Markus Schauermann**, **Lukas Ochmann**, **Frederik Erb** und **Lars Rummel** bedanken. Ich danke euch für die schöne Zeit und die zahlreichen Gespräche, die zu neuen Ideen und Erkenntnissen geführt haben.

Ich danke dem gesamten Team der OC-Analytik (**Anika Bernhardt**, **Stefan Bernhardt**, **Dr. Heike Hausmann**, **Edgar Reitz**, **Dr. Erwin Röcker**, **Steffen Wagner** und **Brigitte Weinl-Boulakhrouf**) für die vielen gemessenen Spektren und Chromatogramme und der Instandhaltung der chiralen Gaschromatographen.

Ich möchte dem Team der Chemikalienausgabe (**Mario Dauber**, **Eike Santowski** und **Rainer Schmidt**) und der Glasbläserei (**Anja Beneckenstein**) für die außerordentlich freundliche Unterstützung und gute Versorgung danken!

Meinen **Eltern** danke ich von Herzen, dass sie mir sowohl Studium als auch die Promotion ermöglicht haben und mir auf diesem Weg immer Unterstützung und Rückhalt entgegen gebracht haben.

Abschließend möchte ich mich bei meiner Freundin **Isabella** bedanken. Ich danke dir für dein Vertrauen, deine absolute Unterstützung, deine Geduld und die vielen aufbauenden Worte nach Rückschlägen im Labor.